JANUARY - MARCH · 1961

VOLUME XXXIV

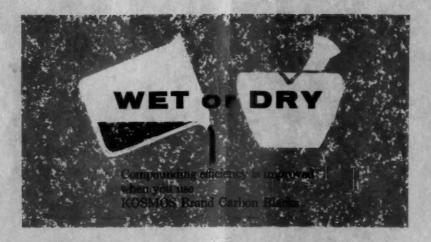
HILIMBED ONE

RUBBER CHEMISTRY

AND TECHNOLOGY

DIVISION OF RUBBER CHEMISTRY
OF THE AMERICAN CHEMICAL SOCIETY







End-Product and Processing Requirements . . .

United's broad range of dispersant-free BAYTOWN black masterbatches is tailored to serve your individual production line needs more economically.



For fast, reliable service please contact:

UNITED CARBON COMPANY, INC.

A Subsidiary of United Carbon Company

AKRON CHICAGO LOS ANGELES BOSTON HOUSTON MEMPHIS

In Canada: CANADIAN INDUSTRIES LIMITED



RUBBER CHEMISTRY AND TECHNOLOGY

Published in Five Issues (January-March, April-June, July-September, October-November & December) under the Auspices of the Division of Rubber Chemistry of the American Chemical Society,

Prince and Lemon Streets,

Lancaster, Pa.

Editor	DAVID CRAIG	Business ManagerG	EORGE	HACKIM
Associate Editor	.S. D. GEHMAN	Advertising ManagerG	EORGE	HACKIM
Associate Editor	.B. L. Johnson	Treasurer	.D. F.	BEHNEY

Vol. XXXIV January-March 1961

No. 1

CONTENTS

	General Section	PAGE
Officers		iii
Sponsored Rubber Groups		vi
Chemical Institute of Canada Rub	ber Division and Sponsored Rub	ber Groups x
New Books and Other Publications		xi
Bibliographies Available in Rubber	Division Library	xii
ISO Recommendations		Xvii
ISO Recommendations. Determination of KOH Numb Determination of Resistance t	er of Latex	XVII
Determination of Resistance to	o Flex Cracking of Vulcanized N	latural or Syn-
thetic Rubber (De Mattia	a Type Machine)	XX
Determination of Resistance to	o Crack Growth of Vulcanized N	atural or Syn-
thetic Rubber (De Mattia	a Type Machine)	
IUPAC The 1961 Gordon Research Conference	ence on Elastomers	xxxii
	Papers	
The Pico Laboratory Abrasion Tes	st. EDWIN B. NEWTON, HERSHE	L W. GRINTER
AND D. SCOTT SEARS		1
Attrited Carbon Blacks and Their	Behavior in Elastomers. III.	Effects in SBR
and Other Rubbers. A. M. G.	ESSLER	16
and Other Rubbers. A. M. G Effects of Carbon Black Structure	on Tire Tread Wear. T. D. Be	OLT AND E. M.
DANNENBERG		43
Features of the Reinforcing Actio	on of Carbon Blacks Deduced I	From the Tear
Propagation of Filled Vulcaniz	ates. A. I. LUKOMSKAYA	57
Rupture of Rubber. VI. Further	r Experiments of the Tear Cri	terion. A. G.
THOMAS		66
Rupture of Rubber. VII. Effects	of Rate of Extension in Tensile	Tests. H. W.
GREENSMITH		76
Rupture of Rubber. VIII. Comp	arisons of Tear and Tensile Rup	oture Measure-
ments. H. W. GREENSMITH Mechanism of Rupture of High Pol		
Mechanism of Rupture of High Pol	lymers. V. E. Gul	101
Approximate Analysis of the Stress	sed State of Rubber Specimens,	Fear Tested by
Various Methods. A. I. Luko Volume Changes and Dewetting i	OMSKAYA	
Volume Changes and Dewetting	in Glass Bead-Polyvinyl Chloric	de Elastomeric
Composites Under Large Deloi	rmations. Thor L. Smith	123
The Effect of Network Flaws on the		
Dynamic Properties of Rubberlik	e Materials and the Isolation	
Vibration. J. C. Snowdon		D-11-04-in-
Determination of the Damping Cha	dio Frequencies, Francis M.	
	no Frequencies. FRANCIS M.	
Cheighton M. Ougos		100

No matter where in the world you are, Cabot can serve you better



of carbon black than anyone else - and sells more - not only in the U.S. but throughout the world. On all six continents. In 58 different countries.

Cabot has more production facilities — abroad — than anyone else. Ships from more countries. Sells in more currencies. And Cabot is continually establishing new plants.

That's why Cabot can serve your carbon black needs better than anyone else — internationally.

Sales representatives in all principal cities of the world



CABOT CORPORATION

125 HIGH STREET, BOSTON 10, MASSACHUSETTS

AKRON . CHICAGO . DALLAS . LOS ANGELES . NEW BRUNSWICK . NEW YORK

Cabot Carbon of Canada, Ltd.

121 Richmond Street West, Toronto 1, Ontario, Canada

Cabot Carbon Limited

62 Brompton Road, London, S.W. 3, England

Cabot France, S.A.,
45, rue de Courcelles, Paris 8, France

Cabet Italiana, S.p.A., Via Larga 19, Milano, Italy

Cabet Europa, 45, rue de Courcelles, Paris 8, France

Joint Ownership of Australian Carbon Black

Pty., Ltd., Millers Road, Altona, Victoria, Australia

CHANNEL BLACKSI Spheron 9 EPC FURNACE BLACKSI Vulcan 9 SAF Vulcan C CF Sterling 99 FF Sterling S SRF THERMAL BLACKSI Sterling FT Sterling AT Sterling AT Sterling AT Regal 600 Regal 300 Vulcan C CF Sterling S SRF THERMAL BLACKS:

Vulcan 3 HAF
Vulcan XC-72 ECF
Sterling V GPF
Sterling L HAF
Polletox NS SPF
Sterling R SPF
Sterling MT-NS
Sterling FT-FF
Sterling MT-FF

Regal SRF

The Elastorelaxometer for Large Reversible Deformation of Elastomeric Systems	
and Polymer Solutions. A. A. Trapeznikov	165
Diene Rubber: Compounding and Testing. WARD A. SMITH AND JAMES M. WILLIS	176
cis-1,4-Polyisoprene Rubber By Alkyl Lithium Initiated Polymerization. Hugh	191
E. DIEM, HAROLD TUCKER, AND C. F. GIBBS	191
Methods. A. I. Yakubchik and A. I. Spasskova	200
Ozonation of Butyl Rubber to Estimate Unsaturation. I. S. Ungar and G. A. Lutz	
Structure of the Spongy Polymer of Isoprene. A. I. Spasskova and D. I.	
RABINOVITCH. Mechanochemical Transformation and Synthesis of Polymers. A. A. Berlin	211
Mechanochemical Transformation and Synthesis of Polymers. A. A. Berlin	215
Compounding SBR for Radiation Resistance. HERBERT R. ANDERSON, JR	228
X-Ray Diffraction Comparison of Radiation Damage in Rubber. W. E. Shelberg	250
AND L. H. GEVANTMAN. Vulcanization of SBR by Gamma Radiation. P. M. Arnold, Gerard Kraus, and R. H. Anneson, In	200
R. H. Anderson, Jr.	265
R. H. Anderson, Jr Determination of Degree of Crosslinking in Natural Rubber Vulcanizates. Part	
III. L. MULLINS	279
Determination of Degree of Crosslinking in Natural Rubber Vulcanizates. Part IV.	
Stress-Strain Behavior at Large Extensions. L. Mullins	290
Determination of Degree of Crosslinking in Natural Rubber Vulcanizates. Part V.	
Effect of Network Flaws Due to Free Chain Ends. L. Mullins and A. G. Thomas.	301
Determination of Degree of Crosslinking in Natural Rubber Vulcanizates. Part	100
VI. Evidence for Chain Scission During the Crosslinking of Natural Rubber	
	309
Electron Spin Resonance Study of the Interaction of Tetramethylthiuram Disul-	
phide (TMTD) with Rubber and Related Compounds. S. E. Bresler, B. A.	010
Dogadkin, E. N. Kazbekov, E. M. Saminskii and V. A. Shershnev	
Some Aspects of High Temperature Vulcanization. G. BIELSTEIN	319
	334
The Shape of Specimen and the Measurement of Permanent Set. Shiro Yabuta	
A New Indentor Hysteresimeter. G. Tangorra	347
Apparatus Study of Pore Formation Kinetics in Vulcanization. M. A. Albam and	
A. P. PISARENKO	357

RUBBER CHEMISTRY AND TECHNOLOGY

RUBBER CHEMISTRY AND TECHNOLOGY is published under the supervision of the Editor, representing the Division of Rubber Chemistry of the American Chemical Society. One object of the publication is to render available in convenient form under one cover important and permanently valuable papers on fundamental research, technical developments, and chemical engineering problems relating to rubber or its allied substances. Another object is to publish timely reviews.

RUBBER CHEMISTRY AND TECHNOLOGY may be obtained in one of three ways:

(1) Any member of the American Chemical Society may become a member of the Division of Rubber Chemistry by payment of the dues (\$6.00 per year) to the Division and thus receive Rubber Chemistry and Technology.

(2) Anyone who is not a member of the American Chemical Society may become an Associate of the Division of Rubber Chemistry upon payment of \$8.50 per year to the Treasurer of the Division of Rubber Chemistry, and thus receive Rubber Chemistry and Technology.

(3) Companies and libraries may subscribe to Rubber Chemistry and Technology at the subscription price of \$9.50 per year.

To these charges of \$6.00, \$8.50 and \$9.50, respectively, per year, postage of \$.30 per year must be added for subscribers in Canada, and \$.90 per year for those in all other countries not United States possessions.

All applications to become Members or Associates of the Division of Rubber Chemistry, with the privilege of receiving this publication, all correspondence about subscriptions, back numbers, changes of address, missing numbers, and all other information or questions should be directed to the Treasurer of the Division of Rubber Chemistry, D. F. Behney, Harwick Standard Chemical Co., 60 South Seiberling Street, Akron 5, Ohio.

Articles, including translations and their illustrations, may be reprinted if due credit is given RUBBER CHEMISTRY AND TECHNOLOGY.

Announcing_

the production of HAF and ISAF carbon blacks at our new ECHO Philblack plant, Orange, Texas. This gives Phillips customers added assurance of a continuing supply of these high quality blacks.

PHILLIPS CHEMICAL COMPANY Rubber Chemicals Sales Division, Akron, Ohio







CHEMI-VIC puts you on the right track against ozone attack!

The basic feature of new CHEMI-VIC is well described in the photograph above. That's CHEMI-VIC on the left, compared to a similar, currently popular elastomer, after 144 hours in an ozone box (100 pphm) at 100° F.

CHEMI-VIC is brand-new – a vinyl reinforced nitrile elastomer. In addition to outstanding resistance to ozone and weather, it offers high physical properties plus exceptional resistance to oil. Moreover, it's light in color

easy to compound and process on standard equipment.

New CHEMI-VIC is available in two grades: CHEMI-VIC 400 for general purposes. CHEMI-VIC 800 for extrusion and calendering application. Typical uses: hose, belting, wire and cable jacketing, weather stripping, integral molded shoe soles. If you would like more information, just write: Goodyear, Chemical Division, Dept. A-9430, Akron 16, Ohio.



Lots of good things come from

GOODFYEAR

CHEMICAL DIVISION

Chemi-Vic-T. M. The Goodyear Tire & Rubber Company, Akron, Ohio

From Eastman... A family of fine products to serve the rubber industry ANTIOZONANTS ANTIOXIDANTS EASTOZONE® 32 Especially useful in static 2.5-DI-TERTexposure applications. BUTYLHYDROQUINONE 2,6-Di-tert-butyl-p-cresol. ADHESIVES Effective in rubber and An excellent non-discoloring and non-staining antioxidant synthetic elastomers; also an EASTMAN excellentipolymerization inhibitor. of low odor and toxicity for 910 ADHESIVE light-colored rubber A fast-setting and synthetic elastomers. adhesive for strong A series of non-discoloring, HYDROQUINONE rubber-to-rubber and food-grade antioxidants. MONOMETHYL ETHER rubber-to-metal bonds. TECQUINOL® Valuable antioxidant and WAXES polymerization inhibitor. Retards polymerization of styrene EPOLENE LV Non-emulsifiable, and gelation of rubber sols. low-molecular-weight, EPOLENE® N polyethylene resins for CELLULOSICS se as calender release EPOLENE HD agents in milling. CELLULOSE ACETATE **EPOLENE C** BUTYPATE For use in abrasion-resistant lacquers for rubber articles. flow and bodying agent PLASTICIZERS for coatings made from urethane. DIBUTYL PHTHALATE INTERMEDIATES ISOBUTYRONITRILE DI-(2-ETHYLHEXYL) Reactants in PHTHALATE the preparation of facilitates reclamation of scrap antioxidants and rubber. Esters for softening agents DI-(2-ETHYLHEXYL) accelerators. and solvents. **ACETALDEHYDE** DIBUTYL SERACATE ACETONE Preparation of hydrocarbon resins POLYMERIC CROTONALDEHYDE DI-(B-HYDROXY- ETHYL) PLASTICIZER ETHER OF HYDROQUINONE ISOBUTYRALDEHYDE NP-10 Cross-linking agent for polyurethanes. PROPIONALDEHYDE NEOPENTYL GLYCOL n-BUTYRALDEHYDE Polyesters of outstanding CROTONIC ACID stability for polyurethane. CHEMICAL PRODUCTS, INC. HYDROQUINONE KINGSPORT, TENNESSEE (tech.)

SALES OFFICES: Eastman Chemical Products, Inc., Kingsport, Tannessee; Aliante; Boston; Buffole; Chicago; Cincinneti; Cleveland; Detroit; Greanboro, N. C.; Noustan; Kansos City, Ma., New York City; Philodelphia; S.; Louis, West Coast: Wilson & Ges. Mayor & Company, San Francisco; los Angeles; Portlond; Solt Los City; South

A new booklet containing more information on the products described here has just been published. For your copy, write to Subsidiary of Eastman Kodak Company



B-58's mid-air refueling hazard reduced by Hycar

As a safeguard against leakage of jet fuels, each B-58 uses sleeves made of Hycar nitrile rubber around the connection with the tanker plane's fueling pipe. Each sleeve has a tube to escort any leaked fuel out of the plane—away from danger.

The flexibility of rubber is needed for this sleeve, but many properties ordinary rubber can't provide are also needed. That's why Hycar was chosen. Tough and long-lasting, it retains flexibility even at low temperatures of high altitudes. And it's highly resistant to change when exposed to all types of petroleum base fuels.

Here's another unusual performance problem solved by Hycar. It may help you solve a problem. For information, write Dept. ME-1, B.F.Goodrich Chemical Company, 3135 Euclid

Avenue, Cleveland 15, Ohio. In Canada: Kitchener, Ontario.



B.F.Goodrich Chemical Company

a division of The B.F.Goodrich Company



BEST FOR RUBBER

AT A SAVINGS



FRENCH PROCESS





LARGE STOCKS





DELIVERED TO YOUR PLANT FASTER BY TRUCK





74 1 0

USE PASCO ZINC OXIDE

PACIFIC

SMELTING

COMPANY

22219 South Western Avenue

TORRANCE, CALIFORNIA

Naugatuck RUBBER CHEMICALS

ACCELERATORS

Thiazoles Thiurams Dithiocarbamates Aldehyde Amines Tuex®* Arazate® Beutene® M-B-T M-B-T-S Ethyl Tuex* Butazate® Hepteen Base® O-X-A-F Monex** **Butazate 50-D** Trimene Base® DELAC-S Ethazate® Trimene® Pentex Pentex Flour Ethazate 50-D Methazate* Xanthates **Vulcanizing Agents** C-P-B® G-M-F Z-B-X Dibenzo G-M-F

ACTIVATOR

D-B-A Accelerator

ANTIOXIDANTS

 Discoloring
 Nondiscoloring
 Seminox®
 Antiozonants

 Aminox®
 Polygard®
 nondiscoloring
 Flexzone 3-C

 Aranox®
 Naugawhite
 Octamine
 Flexzone 6-H

 B-L-E-25
 Naugawhite Powder
 Betanox Special®

Flexamine G V-G-B®

BLOWING AGENTS

Celogen® Celogen-80 Celogen-AZ®

SUNPROOFING WAXES

Sunproof® Regular Sunproof® Improved Sunproof® Jr.
Sunproof®-713 Sunproof® Super

MISCELLANEOUS SPECIAL PRODUCTS

BWH-I – mixture of oils

DDM – dodecyl mercaptan

LAUREX® – zinc laurate

PROCESS STIFFENER *710 –
26.4% hydrazine salt and 73.6% inert mineral filler

THIOSTOP N – 35% aqueous solution of sodium dimethyl dithiocarbamate

TONOX - p, p'-diaminodiphenylmethane

RETARDERS

RETARDER E-S-E-N RETARDER J

*available in Nauget form



Naugatuck Chemical

Division of United States Rubber Company Naugatuck, Connecticut



QUALITY PRODUCTS for the RUBBER INDUSTRY

General Tire's Chemical Division is constantly aware of the needs of the rubber industry, and provides these specially-formulated products to meet those needs. Write or call for further information and generous samples.

GEN-TAC • Vinyl pyridine latex. Assures excellent fabric-to-rubber adhesion using nylon or rayon cords.

KO-BLEND • Latex-compounded masterbatch, 85% insoluble sulfur colloidally dispersed in SBR latex. Cuts whitewall rejects and reworks . . . eliminates spots, streaks and batch softening.

MT • 50 SBR —50 TMTD latex-compounded masterbatch. Gives faster, more even dispersion, allowing full advantage of TMTD accelerator. Assures uniform cure, at no premium cost.

GENTRO . Top-quality cold SBR Polymers.

GENTRO-JET • Cold and oil-extended black masterbatches, for easier processing and more efficient production.

GEN-FLO • Styrene-butadiene, with balanced stabilization system, low odor, and excellent mechanical stability.

ACRI-FLO • Styrene-acrylic, offering excellent adhesion, mechanical stability and UV heat and light stability.

a complete family of top-quality, versatile resins formulated to meet specific needs.

THE GENERAL TIRE & RUBBER COMPANY
CHEMICAL DIVISION . AKRON, OHIO

Creating Progress Through Chemistry



Now On Stream CIS-4*

stable supply of synthetic polybutadiene rubber . . . dramatically improves tire performance. Proved in over 3 million miles of road tests . . .

- CIS-4 gives more mileage than any other tread rubber now used
- CIS-4 excels even natural rubber in resilience
- CIS-4 has low heat build-up . . . equal to natural rubber
- You can depend on the uniform high quality of CIS-4

*A trademark

PHILLIPS CHEMICAL COMPANY

Rubber Chemicals Sales Division, 318 Water St., Akron 8, Ohio

District Offices: Chicago, Dallas, Providence and Trenton
West Coast: Harwick Standard Chemical Company, Los Angeles, California

Export Sales: Phillips Petroleum International Corporation • Sumatrastrasse 27, Zurich 6, Switzerland
Distributors of Phillips Chemical Company Products • 80 Broadway, New York 5, N. Y.



HERE'S HOW WITCO-CONTINENTAL PROTECTS

YOUR CARBON BLACK DOLLAR

THROUGH

Quicker, More Dependable Shipments • Unmatched Care in Packaging
Outstanding Loading and Stacking Techniques
Faster. Cleaner Unloading and Handling

CARBON BLACKS . . . PRODUCED AND HANDLED WITH CARE BY WITCO-CONTINENTAL

Only Witco-Continental gives carbon blacks such kid-glove treatment in packaging and shipping. There's no compromise on quality and no compromise on service. Facilities are maintained in every sales office city for ex-warehouse customers. For outstanding service and personalized attention on all your carbon black orders...be sure to specify WITCO-CONTINENTAL.



There's less chance of shipping delay with Witco-Continental carbon blacks. We print your purchase order number, code or pigment number, type of black and other information, on every bag. Result is easier inventory, checking and handling.

Improved packing and better palletizing are achieved through specially built bag-shaping machines. You choose the type of bag you want.

Valve bags mean better unit loading, cleaner warehousing, faster and easier handling. Witco-Continental's exclusive, patented valve-filling machines insuregreater uniformity of outside bag dimensions.







When carbon blacks leave Witco-Continental plants, you can be sure they're in good condition. We photograph each shipment after loading as a check on correct and damage-free stacking. These photographs, with specially designed loading diagrams attached, are then sent to you as your check on shipping conditions.



Special car liners prevent interlocking of bags and protect them from each other and from the sides of cars or trailers. Convenient, disposable pallets facilitate handling, yet eliminate storage or return costs.



If you prefer shipment by hopper car, Witco-Continental traffic control system means that you can get same-day information on the whereabouts of your shipment from your local sales office. There are 113 carefully maintained hopper cars ready to serve you.



WITCO CHEMICAL COMPANY, Inc. CONTINENTAL CARBON COMPANY



Chicago · Boston · Akron · Atlanta · Houston · Los Angeles San Francisco · London and Manchester, England

DU PONT CHEMICALS and COLORS

DEPENDABLE IN PERFORMANCE... UNIFORM IN QUALITY

ACCELERATORS

Accelerator No. 8 Accelerator 552 Accelerator 808 Accelerator 833 Conac S MRT **MBTS**

MBTS Grains NA-22 Permalux **Polyac Pellets** Tepidone Tetrone A Thionex **Thionex Grains**

Thiuram E Thiuram E Grains Thiuram M Thiuram M Grains Zenite

Zenite Special Zenite A Zenite AM

ANTI-OXIDANTS

Akroflex C Pellets Akroflex CD Pellets

Neozone C Neozone D Permalux

Neozone A Peliets Thermoflex A Peliets Zalba Zalba Special

Aquarex SMO

Aquarex WAQ

AQUAREXES (MOLD LUBRICANTS AND STABILIZERS)

Aquarex D Aquarex G Aquarex L

Unicel ND

Aquarex MDL Aquarex ME Aquarex NS

Unicel NDX

BLOWING AGENTS

Unicel S

RUBBER DISPERSED COLORS

Rubber Red PBD Rubber Green FD **Rubber Red 2BD Rubber Blue PCD** Rubber Yellow GD Rubber Blue GD Rubber Green GSD Rubber Orange OD

ORGANIC ISOCYANATES

Hylene* M Hylene* M-50

Hylene* TM Hylene* MP Hylene* TM-65 PEPTIZING AGENTS

Endor

RPA No. 2 RPA No. 3 **RPA No. 3 Concentrated** RPA No. 6 RR-10

Hylene* T

RECLAIMING CHEMICALS

RPA No. 3 RR-10

SPECIAL-PURPOSE CHEMICALS

BARAK-Retarder activator for thiazole accelerators

Copper inhibitor 58-In-hibits catalytic action of

copper on elastomers ELA-Elastomer lubricating agent

HELIOZONE-Sunchecking inhibitor

NBC-Inhibits weather and ozone cracking of SBR compounds

RETARDER W

Retarder-activator for acidic accelerators

* REG. U. S. PAT. OFF.

DISTRICT OFFICES

Akron 8, Ohio, 40 E. Buchtel Ave. at High St. . . . POrtage 2-8461 Atlanta, Ga., 1261 Spring St., N.W. TRinity 5-5391 Boston 10, Mass., 140 Federal St. HAncock 6-1719
Charlotte 1, N. C., 427 W. 4th St. FRanklin 5-5561 FRanklin 5-5561 Chicago 3, Ill., 7 South Dearborn St. ANdover 3-7000 Detroit 35, Mich., 13000 W. 7-Mile Rd. University 4-1963 Houston 6, Texas, 2601A West Grove Lane . . . MOhawk 7-7429 Los Angeles 58, Calif., 2930 E. 44th St. LUdlow 2-6464 Palo Alto, Calif., 701 Welch Rd. DAvenport 6-7550 Trenton 8, N. J., 1750 N. Olden Ave. EXport 3-7141 In New York call WAlker 5-3290

In Canada contact: Du Pont Company of Canada Limited

E. I. du Pont de Nemours & Co. (Inc.) **Elastomer Chemicals Department**

Wilmington 98, Delaware



Better Things for Better Living ... through Chemistry





The Scott Model LGP sets a new world standard of safety and cleanliness for pressure aging tests of rubber, silicone and other elastomers. Featuring 14 small-volume, seamless pressure cylinders encased in a solid, insulated aluminum block... the safety-designed Model LGP uses no liquid heating medium. No more oil-fire hazards and explosions! No more costly barricades needed to protect facilities or personnel. In addition, each pressure cylinder has a precise-seating, screw-on cap with pressure hose connection, separate purging valve, and a blowout disc for fast, safe release of excess pressure.

No Contamination Individual pressure stop cocks permit examination and removal of test specimen without disturbing conditions in the other pressure cylinders. Positively no migration or contamination from one pressure

cylinder to another! All metal parts of the pressure system are of stainless steel (except blowout discs), eliminating metal contamination of material under test.

Easy Operation Slight hand pressure will open or close each pressure cylinder cap. Sensitive thermo-control switch and suitable insulation assure exact, stable regulation of temperatures. Also has over-riding thermo-switch for double protection. Scott automatic temperature recorders are also available to guarantee conformance with ASTM Methods of Test D-572 and D-454.

WRITE FOR COMPLETE FACTS ON SCOTT'S SAFETY-DESIGNED MODEL LGP

SCOTT TESTERS

THE SURE TEST ... SCOTT



Scott Testers, Inc. • 102 Blackstone Street, Providence, Rhode Island

COLUMBIAN offers an outstanding carbon black for every rubber need...

STATEX® 160 SAF Super Abrasion Furnace

STATEX 125 ISAF Intermediate Super Abrasion Furnace

STATEX R HAF High Abrasion Furnace

STANDARD MICRONEX® MPC Medium Processing Channel

MICRONEX W 6 EPC Easy Processing Channel

STATEX B FF Fine Furnace

STATEX M FEF Fast Extruding Furnace

STATEX 93 HMF High Modulus Furnace

STATEX 6 GPF General Purpose Furnace

FURNEX® SRF Semi-Reinforcing Furnace

And Now MEOTEX* 100 MEOTEX 130 MEOTEX 150

plus outstanding pure iron oxide pigments from our MAPICO IRON OXIDES UNIT

REDS . . . 617, 297, 347, 387, 477 and 567

TANS ... 10, 15 and 20

BROWNS . . . 418, 419, 420, 421 and 422

PLUS YELLOWS ...



COLUMBIAN CARBON COMPANY

380 Madison Avenue, New York 17, N. Y.

JANUARY - MARCH · 1961

VOLUME XXXIV

NUMBER ONE

RUBBER CHEMISTRY

AND TECHNOLOGY

PUBLISHED IN FIVE ISSUES BY THE DIVISION OF RUBBER CHEMISTRY OF THE AMERICAN CHEMICAL SOCIETY



SOOO Tamily to know...

Columbia-Southern White Reinforcing Pigments



Hi-Sil® 233

Hydrated silica providing outstanding tear and abrasion resistance, very high tensile strength, high modulus at a most competitive price.



Silene® EF

Finely divided hydrated calcium silicate for greater abrasion, scuff or mar resistance, improved elongation, higher tensile strength.



Calcene® TM, Calcene® NC

Precipitated calcium carbonate in coated and uncoated grades for improved hot tear resistance, low modulus and higher tensile strength.

You are invited to write for data sheets, working samples and bulletins on these rubber compounding aids.



columbia southern chemicals

CHEMICAL DIVISION

PITTSBURGH PLATE GLASS COMPANY ONE GATEWAY CENTER PITTSBURGH 22, PENNSYLVANIA DISTRICT OFFICES: Boston · Charlotte · Chicago · Cincinnati · Cleveland Dallas · Houston · Minneapolis · New Orfeans · New York · Philadelphia Pittsburgh · San Francisco · St. Louis · IN CANADA: Standard Chemical Limited

THE DIVISION OF RUBBER CHEMISTRY OF THE AMERICAN CHEMICAL SOCIETY

OFFICERS, EXECUTIVE COMMITTEE AND LIBRARIAN

Chairman W. S. Coe, Naugatuck Chemical Division, Naugatuck, Conn.

Vice-Chairman G. E. Popp, Phillips Chemical Company, Akron, O.

Secretary....L. H. Howland, Naugatuck Chemical Division, Naugatuck, Conn.

Treasurer......D. F. BEHNEY, Harwick Standard Chemical Co., Akron, O.

Assistant Treasurer George Hackim, General Tire & Rubber Co., Akron, O.

Editor of Rubber Chemistry and Technology......David Craig, B. F. Goodrich Research Center, Brecksville, O.

Advertising and Business Manager of Rubber Chemistry and Technology George Hackim, General Tire & Rubber Co., Akron, O.

Directors....W. J. Sparks (Past Chairman), H. J. Osterhof (Director-at-Large), J. M. Bolt (Southern Rubber Group), G. W. Smith (Boston), M. H. Leonard (Akron), C. V. Lundberg (New York), R. A. Garrett (Philadelphia), J. A. Carr (Canada), N. R. Legge (Northern California), A. T. McPherson (Washington, D. C.), H. E. Schweller (Southern Ohio), M. J. O'Connor (Fort Wayne), H. D. Shetler (Chicago), R. H. Snyder (Detroit), D. C. Maddy (Los Angeles), J. Frankfurth (Buffalo), R. W. Szulik (Rhode Island), R. T. Zimmerman (Connecticut). Alternate directors: I. G. Sjothun (Akron), W. F. Malcolm (Boston), T. L. Davies (Canada), A. J. Hawkins, Jr. (Los Angeles), J. T. Dunn (New York).

Councilors....W. S. Coe.
(Alternates, C. S. Yoran, 1958-1960; J. D. D'Ianni).

Rubber Division Librarian MRS. SANDRA GATES, Akron University, Akron, O.

COMMITTEES

- Advisory Committee on Local Arrangements....C. A. Smith, Chairman (New Jersey Zine Co., Cleveland, Ohio), S. L. Brams (Dayton Chemical Products, West Alexandria, Ohio), W. H. Peterson (Enjay Co., 15 West 51 Street, New York City).
- Auditing Committee....F. W. Burger, Chairman (Phillips Chemical Co., Akron, Ohio), C. W. Christensen (Monsanto Chemical Company, Akron, Ohio), L. V. Cooper (Firestone Tire & Rubber Co., Akron, Ohio).

- Best Papers Committee....HAROLD TUCKER, Chairman (B. F. Goodrich Research Center, Brecksville, Ohio), H. E. HAXO (U. S. Rubber Company, Research Center, Wayne, N. J.), G. E. POPP (Phillips Chemical Company, Akron, Ohio).
- Bibliography Committee JOHN McGAVACK, Chairman (144 Ames Avenue, Leonia, New Jersey), P. H. Biddison (Firestone Tire & Rubber Company, 352 Wayne Avenue, Akron, Ohio), V. L. Burger (U. S. Rubber Company, Research Center, Wayne, New Jersey), Lois Brock (Research Laboratory, General Tire & Rubber Company, Akron, Ohio), D. E. CABLE (U. S. Rubber Company, Research Center, Wayne, New Jersey), H. E. Haxo (U. S. Rubber Company, Research Center, Wayne, New Jersey), Mrs. Jeanne Johnson (U. S. Rubber Company, Research Center, Wayne, New Jersey), M. E. LERNER (Rubber Age, 101 West 31st Street, New York City), G. S. Mills (U. S. Rubber Company, Research Center, Wayne, New Jersey), Leora Straka (Goodyear Tire & Rubber Company, Akron, Ohio), Mrs. M. L. RELYEA (36 Hopper Avenue, Pompton Plains, New Jersey), C. E. RHINES (U. S. Rubber Company, Research Center, Wayne, N. J.), D. F. BEHNEY (Harwick Standard Chemical Co., 60 S. Seiberling Street, Akron 5, Ohio).
- By-Laws Revision Committee....G. Alliger, Chairman (Firestone Tire & Rubber Co., Akron, Ohio), W. C. Warner (General Tire & Rubber Co., Akron, Ohio), R. A. Garrett (Armstrong Cork Co., Lancaster, Pa.), L. H. Howland (Naugatuck Chemical Division, Naugatuck, Conn.).
- Committee on Committees....T. W. Elkin, Chairman (R. T. Vanderbilt Company, 230 Park Avenue, New York), A. E. Juve (B. F. Goodrich Research Center, Brecksville, Ohio), V. J. Labrecque (Victor Gasket & Mfg. Co., Chicago, Ill.), R. T. Zimmerman (R. T. Vanderbilt Co., 230 Park Avenue, New York City), R. H. Snyder (U. S. Rubber Co., Detroit, Michigan).
- Editorial Board of Rubber Reviews...G. E. P. SMITH, JR. Chairman (Firestone Tire and Rubber Co., Akron, Ohio), J. Rehner, Jr. (Esso Research & Engineering Co., Linden, N. J.), B. L. Johnson (Firestone Tire & Rubber Co., Akron, Ohio), S. D. Gehman (Goodyear Tire & Rubber Co., Akron, Ohio), D. Craig (B. F. Goodrich Research Center, Brecksville, Ohio), W. R. Smith (The Cabot Corporation, Cambridge, Mass.).
- Education Committee....C. V. Lundberg, Chairman (Bell Telephone Laboratories, Inc., Murray Hill, New Jersey), R. D. Stiehler (National Bureau of Standards, Washington, D. C.), W. F. Busse (E. I. du Pont de Nemours & Co., Wilmington, Delaware), H. D. Shetler (Chicago Rawhide Manufacturing Co., 1301 Elston Avenue, Chicago 22, Illinois), H. E. Schweller (Inland Manufacturing Division, General Motors Corporation, Dayton 1, Ohio), R. A. Garrett (Armstrong Cork Co., Lancaster, Pennsylvania), Milton H. Leonard (Columbian Carbon Company, Akron, Ohio).
- Files & Records Committee....J. D. D'IANNI, Chairman (Goodyear Tire & Rubber Co., Akron, Ohio), DOROTHY HAMLEN (University of Akron,

- Akron, Ohio), E. A. Willson (B. F. Goodrich Research Center, Brecksville, Ohio).
- Finance Budget Committee....L. V. COOPER, Chairman (Firestone Tire & Rubber Company, Akron, Ohio), C. W. Christensen (Monsanto Chemical Company, Akron, Ohio), F. W. Burger (Phillips Chemical Company, Akron, Ohio), E. H. Krismann (E. I. du Pont de Nemours & Co., Akron, Ohio), S. B. Kuykendall (Firestone Tire & Rubber Co., Akron, Ohio), D. F. Behney, Ex-officio (Harwick Standard Chemical Co., 60 S. Seiberling Street, Akron 5, Ohio).
- Future Meetings....A. E. LAURENCE, Chairman (R. T. Vanderbilt Co., Akron, Ohio), G. N. VACCA (Bell Telephone Laboratories, Murray Hill, N. J.), J. M. Bolt (Naugatuck Chemical Co., Olive Branch, Miss.).
- Library Operating Committee....Guido H. Stempel, Chairman (The General Tire & Rubber Company, Central Research Laboratories, Akron 9, Ohio), Maurice Morton (University of Akron, Akron, Ohio), Mrs. Sandra Gates (University of Akron, Akron, Ohio), Miss Dorothy Hamlen (University of Akron, Akron, Ohio).
- Library Policy Committee....Guido H. Stempel, Chairman (The General Tire & Rubber Co., Central Research Laboratories, Akron 9, Ohio), Robert L. Bebb (Firestone Tire & Rubber Company, Akron, Ohio), A. M. Clifford (Goodyear Tire & Rubber Company, Akron, Ohio), Maurice Morton (University of Akron, Akron, Ohio), Earl C. Gregg, Jr. (The B. F. Goodrich Company, Akron, Ohio), D. F. Behney, Ex-officio (Harwick Standard Chemical Co., 60 S. Seiberling Street, Akron 5, Ohio).
- Membership Committee....MAURICE J. O'CONNOR, Chairman (O'Connor and Company, Inc., 4667 North Manor Avenue, Chicago 25, Illinois), All Directors from each Local Rubber Group, C. E. Huxley (Enjay Company, Inc., 130 East Randolph Drive, Chicago, Illinois), A. M. Gessler (Esso Research & Engineering Company, Linden, New Jersey), E. M. Dannenberg (Cabot Corporation, 38 Memorial Drive, Cambridge 42, Massachusetts).
- New Publications Committee...R. G. SEAMAN, Chairman (Rubber World, New York City), D. CRAIG (B. F. Goodrich Research Center, Breeksville, Ohio), J. M. BALL (Midwest Rubber Reclaiming Co., 95 Whipstick Road, Wilton, Conn.), G. E. P. SMITH, JR. (Firestone Tire & Rubber Co., Akron, Ohio).
- Nomenclature Committee....RALPH F. WOLF, Chairman (4448 Lahm Drive, Akron 19, Ohio), I. D. Patterson (Goodyear Tire & Rubber Co., Akron, Ohio), F. W. Gage (Dayton Chemical Products Laboratories, W. Alexandria, Ohio), E. E. Gruber (General Tire & Rubber Co., Akron, Ohio), A. T. McPherson (National Bureau of Standards, Washington, D. C.), R. W. Szulik (Acushnet Process Co., New Bedford, Mass.).
- Nominating Committee....LARRY M. BAKER, Chairman (General Tire & Rubber Company, Akron, Ohio), JAMES D. D'IANNI (The Goodyear Tire & Rubber Company, Akron 16, Ohio), KENNETH R. GARVICK (The Mansfield Tire & Rubber Company, P. O. Box 428, Mansfield, Ohio), ROBERT

- G. SEAMAN (Editor, Rubber World, 630 Third Avenue, New York 17, N. Y.), GEORGE VACCA (Bell Telephone Laboratories, Murray Hill, New Jersey).
- Officers Manual...A. E. Juve, Chairman (B. F. Goodrich Research Center, Brecksville, Ohio), B. S. Garvey (Pennsalt Chemicals Corp., Philadelphia, Pa.).
- Papers Review Committee....W. S. Coe, Chairman (Naugatuck Chemical Division, U. S. Rubber Company, Naugatuck, Connecticut), W. J. Sparks (Esso Research & Engineering Company, P. O. Box 51, Linden, New Jersey), David Craig (Editor, Rubber Chemistry & Technology, B. F. Goodrich Research Center, Brecksville, Ohio), L. H. Howland (Naugatuck Chemical Division, U. S. Rubber Company, Naugatuck, Connecticut), G. E. Popp (Phillips Chemical Company, Rubber Chemicals Sales Division, 318 Water Street, Akron 8, Ohio).
- Program Planning Committee....George E. Popp, Chairman (Phillips Chemical Company, Rubber Chemicals Sales Division, 318 Water Street, Akron 8, Ohio), J. D. D'IANNI (The Goodyear Tire & Rubber Co., Akron 8, Ohio), DAVID CRAIG (Editor, RUBBER CHEMISTRY & TECHNOLOGY, B. F. Goodrich Research Center, Brecksville, Ohio), MERTON STUDEBAKER (Phillips Chemical Company, 318 Water Street, Akron 8, Ohio), W. F. Tuley (Naugatuck Chemical Division, U. S. Rubber Company, Naugatuck, Connecticut).
- Selection Committee for the Rubber Science Hall of Fame, University of Akron, representatives of the Division of Rubber Chemistry....A. E. Juve (B. F. Goodrich Research Center, Brecksville, Ohio), RALPH F. WOLF (4448 Lahm Drive, Akron 19, Ohio).
- Tellers....A. C. Stevenson, Chairman (E. I. du Pont de Nemours & Co., Wilmington, Del.), L. T. Eby (Esso Research and Engineering Co., Elizabeth, N. J.), Paul Roach (Texas-U. S. Chemical Co., Parsippany, N. J.).

SPONSORED RUBBER GROUPS OFFICERS AND MEETING DATES

1960

AKRON RUBBER GROUP INC.

Chairman: IRVIN J. SJOTHUN (Firestone Tire & Rubber Company, Akron, Ohio). Vice-Chairman: John Gifford (Witco Chemical Company, Akron, Ohio). Secretary: R. B. KNILL (Goodyear Tire and Rubber Co., Akron, Ohio). Treasurer: B. N. Larsen (Naugatuck Chemical Co., Akron, Ohio). Officers Tenure: August 1, 1960-August 1, 1961. Director to Div. of Rub. Chem., ACS: M. H. Leonard. Meeting Dates: (1961)—Jan. 27, April 6, June 16, Sept. 29, Oct. 20; (1962)—Jan. 26, April 6, June 22.

BOSTON RUBBER GROUP

Chairman: George E. Herbert (Tyer Rubber Company, Andover, Massachusetts). Vice-Chairman: John M. Hussey (Goodyear Chemical Company, Need-

ham Heights 94, Massachusetts). Secretary-Treasurer: George H. Hunt (Simplex Wire & Cable Company, Cambridge 39, Massachusetts). Executive Committee: James J. Breen (Barrett & Breen Co., Boston 10, Massachusetts). Chester Stoekels (Firestone Tire & Rubber Company, Fall River, Massachusetts). Robert Loveland (R. T. Vanderbilt Company, Boston, Massachusetts). George W. Smith (E. I. du Pont de Nemours & Co., Boston, Massachusetts). Officers Tenure: January 1, 1961-January 1, 1962. Meeting Dates: (1961)—February 3, 4, 5; March 17; June 16; October 13; and December 15.

BUFFALO RUBBER GROUP

Chairman: E. F. SVERDRUP (U. S. Rubber Reclaiming Company, Buffalo 5, New York). Vice-Chairman: E. R. Martin (Dunlop Tire and Rubber Corporation, Buffalo 5, New York). Secretary-Treasurer: E. J. Haas (Dunlop Tire and Rubber Corporation, Buffalo 5, New York). Asst. Secretary-Treasurer: R. J. O'Brien (Dunlop Tire and Rubber Corporation, Buffalo 5, New York). Directors: D. Schuler, C. Peffer, J. Frankfurth, R. Lindberg, S. Murray, F. O'Connor. Officers Tenure: December 1960-December 1961. Director to Div. of Rubber Chemistry: J. Frankfurth. Meeting Dates: March 7, May 12, June 13, October 10 and December 12.

CHICAGO RUBBER GROUP, INC.

President: Stanley F. Choate (Tumpeer Chemical Company, Chicago 1, Illinois). Vice-President: T. C. Argue (Roth Rubber Company, 1860 S. 54th Avenue, Cicero 50, Illinois). Secretary: Robert R. Kann (Chemical Division, Goodyear Tire & Rubber Company, 141 West Ohio Street, Chicago 10, Illinois). Treasurer: Harold Stark (Dryden Rubber Division, Sheller Mfg. Corporation, 1014 S. Kildare Avenue, Chicago 24, Illinois). Directors: A. D. Marr, Richard Huhn, Irwin O. Nejdl, Harold Shetler, Stanley Shaw, Frank E. Smith, James Dunne, Melvin Whitfield. Legal Counsel & Exec. Secretary: Edward H. Leahy (333 N. Michigan Avenue, Chicago 1, Illinois). Officers Tenure: September, 1960-September, 1961. Meeting Dates: January 27, March 10, April 28.

CONNECTICUT RUBBER GROUP

Chairman: Frank B. Smith (Naugatuck Chemical Company, Naugatuck, Connecticut). Vice-Chairman: Alexander Murdock, Jr. (Armstrong Rubber Company, West Haven, Connecticut). Secretary: Rial S. Pottes, Jr. (Spencer Rubber Products, Manchester, Connecticut). Treasurer: Frank F. Villa (Whitney Blake Company, Hamden, Connecticut). Directors: Vincent P. Chadwick, Francis H. H. Browning, Ken C. Crouse, Richard Stimets, Carl Lawson. Director to Division of Rubber Chemistry: R. T. Zimmerman. Meeting Dates: February 17, May 19, September 9 and November 17. Officers Tenure: January 1, 1961 to January 1, 1962.

DETROIT RUBBER AND PLASTICS GROUP

Chairman: W. D. Wilson (R. T. Vanderbilt Company, 5272 Doherty Dr., Orchard Lake, Michigan). Vice-Chairman: S. M. Sidwell (Chrysler Engineering Division, P. O. Box 1118, Dept. 821, Detroit 21, Michigan). Treasurer: P. V. Millard (Automotive Rubber Company, 12550 Beech Road, Detroit 39, Michigan). Secretary: R. W. Malcolmson (E. I. du Pont de Nemours & Company, 13000 W. Seven Mile Road, Detroit 35, Michigan). Executive Committee:

W. F. MILLER, E. J. KVET, H. W. HOERAUF, C. H. ALBERS, C. E. BECK, E. I. BOSWORTH, R. C. CHILTON, F. G. FALVEY, E. P. FRANCIS, T. W. HALLORAN, J. F. MASDEN, J. M. MCCLELLAN, R. H. SNYDER, R. C. WATERS, P. WEISS. Officers Tenure: December 1959-December 1960. Director to Div. of Rub. Chem., ACS: R. H. SNYDER (to 1962). Meeting Dates: (1961)—Feb. 17, Apr. 21, June 23, Oct. 5 and December 8.

FORT WAYNE RUBBER & PLASTICS GROUP

Chairman: Allen C. Bluestein (Anaconda Wire & Cable Co., Marion, Indiana). Vice-Chairman: A. L. Robinson (Harwick Standard Chemical Company, 2724 West Lawrence Avenue, Chicago 25, Illinois). Secretary-Treasurer: Carroll Voss (General Tire & Rubber Company, Wabash, Indiana). Directors: Walt Wilson, Arthur Brumfield, Melvin Whitefield, Samuel Armato, Balfour Connell, Jack Lippincott, Alfred Cobbe, Gerard Zwick, Devon Wilson. Meeting Dates: (1961)—February 9, April 13, June 9, September 28, December 7. (1962)—February 8, April 5.

Los Angeles Rubber Group, Inc.

Chairman: W. M. Anderson (Gross Manufacturing Co., Inc., 1711 S. California Avenue, Monrovia, California). Assoc. Chairman: C. M. CHURCHILL (Naugatuck Chemical Division, U. S. Rubber Company, 5901 Telegraph Rd., Los Angeles 22, California). Vice-Chairman: L. W. CHAFFEE (The Ohio Rubber Company, 6700 Cherry Avenue, Long Beach 5, California). Treasurer: J. L. RYAN (Shell Chemical Company, P. O. Box 6066, Lakewood, California). Secretary: C. F. Ashcroft (Cabot Corporation, 3350 Wilshire Blvd. #718, Los Angeles 5, California). Directors: Don Montgomery (1961-1962), Howard R. Fisher (1961-1962), L. E. Peterson (1961-1962), R. L. Wells (1960-1961), HAROLD W. SEARS (1960-1961), HAROLD J. BRANDENBURG (1960-1961), B. R. SNYDER (1961). Asst. Treasurer: ROBERT F. DOUGHERTY (U. S. Rubber Company, 5675 Telegraph Rd., Los Angeles 22, California). Asst. Secretary: W. C. SCHEUERMANN (Plastic & Rubber Products Co., 2100 Hyde Park Blvd., Los Angeles 47, California). Historian & Librarian: Roy N. PHELAN (Atlas Sponge Rubber Co., 1707 S. California Avenue, Monrovia, California). Attorney: CECIL COLLINS (2875 Glendale Blvd., Los Angeles 39, California). Photographer Emeritus: L. E. BUDNICK (The Ohio Rubber Company, 6700 Cherry Avenue, Long Beach 5, California). Official Photographer: BERT SLUYTER (The Ohio Rubber Company, 6700 Cherry Avenue, Long Beach 5, California). Director to Division of Rubber Chemistry: D. C. Maddy (to 1963), Harwick Standard Chemical Company, 7225 Paramount Blvd., Pico Rivera, California. Officers Tenure: December, 1960 to December, 1961. Meeting Dates: (1961)-February 7, March 7, April 4, May 2, October 3 and November 7.

NEW YORK RUBBER GROUP

Chairman: H. J. Peters (Bell Telephone Laboratories, Murray Hill, N. J.). Vice-Chairman: R. Deturk (Cooke Color & Chemical Co., Hackettstown, N. J.). Sgt.-at-Arms: W. Birkitt (Passaie Rubber Co., Clifton, N. J.). Secretary-Treasurer: R. G. Seaman (Rubber World, 630 Third Ave., New York 17, N. Y.). Directors: W. J. O'Brien, Bryant Ross, E. C. Strube, A. H. Woodward, J. T. Dunn, M. A. Durakis, W. R. Hartman, J. E. Walsh, R. T. Ambrose, K. B. Cary, W. C. Carter, A. M. Gessler, E. S. Kern, M. E. Lerner. Officers Tenure: January 1, 1961-January 1, 1962. Director to Div. of Rub. Chem., ACS: C. V. Lundberg (to 1963). Meeting Dates: (1961)—Mar. 24, June

(Summer Outing), Aug. 1, Oct. 20 and Dec. 15. (1962)—Mar. 23, June 7, Aug. (Golf Outing), Oct. 19 and Dec. 14.

NORTHERN CALIFORNIA RUBBER GROUP

Chairman: Virgil C. Price (Burke Rubber Company, 2250 South Tenth Street, San Jose 3, California). Vice-Chairman: Victor J. Carriere (Mansfield Tire & Rubber Company, 4901 East 12th Street, Oakland, California). Treasurer: Gene L. Unterzuber (Oliver Tire & Rubber Company, 1256 65th Street, Oakland 8, California). Secretary: Roger H. Thatcher (Union Rubber Company, 1002 77th Avenue, Oakland 21, California). Directors: Eugene Gador, Henri Krakowski, Robert B. Stewart. Officers Tenure: December, 1960-December, 1961. Meeting Dates: January 12, February 9, March 9, April 13, May 11, June 8, September—open date for Summer Outing, October 12, November 9, December—open for Christmas Party.

THE PHILADELPHIA RUBBER GROUP

Chairman: R. N. Hendriksen (Phillips Chemical Company, Trenton, New Jersey). Vice-Chairman: R. M. Kerr (H. K. Porter Company, Thermoid Division, Philadelphia, Pa.). Secretary-Treasurer: H. F. Smith (Naugatuck Chemical Company, 97 Bayard Street, New Brunswick, New Jersey). Historian: J. B. Johnson (Linear, Inc., Philadelphia, Pa.). Executive Committee: E. C. Brown, K. E. Chester, R. E. Connor, W. J. Macomber, K. F. Quinn, B. Vanarkel. Director to Division of Rubber Chemistry: R. A. Garrett (to 1962). Officers Tenure: January 1, 1961 to January 1, 1962. Meeting Dates: January 27, April 28, August 18, October 13, November 3.

RHODE ISLAND RUBBER GROUP

Chairman: Walter Blecharczyk (Davol Rubber Company, Providence, Rhode Island). Vice-Chairman: Edwin C. Uhlig (United States Rubber Company, Providence, Rhode Island). Secretary-Treasurer: Joseph Vitale (Crescent Wire Company, Pawtucket, Rhode Island). Board of Directors: C. A. Damicone, Joseph M. Donahue, Paul Hastings, Vincent Casey, Tom Crosby, Harry Ebert. Dir. to Div. of Rubber Chemistry, ACS: R. W. Szulik (to 1962). Officers Tenure: January 1, 1961-January 1, 1962. Permanent Historian: Robert Van Amburgh. Meeting Dates: April 6, June 8 and November 2.

SOUTHERN OHIO RUBBER GROUP

President: Howard G. Gillette (Precision Rubber Prod. Corp., Dayton, Ohio). Vice-President: E. N. IPIOTIS (Inland Mfg. Division, G.M.C., Dayton, Ohio). Secretary: John H. Woodward (Inland Mfg. Division, G.M.C., Dayton, Ohio). Treasurer: Donald R. Strack (Inland Mfg. Division, G.M.C., Dayton, Ohio). Directors: F. W. Gage, Harold Schweller, D. L. Allen, C. Bellanca, R. Heist, R. L. Jacobs, M. K. Coulter, J. West, H. S. Karch, W. F. Herberg, J. M. Williams. Director to Division of Rubber Chemistry: H. E. Schweller (1962). Officers Tenure: January 1, 1961—January 1, 1962. Meeting Dates: March 23, June 3, September 28 and Dec. 9.

SOUTHERN RUBBER GROUP

Chairman: Lenoir Black (C. P. Hall Company, 648 Riverside, Memphis, Tennessee). Vice-Chairman: Roswell C. Whitmore (3610 Waldorf, Dallas,

Texas, (Better Monkey Grip Company)). Secretary: R. W. Rice (Firestone Synthetic Rubber & Latex Company, Box 21361, Lake Charles, Louisiana). Treasurer: Martin E. Samuels (Copolymer Rubber & Chemical Corp., Box 2591, Baton Rouge, Louisiana). Officers Tenure: June, 1960-June, 1961. Meeting Dates: (1961)—January 20-21; June 23-24; November 17-18 and (January 26-27, 1962).

WASHINGTON RUBBER GROUP

President: PHILIP MITTON (Materials Branch, U. S. Army Engineer Research and Development Laboratories, Fort Belvoir, Virginia). Vice-President: Thomas A. Tharp (General Tire & Rubber Company, 1120 Conn. Avenue, N. W., Washington, D. C.). Secretary: Daniel Pratt (Code 634 C, Bureau of Ships, Navy Department, Washington 25, D. C.). Treasurer: George G. Richey (National Bureau of Standards, Washington 25, D. C.). Director to Division of Rubber Chemistry: A. T. McPherson (to 1961). Officers Tenure: July 1, 1960 to July 1, 1961. Meeting Dates: January 25, March 8, April 19, May 17.

THE CHEMICAL INSTITUTE OF CANADA RUBBER DIVISION OFFICERS AND SPONSORED RUBBER GROUPS

Chairman: A. Jaychuk (Goodyear Tire & Rubber Co. of Canada Ltd., New Toronto, Ontario). Vice-Chairman: D. W. Hay (Polymer Corporation Limited, Sarnia, Ontario). Secretary-Treasurer: C. M. Croakman (Columbian Carbon of Canada, Toronto, Ontario). Directors: A. Holden (Canada Colors & Chemicals, Montreal, Quebec). W. A. Cline (Canadian General Tower Limited, Galt, Ontario). W. J. Nichol (Dunlop Canada Limited, Toronto, Ontario). Ontario Rubber Group Representative: W. R. Smith (Dominion Rubber Company Limited, Kitchener, Ontario). Quebec Rubber & Plastics Group Representative: J. M. Campbell (Northern Electric Co., Lachine, Quebec).

THE ONTARIO RUBBER GROUP

Chairman: D. G. SEYMOUR (Cabot Carbon of Canada Ltd., Toronto, Ontario). Vice-Chairman: W. R. SMITH (Dominion Rubber Company Limited, Kitchener, Ontario). Secretary: L. V. LOMAS (c/o L. V. Lomas Chemical Company, Toronto, Ontario). Treasurer: BRUCE WILLIAMS (Feather Industries Limited, Toronto, Ontario). Membership Chairman: W. J. Hogg (Naugatuck Chemicals Division, Dominion Rubber Company Limited, Elmira, Ontario).

QUEBEC RUBBER & PLASTICS GROUP

Chairman: J. M. CAMPBELL (Northern Electric Company, Lachine, Quebec).
Secretary: L. V. WOYTIUK (Northern Electric Company, Lachine, Quebec).
Treasurer: R. B. PILMER (Dominion Rubber Company, Mechanical Division, Montreal, Quebec).
Committee Chairmen—Speakers: F. R. Moorehouse (Shawinigan Chemicals Limited, Montreal, Quebec).
Membership: R. VINCENT (Dominion Rubber Company, Montreal, Quebec).
Publicity: R. E. Suksi (Sun Oil Company of Canada Ltd., Montreal, Quebec).
Education: G. L. Bata (Carbide Chemicals Company, Montreal, Quebec).
House Committee: W. L. Leach (Cabot Carbon of Canada Limited, Montreal, Quebec).
Directors: W. M. Schwenger (Dupont Company of Canada, Montreal); A. S. MacLean (Dominion Rubber Company, Montreal).

NEW BOOKS AND OTHER PUBLICATIONS

Penn State Engineering Research Bulletin B-80, Rubber and Tire Friction. H. W. Kummer and W. E. Meyer, The Pennsylvania State University, Department of Mechanical Engineering, Automotive Safety Project, 96 pages including 54 figures. Copies can be purchased through Engineering Publications, 227 Hammond Building, The Pennsylvania State University, University Park, Pa., by ordering Engineering Research Bulletin B-80 at \$3.00 per copy. The following Abstract and Preface are reprinted from pages iii and v of the bulletin.

Abstract.—The mechanism of rubber friction is discussed, and an attempt is made to relate the friction characteristics of a rubber block to those of a slipping and sliding pneumatic tire. Several new or modified explanations of the behavior of tires on dry and wet surfaces are proposed. The effects of pressure or normal load, sliding velocity, temperature, and contaminating and lubricating films on the adhesion and hysteresis components are separately investigated for the rubber block and the rolling, slipping, and sliding tire. Attention is given to such topics as the existence or nonexistence of a static coefficient, the transient behavior of adhesive friction at nonsteady sliding velocities, the rise of the sliding coefficient with sliding velocity, comparison of the coefficients obtained from a sliding and a slipping tire, the meaning of slip, and the dependence of the critical coefficient on slip and vehicle velocity. Also explored are the mechanism of water removal between tire and road surface under wet driving conditions, and the effects of tire geometry, pressure distribution in the footprint, vehicle speed, and water film thickness on the obtainable coefficient. Experimental methods for measuring rubber and tire friction are reviewed. The Penn State brake test trailer is described.

Preface.—Highway traffic safety has become a matter of acute concern in the United States and throughout the civilized world. The growing problem of accident prevention cannot be left to the highway engineer and the psychologist alone; the vehicle itself must be made more foolproof. Recognizing this, the Department of Mechanical Engineering of The Pennsylvania State University has established a research program to approach highway accident prevention through better understanding of the driver-vehicle-road complex and improvement of mechanical controls. The initial activities of this project are directed

toward finding improved means to stop a vehicle that is in motion.

Brakes as such, though they could be better, are not a critical factor in most cases. Rather, it is the operator's misuse of his vehicle's braking capacity on slippery roads that breeds danger or prevents him from extricating himself from a dangerous situation. When excessive application of brake pressure locks some or all of the wheels, skidding or spinning will occur, and jackknifing in the case of articulated vehicles. Obviously, then, prevention of wheel lock by automatic means would greatly enhance the safety of present-day driving, and will be an absolute necessity if vehicle movement is ever subject to some form of remote control.

Antilock systems are in use on aircraft, but there they serve mainly to prevent tire blowout. Transferred to road vehicles, these systems do eliminate the loss of directional control, but they increase stopping distances. To eliminate this disadvantage or reduce it to a tolerable minimum, brake control systems are

needed that have optimum capability for dealing with all situations that may arise in road traffic. The design of such equipment must proceed from a full understanding of the frictional interaction of tire and road.

Prior knowledge of the frictional behavior of pneumatic tires, particularly on wet road surfaces, shows several serious gaps, some of which the authors have attempted to fill. This monograph reports the results of our research, but it also reviews the literature on the subject and offers several new interpretations of existing information. It should therefore be useful to researchers and engineers concerned not only with stopping problems but also with the design of tires and road surfaces.

Several graduate students in the Department of Mechanical Engineering have contributed to the overall picture through thesis research. Their work is acknowledged at appropriate locations in the text. The assistance of Miss Dorothy Anderson, technical editor for the College of Engineering and Architecture, has been extremely valuable. Above all, the research project which produced this monograph owes its existence entirely to financial support by The Pennsylvania State University.

Kautschuk-Handbuch. Volume I. Edited by Siegfried Bostrom. Published by Berliner Union G.m.b.H., Stuttgart, Germany. 1959. Plastics cover; 6¼ by 9 inches; 448 pages; 152 illustrations.—Designed to take the place of Hauser's "Handbook of Rubber Technology," long out of print, the new rubber handbook—compiled in collaboration with more than 40 specialists of leading German, Italian, and Austrian companies—is to be made available in four volumes. This Volume I is the second to be printed. It describes in 13 chapters and numerous sub-sections the different types of natural and synthetic rubbers, their properties, curing methods and curing aids, and gives details of the development of the synthetic materials, to 1958, chiefly in the United States, Canada, and Germany. The economic importance of rubber in American, Asian, and European industry is discussed, country by country, and illustrated by consumption figures to 1957. Helpful and often extensive bibliographies are appended to each chapter.

The print of the book is clear, and the plastics cover neat and utilitarian, but —surprisingly for a reference book—the binding work does not seem very sturdy.

Of the other three volumes, Volume III was the first to be published, and is devoted to rubber technology; manufacturing processes for tires, mechanical goods, footwear, toys, cellular rubbers, thread, erasers, and floorings are described in some detail. Volume II will deal with PVC, butyl rubber, Oppanol, silicones, reclaim, compounding ingredients, and manufacturing aids, textiles, and machinery. The final volume, IV, will consider, among others, belting, hard rubber, rubber-to-metal bonding, dipped goods and rubberized fabrics, latex technology, and chemical and physical tests.

The price for the set of four volumes will be 360 DM., if ordered before the last volume is issued; thereafter the price will be at least 380 DM. The volumes

will not be sold separately. [From Rubber World.]

BIBLIOGRAPHIES AVAILABLE IN RUBBER DIVISION LIBRARY

The following mimeographied bibliographies are available: Peroxide Curing of Polymers (No. 38), 57 references, February 1960; Polyisoprene (No. 37),

192 references, February 1960; Resins-Rubbers (No. 32), 134 references, March 1960; Chemistry of Rubber Adhesives (No. 31), January 1960, 33 references; Bonding of Polyurethanes (No. 33), 36 references, December 1959; Production of Latex Foam-Addenda (No. 34), 88 references, February 1960; Rubber to Fabric Adhesives (No. 35), 146 references, January 1960; Non-Staining Anti-

oxidants (No. 36), 139 references, April 1959.

The following bibliographies also are available: Chemical and Solvent Resistance of Natural and Synthetic Rubber, Neoprene, and Nylon, 260 references, March 1960; Molding of Rubber Parts, 26 references, March 1960; Processibility Evaluation Methods for Rubber, 140 references, March 1960; Measurements of Stress-Strain of Rubber, 68 references, March 1960; Thiuramdisulfides, 84 references; Electroplating and Electrodeposition of Rubbers and Plastics, 52 references, March 1960; Clays in Rubber, 98 references, March 1960; Compression Set and Compression of Rubber, 34 references, March 1960; Aging of Neoprene, 48 references, April 1960; Effect of Ammonia on Elastomers, 23 references, April 1960; Plasticizers and Softeners for Rubber 1907–1942, 275 references, April 1960; O-Rings 1952-1958, 130 references, April 1960; O-Ring Test for Physicals, 3 references, 1960; Rubber Floor Coverings, 42 references, April 1960; Halogenation of Polymers, 79 references, April 1960; Fireproofing Natural Latex Foam Rubber, 10 references, April 1960; Mandrels for Making Latex Tubing and Hose, 40 references, April 1960; Pigments in Rubber, 110 references, April 1960; Non-Amine Antioxidants, 31 items, May 1960; Rubber Latex Dipping 1955-1958, 52 references, May 1960; Reclaiming Foamed Materials, 5 references, 1960; Shrinkage of Molded Goods, 18 references, May 1960; Molding Compositions, 58 references, May 1960; Silicone Materials in Elastomers, 15 references, May 1960; Permeability of Rubber to Gases, 48 references, May 1960; The Effect of Molecular Structure on Physical Properties of Polymers, 293 references, May 1960; Flocked Fabrics, 35 references, June 1960; Battery Box Separators, 118 references, June 1960; Elastomers in Dentistry, 38 references, June 1960; The Analysis and the Nature of the Rubber Phase in Latex, 74 references, June 1960; Thermal Conductivities of Rubbers, 26 references, June 1960; Peptizers in Rubber, 114 references, June 1960; Liquid Rubber in Sculpturing, 7 references, 1960; Mathematical Analysis of Mixing, Milling and Calendering, 21 references, 1960; The History of the Use of Hose, 151 references, June 1960; Procedures and Equipment for High Speed and High Temperature Vulcanization, 27 references, 1960; Active Accelerator Systems, 23 references, July 1960; Glycerine in Rubber Compounding, 9 references, 1960; Friction Tape from Reclaim, 1 reference, 1960; Protective Clothing for Electricians, 7 references, 1960; Rubber in Plates for Railroad Tracks, 11 references, 1960; Urea as Part of the Curing System for Rubber, 4 references, 1960; V-Belts and V-Belt Drives, 241 references, July 1960; Procedures and Equipment of High Temperature and/or High Speed Vulcanization, 27 references, July 1960; Off-the-Road Tires, 116 references, July 1960; General Preparations of Accelerators and Antioxidants, 47 references, August 1960; Elastomeric Pipe Gaskets, 22 references, August 1960; Ozone Testing Methods and Equipment—Addenda, 33 references, September 1960; Tensile Strength Testing Methods and Results, 15 references, September 1960; Abrasion Testing (addendum), 128 references, 1960; Cold Flow and Other Related Properties of SBR, 92 references, November 1960; Shrinking and Swelling of Microporous and Other Rubber Molds, 33 references, November 1960; Dynamic Properties of Visco-Elastic Materials, 127 references, January 1961; Rubber

Springs, 85 references, January 1961; Clays in Rubber, 98 references, 1960; Sand Blast Hose, 1960.

The cost of any bibliography on this entire list is \$2.50 to ACS Rubber Division members and \$5.00 to non-members.

BIBLIOGRAPHY OF RUBBER LITERATURE, 1955-1956. This book is available (\$7.50) from D. F. Behney, Treasurer, Division of Rubber Chemistry, Harwick Standard Chemical Company, Akron, Ohio. The Preface and Table of Contents are as follows.

PREFACE

This is the Eleventh Edition of the Bibliography of Rubber Literature. With its publication coverage of the rubber literature (including patents since 1940) has been accomplished for the period from 1935 through 1956. For the record, the first four of these bibliographies, covering the literature only from 1935 through 1939, were published independently by Rubber Age, and the last seven editions, including the current one, covering the literature and patents from 1940 through 1956, by the Division of Rubber Chemistry of the American Chemical Society.

The last few editions of the Rubber Bibliography reflect the tremendous increase in literature and patents pertaining directly to the rubber industry in all of its manifold ramifications. The current edition, spanning a two-year period only, contains some 7,000 references, as compared with the 9,170 references in the previous edition, which covered the three-year period from 1952 to 1954, inclusive. A better idea of this increase can be seen from comparisons with earlier three-year editions. For example, the 1949–51 edition contained some 6,400 references and the 1946–48 edition contained only some 5,000 references.

That this increase in rubber literature and patents is being sustained can be determined by a quick look into future editions of the Rubber Bibliography. Work has already progressed to the point where we already know that the 1957-58 edition will have some 8000 references (4000 for each year), the 1959 edition will have over 5000 references (for a single year), and the 1960 edition (also covering a single year) will contain some 5400 references. It should be evident that these bibliographies will become even more valuable to the rubber technologist in the future. The ability to keep up with the literature is becoming progressively more difficult.

As in previous editions, the current Rubber Bibliography is based on the rubber references prepared at the Research Center of the United States Rubber Company in bulletin form, plus additional references culled mainly from three additional sources. The latter are: Rubber Abstracts, the comprehensive monthly abstract journal published by the Research Association of British Rubber Manufacturers; the abstract section which appears in each issue of Revue Générale du Caoutchouc, the monthly journal of the French Rubber Institute, and, for the first time, the excellent abstract bulletins compiled by the Brecksville Research Center of the B. F. Goodrich Company.

The letter-number identification system originally conceived by Dr. Donald E. Cable, of the U. S. Rubber Company, has been continued in the current edition, while the Journal Abbreviations used, with a few minor exceptions, follow those established by the American Chemical Society. The practice of giving credit to

the respective members of the Bibliography Committee for each classification, established with the 1949-51 edition, has been continued. This is in full recognition of the fact that each member of the Board of Editors, made up of members of the Bibliography Committee, is charged with the complete preparation of special classifications, up to and including the preparation of work cards for both the author and subject indexes.

The style and format of previous issues has been closely followed in the current edition and again a special effort has been made to indicate where more comprehensive abstracts of any article or patent can be found, particularly those appearing in Chemical Abstracts and Rubber Abstracts. Once again Dr. Cable prepared extensive work cards covering every article which appeared in Rubber Chemistry and Technology pertaining to work published in the 1955-56 period, and an extra special effort was made to insure that references to such articles were included, whether such articles were reproductions or translations of published material or whether they were original from the standpoint of publication. We believe this is a valuable portion of our work.

As indicated in previous editions of the Rubber Bibliography, it is the hope of both the Bibliography Committee and the Executive Committee of the Division of Rubber Chemistry that these bibliographies can be issued on an annual basis as soon as possible. At long last this possibility is in sight. Before this current edition was finished work had already been started on the next one, covering the 1957-58 period. Preparatory work on the 1959 edition, which we hope will be the first annual, is almost completed, and 1960 references are already being put on eards, which is the first step in the tedious job of getting an

edition into print.

None of this progress would be made without the special efforts of Dr. John McGavack, chairman of the Bibliography Committee, nor without the helpful cooperation of the various bibliography editors. The major stumbling blocks lie in the area of copy preparation and the compilation of the author and subject indexes, without which these bibliographies would have limited value. We believe we can overcome these difficulties in the near future and put the Rubber Bibliography on the annual basis it merits and which the rubber industry, in our opinion, needs.

M. E. LERNER, Editor-in-Chief

TABLE OF CONTENTS

	PAGE
Foreword	33
Acknowledgements	35
Preface	37
Journal Abbreviations	39
Makes and American Control of the Co	
Accelerators AGA	65
Adhesives or Rubber Solutions AGE	72
Aging of Rubber AGC	80
Antioxidants for Rubber AGI	84
Belting AGE	92
Carbon Black and Other Reinforcing Agents AGF	100
Chemicals for Latex AGG	109
Chemistry of Rubber AGI	I 110

		PAGE
Clothing—Rubber-Containing	AGJ	122
Compounding Ingredients	AGK	124
Compounding of Rubber	AGL	128
Derivatives of Rubber-Halogen	AGM	136
Derivatives of Rubber-Halogen-Free	AGN	139
Dipped Goods	AGO	140
Electrical Insulation	AGP	142
Fiber-Rubber Products	AGQ	145
Fillers—Non-Reinforcing	AGR	146
Footwear	AGS	152
Gutta-Percha and Balata	AGT	158
Hard Rubber	AGU	159
Hose	AGV	159
Latex Analysis	AGW	162
Latex—Artificial	AGX	164
Latex Chemistry	AGY	169
Latex Compounding	AGZ	171
Latex—Miscellaneous	AHA	172
Latex—Normal or Concentrated	AHB	173
Latex Processes	AHC	174
Latex Products—General	AHD	175
Molds, Presses and Curing Techniques	AHE	178
Paints, Inks and Varnishes Containing Rubber	AHF	179
Physics of Rubber	AHG	181
Plasticizers and Softeners	AHH	196
Processing Operations and Equipment	AHJ	207
Raw Rubber—Cultivation	AHK	214
Raw Rubber—General	AHL	224
Reclaimed Rubber	AHM	230
Rubber as an Engineering Material	AHN	233
Rubber Coverings	AHO	239
Rubber in General	AHP	247
Rubber Products-Miscellaneous	AHQ	255
Rubberlike Plastics:		
PVC Polymers	AHR	280
Polyethylene and Copolymers	AHS	307
Fluorine Polymers	AHT	320
Other Types of Polymers	AHU	326
Sponge and Cellular Rubbers	AHV	336
Sporting Goods	AHW	348
Synthetic Rubber:	AIIW	340
Butyl Rubber	ATIV	951
General Purpose	AHX	351
Miscellaneous	AHY	356
Neoprene	AHZ AJA	359 366
Nitrile Type Rubbers		368
Raw Materials	AJB AJC	370
Silicone Rubber	AJD	371
Thickel	AJD	3/1

	PAG	E
Testing of Rubber-Chemical	JF 38	0
	JG 38	4
	JH 40	2
Textile-Rubber Composite Goods	JJ = 40	3
Tires—General	JK 40	9
Tires-Cords and Fabries	JL 42	3
Toxicology of Rubber Chemicals	JM 42	6
Tubes, Inner	JN 42	9
Vulcanization	JO 43	1
Wire Constructions	JP 43	7
Author Index	44	6
	51	
Subject Index		
Index to Advertisers	57	3

ISO RECOMMENDATIONS

ISO Recommendation

R 127

August 1959

DETERMINATION OF KOH NUMBER OF LATEX

BRIEF HISTORY

The ISO Recommendation R 127, Determination of KOH Number of Latex, was drawn up by Technical Committee ISO/TC 45, Rubber, the Secretariat of which is held by the British Standards Institution (B.S.I.).

Work on the preparation of this method was authorized at the first meeting of the Technical Committee held in London, in June 1948, and was entrusted to the Working Group No. 12, Sampling of Latex.

The Secretariat considered the standard methods adopted by the Member Bodies and proposed a compromise method which was put forward to the Working Group.

The method was considered by the Working Group and by the Technical Committee at the meetings held in The Hague, in September 1949; in Akron, in October 1950; in Oxford, in October 1951; in Paris, in June 1953, and was finally approved as a Draft ISO Recommendation at the Dusseldorf meeting, 5-10 September 1955.

On 29 March 1957, the Draft ISO Recommendation (No. 148) was distributed to all the ISO Member Bodies and was approved, subject to some modifications, by the following 26 (out of a total of 38) Member Bodies:

^o Australia	Hungary	Rumania
Austria	India	Spain
^a Canada	°Indonesia	Sweden
Czechoslovakia	°Ireland	Switzerland
° Denmark	Italy	Union of South Africa
Finland	Japan	United Kingdom
France	*New Zealand	U.S.A.
Germany	Pakistan	U.S.S.R.
*Greece	Poland	

^{*} These Member Bodies stated that they had no objection to the Draft being approved.

No Member Body opposed the approval of the Draft.

The Draft ISO Recommendation was then submitted by correspondence to the ISO Council, which decided, in August 1959, to accept it as an ISO REC-OMMENDATION.

1. SCOPE

This method of test is for natural rubber latex preserved wholly with ammonia or ammonia and formaldehyde. The KOH number for such latex is the number of grams of potassium hydroxide equivalent to the acid radicals combined with ammonia in latex containing 100 g of solids.

This procedure is not necessarily suitable for latexes from natural sources other than *Hevea brasiliensis* or for latexes of synthetic rubber, compounded latex, heat-concentrated latex, vulcanized latex or artificial dispersions of rubber.

2. APPARATUS

The apparatus consists of the following:

- pH meter.—dependent on electrometric measurements and capable of being read to 0.02 unit.
- (b) Glass electrode.—with a linear response up to pH 10.
- (c) Suitable half cell.—a calomel electrode is recommended.
- (d) Mechanical stirrer .- with glass paddle.

3. REAGENTS

3.1 Formaldehyde solution (5 per cent, acid free).—This solution is prepared by diluting concentrated formaldehyde of pharmacopoeia guaranteed purity to 5 per cent strength by adding six times its volume of distilled water and neutralizing with 0.1 N potassium hydroxide solution, using as indicator the faint pink color of phenolphthalein.

As formaldehyde is not very stable, it may be necessary, in the case of an old solution, to determine its strength by adding a known volume of excess ammonia of known alkalinity and determining the residual alkalinity after 15 min. If the strength of the solution is less than 4.5 per cent, the calculated amount of concentrated formaldehyde should be added to bring it to 5 per cent.

180 g of formaldehyde are equivalent to 68 g ammonia.

3.2 Potassium hydroxide solution (0.5 N, carbonate-free).—This solution should be prepared and standardized by methods recommended in textbooks on analytical chemistry.

To ensure that the solution is reasonably free from carbonate, the following precautions are necessary:

3.2.1 A fairly concentrated solution of approximately known strength should first be prepared. For this purpose, each stick of pure potassium hydroxide is held by means of clean stainless steel tongs and rinsed rapidly in a stream of freshly boiled and cooled distilled water. It is immediately added a bulk of boiled distilled water until the approximately required weight has been added.

If there is reason to suspect that more than traces of carbonate are present, a small quantity of the solution, say 10 ml, should be treated with 10 per cent barium chloride solution. A very slight precipitate can be ignored. If carbonate is definitely present, 10 per cent barium chloride solution is added until no further precipitate occurs and the calculated amount of barium chloride solution is then added to the main bulk solution of potassium hydroxide to precipitate all the carbonate. The bulk solution should then be retested for carbonate and also for excess of barium. If the latter is present, it should be removed by adding 10 per cent potassium sulfate solution dropwise until one drop gives no further precipitate. Before dilution of the bulk solution, the precipitate should be allowed to settle and the clear supernatant liquid decanted off.

- 3.2.2 For dilution, freshly boiled and cooled distilled water should be used.
- 3.2.3 Solutions which have to be stored should be kept in air-tight bottles.

4. PROCEDURE

The pH meter is standardized with a buffer of known pH about 9. A suitable buffer is 0.05 N solution of sodium borate (pH = 9.18 at 25° C).

A portion of latex of known solid content and alkalinity containing approximately 50 g of solids is accurately weighed into a 400 ml beaker. The ammonia content is adjusted to 0.5 per cent calculated on the water phase by adding 5 per cent formaldehyde solution (1 ml = 0.0189 g NH_a), while stirring.

Enough boiled and cooled distilled water is added to dilute the latex to about 30 per cent solids. The electrodes are inserted and 5 ml of 0.5 N potassium hydroxide are slowly added, while the solution is stirred slowly with a glass paddle. The reading of the pH meter is recorded.

Careful earthing of the pH meter and of the motor (should one be used to drive the glass stirrer) is necessary to prevent the wandering of the released galvanometer needle about its zero point, due to external electrical and electrostatic interference.

Additions of 1 ml increment of 0.5 N potassium hydroxide are continued, stirring being carried out at the same time. The pH is recorded after each addition. To keep electrical conditions constant, the stirrer should not be turned off until the titration is finished. The endpoint of the titration is the point of inflection of the pH-ml potassium hydroxide titration curve. At this point, the slope of the curve, i.e., the first differential, reaches a maximum and the second differential changes from a positive to a negative value. The endpoint can be calculated with reasonable accuracy from the second differential, assuming that the change from a positive to a negative value bears a linear relation to the addition of 0.5 N potassium hydroxide during the 1 ml interval involved.

5. EXPRESSION OF RESULTS

The KOH number is calculated as follows:

 ${\rm KOH~number} = \frac{{\rm number~of~milliliters~of~potassium~hydroxide} \times N \times 561}{TS \times {\rm weight~of~sample,~in~grams}}$

where TS = percentage of total solids,

N =normality of standard potassium hydroxide solution.

DETERMINATION OF RESISTANCE TO FLEX CRACKING OF VULCANIZED NATURAL OR SYNTHETIC RUBBER (DE MATTIA TYPE MACHINE)

BRIEF HISTORY

The ISO Recommendation R 132, Determination of Resistance to Flex Cracking of Vulcanized Natural or Synthetic Rubber (De Mattia type machine), was drawn up by Technical Committee ISO/TC 45, Rubber, the Secretariat of which is held by the British Standards Institution (B.S.I.).

Work on the preparation of this method was authorized at the first meeting of the Technical Committee held in London, in June 1948, and was entrusted to

the Working Group on "Flex Cracking and Cut-Growth."

It was agreed by the Working Group that the method should be based on that

used in the United Kingdom.

Germany

The method was considered by the Working Group and by the Technical Committee at the meetings held in The Hague (September 1949), in Akron (October 1950), in Oxford (October 1951), in Paris (June 1953) and was finally approved, as a Draft ISO Recommendation, at the Dusseldorf meeting, in September 1955.

On 17 July 1957, the Draft ISO Recommendation (No. 172) was distributed to all the ISO Member Bodies and was approved, subject to some modifications, by the following 26 (out of a total of 39) Member Bodies:

[®]Australia °Greece Austria Hungary Burma India *Canada °Ireland Czechoslovakia Italy ^eDenmark Japan Finland New Zealand France Pakistan

Portugal Romania Spain Sweden Switzerland Union of South Africa

United Kingdom

U.S.A.

One Member Body opposed the approval of the Draft: U.S.S.R.

Poland

The Draft ISO Recommendation was then submitted by correspondence to the ISO Council, which decided, in September 1959, to accept it as an ISO REC-OMMENDATION.

FOREWORD

Repeated bending or flexing of a rubber vulcanizate causes cracks to develop in that part of the surface where tension stress is set up during flexing or, if this part of the surface contains a crack, causes this crack to extend in a direction perpendicular to the stress. Certain soft vulcanizates, notably those prepared from styrene butadiene rubber, show marked resistance to crack initiation, but it is possible for these sample compounds to have a low resistance to crack growth.

It is important therefore to measure both the resistance to crack initiation by flexing and the resistance to crack growth. A method for determining the

^{*} These Member Bodies stated that they had no objection to the Draft being approved.

resistance to crack growth is given in ISO Recommendation R 133, Determination of Resistance to Crack Growth of Vulcanized Natural or Synthetic Rubber (De Mattia Type Machine).

The test described below is intended for use in comparing the resistance of rubbers to the formation and growth of cracks, when subjected to repeated flex-

ing on the De Mattia type machine.

1. APPARATUS

The essential features of the De Mattia type machine are as follows:

There are stationary parts, provided with grips for holding one end of each of the testpieces in a fixed position, and similar but reciprocating parts for holding the other end of each of the testpieces. The travel is 57.15 ± 0.1 mm (2.250 ± 0.005 in.) and is such that the maximum distance between each set of opposing grips is $75.0^{+1.2}_{-0.0}$ mm (3.00 $^{+0.00}_{-0.05}$ in.) (see Figure 1).

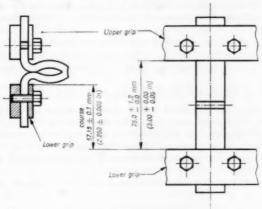


Fig. 1.-De Mattia type machine.

The reciprocating parts are so arranged that their motion is straight, and in the direction of, and in the same plane as, the common center-line of each opposing pair of grips. The planes of the gripping surfaces of each opposing pair of grips remain parallel throughout the motion.

The eccentric which actuates the reciprocating parts is driven by a constantspeed motor to give 300 ± 10 flexing cycles per minute, with sufficient power to flex at least six, and preferably twelve, testpieces at one test. The grips hold the testpieces firmly, without undue compression, and enable individual adjustment to be made to the testpieces to ensure accurate insertion.

Note. It is useful to arrange the testpieces in two equal groups, so that one group is being flexed while the other group is being straightened, thus reducing the vibration in the machine.

2. TESTPIECE

The testpiece is a strip with a molded groove, as shown in Figure 2. The strips may be molded individually in multiple-cavity mold or may be cut from a wide slab having a molded groove.

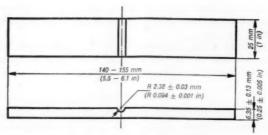


Fig. 2.—Testpiece.

The groove in the testpiece should have a smooth surface and be free from irregularities from which cracks may start prematurely. The groove should be molded into the testpiece or slab by a half-round ridge in the center of the cavity; this half-round ridge should have a radius of 2.38 ± 0.03 mm (0.094 ± 0.001 in.).

The results should be compared only between testpieces having thicknesses agreeing within 0.13 mm (0.005 in.), when measured close to the groove, because the results of the test are dependent upon the thickness of the testpiece.

3. STORAGE OF SAMPLES AND TESTPIECES

The properties of vulcanized rubber change continuously with time, these changes being particularly rapid during the first 24 hours after vulcanization.

Tests should therefore be carried out not less than 24 hours after vulcanization, and for accurate comparisons between different rubbers it may be necessary to ensure that these are tested at substantially the same interval after vulcanization.

Samples and test pieces should be protected from light as completely as possible.

4. NUMBER OF TESTPIECES

At least three, and preferably six, testpieces from each rubber compound are tested, and the results averaged, one or more testpieces being tested simultaneously with those of other rubbers with which the comparison is to be made.

5. PROCEDURE

The pairs of grips are separated to their maximum extent, and the testpieces inserted so that they are flat and not under tension, with the groove in any particular testpiece midway between the two grips, in which that testpiece is held, and on the outside of the angle made by the testpiece, when it is bent.

The machine is started and the test continued with frequent inspection until the first minute sign of cracking is detected; when the number of flexing cycles is recorded, the machine is restarted and stopped after intervals in which the number of flexing cycles is increased in geometric progression, a suitable ratio being 50 per cent on each occasion.

It is not desirable to run the testpiece until complete rupture occurs, the preferred method being to grade the severity of cracking by comparison with a standard scale of cracked testpieces, as described in section 7, "Expression of

results." The comparison includes an assessment of the length, depth and number of cracks.

The results should be recorded as follows:

- (a) the grade of cracking reached by each testpiece on each occasion the machine is stopped;
- (b) the flexing cycles which have been run.

6. TEMPERATURE OF TEST

A precise temperature is not specified and tests are normally performed at room temperature, although elevated temperatures may often be used with advantage.

7. EXPRESSION OF RESULTS

The accuracy of the test result can be greatly improved if quantitative values are calculated. The method recommended, based on references 1° and 2°°, is to provide the operator with photographs of a series of cracked testpieces and also a description of the effects, as a guide in interpreting the photographs.

A copy of the photographs is provided in Figure 3.

- Grade A. A few (less than ten) minute cracks have appeared at scattered points on the surface. A lens is not necessary for examining them, but the unaided eye is unable to detect that they have any depth. They should not be confused with mold-marks or specks of dust on the rubber; the latter should be removed before grading by wiping the testpiece with a moistened finger.
- Grade B. The number of cracks has increased, but they still appear to have no depth; they tend to concentrate along the center-line of the groove and extend nearly the full width of the testpiece.
- Grade C. The cracks begin to show some depth, and their breadth is equal to their length. This grade is regarded as the standard amount of deterioration to which the final result is calculated.
- Grade D. The cracks have now become so concentrated along the center-line that a few have coalesced.
- Grade E. Many of the cracks have now coalesced to form about a dozen cracks 1 to 2 mm long with a length/breadth ratio of about 2 or 3. This is the most severe degree of cracking which is regarded as satisfactory for grading purposes.
- Although the gradings F to K are much more arbitrary, a brief description follows:
- Grade F. Several cracks have coalesced to form one large crack which releases the surface in the center of the testpiece, thus distorting the top and bottom edges of the groove.
- Grade G. The large erack has torn its way nearer to the ends of the groove.
- Grade H. The crack has grown nearer to the ends and has absorbed a number of small ones, thus making its outline indistinct.
- Grade J. The crack has torn nearly to the ends of the groove.
- Grade K. The crack has torn right across the groove.

^{*} Reference 1: R. G. Newton, Transactions of the Institution of the Rubber Industry, 1939, 15, 172; Rubber Chemistry and Technology, 1940, 13, 59; Journal for Rubber Research, 1947, 25, 29.

** Reference 2: W. L. Stevens, India Rubber World, 1940, 102, 5, 36; Rubber Chemistry and Technology, 1942, 15, 159.

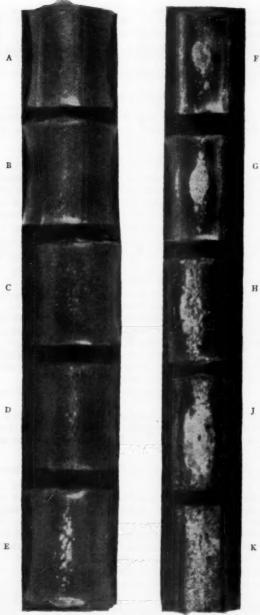


Fig. 3.—Reference standards for grading of cracked testpieces.

xxiv

7.1 Logarithmic method.—Different observers obtain reproducible results in using these gradings, and numerical constants can be associated with the gradings, representing the proportionate increase in time of running to change from one grade to another. If the number of kilocycles for which the machine has run is expressed as a logarithm to the base 10, these constants can be added or subtracted to change from one grade to another (see references 1° and 2**). Thus several gradings can be obtained on the same testpiece for different periods of running; it is convenient to add the constants corresponding to Grades A and B and subtract those for D and E, thus converting all the values to Grade C.

These constants for the gradings are:

A + 0.35B + 0.15C 0.00 D - 0.14E - 0.24

These values were taken from reference 1°, and their use is illustrated by the following examples:

Number of flexing cycles	Log number of kilocycles	Grading	Constant	Flex-cracking resistance
13 500	1.13	A	+0.35	1.48
22 500	1.35	A	+0.35	1.70
31 500	1.50	C	0.00	1.50
40 500	1.61	C	0.00	1.61
49 500	1.70	D	-0.14	1.56
58 500	1.77	D	-0.14	1.63
67 500	1.83	D	-0.14	1.69
85 500	1.93	E	-0.24	1.69

Mean = 1.61Standard error of mean = 0.03

The mean flex-cracking resistance represents the logarithm of the mean number of kilocycles required to produce Grade C cracking, the eight individual values lying between 1.48 and 1.70, i.e., between 30,000 and 50,000 cycles.

7.2 Graphical method.—If no assumption is made as to the manner in which eracking progresses, the results may be treated graphically (see reference 3***). Either the experimental results as observed are expressed in kilocycles or the logarithm of the observed results may be used. When results are to be averaged, the arithmetic mean should be taken, it being noted that the arithmetic mean of the logarithm of the experimental results is equivalent to the geometric mean of the experimental results. It is assumed in the following treatment that either the observed experimental results are being used or that all experimental results have been converted into their corresponding logarithms, the logarithms then being treated as "results".

The method is illustrated in Figure 4.

7.2.1 Considering the individual results for each testpiece obtained in the experiment, the average results corresponding to Grades A, B, C, D and E (call these A, B, C, D and E) are calculated.

*Reference 1: R. G. Newton, Transactions of the Institution of the Rubber Industry, 1939, 15, 172; Rubber Chemistry and Technology, 1940, 13, 694; Journal for Rubber Research, 1947, 16, 29.

**Reference 2: W. L. Stevens, India Rubber World, 1940, 1663, 36; Rubber Chemistry and Technology, 1942, 15, 159.

***Reference 3: J. M. Buist and G. E. Williams, Transactions of the Institution of the Rubber Industry, 1951, 27, 209; Rubber Chemistry and Technology, 1952, 28, 110.

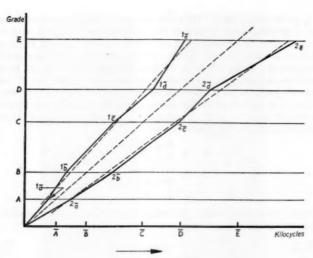


Fig. 4.-Graphical method.

- 7.2.2 A linear scale is placed on the abscissa axis, marked suitably in kilocycles (or logarithms of kilocycles) (see Fig. 4).
- 7.2.3 Five points are marked on the ordinate axis at distances from the origin proportional to Ā, B̄, C̄, D̄ and Ē respectively, the points being identified by the letters A, B, C, D and E. Five lines are drawn parallel to the abscissa axis.
 This may be conveniently accomplished by:
 - (a) marking the points \overline{A} , \overline{B} , \overline{C} , \overline{D} and \overline{E} on the abscissa axis.
 - (b) drawing a straight line inclined to the abscissa axis at a convenient angle,
 - (c) placing a series of lines perpendicular to the abscissa axis through the five marked points and so as to cross the inclined line,
 - (d) drawing through the five points of intersection on the inclined lines a set of five lines parallel to the abscissa axis and denoted A, B, C, D and E as appropriate.
- 7.2.4 The results obtained for each compound are considered separately and the results for the individual testpieces at each of the five grades of cracking arranged. These may be denoted as 1_a, 1_b, 1_c, 1_d, 1_e for compound 1, and 2_a, 2_b, 2_c, 2_d and 2_e for compound 2, etc.
- 7.2.5 The results for each compound are plotted on the prepared graph paper. For example, for compound 1, the first point is the origin, the second point has its ordinate on line A and abscissa 1_a, the third point has its ordinate on line B and abscissa 1_b, etc., until the sixth and last point with its ordinate on line E and abscissa 1_e. Similarly for the other compounds. The points are joined by straight lines to give a set of graphs, one graph for each compound.

- 7.2.6 The best straight line through the points on each graph, ignoring the origin, is drawn.
- 7.2.7 The following information can be obtained from the graph:
 - (a) Crack initiation time: the number of kilocycles at which the straight line graph meets the line A;
 - (b) Crack propagation time: the number of kilocycles at which the straight line graph crosses the line E, minus crack initiation time.

Although the method is intended to be applied to the set of experimental results obtained in each experiment, it may be found in practice that the relative positions of the grade lines are sufficiently reproducible in one laboratory for a set of standard grade lines to be determined for that laboratory.

8. REPORT

The report should state:

- the average time to reach each stage of cracking A to E, given in section 7, "Expression of results",
 - or the mean flex cracking resistance, determined by the logarithmic method.
 - or the crack initiation and propagation, determined by the graphical method:
- (2) the number of testpieces used;
- (3) the temperature of test.

ISO Recommendation

R 133

September 1959

DETERMINATION OF RESISTANCE TO CRACK GROWTH OF VULCANIZED NATURAL OR SYNTHETIC RUBBER (DE MATTIA TYPE MACHINE)

BRIEF HISTORY

The ISO Recommendation ISO/R 133, Determination of Resistance to Crack Growth of Vulcanized Natural or Synthetic Rubber (De Mattia type machine), was drawn up by Technical Committee ISO/TC 45, Rubber, the Secretariat of which is held by the British Standards Institution (B.S.I.).

Work on the preparation of this method was authorized at the first meeting of the Technical Committee held in London, in June 1948, and was entrusted to the Working Group on "Flex Cracking and Cut-Growth".

It was agreed by the Working Group that the method should be based on that used in the United Kingdom.

The method was considered by the Working Group and by the Technical Committee at the meetings held in The Hague (September 1949), in Akron (October 1950), in Oxford (October 1951), in Paris (June 1953) and was finally approved, as a Draft ISO Recommendation, at the Dusseldorf meeting, in September 1955.

On 17 July 1957, the Draft ISO Recommendation (No. 173) was distributed to all the ISO Member Bodies and was approved, subject to some modifications, by the following 27 (out of a total of 39) Member Bodies:

*Australia	*Greece	Portugal
Austria	Hungary	Romania
Burma	India	Spain
*Canada	*Ireland	Sweden
Czechoslovakia	Italy	Switzerland
*Denmark	Japan	Union of South Africa
Finland	New Zealand	United Kingdom
France	Pakistan	°U.S.S.R.
Germany	Poland	U.S.A.

No Member Body opposed the approval of the Draft.

The Draft ISO Recommendation was then submitted by correspondence to the ISO Council, which decided, in September 1959, to accept it as an ISO RECOMMENDATION.

1. FOREWORD

Repeated bending or flexing of a rubber vulcanizate causes cracks to develop in that part of the surface where tension stress is set up during flexing or, if this part of the surface contains a crack, causes this crack to extend in a direction perpendicular to the stress. Certain soft vulcanizates, notably those prepared from styrene butadiene rubber, show marked resistance to crack initiation, but it is possible for these sample compounds to have a low resistance to crack growth.

It is important therefore to measure both the resistance to crack initiation by flexing and the resistance to crack growth. A method for determining the resistance to crack initiation by flexing is given in ISO Recommendation R 132, Determination of Resistance to Flex Cracking of Vulcanized Natural or Synthetic Rubber (De Mattia Type Machine).

The test described below is intended for use in comparing the resistance of rubbers to the growth of cracks, when subjected to repeated flexing on the De Mattia type machine.

1. APPARATUS

The essential features of the De Mattia type machine are as follows:

There are stationary parts, provided with grips for holding one end of each of the testpieces in a fixed position, and similar but reciprocating parts for holding the other end of each of the test pieces. The travel is 57.15 ± 0.1 mm (2.250 ± 0.005 in.) and is such that the maximum distance between each set of opposing grips is $75.0^{+1.2}_{-0.0}$ mm (3.00 $^{+0.00}_{-0.05}$ in.) (see Fig. 1).

The reciprocating parts are so arranged that their motion is straight, and in the direction of, and in the same plane as, the common center-line of each opposing pair of grips. The planes of the gripping surfaces of each opposing pair of grips remain parallel throughout the motion.

The eccentric which actuates the reciprocating parts is driven by a constant-speed motor to give 300 ± 10 flexing cycles per minute, with sufficient power to flex at least six, and preferably twelve, testpieces at one test. The grips hold

[&]quot; These Member Bodies stated that they had no objection to the Draft being approved.

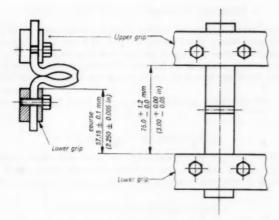


Fig. 1.-De Mattia type machine.

the testpieces firmly, without undue compression, and enable individual adjustment to be made to the testpieces to ensure accurate insertion.

Note. It is useful to arrange the testpieces in two equal groups, so that one group is being flexed while the other group is being straightened, thus reducing the vibration in the machine.

2. TESTPIECE

The testpiece is a strip with a molded groove, as shown in Figure 2. The strips may be molded individually in a multiple-cavity mold or may be cut from a wide slab having a molded groove. The groove in the testpiece should have a smooth surface and be free from irregularities from which cracks may start prematurely. The groove should be molded into the testpiece or slab by a half-round ridge in the center of the cavity. This half-round ridge should have a radius of 2.38 ± 0.03 mm $(0.094 \pm 0.001$ in.).

The results should be compared only between testpieces having thicknesses agreeing within 0.13 mm (0.005 in.), when measured close to the groove, because the results of the test are dependent upon the thickness of the testpiece.

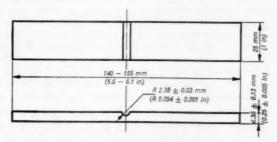


Fig. 2.-Testpiece.

3. STORAGE OF SAMPLES AND TESTPIECES

The properties of vulcanized rubber change continuously with time, these changes being particularly rapid during the first 24 hours after vulcanization.

Tests should therefore be carried out not less than 24 hours after vulcanization, and for accurate comparisons between different rubbers it may be necessary to insure that these are tested at substantially the same interval after vulcanization.

Samples and testpieces should be protected from light as completely as possible.

4. NUMBER OF TESTPIECES

At least three, and preferably six, testpieces from each rubber compound are tested, and the results averaged, one or more testpieces being tested simultaneously with those of other rubbers with which the comparison is to be made.

5. PREPARATION OF TESTPIECE

Each testpiece should be prepared by piercing the bottom of the groove at a point equidistant from the sides, using a suitable jig. The piercing tool should be maintained perpendicular to both the transverse and longitudinal axes and the cut accomplished by a single insertion and withdrawal of the tool. The cut should be parallel to the longitudinal axis of the groove. Lubrication with water containing a suitable wetting agent may be used.

Although it is not necessary to include exact details of a suitable jig for holding the cutting tool, it may be useful to state the basic principles governing the design of such a jig. The testpiece should be held flat in a solid support; the cutting tool should be normal to the support and placed centrally with respect to the groove of the testpiece, with the edge of the chisel parallel to the axis of the groove. Means should be provided for passing the cutting tool through the entire thickness of the rubber, and the support should have a hole of a size just sufficient to permit the cutting tool to project through the base of the testpiece to not less than 2.5 mm (0.1 in.) and not more than 3 mm (0.125 in.).

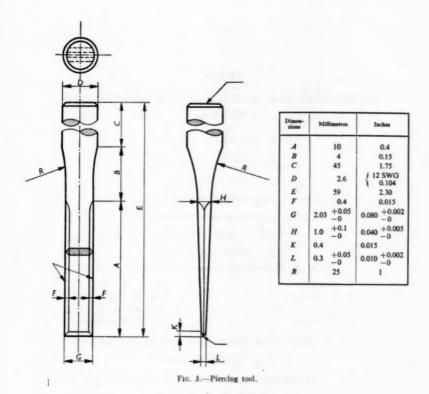
The piercing tool should conform to the dimensions given in Figure 3 below.

6. PROCEDURE

The pairs of grips are separated to their maximum extent, and the testpieces inserted so that they are flat and not under tension, with the groove in any particular testpiece midway between the two grips, in which that testpiece is held, and on the outside of the angle made by the testpiece, when it is bent.

The machine is started and stopped at frequent intervals to measure the length of the crack, e.g., at the 1, 3 and 5 kilocycle periods and at such further or intermediate periods as appear necessary. At each observation the grips are separated to a distance of 65 mm (2.56 in.) and the length of crack measured, preferably using a low-powered microscope, and from the smooth curve obtained by plotting length against number of flexing cycles, readings should be taken of

- (a) the number of kilocycles for the crack to extend from 2 to 4 mm,
- (b) the number of kilocycles for the crack to extend from 4 to 8 mm.
- (c) if desired, the number of kilocycles for the crack to extend from 8 to 12 mm.



7. TEMPERATURE OF TEST

A precise temperature is not specified and tests are normally performed at room temperature, although elevated temperatures may often be used with advantage.

8. REPORT

The report should state:

- (1) the number of kilocycles for the crack to extend from 2 to 4 mm;
- (2) the number of kilocycles for the crack to extend from 4 to 8 mm;
- (3) if desired, the number of kilocycles for the crack to extend from 8 to 12 mm;
- (4) the number of testpieces used;
- (5) the temperature of the test.

IUPAC

INTERNATIONAL SYMPOSIUM ON MACROMOLECULAR CHEMISTRY

C. A. WINKLER, Chairman

(From the 3rd Circular)

Organizing Committee

H. L. WILLIAMS, Chairman

MRS. A. LEE, Secretary

E. A. Crockett-Registration

L. A. McLeod-Program and Publicity

S. Bywater

B. B. Hillary D. G. Ivev

M. H. Jones

S. G. Mason

H. W. Quinn

M. Rinfret

R. T. Woodhams

E. B. BAGLEY, Montreal Sub-Committee Chairman

E. C. GAUDETTE, Liaison

H. Daoust-Special Events and Tours

Assisted by D. D. Patterson

Miss A. MacIver, Ladies Program

Assisted by Mrs. D. K. Jackson

Mrs. D. A. I. Goring Miss Francis Johnston

Miss Justine Sentenne

A. H. Sehon and T. H. Waid, Meeting Facilities

G. L. Bata, Transportation

Canadian High Polymer Forum

K. E. Russell

D. A. I. Goring

L. Breitman

Division of Polymer Chemistry, American Chemical Society

M. Morton

F. H. Winslow

Commission on Macromolecules, I.U.P.A.C.

H. W. Melville

T. Alfrey, Jr.

H. F. Mark

Host

The Canadian High Polymer Forum

Cosponsoring Groups

The Division of Polymer Chemistry of the American Chemical Society

The Commission on Macromolecules of the International Union of Pure and Applied Chemistry

Patrons

The National Research Council
The Chemical Institute of Canada
Canadian Section, Society of Chemical Industry
The Canadian Association of Physicists

Address

The Organizing Committee
International Symposium on Macromolecular Chemistry
P. O. BOX 816
Sarnia, Ontario, Canada
Cables—Macromol, Sarnia

GENERAL PROGRAM

All events will take place at the Queen Elizabeth unless otherwise stated.

WEDNESDAY, JULY 26

Registration desk open, 7:00-10:00 p.m.-Mezzanine floor.

THURSDAY, JULY 27

Registration, 8:00 a.m. to 9:00 p.m.-Mezzanine floor.

Opening ceremonies 9:30 a.m., Prof. C. A. Winkler, Chairman. Opening remarks, greetings, general announcements.

Plenary Lecture, 10:00-11:00 a.m., Professor H. F. Mark, "Polymer Research at Brooklyn Polytechnic".

Opening Luncheon, 12:30 p.m., Prof. C. A. Winkler, Chairman.

Technical Sessions, 2:00 p.m. to 5:00 p.m.

Mixer and Buffet, p.m. A general buffet lunch and evening mixer is being planned. This will take place away from the hotel. Transportation will be provided.

FRIDAY, JULY 28

Registration, 8:00 a.m. to 5:00 p.m.—Mezzanine floor. Technical Sessions, 9:00 a.m. to 12:30 p.m.; 2:00 p.m. to 5:00 p.m.

SATURDAY, JULY 29

Registration, 8:00 a.m. to 5:00 p.m.—Mezzanine floor.
Technical Sessions, 9:00 a.m. to 1:00 p.m.
Tours—City of Montreal, a.m. and p.m.; Seaway Tour, a.m. and p.m.
xxxiii

La Roulotte Travelling Players. Free, p.m. in Dominion Square near hotels. Pantomine Players using mobile stage. Reserved area available for participants of Symposium.

SUNDAY, JULY 30

Registration, 10:00 a.m. to 5:00 p.m.—Mezzanine floor. Tours—Trip to Ottawa, all day; Laurentian Picnic at Le Chatelet, all day.

MONDAY, JULY 31

Registration, 9:00 a.m. to 5:00 p.m.—Mezzanine floor. Technical Sessions, 9:00 a.m. to 12:30 p.m.; 2:00 p.m. to 5:00 p.m. Gournet Banquet, 7:00 p.m.

TUESDAY, AUGUST 1

Registration, 9:00 a.m. to 5:00 p.m.—Mezzanine floor. Technical Sessions, 9:00 a.m. to 12:30 p.m. Closing Luncheon, 12:30 p.m., Professor C. A. Winkler, Chairman. Technical Sessions, 2:00 p.m. to 5:00 p.m. Post Conference Tour Leaves for Ottawa.

OTHER MEETINGS

The Chemical Institute of Canada will hold its Annual Conference and Exhibition at the Queen Elizabeth, August 3rd and 4th, 1961. For details please write the

Chemical Institute of Canada, 48 Rideau Street, Ottawa 2, Ontario, Canada.

The International Union of Pure and Applied Chemistry will hold its Conference and Congress in 1961 in Montreal, the Conference from August 2nd to 5th and the Congress from August 6th to 12th. For details write the

National Research Council, Organizing Committee, IUPAC Congress, Ottawa 2, Ontario, Canada.

The International Calorimetry Conference (cosponsored by IUPAC) will be held in Ottawa, Ontario, Canada, August 14th to 17th, 1961. For details please write:

Dr. J. E. Kunzler, Bell Telephone Laboratories Inc., Murray Hill, New Jersey, U. S. A.

The International Symposium on Microchemical Techniques (cosponsored by IUPAC) will be held August 13th to 18th, 1961, at Pennsylvania State University, University Park, Pennsylvania, U. S. A. For details please write:

Mr. Howard J. Francis, Jr., Pennsalt Chemicals Corporation, P. O. Box 4388, Philadelphia 18, Pennsylvania, U. S. A. The Sixth International Conference on Coordination Chemistry (cosponsored by IUPAC) will be held at Wayne State University, Detroit, Michigan, August 27th to Sept. 1st, 1961. For details please write:

Dr. S. Kirschner, Department of Chemistry, Wayne State University, Detroit 2, Michigan, U. S. A.

TECHNICAL PROGRAM

Speakers are reminded that there is a speaker's room with facilities for testing slides and desks for preparing final texts on the Convention Floor.

The accompanying program is tentative and incomplete. Those attending

the Symposium will receive a final program at the time of registration.

The discussions are to be recorded on sheets which will be given to each questioner and each author after each question and reply. These sheets will be given to the recorders or the Organization Committee at the Registration desk as soon as possible after the paper for incorporation with the final manuscript into the collective volumes. It will be the responsibility of the questioners and authors to complete the forms. Proofs will accompany those of the papers and will be sent to the authors only.

PUBLICATION

Publication of the contributed papers will be in collective volumes of the Journal of Polymer Science. Authors are requested to leave at least two copies of their papers with the Organizing Committee at the Registration desk before the International Symposium closes. Copies of the collective volumes may be purchased from Interscience Publishers.

Invited plenary and sessional lectures will be published in a collective volume. Authors are requested to leave at least two copies of their lectures with the Organizing Committee at the Registration desk before the International Sym-

posium closes.

Extra copies of the Program, Book of Abstracts and List of Members may be purchased for \$3.00 for the three items together as long as the supply lasts.

CORRESPONDENCE

Correspondence relating to the International Symposium on Macromolecular Chemistry, please write:

The Organizing Committee, International Symposium on Macromolecular Chemistry, P. O. Box 816, Sarnia, Ontario, Canada.

PRELIMINARY TECHNICAL PROGRAM

In order that the third circular may reach all participants in good time for study prior to the International Symposium on Macromolecular Chemistry time has not been taken to finalize the organization into sessions by day and time of day. The papers are grouped into five lists each of which will represent a parallel session starting Thursday, July 27 and terminating Tuesday, August 1.

It is likely that only four simultaneous sessions will be required for most of the week and therefore there will be gaps in some of the groups shown. However, authors may judge approximately the time of their presentation by the location in the list. Changes may be made if requested.

The final, detailed program listing the papers in each session with the time and day of presentation will be available at the time of registration. Authors will be advised individually of the exact time of their presentation soon.

The titles, in general, are in the language in which the paper will be presented. The author presenting is italicized.

GROUP 1

PREDOMINANTLY SOLUTION PROPERTIES

The Velocity of Dissolution of Polymers in Solvents. Part 1. Kurt Ueberreiter and F. Asmussen, Fritz-Haber Institut der Max-Planck-Gesellschaft, Berlin-Dahlem, Germany.

Die Auflösungsgeschwindigkeit von Polymeren in Lösungsmitteln Teil 2. F. Asmussen and Kurt Ueberreiter, Fritz-Haber-Institut der Max-Planck-Gesellschaft, Berlin-Dahlem, Germany.

The Dilute Solution Properties of Nylon 66 in Relation to the Solvent Environment. P. R. Saunders, Chemstrand Research Center, Inc., Durham, North Carolina.

Ion-Solvent Interaction in Solutions of Polymeric Ions. Part I. B. E. Conway and J. E. Desnoyers, University of Ottawa, Ottawa, Ontario.

Ion-Solvent Interaction in Solutions of Polymeric Ions. Part II. B. E. Conway and J. E. Desnoyers, University of Ottawa, Ottawa, Ontario.

Polyvinyl Chloride-Diluent Interactions. C. E. Anagnostopoulos and A. Y. Coran, Monsanto Chemical Company, St. Louis, Missouri.

Polyethylene—Diluent Interactions. A. Y. Coran and C. E. Anagnostopou-

los, Monsanto Chemical Company, St. Louis, Missouri.

The Use of High Pressure to Study Polymer-Solvent Interaction. Joe S. Ham, A & M College of Texas, College Station, Texas. Max C. Bolen and James K. Hughes.

Shear Dependence of the Reduced Viscosity-Concentration Slope Constant. L. H. Cragg and H. van Oene, University of Alberta, Edmonton, Alberta.

Light Scattering Studies on Polyethers. I. High Molecular Weight Poly (ethylene oxide). Anthony J. Hyde, Royal College of Science and Technology. Glasgow, Scotland.

Light Scattering by Poly-L-Benzyl Glutamate Solutions Subjected to an Electric Field. Morton L. Wallach, E. I. du Pont de Nemours & Co., Inc., Wilmington, Delaware, and H. L. Benoit, Centre de Recherches sur les Macromolécules, Strasbourg, France.

Solution Behaviour of Poly-Silicie Acid. Sidney A. Greenberg and T. N.

Chang, Portland Cement Association, Skokie, Illinois.

Propriétés Thermodynamiques de Solutions Modérément Concentrées de Polyisobutylène dans le Chlorobenzène. Hubert Daoust et Jacques Léonard, Université de Montréal, Montréal, P. Q.

Contribution à l'étude des Propriétés Thermodynamiques des Solutions de Copolymères. Marguerite Lautout-Magat, C.N.R.S., Paris, France.

The Heat of Mixing in Polyisobutylene-Hydrocarbon Systems. G. Delmas, D. D. Patterson and T. Someynsky, University of Montreal, Montreal, P. O.

The Relation of Optical Rotatory Properties to Structure of Polypeptides. Murray Goodman, Irving Listowsky, Franklin Boardman and Marija Stake, Polytechnic Institute of Brooklyn, Brooklyn, New York.

The Adsorption of Macromolecules at a Liquid Solid Interface. Robert

Ullman, Polytechnic Institute of Brooklyn, Brooklyn, New York.

The Estimation of Diffusivities and Solubilities from Sorption Studies. J. L. Lundberg, M. B. Wilk and Marilyn J. Huyett. Bell Telephone Laboratories, Inc., Murray Hill, New Jersey.

The Dependency of the Ultracentrifugal Sedimentation Coefficient on Concentration. Matatiahu Gehatia, Institut für vegetative Physiologie der Uni-

versität, Frankfurt-Main, Germany.

Equilibrium Ultracentrifuge for Molecular Weight Measurement. J. W. Beams, R. D. Boyle and P. E. Hexner, University of Virginia, Charlottesville, Virginia.

Birefringence in a Strained Viscoelastic Fluid Under Steady State Rotary Conditions. Stanley J. Gill and Frederick R. Dintzis, University of Colorado,

Boulder, Colorado.

Diffusion de la Lumière par les Solutions de Copolymères. H. L. Benoit and M. Leng, Centre de Recherches sur les Macromolécules, Strasbourg, France.

Calibration of Light Scattering Instruments—A Critical Survey and Some Experiments. J. P. Kratohvil, Gj. Dezelic, M. Kerker and E. Matijevic (University of Zagreb, Zagreb, Yugoslavia), Clarkson College of Technology, Potsdam, New York.

Molecular Weight of Polymers from Electrical Resistivity of Solutions. J. R. Purdon and M. Morton, University of Akron, Akron, Ohio.

Zone Fractionation of Polystyrene. Arnold M. Ruskin and Giuseppe Parravano, University of Michigan, Ann Arbor, Michigan.

Diffusion, Thermodiffusion and Thermic Diffusion of Polystyrene in Solution. G. Meyerhoff and K. Nachtigall, Universität Mainz, Mainz, Germany.

A Coaxial Cylinder Elastoviscometer for the Study of Dilute Polymer Solutions. H. van Oene and L. H. Cragg, University of Alberta, Edmonton, Alberta.

The Polymer Literature. E. H. Immergut, Interscience Publishers, New York, New York.

Effect of Branching on Solution Properties and Melt Viscosity of Polyvinyl Acetate. Lindsey M. Hobbs, Lord Manufacturing Company, Erie, Pennsylvania, Guy C. Berry, Mellon Institute, Pittsburgh, Pennsylvania, and Victor C. Long, E. I. du Pont de Nemours & Co., Inc., Wilmington, Delaware. (Work done at University of Michigan, Ann Arbor, Michigan.)

Solution Properties of Linear and Branched Polybutadiene and Trans Polyisoprene Fractions. W. Cooper, G. Vaughan and D. E. Eaves, Dunlop Rubber

Company, Limited, Birmingham, England.

Regularities in the Solution Viscosities, Melt Viscosities and Molecular Weights of Branched Polymers. Warner L. Peticolas, I.B.M., San Jose, California.

Study of Branching in Regular Isoprene Polymers. I. J. Poddubnyi and E. Erenburg, Allunion Scientific Research Institute of Synthetic Rubber, Leningrad, U.S.S.R.

Preparation and Properties of Monodisperse Branched Polystyrenes. M. Morton, T. E. Helminiak, S. D. Gadwary and F. Bueche, University of Akron, Akron, Ohio.

The Viscosity Behaviour of Linear and Branched Dextran Sulphates. W. M.

Pasika and L. H. Cragg, University of Alberta, Edmonton, Alberta.

Polymer Size Distribution and Average Molecular Weights for Reactions Involving Variable Propagation Rates. Henri J. R. Maget, General Electric Company, West Lynn, Massachusetts.

The Determination of Number Criteria of Polymer Heterogeneity. Henryk

Sibinski, Instyut Wlokien Sztucznych i Syntetcznych, Lodz, Poland.

A Study of the Molecular Dimensions of Fractions of High Pressure Polyethylene. H. J. L. Schuurmans, Monsanto Chemical Company, Texas City, Texas.

Lösungszustand und Fraktionierung der Cellulose in dem Modifizierten Eisen-Weinsäure-Lösungsmittel. Kurt Edelmann, Institut für Faserstoff-

Forschung, Berlin-Charlottenburg, Berlin, Germany.

Thermodiffusion Fractionation of Polymers and Determination of Distribution Curves. Ivo Kössler and Jan Krejsa, Czechoslovakian Academy of Science,

Prague, Czechoslovakia.

Fractionnement des Polyamides par une Méthode en Continu. N. Duveau (Société RHODIACETA, Lyon, France) and A. Piguet (Battelle Memorial Institute, Geneva, Switzerland). Presented by F. Ecochard, Société RHODIACETA, Lyon, France.

Effect of Configuration on Binding of Magnesium Ion by Polyacrylic Acid.

Ada Leah Jacobson, University of Alberta, Calgary, Alberta.

Cross-linking of Single Linear Macromolecules. Werner Kuhn and G.

Balmer, Universität Basel, Basel, Switzerland.

Treatment of Intrinsic Viscosities. Michio Kurata (University of Kyoto, Kyoto, Japan), Dartmouth College, Hanover, New Hampshire, and W. H. Stockmayer, Massachusetts Institute of Technology, Cambridge, Massachusetts.

Statistical Computation of Distribution Functions of Dimensions of Macromolecules. F. T. Wall, University of Illinois, Urbana, Illinois, and Thomas F.

Schatzki, Shell Development Company, Emeryville, California.

Studies of the Configuration and Conformation of Vinyl-Type Polymers. II. Temperature Dependence of Infra-red Spectrum of Polyvinyl Chloride in Solution and its Sereo Regularity. *Masatami Takeda* and Kazuyoshi Iimura, Tokyo College of Science, Tokyo, Japan.

Solution Properties of Poly (N-Dimethyl-Aerylamide). L. Trossarelli,

Instituto Chimico dell'Università, Torino, Italy.

A Study of Poly (ethylene oxide) in Solution. Rossi Corrado, Università di Genova, Genova, Italy.

GROUP 2

PREDOMINANTLY BULK POLYMER PROPERTIES

The Dynamic Birefringence of Polymeric Solids. S. Onogi (Kyoto University, Kyoto, Japan), D. A. Keedy and R. S. Stein, University of Massachusetts, Amherst, Massachusetts.

Wärmeleitfähigkeit von Hochpolymeren in Temperaturbereich von -180°C. bis +90°C. Kurt Eiermann und Karl-Heinz Hellwege, Deutsches Kunststoff-

Institut, Darmstadt, Germany.

Proton Magnetic Resonance Studies on Synthetic Rubber. I. Polybutadienes and Polyisoprenes. *Masatami Takeda*, Koji Tanaka and Rumika Nagao, Tokyo College of Science, Tokyo, Japan.

Molecular Motion in Polystyrene and Some Substituted Polystyrenes. A. Odajima, J. A. Sauer and A. E. Woodward, The Pennsylvania State University, University Park, Pennsylvania.

Experimental Determination of the Elastic Modulus of the Crystalline Regions in Oriented Polymers. Ichiro Sakurada, Yasuhiko Nukushina and

Taisuke Ito, Kyoto University, Kyoto, Japan.

Elasticity of Cubic Lattice Chain Networks. W. R. Krigbaum and M. Kaneko, Duke University, Durham, North Carolina, and T. M. Birshtein, Institute for Macromolecular Compounds, Leningrad, U.S.S.R.

Effect of Carbon Black on Chain Mobility of Synthetic Rubbers. Mario Baccaredda and EnzoButta, Instituto di Chimica Industriale e Applicata-

Facolta' Di Ingegneria, Pisa, Italy.

Steric Hindrance as a Structural Factor Affecting Polyester Properties. I. Goodman, J. Mather and J. W. Stimpson, Imperial Chemical Industries, Ltd, Harrogate, Yorkshire, England.

Phase Equilibria of Multicomponent Systems Containing Polydisperse Polymer. Andrzej Broda, Lodzkie Zaklady Chemiczne P. T., Lodz, Poland.

Morphology of Polyethylene Crystalline Complexes. V. F. Holland and Paul H. Lindenmeyer, Chemstrand Research Center, Inc., Durham, North Carolina.

The Relationship Between Crystallization Habit and Crystallization Conditions in Polyethylene. Paul H. Lindenmeyer and V. F. Holland, Chemstrand Research Center, Inc., Durham, North Carolina.

Invited Lecture

The Formation of Big Crystal Structures in Polymers, and their Properties. V. A. Kargin, Academy of Sciences of the U.S.S.R., Moscow, U.S.S.R.

Relationship Between Morphology and Mechanical Properties in Polyolefin Film. S. Hoshino (Ube Industries, Japan), J. Powers and R. S. Stein, University of Massachusetts, Amherst, Massachusetts.

The Morphology and Internal Structure of Poly (ethylene oxide) Spherulites. Fraser P. Price and Ralph W. Kilb, General Electric Research Labora-

tory, Schenectady, New York.

A Study of the Crystalline Structure of Synthetic Fibres Using Dark Field Electron Microscopy. *Robert G. Scott*, E. I. du Pont de Nemours & Co., Inc., Wilmington, Delaware.

Crystals of Cellulose Triacetate and Cellulose. R. St. John Manley, Pulp &

Paper Research Institute of Canada, Montreal, P. Q.

Invited Lecture

Optical Studies of Morphological Changes in Deforming Polyolefines. R. S. Stein, University of Massachusetts, Amherst, Massachusetts.

Kristallisation von aus der Dampfphase Kondensierten Schichten aus CH₂-Kettenmolekeln. Götz Reinhard Lampe und Karl-Heinz Hellwege, Deutsches Kunststoff-institut, Darmstadt, Germany.

Crystallization of Copolymers of Ethylene Glycol and Diethylene Glycol Terephthalate. Ralph C. Golike and Walter H. Cobbs, Jr., E. I. du Pont de

Nemours & Co., Inc., Buffalo 7, New York.

Time-Humidity Superposition in Some Crystalline Polymers. Shigeharu Onogi (Kyoto University, Kyoto, Japan), University of Massachusetts, Amherst,

Massachusetts, Kiichiro Sasaguri, Tomio Adachi and Sadahide Ogiwara, Kyoto

University, Kyoto, Japan.

Gross Structures in Polyethylene Terephthalate Films as Revealed by Etching. W. P. Baker, Jr., E. I. du Pont de Nemours & Co., Inc., Wilmington, Delaware.

A Theoretical Approach to the Glass Transition Phenomena and Comparison with Experiments. A. J. Kovacs, University of Wisconsin, Madison, Wisconsin (Centre de Recherches sur les Macromolécules, Strasbourg, France).

Effect of Pressure on Dielectric Relaxation and Glass Transition Temperature of Polymers. James M. O'Reilly, General Electric Research Laboratory,

Schenectady, New York.

The Effect of Pressure and Temperature on the Specific Volume of Polyethylene. Shiro Matsuoka, Bell Telephone Labs., Inc., Murray Hill, New Jersey.

Higher-Order Transitions in Poly (4-Methyl-1-Pentene). B. G. Ranby, K. S. Chan, N. Y. State College of Forestry, Syracuse, New York, and H. Brumberger, Syracuse University, Syracuse, New York.

Glass Transitions in Mono-substituted Vinyl Homo—and Copolymers. F. P. Reding and J. A. Faucher, Union Carbide Chemicals Company, South Charleston,

West Virginia.

Formation and Characteristics of the Crystalline Cellulose x Modification of Cellulose. O. Ellefsen, The Norwegian Pulp & Paper Research Institute, Oslo, Norway, and N. Norman, Central Institute for Industrial Research, Oslo, Norway.

Thermal X-Ray Diffraction Study or Highly Acetylated Cotton Cellulose. Carl M. Conrad and Joseph J. Creely, Southern Regional Research Laboratory,

New Orleans, Louisiana.

Etude Cristallographique de la Structure de Films de Polytetra fluoroéthylène Greffés de Styrène. Destruction du copolymère Greffé par un Traitement Thermique. Claude Sella, Adolphe Chapiro and Akira Matsumoto, C. N. R. S., Bellevue (S & O), France.

On the Characterization of Stereoregular Polymers. III. Application to Polypropylene. Robert L. Miller, Monsanto Chemical Company, Springfield 2,

Massachusetts.

Studies of the Effects on Crystal Structure of Introducing Aromatic Rings into Linear Polyamides. D. C. Vogelsong, E. I. du Pont de Nemours & Co., Inc., Wilmington, Del.

Specific Heats and Crystallinity of Isotactic and Atactic Polypropylene. M. Dole and R. W. Wilkinson, Northwestern University, Evanston, Illinois.

Adiabatic Crystallization of Amorphous Polycaprolactam. O. Wichterle, J. Sebenda and J. Tomka, Institute of Macromolecular Chemistry, Prague, Czechoslovakia.

On the Stability of Helical Conformations of Simple Linear Polymers. P. De Santis, E. Giglio, A. M. Liquori and A. Ripamonti, Instituto de Chimica Fisica, Unversità di Napoli, Napoli, Italy.

On the Structure and Physiochemical Properties of Stereoregular Polyacrylates and Methacrylates. V. Crescenzi, M. D.'Alagni, A. M. Liquori, P. G.

Orsini and V. Vitagliano, Università di Napoli, Napoli, Italy.

Permeation, Solution and Diffusion of Water in Some High Polymers. V. Stannett and H. Yasuda, State University College of Forestry, Syracuse, New York,

Microvoids in Fibres as Studied by Small-Angle Scattering of X-Rays. W. O. Statton, E. I. du Pont de Nemours & Co., Inc., Wilmington, Delaware.

The Rheology of Polymer Solutions in Oil. Wladimir Philippoff, Esso

Research & Engineering Company, Linden, New Jersey.

Long-Range Intermolecular Coupling in Concentrated Poly-n-Butyl Methacrylate Solutions and its Dependence on Temperature and Concentration. Thomas E. Newlin, Stuart E. Lovell, P. R. Saunders and John D. Ferry, University of Wisconsin, Madison, Wisconsin.

Modification of the Spectral and Semi-conducting Properties of Polyvinylidene Chloride by Ultraviolet Light of Specific Wavelengths. Gerald Oster, Gisela Oster and Marian Kryszewski, Polytechnic Institute of Brooklyn, Brook-

lvn. New York.

Stress Relaxation Phenomena-Multiple Box Distribution Treatment of Relaxation Times. Franklin S. C. Chang, Borg-Warner Corporation, Des Plaines, Illiniois.

Dynamic Mechanical Studies of Irradiated Polypropylene. J. A. Saucer, L. J. Merrill and A. E. Woodward, The Pennsylvania State University, University Park, Pennsylvania.

Some Mechanical Aspects of the Swelling and Drying of Polymers. Bernard Rosen, Westinghouse Electric Corporation, Pittsburgh 35, Pennsylvania.

Methods of Predicting Radiation Induced Changes in the Mechanical Properties of High Polymers. E. G. Fritz, General Dynamics Corporation, Fort Worth, Texas.

Mechanisches Verhalten von Hochpolymeren bei Verschiedener Zeitlicher Form, Art und Grösse der Deformation. G. W. Becker, Physikalisch-Technische Bundesanstalt, Braunschweig, Germany.

Diffusion of Gases in Fluorocarbon Polymers. W. W. Brandt, Illinois

Institute of Technology, Chicago, Illinois.

A Critical Investigation of Polyethylene Gas Permeability. Harvey Alter, Union Carbide Plastics Company and Harris Research Laboratories, Inc., Washington 11, D. C.

On the Influence of the Glass Transition on Diffusion Processes in Irradiated Polymers. Robert E. Barker, Jr., General Electric Research Laboratory,

Schenectady, New York.

The Newtonian Melt Viscosity of Polythene: An Index of Chain Branching. H. P. Schreiber and E. B. Bagley, Canadian Industries Limited, McMasterville, P. Q.

Effect of Molecular Weight Distribution and Branching on the Viscosity of Polyethylene Melts. W. F. Busse and R. Longworth, E. I. du Pont de Nemours & Co., Inc., Wilmington, Delaware.

On the Cutting Mechanism of High Polymers. Akira Kobayashi and Katsumasa Saito, Electrotechnical Laboratory, Tokyo, Japan.

GROUP 3A

PREDOMINANTLY FREE RADICAL POLYMERIZATION

Kinetics of the Thermal Decomposition of Dimethyl-N-(2-cyano-2-propyl)-Ketenimine by Nuclear Magnetic Resonance Spectrascopy. N. Muller, Purdue University, Lafayette, Indiana, and P. Smith and W. C. Tosch, Duke University, Durham, North Carolina.

Examination of Kinetics of Thermal Decomposition of the Peroxides of Methyl Polymethacrylate. E. Turska and S. Polowinski, Polish Academy of Science, Lodz, Poland.

Isotope Effects in the Reactions of Primary Radicals. J. K. Allen, The University, Louisville, Kentucky, and J. C. Bevington, University of Birming-

ham, Birmingham, England.

Permanganate-Oxalic Acid as a Redox Initiator in Aqueous Media. Part I. The Initiating Radical and General Features. Santi R. Palit and Ranjit S. Konar, Indian Association for the Cultivation of Science, Calcutta, India.

Permanganate—Oxalic Acid as a Redox Initiator in Aqueous Media. Part II. Kinetics and D. P. Santi R. Palit and Ranjit S. Konar, Indian Association for the Cultivation of Science, Calcutta, India.

Invited Lecture

Electrochemical Initiation of Polymerization. J. W. Breitenbach and Ch. Srna, Chemisches Institut der Universität, Wien, Austria.

Polymerization Reactions in the Presence of a Metal Salt. Michel B.

Mullier, W. R. Grace & Company, Clifton, New Jersey.

Effects of Cupric Salt on the Polymerization of Aerylonitrile in an Aqueous Solution. *Masamoto Watanabe* and Hiroshi Kiuchi, Toyo Rayon Company, Ltd., Otsu-eity, Japan.

Behaviour of Primary Radicals in Vinyl Polymerization. Tomonobu Manabe

and Seizo Okamura, Kyoto University, Kyoto, Japan.

Kinetics of Polymerization of Vinylidene Chloride. Leon Marker, Orville J. Sweeting, James G. Wepsic, Olin Mathieson Chemical Corporation, New Haven, Connecticut.

Ultracentrifugation Method for Determination of Velocity Coefficients of Vinyl Polymerization. *Nobuo Yamada*, Electrical Communication Laboratory, Tokyo, Japan.

Sur la Polymérisation Catalytique et Radiochimique des Allylsilanes. A. V. Toptchiev, N. S. Nametkin and L. S. Polak, Institut de la Synthése Petrochimique, Académie des Sciences d'U.S.S.R., Moscow, U.S.S.R.

Kinetics of Ethylene Polymerization Initiated by Free Radicals. H. N.

Friedlander, Amoco Chemicals Corporation, Whiting, Indiana.

Copolymerization Studies of the Radiation-Induced Polymerization at Low Temperature. Yoshizo Tsuda, Toyo Rayon Company Limited, Otsu-city, Japan.

Polymerizations Induced by Ionizing Radiation at Low Temperatures. I. Evidence for the Simultaneous Existence of Ionic and Free Radical Mechanisms in the Polymerization of Styrene and 2,4-Dimethylstyrene. Catherine S. Hsia Chen and Robert F. Stamm, American Cyanamid Company, Stamford, Connecticut.

Polymerizations Induced by Ionizing Radiation at Low Temperatures. II. Effects of Change of Phase and Heterogeneity on the Polymerization of Styrene and 2,4-Dimethylstyrene. Catherine S. Hsia Chen, American Cyanamid Company, Stamford, Connecticut.

Graft Copolymerization to Cellulose by Sodium Periodate. Takao Toda,

Toyo Spinning Company, Ltd., Shiga-ken, Japan.

Monomer Reactivities in Radiation-Induced Graft Copolymerization. G. Odian, T. Acker, A. Rossi and E. Ratchik, Radiation Applications, Inc., Long Island, New York.

Invited Lecture

Relative Efficiencies in Graft Copolymerizations. G. Smets, University of

Louvain, Louvain, Belgium.

Influence de la Témperature sur de Greffage du Styrène sur des Films de Polytetrafluoroéthylène et de Poly (chlorure de Vinyle) par la Méthode Radiochimique Directe. Adolphe Chapiro and Akira Matsumoto, Centre National de la Recherche Scientifique, Paris, France.

Kinetics of Mutual Radiation Grafting of Styrene in Ethocel (Ethyl Cellulose) Film. Richard A. Mock and William N. Vanderkooi, The Dow

Chemical Company, Midland, Michigan.

Studies of the gamma-radiation-initiated Polymerization of Ethylene. Richard H. Wiley, N. T. Lipscomb, F. J. Johnston, G. A. Akin and J. E.

Guillet, University of Louisville, Louisville, Kentucky.

Gamma-Ray Induced Solid-State Polymerization of Ring Compounds, S. Okamura, Kyoto University, Kyoto, Japan, and K. Hayashi and Y. Kitanishi, Japanese Association for Radiation Research on Polymers, Osaka, Japan.

Polymerization in the Crystalline State of Methacrylic Acid and of Alkali Metal Acrylates and Methacrylates. H. Morawetz and I. Rubin, Polytechnic

Institute of Brooklyn, Brooklyn, New York.

Cyclopolymerization of Acrylic Anhydride. J. Mercier and G. Smets, Uni-

versity of Louvain, Louvain, Belgium.

The Low Temperature Polymerization of Methyl Methacrylate Initiated by Silver Ethyl. C. E. H. Bawn, W. H. Janes and A. M. North, University of Liverpool, Liverpool, England.

Mechanism of Alternating Intra-Intermolecular Propagation. I. Methacrylic Anhydride. William E. Gibbs and Joseph T. Murray, Wright-Patterson AFB,

Ohio.

Invited Lecture

Some Conformational Aspects of Polymers Obtained through the Alternating Intra-Intermolecular Mechanism. G. B. Butler, University of Florida, Gainesville, Florida.

Inhibited and Retarded Polymerization of Ethyl Methacrylate. B. Lionel Funt and Fred D. Williams, University of Manitoba, Winnipeg, Manitoba.

The Effect of Phenols on the Polymerization of Styrene. M. Godsay, G.

Harpell and K. E. Russell, Queen's University, Kingston, Ontario.

Effect of Asymmetric Centers on the Polymerization of Vinyl Monomers and the Properties of their Polymers. Methacrylyl Alanine, Methacrylyl Glutamic Acid and Acrylyl Glutamic Acid. H. Morawetz and R. K. Kulkarni, Polytechnic Institute of Brooklyn, Brooklyn, New York.

Coplymerization Studies. II. The Effect of High Pressures on Comonomer Reactivity Ratios. R. D. Burkhart and N. L. Zutty, Union Carbide Company,

South Charleston, West Virginia.

Invited Lecture

Some Recent Problems in the Thermodynamics and Reversibility of Addition

Polymerization. K. J. Ivin, University of Leeds, Leeds, England.

Emulsion Polymerization of Vinyl Acetate. S. Okamura, Kyoto University, Kyoto, Japan, and T. Motoyama, High Polymer Chemical Industries, Ltd., Kyoto, Japan.

Initial Rates of Emulsion Polymerization of Styrene with Water-Soluble and Oil-Soluble Initiators. *Helmut Edelhauser*, Universität, Wien, Wien, Austria.

Emulsion Copolymerization of Butadiene and Styrene in the Presence of Carbon Black. A. I. Medalia, E. Hagopian and J. P. Hall, Cabot Corpo-

ration, Cambridge, Massachusetts.

Nature of Molecular-Weight Distribution and Properties of Styrene-Butadiene Rubbers Depending on Polymerization Conditions. I. J. Poddubnyi, M. Mosevitsky, M. Rabinerson and A. Perminov, All Union Scientific Research Institute of Synthetic Rubber, Leningrad, U.S.S.R.

GROUP 3B

PREDOMINANTLY IONIC POLYMERIZATION

New Elastomers Derived from Copolymers of Tetrahydrofuran and Propylene Oxide. L. A. Dickinson, Canadian Armament Research & Development Establishment, Quebec, P. Q.

Anionic Copolymerization. K. F. O'Driscoll, Villanova University, Villa-

nova, Pennsylvania.

Kinetics of Anionic Polymerization of Styrene. J. Scmid and M. Szwarc, State University of New York, Syracuse, New York.

Anthracene—"Living" Polystyrene Complexes. "Dormant" Polymers. M. Levy and M. Szwarc, State University of New York, Syracuse, New York.

Equilibria between Low Molecular Weight Living Polymers and Monomer. A. Vrancken and M. Szwarc. State University of New York, Syracuse, New York.

Invited Lecture

Kinetic Studies and Reaction Mechanisms in Homogeneous Anionic Polymerization. S. Bywater, National Research Council, Ottawa, Ontario.

Copolymères Séquencés Obtenus par Polymérisation Anionique. G. Champetier, M. Fontanille, A. C. Korn and P. Sigwalt, Faculté des Sciences de Paris, Laboratoire de Chimie Macromoléculaire, Paris V, France.

Anionic Polymerization of Acrylonitrile. R. B. Cundall, D. D. Eley and

(Mrs.) J. Worrall, Nottingham University, Nottingham, England.

Polymerization Catalyzed by Lithium and Lithium Alkyl. U. A. Spirin, A. A. Arest-Jakubovich, D. K. Poliakov, A. R. Gantmaher and S. S. Medvedev, Karpov Institute of Physical Chemistry, Moscow, U.S.S.R. (in German).

Anionic Polymerization of Styrene. S. Bywater and D. J. Worsfold, Na-

tional Research Council, Ottawa, Ontario.

Polymerization of Styrene with n-Butyl Lithium and Titanium Tetrachloride. A. Malatesta, J. Megee, R. V. Mihailovich and K. C. Tsou, The Borden Chemical Company, Philadelphia 24, Pennsylvania.

The Effect of Inadequate Mixing on Molecular Weight Distributions in Polymerizations. Morton Litt, Allied Chemical Corporation, Morristown, New

Jersey.

Temperature Effect on Polymer Structure in Diene Polymerization by Alkali Metals. K. B. Piotrovsky, All Union Scientific Research Institute of Synthetic Rubber, Leningrad, U.S.S.R.

Role of Polymer-Catalyst in Coordinated Anionic Polymerization of Di-

xliv

Invited Lecture

Elementarprozesse der Polyreaktionen. F. Patat, Institut für Chemische

Technologie, München, Germany.

Polymerization of Some Epoxy Compounds. A. W. Topchiev, B. A. Krentsel and L. A. Bakalo, Petrochemical Institute of the Academy of Sciences of U.S.S.R., Moscow, U.S.S.R.

Polymerization and Isomerization of Alpha-Olefins on Molybdenum Oxide-Lithium Butyl Catalysts. W. H. McCarty and G. Parravano, University of

Michigan, Ann Arbor, Michigan.

Effect of Silanes on the Polymerization of Propylene by Ziegler Catalysts. Isao Shiihara, Wasaburo Kawai and Taiichi Higuchi, Osaka Industrial Research

Institute, Osaka, Japan.

Polymerization of Ethylene with a "Pre-activated" Aluminum/Titanium (IV) Chloride Catalyst and a Statistical Study of the Polymerization Variables. H. W. Coover, Jr., F. B. Joyner, and N. H. Shearer, Jr., Tennessee Eastman Company, Kingsport, Tennessee.

On the Kinetics of Propylene Polymerization. E. Kohn, H. Schuurmans, J. V. Cavender and R. Mendelsson, Monsanto Chemical Company, Texas City,

Texas.

Invited Lecture

Progress of Stereospecific Polymerization and Asymmetric Synthesis of Macromolecules. G. Natta, Politecnico di Milano, Milano, Italy.

Kinetics of Ethylene-Propylene Copolymerization. H. M. Spurlin, C. A. Lukach and D. L. Christman, Hercules Powder Company, Wilmington, Delaware.

On the Kinetics of Formaldehyde Polymerization and Polyformaldehyde Degradation. N. S. Enikolopov, Institute of Chemical Physics of the U.S.S.R. Academy of Sciences, Moscow, U.S.S.R.

Invited Lecture

High Polymerization of Heterocyclic or Unsaturated Compounds. Junji Furukawa and Takeo Saegusa, Kyoto University, Kyoto, Japan.

Complex Metaphosphate Polymers. R. C. Mehrotra and V. S. Gupta,

University of Gorakhpur, Gorakhpur, India.

Preparation and Decomposition of the Silver and Copper Salts of Certain Phenols. *Harry S. Blanchard*, Herman L. Finkbeiner and Glenn A. Russell, General Electric Research Laboratory, Schenectady, New York.

Polymerization by Oxidative Coupling. II. Oxidation of 2,6-Di-substituted Phenols. Allan S. Hay, General Electric Research Laboratory, Schenectady,

New York.

Polymerization by Oxidative Coupling. III. Mechanistic Type in the Copper-Amine Catalyzed Polymerization of 2,6-Xylenol. G. F. Endres and J. Kwiatek, General Electric Research Laboratory, Schenectady, New York.

The Synthesis of Linear Polyphenylene Sulfide. Robert W. Lenz, Carl E. Handlovits and Harry Smith, The Dow Chemical Company, Midland, Michigan.

Invited Lecture

Les Polymères Organisés. Ch. Sadron, Centre de Recherches sur les Macromolécules, Strasbourg, France.

Fundamentals of Cationic Polymerizations. J. P. Kennedy and R. M. Thomas, Esso Research & Engineering Company, Linden, New Jersey.

Chain-Propagation Constants in the Cationic Polymerization of Styrene. D. C. Pepper and P. J. Reilly, University of Dublin, Dublin, Ireland.

Transfer Processes in the Cationic Polymerization of Isobutene. J. Penfold and P. H. Plesch, University College of North Staffordshire, Keele, England.

Invited Lecture

K. Vesely, Vyzkummy Nstav Makromolekularni Chemie, Brno, Czechoslovakia.

About the Phosphoric Acid Catalyzed Polymerization of Epsilonaminocaproiclactam. Frederic Geleji and Alfred Szafner, Plastics Research Institute, Budapest, Hungary.

Condensation Polymers from 3,9-Bis(7-Carbomethoxyheptyl)-2,4,8,10-Tetraoxaspiro (5.5) Undecane. II. Poly(amide-acetals). E. H. Pryde, D. J. Moore, H. M. Teeter and J. C. Cowan, Northern Regional Research Laboratory, Peoria 5, Illinois.

Polycondensation of Glycerol with Phthalic Anhydride in Presence of Inorganic Boric Compounds. Mario Baccaredda and Gianfranco Nencetti, Università di Pisa, Pisa, Italy.

Structure Property Relationships in Linear Bisphenolpolyesters. André J. Conix, Gevaert Photo-Production N. V., Mortsel, Belgium.

Poly(perfluoroalky) oxetanes—A New Class of Stable Polymers. L. C. Case and C. C. Todd, Purdue University, Lafayette, Indiana.

GROUP 4-5

PREDOMINANTLY CHEMICAL REACTIONS OF POLYMERS

Stabilität von Polyvinylchlorid in der Gegenwart von Nitriersäure. Zoltan Wolkober, Ungarisches Kunststoff-Forschungs Institut, Budapest, Hungary.

The Kinetics of the Oxidation of Cotton with Hypochlorite in the pH Range 5-10. Joseph A. Epstein and Menachem Lewin, Institute for Fibres and Forest Products Research, Jerusalem, Israel.

Functional Groups and Degradation of Cotton Oxidized by Hypochlorite. Joseph A. Epstein and Menachem Lewin, Institute for Fibres and Forest Products Research, Jerusalem, Israel.

Thermal Decomposition of Natural Cellulose in Vacuo. Edward J. Murphy, The Rockefeller Institute, New York, New York.

Observations on the Thermolytic Decomposition of Poly(t-butyl acrylate). Ilya M. Sarasohn, E. I. du Pont de Nemours & Co., Inc., Wilmington, Delaware.

On the Evaporation of Low Molecular Weight Components and an Aspect of Initial Degradation of Polyethylene in Vacuum. Kisaku Nakagawa, Electrical Communication Laboratory, Tokyo, Japan.

Invited Lecture

Photo and High Temperature Degradation of Polymers. H. H. G. Jellinek, Assumption University, Windsor, Ontario.

Investigation of the Mechanism of Radiolysis of Polymers Containing Quaternary Atoms of Carbon. A. N. Pravednikov, E. N. Teleshov, In Shen Kan and S. S. Medvedev. Karpov Physical Chemical Institute, Moscow, U.S.S.R.

Mechanism of the Thermal Degradation of Polymers. E. C. Penski, R. J. McHenry and I. J. Goldfarb, Wright-Patterson AFB, Ohio.

Contribution to the Study of Thermo-oxidative Degradation Mechanism of Some Types of Linear Polyesters. *Ivan Gömöry* and Ján Stímel, Cables & Insulating Materials Research Institute, Bratislava, Czechoslovakia.

Macromolecular Stable Free Nitrogen Radicals. D. Braun, I. Loflund and

H. Fischer, Deutsches Kunststoff-institut, Darmstadt, Germany.

Synthesis and Properties of Poly-Schiff-bases and Their Chelates. J. Charette, C. Decoene and P. Teyssié. (Lovanium University, Léopoldville, Congo) 88 rue des Champs Elysees, Brussels, Belgium.

Invited Lecture

End Group Analysis of Polymers by Interaction with Dyes. Santi R. Palit,

Indian Association for the Cultivation of Science, Calcutta, India.

Light Scattering Studies of Cross-linking Unsaturated Polyesters with Methylacrylate. Lawrence Gallagher and Frederick A. Bettelheim, Adelphi College, Garden City, New York.

Measurements on the Degree of Cross-linking of High-Conversion Post-Gelation Methyl Methacrylate-Methylene Dimethacrylate Copolymers. Jessee C.

H. Hwa, Rohm & Haas Company, Philadelphia 37, Pennsylvania.

The Rupture of Chemical Bonds in Polymers by Swelling Forces. R. J. Ceresa, National College of Rubber Technology, London, England.

An Experimental Verification of Gel Network Formation Theories. Kenneth

W. Scott, Goodyear Tire & Rubber Company, Akron, Ohio.

Use of Dimaleimides as Accelerators for the Radiation Induced Vulcanization of Hydrocarbon Polymers. Part I. Natural Rubber. S. M. Miller, R. Roberts and R. L. Vale, United Kingdom Atomic Energy Authority, Wantage, Berks, England.

Infrared Study of the Reaction of Polyisoprene and Polybutadiene with Sulfur Using Deuterated Polymers. J. J. Shipman and M. Golub (Stanford Research Institute, Menlo Park, California), B. F. Goodrich Research Center, Brecksville, Ohio.

Wechselwirkung von Polyäthylen mit Schwefel. B. A. Dogadkin and A. A.

Donzow, Lomonossow Institut, Moscow, U.S.S.R.

Quantitative Determination of Carboxyl (End) Groups in Vinyl Polymers by the Dye Interaction Method. Santi R. Palit and Premamoy Ghosh, Indian Association for the Cultivation of Science, Calcutta, India.

Formation of Hydroxyl (End) Groups in Polymers and Their Detection by the Dye Test. Santi R. Palit and Asish R. Mukherjee, Indian Association for

the Cultivation of Science, Calcutta, India.

Incorporation of Halogen (End) Groups in Polymers and Their Detection by the Dye Test. Santi R. Palit and Mihir K. Saha, Indian Association for the Cultivation of Science, Calcutta, India.

Etude Expérimentale des Dismutations Rapides que Subissent la Cellulose, la Lignine et le Bois dans l'eau sous Pression audessus de 280°C. (Le Problème de la Lignine). Alfred C. Gillet and Paul Colson, Université de Liège, Belgium.

Hydrodynamic Studies on Carboxymethyl Cellulose in Aqueous Solutions. G. Sitaramaiah and D. A. I. Goring, Pulp and Paper Research Institute of Canada, Montreal, P. Q.

The Polyelectrolytic Nature of Cellulose Gels in Alkali Solutions. A. J. Pennings and W. Prins, Cellulose Research Institute, Syracuse, New York.

New Polyelectrolytes: Synthesis and Preliminary Characterization. Paul E. Blatz, Socony Mobil Oil Company, Inc., Dallas, Texas.

Invited Lecture

The Biological Chemical Synthesis of Polysaccharides. J. K. N. Jones, Queen's University, Kingston, Ontario.

Studies on Some Protein Molecular Constructive Mechanisms. Seichu Goto,

Chemical Laboratory of Goto's Memorial Foundation, Osaka, Japan.

The Molecular Weight of Silk Fibroin in Solution. C. Wippler and A. J. Hyde, Royal College of Science and Technology, Glasgow, Scotland.

Deuterium-Hydrogen Exchange Between Water and Silk Fibroin. John L. Morrison, University of Toronto, Toronto, Ontario.

Invited Lecture

Concepts of Polymer Chemistry Applied to Antibody-Antigen Interactions. Alec H. Sehon, McGill University, P. Q.

Invited Lecture

Reactive Polymers and Their Use for the Preparation of Antibody and Enzyme-Resins. *Georg Manecke*, Fritz-Haber-Institut der Max-Planck-Gesellschaft, Berlin-Dahlem, Germany.

Invited Lecture

Biologically Active Polymers. C. G. Overberger, J. J. Ferraro, P. V. Bonsignore, N. Vorcheimer, F. W. Orttung and B. Kösters, Polytechnic Institute of Brooklyn, Brooklyn, New York.

Polar Effects in the Radiation Chemistry of p-Substituted Polystyrenes. William Burlant, Ford Motor Company, Dearborn, Michigan, and Vinicio

Serment, University of Michigan, Ann Arbor, Michigan.

The Effects of High-Speed Electrons on the Structure of Polyethylene Terephthalate. N. A. Slovokhatova, G. K. Sadovskaya and V. A. Kargin, The Karpov Institute of Physical Chemistry, Moscow, U.S.S.R.

High Molecular Weight Poly(vinylene carbonate) and Derivatives. J. R. Schaefgen and N. D. Field, E. I. du Pont de Nemours & Co., Inc., Wilmington,

Delaware.

The Structure of Sepiomelanin. M. Piattelli and R. A. Nicolaus, University

of Naples, Naples, Italy.

Interaction of Polysaccharides in the Calcium Oxalate Precipitation System. Igo Light and Hans H. Zinsser, Columbia University, New York 32, New York.

Cross-linkage Mechanisms in Tissue Aging. Johann Bjorksten, Bjorksten Research Institute, Madison, Wisconsin, Fred Andrew and Hans H. Zinsser, Columbia University, New York 32, New York.

ADDENDUM

The Determination of the Mechanical Properties of High Polymers at High Speeds of Testing. Kurt Richard, Farbwerke Hoechst AG. Frankfurt (Main)-Hoechst, Germany.

Stereoregularity and Optical Anisotropy of Macromolecules. V. Tsvetcov, Institute of High Molecular Compounds of the Academy of Sciences, Leningrad,

U.S.S.R.

The Investigation of the Cotton Cellulose Polydispersity According to the Molecular Weight. H. U. Usmanow and T. I. Sushkewitch, Academy of Sciences, Tashkent, Uzbekistan, U.S.S.R.

A New Absolute Method for the Molecular Weight Determination of Polymers from Solution Viscosities. S. Gundiah and S. L. Kapur, National Chemical Laboratory, Poona 8, India.

A Study of the Mechanism of Interfacial Polyamidation and Polyesterification. Ernest M. Hodnett and Donald A. Holmer, Oklahoma State University,

Stillwater, Oklahoma.

Chemical Graft Polymerization. Quantitative Analysis of the Cellulose Acetate-Vinyl Monomer System. Murray Goodman and Carl Horowitz, Polytechnic Institute of Brooklyn, Brooklyn, New York.

THE 1961 GORDON RESEARCH CONFERENCE ON ELASTOMERS

Colby Junior College, New London, New Hampshire

July 17-21, 1961

PROGRAM

Monday, July 17

- F. Bueche (University of Akron, Akron, Ohio)-"Tensile Properties of Elastomers"
- P. J. Blatz (California Institute of Technology, Pasadena, California)-"Application of Finite Elastic Theory to the Deformation and Fracture of Rubbery Materials"
- Gerhard Bier (Farbwerke Hoechst, Frankfurt (M), Germany)—"Crystalline and Amorphous Copolymers of Olefins"

Tuesday, July 18

R. T. Woodhams and S. Adamek (Dunlop Research Centre, Toronto, Canada)-

"Unsaturated Ethylene/Propylene Terpolymers"

C. A. Dahlquist, P. W. Trott and R. B. Althouse (Minnesota Mining and Manufacturing Co., St. Paul, Minnesota)-"Viscoelastic Properties of Polyolefin Elastomers"

H. J. Cantow (Chemische Werke Huels, Marl, Germany)-"On the Molecular Structure of Polybutadienes"

Wednesday, July 19

- E. M. Bevilacqua (U. S. Rubber Company, Wayne, New Jersey)—"Chemistry of Elastomer Oxidation"
- A. N. Gent (Natural Rubber Producers' Research Association, Welwyn Garden City, Herts, England)-"The Mechanics of Ozone Cracking of Rubbers"
- W. P. Slichter (Bell Telephone Laboratories, Murray Hill, New Jersey)-"The Study of Elastomers by Nuclear Magnetic Resonance"

Thursday, July 20

David Craig and J. J. Shipman (B. F. Goodrich Company, Akron, Ohio) - "The Conformation of Alkyl and Halogen Substituted 1,3-Butadienes"

C. E. Snyder and J. A. Lovell (Goodyear Tire and Rubber Company, Akron, Ohio) - "Tetrahydrofuran Polymerization: Mechanism and Elastomeric Properties"

E. K. Gladding (E. I. du Pont de Nemours & Company, Wilmington, Delaware) —"A New Hydrocarbon Elastomer"

Friday, July 21

- L. A. Walker (Monsanto Chemical Company, Nitro, West Virginia)—"The Role of N,4-Dinitroso-N-Methylaniline in the Promotion of Rubber-Carbon Black Interaction"
- P. E. Wei, G. G. Wanless and John Rehner, Jr. (Esso Research and Engineering Company, Linden, New Jersey)—"Reaction of Isoparaffins with Sulfur and Di-t-Butyl Peroxide"

GORDON RESEARCH CONFERENCES

The Gordon Research Conferences for 1961 will be held from 12 June to 1 September at Colby Junior College, New London, New Hampshire; New Hampton School, New Hampton, New Hampshire; Kimball Union Academy, Meriden, New Hampshire; and Tilton School, Tilton, New Hampshire.

Purpose.—The Conferences were established to stimulate research in universities, research foundations, and industrial laboratories. This purpose is achieved by an informal type of meeting consisting of scheduled speakers and discussion groups. Sufficient time is available to stimulate informal discussion among the members of each Conference. Meetings are held in the morning and in the evening, Monday through Friday, with the exception of Friday evening. The afternoons are available for recreation, reading, or participation in discussion groups, as the individual desires. This type of meeting is a valuable means of disseminating information and ideas to an extent that could not be achieved through the usual channels of publication and presentation at scientific meetings. In addition, scientists in related fields become acquainted, and valuable associations are formed that often result in collaboration and cooperative efforts between different laboratories.

It is hoped that each conference will extend the frontiers of science by fostering a free and informal exchange of ideas among persons actively interested in the subject under discussion. The purpose of the program is to bring experts up to date on the latest developments, to analyze the significance of these developments and to provoke suggestions concerning the underlying theories and profitable methods of approach for making progress. The review of known information on a subject is not desired.

In order to protect individual rights and to promote discussion, it is an established requirement of each Conference that no information presented is to be used without specific authorization of the individual making the contribution, whether in formal presentation or in discussion. Scientific publications are not

prepared as emanating from the Conferences.

Registration and reservations.—Attendance at the Conferences is by application. Individuals interested in attending the Conferences are requested to send their applications to the Director at least two months prior to the date of the Conference. All applications must be submitted in duplicate on the standard application form, which may be obtained by writing to the office of the Director. This procedure is important because certain specific information is required in order that a fair and equitable decision on the application may be made. Attendance at each Conference is limited to approximately 100 conferees.

The Director will submit the applications of those requesting permission to attend a Conference to the Committee for that Conference. This Committee will

review the applications and select the members in an effort to distribute the attendance as widely as possible among the various institutions and laboratories represented by the applications. A registration card will be mailed to those selected. Advance registration by mail for each Conference is required and is completed on receipt of the card and a deposit of \$15. (Checks are to be made payable to the Gordon Research Conferences.) The deposit of \$15 will be credited against the fixed fee for the Conference if the individual attends the Conference for which he has applied. A registration card not accompanied by

the \$15 deposit will not be accepted.

The Board of Trustees of the Conferences has established a fixed fee of \$100 for resident conferees at each Conference. This fee was established to encourage attendance for the entire Conference and to increase the Special Fund that is available to each Conference Chairman for the purpose of assisting conferees who attend a Conference at total or partial personal expense with their travel or subsistence expenses, or with both. It is to the advantage of all participants to attend a Conference for the entire week. This fixed fee will be charged regardless of the time a conferee attends the Conference—that is, for the periods of from 1 to 4½ days. It is divided as follows: registration fee, \$40 (\$15 for administration and \$25 for the special fund); room and meals, \$60 (including gratuities) for 5 days. An additional charge of \$1 per night per person will be made for a room with private bath or for a single room, of which there are only a limited number. These rooms will be assigned in the order that applications are received. An additional charge will also be made for rooms occupied more than five nights.

The fixed fee will cover registration, room (except room with private bath or single room), meals and gratuities for resident conferees. It will not provide for golf, telephone, taxi, laundry, Conference photograph, or any other per-

sonal expenses.

Conferees are expected to live at the Conference location because one of the objectives of the Conferences is to provide a place where scientists can get together informally for discussion of scientific research of mutual interest. When special circumstances warrant a request to live elsewhere permission must be obtained from the Director. If the request is approved these non-resident conferees will be charged a registration fee of \$50, instead of the resident fee of \$40.

Conferees living at the Conference location who will pay all or part of the fixed fee as a personal expense may request a reduction of \$25 (the amount allotted for the special fund). Application for this special fee (\$75) must be

made when the registration card is returned to the Director.

Accommodations are available for wives who wish to accompany their husbands. All such requests should be made at the time the attendance application is submitted because these accommodations, limited number, will be assigned in the order that specific requests are received. Children under 12 years of age cannot be accommodated. Dogs and other animals will not be permitted in the dormitories.

Special fund.—A special fund is provided by the Board of Trustees from the registration fee and is made available to the Chairman of each Conference for the purpose of assisting scientists who could not otherwise attend or participate because of financial limitations. This fund is provided to increase the participation of research workers. Its use is not limited to scientists who have been invited by the Chairman as a speaker or discussion leader. The money is to be

used as an assistance fund only and may be used to contribute toward traveling expenses or subsistence expenses at the Conference, or both. Total travel and subsistence expenses usually will not be provided.

Cancellation.—The deposit of \$15 will be forfeited if an approved applica-

tion for attendance at a Conference is cancelled.

Program.—The complete program for the 1961 Gordon Research Conferences is published in "Science", 24 March 1961. Reprints are available on request.

Attendance.—Requests for attendance at the Conferences, or for additional information, should be addressed to W. George Parks, Director, Gordon Research Conferences, University of Rhode Island, Kingston, R. I. From 12 June to 1 September 1961 mail for the office of the Director should be addressed to Colby Junior College, New London, New Hampshire.

THE PICO LABORATORY ABRASION TEST

EDWIN B. NEWTON, HERSHEL W. GRINTER AND D. SCOTT SEARS *

B. F. GOODRICH RESEARCH CENTER, BRECKSVILLE, OHIO

In testing the relative wear resistance of tire tread stocks, most of the standard abrasion machines will correctly evaluate different carbon blacks in the same polymer. But they are less successful in the evaluation of blacks in

different polymers. The Pico** method described here does both.

It had its origin in the simple scratch test shown in Figure 1. Judging by the amount of material scratched loose (viewed at about 20 × magnification), it was often possible in a very qualitative way to line up blind samples in the order of their known abrasion resistance. This experience led to the idea that knives might be used as the abrading agent replacing the more commonly used grinding wheels and sandpaper. The microscope also revealed that the material abraded from different stocks did not look the same. That from natural rubber-channel black (NR-EPC) stocks looked like loose dry crumbs; that from cold rubber-super abrasion furnace black (cold SBR-SAF) stocks looked like masticated rubber and was soft enough to be smeared with the knife on to to the surface of the testpiece,—an observation suggesting some means were required, such as dusting the test area during actual abrasion, to prevent this soft loosened material from lubricating the knife edges. Combination of these two ideas with provision for moving the testpiece under dead-weighted knives led to the present machine design.

The apparatus, shown in Figure 2 is an ordinary drill press modified so that the spindle is free to move only in a vertical direction (and available from the Ferry Machine Company, Kent, Ohio). A holder into which the knives are fitted is gripped by the chuck at the lower end of the spindle. The box at the top of the spindle holds the weights. The rubber testpiece, shaped like a flat-topped hat, is held fixed on a turntable driven through reducing gears by a thyratron-controlled motor. This arrangement permits a wide variation in the speed of rotation of the turntable but holds the rotation constant at any selected setting of the control. Turntable revolutions are

followed by mechanical counters.

The dusting powder (such as Tripoli AFR) is conducted down from a shaker (based on an ordinary electric sander) through the two tubes which deliver dust on either side of the knife holder. The mechanics of the dusting procedure is facilitated by holding the knives in a fixed position and rotating

the testpiece rather than reversing this relation.

The abrading knives are of cemented tungsten carbide (such as GE grade 831) and custom ground so that opposite faces are parallel. The sharpened edge is ground to a 60° included angle. Two knives are used and they are mounted parallel on either side of and equidistant from the center of rotation

^{*} Present address: Virginia-Carolina Chemical Corporation, Richmond, Va.
** The laboratory name adopted during development of the method. According to Webster's dictionary it is a word with either of two meanings: (1) a mountain peak; (2) a gambling game.

of the testpiece. This arrangement (Figure 3) allows the leading knife edge (knives are currently \$" long) to attack the test piece at all angles from 0° (tangential) to 71° and the trailing edge to attack from 109° to 180°. The problem of choice of slip angle is thereby eliminated. The geometry is shown in Figure 4.

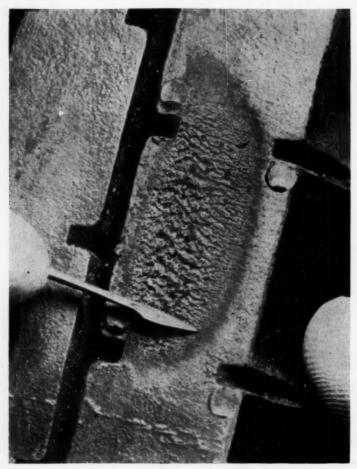


Fig. 1.—Abrasion pattern developed by simple scratch test.

Calibration of the machine at ambient temperature consists essentially of adjusting the severity of the test so that, on a volume loss basis determined gravimetrically, five standard control stocks covering a wide range of abrasion resistance line up (within $\pm 10\%$) with their known performance in road tests. These standard stocks are combinations of three different polymers and three

different carbon blacks. The relative road wear indexes of these five control stocks (shown in Table I), taking the volume loss of the NR-EPC stock as 100, are those found on passenger car tire treads run 60 mph on Texas roads. Such a test, of course, represents only one approximate degree of severity. The abrasion indexes shown were adopted in the first place as a result of a number of discussions with knowledged people working in this field.

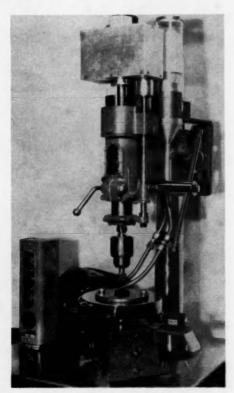


Fig. 2.-Current form of Pico Abrader.

The actual procedure followed to bring the machine into calibration starts with the controlled dulling of a new set of knife blades. The sharpness of the blades is an important factor in determining the severity of the test. The width of the edge is therefore controlled within limits. In this hand operation, the blades are honed with diamond dust to a width of 15 to 18 microns. Progress of this operation is followed with a microscope fitted with a direct illuminator. When this width of edge has been reached, the blades are fastened planeparallel in the holder which is then put in the chuck at the end of the spindle. Each of the five control stocks is then run through a standard procedure: the surface of the test sample is prepared by buffing it flat (that is, parallel to the

bottom surface) with a high speed carborundum wheel made of 30 mesh grit; dead weight on the knives is adjusted to 4.5 kg; the motor control is set to rotate the turntable at 60 rpm; the dust feeding mechanism is started; the turntable motor is started and at the same time the knives are lowered onto the

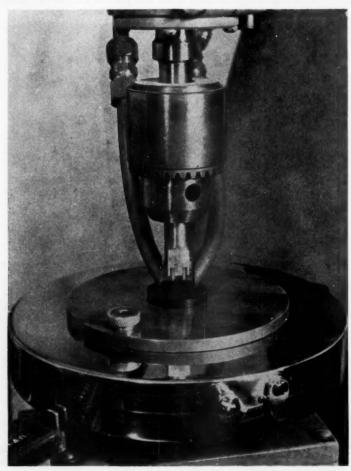


Fig. 3.—Close-up view showing relative positions of knives, test piece and dust tubes

sample to abrade it for 20 revolutions. The turntable is stopped, dust and abraded rubber particles removed by vacuum. The procedure is then repeated but with the turntable revolving in the opposite direction. This forward and reverse procedure is repeated once again for a total of 80 revolutions of the sample. (Each Pico abrasion loss in this paper is based on a total of 80 revolutions of the test piece.) Weight loss of the sample, which is of the order

of 30 mg for the NR-EPC stock, is converted to volume loss by dividing by the sp.g. of the compound. The Pico index is then determined by:

$$\frac{\text{Volume loss of NR-EPC Stock}}{\text{Volume loss of test Stock}} \times 100 = \text{Pico index}$$
 (1)

When all five control stocks fall within their tolerance limits shown in Table I, the machine is regarded as calibrated and ready for the testing of unknown stocks. The calibration procedure is repeated each time after 30 or 40 samples have been tested because the knife edges get duller with use. The redetermined volume loss of the NR-EPC stock is then inserted in Equation (1) for subsequent calculations of Pico index. Eventually (say, after 150 to 200 tests)

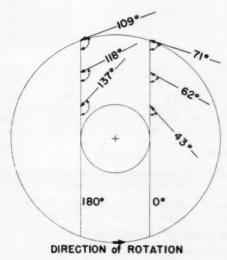


Fig. 4.—Angle of approach of rubber to knife blades during test.

the knives get too dull for acceptable calibration. At this point the indexes all fall on the low side of the tolerances. New knives are than installed and the dull ones sent out for resharpening. Test pieces always develop abrasion patterns²—coarse in the case of stocks showing high abrasion loss, fine in the case of stocks showing low abrasion loss.

The effectiveness of the dusting procedure in minimizing or eliminating skidding of the knives over the sample under test is shown in Table II. Without any other recipe change, 10 parts of paraffin wax were added to each of the five control stocks. This produced in every case, as would be expected, a loss of resistance to abrasion and this is shown by the drop in Pico indexes below those of the untreated controls.

Comparative results of running the five control stocks on several different laboratory abrasion machines^{3, 4, 5} are shown in Table III. The indexes, except those of the Pico machine, do not correlate very well with road test results. But, as shown in Table IV, if the comparison is confined to differentiation of

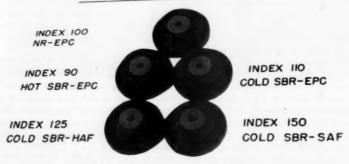
TABLE I RECIPES FOR PICO STANDARD CONTROL COMPOUNDS

		Cor	mpound design	ation	
	Hot SBR-EPC	NR-EPC	Cold SBR-EPC	Cold SBR-HAF	Cold SBR-SAF
Hot SBR 1000* NR 50-50 blend	100.0	_	_	_	
RSS No. 1 and		100.0			
No. 1 pale crepe	_	100.0			_
Cold SBR 1500**			100.0	100.0	100.0
EPC Black	40.0	50.0	50.0	_	-
HAF Black	-	_	_	50.0	
SAF Black	-		_		50.0
Zinc oxide	5.0	5.0	5.0	5.0	5.0
Stearic acid	-	3.0	1.5	1.5	1.5
Process oil***		-	5.0	5.0	5.0
Phenyl β naphthyl					
amine	annearism.	1.0	-	-	
Benzo-thiazyldisulfide	*********	1.0			-
N-cyclohexyl-2- benzo-thiazyl-					
sulfenamide	1.2		1.2	0.9	0.9
Sulfur	2.0	3.0	2.0	2.0	2.0
Specific gravity	1.13	1.13	1.15	1.15	1.15
Cure for Pico test					
Pieces (determined by stress strain data but					
averages would be)	60 min at 302° F	60 min at 280° F	75 min at 302° F	75 min at 302° F	90 min at 302° F
Road wear and nominal Pico index	90	100	110	125	150
Pico index tolerance	81-99	100	99-121	112-138	135-165

* National Bureau of Standards (N.B.S.) sample No. 387.

** N.B.S. sample No. 386. *** Circosol 2×H or equivalent.

CALIBRATION STANDARDS



INDEX TOLERANCE ± 10%

carbon blacks in a single polymer, only the NBS machine2 in this series pro-

duced misleading results.

Correlation of Pico indexes with road wear results is shown in Figure 5. These have been collected over a period of time, most of the data being 6 or 7 years old, by the following procedure. First, the machine was brought into calibration as described before. Pieces of the tread ribs from the tires which

Table II

Effect of 10 Parts Paraffin on Pico Indexes of Standard Stocks

	Without paraffin	With paraffin
NR-EPC	100	64
HOT SBR-SPC	93	71
Cold SBR-EPC	112	72
Cold SBR-HAF	125	92
Cold SBR-SAF	148	107

had been run 60 mph on Texas roads were cut both from the control section and from the test section. The pieces were then cemented on to rubber bases to fit the sample holder. The surface of each such assembly was buffed flat as in the usual sample preparation and then tested. The Pico indexes shown in Figure 5 were therefore determined on the treads of the tires which had actually been road tested. This long series of test tires included four different

Table III

Evaluation of Standard Compounds on Various
Abrasion Machines

	Road wear rating	Pico	N.B.S.	Angle	Lambourn
NR-EPC	100	100	100	100	100
HOT SBR-EPC	90	$90 \pm 10\%$	105	136	155
Cold SBR-EPC	110	$110 \pm 10\%$	87	133	330
Cold SBR-HAF	125	$125 \pm 10\%$	1500	159	425
Cold SBR-SAF	150	$150 \pm 10\%$	2400	218	510

rubbers and blends, and had a spread of abrasion indexes from about 60 to 140. Out of a total of 55 tires, 62% fell within $\pm 10\%$ of a true correlation.

Four factors control the severity of the Pico test run at ambient temperatures—the type of dusting powder; the sharpness of the knives; the speed of rotation of the test piece; the weight on the knives.

The effectiveness of a dusting powder is related to its mass hardness. Dusting powders such as china clay, mica and graphite reduce severity of test to

Table IV

Evaluation by Different Abraders of Various
Blacks in the Same Polymer

	Pieo	N.B.S.	Angle	Lambourn
Cold SBR-EPC	100	100	100	100
Cold SBR-HAF	114	1725	120	129
Cold SBR-SAF	136	2800	164	165

CORRELATION ROAD WEAR AND PICO DATA

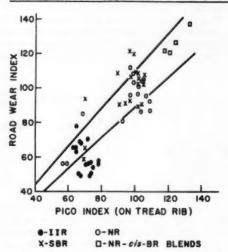


Fig. 5.—Correlation of road wear and Pico abrasion data.

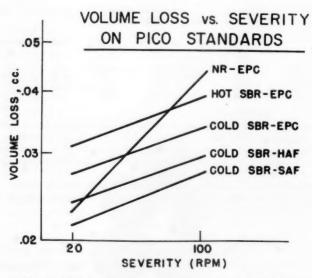


Fig. 6.—Volume loss vs. severity (speed) of test on Pico standard stocks. (Load constant at 4.5 kg.)

the point that calibration of the machine is not possible. Starches, carbon black, and liquids such as water and alcohol almost prevent abrasion under normal conditions. But the two dusts in current use—Tripoli AFR powder which is commercially available; and a high-surface-area fibrous silica from an electric are process—are quite satisfactory. So far, our experience with the dusting powders can be summed up by saying—materials which on Mohs' scale show hardnesses in the region of 6.5 to 7.5 permit calibration of the machine whereas those of 3.5 hardness or less are not satisfactory.

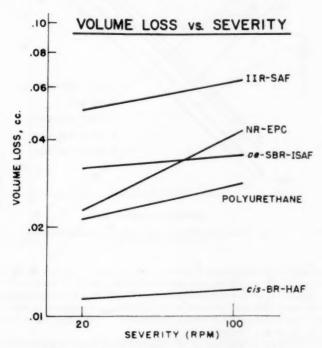


Fig. 7.—Volume loss vs. severity (speed) of test on various stocks, (Load constant at 4.5 kg.)

The second factor, that of knife sharpness, has been discussed before. The two remaining factors, speed of abrasion and weight on the knives, are both subject to close control, individually and in combination.

The effects of volume loss of various types of stocks resulting from a progressive increase in speed of abrasion (rpm of sample) but at constant 4.5 kg load are shown in two Figures, 6 and 7, for clarity. The volume losses of all the stocks increase with increase in severity but the slopes of the lines remain roughly parallel except that of the NR-EPC stock which rises sharply. Advantage can be taken of this differential effect in the case of knives which have become just dull enough so that the assigned indexes of the standard stocks

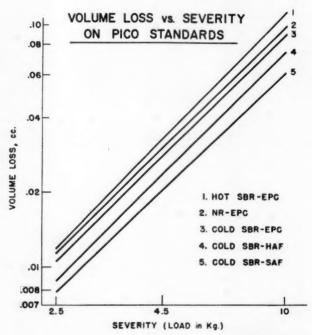


Fig. 8.—Volume loss vs. severity (load) of test on Pico standard stocks. (Speed constant at 60 rpm.)

cannot be brought into line at 60 rpm with 4.5 kg load. By increasing the speed of rotation of the test piece, the standard stocks can be "tuned into" calibration. Results of such a series are shown in Table V. Indexes in line 1 at the standard speed (60 rpm) indicate a dull set of knives; indexes in line 3 (run at 72 rpm) show the machine is back in calibration. Indexes on line 4 (at 74 rpm) show the effect can be carried too far.

The effects on volume loss of the same series of stocks resulting from a progressive increase in weight on the knives but at constant 60 rpm speed are

TABLE V
RECALIBRATION OF DULL KNIVES
Load 4.5 kg

Speed	NR-EPC 100*	Hot SBR-EPC 81-99*	Cold SBR-EPC 99-121*	Cold SBR-HAF 112-138*	Cold SBR-SAF 135-165*
60 rpm	100	85	93	107	111
66	100	92	105	122	138
72	100	92	109	131	146
74	100	103	120	131	144

^{*} Tolerance, Pico index.

shown⁶ in Figures 8 and 9. All of the standard control stocks (Figure 8) show progressive increase in volume loss with increasing weight but the slopes of the lines are essentially the same. This is not the case with the other stocks in the series (Figure 9). The cast polyurethane stock, which is better than the NR-EPC stock at low severity, is poorer at high severity. The reverse is

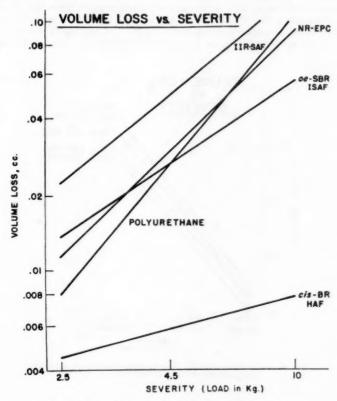


Fig. 9.—Volume loss vs. severity (load) of test on various atocks. (Speed constant at 60 rpm.)

true of the oil extended SBR stock (oe-SBR). The butyl stock (IIR) relative to the NR-EPC stock improves somewhat at high severity and the cis-1,4-polybutadiene stock (cis-BR) is outstanding in this respect.

In the road testing of tires, the very processes which occasion the highest abrasion losses—braking, acceleration and especially cornering—involve not only changes in velocity but an alteration of weight distribution to different parts of the tread in contact with the road surface. The interplay of these two kinds of severity complicates any testing program because, as already shown,

different polymers react with relatively different degrees of resistance to each of these two kinds of severity. It follows, therefore, that a combination of these two conditions should be used and the results of one way of doing this are shown in Figures 10 and 11. In such a progression from low severity (30 rpm and 2.5 kg load) to high severity (112 rpm and 9 kg load) many crossovers are seen. In the case of the standard controls (Figure 10), all the stocks are poorer at low severity and better at the highest severity than the NR-EPC stocks—excepting the cold SBR-SAF stock; and even here a projection of its volume loss line to a lower severity than actually used indicates a possible crossover. Volume losses in Figure 11 show the oe-SBR and the cis-BR stocks

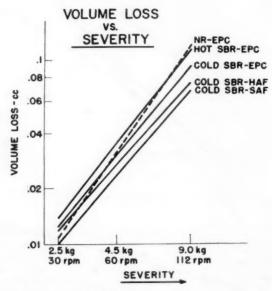


Fig. 10.—Volume loss vs. severity (various combinations of load and speed) of test on Pico standard stocks.

definitely improving, the IIR improving somewhat and the polyurethane getting worse in comparison with the NR-EPC stock at high severity. The data in Figures 10 and 11 are replotted more strikingly as Pico indexes in Figure 12 where the NR-EPC loss at each severity is taken as an index of 100.

The calculated pressures on a static test piece under the knife edges and the speed of travel of the tips of the knives over the rubber during an actual test are much greater than one might at first suppose. Taking into account only the 15 micron width of the knife edge, the pressure on the rubber so contacted under a 4.5 kg load is of the order of 10,000 psi. Again considering a 15 micron width, the tip of the knife at 60 rpm passes over a point on the outer circumference of the abrasion pattern in only 0.3 microsecond. It is reasonable

to suppose that the localized but transient temperatures developed at the knife edges during abrasion testing are much higher than ambient temperature.

If we are, in fact, dealing with such high speed testing, whether this be a high speed tensile or a high speed tearing process, it may be suggestive at this point to introduce Figure 13. This shows that as the state of cure of the NR-EPC

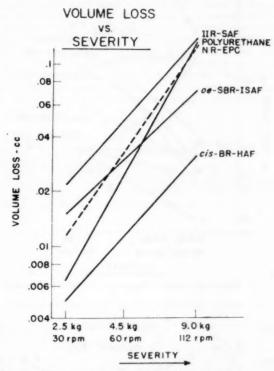


Fig. 11.—Volume loss vs. severity (various combinations of load and speed) of test on various stocks.

stock progresses, the maximum of the high speed tensile curve coincides with the minimum in the abrasion volume loss curve. This result could indeed be entirely fortuitous because that is all the data we have on this relation. The reason for bringing it up at this time is to direct attention to an interesting field wherein the versatility of the Pico abrasion method is used in conjunction with high speed tensile⁷ and high speed tearing⁸ test to further explore mechanisms of abrasion.

SUMMARY

The Pico abrasion tester can be adjusted to simulate wide conditions of severity. It can also be adjusted to approximate the severity of test encoun-

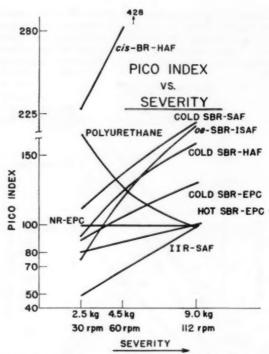


Fig. 12.—Volume losses shown in Figures 10 and 11 plotted as Pico indexes.

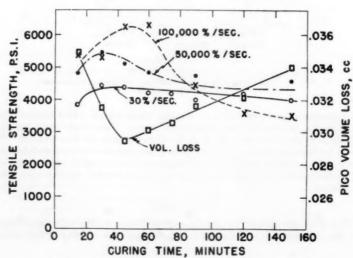


Fig. 13.—High speed tensile strength and Pico abrasion loss vs. time of cure of NR-EPC (Table I) testpiece.

tered in ordinary 60 mph road tests to give laboratory data which agree fairly well with road results. It can evaluate tread stocks made with different polymers quite as well as evaluate different carbon blacks in the same polymer.

ACKNOWLEDGMENTS

The authors express their thanks to Mr. Roy Vance, Columbian Carbon Co., for running our control stocks on the Lambourn abrader and to Mr. Lynn Harbison, Phillips Chemical Co., who ran our control stocks on the angle abrader (data in Table III); to Mr. Frank Snyder for the two high speed tensile curves he ran for us on a ballistic machine of his own design (Figure 13); to many of our colleagues for assistance and for discussions-among them, M/s A. E. Juve, J. H. Macey, M. A. Reinhart, Ross Shearer, W. H. Showen; to Mr. F. Verlaney for the photographs; to Mr. W. H. Willard for the drawings; and especially to Mr. B. J. Miksch who ran the testing machine for us.

REFERENCES

Biard and Svetlik, India Rubber World 127, 363 (1952).
 Schallamach, Rubber Chem. and Technol. 26, 230 (1953).
 Sigler and Holt, India Rubber World 82, 63 (Aug. 1930) [NBS Abrader].
 Vogt, Ind. Eng. Chem. 20, 302 (1928) [Angle Abrader].
 Lambourn, Trans. Inst. Rubber Ind. 4, 210 (1928) [Lambourn Abrader].
 Data plotted according to the method of Geesink and Prat, Rubber Chem. and Technol. 31, 166 (1958).
 van Rossem and Beverdam, Rubber Chem. and Technol. 4, 147 (1931); Villars, Rubber Chem. and Technol. 24, 144 (1951); Fromandi, Ecker and Heidemann, Proceedings International Rubber Conference Washington (1959), page 177.
 Kainradl and Händler, Rubber Chem. and Technol. 33 (Dec. 1960).

ATTRITED CARBON BLACKS AND THEIR BEHAVIOR IN ELASTOMERS. III. EFFECTS IN SBR AND OTHER RUBBERS *

A. M. GESSLER

CHEMICALS RESEARCH DIVISION, ESSO RESEARCH AND ENGINEERING COMPANY,

LINDEN. NEW JERSEY

The modification of carbon blacks by severe attrition through ball or two roll (rubber) milling was described in the first paper¹ of this series. Unexpectedly large increases in the surface area of the blacks were shown to attend the attrition. These increases were attributed partly to the breakage of secondary aggregate structure, and partly to abrasion or fragmentation occurring at the surfaces of individual particles. Oxidation of the blacks, the extent of which was shown to increase linearly with the surface area of the blacks, was envisioned as arising from free radical activity, unpaired electrons being made available from the homolytic cleavage of carbon to carbon bonds in the course of the attrition. The acidity of the blacks, as indicated by pH, was shown to increase with the oxidation. Oil absorption measurements, finally, were used to indicate the dissipation of secondary or aggregate structure in attrited carbons.

A second paper in this series² showed the effects of attrited blacks on the properties of butyl. Improved stress-strain and dynamic properties, it was proposed, resulted from an increased reinforcing capacity associated with both the physical and chemical changes rendered in the blacks by attrition. The intrinsic conflict in butyl cures between abrasion resistance on the one hand and hysteresis on the other was shown to be resolved, good abrasion resistance as well as good dynamic properties being provided with attrited blacks in samples cured for relatively short times. The advantages of attrited blacks were further reported to be maintained over a wide range of black concentrations. As a result, the use of higher loading levels was suggested for these blacks as a means for gaining economic advantages over the corresponding standard blacks. Finally, the sharp response of butyl-attrited black systems to unpromoted heat treatment². 4 was cited as further evidence for increased chemical activity in the attrited blacks.

The present paper considers the effects of attrited blacks in SBR and other elastomers with much higher unsaturation than butyl. With natural, acrylonitrile-butadiene, and chloroprene rubbers, for which illustrative data are presented, the approach is direct, and involves straight forward consideration of the blacks. With SBR, however, the anticipated effects of attrited blacks are not directly achieved. Cure with these blacks is severely retarded. Considerable discussion, therefore, is devoted first to the vulcanization behavior of SBR-attrited black systems, and second and more especially, to the unusual

^{*} Presented at the Division of Rubber Chemistry (ACS) meeting in New York, September, 1960. Reprinted from Rubber Age 88, 958 (1961).

cure activating influence which is obtained when glycerol or other polyols are added in these mixtures.

The good dispersion of carbon black in elastomers is a requisite to obtaining optimum vulcanizate quality. This is especially true with attrited blacks. These blacks, since they are fluffy (not pelleted or otherwise densed) and have low secondary structure and high surface area, require particular care in handling. For the work reported here (and in the previous paper) compounds were prepared on an open mill, the black being added slowly and as uniformly as possible along the length of the mill nip. The batch, in addition, was cut from time to time in the course of the mixing, but never before the disappearance of all free black. As a general rule, an effort was made to keep the amount

TABLE 1
BASE FORMULATIONS

Styrene-butadiene rubber		Natural rubber	
SBR 1500 Phenyl-2-naphthylamine Black Stearic acid Zinc oxide Sulfur 2,2'-Benzothiazolyl disulfide*. MBTS Zinc diethyldithiocarbamate*, ZnDMDC	100.0 0.5 50.0 1.0 5.0 2.0 1.5 0.15	Smoked sheets Phenyl-2-naphthylamine Black Stearie seid Zine oxide Sulfur Mercaptobenzothiazole ^c , MBT	100.0 0.3 50.0 3.0 5.0 3.0 1.0
Compounds cured at 300° F		Compounds cured at 287° F	
Acrylonitrile butadiene rubber		Chloroprene rubber	
Hyear OR 15 Black Stearic acid Zinc oxide Sulfur 2,2'-Bensothiazolyl disulfide® Diphenylguanidine∉ Dibutyl phthalate	100.00 50.0 1.0 5.0 1.5 1.0 0.25 5.0	Neoprene GN Black Magnesia Phenyl-1-naphthylamine Zinc oxide Sulfur Diphenylguanidine	100.0 50.0 4.0 2.0 5.0 1.0
Compounds cured at 287° F		Compounds cured at 287° F	
1	Butyl rubb	er	
Enjay Butyl Black Stearic acid Zinc oxide Sulfur Tetramethylt 2,2'-Benzothi	thiur am di		

a Altax, MBTS. Zimate, ZnDMDC. Captax, MBT. DPG. Tuads, TMTD.

of black falling through the mill into the pan at an absolute minimum, and particularly, to avoid the formation of compacted plates in this by-passed black. Longer mixing times than those normally employed with standard blacks were therefore employed. This fact, though it may constitute cause for practical concern, was not a deterrent in our work, the object of which was, taking first things first, to assay the intrinsic potentialities of attrited blacks, and not the prospects for their immediate adaptability to accepted commercial processes.

Unless otherwise stated, the studies in this paper are restricted to the compound formulations shown in Table 1. The words "attrited" and "ball milled," as in the previous paper, are used interchangeably to refer to blacks which were ball milled in steel assay jars (14 gallon capacity) under standard conditions as already described.

RETARDATION CURE OF SBR WITH ATTRITED BLACKS

General effects.—In the absence of the selected additives which will be discussed in a later section, a surprising and yet primary effect of attrited blacks in SBR is to retard cure. Table 2 shows a typical set of results for SBR vulcanizates with a series of ball milled HAF blacks. Cure retardation effects are seen to increase with the time of carbon black attrition. Modulus and Shore hardness are sharply decreased; extensibility is greatly increased. In addition, undesirable softening of the vulcanizate due to insufficient cure is

Table 2

Effect of Attrited HAF Blacks on Properties of SBR (Compounds Cured 45 Minutes at 300° F)

(COMI OCHES	COMID 10	ATAMIN C A ESTO	A1 000 1	,	
Time of ball milling, hours	0	4	8	12	24
Surface area of black, M ² /g Oxygen content of black, wt. % pH of black Properties of SBR vulcanizate	80.0 0.58 6.9	90.0 0.81 4.5	95.0 1.04 4.3	108.0 1.18 4.1	136.0 1.72 3.5
Modulus (psi) at 100% 300% 500% 700%	415 2325	200 825 2000 3430	190 750 1865 3215	165 545 1410 2505	150 355 855 1850
Tensile strength, psi	3495	3460	3430	3220	1925
% elongation	425	705	740	800	815
Dynamic properties					
$nf \times 10^{-6}$, poises \times CPS $K \times 10^{-7}$, dynes/cm ² % relative damping	4.28 11.3 26.3	$\begin{array}{c} 3.67 \\ 8.19 \\ 30.4 \end{array}$	$3.87 \\ 8.43 \\ 31.0$	$\frac{3.49}{7.66}$ $\frac{30.9}{30.9}$	$\begin{array}{c} 3.01 \\ 6.38 \\ 31.8 \end{array}$
Shore hardness	53	46	43	42	35

apparent in the decay of dynamic properties. Reductions in dynamic modulus, K, are disproportionately larger than the reductions in internal viscosity, η , with the result that relative damping is increased, according to the equation⁵:

% relative damping =
$$200/[1 + (2K/\pi^2\eta f)]$$

where f refers to frequency in cycles/second.

Comparison with butyl.—Cure retardation with attrited blacks in SBR is further demonstrated by comparing similar butyl and SBR systems. This is done in Figure 1, using the same series of blacks as in Table 2. Modulus in the case of SBR is decreased more than 65 per cent with HAF black ball milled just long enough (4 hours) to increase its surface area from 80, its original value, to 90 M²/g. This is a nominal change when the full extent of the surface area changes attending the attrition, and plotted along the abscissa, is considered. Modulus with butyl, by contrast, is decreased less than 15 per cent with the same ball milled black, and the decrease in this case is attributed to reduced aggregate structure in the black rather than to cure rate differences. It is interesting, finally, to note that the curves for butyl and SBR in Figure 1 are very nearly parallel as the surface area of the attrited black is increased from 95 to 136 M²/g. The effects of attrition apparently yield similar changes in the modulus of both rubbers in this range of the attrition spectrum.

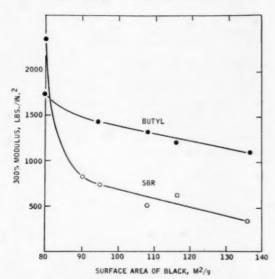


Fig. 1.—The effect of surface area of attrited HAF black on the modulus of butyl and SBR. Compounds cured 45 minutes at 300° F.

Cure retardation with attrited blacks in SBR is a general and consistent phenomenon. Figure 2 shows that effects similar to those just reported for ball milled HAF black are also obtained with ball milled SRF, FEF, and SAF blacks. It is noteworthy that the break in these curves, following the initial and sharp decay of modulus, is not uniquely associated with the surface areà of the black.

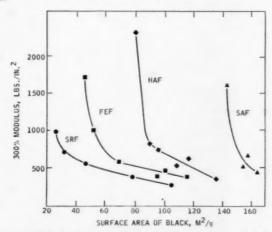


Fig. 2.—The effect of surface area of attrited blacks on modulus of SBR. Compounds cured 45 minutes at 300° F.

Effect of carbon black acidity.—The pH of carbon black decreases very rapidly during the early stages of severe attrition. With high structure furnace blacks such as FEF, HAF, ISAF, or SAF, more than 75 per cent of the total pH change is achieved in the first 4 to 8 hours of ball milling. This pH change, furthermore, can be correlated with the modulus change in the resulting vulcanizate. Figure 3 shows such a relationship using the butyl and SBR systems referred to in Figure 1, and expressing pH reciprocally, as the hydrogen ion concentration in moles/liter. Clearly, the SBR cure system is much more sensitive to carbon black acidity than is that of butyl. This sensitivity, though it is not understood, apparently accounts for the unique behavior of SBR with attrited blacks. Natural, acrylonitrile-butadiene, and chloroprene rubbers, like butyl, exhibit no similar cure retardation effects.

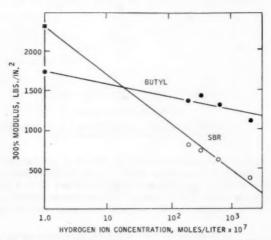


Fig. 3.—The relationship between vulcanizate modulus and hydrogen ion concentration of the black in butyl and SBR. Compounds cured 45 minutes at 300° F.

Up until the time that work was initiated with SBR, reduced modulus in vulcanizates with attrited blacks was associated almost entirely with reduced aggregate or secondary structure in the black. Justification for this association was found in the fact that modulus is known to decrease when secondary structure is reduced without changing the pH or other properties of the black. Since the dissipation of black structure, as it is measured by oil absorption tests, and the regression of pH follow parallel courses during the attrition, it is impossible at this time to separate the influence of each on modulus. Experimental evidence6 indicates, however, that modulus losses resulting from reduced black structure alone are very nearly constant (300-500 psi) regardless of the polymer. Critical cure differences between SBR and butyl therefore seem to be a reflection of differences in the sensitivity to acidity in the black, as is indicated in Figure With this in mind, limitation of the oxidation, and hence the acidity, of severely attrited blacks is suggested as an approach to "tailoring" these blacks for SBR. If oxidation is the result of free radical activity, as we have proposed1, the use of free radical acceptors in the attrition reaction might constitute a means for accomplishing this purpose.

SOME GENERAL GLYCEROL EFFECTS

The cure of SBR with attrited blacks is greatly improved when polyols, like glycerol, are added in the compound. This effect, which will be dealt with in detail in the next several sections of this paper, is preceded here with a short discussion of the literature pertaining to the use of glycerol in rubber and other elastomers.

The use of glycerol in rubber has recently been reviewed. Glycerol and other polyols are employed as auxiliary agents in the development of optimum mechanical properties. Chemisorption at the surface of active fillers and direct chemical reactions involving the vulcanization system are proposed as

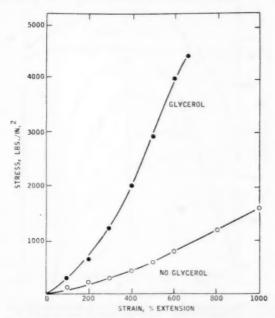


Fig. 4.—Stress-strain of SBR-attrited black vulcanizates with and without glycerol. Compounds cured 15 minutes at 300° F.

mechanisms for this effect. Howland and coworkers⁸ studied aqueous phase diluents in the emulsion polymerization of styrene-butadiene rubber, and found that polymers synthesized in the presence of glycerol exhibited abnormally high stiffening in tread type compounds, and cured considerably more rapidly than standard SBR. They offered no explanation for this result, but reported that similar effects were not obtained when methyl alcohol was used in place of glycerol. The increased vulcanization rate and higher modulus and tensile strength in SBR-hydrated silica systems containing ethylene glycol were also demonstrated¹⁹. Hausch¹⁰-found that the addition of glycols or amines to silica decreased the adsorption of malachite green on the pigment, and proposed that glycols and amines reduced the accelerator adsorption in mixtures of Hevea and silica, and thereby led to improved vulcanizates. Previous work

in these laboratories¹¹ showed that glycerol in conventional butyl-silica systems yielded little improvement in vulcanizate quality. In butyl-silica systems which were heat treated, however, glycerol produced vulcanizates with improved modulus, tensile strength, and dynamic properties. Polyol activation of thermal interaction between the filler and polymer was envisioned. Finally, Tinyakova and coworkers in Russia have proposed that hydrogen sulfide formed by the reduction of sulfur with polyols is an explanation for cure acceleration effects which are obtained with these agents¹². Data from solution studies were offered to support this proposition.

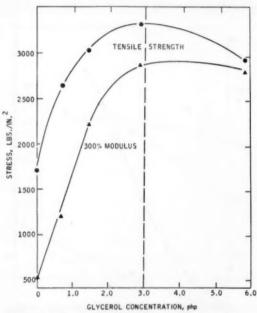


Fig. 5.—Effect of glycerol concentration in SBR with attrited FT black on modulus and tensile strength. Compounds cured 30 minutes at 300° F.

GLYCEROL ACTIVATION OF CURE

The greatly enhanced properties which result in SBR-attrited black vulcanizates when glycerol is present have already been mentioned. Curves in Figure 4 show this effect, and demonstrate the improved stress-strain properties which result from the use of glycerol (3.0 phr) in an SBR compound with ball milled HAF black. The ball milled black used in this work, and in all subsequent work in this paper dealing with HAF black, was characterized by the following analytical data: surface area = $106~\mathrm{M}^2/\mathrm{g}$, weight % oxygen = 1.57, slurry pH = 4.0, oil absorption = $0.61~\mathrm{cc/g}$. Typical properties for a standard HAF black are listed in Table 2. The oil absorption value for the standard black is $1.08~\mathrm{cc/g}$.

The effect of glycerol concentration was studied in SBR compounds containing 40 volumes (72.0 phr) of ball milled FT black (surface area = 128 M²/g,

weight % oxygen = 1.97, slurry pH = 4.35). Since this work involved other considerations, which are outside the scope of this paper, the base formulation in Table 1 was changed to contain increased quantities of sulfur and accelerators: sulfur—2.5, MBTS—1.75, zinc diethyldithiocarbamate—0.2. Modulus and tensile curves in Figure 5 show the results which were obtained. In accordance with these data, glycerol concentration at 3.0 phr was taken as the standard for the work reported in this paper. No attempt was made to investigate the interrelation between the optimum glycerol requirement and the concentration and type of black. It is nevertheless recognized that systematic study of these parameters might be of great value in understanding more clearly the role played by glycerol in SBR-attrited black systems.

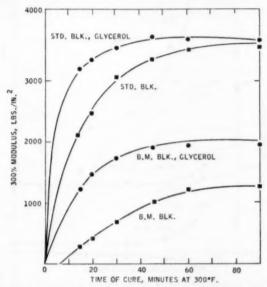


Fig. 6.-Effect of glycerol on cure of SBR with standard and ball milled HAF blacks.

The powerful cure activating effect of glycerol is unique in SBR systems with attrited blacks. Glycerol increases the rate of cure in systems with standard black, but it has little or no effect on the ultimate state of cure. The upper curves in Figure 6 show that modulus increases at early cure times when glycerol is present in this kind of compound. However, the difference virtually disappears when the cure time is extended to 60 minutes or longer, modulus values then tending to be the same, regardless of the presence of glycerol. By contrast, SBR-attrited black compounds containing glycerol (lower curves in Figure 6) display not only increased cure rate, as is indicated by the steeper slope in the early portions of the glycerol curve, but the ultimate modulus, after both curves have leveled, is 58 per cent higher in this case. Both cure rate and cure state effects are attributed to glycerol in these systems.

The equilibrium swelling capacities of the vulcanizates used in the work of Figure 6 were measured in toluene (48 hours at $25 \pm 0.5^{\circ}$ C). The results in

Figure 7 corroborate the conclusions drawn from the modulus data in Figure 6. With standard black, volume swell values, particularly for samples at long cure times, tend to be the same for compounds with and without glycerol. With attrited black, however, the presence of glycerol leads to vulcanizates with higher crosslink density and significantly lower swelling capacity. The reversal in the swell curve shown in Figure 7 for the ball milled black vulcanizate without glycerol is not paralleled by the corresponding modulus curve in Figure 6. No explanation for the divergence can be offered. Reversion, in the sense of

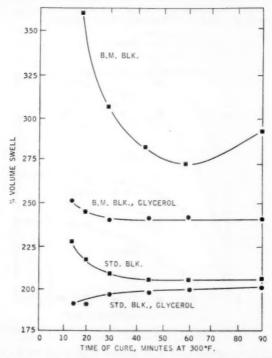


Fig. 7.-Effect of glycerol on cure of SBR with standard and ball milled HAF blacks.

softening, is generally not experienced with styrene-butadiene rubbers, which tend to harden or resinify on extended curing or on heat aging. The slight increases in volume swell occurring when the vulcanizates with standard black and glycerol are cured for longer times is also unexpected. However, since the samples were weighed originally but not finally after drying, the influence of extractable matter may be a factor in these results.

The unique nature of the glycerol cure activation effect in SBR-attrited black systems is further demonstrated when the results in Figure 6 are compared with those obtained from similar experiments with butyl or natural rubber. Figure 8 shows that in butyl compounds containing standard black, the modulus of the glycerol systems is uniformly lower. This suggests a simple

diluent or plasticizer action as the role of glycerol in these vulcanizates. The loss of modulus which glycerol produces in butyl compounds containing ball milled black, however, is larger than would be expected from diluent action alone, and increases with the time of cure. Thus, the glycerol effect in butyl is not only very much smaller than that in SBR but, oddly enough, in the opposite direction. In the presence of glycerol, modulus is depressed in butyl, and enhanced in SBR. This is especially true in systems with attrited blacks.

Detailed tensile and cure data from these experiments with SBR and butyl are presented in Tables 3 and 4, respectively. Careful inspection of the values in the first four columns of each of these tables will convince the reader that SBR and butyl are indeed different in their response to the separate influences of attrited black and glycerol. The remarkable and striking results in Table 3 have been referred to already, but in much less detail. It is noteworthy in

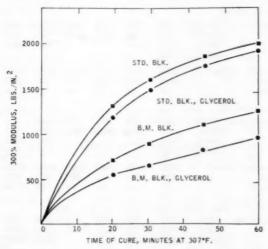


Fig. 8.-Effect of glycerol on cure of butyl with standard and ball milled HAF blacks.

Table 4 that tensile strength and extensibility suffer very little change as a result of glycerol addition when butyl is compounded with standard black. This seems to support the propositon which was suggested by the modulus data, namely, that the glycerol effect is simply a plasticizer or diluent effect. Much greater changes in tensile strength and elongation are observed when glycerol is added in the butyl compound with attrited black. These results, like the modulus data, imply that important changes in either the cure or reinforcement systems, or both, attend the use of glycerol in this case.

The uniqueness of the glycerol cure activation effect in SBR systems containing attrited blacks is associated with both the polymer and the black, as already described. Additional support for this statement is found in the fact that similar results are not obtained with natural or acrylonitrile-butadiene rubbers. Attrited blacks do not lead to cure rate difficulties in these elastomers, and the addition of glycerol produces insignificant changes in the quality of the vulcanizates, regardless of the nature of the black.

In attributing the uniqueness of the glycerol effect in SBR to the polymer and the black, the possibility had to be considered that the activity of glycerol might instead be related to the particular chemical environment of the cure, i.e., to the chemical activity of the accelerator or accelerator combination used to make the cure. SBR vulcanizates containing ball milled black were therefore prepared with the accelerator systems which were used in butyl and na-

TABLE 3

CURE STUDY SHOWING EFFECT OF GLYCEROL IN SBR
WITH STANDARD AND ATTRITTED HAF BLACKS

			Not hea	treated			Heat	treated	
Condition of black		Ball 1	milled	Star	ndard	Ball	milled	Star	ndard
Glycerol, phr Cured 15 min at 300°		_	3.0	_	3.0		3.0		3.0
Modulus lbs/in. ² at	100% $300%$ $500%$ $800%$	135 305 610 1220	325 1235 2910	430 2090	690 3205	200 575 1815	200 625 1960	410 2410	600 3360
Tensile strength, lbs % elongation Shore hardness	/in. ²	1610 1000+ 49	4445 655 61	3650 490 63	$\frac{3670}{360} \\ 68$	3135 735 47	3735 740 48	$ \begin{array}{r} 3735 \\ 460 \\ 62 \end{array} $	$\frac{3800}{355}$
Cured 20 min at 300°	F								
Modulus lbs/in.² at	100% $300%$ $500%$ $700%$	130 430 1005 1790	375 1505 3505	485 2475	670 3355	205 850 2665	215 960 2825	$\frac{470}{2785}$	695 3680
Tensile strength, lbs % elongation Shore hardness	/in.²	2620 925 51	$4415 \\ 585 \\ 62$	3910 460 64	$ \begin{array}{r} 3655 \\ 330 \\ 69 \end{array} $	$\frac{4000}{625}$ $\frac{47}{47}$	4115 670 49	$\frac{3860}{420} \\ 61$	$ \begin{array}{r} 3820 \\ 320 \\ 65 \end{array} $
Cured 30 min at 300°	F								
Modulus lbs/in. ² at	$\frac{100\%}{300\%}$ $\frac{500\%}{}$	215 695 1815	395 1750 4090	660 3065	755 3565	250 1190 3525	$\frac{260}{1290}$ $\frac{3665}{3}$	570 3170	730 3665
Tensile strength, lbs. % elongation Shore hardness	/in.2	3630 755 53	4340 530 63	3790 380 66	3710 320 68	4370 590 50	4545 600 50	$3985 \\ 380 \\ 64$	3665 300 66
Cured 45 min at 300° l	F								
Modulus lbs/in.² at	100% 300% 500%	$260 \\ 1035 \\ 2655$	$390 \\ 1910 \\ 4335$	$\begin{array}{c} 650 \\ 3350 \end{array}$	785 3755	$\begin{array}{c} 275 \\ 1645 \end{array}$	$265 \\ 1695 \\ 4265$	620 3430	750
Tensile strength, lbs, % elongation Shore hardness	/in.2	4450 690 56	4515 530 63	3935 365 68	3755 300 69	4525 510 53	4730 535 55	3765 335 66	3700 290 67
Cured 60 min at 300° l	q.								
Modulus lbs/in.2 at	$100\% \\ 300\% \\ 500\%$	305 1250 3115	390 1950	675 3495	770 3695	$285 \\ 1850 \\ 4810$	$300 \\ 1870 \\ 4400$	660 3600	705
Tensile strength, lbs, % elongation Shore hardness		4675 565 60	$4430 \\ 520 \\ 64$	3775 325 68	3695 300 69	4810 500 54	4400 500 57	3725 320 67	3720 295 68

Table 4

Cure Study Showing Effect of Glycerol in Butyl with
Standard and Attrited HAF Blacks

		Not heat treated				Heat treated			
Condition of black		Ball n	Ball milled Stand		dard	lard Ball milled		Stan	dard
Glycerol, phr Cured 20 min at 307°	F		3.0	_	3.0	-	3.0	_	3.0
Modulus lbs/in. ² at	$100\% \\ 300\% \\ 500\%$	200 740 1900	$175 \\ 580 \\ 1400$	$350 \\ 1350 \\ 2315$	$330 \\ 1220 \\ 2240$	$200 \\ 980 \\ 2510$	$\frac{200}{700}$ 1800	$360 \\ 1370 \\ 2335$	$330 \\ 1270 \\ 2300$
Tensile strength, lbs % elongation Shore hardness	/in.*	$3050 \\ 710 \\ 52$	2850 775 54	2400 540 64	2430 570 63	3400 670 48	$3000 \\ 720 \\ 51$	$2480 \\ 560 \\ 62$	2470 565 62
Cured 30 min at 307°	F								
Modulus lbs/in. 2 at	$100\% \\ 300\% \\ 500\%$	$225 \\ 920 \\ 2250$	$\frac{220}{700}$ $\frac{1670}{}$	450 1625	400 1500	$230 \\ 1250 \\ 2850$	$225 \\ 950 \\ 2200$	440 1650	400 1600
Tensile strength, lbs % elongation Shore hardness	/in. ²	$\frac{3000}{660}$ $\frac{53}{53}$	2870 705 53	$2300 \\ 440 \\ 66$	$2300 \\ 460 \\ 65$	$3235 \\ 580 \\ 50$	2890 660 55	$2375 \\ 450 \\ 65$	2360 455 65
Cured 45 min at 307°	F								
Modulus lbs/in. 2 at	$100\% \\ 300\% \\ 500\%$	$\begin{array}{c} 275 \\ 1150 \\ 2600 \end{array}$	350 880 2035	530 1900	430 1810	275 1475 3050	$260 \\ 1110 \\ 2370$	515 1930	475 1875
Tensile strength, lbs % elongation Shore hardness	/in. ²	3000 575 56	2775 660 55	2275 380 67	2200 370 67	3150 515 53	2700 585 54	2335 370 68	2260 480 67
Cured 60 min at 307°	F								
Modulus lbs/in. ² at	100% $300%$ $500%$	270 1315 2800	$250 \\ 1000 \\ 2175$	$\frac{550}{2050}$	475 1980	290 1600	$280 \\ 1190 \\ 2475$	$\frac{550}{2050}$	510 1975
Tensile strength, lbs % elongation Shore hardness	/in.2	2900 535 54	$2700 \\ 615 \\ 55$	$2225 \\ 340 \\ 68$	2310 365 64	3000 475 54	2600 525 55	$2235 \\ 340 \\ 64$	2260 360 67

tural rubber, and which gave neither cure retardation nor glycerol activation effects in these polymers. Table 5 shows that in the absence of glycerol, attrited black retards the cure of SBR to very nearly the same extent for the three accelerator systems studied. Similarly, the magnitude of the glycerol activation effect appears to be about the same in the three cases shown. From this, the dependence of these phenomena on the polymer composition and the black type seems assured.

It is interesting to note in Table 6 that SBR, when cured with dicumyl peroxide (Di Cup at 1.0 phr) without sulfur or accelerators, suffers little or no cure retardation with attrited blacks. This observation is contrary to expectation since acidic compounds are generally not recommended for use in peroxide cured vulcanizates¹³. Glycerol yields relatively small cure activation effects in peroxide cured SBR. Though glycerol has a greater activity in the attrited black compound (Table 6), the vulcanizate changes which it produces are small when compared with the changes in the corresponding sulfur cured compound.

Table 5

Comparison of Glycerol Effect in SBR Compounds
with Different Accelerator Systems

Glycerol, phr		-	3.0	-	3.0		3.0
MBTS		1.5	1.5	-	_	1.0	1.0
ZnDEDC MBT		0.15	0.15	1.5	1.5		_
TMTD			_			1.0	1.0
Cure at 300° F, min			15		30		20
Modulus, lbs/in. ² at	100% $300%$ $500%$ $700%$ $900%$	140 315 705 1210 1750	240 1220 2930	150 300 610 935	370 1445 3470	150 310 720 1240 1935	365 1550 3515
Tensile strength, lbs/ % elongation Shore hardness	in.2	1850 950 54	3685 590 58	1200 960 50	3950 565 63	$2250 \\ 985 \\ 51$	3600 515 65

In further consideration of the glycerol effect, SBR-attrited HAF black systems were studied with other hydroxy compounds substituted for glycerol. The standard formulation was used in this work, and the concentration of the substituted polyols was taken as a molar equivalent of glycerol at 3.0 phr. Results are given in Table 7, listing the hydroxy compounds in order of increasing cure activity as judged by the 300% modulus.

Aromatic hydroxy compounds (mono, di, and trihydric phenols) are generally undesirable. Cure is not obtained at all with three of these, even when the vulcanization time is extended to 60 minutes. Two others give little or no improvement over the control compound which was prepared without polyol addition. Hydroquinone alone shows positive results in terms of increased modulus, increased tensile strength, and reduced extensibility. Since phenols are weak acids, and since the vulcanization of SBR is sensitive to acid (Figure 3), one might suspect that phenol reponses are related to phenol acidity. That this is not the case is evident from the widely different results obtained with catechol, resorcinol, and hydroquinone, all of which have roughly the same dissociation constants.

Monohydric alcohols such as n-propyl alcohol or lauryl alcohol yield little if any enhancement of cure, even when their concentrations are increased to

TABLE 6

EFFECT OF ATTRITED HAF BLACK AND GLYCEROL IN SBR
COMPOUND CURED WITH PEROXIDE

Condition of black		Ball 1	nilled	Standard		
Glycerol, phr		_	3.0	_	3.0	
Modulus, lbs/in. 2 at	100% 300% 500% 700%	160 475 1400 2350	175 670 1850 3125	190 690 1540	175 725 1580	
Tensile strength, lbs	/in.2	2750	3125	2025	1925	
% elongation		785	700	680	630	
Shore hardness		53	55	58	55	

Table 7

Effect of Selected Hydroxy Compounds Substituted for Glycerol in SBR-Ball Milled HAF Systems Cured for 20 Minutes at 300° F

	Modulus, lbs/in.3					
	200%	300%	500%	strength, lbs/in.2	gation,	hard- ness
Catechol (1,2-dihydroxyphenol)	4			No cure		
Pyrogallol (1,2,3-trihydroxyphenol)	+			- No cure		
Phloroglucinol (1,3,5-trihydroxyphenol)	+			No cure		
Water	310	475	1075	2250	825	51
Lauryl alcohol (3 moles)	215	480	1335	3050	760	
CONTROL (no additive)	300	500	1185	2550	855	50
Diethylenetriamine	325	500	925	1875	740	58
n-Propyl alcohol	310	520	1260	2500	790	50
Resorcinol (1,3-dihydroxyphenol)	350	530	1110	3015	860	58
Phenol	350	550	1280	2590	790	52
n-Propyl alcohol (3 moles)	325	550	1350	2830	810	51
Lauryl alcohol	330	575	1490	3240	800	48
Water (3 moles)	350	580	1400	2765	790	50
Hydroquinone (1,4-dihydroxyphenol)	440	750	1720	3150	720	58
Trimethylene glycol (propandiol-1,3)	605	1215	3140	4225	590	68
GLYCEROL	710	1500	3625	4500	590	58
Ethylene glycol	900	1750		3500	470	62
1,2,6-Hexanetriol	985	1900	-	3615	455	62

provide the same number of hydroxyl groups as glycerol. Aliphatic polyols, however, generally appear extremely effective. Ethylene glycol and 1,2,6-hexanetriol promote cure to a greater extent than does glycerol, despite the fact that lower tensile is obtained with these polyols than with glycerol. Experi-

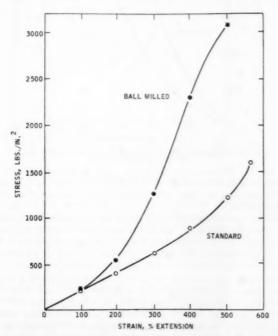


Fig. 9.—Stress-strain properties of SBR for vulcanizates with standard and ball milled FT blacks.

ments with trimethylene glycol (propendiol-1,3) indicate that the reactivity of polyols is not necessarily associated with the 1,2 structure of the hydroxyl groups which is characteristic of glycerol, ethylene glycol, and 1,2,6-hexanetriol.

Hausch⁹ showed that in Hevea the adsorption of malachite green on silica was reduced by both polyols and polyamines. Since no similarity appears in the cure activating effect of diethylenetriamine and the polyols in Table 7, the activity of the latter must be attributed to something more than the placation of adsorptive tendencies on the part of the filler. Polyols are believed to be

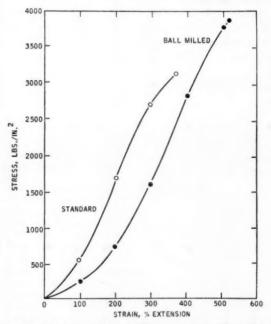


Fig. 10.—Stress-strain properties of SBR for vulcanizates with standard and ball milled FEF blacks.

involved somehow in interactions with the polymer, the black, and the curing systems. Polyamines, at least diethylenetriamine, are not similarly involved in these interactions.

When the compounds are properly cured in the presence of glycerol or other polyols, as has been described, attrited blacks lead to SBR vulcanizates with improved properties. The nature of these improved properties is discussed in the next several sections of this paper. For this discussion, attrited black compounds were prepared with glycerol as already specified (3.0 phr). Due to the increased shortness and hardness which results when glycerol is added in SBR systems with standard black (Table 3), no glycerol was used in the preparation of these systems. Vulcanizates were cured for 30 minutes at 300° F.

As was the case with butyl², SBR vulcanizates containing attrited blacks are characterized by increased tensile strength and extensibility. For the coarser blacks, such as FT black (Figure 9), the stress-strain curve is shifted in

the direction of increased stress. Activation of the black by ball milling in this case is believed to lead to increased numbers of polymer-carbon attachments. As a result, the reinforcing action of the black is greatly increased. FT black is a subnormal structure black. The geometry of its particle distribution, i.e., its secondary aggregate structure or oil absorption capacity, is not appreciably changed by ball milling. Similar results are obtained with MT black.

The formation of increased numbers of polymer-carbon attachments which is claimed for ball milled FT black systems, is claimed for attrited black systems generally. The interaction of carbon black with polymer free radicals formed during milling is one possible mechanism¹⁴ for bringing about these attachments. This concept was invoked in the discussion of attrited blacks in

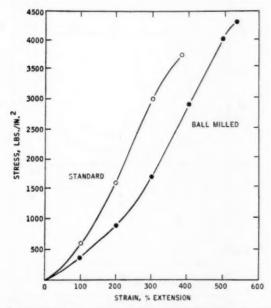


Fig. 11.—Stress-strain properties of SBR for vulcanizates with standard and ball milled HAF blacks.

butyl². However, the possibility for carbon-polymer interaction during vulcanization, by free radical mechanism¹⁸, or more probably, by complex oxidation-reduction schemes which also involve sulfur¹⁶, seems much more likely with SBR. The unique nature of the cure retardation and concomitant glycerol activation effects in sulfur cured SBR-attrited black systems is evidence which seems to be entirely in accord with the requirements for this latter mechanism.

With finer blacks, and specifically, the high structure furnace blacks, the stress-strain curve is shifted in the direction of reduced stress. Figures 10 and 11 show results for FEF and HAF blacks, respectively. Reduced stress in these systems is attributed to the dissipation of secondary or aggregate structure in the blacks. The effect of the increased surface activity of the attrited

blacks is believed to be overshadowed, in these cases, by viscosity effects, the viscosity of the elastomer-black matrix being much less in the absence of sec-

ondary or aggregate carbon structure.

The dependence of vulcanizate modulus on the structure, i.e., the geometric complexity, of the dispersed carbon black was recognized in the previous work with butyl². A similar situation obtains with SBR. Once the geometric complexity of the black is reduced to a nearly constant state by attrition, the vulcanizate modulus at uniform carbon black concentration tends to seek a common level, regardless of the surface area or the surface activity (oxygen content)

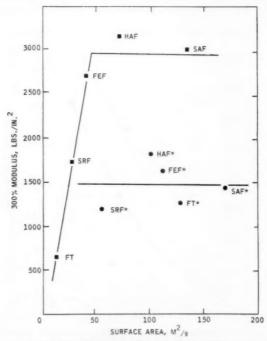


Fig. 12.—Effect of surface area of several blacks on the modulus of SBR for vulcanizates with standard and ball milled blacks.

of the attrited black. This behavior, which is shown in Figure 12, is the same as that shown for butyl in the previous paper. Because of the greater sensitivity of the cure in SBR, the points for SBR vulcanizates with attrited blacks are somewhat more scattered than those for the corresponding butyl systems. Similarly, greater modulus increases are observed as the structure or geometric complexity of the standard blacks increases from FT to SFR, up to the high structure furnace blacks, FEF, HAF, and SAF. These latter standard blacks have roughly the same, strong aggregation habits, and give roughly the same high values for vulcanizate modulus.

If viscosity and relaxation effects are indeed related to the geometric complexity of the carbon black, as we have suggested, they should be apparent in

the raw mixtures of polymer and black, and should become larger as the concentration of the black is increased. This is confirmed by the Mooney viscosity plots in Figure 13. Lower viscosity is obtained with attrited black. And the curves diverge for mixtures of SBR with standard and attrited HAF blacks, respectively. The viscosity of the standard black system, only 10 Mooney points higher at 20 volumes loading, is 80 points higher at 60 volumes loading. This clearly demonstrates the decreased viscosity which results in an elastomer compound when the high degree of structure ordinarly present in a black like HAF black is destroyed. It is this viscosity change, we believe, which leads

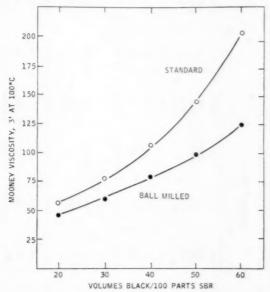


Fig. 13.—Mooney viscosity for SBR systems with varying concentrations of standard and ball milled HAF blacks.

to the downward displacement of the stress-strain curves in Figures 10 and 11. It is an advantage of attrited blacks which is clearly apart from their reinforcing action in the vulcanizate.

The increased length and strength of SBR vulcanizates containing attrited blacks are evident at normal filler loading levels (30 volumes), but become more pronounced when the carbon black concentration is increased to 40, 50, or 60 volumes. Test results are shown in Table 8 for SBR systems with standard and ball milled HAF blacks. Data are presented for both control (not heat treated) and heat treated systems. The enhanced tensile properties which are shown in Table 8 to result from the use of attrited black are illustrated by plotting tensile product (tensile strength × elongation) curves, as in Figure 14. These curves, referring to samples before (solid lines) and after (dotted lines) heat treatment, indicate that the concentration of attrited black can be increased by 15 to 25 volumes over that of the standard black before tensile product is reduced to values typical of those ordinarily obtained for standard black compounds.

Table 8

Eppect of Filler Concentrations on the Tensile Properties of SBR with Standard and Attrited HAF Blacks

				Not Heat Treated	eated					
Volumes of black	04	20	60	30		40	Z,	20	9	09
Condition of black	Std.	B.M.e	Std.	B.M.	Std.	B.M.	Std.	B.M.	Std.	B.M.
Modulus, lbs./in.º, at 100%	315	260	605	360	1105	495	1610	680	1	096
200%	915	580	1835	850	3000	1400	1	2000	1	2770
300%	1800	1190	3180	1755	1	2690	-	3450	1	
400%	2825	2180		2935	1	3890	I	1	1	
Tensile strength, lbs./in.?	3315	3330	3915	4380	3340	4110	2625	3750	1975	3415
% elongation	445	200	375	520	235	425	170	355	105	270
Shore hardness	58	56	89	62	78	20	28	22	00	28
Electrical resistivity, ohm cm	2.9 ×10"	3.8 ×1010	4.7×107	8.6 ×107	4.3×10 ⁷	5.7×10 ⁷	3.7×107	4.6×107	4.1 ×107,	5.2×10 ⁷
				Heat Treated	per					
Modulus, ibs./in.º, at 100%	390	165	695	230	1430	335	2000	550	1	685
200%	1335	330	2215	625	1	965	1	1150	1	2000
300%	2550	735	3730	1585	-	2195	1	3450	1	
400%	1	1510	1	3010	1	3720	1	1	1	
Tensile strength, lbs./in.?	3025	3620	3925	4545	3210	4280	2510	3915	2040	2765
% elongation	330	009	302	555	190	470	135	350	75	260
Shore hardness	29	48	29	22	75	09	83	99	06	73
Electrical resistivity, ohm em	3.9×1014	9.1 ×104	3.8 × 1011	8.6×1014	1.1 ×10	2.3 ×104	4.1 × 107	4.3 ×10"	3.1×10 ⁷	2.2 ×1010
• Ball milled.										

Unusually high values of tensile product, values approaching 200×10^{-4} , are obtained only with attrited black. The possible effect of this result on abrasion resistance¹⁷ is noteworthy. Finally, it is interesting in Figure 14 to compare the heat treatment response. The detrimental response with standard black indicates a disadvantage which may describe the fate of SBR in conventional Banbury mixing. More will be said about this later in the section on heat treatment responses.

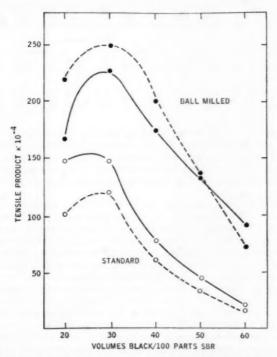


Fig. 14.—Tenaile product of SBR vulcanizates with varying concentrations of standard and ball milled HAF blacks. Solid and dashed lines refer to control and heat treated systems, respectively.

Shore hardness data in Table 8 stress the increased softness obtained with attrited black. The electrical resistivity values in the table indicate that attrited black, even at high levels of loading, is fairly uniformly dispersed by the action of heat treament. This result agrees with the concept of increased black activity, pigment-polymer associations being held as a requisite for the immobilization of black particles which, otherwise, might recluster to form carboncarbon associations in the course of the vulcanization reaction¹⁸.

The dynamic properties of SBR are improved with attrited blacks. Data in Table 9 give results obtained from tests with the modified Yerzley oscillograph⁵. The compounds used in this work were the same as those used in the carbon concentration study above. A plasticizing oil (Sun Circo Light, 10 phr) was added to the base formulation to facilitate the testing of the highly loaded samples.

TABLE 9

EFFECT OF FILLER CONCENTRATION ON THE DYNAMIC PROPERTIES OF SBR WITH STANDARD AND ATTRITED HAF BLACKS

				1	ot Hea	t Treate	ed			
Volumes of black	2	00	3	10	4	10		50	(30
Condition of black	Std.	B.M.	Std.	B.M.	Std.	B.M.	Std.	B.M.	Std.	B.M.
Dynamic properties in SBR										
$\eta f \times 10^{-4}$, poises \times CPS $K \times 10^{-7}$, dynes/cm ² % relative damping	$2.05 \\ 6.98 \\ 25.3$	$1.26 \\ 6.29 \\ 18.0$	3.62 10.2 29.9	$\begin{array}{c} 2.27 \\ 6.87 \\ 28.0 \end{array}$	6.84 14.6 37.4	4.32 10.4 33.9	11.5 20.4 43.6	6.18 13.3 37.1	17.8 30.9 44.2	10.6 18.1 45.0
					Heat 7	Treated				
Volumes of black	2	0	3	0	4	0	į	50	(30
Condition of black	Std.	B.M.	Std.	B.M.	Std.	B.M.	Std.	B.M.	Std.	B.M.
Dynamic properties										
$\pi f \times 10^{-6}$, poises \times CPS $K \times 10^{-7}$, dynes/cm ² % relative damping	1.75 7.40 20.9	1.47 5.33 24.0	3.24 9.34 29.2	1.96 6.64 25.4	5.75 13.8 34.1	2.99 8.15 30.7	10,0 18.4 42.3	4.70 10.9 35.1	16.5 28.6 44.4	7.65 14.0 42.4

The use of attrited black decreases both ηf and K. Changes in relative damping, though much smaller than for the corresponding butyl systems², indicate that reduced internal viscosity and increased dynamic softness are realized in attrited black systems without loss in the overall rubberlike properties. Heat treatment renders some further improvement in the dynamic qualities of the vulcanizates.

Goodrich flexometer tests were run with the above samples containing 30 and 40 volumes of black, respectively. Tests were run at 100° C using 145 lbs/in.² load with a $\frac{1}{8}$ " stroke. In the absence of heat treatment, no sacrifice in flexing properties results from the use of attrited blacks (Table 10). No increases in dynamic drift, compression set, or ΔT are obtained, despite the larger imposed compression which these samples sustain due to their greater softness. Heat treatment renders these attrited black samples too soft for the testing conditions, severe static and dynamic deformations leading to relatively high values for compression set in the resulting samples. This difficulty would probably be corrected if the stiffness of the vulcanizates were increased by omission of the plasticizing oil. Clearly, there is no evidence in the ΔT values for intrinsic hysteretic failure with heat treated attrited black systems.

Cyclic extension-retraction tests run at constant extension (150%) with the Instron tester demonstrated another advantage for attrited blacks in SBR. Curves in Figure 15 show the first and sixth extension-retraction cycles for vulcanizates with standard and ball milled HAF blacks, respectively. The first

TABLE 10

FLEXING PROPERTIES OF SBR WITH STANDARD AND ATTRITED HAF BLACKS

		Not hea	t treated		Heat treated				
Volumes of black	3	0	4	0	3	10	4	10	
Condition of black	Std.	B.M.a	Std.	B.M.	Std.	B.M.	Std.	B.M.	
Static compression, in. Initial dynamic compression, in. Dynamic drift, in. Compression set, % 2 T. ° C	0.186 0.131 0.013 3.2 13.0	$0.261 \\ 0.201 \\ 0.012 \\ 3.8 \\ 12.0$	0.151 0.096 0.018 6.0 20.0	0.215 0.171 0.021 5.1 16.0	0.236 0.181 0.024 7.0 17.0	0.324 0.286 0.021 11.8 15.0	0.169 0.113 0.011 3.5 17.0	0.308 0.266 0.050 15.0 21.0	

a Ball milled.

cycles are indicated by solid lines, and the sixth cycles by dotted lines. Open circles denote standard black, and solid circles denote ball milled black.

Figure 16 shows that the decay of stress on prestressing (the Mullins effect) is less with attrited than with standard black. The plot is constructed using values taken from the extension curves of each extension-retraction cycle, stress decay being expressed in terms of the absolute loss in modulus at 125% elongation. The total changes in going from the original to nearly steady state condition amount to 43 and 29 per cent for standard and attrited black systems,

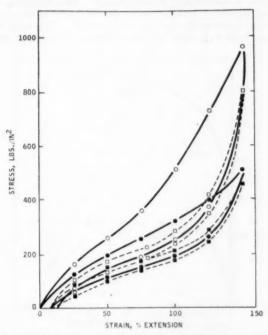


Fig. 15.—Cyclic stress-strain curves for SBR vulcanizates with standard and ball milled HAF blacks.

respectively. The substitution of carbon-polymer attachments for the weaker carbon-carbon attachments is suggested as an explanation for the superior performance of attrited black compounds in this test.

The heat treatment of SBR-carbon black mixtures generally leads to vulcanizates with increased modulus and reduced extensibility. With channel black, a thermal interaction response, similar to that obtained with butyl, but much smaller in magnitude, is obtained. Care must be taken, however, to limit the heat treatment, both with respect to time and temperature, if resinification and related, undesirable oxidative effects are to be avoided.

In contrast to butyl, the thermal interaction of SBR occurs, even if only to a limited extent, with furnace as well as channel blacks. Table 3 shows that conventional heat treatment responses are obtained with standard HAF black, regardless of whether glycerol is present in the compound or not. If 300%

modulus is taken as the criterion, the resultant modulus increases are less than 15 per cent. In the absence of glycerol, the heat treatment of SBR with attrited HAF black (Table 3) yields much greater thermal interaction responses. The enhanced activity of oxy blacks is thus confirmed, the modulus at 300% being increased in this case by 48 to almost 100 per cent, depending on the cure.

The presence of glycerol in mixtures of SBR with attrited black leads to an unexpected reversal in the heat treatment response (Figure 17). Modulus is decreased (downward pointing arrows), the decrease being largest in the earliest cure, and tending to disappear in the longest cure. Heat treatment of the same system without glycerol (upward pointing arrows) produces increases in modulus which become larger as the cure time is increased. Thus heat treatment of the two systems leads to a single level for modulus. This is a surprising result

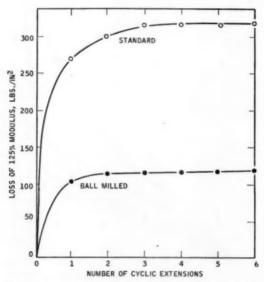


Fig. 16.—Loss of modulus on cyclic extensions for SBR vulcanizates with standard and ball milled HAF blacks.

for which no explanation can yet be given. Examination of columns 5 and 6 in Table 3 reveals also that there is essentially no difference in the stress-strain properties of heat-treated SBR-attrited black compounds prepared with and without glycerol, respectively. Heat treatment was carried out by hot milling the polymer-carbon black masterbatch for 10 minutes at 300–310° F on an open mill. Stearic acid, and glycerol when used, were also added in the masterbatch. This is a mild form of heat treatment. It produces results which tend to be similar to those obtained in Banbury operations, where the times generally are shorter (after initial incorporation of the black), but the stock temperatures are higher.

Effects similar to those in fully cured butyl and SBR compounds are obtained when attrited blacks are used in other elastomers. Results shown in Table 11 illustrate vulcanizate changes resulting from the substitution of at-

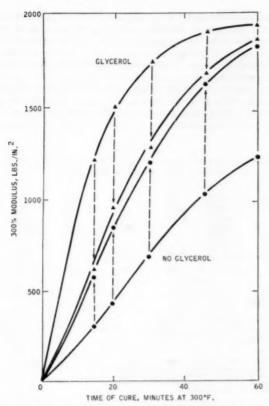


Fig. 17.—Effect of heat treatment on modulus of SBR-attrited HAF black systems with and without glycerol, respectively .

Table 11

Effect of Attrited HAF Black in Natural, Acrylonitrile, and Chloroprene Rubber

Elastomer	Smoke	ed sheet	Hycar	OR 15	Neopr	ene GN
Condition of black	Standard	Ball milled	Standard	Ball milled	Standard	Ball milled
Modulus, lbs/in.2, at 100% 200% 300% 400%	625 1560 2610	350 875 1755 2800	650 1810 3000	400 950 2000 3065	860 2300	600 1550 2565
Tensile strength, lbs/in.9	3465	3505	3775	4240	2780	3065
% elongation	380	470	405	565	280	380
Dynamic properties						
7/×10 ⁻⁴ , poises ×CPS K×10 ⁻⁷ , dynes/cm ² % Relative damping	$\begin{array}{c} 2.45 \\ 11.2 \\ 19.6 \end{array}$	1.32 6.46 18.3	6.77 16.4 33.8	5.33 13.7 32.3	9.05 17.1 41.4	13.6 34.5
Electrical resistivity, ohm cm	2.0×10*	8.3×10°	5.1×10°	7.1×10 ¹⁰	1.7×10^{9}	2.3×10^{10}
Tensile produce ×10 ⁻⁴	131.7	164.7	152.9	239.5	77.8	116.5

trited for standard HAF black in natural, acrylonitrile-butadiene, and chloroprene rubbers. The compounds were cured for 45 minutes at 287° F. As already stated, cure retardation problems were not encountered with these polymers. The use of glycerol was not only not required, but, except in the special case described below, produced no significant improvement in the quality of the vulcanizates.

In the work done with natural rubber, difficulty was experienced in reproducing test results with attrited black compounds. Tensile strength, for example, was found to vary considerably in similar batches prepared under seemingly identical conditions, but at separate times. A final set of experiments was

TABLE 12 EFFECT OF MIXING CONDITIONS ON PROPERTIES OF NATURAL

RUBBER	WITH	ATTRITED	HAF BLACK		
	1	2	3	4	5
400%	330 780 1475	430 935 1715 2665	360 825 1600 2600	415 935 1790 2910 3975	415 945 1770 2745
1.2	2360	3380	3390	4235	3765
	400	480	490	530	510
	57	61	59	64	63
	8.9	7 9,	80 7.69		1.84 8.40 19.6
	100% 200% 300% 400% 500%	100% 330 200% 780 300% 1475 400% 500% 12 2360 400 57 CPS 3.2	1 2 100% 330 430 200% 780 935 300% 1475 1715 400% 2665 500% 1.2 2360 3380 400 480 57 61 CPS 3.20 3.20 3 8.97 9.	1 2 3 100% 330 430 360 200% 780 935 825 300% 1475 1715 1600 400% 2665 2660 1.2 2360 3380 3390 400 480 490 57 61 59 CPS 3.20 3.02 2.0 2 8.97 9.80 7.66	1 2 3 4 100% 330 430 360 415 200% 780 935 825 935 300% 1475 1715 1600 1790 400% 2665 2600 2910 500% 3975 1.2 2360 3380 3390 4235 400 480 490 530 57 61 59 64 CPS 3.20 3.02 2.05 1.92 3 8.97 9.80 7.68 8.63

Mixing Conditions:

1) Polymer broken down prior to addition of black.

2) Like 1), except glycerol (3.0 phr) added with black.

3) Polymer not broken down prior to addition of black.

4) Like 3), except glycerol (3.0 phr) added with black.

5) Concentrated masterbatch prepared.

undertaken, therefore, to determine what effect might be obtained if the mixing procedure was purposely changed. Accordingly, natural rubber was mixed with attrited HAF black under the following conditions:

Condition 1. The raw rubber was premasticated by passing it once through a tight 6 inch × 12 inch mill (0.007 inch clearance) at 80-90° F. The rubber was then immediately banded, and milled continuously with active rolling bank until the band was smooth. This required 3 to 4 minutes. Cooling water, which was not used up until this time, was then turned on, and the addition of black was initiated. Normal mixing procedures were then followed to complete preparation of the batch.

Condition 2. The procedure of Condition 1 was followed in every detail, except that glycerol (3.0 phr) was added with first additions of the black.

Condition 3. The raw rubber was premasticated and banded as in Condition 1. Cooling water, however, was then turned on, and the black addition started immediately, while the band was still rough, the polymer not yet broken down as in Condition 1. After all the black was added, milling was continued for 4 minutes, the time consumed in the previous cases to effect polymer breakdown prior to the addition of black. Normal mixing procedures were then followed to complete preparation of the batch.

Condition 4. The procedure of Condition 3 was followed in every detail, except that glycerol (3.0 phr) was added with first additions of the black.

Condition 5. The procedure of Condition 2 was followed in every detail, except that the black charge was increased from 50 to 100 phr in the preparation of the original masterbatch. The masterbatch was then diluted with virgin rubber to obtain the required black loading (50 phr). The virgin polymer used for dilution was premasticated and banded as in Condition 3. Normal mixing procedures were followed thereafter to complete preparation of the batch. All the compounds were cured for 20 minutes at 287° F.

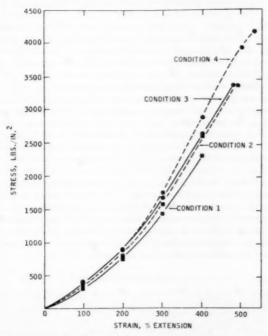


Fig. 18.—Effect of mixing procedure on stress-strain properties of natural rubber vulcanizates with attrited HAF black.

The problem of attrited black utilization in natural rubber is apparently a problem of dispersion—in its broadest sense. If mixing is more severe, as in Conditions 3 and 4, better dispersion of the black is apparently obtained. The improved vulcanizate quality which therefore results is seen by comparing the curves for Conditions 1 and 3 on the one hand, and 2 and 4 on the other, in Figure 18. Table 12 contains a detailed compilation of all the data obtained from the experiments just described. Concentrated masterbatching (Condition 5) is another method for increasing the severity of the milling action. Good utilization of the black is therefore provided.

Dispersion appears also to be aided by the use of additives. Glycerol in mixtures of attrited black with Hevea is cited as an example. Profound cure effects, such as those encountered with SBR, are not obtained in these systems.

But the increases in vulcanizate length and strength which are obtained without other significant changes in the stress-strain curve (Figure 18) are, in the writer's opinion, unmistakable evidence of improved dispersion.

SUMMARY

The cure of SBR is severely retarded in compounds with attrited blacks. This retardation, not found in butyl, natural, and acrylonitrile-butadiene polymers containing the same blacks, is associated with the sensitivity of SBR to acidity on the part of the black. The cure of SBR-attrited black compounds is sharply activated when glycerol or other aliphatic polyols are added in the compounds. The glycerol activation effect is unique with respect to both the polymer and the black. It is not obtained with SBR containing standard blacks, or with other elastomers, regardless of the black. Cure retardation and glycerol activation effects occur also only in attrited black-SBR systems which They are not observed in peroxide cures. A combined are cured with sulfur. reinforcement-vulcanization reaction is therefore envisioned to include the polymer, the black, sulfur, and glycerol as the reactants.

When the compounds are properly cured with glycerol, attrited blacks lead to SBR vulcanizates with improved properties. The results are generally similar to those observed with butyl. Tensile strength and extensibility are increased. The vulcanizates are softer, as is evident from their reduced modulus and shore hardness. The dynamic properties are improved, both the dynamic modulus and the internal viscosity of attrited black-SBR vulcanizates being less than is ordinarily obtained with standard blacks. The increased activity of attrited blacks leads to greater heat treatment responses when glycerol is not present in the compound. The heat treatment of SBR containing both attrited black and glycerol results in a reversal of the normal heat treatment response. The reason for this reversal is not understood.

Attrited blacks in natural, acrylonitrile-butadiene, and chloroprene rubbers give results similar to those in butyl. Cure retardation and glycerol activation effects are not encountered with these elastomers.

ACKNOWLEDGMENT

The author is grateful to F. P. Baldwin, I. Kuntz, and J. Rehner, Jr. of these laboratories for helpful discussion relating to the subject matter of this paper, and for review of the manuscript. He most gratefully acknowledges the assistance of J. C. Scarpa in carrying out the experimental work.

REFERENCES

- **REFERENCES**

 1 Gessler, A. M., Rubber Age, 86, 1017 (1960).
 2 Gessler, A. M., ibid., 87, 64 (1960).
 3 Gessler, A. M., ibid., 74, 59 (1953).
 4 Zapp, R. L., and Gessler, A. M. ibid., 74, 243 (1953).
 5 Baldwin, F. P., ibid., 67, 51 (1950).
 5 Baldwin, F. P., ibid., 67, 51 (1950).
 6 Cabot Technical Report, RC-103, March 1960 (Regal 300).
 7 Smith, D. A., Rubber and Plastica Age, 41, 56 (1960).
 8 Howland, L. H., Reynolds, J. A., and Brown, R. W., Ind. Eng. Chem., 45, 2738 (1953).
 9 Allen, E. M., Gasge, F. W., and Wolf, Ralph F., Rubber World, 120, 577 (1949).
 10 Gessler, A. M., and Rehner, John, Jr., Rubber Age 77, 875 (1955).
 11 Tinyakova, E. I. et al., Zhur. Obshchei Khim. 26, 2476 (1956).
 12 Tilyakova, E. I. et al., Zhur. Obshchei Khim. 26, 2476 (1956).
 13 Effect of Carbon Blacks on Di-Cup Requirements' Data Sheet No. 7-16-56 Hercules Powder Company.
 14 Watson, W. F., Ind. Eng. Chem. 47, 1281 (1955).
 15 Watson, J. W., Trans. Inst. Rubber Ind. 32, 204 (1956).
 16 Studebaker, M. L., Rubber Age, 77, 69 (1955).
 17 Zapp, R. L., Rubber World, 133, 59 (1955).
 18 Ford, F. P. and Gessler, A. M., Ind. Eng. Chem. 44, 819 (1952).

EFFECTS OF CARBON BLACK STRUCTURE ON TIRE TREAD WEAR*

T. D. BOLT AND E. M. DANNENBERG

GODFREY L. CABOT, INC., BOSTON, MASSACHUSETTS

The purpose of this work was to study the effects of carbon black "structure" on the mechanical properties of rubber compounds including road wear performance. Recent progress in the carbon black industry has made possible extensive "structure" variations in the particle size range of any of the oil furnace black grades. These structure changes involve different degrees of primary chainlike aggregation produced during the actual combustion process.

Tire compounders and design engineers continue to seek tire constructions and tread stocks possessing high wear resistance, good traction properties, freedom from excessive cracking, soft and comfortable riding and good driving qualities. An improvement in one of these features frequently results in the deterioration of others. For this reason, the selection of a tread stock is necessarily a compromise where the most critical requirements play the most dominant role.

In recent years more emphasis has been placed on quieter and more comfortable riding performance of passenger tires. Such tires require treads that grip the road strongly and minimize the squeal on corners; reduce the pounding on pavement expansion joints, the rumble on rough road surface, and the whine on the highway—in short, tread compounds which help in avoiding any noises detracting from the smooth, silent operation of the modern automobile. Tire designers and rubber compounders have made notable advances in the development of soft and noiseless passenger tires.

The recent introduction of lower structure, lower hardness reinforcing carbon blacks gives rubber compounders a new approach to the problem of providing the soft treads for the quieter riding tires. Whether these new reinforcing low structure tread blacks achieve the popularity of currently popular grades depends, of course, on whether their advantages outweigh some of their disadvantages. Extensive road testing has already established that the structure level of present-day oil furnace process tread blacks can be reduced to some extent without encountering appreciable loss in wear resistance under normal wearing conditions. Extreme reductions in primary structure properties and excessively severe road wear conditions can result in a noticeable loss in wear resistance.

The present study describes a passenger tire road test program, the object of which was to determine the effect of wide carbon black structure variations on tread wear performance. The carbon blacks used were comparable in particle size to a standard high structure ISAF (Intermediate Super Abrasion Furnace) black (Vulcan 6). The next lower structure black was Regal 600, classified as a normal structure black relative to high structure ISAF black. Two experimental blacks, X-3 and X-5, having successively lower than normal

^{*} Presented at the Division of Rubber Chemistry (ACS) meeting, September (1960), in New York,

structure levels and classified as low structure blacks, were included in the study. These blacks were compared at various loadings in oil-extended SBR tread stocks.

Particle size and surface area characteristics.—Numerous references have characterized the effects of carbon blacks in rubber by the size of the individual carbon black particles, the nature and extent of their surface, and the degree and strength of their particle-to-particle aggregation¹⁻⁷.

Table I lists some of the characteristic properties of the blacks used in this study. The average particle diameters, measured from electron photomicrographs, the nitrogen adsorption surface areas, and their nigrometer color values

TABLE I
PARTICLE SIZE CHARACTERISTICS

Carbon black	Particle diameter, electron microscope surface average da, mµ	Surface area, m³/gram Nitrogen adsorption	Nigrometer color
Vulcan 6 (ISAF)	33.1	121	87.0
Regal 600	31.2	105	86.8
Exp. Black X-3	32.3	123	85.3
Exp. Black X-5	31.0	125	85.0

place these four carbon blacks in the ISAF black particle size range. Regal 600 has a somewhat lower surface area than Vulcan 6 and the experimental blacks, indicating lower surface porosity since particle size is not increased²⁻³.

Particle aggregation—structure.—One type of particle aggregation appears in electron micrographs as fused chains of particles. These particle-to-particle chains, probably formed early in the carbon black particle growth process in the flame, are strong enough to resist rupture by the high shearing forces encountered during milling into rubber. These structures can, however, be broken by the higher shearing forces encountered during roll milling or ball milling of the dry black^{8, 9}.

TABLE II STRUCTURE CHARACTERISTICS

Carbon black	Oil absorption, ec/gram	Extrusion shrinkage,
Vulcan 6 (ISAF)	1.37	37
Regal 600	0.97	43
Exp. Black X-3	0.83	49
Exp. Black X-5	0.63	51

An indication of the structure of a carbon black can be obtained from oil absorption measurements. The minimum amount of linseed oil required to form a stiff coherent mass⁴ has been defined as the oil absorption value. The structure of a black is also evident from its effect on the processing shrinkage of a rubber compound¹⁰. Table II shows the blacks arranged in the order of decreasing structure as judged from their oil absorption values and their extrusion shrinkage values obtained with a 65 phr loading in SBR-1000.

Particle agglomeration—dispersion.—Another type of particle aggregation consists of loose agglomerates of individual particles and particle chains from

pelleting of the black or from mechanical compaction of the dry black during the process of incorporation in rubber. These agglomerates must be thoroughly dispersed in rubber to individual particles and primary particle chains to achieve the full reinforcement potential of the carbon black.

Decreasing carbon black structure is accompanied by an increasing tendency to form denser agglomerates which are more difficult to disperse. That the lower structure blacks pack more readily is reflected in their higher pour (bulk) densities as shown in Table III. The greater strength of the denser agglomerates is displayed by their lower dispersion ratings, as calculated by the

Table III

Particle Agglomeration Characteristics

Carbon black	Pour density. lbs/cu ft	Disperion rating, % 6 μ Agglomerates
Vulcan 6 (ISAF)	21	99
Regal 600	26	90
Exp. Black X-3	31	73
Exp. Black X-5	33	58

method of Leigh-Dugmore¹¹. These SBR-1710 stocks contained 60 phr black and were mixed in a laboratory "B" Banbury on a conventional single-stage 6-minute cycle.

In order to evaluate the blacks properly, it is necessary to insure that the lower structure blacks are as well dispersed as the control ISAF black. One technique for obtaining better dispersion is the use of a high concentration carbon black Banbury-mixed masterbatch and subsequent dilution of this Stage I mix to the desired black level. Excellent dispersion ratings have been achieved with Regal 600 by using a high black loading (70–110 phr) incorporated in the first-stage masterbatch of a two-stage mixing procedure. In the second stage sufficient SBR is added to dilute the mixture to the desired black loading.

EXPERIMENTAL PROCEDURE AND RESULTS

The four carbon blacks were evaluated in the following formulation and loadings.

		Formula	tion			
	Ster Zin Fle:	R-1710 aric acid c oxide xamine tocure fur	3 1 1	5 .5 .0 .0 .2 .0		
Carbon blacks			Los	dings		
ISAF Black Regal 600 Exp. Black X-3 Exp. Black X-5	55	60 60 60 60	69 69 69	78 78 78	82.5 82.5	90 90

The following data illustrate the mixing procedure for the first stage masterbatches for the 60, 78 and 90 phr black loaded compounds. 1A Banbury, 60 rpm, 70 psi ram pressure cooling water on full.

Black loading	60 phr	78 phr	90 phr
SBR 1710	137.50	137.50	137.50
Carbon black	82.50	107.20	123.80
Stearic acid	2.06	2.06	2.06
Zinc oxide	4.13	4.13	4.13
Flexamine	1.38	1.38	1.38
Cycle, minutes		Ingredient	
0		10, d black	
		cid, ZnO, antioxi	dant
2 3	Remain	ing black	
3	Sweep		
4.5	Dump,	mill, cool and age	

The remaining SBR 1710 and the curatives were then incorporated in the second stage final mix to give the desired black loading as follows.

Black loading	60 phr	78 phr	90 phr
Master above	165.5	183.5	195.5
SBR 1710	37.5	37.5	37.5
Santocure	1.2	1.2	1.2
Sulfur	2.0	2.0	2.0
C	ycle	1A Ba mix, n	nbury
Master a	bove	()
SBR 171	0		
Santocur	e/sulfur		2
	d sheet off	3	3

Excellent dispersion ratings were obtained with Vulcan 6, Regal 600, and Black X-3. The dispersions with Black X-5 are only fair as shown in the following:

	I	Dispersion ra	tings % Bl	ack in <6,	agglomerat	es
Black loading, phr	55	60	69	78	82.5	90
Vulcan 6 Regal 600	99	99 99	99 99	99	99	
Exp. Black X-3		98	99	99	98	99
Exp. Black X-5		91	87	91		89

Laboratory test results.—The concept of carbon black structure has been used to explain anomalous behavior in rubber of acetylene black, lampblacks, and oil furnace blacks in comparison with gas furnace, channel, and thermal blacks. Anomalies have been found in Mooney viscosity, loading capacity, processing smoothout, modulus, hardness, electrical resistivity, and, to a lesser extent, in tensile strength, rebound, and abrasion resistance. It is of interest to compare the behavior of a series of oil furnace blacks differing primarily in their structure and having essentially the same particle size. Their behavior generally confirms previous observations.

Figure 1 shows the decrease in extrusion shrinkage of tread stocks with increasing loading and increasing degree of carbon black structure. The differences in shrinkage are most evident at the higher black contents. The mixing procedure favorably influenced the extrusion behavior with the lower structure blacks since, the extrusion shrinkage was reduced with an attendant improvement in surface smoothness by the use of a high viscosity mixing technique.

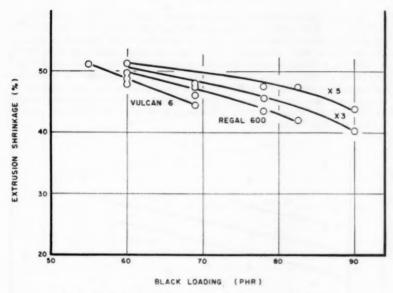


Fig. 1.—Effect of carbon black structure and loading on extrusion shrinkage.

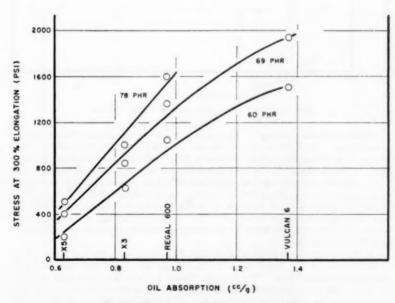


Fig. 2.—Effect of carbon black structure on modulus.

The relationship between modulus and oil absorption of the blacks is seen in Figure 2. The extent of the decrease in modulus which occurs by reducing the oil absorption of the blacks from 1.3 cc/gram to 0.6 cc/gram is striking. The modulus at 300% elongation of the road test compounds range from 300 psi to 1900 psi. Modulus levels which are scarcely more than are expected from a gum stock are obtained at 60 phr loading with the experimental black X-5. Although it is possible to produce carbon black grades over this complete oil absorption range, the structure level of presently available commercial normal structure ISAF blacks has been determined to provide the minimum sacrifice of tread wear performance.

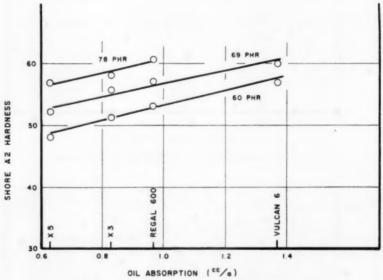


Fig. 3.-Effect of carbon black structure on Shore hardness.

Figure 3 shows a similar relationship between vulcanizate hardness and oil absorption. Tread hardness values are decreased by approximately three points by substituting normal structure Regal 600 at equal loading for ISAF black. The hardness of the road test compounds range from 47 to 62.

It is worthy of note that no significant effect on tensile strength was found with the ISAF black, Regal 600, or the experimental black X-3. With all these black compounds a small decrease in tensile level at the highest black loadings was found, as would be expected. The stocks containing the experimental black X-5, however, did show lower tensile strengths which are attributed to poor black dispersion.

A small decrease in rebound resilience with decreasing black structure may be seen in Figure 5. Regal 600 tends to fall slightly on the high side of the oil absorption-rebound line. The data in Figure 5 show the lower heat buildup of Regal 600 more clearly. No significant effect of black structure on heat buildup was found in these vulcanizates. The low heat rise of the Regal 600

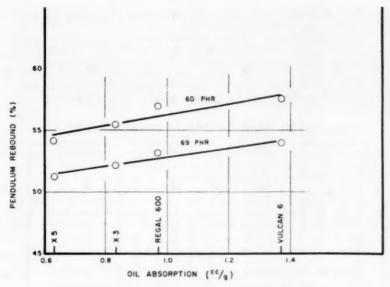


Fig. 4.—Effect of carbon black structure on rebound resilience.

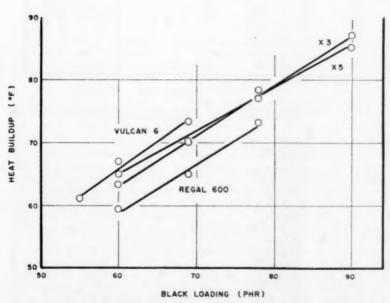


Fig. 5.—Effect of carbon black type and loading on Goodrich flexometer heat buildup.

compound is attributed to the lower total surface area of this black and to the

higher state of cure of its tread compounds.

DeMattia flex cracking resistance has been shown to be strongly influenced by modulus level. It would be expected that low structure should improve and increased loading of carbon black should detract from cracking resistance. The data in Table V tend to confirm these effects although the differences are small. The cut growth resistance with the lower structure carbon blacks at higher loading is comparable with that of the ISAF black reference compounds.

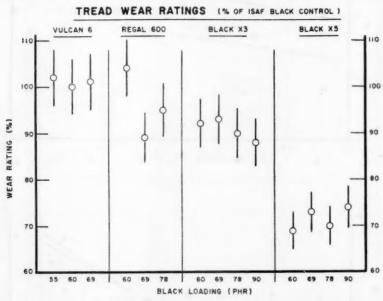


Fig. 6.—Average ratings and 95% confidence limits for road test program. Effects of carbon black structure and loading on tread wear resistance.

Tire testing procedure.—The above stocks were used in retread tire tests. Two types of retreaded tires were involved in tread wear screening tests. In one type the tread stocks were remilled and sheeted on a laboratory roll mill. These were used to replace the original treads on new 7.50-14/4-ply tires which were removed by buffing. A three-part tread construction was used which always included an ISAF black (Vulcan 6) tread compound as the reference standard. The recapped tires were vulcanized in a special shallow depth, broad rib, flat groove tread design for 40 minutes at 292° F external temperature with an internal curing band at 337° F. Prior to start of the actual measured period, each tire was subjected to a 900-mile breakin period during which each tire was rotated among all four wheel positions. The road tests were conducted at 60 mph, 24 psi cold inflation pressure, and 1085 lbs wheel load with standard X-rotation among wheel positions each 450 miles for a balanced rotation cycle of 1800 miles. Tread depth measurements were made at the completion of each complete rotation cycle.

In the second type of passenger retread tire test, the uncured tread stocks were remilled and pressed into the profile of wing camelback and placed on the buffed surface of new 6.70-15/4-ply tires. A two-part tread construction was used with one of the tread sections serving as the ISAF black reference compound. The retreaded tires were cured for 70 minutes at 292° F external temperature using a conventional tread design. Road test conditions were 60 mph, 26 psi cold inflation pressure, and 1230 lbs. wheel load with standard X-rotation among wheel positions. The tread depth was measured at each wheel position change at 1080 miles. A balanced rotation cycle consisted of 4320 miles.

Road test results.—The tread wear of passenger car tires is influenced by innumerable factors. These include the vehicle weight, mechanical condition, driving and braking torque, driver habits, the wheel positions, tire inflation pressures, road surface, number and radii of turns and the climatic conditions. It is scarcely surprising that any tread compound when subjected to such widely varying service conditions should give quite different rates of wear. The evaluation of the relative performance of any two tread compounds by controlled road test procedures usually employs service conditions giving rapid wear in order to complete the road test within the least time and at the lowest cost.

TABLE V

DEMATTIA FLEX	CRACKING	(KILOCYCLES	то 0.8 п	N. CUT	GROWTH)
Black loading, phr	55	60	69	78	90
Vulcan 6 (ISAF) Regal 600	24	26 30	15 25	23	
Exp. Black X-3 Exp. Black X-5		32 38	31 35	33 30	26 31

The wear rating of a tread compound relative to a reference compound is not constant under all test conditions but is dependent on the "severity of service," commonly described in terms of miles/mil depth loss or of mile loss/1000 miles of the reference compound^{12–16}. By careful control of the fleet test conditions, and by a statistical plan of the experiments and analysis^{14–18} of the data, one obtains the degree of test precision which is useful in estimating the presence of any significant differences in the relative tread wear ratings of the experimental compounds. The ratings obtained are applicable only to the particular road test analyzed. It is preferable to conduct the individual tests in road test programs under several severities of service for a more general assessment of tread wear performance.

A retread passenger tire screening test was conducted on tires with threepart treads to evaluate the tread wear rating of fourteen compounds. The depth loss per 1800 miles of the control compound on each tire and the variance analysis performed on the logarithms of the data are given in Table VI. The compound wear ratings and the variance analysis are shown in Table VII.

Figure 6 shows the average treadwear ratings of the compounds and the confidence limits of the averages for the road test program. The 95% confidence limits are indicated by the short vertical line across each rating point. The effect of carbon black content is presented by the group of rating points under each type of black. Within the range of loadings studied, there is little effect on treadwear by increasing the carbon black content. The loading capacity with normal structure blacks is higher than with the high structure

TABLE VI

RATE OF WEAR OF REFERENCE TREAD COMPOUNDS (MILS DEPTH LOSS PER 1800 MILES)

Test						01-				c0 4				4.		
Reference compound	09	60 phr ISAF Black	AF Blac		09	60 phr ISAF Black	AF Blac	[_	69	phr IS	69 phr ISAF Black		69	69 phr ISAF Black	F Black	
Tire. Rotations	-	21	00	F	00	9	1	(∞	6	10	11	12	13	14	15	16
	25.5	28.9	17.7	14.1	24.4	27.1	31.4	29.2	16.4	16.6	25.3	19.9	16.5	21.3	17.4	22.8
N 00	18.7		16.8	18.9	18.7	21.0	18.9	17.1	29.5		25.5	17.3	18.0	24.2	17.1	17.1
4	26.3	25.1	28.1	27.3	26.0	25.4	24.6	24.5	30.5		42.3	25.4	25.2	46.4	28.6	26.1
Geometric average	23.9	25.4	25.4 21.2	20.7	21.3	23.8	21.8	21.2	25.6		22.3 30.5	19.5	18.8	25.6	18.9	20.0
Program average		7	Test 1 and 2	and 2	22.4					1	Test 3 and 4	und 4	22.3			
					(On	Analysis of Variance on Logarithms of Dat	of Va	Analysis of Variance (On Logarithms of Data)								
					Te	Tests 1 and 2	2 p					Tests 3 and 4	\$ P			
Source of variance	iance		JÞ	Variance		Variance ratio (F)	(F)	Sig. at 5% level		Variance	ince	Variance ratio (F)	(F)	Sig. at	ق م	
a) Test b) Tres c) Rotation d) Rotation × tests e) Residual	× test	30	73334	.001069 .003921 .027263 .024632 .004220	0-880	0.04 (a/d) 0.93 (b/e) 1.11 (c/d) 5.84 (d/e)	a/d b/e d/e)	$\mathbf{x}\mathbf{x}\mathbf{x}\mathbf{x}$.037813 .072711 .024092 .012531	813 711 092 531 437	3.02(a/d) 7.01(b/e) 5.80(c/d) 3.64(d/e)	a/d) b/e) c/d) d/e)	N N N N		
Total			31													
Coefficient of variation of residual error	variat	tion of		7	0.0042	$\sqrt{0.004220 \times 2.3 \times 100}$ = 15%	2.3 × 1	00			√0.00°	$\sqrt{0.003437} \times 2.3 \times 100$ = 13.6%	3 × 10	0		

TABLE VII
THEAD WEAR RATINGS OF COMPOUNDS
(%, OF REFERENCE COMPOUND)

					(% or	(% OF REFERENCE COMPOUND)	E COMPC	(QNDO				;	1	
		Vulcan 6		-	Regal 600			Exp. Black X-3	ck X-3			Exp. Black X-5	ck X-5	
Tests 1 & 2 Rotation	55	09	60	8	60	18	09	69	78	06	09	66	78	96
Tomanou I	0 00		0 40	. 40.	0 10	0 10	* 011	0 000	* 000		000	000	000	404
- 0	88.3		87.3	107.4	94.0	94.6	112.5	100.0	100.7	97.5	82.2	86.0	79.6	10.4
77	86.1	1	101.3	95.4	91.7	105.4	96.0	0.66	89.5	85.3	2.99	67.5	2.79	70.9
8	119.0	1	8.101	105.5	86.3	95.9	9.101	101.1	85.4	82.0	62.9	80.1	76.3	85.0
4	95.8	1	104.1	103.7	29.6	87.8	100.4	98.2	77.4	75.1	64.9	69.7	61.4	9.89
Average	8.66	1	101.1	103.0	87.9	95.9	102.6	99.7	88.3	85.0	6.69	75.8	6.69	75.2
Tests 3 & 4														
Rotation														
-010	107.7	97.0	11	98.1	85.9	91.5	98.5	100.6	92.2	97.5	76.3	68.5	73.8	87.4 72.0
04	109.0	6.701	11	116.5	94.0	104.3	74.1	95.5	103.6	94.6	0.09	69.6	71.7	71.3
Average Overall average	103.5	104.6	1	108.5	94.3	99.9	86.5	91.8	95.0	97.1 91.0	70.2	73.9	74.3	76.0
					An	Analysis of Variance	Variance							
					T	Tests 1 and 2	64			T	Tests 3 and 4	1.4		
Sou	Source of	of fo	Degrees of freedom	Variance	nce	Variance ratio (F)		Sig. at	Varia	ariance	Variance ration (F)		Sig. at 5% level	
c. D. Rol	Compounds Rotations Residual		12 36 51	638.98 311.07 44.01	007	14.52		SS SS	739 9 818	739.23 9.10 81.19	9.10	0	N N N N	
Stand	Standard deviation of residual error(s)	tion of re	esidual er	rror(8)	П	± V44.01 = ± 6.6%	=± 6.69	%	11	± √81.19 = ± 9%	6 == 6	%		
Comb	Combined standard deviation	dard dev	iation			9	1	± 8.0%	%0					
0/00	onnoence	mm165 10	or compo	20 70 connucince minus for compound averages		= ± 3 × 1/ NB	n/2	₩ 0.4%	0/4					

Test route . . .

Carbon black.....

TABLE VIII RATE OF WEAR OF CONTROL HALF TREAD (MILS DEPTH LOSS PER 1000 MILES)

Test route		Fast wear				Normal wear			
Tire	. 1	2	3	4	5	6	7	8	
Test period									
1	18.0	29.0	24.0	31.0	33.0	23.5	12.	5 13.0	
2	27.5	27.0	14.5	16.5	19.5	16.0	15.0	7.0	
2 3 4	19.5	19.5	32.0	18.5	27.5	17.0	15.5	5 18.5	
4	_	23.5		31.0	21.5	23.0	6.0	13.5	
			Analysis (On logari						
Source of variance	Degrees of freedom		Sum of squares	Variance		Variance ratio (F)		Sig. at 5% level	
Tires	7		.299273	0.	042753	2.75		NS	
Periods	2		.061556	061556 0.		1.9		NS	
Residual	14		.217307	0.	0.015522				

23 Coefficient of variation

Regal 600

82.5

of residual error = $\sqrt{0.015522} \times 2.3 \times 100 = 28.6\%$

.578136

ISAF black. They provide additional latitude in compound development by making possible increased black loadings for cost reduction.

There is a trend evident in Figure 6 of decreasing tread wear rating with decreasing carbon black structure. All of the wear ratings with the lowest structure black X-5 are inferior to the control. The 78 and 90 phr X-3 black

TABLE IX TREAD WEAR RATINGS

Black X-3

Normal wear

Regal 600 Black X-3

60

Fast wear

2 3 4 Average		79 67 75 75	103	100 105 107	62 62 61 62	93,89 98,83 86,84 87	81 124 71 104	;	93 108 88 77 92
				Analys	is of variance				
		60 phr carb	on bla	iek			82.5 phr carbon black		
Source	D.F.	Variance	F	Sig. at 5% level	Source	D.F.	Variance	F ratio	Sig. at 5% level
Compounds Test route Rotations C×TR TR×R Residual	1 3 1 3 6	638 3452 332 0 333 306	11	NS VS NS NS	$\begin{array}{c} \textbf{Compounds} \\ \textbf{Tests} \\ \textbf{Rotations} \\ \textbf{C} \times \textbf{R} \\ \textbf{C} \times \textbf{T} \\ \textbf{T} \times \textbf{R} \end{array}$	1 1 3 3 1 3	1764 72 39 87 21 80	13.9	VS
	15				Residual	3	127		
Pooled Residual	10	283			Pooled	15 10	90.5		
Std. deviation of residual			±√2	$283 = \pm 16.4$	8%	±	$\sqrt{90.5} = \pm 9$.5%	
95% confidence limits $\pm 16.8 \times t/\sqrt{4} =$			±18.7%	#	$\pm 9.5 \times t/\sqrt{8} = \pm 7.4\%$				

compounds are also significantly poorer than the control compound. The differences, if any, between the other compounds and the control cannot be determined with the available data. The poor dispersion of the X-5 black may have contributed to a part of its loss in wear rating but the extent of the decrease is too large for this factor to serve as the complete explanation.

Another passenger tire screening test was conducted on retread tires to compare 60 phr and 82.5 phr loadings of Regal 600 and the experimental black X-3. A 60 phr ISAF black compound was used as the control half tread on each tire. Road tests were run on a regular highway passenger tire test route and on a special test route selected to give a fast rate of wear. The special test route contained numerous sharp curves and a more abrasive surface than the regular test route.

The depth loss per 1000 miles of the control half treads and the variance analysis of the logarithms of the data are shown in Table VIII. The relative wear ratings of the compounds and the variance analyses are given in Table IX. The coefficient of variation of the control is larger than in the previous road test program since the depth loss measurements were made at each wheel position. Differences among the compounds were detected on the fast rate of wear test route but not on the regular passenger tire test route. The normal structure Regal 600 and low structure black X-3 at 60 phr had significantly lower ratings than the control under the severe service conditions.

Increasing the black loading gave better treadwear with both Regal 600 and black X-3 on the fast wear test route. The 82.5 phr black X-3 compound is significantly poorer than the control, but the difference, if any, between the Regal 600 and the control cannot be determined at a high confidence level with the available data. The higher loading of the normal structure Regal 600 gave treadwear rating comparable with the control on both the regular test route and the fast wear test route.

SUMMARY

Oil furnace process carbon blacks have been produced which differ widely in the extent of their primary chainlike aggregation.

The effect of the carbon black structure on rubber properties and road wear was evaluated in oil-extended SBR passenger tire tread compounds. The decrease in primary particle aggregation increases the tendency to form strong, dense, secondary agglomerates which require mixing techniques designed to insure that they are well dispersed. The behavior in rubber of a series of oil furnace blacks differing primarily in their structure is most apparent in processing, shrinkage, modulus and hardness. There are small effects on rebound and flex cracking resistance but no significant effects on tensile strength and heat buildup. Carbon black structure can be reduced to some extent without encountering significant loss in road wear resistance under normal wearing conditions. Some decrease in road wear performance occurred under very severe road test conditions. The use of higher black loadings of the normal structure blacks gave good wear resistance under both normal and severe service conditions.

ACKNOWLEDGMENT

We wish to express our gratitude to Godfrey L. Cabot, Inc. for permission to publish this information. The authors also wish to acknowledge the very helpful assistance of Mrs. Fern C. Church in assembling the statistical data presented in this paper.

REFERENCES

- REFERENCES

 1 Dannenberg, E. M., Rubber Age 86, 431 (1959).
 2 Smith, W. R. and Polley, M. H., J. Phys. Chem. 60, 689 (1956).
 3 Dannenberg, E. M. and Boonstra, B. B. S. T., Ind. Eng. Chem. 47, 339 (1955).
 4 Sweitzer, C. W. and Goodrich, W. C., Rubber Age 55, 469 (1944).
 5 Braendle, H. A., Steffen, H. C., and Sheppard, J. R., Ind. Rubber World 119, 57 (1948).
 5 Sweitzer, C. W., Trans. Inst. Rub. Ind. 2, 77 (1955).
 7 Sweitzer, C. W., Trans. Inst. Rub. Ind. 2, 77 (1955).
 8 Boonstra, B. B. S. T. and Dannenberg, E. M., Ind. Eng. Chem. 46, 218 (1954).
 9 Dobbin, R. E. and Rossman, R. P., Ind. Eng. Chem. 38, 1145 (1946).
 9 Dannenberg, E. M. and Stokes, C. A., Ind. Eng. Chem. 41, 812 (1949).
 10 Leigh-Dugmore, C. H., Rubber Chem. 4 Technol. 29, 1303 (1956).
 11 Baird, C. C. and Svetlik, J. F., India Rubber World 127, 363 (1952).
 12 Buist, J. M., Trans. Inst. Rubber Ind. 26, 192 and 288 (1950).
 13 Geesink, H. A. O. W. and Prat, CL. P., Rubber Chem. 4 Technol. 31, 166 (1958).
 14 Geesink, H. A. O. W. and Prat, CL. P., Rubber Chem. 4 Technol. 31, 166 (1958).
 15 Amon, F. H. and Dannenberg, E. M. Rubber World 131, 627 (1955).
 16 Bussemaker, O. F. K., Dannenberg, E. M., Prat, C. and Westlinning, H., Proc. Int. Rubber Conf. (Washington) 117 (1959).
 17 Stiehler, R. D., Steel, M. N. and Mandel, J., Rubber Age 73, 201 (1953).

FEATURES OF THE REINFORCING ACTION OF CARBON BLACKS DEDUCED FROM THE TEAR PROPAGATION OF FILLED VULCANIZATES *

A. I. LUKOMSKAYA

SCIENTIFIC RESEARCH INSTITUTE OF THE TIRE INDUSTRY, MOSCOW, USSR

In considering the various studies that have been made on the mechanism of reinforcement of vulcanizates by carbon black we cannot but notice the contradictory conclusions drawn, which show that we do not have a sufficiently clear picture of the phenomena. All the authors acknowledge the necessity for interaction between the rubber hydrocarbon and the filler, but they hold different opinions as to the basic cause of reinforcement. Thus some of them consider that the presence of a strong bond between the rubber and the filler is necessary¹; others² point out a direct connection between the capacity of the carbon black for the formation of reticular chain structures²-5 and the high strength properties of carbon black filled vulcanizates; yet others note the presence of a large number of particles of filler per unit volume¹. 6 or other factors².

Another equally unexplained question is that of the nature of the interaction of the rubber with the filler; so far it is not possible to say with conviction whether it is of chemical or physical character^{1, 5, 7, 11}. If chemical interaction of the rubber with the filler actually takes place, it apparently does not occur by way of the sulfur bridges as is ordinarily assumed by the supporters of the chemical bond theory⁸. Confirmation of this conclusion is found in the fact that the dipole moment of the vulcanizates does not change in the presence of fillers^{5, 10}; in addition, if we accept in any measure the utility of investigation of the behavior of low-molecular analogues of the rubber hydrocarbon as being models of it, then it is interesting to note that the reaction of squalene with carbon black does not depend upon the presence of sulfur in the system¹². In connection with the conceptions of the part played by the carbon black structures, the question of the relative strength of the carbon black-carbon black and rubber-carbon black bonds^{6, 10, 13, 14} also becomes important.

As a direct result of the reinforcement we get an increase in stiffness and in such strength properties of the vulcanizates as tear propagation resistance, tensile strength, abrasion resistance, and so on. Therefore the character of the dependence of these properties upon this or that factor may be utilized to explain the essential nature of the phenomenon. In particular, in the present communication we consider the results of tear propagation of filled vulcanizates in connection with changes in temperature and rate of deformation.

EXPERIMENTAL

The experiments were carried out in the temperature range from 40° to 100° C and the range of rates of extension from 40 to 1000 mm/min on testpieces

^{*} Translated by R. J. Moseley from Vysokomolekulyarnye Soedineniya, Vol. 1, No. 9, pages 1287-1294, 1959.

A, B, and C (crescent-shaped and angular), the dimensions and shape of which are recommended by ASTM specifications¹⁵, and also on testpieces used at Delft—strips with nicks in the center¹⁶, and ring-shaped testpieces with two diametrically opposite nicks starting from the edge, of the type recommended by the German standards¹⁷ (Figure 1). With testpieces A, B, and C we varied the thickness t and the length of the nick c. We investigated the tear propagation of sulfur vulcanizates of natural rubber, sodium butadiene rubber (SKB) and butadiene styrene rubber (SKS-30) with varying amounts of Ukhta thermal or contact gas blacks. (Translator's Note. The author later refers to the latter simply as channel black, when obviously 'contact gas black' is intended.)

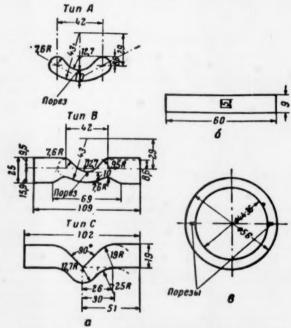


Fig. 1.—Types of testpieces for tear propagation testing: a—ASTM¹⁵; b—Delft pattern ¹⁶; c—ring specimens.

The time of cure in the press at 143° C was determined by the optimum for tear propagation resistance, according to GOST 262-53. In our experiments we recorded the load-extension curve, and noted particularly the load and total deformation of the testpiece at the instant of the commencement of tear propagation.

In the present communication we restrict outselves to those data which are of interest for the problem of reinforcement. If we compare the character of tear propagation in filled and unfilled vulcanizates, we may note the following

essential features.

1. Within the ranges of temperatures and rates employed, all types of testpieces of unfilled vulcanizates propagated the tear in the overwhelming majority

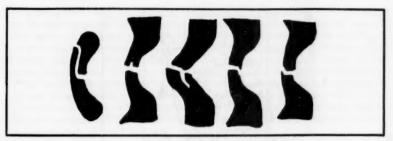


Fig. 2.—Knotty tearing of filled vulcanisates of various types.

of cases perpendicular to the direction of extension. The torn surface of the testpiece may be either smooth or rough, depending upon the rate and temperature of testing. With lower temperatures and high rates it is smooth, and at higher temperatures and low rates it is rough.

2. Filled vulcanizates within definite ranges of temperature and rate give knotty tears; the direction of failure becomes almost or entirely parallel to the direction of extension, and then turns again to the direction of the original nick of the testpiece, i.e. perpendicular to the extension. Examples of knotty tear-

ing are shown in Figure 2.

The existence of knotty tearing in vulcanizates with channel gas black was noted by Busse¹⁸, who ascribed the phenomenon to the formation of 'mechanical fibers' in the presence of an active filler, and pointed out that knotty tearing does not take place at very high rates of deformation. In actual fact it seems that at lower rates, depending upon the type of rubber and filler, knotty tearing is observed only in specific ranges of temperature and rate, which are not peculiar to vulcanizates with contact gas black; knotty tearing is also characteristic of vulcanizates with a comparatively low activity filler such as thermal black.

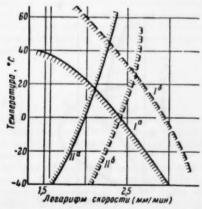


Fig. 3.—Ranges of existence of knotty tearing by temperature and rate (on left of curves) for filled veight of contact black; II—with 40 parts by weight of contact black; II—with 40 parts by weight of thermal black in tests of type B testpieces: a—without nick, b—with I m nick.

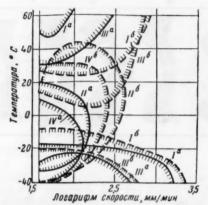


Fig. 4.—Ranges of knotty tearing (inside the curves; the direction is indicated by strokes) of filled vulcanizates based on I—SKB with 60 parts by weight of contact black; II—SKB with 60 parts by weight of thermal black; II—SKS-30 with 50 parts by weight of contact black and IV—SKS-30 with 50 parts by weight of thermal black in tests of type B testpieces: a—without nick, b—with 1 mm nick.

The first indication of this fact is found in the investigations of Greensmith¹⁹ on the tear propagation of filled rubber and GR-S vulcanizates with furnace and thermal blacks on specimens with the simple extension type of deformation. He considers the phenomenon of knotty tearing to be a consequence of the formation of a 'strengthening structure', which leads to a considerable increase in the effective diameter of the tip of the nick in the testpiece.

In Figures 3 to 5 we show the temperature and rate ranges where we observe knotty tearing of the carbon black vulcanizates under investigation. Vulcanizates of natural rubber (Figure 3) give knotty tearing at low rates of deformation. In the case of vulcanizates with contact gas black the knotty tearing range includes higher rates than in the case of thermal black. For the testpieces

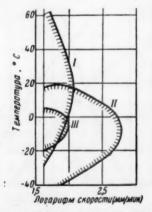


Fig. 5.—Ranges of knotty tearing of vulcanizates filled with contact gas black; I—of natural rubber with 10 parts by weight of carbon black; III—of SKB with 15 parts by weight of carbon black; III—of SKS-30 with 15 parts by weight of carbon black in tests of type B testspieces without nick.

with a nick, the knotty tearing range is shifted to higher ratios in comparison with the analogous range for testpieces of the same type but without a nick. Vulcanizates of SKB and SKS-30 with considerable amounts of channel black have two ranges of knotty tearing (Figure 4), the first at high temperatures and relatively low rates, the second at low temperatures and higher rates. With thermal black instead of contact gas black the same vulcanizates are characterized by the presence of only one range of knotty tearing, occurring at medium rates and temperatures. As in the case of vulcanizates of natural rubber, for the testpieces with a nick the range of knotty tearing is shifted towards higher rates and is considerably widened as far as temperatures are concerned in comparison with testpieces of the same type without a nick.

Reduction in the amount of contact gas black in the compounds brings them closer in properties to those with thermal black; for synthetic rubber vulcanizates the high-temperature range of knotty tearing disappears; the low temperature range shifts towards medium temperatures, while the upper limits

of the rates are reduced (Figure 5).

3. The position and width of the knotty tearing range are considerably influenced by the type of testpiece. The widest range is found with C testpieces, followed by B and A, and the least wide with Delft testpieces. On increasing the length of the nick in the testpieces the ranges for knotty tearing widen in every case.

4. The tear propagation resistance of testpieces without a nick (σ_0) , like the index of tensile strength, decreases as the temperature increases and in-

creases as the rate is increased.

With various types of testpiece of unfilled vulcanizates, and also of filled vulcanizates, in those ranges of rate and temperature where they do not give knotty tearing, it was demonstrated that the tear propagation resistance of nicked testpieces (σ) is a function of the thickness t and the width b of the testpiece, and also of the length of the nick c:

$$\sigma = \sigma_0 e^{-a \left[1/t, 1/b, (b-\varepsilon)\right]} \tag{1}$$

having a concrete form in various cases; σ_0 is the tear propagation resistance of a testpiece without a nick, of the same shape and dimensions—the magnitude σ_0 depends upon the rate of extension v and the absolute temperature T, analogously with the tensile strength, changing according to the factors which were found by Dogadkin and Sandomirskii.

$$\sigma_0 = \sigma \cdot e^{U/RT}, \tag{2}$$

$$\sigma_0 = av^n \tag{3}$$

Here a, n and U are constants of the material and R the gas constant.

For filled vulcanizates these relations are not followed in the range of knotty tearing; the tear propagation resistance is significantly higher than that calculated from Equations 1-3.

5. Knotty tearing is of course not encountered at very high rates and low temperatures. Here the work of deformation before the beginning of tearing of the filled vulcanizates has substantially reduced values, approximating those characteristic of unfilled vulcanizates.

6. In investigating the effect of prior (repeated) extension of a material we subjected sheets to fatigue from which we later blanked out Delft testpieces

perpendicular and parallel to the direction of extension. It was observed that natural rubber vulcanizates with contact gas black give higher figures for tear propagation resistance if the tear propagation takes effect perpendicular to the direction of prior deformation (Figure 6). With natural rubber vulcanizates with thermal black and with filled vulcanizates of SKS-30 and SKB this effect is not noticed in practice. It is very interesting that in the case of the Delft testpieces prior deformation does not displace the ranges of knotty tearing either for rates or for temperatures. We did not investigate the other types of testpiece in tests with prior stretching.

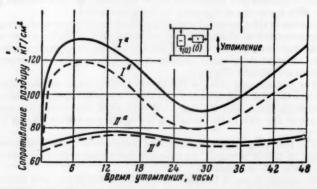


Fig. 6.—Dependence of tear propagation resistance of Delft testpieces upon time and direction of repeated extension (extension by 25%). I—for vulcanizates filled with contact gas black, based on natural rubber; II—for vulcanizates filled with thermal black, based on natural rubber, in tear propagation: a—perpendicular to the direction of extension; b—parallel to the direction of extension.

DISCUSSION OF RESULTS

The failure of a uniform material takes place at its most highly stressed section, and that of a nonuniform material, for a uniform distribution of the stresses, at its weakest section. With nonuniform distribution of the stresses the nonuniform material fails at that point where the stresses reach its limit of strength. In the tear propagation of testpieces like those shown in Figure 1, the maximum destructive stresses act from the tip of the nick (or from an analogous portion of stress concentration) along the direction of extension.

The change in the direction of failure in knotty tearing may be connected with nonuniformity of structure of the deformed material, which is a cause of anisotropy of strength in small portions of the material. A similar explanation of knotty tearing was put forward by Mason¹⁹. Prior deformation, giving rise to anisotropy of the material, likewise gives nonuniformity of structure, but of a different character. In contrast with the previous case, with nonuniform structure of the material we do not distinguish definite directions with identical properties.

Nonuniformity of stress distribution cannot in itself be the cause of knotty tearing; with increase in the nonuniformity of stresses, caused by an increase in the length of the nick or increased complication of the shape of the testpiece, the ranges of knotty tearing may be displaced or widened, but new ranges are not formed, as is seen by comparing them for testpieces of different type. Knotty tearing is characteristic only of rubbers filled with carbon black. Since

knotty tearing is not observed under all conditions of deformation, the presence of carbon black is a necessary, but not self-sufficient, condition for its existence. The ranges of knotty tearing occur at lower rates and higher temperatures, which indicates the possibility of the existence of some kind of processes, proceeding over a period and becoming most evident when their rates are comparable with the rates of deformation.

In the literature there are described a whole series of facts about the existence of ranges of temperature and rates of deformation in which the properties of filled vulcanizates approximate those of unfilled, i.e. ranges where as in the case where knotty tearing is not observed, the effect of the fillers is not very evident: the independence of the conventional equilibrium modulus of carbon black vulcanizates²¹ and of the distribution parameter of the times of dipole relaxation (at temperatures above 100°)¹⁰ upon the degree of filling: the approximation of the stiffness of filled vulcanizates to the corresponding indices of unfilled vulcanizates under repeated deformations², and of the strength in failure in a direction parallel to the prior deformation²²; the identical heat effect per unit of work in the adiabatic deformation of filled and unfilled vulcanizates²³; the drawing together of the values of work of deformation exerted up to the beginning of tear propagation for filled and unfilled vulcanizates at high rates of tearing, found in the present investigation, and a number of other data⁵.

With high contents of contact gas black in vulcanizates of the synthetic rubbers SKB and SKS-30 there occur two ranges of knotty tearing (Figure 4), which may be explained by two types of time processes, one of which takes place on larger portions, at higher temperatures and low rates, and the other on smaller portions, at lower temperatures and high rates. The high temperature range of knotty tearing disappears when we reduce the amount of contact gas black (Figure 5) and is not observed at all in compounds with thermal black. As is well-known, a carbon black chains are lacking in the vulcanizates in such cases. Therefore, apparently, the processes of the first type must be connected

with the presence of carbon black chains in the vulcanizates.

The ranges of knotty tearing, situated at lower temperatures and observed at any given content whether of contact or thermal black (Figures 4 and 5) are in all probability connected with the presence of carbon black particles. For vulcanizates with contact gas black they are displaced towards higher rates and low temperatures in comparison with vulcanizates containing thermal black (Figure 4). An analogous displacement is brought about by increasing the length of the nick in the testpieces and by increasing the complication of the shape of the testpiece, which involves increasing the nonuniformity of the stress distribution.

By comparing Figures 4 and 3, it is possible to explain the disappearance of one of the ranges of knotty tearing in natural rubber vulcanizates with high content of contact gas black. Here there emerges quite clearly the analogy of the low temperature range in vulcanizates of synthetic rubber and of all the temperature ranges investigated in vulcanizates of natural rubber. From this it follows that with the testing rates and temperatures employed in practice only the presence of carbon black particles, and not that of chains, is of significance. This possibly explains in part the relatively lower reinforcement in carbon black vulcanizates of natural rubber in comparison with carbon black vulcanizates of synthetic rubbers.

Such is the additional data on the reinforcing effect of carbon blacks obtained by investigation of the tear propagation behavior. It shows that reinforcement must not be regarded, as has usually been understood, as the result solely of a reduction in the deformability and increase in the strength as a result of interaction of the rubber polymer with the filler. Reinforcement is connected also with an increase in the path of failure as a result of the alteration in the structure of the material. This alteration takes place when carbon black particles and chains are present in the vulcanizate, influencing the time processes which take place in the deformation of filled vulcanizates.

CONCLUSIONS

1. The reinforcing action of carbon blacks is most clearly apparent in the knotty tearing of carbon black rubbers.

2. Knotty tearing is characteristic of rubbers filled with carbon black in definite ranges of deformation and temperature, the position of which depends upon the type of rubber and carbon black.

3. With high contents of contact gas black in vulcanizates of sodium butadiene (SKB) and butadiene sytrene (SKS-30) rubbers two ranges of knotty tearing occur. The first is situated at relatively high temperatures and low rates and the second at relatively low temperatures and higher rates. Reduction in the content of black in these vulcanizates leads to the disappearance of the high temperature range of knotty tearing and the displacement of the lowtemperature range towards higher temperatures and low rates. This position of the ranges (at medium rates and temperatures) is characteristic also of the said synthetic rubbers containing thermal black.

4. The first range of knotty tearing of filled SKB and SKS-30 vulcanizates with contact black is linked with the presence in them of carbon black chains, while the second range, existing also with vulcanizates with thermal black, is connected with the presence of carbon black particles.

5. Within the ranges of ates from 40 to 1000 mm/min and of temperatures from 40 to +100° C filled vulcanizates of natural rubber have one range of knotty tearing situated at lower rates. In the case of the presence in them of contact gas black the range is shifted towards higher rates than in the case of

6. Increasing the length of the nick in testpieces being tested for tear propagation leads to a shift in the range of knotty tearing towards higher rates and widens it with respect to temperatures. This same effect is noted on altering the shape of the testpiece, starting with the Delft testpieces and proceeding to types A, B, and C¹⁵, i.e. increasing the nonuniformity of stress distribution in the deformed testpieces.

REFERENCES

- Blanchard, A. F., and Parkinson, D., Proc. Second Rubber Technol. Conf., London, 1948, p. 414; Trans. Inst. Rubber Ind. 23, 259 (1948); Blanchard, A. F., Trans. Inst. Rubber Ind. 32, 124 (1956).
 Mullins, L., J. Rubber Research 16, 275 (1947); J. Phys. & Colloid Chem. 54, 239 (1950); Trans. Inst. Rubber Ind. 32, 23 (1956).
 Mullins, L., and Tobin, N. R., Proc. Third Rubber Technol. Conf., London, 1954, p. 397.
 Dogadkin, B. A., Pechkovskays, K. A., and Milman, Ts., Kolloid. Zhur. 14, 250; 346 (1952); Rubber Chies. & Technol. 26, 821 (1953).
 Dogadkin, B. A., and Pechkovskays, K. A., Proc. Third All-Union Conf. on Colloid Chem., Akad. Nauk SSSR, 1956, p. 371; Dogadkin, B. A., and Lukomskays, A. I., ibid., p. 363.
 Guth, E., Proc. Second Rubber Technol. Conf., London, 1948, p. 353.
 Tarkinson, D. Trans. Inst. Rubber Ind. 19, 131 (1943); Ibid. 21, 7 (1945). "Advances in Colloid Science", Vol. II, Interscience Publishers, Inc., New York, 1946, p. 389.
 Staarns, R. S., and Johnson, B. L., Ind. Eng. Chem. 43, 146 (1951).
 Studebaker, M. L., and Nabors, L. G., Rubber Age 80, 1027 (1957).
 Dogadkin, B. A., and Lukomskays, A. I., Doklady Akad. Nauk SSSR 88, 1015 (1953); Rubber Chem. & Technot. 28, 291 (1955); Kolloid Zhur. 15, 183; 259 (1953); ibid. 16, 36 (1954).
 Havenhill, R. S., Carlson, L. E., and Rankin, J. J., Rubber Chem. & Technot. 22, 477 (1949); Trans. Inst. Rubber Ind. 27, 339 (1951); Havenhill, R. S., Carlson, L. E., Emery, H. F., and Rankin,

-

- J. J., Ind. Eng. Chem. 45, 1128 (1953); Havenhill, R. S., Carlson, L. E., and Rankin, J. J. Rubber Age 79, 75 (1956).

 12 Studebaker, M. L., and Nabors, L. G., Rubber Age 80, 1027 (1957).

 13 Ladd, W. A., and Wiegand, W. B., Rubber Age 57, 299 (1945).

 14 Dobbin, R. E., and Rossman, R. P., Ind. Eng. Chem. 38, 1145 (1946).

 15 ASTM Designation: D624-54, "ASTM Standards on Rubber Products", American Society for Testing Materials, Philadelphia, 1960, p. 349.

 15 International Standards Organisation/TC 45 (Secretariat 185) 293, 1956; Nijveld, H. A. W., Proc. Second Rubber Technol. Conf., London, 1948, p. 256.

 15 DIN, Specification 53504.

 16 Busse, W. F., Ind. Eng. Chem. 26, 1194 (1934); Rubber Chem. & Technol. 8, 122 (1935).

 18 Greensmith, H. W., J. Polymer Sci. 21, 175 (1956); P. Mason in discussion of paper by H. W. Greensmith in "The Rheology of Elastomers" Pergamon Press, London, 1958, p. 113.

 28 Dogadkin, B. A., and Sandomirskii, Kolloid Zhur. 13, 287 (1951).

 29 Rennikovskii, M. M., Priss, L. S., and Dogadkin, B. A., Kolloid Zhur. 16, 211 (1954).

 29 Janssen, H. J. J., Proc. Third Rubber Technol. Conf., London, 1954, p. 351.

 29 Votinov, M. P., and Kuvshinskii, E. V., Zhur. Tekh. Fiz. 27, 2307 (1957).

RUPTURE OF RUBBER. VI. FURTHER EXPERIMENTS OF THE TEAR CRITERION *

A. G. THOMAS

THE NATURAL RUBBER RESEARCH AND DEVELOPMENT BOARD WELWYN GARDEN CITY, HERTS, ENGLAND

1. INTRODUCTION

In previous papers (I to V of this series)1-5, a tear criterion for rubbers has been proposed based on an energy balance approach. This equates the energy required to form new surfaces (the tearing energy) with the loss of elastic strain energy in the test piece. The tearing energy T is assumed to be characteristic of the material and so independent of the overall shape of the test piece. It is thus the fundamental property controlling tear behavior. The correctness of this approach was investigated by making tear measurements on test pieces of different shapes but of the same material and examining the constancy of the T values obtained1,5. The results were consistent with the theory but not wholly conclusive, due primarily to the particular tearing behavior of the materials used (natural rubber gum vulcanizates). Another limitation was that accurate T values could be obtained only if they could be calculated directly from the measured tearing forces or elongations, and the required relationships were known for only two types of test piece. Clearly, the more test pieces available for comparison and the more they differ from each other in shape, the more stringent the test of the basic theory. In the present paper a third test piece is described, the necessary theory given, and experimental results presented on the three test pieces. By comparing the results from these test pieces, which are of widely different shapes, a critical test of the theory is possible.

The choice of the experimental material is influenced by several factors. Previous measurements have been made on natural rubber gum compounds¹, which have the advantage of possessing excellent elastic properties but whose rupture characteristics are such that tearing occurs at a critical load. In contrast, a gum GR-S tears more or less steadily at a rate depending on the load³, a characteristic which is experimentally advantageous for the particular test pieces described here. It was therefore used in this investigation.

2. COMPARISON OF THE "PURE SHEAR" AND "SIMPLE EXTENSION" TEAR TEST PIECES

The proposed tear criterion states that the amount of work necessary to make a cut of length c grow by a small amount Δc , thus creating an area $t\Delta c$ of new surface, is equal to $Tt\Delta c$, where T is a constant of the material and independent of the overall shape of the test piece and t is the thickness. If this cut growth occurs without the applied forces on the test piece moving, the energy is derived only from the elastic strain energy in the test piece. The criterion can thus be written as

$$-1/t(\partial W/\partial c)_l = T \tag{2.1}$$

^{*} Reprinted from the Journal of Applied Polymer Science, Vol. 3, pages 168-174, 1960.

where W is the total strain energy and the subscript l indicates that the differentiation is carried out with the applied forces not moving and so doing no work.

In part I the quantity $1/t(\partial W/\partial c)_l$ was calculated for two test pieces, called "simple extension" and "pure shear" (Figures 1 and 2) in terms of their dimensions, the elastic properties of the material, and the applied forces or strains. The dimensions of the simple extension test piece are such that there are regions in simple extension in the arms and a substantially unstrained region beyond

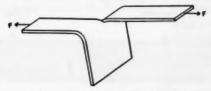


Fig. 1.—Simple extension tear test piece.

the tip of the cut. The calculation for this test piece gives [Equation (6.8 in I)]:

$$- (\partial W/\partial c)_{l} = 2\lambda F - E_{s}A_{0}$$
 (2.2)

where F is the applied force, λ the extension ratio in the arms, E_0 the elastically stored energy per unit volume in the arms, and A_0 the unstrained cross sectional area of the test piece. The pure shear test piece must have regions A unstrained and a region B in pure shear. The calculation for this test piece gives [Equation (6.10) in I]:

$$-1/t(\partial W/\partial c)_{l} = E_{s}l_{0} \tag{2.3}$$

where E_{\bullet} is the elastically stored energy per unit volume in the pure shear region and l_0 is the unstrained length of the test piece.

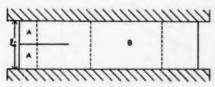


Fig. 2.-Pure shear tear test piece.

In part I, experiments were done to test Equations (2.1)-(2.3) using natural rubber pure gum vulcanizates. A test piece of this material pulled slowly at room temperature tears catastrophically, giving a single value of T. A GR-S gum rubber, however, tears continuously³, the rate of tearing depending strongly on the applied load. In this case, therefore, T has no unique value but is a function of the rate of tearing τ , and comparisons have to be made over a range of τ and T.

The same GR-S vulcanizate was used for all the measurements reported in this paper, the formulation being given in Table I. The dependence of T on r for a simple extension test piece was found by the method described in part III, viz., by pulling the test piece at known rates of clamp separation and measuring

the average tearing forces developed. The T values were calculated from the forces by Equation (2.2), and the results are shown as the full curve in Figure 3.

The corresponding measurements on the pure shear test piece were made as follows. The apparatus for extending the test piece was similar to that described in II, consisting of two parallel clamps, about 30 cm long, the separation of which could be varied by screws. With l_0 about 5 cm, the strain distribution

TABLE I

Component	Parts		
Polysar S	100		
Zinc oxide	5		
Stearic acid	2		
Nonox H.F.N.	1		
Santocure	1		
Sulfur	1.75		

Cure: 145° C for 50 min

conditions for this test piece were satisfied for 5 cm < c < 15 cm, with wider tolerances for smaller l_0 values. The test pieces were strained to a suitable extent and λ_s calculated from the measured separations of marks on the rubber. The incision was then made, and during the subsequent tearing the passage of the tip past reference marks on the rubber was timed, giving r. To find T, E_s must be known in terms of λ_s . This relation was found by integrating graphically under the pure shear stress-strain curve obtained by the method of Rivlin

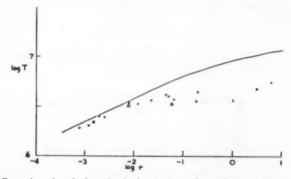


Fig. 3.—Comparison of results from the simple extension and pure shear test pieces: (——) simple extension test piece with constant rate of grip separation: (\blacksquare) simple extension test piece with use of constant force apparatus; pure shear test piece for (\triangle) $l_0 = 5.0$ cm; (+) $l_0 = 3.0$ cm; (\times) $l_0 = 1.5$ cm.

and Saunders⁷. Equations (2.3) and (2.1) then gave *T*. Test pieces of lengths 1.5, 3.0, and 5.0 cm were used, and the results are shown in Figure 3, where they may be compared with those obtained from the simple extension test piece.

The results show (1) that the pure shear measurements are self-consistent, the results for test pieces of different lengths agreeing with each other; (3) that there is approximate agreement with the simple extension measurements below rates of about 10^{-2} cm/sec; and (3) that above this critical rate r_c , however, there is marked disagreement between the behavior of these two test pieces, the pure shear test piece giving much higher rates of tear. The manner of

tearing of the pure shear test piece undergoes a fairly abrupt change at r_c . At lower rates, r fluctuates somewhat, but it is rarely more than about three times the average. Above r_c , the rate fluctuates between low values ($\sim 10^{-2}$ cm/sec) and much higher ones ($\sim 1-10$ cm/sec), and the tearing has a "stick-slip" character. The average rate observed in this region is governed by the relative times the tear is in the "stick" or "slip" states. The appearance of the torn surfaces correlates with these rate changes. Below r_c the surfaces are rough and irregular, but above it in the "slip" regions they are much smoother and reflect light specularly; in "stick" regions they are rough. The photographs in Figure 4 illustrate this.



Fig. 4.—Photographs of torn surfaces (left) torn at low rates; (right) torn at high rates.

The large fluctuation in tearing rate observed with the pure shear test piece above r_c suggests that the discrepancy between this and the simple extension test piece may arise from the different averaging procedures. The method of measurement with the latter test piece is to separate the arms at a known constant rate and measure the resulting force. The latter is not constant, fluctuating by about $\pm 20\%$ in this region; also the actual rate of cut growth varies considerably due to the compliance of the test piece and the force measuring device. Thus both r and T are averages. In the pure shear case, T is governed by the strain in the test piece and, apart from the slight inertial effect of the

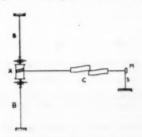


Fig. 5.—Constant force apparatus.

rubber, should be constant with time and independent of r. This measurement therefore gives an average at constant T in contrast with the simple extension case, in which both T and r fluctuate.

To find if this explanation of the discrepancy is correct, measurements were made on the simple extension test piece under conditions nearer to constant T, i.e., constant applied force F. A dead load applied by a weight is not satisfactory if stick-slip behavior is expected, as the accelerations may be comparable with the gravitational acceleration. A device, shown in Figure 5, was therefore constructed to produce a substantially constant force with little associated inertia. An aluminum drum A, about 0.5 cm in diameter, was connected to rubber strips about 30 cm long, and a thin nylon monofilament wound on it. This was connected to one arm of the test piece C, the other arm being joined

to a cantilever spring S. This carried a mirror M, so that, by use of a lamp and scale, the force could be found. The rubber strips were twisted by devices at their ends (not shown) and so transmitted a force to the test piece. The inertia associated with the drum and the elastic strips was small, being comparable to that of the test piece itself. As the test piece tore, the strips untwisted and the force fell, but this change was kept to within 5% of the mean.

Test pieces with dimensions of about $10 \times 3 \times 0.1$ cm were used. The results, given in Figure 3, show that the discrepancy with the pure shear measurements is now greatly reduced. The remaining differences may be due to the appreciable inertia still present, mostly in the test piece itself, as the force indicated by the spring still showed noticeable fluctuations. The substantial

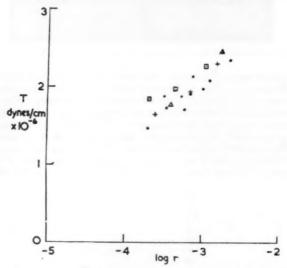


Fig. 6.—Comparison of results from simple extension and pure shear test pieces at low tearing rates: (\bullet) simple extension; pure shear for (\boxdot) $l_0 = 5.0$ cm, (\triangle) $l_0 = 3.0$ cm, (+) $l_0 = 2.0$ cm.

improvement obtained does, however, indicate that the original discrepancy was due primarily to the suggested cause and not to a basic deficiency in the theory.

3. FURTHER RESULTS ON THE PURE SHEAR AND SIMPLE EXTENSION TEST PIECES

In view of the tear behavior of GR-S at tearing rates greater than 10⁻² cm/sec, accurate comparisons of different test pieces are best carried out below this rate. The results of Section 2 show approximate agreement in this range, but more results are needed to establish this definitely.

The present experiments were all done on test pieces cut from the same sheet of rubber (prepared as before) to minimize variations. The simple extension measurements were made by hanging weights on the test pieces and observing the rate of movement of the arms. The pure shear measurements were carried out as described in Section 2 on three different sizes of test piece.

The experiments were done at room temperature, which was $20\pm2^{\circ}$ C. This variation was found to have a perceptible effect, so subsidiary measurements were made at 17 and 25° C which indicated a change in T with temperature of 0.075 kg/cm/° C for a fixed rate of tearing. The results were then corrected to 20° C.

The results for both the simple extension and pure shear test pieces are shown in Figure 6. The agreement between these two test pieces and between the pure shear test pieces of different sizes is very satisfactory, all giving results consistent with the same T-r relation.

4. CALCULATIONS ON THE SPLIT TEAR TEST PIECE

In this section a new tear test piece is described and its elastic properties calculated so that the tear criterion may be applied.

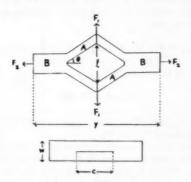


Fig. 7.-Split tear test piece.

The test piece is shown in Figure 7. It is deformed by two pairs of forces F_1 and F_2 , and its dimensions are such that there are regions A and B in simple extension. The force S in region A makes an angle θ with the test piece axis, and the extension ratios in regions A and B are λ_1 and λ_2 , respectively.

For the tear criterion to be applied, $(\partial W/\partial c)_{l,y}$ must be known in terms of directly measurable quantities.

We have

$$dW = (\partial W/\partial c)_{l,y}dc + (\partial W/\partial l)_{c,y}dl + (\partial W/\partial y)_{c,l}dy$$
 (4.1)

and

$$F_1 = (\partial W/\partial l)_{c,y}$$

$$F_2 = (\partial W/\partial y)_{c,l}$$
(4.2)

Hence, by substitution,

$$(\partial W/\partial c)F_{1,F_{2}} = (\partial W/\partial c)I_{1,y} + F_{1}(\partial U/\partial c)F_{1,F_{2}} + F_{2}(\partial y/\partial c)F_{1,F_{2}}$$
(4.3)

As regions A and B are in simple extension, the complex strains around the points of applications of F_1 and around the ends of the cut will not vary with c, provided F_1 and F_2 are constant. If c increases by Δc , for example, the regions at the ends of the cut will move outwards by Δc but will still have the

same total stored energy, the net effect being for regions A to grow at the expense of regions B. Under these conditions

$$F_1 = 2S \sin \theta$$

$$F_2 = 2S \cos \theta$$
(4.4)

$$(\partial l/\partial c)F_{1,F_{2}} = \lambda_{1}\sin\theta \tag{4.5}$$

$$(\partial y/\partial c)F_1F_2 = \lambda_1 \cos \theta - \lambda_2 \tag{4.6}$$

$$(\partial W/\partial c)F_1F_2 = wt(E_1 - E_2) \tag{4.7}$$

In Equation (4.7), E_1 and E_2 are the stored energies per unit volume in the regions A and B, respectively. They can be found from λ_1 and λ_2 by using the measured stress-strain relation for the rubber. Substituting Equations (4.5)–(4.7) in Equation (4.3), yields

$$-(\partial W/\partial c)_{l,y} = F_1 \lambda_1 \sin \theta + F_2(\lambda, \cos \theta - \lambda_2) - wt(E_1 - E_2)$$
 (4.8)

and, from Equation (4.4) we obtain

$$an \theta = F_1/F_2 \tag{4.9}$$

Thus, Equations (4.4), (4.8), and (4.9), together with the stress-strain curve, give $(\partial W/\partial c)_{t,y}$ in terms of F_1 and F_2 .

If $F_2 = 0$, the test piece becomes equivalent to two simple extension test pieces joined together, and Equation (4.8) reduces to Equation (2.2), apart from the factor of 2. When F_2 is comparable with F_1 , the behavior of the test pieces is very different, and it is in this range that comparisons will be made.

A very useful approximation to Equation (4.8) can be made when λ_1 is not much greater than λ_2 . Putting $\lambda_1 = \lambda_2 + \Delta \lambda$, we have approximately

$$wt(E_1 - E_2) = \Delta \lambda (F_2 + 2S)/2$$
 (4.10)

From Equation (4.4) we have

$$2S = \sqrt{F_1^2 + F_2^2} \tag{4.11}$$

and, substituting (4.9), (4.10), and (4.11) in Equation (4.8), we obtain

$$- (\partial W/\partial c)_{l,y} = \tilde{\lambda}(\sqrt{F_1^2 + F_2^2} - F_2)$$
 (4.12)

where $\tilde{\lambda} = \frac{1}{2}(\lambda_1 + \lambda_2)$. Comparison of the exact relation, Equation (4.8), with Equation (4.12) for a rubber obeying the statistical theory indicates that Equation (4.12) is a good approximation; for example, with $\lambda_1 = 3.0$ and $\lambda_2 = 1.5$, it is in error by less than 2%. In the experiments on this test piece the error from this cause is even less.

The relation (4.12) can be conveniently represented graphically by $-(\partial W/\partial c)_{l,y}(F_2/\bar{\lambda}F_1^2)$ as a function of F_1/F_2 , and this is given in Figure 8. As F_1/F_2 approaches zero, the ordinate tends to $\frac{1}{2}$, and, in fact, departs relatively slightly from this for values of F_1/F_2 met with in the experiments.

5. EXPERIMENTS ON THE SPLIT TEAR TEST PIECE

Consideration of this test piece suggests that a tear growing along the central line will be unstable, tending to deviate towards the edge, and experiment confirms this. To overcome this difficulty, the test pieces were scored along the intended path of the tear. By holding the rubber sheet in a special jig and using a razor blade in a holder running on guides, accurately aligned score marks could be made on both faces to a controlled depth. If the unscored thickness was about half the original, the tear was found to be stable.

Preliminary measurements were made to ensure that the elastic conditions postulated in Section 4 were fulfilled. Equation (4.5) is the crucial relation, and this could be easily checked by measuring the separation l of the grips as a function of c for various combinations of F_1 and F_2 . The slope $(\partial l/\partial c)F_1,F_2$ is $\lambda_1 \sin \theta$ according to Equation (4.5); θ can be found from Equation (4.9), and

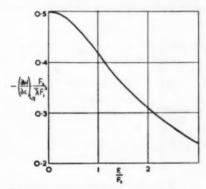


Fig. 8.—Theoretical relation for split test piece from Equation (4.12).

 λ_1 from the stresses and the measured stress-strain curve. The measured value of $(\partial l/\partial c)F_{1,F_{2}}$ and $\lambda_{1}\sin\theta$ agreed to within 5%, provided c/w>3 and $\lambda_{1}>1.15$. Both these conditions were amply fulfilled in the subsequent experiments.

The test pieces used for the tearing measurements were about 1 cm wide, 12 cm long, and 2 mm thick; the unstrained cut lengths were about 5 cm initially. The unscored thickness was found by microscopic measurement of the torn surface and was usually about 0.8 mm. Marks were made on the test piece in the unstrained state so that the rate of cut growth r could be found by timing the passage of the tip past them, as the rate must, of course, be referred to the unstrained state.

The test pieces were loaded under various combinations of F_1 and F_2 and the corresponding rates of tearing measured. These were always below the critical rate $r_c \, (\sim 10^{-2} \, \mathrm{cm/sec})$, so that the tearing was steady. The values of T were calculated from Figure 8 and Equation (2.1), $\bar{\lambda}$ being found from the measured stress-strain curve of the material. In Equation (2.1), the torn thickness must now be used.

In order to check the tear criterion, the above results were compared with those from simple extension test pieces. It was necessary for these to be scored in a similar manner, as it was possible that this might affect the tearing process.

The simple extension test pieces were cut from the same sheet and tested as described in Section 3. The results from both test pieces are shown in Figure 9, correction having been made for slight variations in ambient temperature from 20° C. The agreement is again very satisfactory.

Although the above comparison was made with the use of scored test pieces throughout for consistency, the T-r relation obtained differs in fact very little

from that found for the unscored ones (Figure 6).

The results from the three tear test pieces at low tearing rates are all mutually consistent when expressed in terms of the tearing energy, despite their very different shapes. This agreement is good evidence for the fundamental nature of this parameter.

The discrepancy at high tearing rates found initially between the pure shear and simple extension results could be largely eliminated by applying the tearing force to the latter test piece so that fluctuations in rate and tearing force were

This quite marked effect on the results from this test piece of the

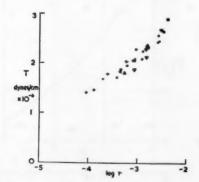


Fig. 9.—Comparison of results from simple extension and split tear test pieces: (\bullet) simple extension; split test piece with (\boxdot) $F_2 = 0.7$ kg, (\bigtriangledown) $F_2 = 0.6$ kg, (+) $F_2 = 0.5$ kg, (\triangle) $F_2 = 0.4$ kg, (\bigcirc) $F_2 = 0.3$ kg

method of applying the load indicates that the significance of such measurements must be assessed cautiously if there is any tendency for stick-slip behavior. In part III, stick-slip tearing was ascribed to the formation of a strengthening structure at low rates of tear that had insufficient time to form at high rates, giving a negative slope to the T-r relation. This explanation could also hold for the exaggerated effect found here, although the magnitude is rather surprising for a material which is supposed to be noncrystallizing. The change in the appearance of the torn surface from rough to smooth at the critical tearing rate τ_c suggests that the change in T is associated primarily with a change in the effective radius of the tear tip².

The validity of the tearing energy concept has now been tested under a variety of conditions: (1) for catastrophic tearing of natural rubber¹, (2) for cut growth in natural rubber⁵, and (3) steady tearing of GR-S. The same concept appears to be valid for the hard plastics, polymethyl methacrylate and polystyrene (Benbow and Roesler⁸). The original work along these lines by Griffith⁹ was on glass. The theory, therefore, appears to be of quite wide

application.

SYNOPSIS

A criterion for the tearing of rubber based on an energy balance approach, proposed previously, has been critically examined experimentally. This criterion implies that the energy required to form unit area of surface by tearing should be a constant of the material, and it can be tested by finding if tearing results from test pieces of different shapes are self-consistent. Previous work has indicated that the criterion is approximately correct for natural rubber, and the present paper gives a much more rigorous check for a noncrystallizing and therefore more convenient material (GR-S). The results from three test pieces of widely different shapes show excellent agreement. The material used exhibited an abrupt change in the mode of tearing as the tearing energy increased through 3 × 106 ergs/cm², the rate of tearing suddenly increasing from about 10-2 to 10 cm/sec. This correlated with a change in the appearance of the torn surfaces from rough to smooth.

ACKNOWLEDGMENT

This work forms part of a program of research undertaken by the Board of the British Rubber Producers' Research Association.

REFERENCES

- ¹ Rivlin, R. S., and Thomas, A. G., *J. Polymer Sci.*, **10**, 291 (1953).

 ² Thomas, A. G., *J. Polymer Sci.* **18**, 177 (1955).

 ³ Greensmith, H. W., and Thomas, A. G., *J. Polymer Sci.* **18**, 189 (1955).

 ⁴ Greensmith, H. W., *J. Polymer Sci.* **21**, 175 (1956).

 ⁵ Thomas, A. G., *J. Polymer Sci.* **31**, 467 (1968).

 ⁶ Greensmith, H. W., private communication.

 ⁷ Rivlin, R. S., and Saunders, D. W., *Phil. Trans. Roy. Soc. London* **A243**, 251 (1951).

 ⁸ Benbow, J. J., and F. C. Roesler, *Proc. Phys. Soc. (London)* **B70**, 201 (1957).

 ⁹ Griffith, A. A., *Phil. Trans. Roy. Soc. London* **A221**, 163 (1920).

RUPTURE OF RUBBER. VII. EFFECT OF RATE OF EXTENSION IN TENSILE TESTS *

H. W. GREENSMITH

THE NATURAL RUBBER RESEARCH AND DEVELOPMENT BOARD, WELWYN GARDEN CITY, HERTS, ENGLAND

INTRODUCTION

There are few published measurements on the effect of rate of extension in tensile rupture tests on rubber vulcanizates. The most extensive data on a single vulcanizate are those of Dogadkin and Sandomirskii¹ and of Smith². These measurements were made on GR-S gum vulcanizates and covered a similar range of rates of extension, from about 0.02 to 20%/sec. Ring specimens were used in both cases, and tensile strength and breaking extension were measured over a wide temperature range. Villars³ has made tensile strength and breaking extension measurements on double dumbbell specimens of several gum and filled vulcanizates extended at various rates in the range 10,000 to 100,000%/sec. Kainradl and Handler⁴ have reported tensile strength measurements for several filled vulcanizates, obtained with dumbbell specimens extended at four different rates of extension covering a range from about 1 to 100,000%/sec. All these results indicate that tensile strength and breaking extension can vary appreciably with the rate of extension of the specimen. Complete load-extension curves are not given in any of these papers.

In the present paper an autographic method is described for obtaining the load-extension curves of ring specimens extended at various rates from about 0.1 to 2000%/sec. Results showing the effect of the rate of extension on the tensile strength and breaking extension and on the load-extension curve are given for GR-S vulcanizates. The data were obtained primarily for the comparisons of tear and tensile rupture measurements given in a subsequent paper

(Part VIII)5.

EXPERIMENTAL

METHOD OF MEASUREMENT

The main features of the tensometer which was used are shown schematically in Figure 1. The ring specimen was looped, as shown, over two small rollers, one roller being mounted on an auxiliary crosshead attached to the main crosshead of the tensometer, the other roller and its mounting being coupled to a cantilever spring which measured the force on the ring. The tensometer drive consisted of an endless chain mounted on a pair of sprocket wheels immediately below the crossheads and driven via a multispeed gear box by a variable-speed motor. The chain was driven continuously at the chosen speed, and the main crosshead was set in motion by depressing a pin in the crosshead so as to engage with the links of the chain. Provision was made for the pin to move out of engagement with the chain at the end of the crosshead traverse. A slotted coupling between the main and auxiliary crossheads ensured that the auxiliary

^{*} Reprinted from the Journal of Applied Polymer Science, Vol. 3, pages 175-182, 1966.

crosshead was not set in motion until the main crosshead was moving at uniform speed. The deflection of the cantilever spring was magnified by an optical lever (not shown), and the deflection of the light spot was recorded on a drum camera geared to the chain drive, the curve traced out on the drum camera film giving, therefore, the force on the ring as a function of the distance travelled by the crosshead.

The cantilever spring system was sufficiently stiff for the displacement of the roller coupled to the spring to be negligible in comparison with the extended length of the specimen. The response time of the spring system was about 2 msec. The rollers were 6 mm in diameter, machined from reinforced resin material, and rotated on steel pins. The reproducibility of load-extension measurements indicated that the rollers adequately equalized tensions in the ring specimens. The ring specimens were immersed during extension in a water or alcohol bath maintained at the test temperature to $\pm 1^{\circ}$ C. Crosshead speeds from about 6×10^{-3} to about 60 cm/sec could be obtained. The speeds were calculated from the motor speed as measured by a tachometer.

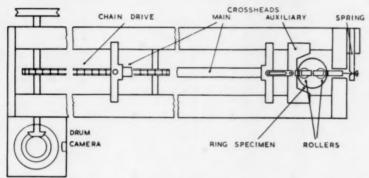


Fig. 1.—Schematic diagram of tensometer.

Ring specimens were cut out from a sheet of vulcanizate by means of double-bladed cutters. Rings of 2 and 3 cm internal diameter were used, the larger rings being employed for vulcanizates of relatively low breaking extension. The thickness of the rings, i.e., the difference between the external and internal radii, was about 0.7 mm and the width was 1.5–3 mm, depending on the thickness of sheet from which the rings were cut. The mean cross-sectional area of the ring was derived from the weight and internal diameter and the density of the vulcanizate.

Extensions were calculated from the increase in length of the ring as given by the force-distance record, taking as the initial length of the ring the mean circumferential length. It was observed that a portion of the ring in the region of contact with the rollers was not fully extended, and it was estimated that this would cause the extensions calculated as described above to be about 5% low. This was the main source of error in the measurement of the extension of the ring. Loads/unit undeformed area were calculated on the basis of the mean undeformed cross-sectional area.

The number of rings extended at each rate of extension varied from three to six, depending on the scatter in the values for breaking load and extension.

TABLE I

	C	ompounding reciporate by weight	pe	
Vulcanizate	A	В	C	Cure
Polysar S	100	100	100	50 min.
HAF black	***************************************	50	-	145° C
SRF black	-	_	50	
Sulfur	1.75	1.75	1.75	
Zinc oxide	5	5	5	
Stearic acid	2	2	2	
Santocure	1	1	1	
Antioxidant	1	1	1	
Dutrex R	_	6	6	

Mean values for the tensile strength (the breaking load/unit undeformed area) and breaking extension at each rate of extension were obtained from the measurements on the individual rings. The tensile strengths obtained with the ring specimens were found to be equal to or, more usually, somewhat higher than tensile strengths obtained with die-cut dumbbell specimens for approximately equal rates of extension.

VULCANIZATES

The vulcanizates were prepared from GR-S (Polysar S) polymerized at 50° C and containing 23% of styrene. The compounding recipes and cures are given in Table I. Vulcanizate A was a gum compound, and vulcanizates B and C were filled compounds containing, respectively, High Abrasion Furnace (HAF) and Semireinforcing Furnace (SRF) carbon black.

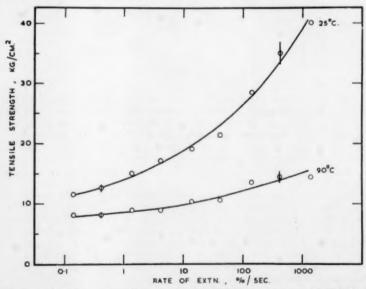


Fig. 2.—Mean values of tensile strength vs. rate of extension for the gum vulcanizate A at 25 and 90° C.

Vertical bars indicate standard deviation.

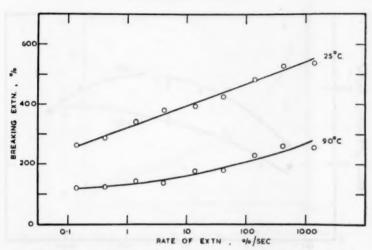


Fig. 3.—Mean values of breaking extension vs. rate of extension for the gum vulcanizate A at 25 and 90° C.

RESULTS

TENSILE STRENGTHS AND BREAKING EXTENSIONS

Tensile strength measurements for the gum vulcanizate A at 25 and 90° C are shown plotted against the rate of extension in Figure 2; breaking extension measurements are shown in Figure 3. The results at 25° C represent mean

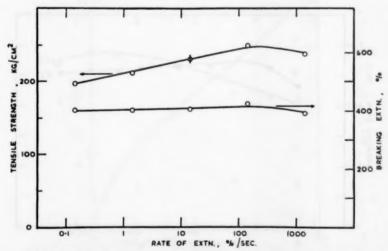


Fig. 4.—Mean values of (top) tensile strength and (bottom) breaking extension vs. rate of extension for the filled vulcanizate B at 25° C. Vertical bar indicates standard deviation.

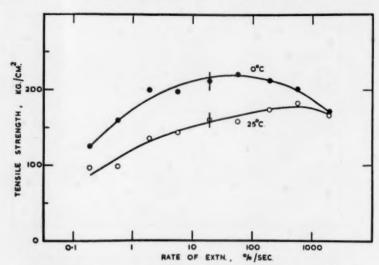


Fig. 5.—Mean values of tensile strength vs. rate of extension for the filled vulcanizate C at 0 and 25° C. Vertical bars indicate standard deviation.

values for three specimens and those at 90° C represent mean values for four to six specimens. With this vulcanizate the tensile strength and breaking extension increase uniformly with the rate of extension.

Results for the filled vulcanizate B at 25° C are given in Figure 4, these being mean values for three specimens. The tensile strength appears to pass

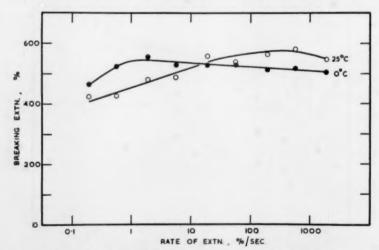


Fig. 6.—Mean values of breaking extension vs. rate of extension for the filled vulcanizate C at 0 and 25° C.

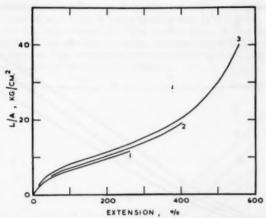


Fig. 7.—Curves of load/unit undeformed area (L/A) vs. extension for the gum vulcanizate A at 25° C at rates of extension of (1) 0.14, (2), 14, and (3) 1400%/sec.

through a maximum as the rate of extension is increased, but the breaking extension shows very little variation with the rate of extension.

Results for the filled vulcanizate C at 0 and 25° C are shown in Figures 5 and 6, these being mean values for four to six specimens. A pronounced maximum in the tensile strength is observed at 0° C, and there are indications of a maximum also at 25° C; the maximum at 25° C occurs at a higher rate of extension

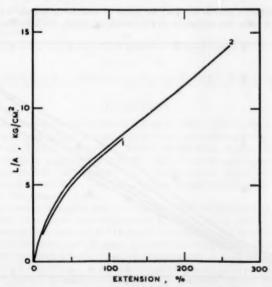


Fig. 8.—Curves of load/unit undeformed area (L/A) vs. extension for the gum-vulcanizate A at 90° C at rates of extension of (1) 0.14 and (2) 1400%/sec.

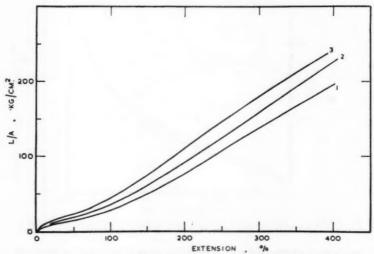


Fig. 9.—Curves of load/unit undeformed area (L/A) vs. extension for the filled vulcanizate B at 25° C at rates of extension of (1) 0.14, (2) 14, and (3) 1400%/sec.

than that at 0° C. The breaking extensions show rather less variation with the rate of extension.

LOAD-EXTENSION CURVES

Load-extension curves for various rates of extension are shown in Figures 7-11. Apart from the variation in the breaking point, the effect of the rate of

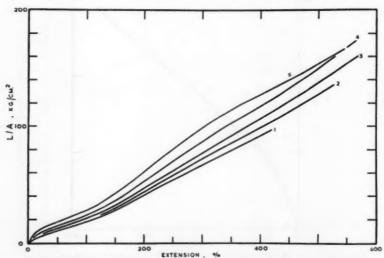


Fig. 10.—Curves of load/unit undeformed area (L/A) vs. extension for the filled vulcanizate C at 25° C at rates of extension of (1) 0.19, (2) 1.9, (3) 19, (4) 190, and (5) 1900%/sec.

extension on the load-extension curves for the gum vulcanizate A is small. The effect of the rate of extension is more pronounced in the filled vulcanizates, particularly in the vulcanizate C. The initial slope of the load-extension curves for the filled vulcanizates increases progressively with the rate of extension, but the slope at high extensions near the breaking point passes through a maximum as the rate of extension is increased.

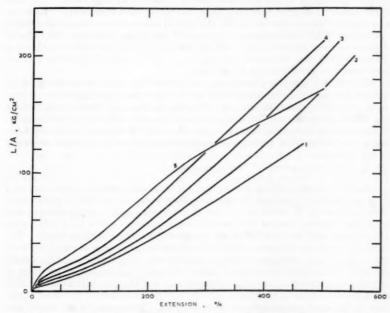


Fig. 11.—Curves of load/unit undeformed area (L/A) vs. extension for the filled vulcanisate C at 0° C at rates of extension of (1) 0.19, (2) 1.9, (3) 19, (4) 190, and (5) 1900%/sec.

DISCUSSION

The experimental results for the GR-S gum vulcanizate A, showing that the tensile strength and breaking extension increase with the rate of extension, are in accord with earlier findings^{1, 2}. Smith² found that tensile strengths and breaking extensions measured at different temperatures and rates of extension could be superposed according to the transformation scheme employed by Williams, Landel, and Ferry⁶ for small-strain viscoelasticity data, and this is true also for the present results.

The high tensile strengths attained by the filled vulcanizates in comparison with the gum vulcanizate are evidence of the reinforcing action of the filler. The occurrence of a maximum in the tensile strength as the rate of extension is increased indicates that part, at least, of this reinforcing action develops during extension and requires a finite time for development so that it does not occur at high rates of extension. A similar explanation has been given to account for the tear behavior of filled vulcanizates. The results for the vulcanizate C, showing that the maximum in the tensile strength shifts to higher rates of ex-

tension as the temperature is increased, suggest that the time required for the development of the reinforcing action decreases as the temperature is increased. Tensile strength data for filled vulcanizates do not appear to transform according to the scheme of Williams, Landel, and Ferry.

A possible alternative explanation of the observed decrease in the tensile strength of the filled vulcanizates at high rates of extension is that it is caused by the heating-up of the specimen during extension at high rates. Previous observations3, 4 suggest, however, that this explanation is unlikely. Kainradl and Handler4 found that the tensile strength of a butadiene/styrene vulcanizate containing ISAF black increased again with the rate of extension for rates of extension above 10,000%/sec. Villars3 also found that, for rates of extension above 10,000%/sec, the tensile strength of a GR-S carbon black-filled vulcanizate increased with the rate of extension.

The effect of the rate of extension on the load-extension curves for the gum vulcanizate is that to be expected from the viscoelastic properties of the material and this applies also, at low extensions, to the load-extension curves for the filled vulcanizates. The changes in the shape of the curves for the filled vulcanizates at higher extensions suggest that the development of the reinforcing action of the filler during extension is accompanied by changes in stressstrain behavior.

SYNOPSIS

An autographic method is described for obtaining load-extension curves of ring specimens extended at various rates from about 0.1 to 2000% per second. Results showing the effect of the rate of extension on the tensile strength and breaking extension and on the load-extension curve are given for a GR-S gum vulcanizate and for two GR-S vulcanizates containing carbon black. The tensile strength of the gum vulcanizate, at the temperatures at which the tests were carried out, increases uniformly with the rate of extension, but the tensile strength of the filled vulcanizates passes through a maximum. The effect of the rate of extension on the load-extension curve of the gum vulcanizate is that to be expected from the viscoelastic properties of the material; the effect in the case of the filled vulcanizates is more complex. These results are briefly discussed.

ACKNOWLEDGMENT

This work forms part of a program of research undertaken by the Board of the British Rubber Producers' Research Association.

REFERENCES

Dogadkin, B. A., and Sandomirskii, D. М., Rubber Chem. Тесниог. 25, 50 (1952).
 Smith, T. L., J. Polymer Sci. 32, 99 (1958).
 Villars, D. S., J. Appl. Phys. 21, 565 (1950).
 Kainradl, P., and Handler, W., paper presented to Deutsche Kautschuk Gesellschaft Conference, Cologne 1958

Greensmith, H. W., J. Appl. Polymer Sci. 3, 181 (1960).
 Williams, M. L., Landel, R. F., and Ferry, J. D., J. Am. Chem. Soc. 77, 3701 (1955).
 Greensmith, H. W., J. Polymer Sci. 21, 175 (1956).

RUPTURE OF RUBBER. VIII. COMPARISONS OF TEAR AND TENSILE RUPTURE MEASUREMENTS *

H. W. GREENSMITH

THE NATURAL RUBBER RESEARCH AND DEVELOPMENT BOARD WELWYN GARDEN CITY, HERTS, ENGLAND

INTRODUCTION

In previous papers of this series¹⁻³ a criterion for tearing of thin sheets of rubber vulcanizates was established on the basis of a characteristic tearing energy, the criterion being applicable either to the initiation of tearing at an incision or to the continuous propagation of a tear. An interpretation of the tearing energy in terms of the strength of a rubber as measured in tensile rupture tests was given², and in the present paper this is used in an attempt to relate tear and tensile rupture measurements, taking into account the observed effects of the speed of the test on such measurements⁴⁻⁶. Data obtained from the tensile rupture measurements given in the preceding paper⁶ (Part VII) are first compared with the energy to initiate tearing at an incision with a tip of semicircular form. The data are then compared with the tearing energy for tears propagated at various rates.

RELATIONS BETWEEN TEAR AND TENSILE RUPTURE MEASUREMENTS

According to the criterion¹, the condition for tearing to occur when the applied forces do no work is

$$-(1/h)(\partial W/\partial c)_l = T$$

where h is the thickness of the test piece in the undeformed state, c is the length of the incision or tear in the undeformed state, W is the total strain energy in the test piece, and T is a characteristic tearing energy. The subscript l denotes differentiation carried out under constant displacement of boundaries over which forces are applied. Thus, $-(1/h)(\partial W/\partial c)_l$ represents the supply of energy for tearing and T the energy expended, T being interpreted as a dissipation of energy. Thomas² has derived the relation between the strain distribution around the tip of an incision and $-(1/h)(\partial W/\partial c)_l$. From this relation be obtained for the energy to initiate tearing at an incision with a semicircular tip:

$$T \simeq Ed$$
 (1)

where E is the work done/unit volume in deforming the rubber at the tip to breaking point and d is the diameter of the tip in the undeformed state; d is assumed to be sufficiently large in comparison with the thickness of the test piece for the tip to be substantially in simple extension. Thomas confirmed experimentally that T was proportional to d and that T/d was comparable with the work to break/unit volume E measured in a tensile rupture test.

^{*} Reprinted from the Journal of Applied Polymer Science, Vol. 3, pages 183-194, 1960.

The approximate validity of Equation (1) for the initiation of tearing at an incision gives grounds for considering the equation to be applicable also in continuous tearing, d now being regarded as an effective diameter of the tip of the tear and a property of the material. Thomas² considered that an effective diameter could be ascribed to the tip of a tear on the grounds that irregularities develop at the tip and extend the zone over which high strains must be developed to produce rupture. In accord with this supposition, the value of d required to fit tear and tensile rupture measurements was found to be comparable in magnitude with the irregularities observed in the torn surface². In applying Equation (1) to continuous tearing it is supposed that, as the tear increases in length by an amount Δc , a volume of rubber $h\Delta cd$ is deformed to breaking point and an amount of work $Eh\Delta cd$ is done. It is further supposed that none of the work done is recovered, strain energy stored in the volume $h\Delta cd$ being dissipated when rupture occurs, so that $Eh\Delta cd$ may be equated with the energy $Th\Delta c$

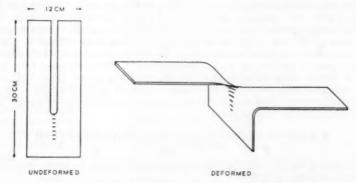


Fig. 1.—Test piece used for measuring the strain near the tip of an incision.

expended in the growth of the tear. In the type of tear test piece considered in the present context, the tear is propagated into undeformed material, and E is therefore the work done/unit volume in taking the rubber from the undeformed

state to the breaking point.

The rate of extension of the rubber at the tip of a tear will vary with the rate of propagation of the tear. An approximate relation between the rate of propagation and the rate of extension at the tip may be derived as follows. It is assumed that, for a tear propagating at a speed R, the strain in the neighborhood of the tip falls to zero at a certain distance l_0 ahead of the tip and that l_0 is proportional to the effective diameter of the tip, d. Assuming also that the rubber in the region of the tip is approximately in simple extension and denoting the extension ratio at the tip by λ_l , the rate of extension V of the rubber approaching the tip is given by:

$$V \simeq (\lambda t - 1)R/l_0$$

which, on rearrangement, yields:

$$R \simeq [(l_0/d)/(\lambda_t - 1)]Vd \tag{2}$$

The value of $l_0/d(\lambda_t - 1)$ in Equation (2) was obtained as described below from measurements of the static strain distribution near the tip of an incision in a test piece of the type used for tear measurements. Evaluation of $l_0/d(\lambda_t - 1)$ in this way restricts the application of Equation (2) to low rates of propagation.

A test piece of the shape shown in Figure 1 was cut from a sheet of natural rubber gum vulcanizate of about $1\frac{1}{2}$ mm thickness. The tip of the incision was semicircular and 1.5 cm in diameter. Lines about 2 mm in length were marked on the test piece, as shown, and the lengths of the lines and their respective distances from the tip of the incision were measured with a travelling microscope. The test piece was then extended as shown and the lengths of the lines were again measured to give the extension ratio λ at various distances from the

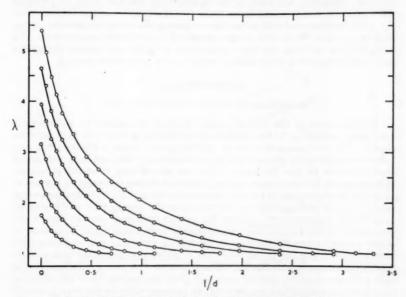


Fig. 2.—Variation of the extension ratio λ with distance l from the tip of an incision; d is the diameter of the tip.

tip of the incision. λ is plotted against l/d in Figure 2, l and d being, respectively, the distance from the tip and the diameter of the tip referred to the undeformed state. The extension ratio does not decrease linearly with distance from the tip as assumed in deriving Equation (2). However, if l_0 is defined as the distance at which λ falls to some low value (say, 1.1 or 1.01), $l_0/d(\lambda_t - 1)$ is found to be nearly independent of the extension ratio λ_t at the tip. Equation (2) may then be written:

$$R \simeq AVd$$
 (3)

where A is treated as a constant and V now represents an average rate of extension for the rubber approaching the tip of the tear. In applying Equation (3), A has been assigned a value of 0.75, this being the value of $l_0/d(\lambda_t-1)$ when l_0 is taken as the distance at which λ falls to 1.01.

Equations (1) and (3) are used, in the experimental comparisons of tear and tensile rupture measurements, to relate the tearing energy for tears propagated at various rates and the work to break/unit volume measured in tensile rupture tests on specimens extended at various rates. In the tensile rupture tests the specimens were extended at uniform rates, and, in using Equation (3), it is assumed that the effect on the strength properties of the material of a non-uniform rate of extension of average value V is to a first approximation the

same as extension at a uniform rate V.

In the case of tearing at an incision a relation equivalent to Equation (3) between the rate of extension of the rubber at the tip of the incision and the overall rate of extension (or rate of loading) of the test piece is not readily derived. However, the time taken in extending the test piece to breaking point provides a measure of the average rate of extension of the rubber at the tip of the incision, and this is used in comparing the energy to initiate tearing with the work to break/unit volume measured in the tensile rupture tests. In using the time to break the same assumption as to the equivalence of uniform and nonuniform rates of extension is made as for continuous tearing.

EXPERIMENTAL

MEASUREMENTS FOR CONTINUOUS TEARING

Measurements of the tearing energy for tears propagated at various rates were made according to the method which has been described in a previous paper4. The test pieces were of the general shape shown in Figure 1 but contained a simple cut in place of the large incision and were cut from vulcanized sheet of about 18 mm thickness. The test pieces were extended at various uniform speeds in a tensometer, being immersed during extension in a water or alcohol bath maintained at the test temperature to ±1°C. The tearing energy and the rate of propagation were derived from the tearing force and the crosshead speed, respectively4. Except for certain instances pointed out in the description of the results, the measurements were made under conditions of stable tearing4 where fluctuations in the tearing force and rate of propagation were small and random in nature. The experimental procedure under stable tearing conditions was as follows. Three or more test pieces were extended at each tensometer speed, and for each test piece the tearing force was noted at intervals once tearing had commenced; an average value for the tearing energy was then derived from the combined force readings. The rate of propagation, as derived from the tensometer crosshead speed, also represents an average value.

MEASUREMENTS FOR TEARING AT AN INCISION

Test pieces similar in shape to that shown in Figure 1 were used, these being cut from vulcanized sheet of about $1\frac{1}{2}$ mm thickness. The test pieces were 10 cm by 4 cm and contained an incision 7 cm long with a semicircular tip of about 2 mm diameter. The tip of the incision was formed with a circular cutter, and

the diameter of the tip was measured with a travelling microscope.

Test pieces were extended at various uniform speeds in the tensometer described in the preceding paper⁶. The force on the test piece at the point of tearing, from which the energy to initiate tearing was derived¹, and the time taken in extending the test piece to breaking point were obtained from the recorded force-distance curve. A water or alcohol bath was used for temperature control, as described in the preceding section.

TENSILE RUPTURE MEASUREMENTS

The work to break/unit volume was derived by graphical integration of the area under the load-extension curves as given in the preceding paper⁶. Mean values for the work to break/unit volume at each rate of extension were obtained from the results on the individual specimens.

MATERIALS

The mixes and cures for the vulcanizates that were used have been described in the preceding paper. The vulcanizates were all compounded from GR-S (Polysar S), vulcanizate A being a gum compound and vulcanizates B and C filled compounds containing, respectively, HAF and SRF carbon blacks in the

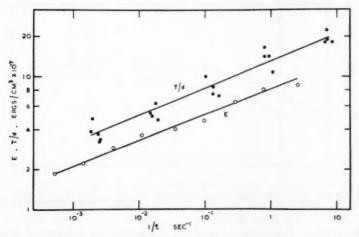


Fig. 3.—Comparison of the work to break/unit volume E and the energy T to initiate tearing at an incision for vulcanizate A at 25° C. Here t is the time taken in extending the test piece to breaking point, and d is the diameter of the tip of the incision.

ratio of 50 parts per hundred of rubber. Several 30 cm × 30 cm sheets of each vulcanizate were prepared from a single mixing, sufficient for all the measurements. For experimental convenience separate sheets were used for each of the various sets of measurements.

RESULTS

COMPARISON OF MEASUREMENTS FOR TENSILE RUPTURE AND TEARING AT AN INCISION

Mean values for the work to break/unit volume E measured in tensile rupture tests on the gum vulcanizate A at 25° C are shown plotted against 1/t in Figure 3, t being the time taken in extending the specimens to breaking point. The values of E plotted are those given in Table II. The breaking time t was obtained from the rate of extension of the specimen, as given in Table II, and the corresponding mean value for the breaking extension as given in the preceding paper⁶. Values of T/d obtained in tear initiation tests on this vulcan-

izate at 25° C are also shown in Figure 3, d being the diameter of the tip of the incision and T the energy to initiate tearing. The values of T/d have been plotted individually for each test piece. Similar data for the filled vulcanizate C at 25° C are shown in Figure 4; the values for E in this case are those given in Table IV.

As will be seen from Figures 3 and 4, T/d and E are of comparable magnitude. The agreement, however, is not as close as would be expected from the theory leading to Equation (1). The probable reason for the discrepancy has been indicated by Thomas². The apparent strength of the material would be expected to decrease as the size of specimen effectively tested is increased if the specimen contains flaws. As the size of specimen effectively tested in tearing at the incision was much smaller than the size of specimen used in the tensile

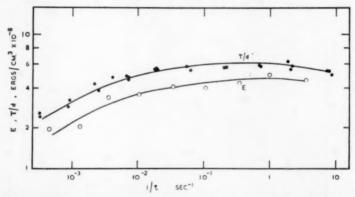


Fig. 4.—Comparison of the work to break/unit volume E and the energy T to initiate tearing at an incision for vulcanizate C at 25° C. Here t is the time taken in extending the test piece to breaking point, and d is the diameter of the tip of the incision.

rupture tests. T/d should accordingly be greater than E. It will be seen from Figures 3 and 4 that T/d is in fact greater than E; this has also been observed for natural rubber vulcanizates².

T/d and E show the same variation with the breaking time t, within the experimental scatter. This suggests that the assumption that the strength of the material depends only on the average rate at which the material is extended to the breaking point is valid as a first approximation.

COMPARISON OF MEASUREMENTS FOR TENSILE RUPTURE AND CONTINUOUS TEARING

In the following comparisons of tear and tensile rupture measurements an attempt is made to account for the variation of the tearing energy with the rate of tear propagation in terms of the variation in the effective diameter of the tip of the tear and the variation in the strength of the material with rate of extension as obtained from the tensile rupture tests. Values for the tearing energy T and rate of tear propagation R have been derived by means of Equations (1) and (3) from the values of the tensile work to break/unit volume E and rate of extension V, and these values are compared with the experimental tear data. The values for the effective diameter of the tip of the tear, d, used in Equations

(1) and (3) were chosen to give the best fit between the derived and experimental tear parameters. In some instances it was found that agreement could be obtained if d was assumed to be constant, but in others it was necessary to assume that d varied with the rate of tear propagation. Qualitative confirmation of the assumptions has been sought from the appearance of the torn surfaces.

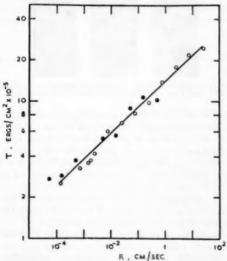


Fig. 5.—Variation of the tearing energy T with rate of propagation R for vulcanizate A at 90° C: (\bigcirc) experimental vulces; (\bigcirc) values derived from the tensile rupture measurements of Table I for a value for the effective diameter of the tip of the tear, A, of 0.48 mm.

The gum vulcanizate A provides instances where either the entire or the main contribution to the variation of the tearing energy with the rate of tear propagation is to be attributed to the variation of the work to break/unit volume with rate of extension. The filled vulcanizate B illustrates the other extreme, where the variation of the tearing energy with the rate of tear propagation is to be attributed largely to variation of the effective diameter of the tip of the tear. At certain test temperatures the tearing energy for the filled vul-

Table I Tensile Rupture Measurements for Vulcanizate A at 90° C

Rate of extension V , see ⁻¹	1.4 × 10 ⁻⁸	4.1 × 10 ⁻³	1.4 × 10 ⁻³	4.1 × 10 ⁻²	1.4 × 10 ⁻¹	1.4× 10 ⁻¹	1.4	4.1	14
Work to break/unit volume E , ergs/cm ³ ×10 ⁻⁶	5.7	6.0	7.8	7.3	11.1	11.6	18.4	22.3	21.5

canizate C shows a maximum value at a particular rate of tear propagation. Similar behavior is observed in the tensile rupture properties, and the attempt to relate these maxima affords a critical test of Equations (1) and (3).

MEASUREMENTS ON THE GUM VULCANIZATE A AT 90 AND 25° C

Tear measurements made on the gum vulcanizate A at 90° C are shown in Figure 5, together with values for the tearing energy and rate of tear propaga-

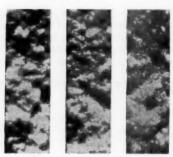


Fig. 6.—Torn surfaces of vulcanizate A at 90° C for rates of propagation (reading from left to right) of 10^{-3} , 2×10^{-3} and 1 cm/sec. The length of the surface shown is ca, 5 mm.

tion derived from the tensile rupture measurements of Table I for a value of 0.48 mm for the effective diameter of the tip of the tear, d. The appearance of the torn surface at various rates of propagation is shown in Figure 6. As the roughness of the torn surface does not vary appreciably with the rate of propagation over the comparison range, the assumption that d is constant is reasonable. The derived and observed tear data are in agreement within the experimental scatter, and it appears, therefore, that the variation of the tearing energy with the rate of tear propagation can be accounted for, in the range for which the comparison has been made, in terms of the variation in the work to break/unit volume with the rate of extension of the material.

Tear measurements made on the gum vulcanizate A at 25° C are shown in Figure 7, together with values for the tearing energy and rate of propagation

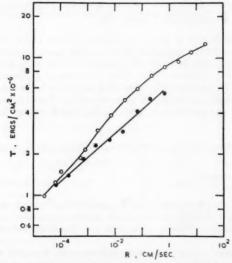


Fig. 7.—Variation of the tearing energy T with rate of propagation R for vulcanizate A at 25° C: (○) experimental values; (●) values derived from the tensile rupture measurements of Table II for a value for the effective diameter of the tip of the tear, 4, of 0.04 mm.

derived from the tensile rupture measurements given in Table II, a value for d of 0.64 mm being used. The variation in the work to break/unit volume does not, in this instance, account entirely for the observed variation in the tearing energy, in contrast with the results at 90° C (cf. also Figure 3). Better agreement was obtained by assuming that d varies with the rate of propagation. The values assumed for d and the corresponding values for the rate of propagation derived from Equation (3) are shown in Table II. The assumed variation in d is not inconsistent with the observed change in the torn surface, as may be

TABLE II
TENSILE RUPTURE MEASUREMENTS AND RELATED DATA
FOR VULCANIZATE A AT 25° C

Rate of extension V , \sec^{-1}	1.4× 10 ⁻³	4.1× 10-4	1.4×10^{-2}	4.1 × 10 ⁻²	1.4 × 10 ⁻¹	4.1 × 10 ⁻¹	1.4	4.1	14
Work to break/unit volume E, ergs/cm ³ ×10 ⁻⁷	1.85	2.2	2.9	3.6	4.0	4.7	6.5	8.0	8.6
Effective diameter d, mm Rate of propagation R, cm/	0.64	0.71	0.78	0.83	0.89	0.96	1.00	1.02	1.10
sec (derived from V and d)	6.6 ×	2.2 ×	8.1 ×	2.6 ×	9.3 X 10 ⁻³	3.0 ×	1 × 10-1	3.3 X	1.1

seen from Figure 8. At rates of propagation below about 10^{-3} cm/sec the torn surface is similar to that at 90° C; it becomes progressively more jagged in appearance as the rate of propagation is increased from 10^{-3} to about 1 cm/sec and then becomes somewhat smoother as the rate of propagation is increased further. It appears, therefore, that the observed variation in the tearing energy may be qualitatively ascribed to variation in the work to break/unit volume and, to a lesser extent, to variation in the effective diameter of the tip of the tear.

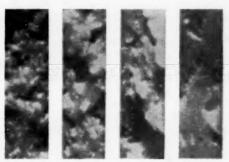


Fig. 8.—Torn surfaces of vulcanizate A at 25° C for rates of propagation (reading from left to right) of 10⁻⁴, 2×10⁻³, 2×10⁻³, and 20 cm/sec. The length of the surfaces shown is ca. 5 mm.

At rates of propagation above 10^{-2} cm/sec fairly large fluctuations in the tearing force and rate of propagation are observed during growth of the tear^{4,3}, these being associated with the intermittent jaggedness of the torn surface. In these circumstances the values obtained for the tearing energy and rate of propagation depend to some extent on the averaging method. This, however, does not affect the qualitative conclusions drawn above.

The effective diameter of the tip of the tear at low rates of propagation at 25° C should be comparable with that at 90°, as the torn surfaces are similar. The values obtained for the effective diameter, 0.64 and 0.48 mm, respectively,



Fig. 9.—Appearance of the tip of a tear in vulcanizate A. The tear was grown slowly (rate of propagation $<10^{-3}$ cm/sec) at room temperature. The thickness of the test piece at the tip (in deformed state) is ca. 1 mm.

are in reasonably close agreement in view of the fact that the specimens used in the various sets of measurements were cut from different sheets of the vulcanizate. Under these conditions of tearing the torn surface has a granular appearance, as will be seen from Figures 6 and 8, the largest irregularities being an appreciable fraction of a millimeter in height or depth. The corresponding appearance of the tip of the growing tear is shown in Figure 9. It will be seen that there is no sharp line of demarcation between the ruptured surfaces; rupture occurs at points scattered over a relatively wide area around the tip.

MEASUREMENTS ON THE FILLED VULCANIZATE B AT 25° C

Tear measurements for this vulcanizate at 25° C are shown in Figure 10. Two levels of tearing energy are observed, a level as at A—associated with a

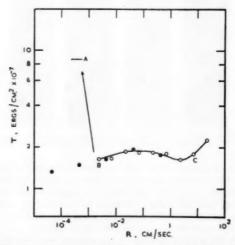
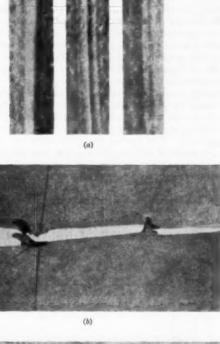


Fig. 10.—Variation of the tearing energy T with rate of propagation R for vulcanizate B at 25° C: (\bigcirc) experimental values; (\bigoplus) values derived from the tensile rupture measurements of Table III for a value for the effective diameter of the tip of the tear, A, of 0.40 mm.

greatly enlarged tip—and a level as in the region BC. The region BC will be considered first.

The appearance of the torn surface for various rates of propagation in the region BC is shown in Figure 11a. The torn surface has a small-scale roughness and larger-scale ridges and grooves with a height or depth of the order of a tenth



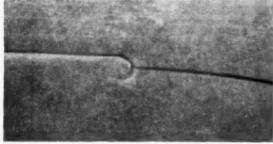


Fig. 11.—Torn surfaces of vulcanizate B at 25° C (a) for rates of propagation (reading from left to right) of 2×10^{-1} , 7×10^{-2} , and 7 cm/sec. The length of the surface shown is ca. 5 mm. (b) Knotty tear. (c) Semicircular knot.

TABLE III

TENSILE RUPTURE MEA	SUREMENTS	FOR VULC	CANIZATE	В ат 25°	C
Rate of extension V , \sec^{-1}	1.4×10^{-3}	1.4×10^{-2}	1.4×10^{-1}	1.4	14
Work to break/unit volume E , ergs/cm ³ ×	2.4	0.7		4.0	4.9

of a millimeter. As the overall roughness of the surface does not vary appreciably with the rate of propagation, the effective diameter of the tip of the tear, d, may be expected to be substantially constant. Values for the tearing energy and rate of propagation derived by means of Equations (1) and (3) from the tensile rupture measurements given in Table III for a value for d of 0.40 mm. are shown in Figure 10. These values are in good agreement with the experimental values for the region BC.

Knotty tearing occurs if the rate of propagation is reduced below the point B shown in Figure 10, and the energy required for continuous propagation of the tear rises to a level as shown at A. Knotty tearing is a form of stick-slip tearing⁵ in which an intermittent enlargement of the tip of the tear occurs, as shown in Figure 11b. The tearing energy as shown at A in Figure 10 is that measured at the point of catastrophic tearing from the enlarger tip or "knot," and the effective diameter d associated with this tearing energy is that appropriate to the knot. The values obtained for the effective diameter of knots in this vulcanizate with a value for E of 3.6×10^8 ergs/cm³ in Equation (1) together with the appropriate value for the tearing energy were of the order of 2 mm, being comparable in magnitude with the lateral spread of the cracks forming the knot. In some instances, where the knot was close to semicircular form, quantitative comparison of the derived value of d with the measured diameter was possible. An example of such a knot is shown in figure 11c; the derived value for d was 2.4 mm in this case, and the measured diameter was 1.8-2.0 mm.

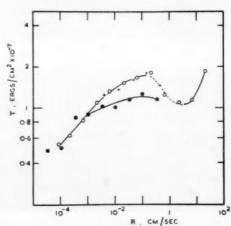


Fig. 12.—Variation of the tearing energy T with rate of propagation R for vulcanizate C at 25° C: (\bigcirc) experimental values; (\bigoplus) values derived from the tensile rupture measurements of Table IV for a value for the effective diameter of the tip of the tear, d, of 0.25 mm; (+) values derived from the tensile rupture measurements for a value of d which varies as shown in Table IV.

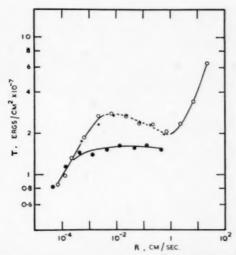


Fig. 13.—Variation of the tearing energy T with rate of propagation R for vulcanizate C at 0° C: (\bigcirc) experimental values; (\blacksquare) values derived from the tensile rupture measurements of Table V for a value for the effective diameter of the tear, d, of $0.32~\mathrm{mm}$; (+) values derived from the tensile rupture measurements for a value of d which varies as shown in Table V.

MEASUREMENT ON THE VULCANIZATE C AT 25 AND 0° C

Tear measurements for the filled vulcanizate C at 25 and 0° C are shown in Figures 12 and 13, respectively. The curves of tearing energy against rate of tear propagation at these temperatures show similar features, but the maximum in the tearing energy occurs at a lower rate of propagation at 0° than at 25° C. The broken lines denote stick-slip tearing, and the measurements in this region are to be regarded as providing a qualitative, rather than a strictly quantitative, representation of the variation of the tearing energy with the rate of tear propagation^{4, 5}. The method of measurement for stick-slip tearing conditions has been described previously^{4, 5}.

As the roughness of the torn surface at these temperatures varies somewhat with the rate of tear propagation, variation in the effective diameter of the tip of the tear, d, would be expected but, to illustrate the contribution from the variation in the work to break/unit volume, d is initially treated as a constant. Values for the tearing energy and rate of tear propagation derived from the tensile rupture measurements of Tables IV and V with values for d of 0.25 and 0.32 mm at 25 and 0° C, respectively, are shown in Figures 12 and 13. These

TABLE IV

Tensile Rupture Measurements and Related Data for Vulcanizate C at 25° C

Rate of extension V , sec ⁻¹	1.9×	5.7×10^{-3}	1.9 ×	5.7×	1.9×	5.7 × 10 ⁻¹	1.9	5.7	19
Work to break/unit volume E, ergs/cm ³ ×10 ⁻³ Effective diameter d, mm	1.9 0.25	2.1 0.25	3.4 0.25	3.6 0.26	4.1	4.0	4.5 0.35	5.0 0.36	4.6 0.32
Rate of propagation R , cm/ sec (derived from V and d)	3.6 ×	1.1 X	3.6 X	1.1 ×	4.4 X	1.4 ×	5.0 X	1.5 X	4.6×
see (derived from 7 and 6)	10-3	10-4	10-6	10-3	10-9	10-2	10-3	10-1	10-1

derived values show qualitatively the same trends as the experimental tear data. Values for the tearing energy and rate of tear propagation derived on the assumption that d varies with the rate of propagation are also shown in Figures 12 and 13, and these give a reasonably good representation of the experimental tear data. The values assumed for d and the corresponding values derived for the rate of tear propagation are shown in Tables IV and V. As will be seen from the torn surfaces shown in Figures 14 and 15, the assumed variation in d

Table V $\begin{array}{c} \text{Table V} \\ \text{Tensile Rupture Measurements and Related Data} \\ \text{for Vulcanizate C at } 0^{\circ} \text{ C} \end{array}$

Rate of extension V , \sec^{-1}	1.9× 10-4	5.7× 10 ⁻⁴	1.9 × 10 ⁻³	5.7× 10 ⁻¹	1.9×10^{-1}	5.7×10^{-1}	1.9	5.7	19
Work to break/unit volume E, ergs/cm ³ ×10 ⁻⁸ Effective diameter d, mm	2.6 0.32	3.6 0.32	4.6 0.38	4.4 0.52	4.7	5.1 0.52	4.9	5.1 0.45	4.8
Rate of propagation R , cm/ sec (derived from V and d)	4.6 × 10-4	1.3 × 10 ⁻⁴	5.5 × 10 ⁻⁴	2.2 × 10 ⁻³	8.1 × 10 ⁻³	2.2× 10 ⁻²	7.1× 10 ⁻²	1.9 ×	5.9 ×

with the rate of tear propagation is, in each case, qualitatively consistent with the variation in the roughness of the torn surfaces, the roughness being greatest at the rate of propagation for which the tearing energy is a maximum. Furthermore, the use of higher values of d at 0° than at 25° C is consistent with the greater roughness of the torn surfaces at 0° C.

It is apparent from Figure 12 and Table IV that in the above representation the tearing energy maximum at 25° C is associated both with a maximum in the effective diameter of the tip of the tear and with a maximum in the work to

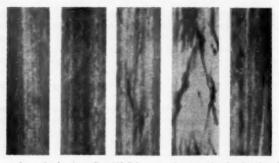


Fig. 14.—Torn surfaces of vulcanizate C at 25° C for rates of propagation (reading from left to right) of 10^{-4} , 2×10^{-3} , 2×10^{-3} , 2×10^{-3} , and 2 cm/sec. The length of the surface shown is ca. 5 mm.

break/unit volume for the material (also with a maximum in tensile strength⁶). It will be seen from Figure 13 and Table V that, at 0° C also, the tearing energy maximum is associated with a maximum in the effective diameter of the tip of the tear. Although in this case there is not a well-defined maximum in the work to break/unit volume, there is a well-defined maximum in the tensile strength⁶ at a rate of extension in the neighborhood of 0.57 sec⁻¹. This rate of extension, it will be seen from Table V, is close to that at which d is a maximum. Hence, in the above representation, the tearing energy maximum at 0° C is also closely associated with a maximum in tensile strength.

DISCUSSION

The comparisons of tear and tensile rupture indicate that the tearing energy for low and moderate rates of propagation of the tear can be plausibly related to the strength of the material as measured in tensile rupture tests on the assumption of an effective diameter for the tip of the tear. It has been seen that, apart from knotty tearing, values for the effective diameter d of a few tenths of a millimeter were required to fit the tear and tensile rupture measurements. Such values are reasonable, as judged by the irregularities in the torn surfaces. The values for d refer to tears in rubber sheet of about $1\frac{1}{4}$ mm thickness. Smaller values of d would be expected for thinner sheets, as the irregularities in the torn surface would be expected to diminish as the thickness of the sheet is decreased. In the case of knotty tearing, where the tip of the tear tends to develop a regular form due to the anisotropy of the material in the stretched state, to the value assumed for d, it has been seen, can be confirmed by direct measurement of the tip diameter.

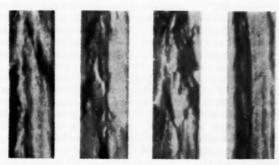


Fig. 15.—Torn surface of vulcanisate C at 0° C for rates of propagation (reading from left to right) of 10^{-4} , 7×10^{-4} , 7×10^{-3} , and 7×10^{-1} , cm/sec. The length of the surface shown is ca. 5 mm.

It was assumed in applying Equation (1) to continuous tearing that (a) the rubber around the tip of the tear is in simple extension and also that (b) the strength of a tensile rupture specimen is the same as that of the much smaller specimen effectively tested in tearing. The first assumption would not be expected to be strictly valid where the irregularities at the tip of the tear are small in comparison with the thickness of the test piece. It is not certain what the effect would be on the value obtained for the effective diameter of the tip of the tear. It has previously been indicated that the second assumption may not be strictly valid, i.e., the apparent strength of the material may decrease as the size of the specimen effectively tested is increased. The effect would be to give an exaggerated value for the effective diameter of the tip of the tear. An indication of the probable magnitude of the exaggeration may be obtained from Figures 3 and 4, where measurements for tensile rupture and tearing at an incision are compared.

It has been supposed, in applying Equation (1) to continuous tearing, that dissipation of energy is confined to the material around the tip of the tear which has been brought to the breaking point or to high extensions close to the breaking point. Additional dissipation of energy will occur, however, in regions adjacent to the tip where, as the tear advances, the material is subjected to moderate extensions and is then relaxed. This additional dissipation of energy

may well be considerable at high rates of propagation where rapid deformation occurs. Accordingly, Equation (1) would not be expected to be applicable at high rates of propagation without the addition of an extra term. Also, Equation (3) would not be expected to be applicable under these conditions, as has been indicated previously. Some additional dissipation of energy may occur as envisaged above in filled vulcanizates even at low rates of propagation. effect would be to give a value for the effective diameter of the tip of the tear which was rather high in comparison with the roughness of the torn surface.

SYNOPSIS

The energy to initiate tearing at an incision with a tip of semicircular form was shown in a previous paper to be approximately equal to Ed, E being the work to break/unit volume as measured in a tensile rupture test and d the diameter of the tip of the incision. In the present paper this relation is used to compare the effects of the speed of test on tear and tensile rupture measurements. It is shown that the variation of the work to break/unit volume with the speed of test adequately accounts for the effect of the speed of test on the energy to initiate tearing at incisions with tips of semi-circular form. It is assumed that the relation applies also in continuous tearing, d being in this case the effective diameter of the tip of the tear, and it is shown that the variation of the tearing energy with the rate of tear propagation, at low and moderate rates of propagation, may be plausibly accounted for in terms of the variation of the work to break/unit volume with the speed of test and variation of the effective diameter of the tip of the tear, d. Values of d of a few tenths of a millimeter were generally required to fit the tear and tensile rupture measurements, the values being, as expected, comparable in magnitude with the irreularities in the torn surfaces. It is shown that in certain instances the values assumed for d may be confirmed by direct measurement of the diameter of the tip of the tear.

ACKNOWLEDGMENT

This work forms part of a program of research undertaken by the Board of the British Rubber Producers' Research Association.

REFERENCES

¹ Rivlin, R. S., and Thomas, A. G., *J. Polymer Sci.* **10**, 291 (1953). ² Thomas, A. G., *J. Polymer Sci.* **18**, 177 (1955). ³ Thomas, A. G., *J. Appl. Polymer Sci.* **3**, 166 (1960). ⁴ Greensmith, H. W., and Thomas, A. G., *J. Polymer Sci.* **18**, 189 (1955). ⁵ Greensmith, H. W., *J. Polymer Sci.* **21**, 175 (1956). ⁶ Greensmith, H. W., *J. Appl. Polymer Sci.* **3**, 173 (1960).

MECHANISM OF RUPTURE OF HIGH POLYMERS *

V. E. Gul.

In connection with the wide distribution of high molecular weight compounds and the great successes in the field of synthesis of these materials, the study of the general principles of the processes of irreversible deformation and rupture of high polymer materials may be included among the important tasks of science and technology. In some cases it is desired to increase to the maximum the strength of the high molecular weight material, as for example in preparing articles from synthetic fibers, rubbers, plastics, etc., while on the other hand in others an increase in strength is undesirable. Thus, for example, food products, into whose composition high molecular weight materials are introduced, should naturally not be too strong. The preparation of reclaim from used rubber articles includes grinding. Here it is attempted to find such a combination of grinding conditions that will proceed with the minimum consumption of energy.

In order to have the possibility of increasing or decreasing the strength of the high molecular weight substances, it is necessary to clarify the mechanism of ruptures and to know what is the relation between the forces of reaction between the structural elements of the material and tensile strength.

CALCULATED AND THEORETICAL VALUES OF TENSILE STRENGTH

Attempts to calculate the tensile strength on the basis of the cohesive forces in crystal lattice have led to great discrepancy with the experimentally observed values of tensile strength. Such attempts have been made repeatedly.

In 1923, Zwicky¹, as a result of calculations of the cohesive forces in a crystal of table salt did not obtain the experimental strength value of 0.531 kg/mm², but instead a value almost 400 times as high, 200 kg/mm². The author considers that in the calculation of tensile strength one should take into account the thermal motion, bringing the structural elements closer to the energy state which it has before the break.

Attempts were made by Griffiths² to present a mechanism of break with which it would be possible to explain the differing calculated and experimental values of the energy of break. He assumed that there are cracks in a crystal, and calculated at what value of stress perpendicular to a crack the equilibrium would be disrupted and crack growth would start. The calculation proposed by Griffiths, however, cannot pretend to strict accuracy. Analogous attempts were made by Smekal².

The hypothesis of Griffiths as to the existence of microcracks found confirmation in the splendid experiment of Ioffe and coworkers, and was developed considerably in the work of these researchers. Ioffe, Kirpicheva and Levitskaya4 determined the strength of a crystal of table salt, the surface of which was being washed by hot water. The hot water rapidly dissolved the surface of the

^{*} Translated from Uspekhi Khimii i Tekhnologii Polymerov, Sbornik, 2, 202-22 (1957).

crystal, smoothing it and freeing it from cracks. The limit of the tensile strength measured under these conditions reached 80% of the theoretical value.

A. F. Ioffe used still another method of deformation to avoid the effect of surface cracks. Spheres, prepared from salt, which were first cooled in liquid air, were then transferred quickly to molten tin. Thereby the external layers of the spheres were heated before the internal ones and, in expanding, subjected the central layers to strains from all sides. Calculations have shown that the multidirectional strains in the center of the spheres reached 60 kg/mm², but no shattering was observed, and consequently the strength limit of the salt exceeds this value.

These experiments have shown clearly the presence of flaws and microcracks in crystalline bodies, and the large part which they play in the mechanism of rupture. On the edges of such defective points the stresses have an increased value as compared with the average.

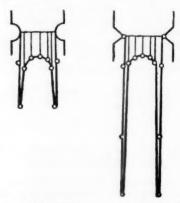


Fig. 1.—Diagram of the distribution of stresses in samples with notches.

Figure 1 shows a diagram of stresses in samples with notches. The ordinates of the curves express the stresses in points situated at different distances from the surface of the sample in a cross-section passing through the notch. As Figure 1 shows, with a sharp shape of the apex of the notch, the maximum stress value exceeds its average value by several times. The maximum stress at the apex of the crack surface may prove in many cases greater than the value determined by the relation of deformation load to the cross-section of the weakened sample. The crack will grow not through the action of the average stress, but through the action of the maximum stress. Simultaneously with the growth of the crack, the average stress value increases. Thus is explained the gap existing between the experimental and theoretical values of the strength of monocrystals.

The statistical theory of brittle strength was formulated by Aleksandrov and Zhurkov⁵. According to the concepts developed by them, the break does not occur simultaneously along the whole surface of rupture, but gradually. The break starts in the most dangerous focus of rupture, at which the overstress reaches a value comparable to the theoretical strength value. Then the rupture starts in new defective places. The growth of cracks is concluded by

the rupture of the material.

In both crystalline and amorphous materials there are flaws within the article and on its surface. The engineering strength of the article is determined largely by its surface flaws. The condition of the surface, determined by the processing of the sample and by the presence of substances on its surface may

change to a substantial degree the condition for crack growth.

Some interesting work was carried out by Rebinder and Aslanova⁶. In clarifying the influence of surface-active media on the strength of solid bodies, they were able to show that because of the leveling of the danger of surface cracks in surface-active media, the cracks start to become deformed reversibly, whereupon the glass samples show elasticity. It should be noted that Rebinder has formulated the basic concepts of the mechanism of the action of surface-active materials on the mechanical properties of solid polymers.

One of the basic concepts of the statistical theory of brittle strength amounts to the fact that the most dangerous flaws are encountered more rarely than the less dangerous ones, while the strength is governed by the most dangerous flaw of those found on the surface. Hence the specimens whose cross-sections are

small (for example, fine fibers) have an increased strength.

To the degree that a specimen is stretched, the stress increases, as a result of its becoming thinner. If the material is plastic, however, the rate of increase in the stress is retarded by reason of the fact that the particles of the material regroup in striving to assume a position of less stress. When the rate of increase in the stresses becomes greater than the rate of resolution of the overstresses, then the nonhomogeneities create overstresses leading to a break. In principle this system is also applicable to crystals, since it has been shown that crystals can flow. As regards the mechanism of the formation of cracks, however, there is no united opinion on this up to the present. Apparently different mechanisms are characteristic of different materials. For metals, the part of cracks is played by regions of loose contact between grains of microcrystals7. If, however, we consider not polycrystals but a monocrystal, then the weak positions may be considered the points which yield plastic displacements on the surface8. Cracks may likewise be formed on inclusions or nonhomogeneities, which are characterized by indexes of mechanical properties differing from the indexes characterizing the material or the specimen as a whole9.

The statistical theory of strength offered the possibility of calculating more accurately a tensile strength value which will decrease the difference between

the theoretical and experimental values of tensile strength.

In developing the theory of brittle strength, Smekalli clarifies the notably regular structures formed on the surface of the break in glass or quartz rods by the creating of elastic waves accompanying the break. The frequency of these waves, which is obtained by measuring the structure at a known velocity of their passage, was found to be of the order of 10^{10} hertz. The experimental confirmation of the existence of ultrashort waves in the break of solid materials is given by Schardin⁴².

Before answering the question of whether it is possible to calculate the value of tensile strength of polymers on the basis of the known values of the cohesive forces between macromolecules, one should give attention to the fact that cohesive forces of two different types exist in high polymers: chemical forces and forces of intermolecular interaction. When a specimen consisting of long flexible molecules breaks, either the chain molecules of the polymer have broken, or else a rupture has occurred in the intermolecular bonds whereby the

macromolecules have become displaced with respect to one another. It is

also possible for both processes to occur simultaneously.

The mechanism of break of a material depends on which type of bond proves more stable in a given testing method. This can be ascertained by calculating the strength of the chemical bonds and the total strength of the forces of intermolecular interaction. For this it is necessary to take into account the length of the chain molecules of the polymer, since the forces of intermolecular interaction are summed according to the chain length. It is also necessary to take into account the chemical nature of the link of the polymer molecule, which conditions the nature of the intermolecular forces and the capability of the polymer to crystallize. The specific characteristics of the break of crystalline and crystallizing polymers are not considered in the present paper.

The relation between the mechanical properties of the polymer and the chain length has been studied in the work of many researchers¹⁰. Thus for example Mark¹¹ indicates that in order to obtain some mechanical strength in the polymer, a certain minimum value of the degree of polymerization is necessary, which is different for different classes of polymers. It is least of all for polyamides and proteins, and reaches considerable values for polyhydrocarbons. With a further increase in chain length the strength increases regularly. When the value of the degree of polymerization of polyhydrocarbons reaches approximately 250, the relation between tensile strength and molecular weight becomes less distinct, and with degrees of polymerization above 600–700 the tensile strength is practically independent of chain length. Undoubtedly the nature of this relationship is similar for different polymers, but the conditions of deformation and the quantity of the intermolecular interaction of polymers exerts a substantial influence on the degree of polymerization values mentioned.

For an approximate determination of the strength of the chemical bonds and the forces of intermolecular interactions, it is necessary to assume certain values of molecular weight and degree of poly-dispersion of the given polymer for given conditions of deformation. Such a calculation applicable to cellulose fibers was carried out by Mikhaïlov and Kargin¹². They showed that, in the first place, the theoretical strength exceeded the actual strength by many times, and secondly that under the given conditions of deformation a break at the —OH . . . OH— bonds (at a comparatively low molecular weight) is uneconomical of energy, since the summated energy of the —OH. . . OH— bonds is many times greater than the corresponding energy of rupture at C—O bonds.

The large difference between the theoretical and experimental strength values of Mikhaïlov and Kargin are explained by the fact that in the break of actual fibers the rupture does not occur simultaneously throughout the whole section, but rather the fiber breaks in sections because of structural nonhomogeneities. Under nonhomogeneities are understood the differing size and shape of chains and the presence of partial orientation in them.

THE INFLUENCE OF CRYSTALLIZATION AND FILLERS ON THE STRENGTH OF HIGH POLYMERS

The orientation and crystallization of high polymers have an especially essential importance for the strength of these substances. Aleksandrov and Lazurkin¹³ have set up an experiment which makes it possible to ascertain whether or not the fine particles of crystalline rubber which are very closely bound to the amorphous phase cause a strengthening of the material. They started from the position that the mechanical properties of the rubber crystals

should be similar to the mechanical properties of paraffin or stearic acid. In this experiment an unloaded vulcanizate of polybutadiene rubber was swelled in molten paraffin or stearic acid. After the swelling, the strength of the swelled samples was measured at temperatures 2–3° C above and below the melting point of paraffin or stearic acid. In the former case the strength was low, but on cooling, at the moment of crystallization of paraffin or stearic acid, the tensile strength of the vulcanizate sharply increased, exceeding by a factor of 4–11 the value of the strength at a temperature above the melting point of the crystals.

In the rapid deformation of crystallizing rubbers, when the crystallization cannot occur in the proper manner, Aleksandrov and Lazurkin observed a decrease in the work of breaking. In the vulcanization of rubber, the capability of the rubbers to crystallize decreases. Here a drop in tensile strength is

bserved.

A thorough investigation of the influence of vulcanization on the strength of vulcanizates was carried out by Dogadkin and Karmin¹⁴, who showed that the strength of vulcanizates is determined by the number of crosslinks formed between the chain molecules. With low degrees of vulcanization, an increase in the number of crosslinks is accompanied by an increase in strength. When sufficiently high degrees of crosslinking of the chain molecules are reached, orientation and crystallization are realized. A further increase in the number of crosslinks in the vulcanizate is accompanied by a drop in the strength.

Both in the work of Dogadkin and of Karmin, and in the research of Lukin and Kasatochkin¹⁵, it has been shown that for the vast majority of vulcanizates the tensile strength is a linear function of the content of crystalline phase (with limited orientation) in the vulcanizate, which phase is created at the moment of break as a result of deformation. It is from this point of view that, in the work of Dogadkin and his coworkers¹⁶, the reinforcing action of fillers, and of the chain structures formed in the rubber-filler system, on the surface of which the orientation of rubber molecules occurs, is considered. In the places where overstresses are created (as a result of a nonhomogeneity of structure) a separation of parts of the chain molecule from the surface of the crystal or filler occurs, and the quantity of overstress decreases accordingly. The nonhomogeneity of distribution of stresses is also reduced thereby. The structural nonhomogeneity of the material, on the other hand, causes a nonhomogeneous distribution of stresses.

Consequently the structural nonhomogeneity is one of the basic causes of the low strength value as compared to the theoretical values calculated for a regular structure. In a number of cases the inert fillers cannot form mobile bonds with chain molecules, but instead they separte the links of the chain molecules, and the strength of the material drops.

DIFFERENT MECHANISMS OF HIGH POLYMER BREAK

In order to be able in each concrete case to answer the question, what bonds to which degree cause the tensile strength of a polymer under given deformation conditions, it is necessary to consider the basic mechanisms of break in high polymers, and particularly the nature of the deformations accompanying the process of rupture of a sample. If the rupture sets in before any notable development of plastic and elastomeric deformation can occur, then a mechanism of brittle break takes place, which has been studied in a number of works^{1–5}. The mechanism of brittle break is observed in the break of polymers at a high

speed or at temperatures below the glass transition temperature. Under these conditions, neither plastic nor high-elasticity deformation can dvelop, and no

slipping of the chain molecules with respect to one another occurs.

A consideration of the surface of a brittle break in polymers such as polymethyl methacrylate and polystyrene, and an analysis of the results obtained, enabled Regel¹⁷ to confirm the applicability of the concepts of the statistical theory of brittleness to the sequential nature of the process of rupture in time. Regal showed that in the samples studied by him there were a large number of flaws. The rupture started with the most dangerous of these. To the degree that the primary cracks grow, the average stress on the actual section of the specimen increases. An overstress on other flaws reaches the critical value, and also the growth in the cracks starts with them. Generally the shiny zones of the break started at the surface of the specimen; this attests to the fact that the most dangerous flaws are located on the surface of the specimen. The phenomenon of cracking has also received the attention of other authors¹⁸ who did not, however, trace the process of crack growth.

In a recent monograph Späth⁴⁸ proposes the formation of microcracks as a result of the interaction of external forces, in which the bonds uniting adjacent portions of chain molecules predominate. The rupture of such bonds is accompanied by the creation of ultrashort waves which cause local breaks.

Observations made on a large number of samples have shown that in all cases the plane of the cracks is perpendicular to the direction of action of the external forces. The surface of the break may be divided into two parts: the shiny and the rough. Around the shiny zone there are situated curves similar to parabolas or hyperbolas (Figure 2). [This figure was not clear enough to reproduce here. An analysis of these data enabled Regel to establish that the lines where two cracks growing at the same rate meet, if they did not start growing simultaneouly, will be hyperbolas. Not all the cracks are formed instantaneously after the application of a load. With a rise in temperature or an increase in the stress, there is an increase in the rate of formation and the rate of growth of the cracks. The number of cracks reaches some limit and does not increase further, but the average size of the cracks increases steadily, thus attesting to the gradual depletion of all the defects which can be converted into cracks. At the same time the stress gradually decreases in the surface layer. Thus the rupture of polymers in the vitrified state occurs by the mechanism of brittle break. In contrast to simple glasses, however, high molecular weight substances in the range between the glass transition temperature and the brittle point retain the ability to allow considerable deformation.

The deformations observed in polymer glasses are not plastic, since they are reversible and disappear after the specimens are heated. As Lazurkin and R. L. Fogelson¹⁹ have shown, these deformations are elastomeric, but are developed under special conditions where, despite the comparatively low temperature, the mobility of the links of the chain molecules increases by reason of the prevalence of intermolecular interactions with the aid of external deforming forces. At comparatively low temperatures, by reason of the low thermal motion energy of the chain molecules, they do not change their mutual arrangement, and only vibrate around points corresponding to the minimum

potential energy.

The application of external forces offers a possibility of a change of the links of the chain molecules into new positions. Here the tangles of the chain molecules elongate and a reversible deformation is noted which has been given the designation of forced elasticity. The mechanism of rupture in materials

showing forced elasticity we shall designate as the mechanism of forced elastic rupture. It is characteristic of this mechanism that if the deformed specimen after the formation of cracks is relieved of the load and is warmed up, then the cracks become invisible; they are "healed over". However, the flaws remain, and in such a sample on repeated deformation the initial pattern of cracks is reproduced.

In a forced-elastic rupture of polymers, apparently, the intermolecular bonds are broken at one stage of the break, and the chemical bonds at another. The forced-elastic deformation causes a stretching of fine cracks into rhombic ones, which is accompanied by a partial smoothing out of the peaks of over-

stresses.

At sufficiently high temperatures and corresponding deformation rates, the linear polymers may show plastic and viscous reversible deformations. In this sort of rupture of polymers, the mechanism of which we shall arbitrarily designate as "plastic", a slipping of the groups of the chain molecules with respect to one another occurs. Here the cross section is reduced until the time that the rate of resolution of overstresses becomes less than the rate of their growth, and the slipping of the groups of the chain with respect to one another ends in rupture of the specimen. Such a mechanism can be observed by deforming plasticized rubbers at room temperature.

Ordinarily rubberlike polymers show not only plastic deformation and viscous flow but also viscoelastic deformation. Polymers with a developed spatial structure, for example cured rubber, cannot exhibit a "plastic" irreversible deformation. In their rupture only elastomeric deformation is observed.

Bartenev²¹ set about clarifying the mechanism of rupture of rubber vulcanizates and came to the conclusion that in cured rubber under the action of a load, tears also are formed and grow. The essential feature of the break of cured rubber, it seems to us, is the necessity of overcoming both chemical and intermolecular bonds in the break. Hence a plastic mechanism for the rupture of such polymers is impossible. Barteney proposed to call the break of such polymers elastic if it is accompanied by elastomeric deformations. He directed attention to the fact that an elastic break, like a brittle one, is characterized by a nonsimultaneous separation of the material into parts. He distinguishes two stages of the break; slow and rapid. If we observe the surface of the break, then, according to Barteney, the slow stage corresponds to the rough zone, and the rapid one to the shiny zone of the break21. One mechanism of rupture in the stage of slow break is characteristic of high polymers in the elastomeric state. In this case, at the apex of the tear, fibers or rods of the breaking polymer are formed. When the temperature is lowered, the mechanism of rupture is different, namely, a rpaid elastic break occurs without the formation of a roughened zone. Bartenev notes that in the first and second cases the break occurs in a strongly oriented material. He indicates the great similarity between brittle and elastic break. In both cases the cross section of the sample before and after the break does not change. The surface of the break is situated perpendicularly to the direction of stress, there is a wide scatter in the test results and an analogous dependence of tensile strength on the rate and time factors is The presence of a rough zone, corresponding to a slow stage of break (not a rapid one as in the case of brittle materials) is characteristic of elastomeric rupture.

Depending on the molecular weight, quantity of linear polymer, the rate of break, and the temperature, both a "plastic" and a high-elasticity break may be achieved. With a change in the deformation conditions, the "plastic"

break may be converted into an elastic one.

The presence of a shiny surface and of a pattern of lines brings Bartenev to the conclusion that the extension of the front of the cracks created in the rapid stage proceeds by a direct scission of chemical bonds. He notes that the standard testing of industrial rubber stocks and high-modulus vulcanizates on a stress-strain machine should be referred to the "rapid" elastomeric break with the formation of only one shiny zone of break. With a sufficiently slow deformation of low-modulus stocks, rods or fibers may be formed in the process of break. The fibrous structure is distinctly visible on a photograph of the break of a vulcanizate (Figure 3). A number of authors have shown^{22–26} that the elastic break is accompanied by an increase in strength at a reduced temperature. Somewhat below the glass transition temperature the tensile strength and elongation at break reach their maximum value.



Fig. 3.—Appearance of growing tear in a low-modulus vulcanizate of SBR-SKS-30; side view (from the data of Bartenev and Belostotskaya).

The original values of the molecular weight of the rubber determine the tensile strength of the vulcanizates obtained, as has been shown convincingly in a number of papers. Novikov and coworkers²⁷ have explained this by the more regular spatial network formation in the high molecular weight fractions as compared with the low molecular weight fractions. Flory²⁸ has shown that with an equal number of crosslinks the quantity of free ends which have not entered into the network will be considerably greater if low molecular weight fractions are used instead of high molecular weight ones. On the basis of these data, Novikov postulates that in vulcanizates, in going from low to high molecular weight fractions of the original rubbers, the nature of the interaction between rubber and carbon blacks changes.

THE KINETICS OF POLYMER BREAK

The basic mechanisms of polymer rupture considered lead to the conclusion that, with the exception of cases of very rapid break of polymers at low temperatures, the rupture of samples is ordinarily accompanied by a gradual scission of the bonds between "bundles" of molecules. One may distinguish two limiting cases. In the first a fairly rapid loading of the material causes the structural elements to be unable to regroup, and the rupture occurs on the surface by scission of both chemical and intermolecular bonds. The forces nec-

essary in order to break the former are many times greater than for the latter; the force also determines the industrial strength of the material under such conditions. In the second case, with a sufficiently slow deformation of the linear polymer—if the values of its molecular weight and experimental temperature are such that a slipping of the groups of chain molecules with respect to one another takes place—a break occurs which is accompanied by a rupture of only the links of intermolecular interaction. Here one should also consider the intensity of the intermolecular interactions. The very same testing in the case of polar polymers may approximate the conditions of brittle break, but in the case of rubberlike polymers may approximate the conditions of elastic break.

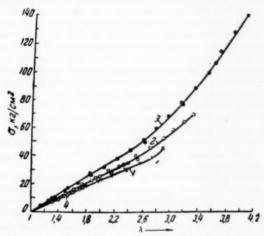


Fig. 4.—Curves of stress (σ) vs. relative length λ for: I—SKN-18; figures mean 18, 26 and 40 parts acrylonitrile); \mathcal{Z} —SKN-26; \mathcal{Z} —SKN-40 (rate of deformation; 1 cm/min); \mathcal{Z} —all three vulcanizates when equilibrium values are achieved. Ordinate: σ , kg cm².

Under actual conditions, polymers apparently break in such a way that a break of both chemical and of intermolecular bonds occurs. In this connection the most general case is represented by the usual testing for the purpose of determining ultimate tensile strength in stretching vulcanizates. Hence with vulcanizates as an example we have made an attempt to study the essential features of polymer rupture.

First of all it is necessary to find the ratio between the tensile strength of the chemical and intermolecular bonds in the process of crack growth or, more accurately, in the process of rupture under different conditions of deformation of an actual polymer. For this purpose, the tensile strength was determined by stretching three vulcanizates of nitrile rubbers with the same chemical crosslink density between the chain molecules, but with different contents of the polar nitrile groups.

Gul, Sideva and Dogadkin²⁹ determined the tensile strength by extension:
(a) at the final deformation rate, and (b) by deforming the specimens to break in such a way that each successively imposed deformation value corresponds to the equilibrium stress value. It was found that under equilibrium deformation conditions all three of the vulcanizates tested were characterized by the same

tensile strength. The marked difference in the intensity of the intermolecular interactions with such a method of testing did not influence the results (Figure 4). All three vulcanizates had the same crosslink density; consequently under these deformation conditions the tensile strength in all three vulcanizates is caused by the same strength of the chemical bonds in the spatial network of the vulcanizate. The deformation of these same vulcanizates at the final rate showed a marked difference in behavior. The greater the intensity of the intermolecular interactions, i.e., the greater the concentrations of polar nitrile groups in the rubber molecules, the higher the deformation curves run and the higher the stress at which the break of the vulcanizates occurs.

The deformation was achieved in the Dogadkin-Gul apparatus, in which it was possible to check the effect of oxygen on the strength of vulcanizates. Here it was found that within the limits of experimental error the strength of vulcanizates in air and in the absence of oxygen was practically the same.

In all cases where the vulcanizates described are tested at the final deformation rate, the tensile strength is higher to the degree that the intermolecular interactions are more intense; the temperature is lower and the rate of deformation is higher; in these cases the tensile strength is always higher than the value

obtained with the equilibrium method of deformation.

To the tensile strength, which shows the forces of the main chemical valences, is added the resistance of the van der Waals forces. The latter is felt more strongly to the degree that the rate of deformation is higher. Apparently the stress at the apex of the crack or tear is a composite of the resistance to the forces of the main chemical valences and the van der Waals forces. This follows from simple reasoning.

Let us consider a specimen with a nominal cross section of S. When the flaws in the sample are taken into account, the cross section should be diminished by the amount s. The deforming force F applied to the specimen may be referred to the nominal or the true value of the cross section. In the first case the value of the nominal stress P is obtained, and in the second that of the true one σ :

$$F = P \cdot S = \sigma(S - s) \tag{1}$$

If the stress at the point of the break π is μ times as great as the mean value of the true stress σ , and $s/S = \gamma$, then the following equation is found to be correct:

$$\pi = \mu \sigma = \mu \frac{S}{S - s} P = \left(\mu \frac{1}{1 - \gamma}\right) P \tag{2}$$

An analysis of the dependence of stress at the point of the growth of the break π on the nominal stress P leads to the conclusion that if P is a sum of the resistance to forces of the main chemical affinity and the van der Waals forces, then the resistance of the material to rupture at the apex of the crack or tear is made up of the resistance to forces of both types. It is found from the work carried out by Chiesa²⁰ that in the usual dynamic testing before final break, in practice the stress is measured at the place where the rupture grows, which is the maximum stress measured (at the time of testing). As will be shown in the following, the break proceeds by the performance of the successive elemental acts of rupture.

In the case of the rupture of a polymer with a network structure, the material at the point where the break grows is oriented³¹, though the very same

chain molecule may be situated in several layers at the same time.

Immediately before rupture, the stress applies to the bonds caused by van der Waals forces as well as to chemical bonds.

Then the chains are displaced, the bonds of both types begin to be deformed. At the moment of break the load is distributed in such a way that part of it falls on the bond of the main chemical valences and part on the bond brought about by the van der Waals forces. If one achieves deformation conditions such that all the physical bonds (resulting from van der Waals forces) escape the action of the load, then only the chemical bonds will break subsequently. By applying a series of deformation values and achieving a relaxation of the stresses resulting from the physical bonds, it is possible to reach the moment of break with a practically complete exclusion of the influence of physical bonds. A case close to this for vulcanizates was observed by Gul, Sideva and Dogadkin²⁹. Since the relaxation of bonds brought about through the van der Waals forces proceeds far more slowly than the relaxation of bonds brought about by the main chemical valences²², the static fatigue of the network of the main chemical valences may be neglected in this case.

Let us consider the mechanism of rupture of a highly elastic polymer with a network structure. Here we exclude the influence of factors such as crystallization, loading with fillers, etc. and plasticization. In this case the rupture of polymers by growing cracks proceeds in such a way as to exclude the marked development of plastic deformation, but such as not to exclude the development of elastomeric deformation. The role of interweaving of chains in this case is played by the intermolecular bonds resulting from the forces of the main

chemical valences.

In the case of tearing, where the rupture of the material at the apex of the crack precedes its separation into rods³³, it is also necessary at the same time to overcome bonds of both types.

In relation to all that has been said above, we consider the nominal resistance of a vulcanizate to rupture as a summation consisting of terms representing the resistance of the main chemical valences and van der Waals forces. The stress at the apex of a crack or tear π is also a composite of the resistance to

forces of the first type π_x and of the second π_M .

The quantity π_M depends on the experimental temperature, the deformation rate and the degree of swelling. By considering the rupture and restoration of the bonds of intermolecular interaction resulting from the fluctuation in thermal motion, we came to the conclusion that π_M , analogous to resistance to viscous flow, should be inversely proportional to the probability of the rupture of bonds and directly proportional to the rate of growth of the break v. The more probable the rupture of bonds, the greater the frequency at which it occurs, and consequently the more intermolecular interaction bonds will be broken by the thermal motion of kinetic units in the time during which the deforming stress acts. In this way the resistance of the material to rupture will be weakened. The frequency of the fluctuation in the thermal energy, leading to the rupture of bonds, $v = v_0 e^{U/RT}$ (where v_0 is the rate of oscillation of a structural unit around a position characterized by a minimum potential energy), and hence $\pi_M = K' e^{U/RT} \cdot v$ where K' is a practically constant quantity for a given type of bonds. Thus

$$\pi = \pi_x + \pi_M = \pi_x + K' \cdot e^{U/RT} \cdot v \tag{3}$$

In converting from π to P, we express the nominal resistance to break in the form of a sum³⁴:

$$P = P_z + K \cdot e^{U/RT} \cdot v \tag{4}$$

It follows from Equation (4) that for vulcanizates the following temperature relation should be observed:

$$\ln (P - P_x) = \ln Kv + \frac{U}{R} \cdot \frac{1}{T}$$
(5)

Figure 5 shows data obtained by us together with Farberova³⁵ on nitrile rubbers.

It was of interest to compare the experimental data on the dependence of tensile strength P upon the rate of deformation of the sample v_1 , as obtained by Dogadkin and Sandomirskii²⁵, with Equation (4). For such a comparison it is necessary to express analytically the interrelation existing between v and the rate of deformation of the specimen v_1 .

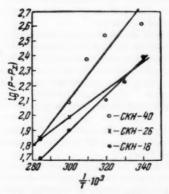


Fig. 5.—The dependence of log $(P-P_z)$ on 1/T. Abscissa: $1/T \times 10^z$; ordinate log $(P-P_z)$. Legends top to bottom: SKN-26, SKN-18.

As a working hypothesis, we assumed that

$$\frac{dv}{v} = \frac{n^{dv_1}}{v_1} \tag{6}$$

where n is the proportionality factor.

Equation (6) shows that the relative increase in the deformation rate of a material at the point where the break grows is proportional to the relative increase in the deformation rate of the specimen. Then

$$\pi = \pi_x + K' \cdot e^{U/RT} \cdot v_1^n \tag{7}$$

Recently by a method of high-speed motion pictues we were able to determine the rate of growth of a break and a notch at different deformation rates. Figure 6 represents some frames of the high-speed motion pictures of the break of a specimen of an SKN vulcanizate by tearing. By interpreting the motion picture photographs taken of vulcanizates, it was found possible to follow the change in the rate of growth of a break or notch in the process of deformation up to the moment when the specimen separates into two pieces. Figure 7

expresses the change in the rate of growth of a break in a vulcanizate of SKN-18 at different stretching rates (curve I, 1000 mm/min; II, 500 mm/min; and III 200 mm/min). Figure 8 shows the elemental relation $v = f(v_1)$ obtained by the method of high speed motion pictures, and confirming within the given limits the existence of a relation of the type $v = Av_1^n$.

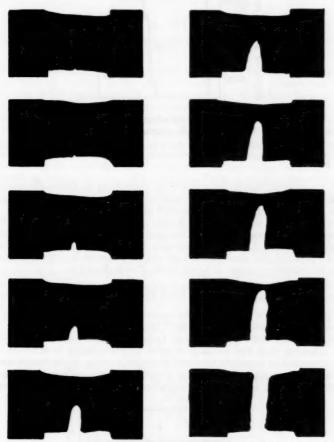


Fig. 6.—Some frames of a motion picture of the break of a vulcanizate sample with a notch (obtained by the author jointly with Krutetakaya and Kurskil).

In converting from π to P, we obtain an equation in the following form

$$P - P_x = K \cdot e^{U/RT} \cdot v_1^n \tag{8}$$

or

$$\log (P - P_z) = \log K + \frac{U}{RT} + n \log v_1 \tag{9}$$

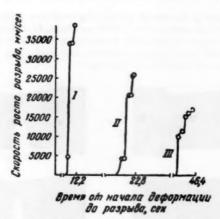


Fig. 7.—Kinetics of growth of a break in a SKN-18 vulcanizate (obtained jointly with Krutetskaya and Kursk). Abscissa: time from start of deformation to break, seconds; ordinate: rate of growth of break, mm/sec.

If we consider that in the experiments carried out by Dogadkin and Sandomivskii $P \ge P_x$, then it may be considered that theory agrees well with experiment, as is seen from the data presented in Figure 9.

In accordance with Equation 8, the resistance to break by the forces of intermolecular interaction should decrease with a diminution in the cohesion energy. Actually, if the specific cohesion energy of the material is E_0 and the volume in which the elemental act of rupture proceeds is a, then the limiting value of activation energy of break where $P \to 0$ should be

$$U_0 \cong aE_0 \tag{10}$$

if $P \ge P_x$. With a decrease in the specific cohesion energy, the value of U_0 decreases, and consequently so does U, since $U = U_0 - aP$.

We, together with Felyukin and Dogadkin, have obtained experimental data attesting that the swelling of different vulcanizates in different liquids is accompanied by a general tendency toward a decrease in the tensile strength. The deviations, with a special choice of liquids and strictly regulated degrees of swelling, were first discovered and explained by us³⁷. Figure 10 presents some

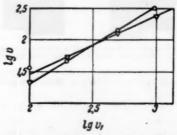


Fig. 8.—Dependence of rate of rupture growth (v) on the rate of stretching (v_1) (obtained jointly with Krutetskaya). Abscissa: $\log v_1$; ordinate: $\log v$.

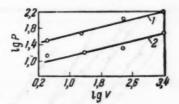


Fig. 9.—Dependence of the logarithm of tensile strength (in the actual cross section) on the logarithm of the rate of stretching: $I-20^{\circ}$ C; $2-80^{\circ}$. Abscissa: $\log v$; ordinate: $\log P$.

experimental data illustrating the general tendency of the tensile strength to decrease with an increase in the degree of swelling. It is characteristic that the decrease in the tensile strength values slows down when fairly large degrees of swelling are reached; this is in agreement with Equation (9).

According to the concepts developed, the break of a vulcanizate proceeds after the material has received a quantity of energy sufficient for overcoming the resistance from the forces of the main chemical affinity and the forces of intermolecular interaction. This quantity of energy is made up of the mechanical energy from the operation of the external deforming forces and from the energy of thermal motion. Each particular rate of deformation of the material at the point where the break grows corresponds to a certain value of the work of the external force consumed in overcoming the bonds between the links of the chain molecules. The rate of deformation of the material at the point of the growth of the rupture changes continually in the course of time. The ratio between the work consumed in the breaking of bonds and that in rupturing bonds brought about by the energy of thermal movement also changes. However, for each set of deformation conditions there is a certain ratio between the portions of mechanical energy and of heat energy consumed in the breaking of bonds. Such a ratio can also exist at a certain constant value of the deformation rate of the material at the point where the break grows, if the de-

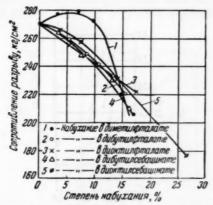


Fig. 10.—The dependence of the tensile strength, in stretching vulcanizates of SKS-30, upon the degree of swelling (obtained jointly with Felyukin and Dogadkin). Abscissa: degree of swelling, %; ordinate: tensile strength, kg/cm². Legends on graph: 1-⊕—swelling in dimethyl phthalate; 2-O—swelling in dibutyl phthalate; 3-X—in dioctyl phthalate; 4-X—in dibutyl sebacate; 5-X—in dioctyl sebacate.

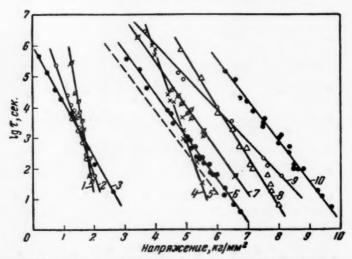


Fig. 11.—Dependence of time to break upon stress: I—vulcanizate without carbon black (Buna 8); \mathcal{E} —plasticated material (polygray) chloride); \mathcal{E} —vulcanizate without carbon black (NBR); \mathcal{E} —aluminum foil; \mathcal{E} —organic glass; \mathcal{E} —pdystyrene; \mathcal{E} —celluphane; \mathcal{E} —celluloid; \mathcal{E} —cellulose acetate; \mathcal{E} 0—nitrocellulose. Abscissa: stress, $\mathcal{E}_{\mathcal{E}}$ /mm²; ordinate: log r, seconds.

formation conditions are such that this rate is constant. The corresponding constant mean value of the rate of growth of the break is designated by the letter v in Equation (6). Thus the constant value of the deformation rate v_1 corresponds to the mean constant value of v. In other words, v is the value of the average rate of growth of the break.

If the rate of deformation v_1 changes in the process of rupture of a vulcanizate, then this variable value may be replaced by a constant one at which the break occurs after the same period of time as with the variable rate. It has been shown experimentally that there is a simple relation between the mean

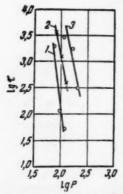


Fig. 12.—Dependence of time to break (min) on deforming stress P (kg/cm²) for nitrile rubbers at room temperature: 1—SKN-18; 2—SKN-26; 3—SKN-40. Abscissa; log P; ordinate log r.

integral rate of deformation and the time to break τ during which the material is deformed, under the deformation conditions adopted by us:

$$v_1 = \frac{K_2}{\tau^m} \tag{11}$$

where K_2 and m are constants determined experimentally⁴⁰. Substituting τ for v_1 in Equation (9), we get:

$$\ln (P - P_x) + \ln K K_2^n - mn \ln \tau + \frac{U}{RT}$$
 (12)

In its general form the activation energy of the process of break depends on the stress P, and hence Equation (12) may be presented in the form:

$$\ln \tau = -\frac{1}{mn} \ln (P - P_x) + \frac{1}{mn} \ln K K_2^n + \frac{U_0}{mnRT} - \frac{aP}{mnRT}$$
 (13)

or

$$\ln \tau = \left[\frac{1}{mn} \ln K K_{2}^{n} + \frac{U_{0}}{mnRT} \right] - \frac{1}{mn} \ln (P - P_{z}) - \frac{aP}{mnRT}$$
 (14)

It follows from Equation (14) that for large values of P, where $\ln (P - P_z) \le aP/RT$, there is a practically linear relation between $\ln \tau$ and P. Such results were obtained by Zhurkov and Narzulaev³⁸. These are shown in Figure 11. For low values of P, where $aP/RT \le \ln (P - P_z)$, the relation is close to linear in the coordinates of $\ln \tau$ plotted against $\ln P$. This position agrees with the results of experiments carried out by ourselves together with Dogadkin and Sandomirskii (see Figure 12), as well as with the data of Holland and Turner³⁰ for the case of the brittle break of glasses.

It follows from Equation (14) that $\log \tau$ and 1/T have a linear relationship. This conclusion also agrees well with experiment. Thus, for example, Zhurkov and Narzulaev obtained an empirical relation which proved to be linear in coordinates of $\log \tau$ versus 1/T (Figure 13).

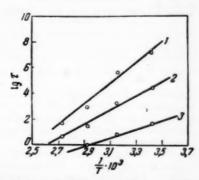


Fig. 13.—Dependence of time to break upon temperature at a constant stress σ for polystyrene: $1-\sigma=2$ kg/mm²; $2-\sigma=4$ kg/mm²; $3-\sigma=6$ kg/mm². Abscissa: $1/T\times 10^{2}$; ordinate: $\log \tau$

REFERENCES

Zwicky, F., Phys. Z. 24, 131 (1923).
 Griffiths, A. A., Phil. Trans. A221, 163 (1921).
 Smekal, A., Z. Tech. Phys. 1, 535 (1926); Phys. Z. 27, 837 (1926).
 Ioffe, A. F., Kirpicheva, N. V., and Levitskaya, M. A., Zhur. Russ. Fiz.-Khim. Obshch. 56, 489 (1924).
 Aleksandrov, A. P. and Zhurkov, S. N. "Vavlenie khrupkovo razryva (Phenomena of Brittle Break)",

Aleksandrov, A. P. and Zhurkov, S. N. "Vavienie khrupkovo razryva (Phenomena of Brittle Break)", GTTI, 1923.
Aslanova, M. S. and Rebinder, P. A., Doklady Akad. Nauk SSSR 96, 2, 299 (1954); Aslanova, M. S., Ibid, 95, 6, 1215 (1954).
Pines, B. Ya., Zhur. Tehk. Fiz. 16, 981 (1946).
Stepanov, A. V., "Sbornik k 70-letiyu akademika A. F. Ioffe (Symposium on the 70th Birthday of Academician A. F. Ioffe)," Izd. AN SSSR. 1950, p. 341; Izvest. Akad. Nauk SSSR, Ser. Fiz. 17,

Stepanov, A. V., "Sbornik k 70-letiyu akademika A. F. Ioffe (Symposium on the 70th Birthday of Academician A. F. Ioffe)," Izd. AN SSSR. 1950, p. 341; Izvest. Akad. Nauk SSSR, 8er. Fiz. 17, 271 (1953).
 Aleksandrov, A. P., Vestnik Akad. Nauk SSSR 7/8, 51 (1944).
 Zapp, R. L. and Baldwin, F. P., Ind. Eng. Chem. 38, 948 (1946); Jonson, B. L., Ind. Eng. Chem. 40, 351 (1948); Yanko, J. A., J. Polymer Sci. 3, 576 (1948); Novikov, A. S., Khalkina, M. B., Dorokhina, T. V. and Arkhangel akaya, M. I., Kolloid Zhur. 15, 1, 51 (1953).
 Mark, H., Ind. Eng. Chem. 34, 11, 1343 (1942).
 Mikhailov, N. V. and Kargin, V. A. "Trudy chetvertol konferentail po vysokomolekulyarnym coldineniyam (Transactions of the Fourth Conference on High Molecular Weight Compounds)", Isd Akad. Nauk SSSR, 1948, p. 115.
 Aleksandrov, A. P. and Lazurkin, Yu. C., Dokkady Akad. Nauk SSSR 45, 308 (1944).
 Dogadkin, B. A. and Karmin, B. K., Kolloid. Zhur. 8, 348 (1948).
 Lukin, B. V. and Kasatochkin, V. I., Zhur. Teth. Fiz. 16, 1383 (1946).
 Dogadkin, B. A. eckovskaya, K., and Dashevskii, M., Kolloid. Zhur. 10, 5 (1948); Pechkovskaya, K., Pupko, S. and Dogadkin, B., Kolloid. Zhur. 12, 5 (1950).
 Howard, R. H., Trans. Farad. Soc. 38, 394 (1942); 39, 267 (1943); Gareya, C. and Borysowski, Z., Proc. Phys. Soc. 61, 446 (1948).
 Lazurkin, Yu. S. and Fogelson, R. L., Zhur. Teth. Fiz. 21, 267 (1951).
 Bartenev, G. M., Doklady Akad. Nauk SSSR 84, 487 (1952); Zhur. Teth. Fiz. 24, 10, 1773 (1954).
 Bartenev, G. M., Doklady Akad. Nauk SSSR 84, 487 (1952); Zhur. Teth. Fiz. 24, 10, 1773 (1954).
 Bartenev, G. M., Wspekhi Khim. 24, 7, 315 (1955).
 Bartenev, G. M., Wspekhi Khim. 24, 7, 315 (1955).
 Bartenev, G. M., Wspekhi Khim. 24, 7, 315 (1955).
 Bartenev, G. M., Wspekhi Khim. 24, 7, 315 (1955).
 Bartenev, G. M., Wspekhi Khim. 24, 7, 315 (1955).
 <

Moscow, 1952.

**Carswell, T. and Nason, H., "Effect of Environmental Conditions on the Mechanical Properties of Organic Plastics", USA, 1944.

**Dogadkin, B. A. and Sandomivskii, D. M., Kolloid Zhur. 13, 4 (1951).

**Boonstra, B. S., Rubber Chem. And Technol. 23, 338 (1950).

**Novikov, A. S., Khalkina, M. B., Dorokhina, T. V. and Arkhangel'skaya, M. I., Kolloid, Zhur. 15, 1, 51 (1953).

**Sifory, P., Ind. Eng. Chem. 38, 417 (1946).

**Gul, V. E., Sideva, N. Ya. and Dogadkin, B. A., Kolloid, Zhur. 13, 6, 422 (1951); Dogadkin, B. A. and Gul, V. E., Sideva, N. Ya. and Dogadkin, B. A., Kolloid, Zhur. 13, 6, 422 (1951); Dogadkin, B. A. and Gul, E. E., Ibid, 12, 3, 184 (1950).

**Chiesa, A., Deutsche Kautschuk-Gesellshaft, Meeting, Hamburg, June 1956.

**Kobenko, P. P., "Amorinye veshchestva (Amorphous Substances)", Izd. AN SSSR, 1952.

**Tobolsky, A. V. and Andrews, H. P., Rubber Chem. and Technol... 18, 4 (1945).

**Bartenev, G. M. and Belostotskaya, G. I., Zhur. Tekh. Fiz. 24, 1773 (1954).

**Gul, V. E., Doklady Akad. Nauk SSSR 85, 1, 145 (1952).

**Gul, V. E., and Farberova, I. I., Kolloid, Zhur. 18, 6 (1956).

**Aleksandrov, A. P., "Trudy I—112—I konferentsil po vysokomolekvlyarnym soedineniyam (Transactions of the 1st and 2nd Conferences on High-Molecular Weight Compounds)", Izd. AN SSSR, 1945.

**Gul, V. E., Fedyukin, D. L. and Dogadkin, B. A., Kolloid, Zhur. 15, 1 (1953).

**Shurkov, S. N. and Naraulaev, B. N., Zhur. Tekh. Fiz. 23, 1677 (1953).

**Holland, A. and Turner, W., J. Soc. Glass Techn. 24, 46 (1940).

**Smekal, A., Phys. Z. 41, 475 (1940); J. Am. Ceram. Soc. 37, 52 (1954).

**Sebardin, H., Kunststoffe 44, 48 (1954).

**Spath, W., "Gummi und Kunststoffe (Rubber and Plastics)," Stuttgart, 1956.

APPROXIMATE ANALYSIS OF THE STRESSED STATE OF RUBBER SPECIMENS, TEAR TESTED BY VARIOUS METHODS *

A. I. LUKOMSKAYA

RESEARCH INSTITUTE FOR THE TIRE INDUSTRY, MOSCOW, USSR

By a tear we usually understand the propagation of cracks, leading to the failure of a specimen or article which is under stress. In tear testing the concentration of stresses is effected either by a special shape of the specimens or by the application of cuts on them.

1. A theoretical investigation of stress distribution in an elastomeric isotropic material has been carried out for the case of the deformation of thin sheets with a hole of known radius. These results are difficult to apply in analysis of stresses in the region of the part of a razor cut or of an analogous part of standard specimens (Figure 1) being tear tested.

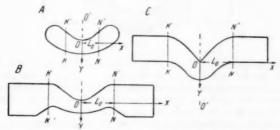


Fig. 1.—Specimens of types A and B with cuts of length 2 mm, and of type C (with no cut) in the undeformed state.

2. Particular interest attaches to the determination of the stresses and deformations in the part where they are concentrated at the moment of starting the tear. It is natural to assume that the tear begins when the stresses and deformations in the point of the cut reach tearing values. With a view to checking on the existence of the indicated connection between the phenomena of tear initiation and tear propagation we applied the following approximated method of analysis.

3. On the surface of the specimens in the undeformed state apply a millimetric rectangular grid. The origin of the rectangular Cartesian system of coordinates O is located in the pont of the cut of type A and B specimens or in the point of the angle of the type C specimens in the center plane along their surface (Figure 1). The axis OY (positive direction downwards) corresponds with the axis of symmetry of the specimen O'O. The stretching is carried out in the direction of the axis OX. The specimen is clamped along the lines KK and NN' each at a distance L_0 from the axis OY. Deformation takes place up

^{*} Translated by R. J. Moseley from Doklady Akad. Nauk SSSR, 127, No. 6, 1207-9 (1959); RABRM translation No. 762.

to the instant of starting of the tear, marked by the appearance of an uncolored strip in the previously colored point of the cut or angle. After maintaining the specimen at this deformation for a prolonged period any one of the points of the rectangular grid with initial coordinates x_0 , y_0 , and z_0 changes into the corresponding point x, y, z (for convenience of numbering the origin of the coordinates O remains in the point or angle. It is found by experience that in thin specimens the displacement of the points on their surface hardly depends at all on the thickness of the specimen, i.e. the picture of the deformation with the surface may be transferred into the middle plane along the thickness, where the displacements are equal to:

$$x - x_0 = u = \Theta_1 (x_0, y_0)$$

$$x - y_0 = v = \Theta_2 (x_0, y_0)$$

$$z - z_0 = w = \Theta_z (x_0, y_0, z_0) = 0$$
(1)

4. In Figure 2 (A specimen of type C of unfilled sodium-butadiene rubber at the instant of commencement of tearing) we show the displacements of the points of the rectangular millimetric grid, represented by the Equations (1). The values of the functions (1) are selected empirically^{3, 4}, on the basis of the observed picture of deformation. Supplementary conditions arising from



Frg. 2

experiment: 1) the lines KK and NN' or the points $\pm x_0 = \pm L_0$ change into $\pm x = \pm L$ for all values of y_0 ; 2) $(\partial u/\partial y_0)_{x_0} = \pm L_0$; 3) the picture of the deformation is symmetrical relative to the coordinate planes YOZ and XOY, or, if we consider this in the middle of the plane $(Z_0 = Z = 0)$, relative to the axis OY; the points $x_0 = 0$ maintain the values x = 0.

5. To find the components of the "tensor" of deformation ϵ_{ik} we use the equations of the nonlinear theory of elasticity^{5, 6}. The connection between the components of the tensors of stress σ_{ik} and of deformation ϵ_{ik} are expressed by the elastic potential F, more or less satisfactory forms of which for rubber have been proposed by Mooney⁷ and Priss⁸. F is a function of the principal extension ratios and of the constants C_1 and C_2 , a method of finding which was developed by Rivlin and Saunders⁹. The adoption of this connection is based upon assumption of the establishment of equilibrium between the stresses and deformations and assumption of isotropicity of the material in the undeformed state.

6. In determining the numerical values of λ_i and their directions in an arbitrary point x_0 , y_0 , z_0 we use the theory of finite deformations developed by Kutilin⁵.

The "affinor" of the deformation under consideration, Φ , is equal to

$$\Phi = \left(1 + \frac{\partial u}{\partial x_0}\right) \mathbf{i}\mathbf{i} + \left(1 + \frac{\partial v}{\partial y_0}\right) \mathbf{j}\mathbf{j} + \left(1 + \frac{\partial w}{\partial z_0}\right) \mathbf{k}\mathbf{k}
+ \frac{\partial v}{\partial x_0} \mathbf{i}\mathbf{j} + \frac{\partial u}{\partial y_0} \mathbf{j}\mathbf{i} + \frac{\partial w}{\partial x_0} \mathbf{i}\mathbf{k} + \frac{\partial w}{\partial y_0} \mathbf{j}\mathbf{k} \quad (2)$$

where i, j, k are unitary cross-cuts of the axes OX, OY and OZ.

As a result of this the symmetric affinor Φ_e has the form:

$$\Phi_{c} = \left(1 + \frac{\partial u}{\partial x_{0}}\right) \mathbf{i}\mathbf{i} + \left(1 + \frac{\partial v}{\partial y_{0}}\right) \mathbf{j}\mathbf{j} + \left(1 + \frac{\partial w}{\partial z_{0}}\right) \mathbf{k}\mathbf{k} + \frac{1}{2} \left(\frac{\partial u}{\partial y_{0}} + \frac{\partial v}{\partial x_{0}}\right) \\
\times (\mathbf{i}\mathbf{j} + \mathbf{j}\mathbf{i}) + \frac{\partial w}{\partial x_{0}} (\mathbf{i}\mathbf{k} + \mathbf{k}\mathbf{i}) + \frac{\partial w}{\partial y_{0}} (\mathbf{j}\mathbf{k} + \mathbf{k}\mathbf{j}) \quad (3)$$

The numerical values λ_1 , λ_2 , and λ_3 are found from the expressions for the 1st, 2nd and 3rd invariants of the symmetric affinor, and also from the condition of maintenance of constancy of volume with the deformation λ_1 , λ_2 , $\lambda_3 = 1$.

TABLE 1

Comparison: Stress σ_1 and Deformation λ_1 at Instant of Commencement of Tearing in the Point of a Cut in Type A and B Specimens and of the 'Angle' of Type C Specimens; Ultimate Tensile Strength σ_{su} and Relative Deformation at Break ϵ_s for Unyilled Rubbers

		Vulcanized rubbers based on			
Type of specimen	Index	Natural rubber	Sodium- butadiene rubber	Styrene- butadiene- rubber	
GOST 270-53	σ_{xu} ϵ_{xu}	$\frac{2420}{9}$	87.5 6.0	$126 \\ 6.5$	
ASTM D624-54 type A	σ_1 λ_1	3000 10.5	89 7.5	128 8.1	
ASTM D 624–54, type B	$\sigma_1 \\ \lambda_1$	4080 12	97.5 8.0	146 8.3	
ASTM D 624–54 type C	σ_1 λ_1	6100 16.5	107.5 8.2	137 8.5	

The direction cosines α_i , β_i and γ_i of the principal axes of deformation λ_i are calculated from the equations

$$\left[\left(1 + \frac{\partial u}{\partial x_0} \right) - \lambda_i \right] \alpha_i + \frac{1}{2} \left(\frac{\partial v}{\partial x_0} + \frac{\partial u}{\partial y_0} \right) \beta_i + \frac{\partial w}{\partial x_0} \gamma_i = 0$$

$$\frac{1}{2} \left(\frac{\partial v}{\partial x_0} + \frac{\partial u}{\partial y_0} \right) \alpha_i + \left[\left(1 + \frac{\partial v}{\partial y_0} \right) - \lambda_i \right] \beta_i + \frac{\partial w}{\partial y_0} \gamma_i = 0$$

$$\frac{\partial w}{\partial x_0} \alpha_i = \frac{\partial w}{\partial y_0} \beta_i + \left[\left(1 + \frac{\partial w}{\partial z_0} \right) - \lambda_i \right] \gamma_i = 0$$

$$\alpha_i^2 + \beta_i^2 + \gamma_i^2 = 1 \quad (i = 1, 2, 3)$$
(4)

7. In practice no real angle exists in type C specimens (in the opposite case the stress in it at infinitely small deformation must be of infinitely great magnitude). The radius of curvature of the 'angle' of or the point of the cut is not known. Empiric values of the Functions (1) are selected with some or other approximation. Bearing this in mind, it is desirable to determine the stresses and deformations in the point $x_0 = y_0 = z_0 = 0$ (the point of the cut or angle) by extrapolation to zero of their corresponding dependences upon the distance

to the point of the cut. It is most simple to carry out such an extrapolation for the points on axis OY, where the directions of the main axes of deformation coincide with the axes of the coordinates and $\lambda_1 = 1 + \frac{\partial u}{\partial x_0}$; $\lambda_2 = 1 + \frac{\partial u}{\partial x_0}$ $\partial v/\partial y_0$; $\lambda_3 = 1 + \partial w/\partial z_0$.

8. The results of the analysis are given in Table 1. In spite of their approximate character, it is easy to see that there is satisfactory agreement between the true values of the ultimate tensile strength σ_{zu} and the stress σ_1 in the direction of the axis of extension in the point of the cut of the specimen at the instant of commencement of tearing. The same applies to the corresponding values of the relative elongation at break ϵ_z and the main degree of deformation $\lambda_1:\lambda_1\approx\epsilon_z+1$.

ABSTRACT

This paper describes analyses made of the stress and strain changes in the 3 standard ASTM tear specimens and a GOST 270-53 specimen up to the time of tearing. Using the nonlinear theory of elasticity the stresses are calculated and show reasonable agreement with ultimate tensile strength figures. The results refer to natural, sodium-butadiene and styrene-butadiene rubbers.

REFERENCES

- Rivlin, R. S., and Thomas, A. G., Phil. Trans. Roy. Soc. A243, No. 865, 289 (1951).
 GOST 262-53: ASTM D624-54: DIN 53515: B.S. 903, Method 2 B 20.
 Semendyaev, K. A., "Empire Formulae", 1933.
 Worsing, L. and Heffner, J., "Methods of Treatment of Experimental Data" (translation into Russian, 1953).
 Kulinin, D. I., "Theory of Finite Deformations", 1947.
 Novoshilov, V. V., "Principles of the Non linear Theory of Elasticity", 1948.
 Mooney, M., J. Appl. Phys., 11, 582 (1940).
 Priss, L. S., Doklady Akad. Nauk SSSR 116, No. 2, 225-8 (1957). (RABRM Transl. 638): Zhur. Tekh. Fiz. 28, No. 3, 636-46 (1958). (English transl. available.)
 Rivlin, R. S. and Saunders, D. W., Phil. Trans. Roy. Soc. A243, No. 865, 251 (1951); Trans. Faraday Soc. 44, 200 (1952).

VOLUME CHANGES AND DEWETTING IN GLASS BEAD-POLYVINYL CHLORIDE ELASTOMERIC COMPOSITES UNDER LARGE DEFORMATIONS *

THOR L. SMITH

JET PROPULSION LABORATORY, CALIFORNIA INSTITUTE OF TECHNOLOGY, PASADENA, CALIFORNIA

INTRODUCTION

Elastomeric materials loaded with inert filler have rheological properties which, on the one hand, are qualitatively like those of unfilled polymeric materials, but which, on the other hand, are unique to filled systems. Their stress-strain curves usually have several distinct regions which are similar to those for certain unfilled polymeric materials. The curves have an initial region in which the stress increases with strain, and here the modulus depends primarily on the amount of filler and the properties of the binder. In the second region, the stress may be roughly independent of the strain or may increase at a rate markedly less than that in the initial region. The transition between these two regions may be either gradual and hardly perceptible or sharp, with a well-defined yield point. Thus, in these two regions, the stress-strain curves may be like those for typical unfilled rubbers or for plastics, or they may resemble the curves for rubbers at low temperatures, which cold draw or neck. In the third region the stress increases more rapidly with strain than in the second region and continues to increase until the specimen breaks; again, this is similar to what is observed for certain plastics and rubbers. Thus, both filled and unfilled systems can have sigmoidal stress-strain curves which may or may not have distinct yield points.

However, filled systems, and especially those in which the binder wets, but does not react chemically with the filler, exhibit the sigmoidal-type stress-strain curve for different reasons than do rubbers and plastics. In filled systems, the binder adheres to the filler initially, which reinforces or strengthens the system. However, in the transition and second regions of the stress-strain curve, adhesive bonds between the filler and binder break, a process called dewetting, and vacuoles form around the filler particles. After the adhesive bonds are essentially all broken, a further increase in strain only stretches the binder

further and enlarges the vacuoles.

Perhaps the best method of studying dewetting is to measure the volume of the filled system as a function of elongation. When an unfilled rubber is stretched, its volume remains essentially constant, provided crystallization does not occur. However, when a filled system is stretched, and vacuoles form, the volume increase may be large: e.g., 50 to 100%, or possibly more. The measurement of this volume increase by means of a sensitive dilatometer can give a precise value for the elongation at which the dewetting begins, and possibly that at which it is complete.

^{*} Reprinted from Trans. Soc. Rheology 3, 113~136 (1959). This paper presents the results of one phase of research carried out at the Jet Propulsion Laboratory, California Institute of Technology, under sponsorship of the Department of the Army, Ordnance Corps (Contract No. DA-04-495-Ord 18). The present address of the author is, Stanford Research Institute, Menlo Park, California.

Additional information can be derived from a study of the volume changes. Since the data show precisely the elongation at which adhesive failure begins, methods for modifying the adhesive strength can be investigated. Further, the temperature dependence of the adhesive strength can be studied by carrying out tests at different temperatures. If certain assumptions are made, an estimate can be obtained of the elongation of the binder between adjacent filler particles at the time when dewetting occurs. This result, when combined with the stress-strain properties of the unfilled binder, gives an indication of

the stress required to break the adhesive bonds.

Relatively few dilatometric studies have been made of the volume changes that occur during the stretching of filled materials. Holt and McPherson¹ made a careful study of the stretching of unfilled vulcanized rubber and the volume changes resulting from crystallization; also, a few studies were made of a gum stock filled with whiting and a carbon black. These investigations were extended by Jones and Yiengst², who studied the volume changes that occurred when various pigmented-rubber systems were stretched in a dilatometer similar to one used by Holt and McPherson. More recently, some data were obtained in a similar manner by Bryant and Bisset³ for several filled rubber vulcanizates. Prior studies relating to vacuole formation in filled rubbers were made by Schippel⁴, Green⁵, Vogt and Evans⁶, and DePew and Easley⁻.

The present study was made to extend previous work and to obtain data at several temperatures. Filled systems composed of small glass beads dispersed in a polyvinyl chloride-dioctyl sebacate rubber were stretched in a dilatometer at 0, 25, and 50° C. Less precise data were also obtained by stretching specimens and measuring the change in their width and length. A simple equation was derived to relate the volume fraction of filler to the yield strain obtained

from the dilatometric data.

EXPERIMENTAL

MATERIALS

Glass beads.—The glass beads were obtained from the Minnesota Mining and Manufacturing Company; their No. 1160 beads were used in nearly all the composites studied. These beads were essentially spherical and were analyzed for size and polydispersity by means of a Micromerigraph. The beads had a weight-average diameter of approximately 40 μ , and about 94 wt-% of the beads had diameters between 20 and 60 μ .

Limited studies were made with beads Nos. 118, 116, 114, and 112. From rough Micromerigraph data, it appeared that these beads had weight-average diameters of about 50, 80, 105, and 140 μ , respectively. (The size of the No. 112 beads was not measured, but a diameter of 140 μ was assumed after comparing data supplied by the manufacturer with measurements obtained on the

Micromerigraph for beads Nos. 118, 116, and 114.)

Elastomer.—The elastomer was prepared from equal weights of a polyvinyl chloride plastisol (Geon 121) and dioctyl sebacate and contained 2.5% lead stearate as stabilizer. To obtain a uniform dispersion, the solids were slowly added to the dioctyl sebacate while it was stirred mildly by a Brookfield counterrotating stirrer. The mixture was then vigorously stirred for 10 min by the Brookfield stirrer running at a high speed. The resulting dispersion was cast into trays, degassed for about 30 min (or until no more gas was evolved), and then cured for about 1 hr at 180° C. The cured sheets, about \{ \frac{1}{8}} in. thick, were visibly homogeneous and completely bubble-free.

Composites.—In preparing the glass-bead composites, the polyvinyl chloride disperson was mixed as described above, and then degassed. The glass beads were next added slowly while the dispersion was stirred at low speed. The re-

sulting mixture was cast into trays, degassed, and then cured.

In addition to sheets of the composites, elongated ringlike specimens were prepared for testing in the dilatometer. The shape and dimensions of the rings are shown in Figure 1. Specimens of this shape were chosen in preference to circular rings, since they could be stretched in the dilatometer without first being flattened, which might disrupt some adhesive bonds between the beads and binder. The rings were prepared by casting the uncured composite into an open mold machined in a small block of aluminum. After the dispersion was poured into the mold, it was degassed again; the excess was then scraped from the surface of the mold, and the mold was placed on a hot plate to effect cure. Highly uniform rings, which ordinarily differed in weight by less than 5%, were prepared in this way.

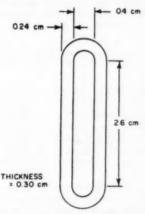


Fig. 1.—Elongated-ring specimen used in dilatometer.

One disadvantage of rings is that the strain in a stretched specimen is not uniform, since the outside of the ring is elongated more than the inside. The rings used had an outside-to-inside-circumference ratio of about 1.23; therefore, the average circumference was used to calculate an average strain or extension ratio from the extension of a ring.

The cured composites were essentially free of voids, as determined by density measurements, and the beads appeared to be uniformly dispersed. However, composites prepared from beads Nos. 112 and 116 had a thin resin-rich surface,

which indicated that these beads had settled somewhat after mixing.

The densities of representative samples of the composites prepared with No. 1160 beads were obtained by hydrostatic weighing. These values are compared in Table I with the theoretical densities calculated from density values of 2.39 and 1.135 g/ml for the beads and the elastomeric binder, respectively. The calculated and measured densities agreed within a few per cent, except for the composite having 50 wt-% beads. The reason for this disagreement is not known; it probably is the result of some error, since no other evidence was ob-

tained which indicated voids in any samples for which data are reported. (Densities were measured on only one set of samples, and many samples were

prepared during the study.)

Polyurethane foam fubber.—To prepare the foam, a castable polyurethane elastomer filled with 59% by volume of a water-soluble inorganic salt was first prepared. About 70% of the salt had an average particle diameter of 150 μ , and 30% had an average diameter of 15 μ . The foam was obtained by extracting the salt from the filled elastomer with boiling water. The foam was dried carefully and chemically analyzed to verify that the salt had been extracted completely.

APPARATUS AND PROCEDURE

Dilatometer.—A dilatometer was constructed which was similar to the one used by Holt and McPherson¹ and by Jones and Yiengst². It consisted of a metal tube which had rubber O-rings and screw caps on each end. A piece of drill rod passed completely through the metal tube and screw caps. Inserted in each screw cap was a threaded stuffing box, which prevented leakage of the

Table I

Experimental and Calculated Densities of Composites
Containing No. 1160 Glass Beads

Glass- bead content.	Glass- bead content.		Density, g/ml	
wt-%	vol-%	Experimental	Calculated	Differe
25	13.7	1.273	1.308	-0.035
50	32.2	1.355	1.541	-0.186
60	41.5	1.645	1.657	-0.012
70	52.5	1.840	1.794	0.046
75	58.9	1.895	1.875	0.020
80	65.4	1.975	1.955	0.020

dilatometer fluid and yet allowed the rod to be moved up and down. The metal tube had a side arm, to which a calibrated glass capillary and an auxiliary reservoir were attached. To hold the ring test specimen in the dilatometer, a metal hook was attached on the inside, near the top of the metal tube, and a similar hook was attached to the drill rod.

In making measurements, the top screw cap was removed, and a ring specimen was hung over the hook attached to the inside of the metal tube. The screw cap was then replaced, and the dilatometer was filled with water from the auxiliary reservoir. A small vent hole in the upper screw cap permitted the escape of any trapped air, after which the vent hole was plugged, and the auxiliary reservoir was isolated from the main part of the apparatus. To test for leaks, the water level in the capillary was observed while the drill rod was moved down and up. The drill rod was next moved to the appropriate position and then rotated until its attached hook moved inside the ring and was in the same vertical plane as the upper hook. The rod was slowly moved down until fiducial marks on the exposed portion of the rod and on a reference rod indicated that the ring was snugly fitted between the hooks and ready to be tested. Next, the rod was moved down stepwise to stretch the ring. After each step, the water level in the capillary was read, and the position of the fiducial mark on the rod was measured by a cathetometer. This procedure was continued until the ring had been stretched about 200%.

Some data were obtained with another dilatometer, which was similar except that the tube was made of Lucite tubing, rather than metal. In this dilatometer, the extension of the ring could be observed visually. Occasionally, the extension of a ring was measured directly by the cathetometer, and the results agreed closely with values obtained from the fiducial mark on the rod. However after two Lucite tubes had cracked, the tube was replaced by a metal one,

To obtain data at 0, 25, and 50° C, the dilatometer was placed in a water bath controlled to ± 0.1 ° C or less. A few runs were made at -19° C; in these, a silicone fluid was substituted for water as the confining liquid in the dilatometer. Accurate temperature control of the thermostat was always maintained in order to prevent small temperature fluctuations during an experi-

ment from changing the water level in the capillary.

Dimension measurements.—Some studies were made by measuring the elongation and width of rectangular tensile specimens which were stretched stepwise. Bench marks were inked on a specimen, and the separation of these marks was measured by a cathetometer after each incremental elongation of the specimen. The width of the specimens was measured by a micrometer. Although this simple procedure is not as precise as the dilatometric method, it provided reasonably accurate data.

THEORETICAL

POISSON'S RATIO

The deformation of an elastic material in pure homogeneous strain may be characterized by three principal extension ratios. For example, suppose that an undeformed rectangular parallelepiped, having length L_0 , width W_0 , and thickness T_0 , is deformed by loads applied perpendicularly to its opposite faces. The resulting deformation is given by the principal extension ratios $\lambda_1 = L/L_0$, $\lambda_2 = W/W_0$, and $\lambda_3 = T/T_0$, where L, W, and T are the new length, width, and thickness. Thus, the volume change is given by the relation

$$V/V_0 = \lambda_1 \lambda_2 \lambda_3 \tag{1}$$

where V and V_0 are the volumes of the deformed and undeformed material. When an isotropic material is subjected to tension or compression, λ_2 equals λ_3 . If no volume change occurs, the following relation holds:

$$1 = \lambda_1 \lambda_2^2 \tag{2}$$

This leads to the equation

$$d\lambda_2/d\lambda_1 = -\lambda_2/2\lambda_1 = d\epsilon_w/d\epsilon_1 \tag{3}$$

where ϵ_w is the lateral strain, and ϵ_1 is the longitudinal strain. According to classical elasticity, based on small-deformation theory, Poisson's ratio ν equals $-d\epsilon_w/d\epsilon_1$, and Equation (3) shows that this ratio varies with the extension, even though it is assumed that no volume change occurs. However, (3) can be integrated to give

$$\ln \lambda_2 / \ln \lambda_1 = -\frac{1}{4} \tag{4}$$

where $\ln \lambda_2$ and $\ln \lambda_1$ are the Hencky, or logarithmic, lateral and longitudinal strains. Thus, Poisson's ratio, defined in terms of the logarithmic measure of strain, is independent of the extension and equals $\frac{1}{2}$, provided that the volume

remains constant. Certain valid reasons are recognized for not defining Poisson's ratio in terms of logarithmic strain. However, Poisson's ratio defined in terms of logarithmic strain is used in this paper only as a convenient index for rate of volume change, even though some other name should, perhaps,

be given to this quantity.

Poisson's ratio, defined in terms of logarithmic strain, is a convenient number to use in specifying volume changes that occur when an elastic material is subjected to large deformations. The volume change that occurs during a tensile or compressive deformation is given by the following equation, derived by differentiating Equation (1) after noting that λ_2 equals λ_3 :

$$\frac{d \ln V/V_0}{d \ln \lambda_1} = 1 + 2 \frac{d \ln \lambda_2}{d \ln \lambda_1} = 1 = 2\nu \tag{5}$$

where Poisson's ratio ν , which may be a function of λ_1 , is defined as follows:

$$\nu = - d \ln \lambda_2 / d \ln \lambda_1 \tag{6}$$

YIELD STRAIN

Certain filled elastomers, like glass bead-polyvinyl chloride composites, can be stretched to a limited extent without showing any appreciable volume change. However, at a reasonably well-defined yield strain, dewetting occurs, and the volume of the sample increases continuously with further stretching. The yield strain can be related to the volume fraction of filler by an equation based on certain simplifying assumptions.

Consider a unit cube of an elastomer filled with n^3 spherical particles, each having a radius r and a modulus which is large compared with that of the elastomeric binder. Assume that these spheres are uniformerly dispered, and that their centers lie in a cubic close-packed array: i.e., if the radius of each sphere were enlarged until all spheres touched, a cubic close-packed array would

result.

Now consider a line through the centers of the n spheres in one row. The length of the line is unity, the fraction of the line occupied by spheres is 2rn, and the fraction occupied by binder is d_0 . Thus,

$$2rn + d_0 = 1 \tag{7}$$

The volume fraction of spheres V_f can be shown, by considering the geometrical properties of cubic close-packed arrays, to be

$$V_f = \frac{4\sqrt{2}}{3} \pi (rn)^3$$
 (8)

By combining Equations (7) and (8), the following expression is obtained:

$$\left(\frac{3\sqrt{2}}{\pi}\right)^{\frac{1}{2}}V_{f^{\frac{1}{2}}} + d_{0} = 1$$
 (9)

If the cube containing the filler is stretched a distance Δl , and if dewetting does not occur, then the following equation can be written:

$$1.105V_f^{\frac{1}{2}} + d_0 + \Delta l = 1 + \Delta l \tag{10}$$

where $1.105 = (3\sqrt{2}/\pi)^{\frac{1}{3}}$. Equation (10) can be rearranged to give

$$1.105V_{f}^{\frac{1}{2}} + (1 + \epsilon_{r}) d_{0} = 1 + \epsilon \tag{11}$$

where ϵ_r is the strain in the binder between adjacent spheres and equals $\Delta l/d_0$, and ϵ is the strain imposed on the unit cube and equals Δl . Now, by substituting in Equation (11) the value of d_0 given by Equation (9), the following relation is obtained:

$$\epsilon = \epsilon_r (1 - 1.105 V_f^{\frac{1}{2}}) \tag{12}$$

This equation gives ϵ/ϵ_r (the ratio of the over-all strain imposed on the sample to the strain in the binder along the line between the centers of adjacent spheres) in terms of the volume fraction of spheres. Now, assume that dewetting occurs when ϵ_r reaches a critical value $\epsilon_{r,c}$, which is assumed to be independent of the amount of filler. Thus, the observed yield strain ϵ_c is given by the equation

$$\epsilon_c = \epsilon_{r,c} \left(1 - 1.105 V_f^{\dagger} \right) \tag{13}$$

When no filler is present, this equation shows that $\epsilon_c = \epsilon_{r,c}$, and, when V_f equals 0.74 (the volume fraction of spheres in a cubic close-packed array), that $\epsilon_c = 0$.

RESULTS AND DISCUSSION

PRELIMINARY STUDIES

A tensile specimen of the polyurethane foam rubber was stretched in incremental steps, and the width and per cent elongation were measured for elonga-

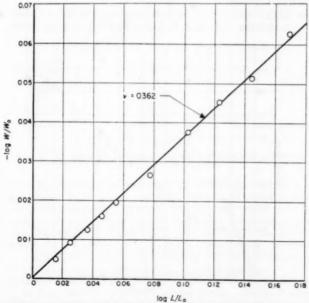


Fig. 2.—Variation in width and length during extension of foam rubber specimen.

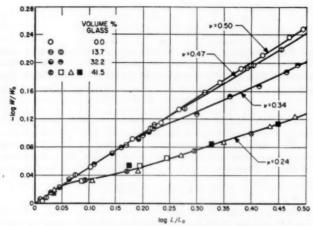


Fig. 3.-Variation in width and length during extension of glass bead composites.

tions up to about 50%. Figure 2 shows that $-\log W/W_0$ is directly proportional to $\log L/L_0$, and that Poisson's ratio is 0.362. When similar measurements were made on a polyurethane elastomer, Poisson's ratio was found to be 0.50 over the entire range of extensions covered. The behavior of the foam is like that of a filled elastomer after dewetting is complete, in that Poisson's ratio is independent of extension.

Similar measurements were made on specimens of the polyvinyl chloride composites containing 13.7, 32.2, 41.5, and 58.9 vol.-% glass beads. (These

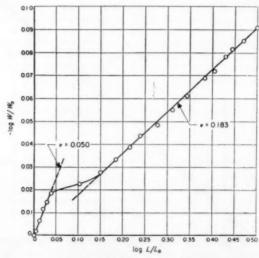


Fig. 4.—Variation in width and length during extension of composites containing 58.9% glass beads. (Legend on first section of curve should read: ν = 0.500.)

volume per cents, and others given in this paper, were calculated from the known weight per cents of binder and glass beads.) The data from these preliminary tests are shown in Figures 3 and 4; data on the unfilled polyvinyl chloride elastomer are also included in Figure 3. In small deformations, Poisson's ratio for all polyvinyl chloride composites is 0.50, within the experimental error, and, for the unfilled elastomer, it is 0.50 over the entire range of extensions (i.e., 0 to 200%). For the composites, however, dewetting begins at some critical extension; after a transition region, $-\log W/W_0$ again increases linearly with $\log L/L_0$, but at a reduced rate. The slope of the final linear portion of a curve equals Poisson's ratio, which is seen to increase from 0.24 to 0.50 as the glass content is decreased.

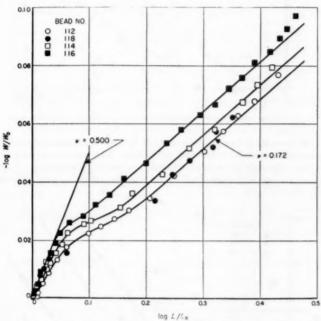


Fig. 5.—Variation in width and length during extension of composites containing 52.5% glass beads of different sizes.

After a sample of the composite containing 41.5% glass had been stretched 200%, it was allowed to recover to within 3% of its initial length, and the measurements were then repeated. Poisson's ratio was now found to be 0.24 over the entire extension range. Although this result does not definitely prove that the dewetting was complete during the first extension, it does show that the adhesive bonds did not reform when the sample recovered. However, some qualitative observations indicated that adhesive bonds can reform in a recovered specimen, provided a sufficiently long period elapses.

Some data, shown in Figure 5, were also obtained on composites containing 52.5 vol.-% of Nos. 112, 114, 116, and 118 glass beads. Again, Poisson's ratio was constant at both small and large deformations. The value was approxi-

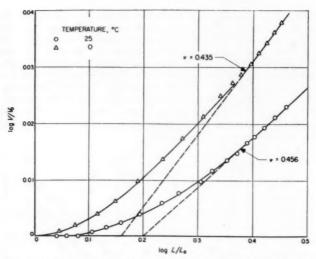


Fig. 6.—Volume increase during extension of composites containing 13.7% glass beads.

mately 0.50 in small deformations and 0.172 in large deformations, even though the composites contained different-sized beads. The composites had different yield values, although the values obtained are not very accurate. In general, yield values are not very reproducible, but Poisson's ratio in large deformations is usually reproducible.

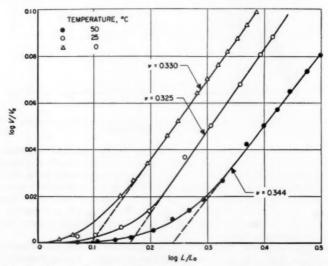


Fig. 7.—Volume increase during extension of composites containing 32.2% glass beads.

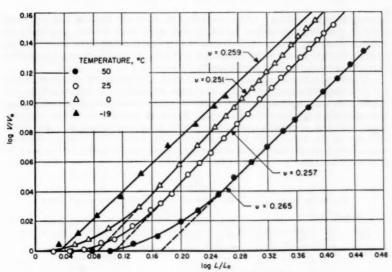


Fig. 8.—Volume increase during extension of composites containing 41.5% glass beads.

DILATOMETRIC STUDIES

More precise and extensive data on Poisson's ratio and the yield strain were obtained by use of the dilatometer. First, an unfilled polyvinyl chloride ring was elongated to 150% in incremental steps in the dilatometer. The volume increase observed was exceedingly small, approximately 0.23%, and gave a Poisson's ratio of about 0.499. This value is in close agreement with the value of 0.500 reported by Holt and McPherson¹ for vulcanized natural rubber at

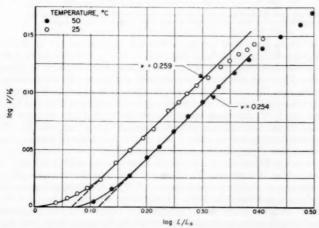


Fig. 9.—Volume increase during extension of composites containing 52.5% glass beads.

extensions up to 300%. Other experiments made on the unfilled polyvinyl chloride elastomer, stretched to 200% and more, also showed essentially no volume changes. It is thus concluded that, when the binder itself is extended, volume changes do not occur (at least not at 25° C) either because of formation

of voids or resulting from crystallization.

Volume changes as a function of extension were measured dilatometrically for the composites containing 13.7, 32.2, 41.5, and 52.5 vol.-% glass. Measurements were made at 0, 25, and 50° C for the composites containing 32.2% glass; the composites having 13.7 and 52.5% glass were tested at only two temperatures; and the composite containing 41.5% glass was tested at -19° C, in addition to the three other temperatures. Ordinarily, duplicate experiments were made, but only the results of single experiments are shown in Figures 6 to 9, plotted as $\log V/V_0$ vs. $\log L/L_0$.

TABLE II
POISSON'S RATIO AND YIELD STRAIN FOR GLASS BEAD COMPOSITES

Glass-	bend co	ntent							
Bead	wt-	vol-		Poisson	s ratio »			Yield strain	te
No.	%	%	0° C	25° C	50° C	~25° C	0° C	25° C	50° C
1160	25	13.7	0.435	0.456	-	0.47	0.44	0.58	-
			0.432	0.463	_		0.45	0.75	-
				0.419	-			0.68	-
1160	50	32.2	0.330	0.325	0.344	0.34	0.24	0.46	0.73
			0.326	0.313	-		0.25	0.57	
				0.310	-			0.50	_
1160	60	41.5	0.234	0.268	0.265	0.24	0.24	0.23	0.49
			0.251	0.257	0.275		0.19	0.31	0.35
1160	70	52.5	_	0.259	0.254	0.16	-	0.17	0.30
				0.265	-		_	0.09	
			-	0.256			-	0.12	_
1160	75	58.9				0.19		0.10^{6}	
112	70	52.5				0.172		0.08^{b}	
114	70	52.5				0.172		0.10^{6}	
116	70	52.5				0.172		0.12^{6}	
118	70	52.5				0.172		0.06(?)	

Preliminary data obtained by measuring the width and length of stretched specimens.
 Yield strains obtained from interpolated "break-away" points in Figures 4 and 5.

These figures show that the data from any experiment can be divided into three sections, similar to those in Figures 3 to 5. In the first section, which is for small deformations, little or no volume increase occurs as a specimen is extended. The next section is the transition region, in which dewetting of the filler occurs, and the volume increases at a progressively increasing rate as the sample is extended. In the final section, the dewetting is believed to be complete and $\log V/V_0$ increases linearly with the logarithmic strain. Figure 9 shows that the rate of volume increase drops off at high extensions. This behavior is believed to result from water in the dilatometer diffusing into the vacuoles or other defects in the stretched specimen.

By the use of Equation (5), Poisson's ratio was calculated from the slope of the linear section of a curve. The linear section was also extrapolated to zero volume change to obtain a yield strain. Values for Poisson's ratio and the yield strain are presented in Table II, together with the values for Poisson's ratio which were obtained in the preliminary experiments by measuring the width and length of a specimen. At -19° C, Poisson's ratio and the yield strain for the 41.5%-glass composite were 0.259 and 0.08, respectively. The

data in Table II show that the duplicate values for Poisson's ratio are in close agreement, and that the values obtained from the preliminary experiments agree closely with those obtained dilatometrically, except for the composite containing 52.5% glass. Within the experimental error, Poisson's ratio is probably independent of temperature, although the data suggest that it may increase slightly with temperature. Although the data on a single ring specimen are very precise, the reproducibility of results on identically prepared ring specimens is not accurately known. Thus, it is believed that the variation in Poisson's ratio may be partly due to slight variations in specimen density, which would indicate the existence of microscopic voids in the specimens, and

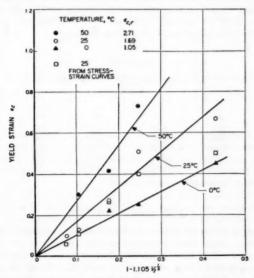


Fig. 10.-Variation of yield strain with volume fraction of glass beads.

partly due to nonuniform dispersion of the beads in the different specimens. The small experimental error in obtaining the strain in a ring, partly due to the use of fiducial marks outside the dilatometer, would not affect Poisson's ratio, although it would lead to error in the yield strain.

Table II shows that the yield strain depends rather strongly on temperature, although its reproducibility is poor. The poor reproducibility is not unexpected, since dewetting is a sensitive and highly rate-dependent process. Small differences in the microscopic structure or mechanical treatment of a specimen can easily cause marked variations of the strain range in which dewetting occurs. However, the temperature dependence of the yield strain is expected, since the modulus of the binder is temperature dependent.

To show how accurately Equation (13) predicts the variation of the yield strain with the volume fraction of filler, average values of the yield strain ϵ_c are plotted against $1-1.105V_f^{-1}$ in Figure 10. This figure also shows yield strains at 25° C obtained from stress-strain curves measured on the Instron tester at a strain rate of 0.6 min⁻¹. The stress-strain curves had two near linear

portions: at strains somewhat less d strains ansomewhat greater than the yield strain. These linear portions were connected either by a curve of gradually decreasing slope or by a curve which passed through a maximum; the latter type of curve was like those for plastics which cold draw. From both types of curves, the yield strain was obtained by extrapolating both linear portions until

they intersected.

Although the points in Figure 10 scatter considerably, the lines drawn are reasonably consistent with the data and have slopes of 1.05, 1.69, and 2.77 at 0, 25, and 50° C, respectively. These slopes, according to Equation (13), should equal $\epsilon_{c,r}$, the strain of the binder between adjacent particles immediately preceding adhesion failure. From the stress-strain curves of the unfilled binder, it was found that these strains correspond to stresses of 550, 470, and approximately 430 psi at 0, 25, and 50° C, respectively. Thus, the adhesion force appears to show little or no temperature dependence.

Table III
Tensile Data for Glass Bead Composites at 25° C

Glass bead content, vol-%	σe, pai	40	E_0 , pei	E_a , pei	$E_a(V_b - 0.26)^{-1}$
13.7	230	0.50	450	285	473
32.2	240	0.40	580	140	334
41.5	146^{a}	0.26^{a}	560	114	351
52.5	90a	0.11^{a}	820	94	437
58.9	63 ^a	0.06^{a}	1050	75	503

⁶ Obtained by double extrapolation, as explained in text.

STRESS-STRAIN BEHAVIOR

Only limited stress-strain data were obtained on the composites and unfilled binder. However, some data measured on the Instron tester at 25° C are given in Table III. This table gives the yield stress σ_c , the yield strain ϵ_c , the initial modulus E_0 , and the modulus after yield E_a ; the latter modulus was taken as the slope of the linear portion of the σ - ϵ curves after yield. (Values of σ_c and ϵ_c for the three composites having the most filler were obtained by interpolation, as explained previously.) It is seen that the yield stress and strain decreases, and the initial modulus increases, with filler content; however, the modulus does not increase very rapidly, considering the large variation in filler content.

The modulus after yield decreases with filler content, as expected, since now the filler only dilutes the binder and has no reinforcing effect. If it is assumed that the filler only dilutes the binder, it seems reasonable to suggest that E_a is proportional to $V_b - 0.26$, where V_b is the volume fraction of binder. The factor 0.26 is introduced, since if the spheres were monodisperse, the maximum volume fraction of spheres would be 0.74, and thus 0.26 would be the minimum fraction of binder that could be present in a well-consolidated composite. The assumption that E_a is proportional to $V_b - 0.26$ means that E_a is zero when V_b equals 0.26, which seems reasonable. With these several assumptions, the following equation results:

$$E_a = 1.35 E_b (V_b - 0.26) (14)$$

where E_b is the modulus of the unfilled binder. Values of $E_a(V_b - 0.26)^{-1}$, given in the last column of Table III, are seen to be relatively constant: none vary by more than 20% from the average, which is 420. When this average value is divided by 1.35, a value of 310 psi is obtained for the modulus of the unfilled binder, which compares favorably with an experimental value of 386.

Tensile data for the composite having 32.2% filler and the modulus for the unfilled binder, as measured at a strain rate of 0.6 min⁻¹ and at a series of temperatures, are given in Tables IV and V. The data given in Tables III to V

Table IV

Temperature Dependence of Mechanical Properties for the Composite Containing 32.2% Glass Beads

Temperature,	σ _c , psi	£e	E_0 , psi	E_a , pai
-40	220	0.07	3200	660
-23	240	0.15	1500	360
- 7	240	0.24	975	240
- 1	280	0.30	905	184
27	240	0.40	580	140
43	168	0.52	320	115
60	73	0.32	225	116

depend on the strain rate, sometimes markedly. The most marked dependence on strain rate is shown by the section of the stress-strain curve for a composite in the yield or dewetting region. Since a complete study was not made, the effect of the strain rate and the reproducibility of the tensile data are not accurately known.

An analysis of E_0 and E_a in Table IV and of E_b in Table V for the unfilled binder shows that these three quantities have the same temperature dependence. Since these quantities are determined by the properties of the binder, this behavior is expected. However, the yield stress in Table IV appears inde-

Table V
Temperature Dependence of the Modulus for the Unfilled Binder

Temperature, ° C	Es, psi
-48	2800
-34	1580
4	585
27	386
49	230
71	132

pendent of temperature within experimental error, with the exception of values at 43 and 60° C. This temperature insensitivity implies that the filler-binder adhesive strength is temperature-independent. A similar conclusion was reached, but in a different way, by analysis of the data in Figure 10.

COMPARISON WITH LITERATURE DATA

Bryant and Bisset³ made an interesting study of vulcanizates which contained up to 55% by volume of mineral fillers having particle size greater than 1μ (apparently in the range 20 to 40 μ). They measured stress-strain curves and volume changes that occurred when specimens were extended in a dilatom-

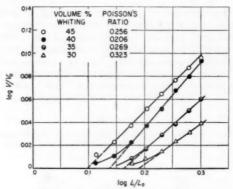


Fig. 11.—Replotted data of Bryant and Bisset for a pale crepe vulcanizate containing different amounts of whiting.

eter. These investigators also studied the effect of per cent filler, particle size (over a rather limited range), degree of cure, and wetting agents for pale crepe and SBR vulcanizates loaded with whiting and other mineral fillers. Qualitatively, their results are similar to those reported here for the glass bead composites, except that they often found an extended plateau in the stress-strain curve following the initiation of dewetting. When this occurred, the dewetting extended over a larger range of strain than that found for the glass bead composites, although the length of the plateau decreased with increasing particle size.

The dilatometric data of Bryant and Bisset for a pale crepe vulcanizate containing between 30 and 45% whiting are shown in Figure 11, replotted as $\log V/V_0$ vs. $\log L/L_0$. This figure shows that the Bryant and Bisset data, like those for the glass bead composites, can be characterized by the constant values of Poisson's ratio listed in Figure 11. Yield values ϵ_c were also obtained

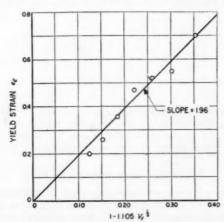


Fig. 12.-Variation of yield strain with volume fraction of whiting in pale crepe vulcanizates.

for the vulcanizates containing between 20 and 45% whiting by extrapolating their linear curves of volume change vs. elongation to zero volume change. The yield values are plotted against $1 - 1.105V_f^{\dagger}$ in Figure 12, which shows that Equation (13) fits the Bryant and Bisset data much better than the data for

the glass bead composites shown in Figure 10.

Jones and Yiengst² made a dilatometric study of vulcanized rubber filled with zinc oxide and barytes. The effect of particle size was studied by using five zinc oxides having particle diameters between 0.10 and 0.40 μ , and, to a lesser extent, by using barytes having particle sizes between 1 and 12 μ . Jones and Yiengst also studied the effect of cure time of the rubber. These factors affected the volume-elongation curves as might have been expected: i.e., the yield strain was decreased by increasing the cure time and the particle size. The Jones and Yiengst data, however, seem to show that samples prepared with different cure times and with fillers of different particle sizes had the same

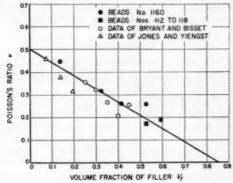


Fig. 13.—Variation of Poisson's ratio for several filled systems after dewetting.

Poisson's ratio at large extensions, where the dewetting was essentially complete. If this is correct, Poisson's ratio, after complete dewetting, depends primarily on the volume per cent filler, and not on the particle size of the filler or on the modulus or nature of the elastomer binder.

To test this hypothesis, values of Poisson's ratio for several composites are plotted in Figure 13 against the volume fraction of filler. Included are the average values obtained at 25° C for the glass bead composites and the data of Bryant and Bisset² given in Figure 11. To obtain Poisson's ratio from some data of Jones and Yiengst², their dilatometric data on vulcanizates containing 0.074, 0.138, and 0.194 volume fraction of 0.40 μ zinc oxide were replotted, and the results are also included in Figure 13. This figure suggests that Poisson's ratio is a linear function of the volume fraction of filler and is independent of the nature of the binder and filler. Since few data are shown for composites containing filler of different particle sizes, it is premature to speculate on the effect of particle size.

SYNOPSIS

The mechanical properties of five composites containing up to 60% by volume of glass beads (40 to 80 μ in diameter) embedded in a polyvinyl chloridedioctyl sebacate rubber were studied under large deformations. Elongated

ringlike specimens were extended in a dilatometer at 0, 25, and 50° C, and the volume increase was measured as a function of extension. At small extensions, the volume remained constant; above a critical extension or yield point, however, the volume increased because of the formation of vacuoles around the beads. Above the yield point, Poisson's ratio (defined in terms of Hencky strain) was calculated from the rate of volume change with extension and was found to be independent of extension and temperature, but to decrease linearly with the volume fraction of glass. The yield point varied with the temperature and also with the volume fraction of beads, as predicted by a theoretical equation. Some stress-strain data for the composites are presented and discussed in relation to the dilatometric data and the vacuole formation which results from failure of the adhesive bonds between the rubber and the glass beads.

ACKNOWLEDGMENT

It is a pleasure to acknowledge the assistance of Mr. Dale Jeffries, who constructed the dilatometer and carried out the experimental work.

REFERENCES

Holt, W. L., and McPherson, A. T., J. Research Natl. Bur. Standards, 17, 657 (1936).
 Jones, H. C., and Yiengat, H. A., Ind. Eng. Chem. 32, 1354 (1940).
 Bryant, K. C., and Bisset, D. C., Proceedings of the Third Rubber Technology Conference (1954), T. H. Messenger, ed., Heffer, Cambridge, England, p. 655.
 Schippel, H. F., Ind. Eng. Chem., 12, 33 (1920).
 Green, H., Ind. Eng. Chem., 13, 1029 (1921).
 Vogt, W. W., and Evans, R. D., Ind. Eng. Chem., 15, 1015 (1923).
 DePew, H. A., and Easley, M. K., Ind. Eng. Chem., 26, 1187 (1934).

THE EFFECT OF NETWORK FLAWS ON THE ELASTIC PROPERTIES OF VULCANIZATES *

J. SCANLAN

RESEARCH ASSOCIATION OF BRITISH RUBBER MANUFACTURERS, SHAWBURY, SHREWSBURY, SHROPSHIRE, ENGLAND

Flory has pointed out that any real polymer network contains terminal chains bound at only one end to a crosslink, the other end being a free end, and that such chains contribute nothing to elastic recovery. Flory suggested that such elastically ineffective material could be allowed for by deducting from the total number of crosslinks introduced into the vulcanizate the number N which are required to bind the N primary elastomer molecules into one giant molecule. Then the number of elastically effective chains N_e is given by

$$N_e = 2(\nu - N) = 2\nu[1 - (2M_c/M)] \tag{1}$$

 ν being the total number of crosslinks, M the molecular weight of the primary elastomer molecules, and M_c the molecular weight of the chain segments between crosslinks.

The present paper gives a new mathematical treatment of the relationship between the elastic modulus of a rubber vulcanizate and the molecular weight of the primary molecules which is intended to take precise account of the wastage of material in elastically ineffective loose ends, no matter how complex in structure these are. Allowance is also made for the presence in the vulcanizate of material completely detached from the main network, the so-called sol, which also contributes nothing to the resistance of the vulcanizate to deformation.

In correspondence Professor Flory and the present author have agreed that the essential difference between the theory now developed and the earlier one given by Professor Flory lies in the status assigned to trifunctional junctions. The present theory considers a trifunctional junction to be equally effective as a constraint on the three elastically active chains concerned as a tetrafunctional junction would be, while the earlier theory allows it only a lesser effectiveness.

The first case considered is that of a vulcanizate in which the original elastomer molecules are linear with a random distribution of lengths, i.e., the fraction of the total number of chains with x monomeric units N_x is given by

$$N_x = p(1 - p)^{x-1}$$

 $p^{-1} = \bar{x}$ (2)

where \bar{x} is the average number of monomeric units per primary molecule. It is assumed also that the crosslinking joins together pairs of monomer units chosen at random among all the possible pairs. Then it can be shown² that the fraction s_1 of free ends of chains which are in the sol (equal to the fraction of the number of primary molecules in the sol) satisfies the equation

$$s_1 = (1 - \alpha) + \alpha s_1^3 \tag{3}$$

^{*} Reprinted from J. of Polymer Sci. 43, 501-508 (1960).

where α , the probability that a crosslink rather than a free end is encountered on preceeding in one direction along a chain from a monomeric unit chosen at random, is given by

 $\alpha = M/(M + M_c) \tag{4}$

Beyond the gel point, the physically significant root of Equation (3) is

$$s_1 = -\frac{1}{2} + \left[\frac{1}{4} + (M_c/M)\right]^{\frac{1}{2}}$$
 (5)

The weight fraction of the vulcanized elastomer which is elastically active is easily deduced. A chain segment in the sol is necessarily elastically inactive, and, further, any chain segment which is part of a loose end of material (however complex in structure) joined at only one point to the main network is also inactive. Thus, only chain segments joined to the main network at both ends are elastically active. If such a chain segment is cut, both the new chain ends formed are still part of the gel, and the probability of this being the case when a chain segment chosen at random is cut is

$$(1-s_1)^2$$
 (6)

The assumption that free ends and crosslinks are distributed at random means that the average size of the chain segments is the same regardless of situation; the quantity $(1 - s_1)^2$ is then also the weight fraction of elastically active material.

However, not all the elastically active chain segments, in the sense in which the term has been used above (where chain segment meant that part of a polymer molecule between one free end or crosslink and another), can be considered as effective chains regarding their contribution to the elastic modulus calculated from the theory of elasticity¹. As Flory has pointed out, two chain segments separated by a crosslink of which the other two chain segments have free ends can form together at most one effective chain in the latter sense. The crosslink joining these two segments only enables them to act together as parts of one longer effective chain.

The crosslinks which are effective in distributing the stresses applied to the vulcanizate among the chains of the network may be divided into two types, those having four elastically active chain segments radiating from them and those having only three, the remaining chain segment being part of a loose end. By similar reasoning to that used previously, the probability that a chain segment starting at a crosslink leads to a loose end is s₁, and thus the probability that a crosslink chosen at random has all four of its chain segments active is

$$(1-s_1)^4 \tag{7}$$

and the number of such crosslinks is

$$\nu_4 = \nu (1 - s_1)^4 \tag{8}$$

Similarly, the number of crosslinks having three active chain segments is

$$\nu_3 = 4\nu s_1 (1 - s_1)^3 \tag{9}$$

Now the number of effective chains is

$$N_e = \frac{1}{2} \{ 4\nu_4 + 3\nu_3 \} \tag{10}$$

and hence

$$N_e = (\nu/2)[4(1-s_1)^4 + 3.4s_1(1-s_1)^3]$$

= $2\nu(1-s_1)^3(1+2s_1)$ (11)

Flory has not given explicitly end corrections taking into account the presence of sol in the vulcanizate. Such a correction according to the Flory theory is required for comparison with the present results and will now be derived for the particular case of interest. In Flory's theory¹, Equation (1) should refer exclusively to the gel, i.e.,

$$N_{\bullet} = 2(\nu' - N') \tag{12}$$

where ν' and N' are the numbers of crosslinks and primary molecules in the gel. Now

$$N' = (1 - s_1)N (13)$$

and the probability that a crosslink chosen at random is in the sol is s14, so that

$$\nu' = \nu (1 - s_1^4) \tag{14}$$

Hence

$$N_s = 2\nu \left[(1 - s_1^4) - (1 - s_1)(N/\nu) \right]$$

= $2\nu \left[(1 - s_1^4) - 2(1 - s_1)(M_c/M) \right]$ (15)

which may be reduced with the help of Equation (5) to

$$N_s = 2\nu (1 - s_1)^3 (1 + s_1) \tag{16}$$

Tobolsky, Metz, and Mesrobian³ have presented a treatment of the effect of introducing cuts into a vulcanizate which is based on a simpler and less realistic concept of effective chains as being all chain segments between two crosslinks, from which can be deduced simply the relationship

$$N_e = 2\nu \exp\left\{-M_c/M\right\} \tag{17}$$

Berry and Watson⁴ have pointed out, however, that Tobolsky's treatment effectively assumes all the chain segments to have the same length, and they, assuming crosslinking to be a random reaction, have given a more appropriate form of equation which can be written

$$N_{\bullet} = 2\nu M/(M + M_c) \tag{18}$$

In Figure 1 are given plots of $N_e/2\nu$ against M_c/M as calculated from the different theoretical treatments. It may be noted that the present theory gives a slope at $M_c/M=0$ equal to that given by the treatments of Tobolsky and Berry and Watson which is one-half that from Flory's theory. For normal vulcanizates, which will have M_c/M in the region of 0.05, the present theory differs considerably from that of Flory and is close to those of Tobolsky and Berry and Watson. On the other hand, the values of $M_c/M=0.4$ or more, (such as may well be obtained in vulcanizates degraded by scission of the polymer chains), the Flory theory is more satisfactory than these simpler treatments, which are greatly in error at high sol contents.

The treatment given above may readily be applied to the cases of branch units in the polymer of functionality other than four (cf. ref. 2). The appropri-

ate end corrections for random crosslinking of other than random distributions of primary chain lengths may be derived by a similar treatment based on the method used by Flory⁵ and later Charlesby⁶ for the derivation of the sol-gel ratios for such systems. As an example, the treatment for the random crosslinking of linear polymer chains initially all of the same length will be given briefly. In order to simplify the mathematics, the chains will be treated from the outset as continuous rather than as composed of a limited number of units; this permits integrations to replace summations. Such an approximation is implicit in the definition of α used above and has always been used to derive explicit sol-gel relations in the past.

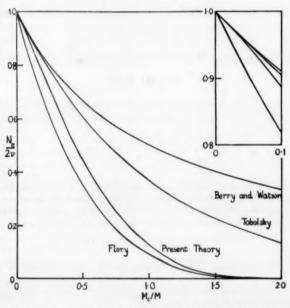


Fig. 1.—Comparison of previous treatments with the present theory for the case of random chain lengths. The inset shows enlarged the initial part of the curve which covers undegraded vulcanizates.

A chain of total length l which has a crosslink at a point distance x from one end is considered. The chain segment from this crosslink in the direction of decreasing x can be elastically active if and only if it has at least one crosslink which joins it to another chain in the gel. The distribution of numbers of crosslinks attached to a chain segment of length x will be a Poisson one, i.e., the probability that there are c crosslinks is

$$(x\gamma/l)^{o}(e^{-x\gamma/l}/c!) \tag{19}$$

where $\gamma = M/M_c$ is the crosslinking index, i.e., the average number of crosslinked units per chain. The probability that at least one of these is joined to a chain in the gel is $1 - s^c \tag{20}$ The probability that this chain segment is elastically active, provided that there is at least one other active segment joined at the crosslink in question, is

$$w(x) = \sum_{e=0}^{\infty} (x\gamma/l)^{e} (e^{-x\gamma/l}/c!) (1 - s^{e})$$

$$= 1 - e^{x\gamma(s-1)/l}$$

$$= 1 - s^{x/l}$$
(21)

where the last form arises since6

$$s = e^{-\gamma (1-s)} \tag{22}$$

The probability that both parts into which the chain is divided by the crosslink are elastically active is then

$$w(x) w(l-x) \tag{23}$$

Averaging over all values of x gives

$$(1/l) \int_0^l w(x)w(l-x)dx = 1 + s + [2(1-s)/\ln s]$$
$$= 1 + s - (2/\gamma)$$
(24)

Similarly, the probability that only one of the chain segments can be active regardless of the position of the crosslink is

$$(2/l) \int_{0}^{l} [1 - w(x)]w(l - x)dx = 2\left(\frac{s - 1}{\ln s} - s\right)$$
$$= 2[(1/\gamma) - s] \tag{25}$$

The probability that a crosslink has four active segments is then

$$[1+s-(2/\gamma)]^2$$
 (26)

and the probability that it has only three is

$$4[1 + s - (2/\gamma)][(1/\gamma) - s]$$
 (27)

The number of active chains is then

$$N_{s} = (\nu/2) \{ 4[1 + s - (2/\gamma)]^{2} + 3.4[1 + s - (2/\gamma)][(1/\gamma) - s] \}$$

$$= 2\nu[1 + s - (2/\gamma)][1 - 2s + (1/\gamma)]$$
(28)

The corresponding relation according to the Flory theory is

$$N_{\epsilon} = 2(\nu' - N')$$

$$= 2[\nu(1 - s^{2}) - N(1 - s)]$$

$$= 2\nu(1 - s)[1 + s - (2/\gamma)]$$
(29)

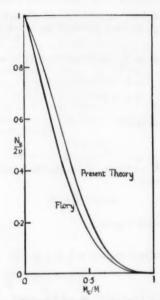


Fig. 2.—Theoretical results for uniform length chains.

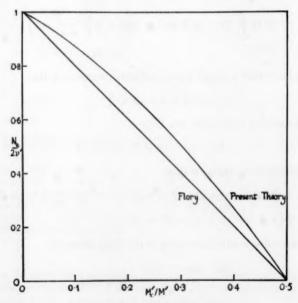


Fig. 3.—End corrections referred to gel only.

The results of this treatment for the case of uniform chains are given in Figure 2. In general they are similar in form to those for random-length chains, with the necessary difference that the gel point at which all the material becomes soluble is $M_c/M = 1$ for uniform chains but is $M_c/M = 2$ for randomlength chains. The difference in chain length distribution leaves the initial slopes of the curves unchanged, and so again the Flory theory predicts an initial decrease in the number of effective chains twice as rapid as does the theory now presented.

The differences between the present theory and that of Flory are perhaps more clearly illustrated in Figure 3, which has been calculated for the gel only rather than for the system as a whole; thus the primed quantities ν' , M_c' , and M' refer to the gel only. The Flory theory then gives a linear plot according to Equation (12) which is invariant whatever the primary chain length distribution, and the gel point is always reached at $M_c/M = 0.5$. Only the curve according to the present theory for an initially random distribution of lengths is presented; the result for uniform chains, although not quite identical, is very similar in this form.

SYNOPSIS

A treatment is given of the effect of network flaws due to the finite chain length of the primary elastomer molecules on the elastic properties of rubber vulcanizates. In this treatment full allowance is made for the elastically inactive material which exists either as sol ar as loose ends of the network. The cases of linear primary molecules with either a random distribution of lengths or with uniform lengths are considered, and the results are compared with those of earlier theoretical treatments.

ACKNOWLEDGMENT

The work described above arose from discussion of the problem with Dr. L. Mullins and Mr. A. G. Thomas to whom the author wishes to express his thanks.

REFERENCES

- Flory, P. J., Chem. Revs. 35, 51 (1944).
 Scanlan, J., and Watson, W. F., J. Polymer Sci. 27, 559 (1958).
 Tobolsky, A. V., Metz, D. J., and Mesrobian, R. B., J. Am. Chem. Soc. 72, 1946 (1950).
 Berry, J. P., and Watson, W. F., J. Polymer Sci. 18, 201 (1955).
 Flory, P. J., J. Am. Chem. Soc. 69, 30 (1947).
 Charlesby, A., J. Polymer Sci. 11, 513 (1953).

DYNAMIC PROPERTIES OF RUBBERLIKE MATERIALS AND THE ISOLATION OF MECHANICAL VIBRATION *

J. C. SNOWDON

FLUID AND SOLID MECHANICS LABORATORY, UNIVERSITY OF MICHIGAN, ANN ARBOR, MICHIGAN

Experiments to determine the dynamic mechanical properties of rubberlike materials frequently employ a sample of material sandwiched between two flat, parallel, and rigid surfaces. The sample is normally bonded to these surfaces or restrained from motion parallel to them by a perpendicularly applied static force. Figure 1 shows diagrammatically a sample attached to parallel rigid plates, which vibrate sinusoidally either in their own plane [Figure 1(a)] or in a perpendicular direction [Figure 1(b)]. In each case the lateral surfaces of the sample are unconstrained.

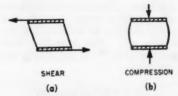


Fig. 1.—Rubberlike material stressed (a) in shear and (b) in compression.

The rubberlike material is commonly said to be stressed in shear in Figure 1(a) and stressed in compression in Figure 1(b). Actually, the rubberlike material in Figure 1(a) will not experience a homogeneous shear deformation unless its thickness is small compared to the sample dimensions in every perpendicular direction. Again, the rubberlike material in Figure 1(b) will not experience purely homogeneous compression because the lateral surfaces of the sample are not subject to an applied stress, and motion at and parallel to the interfaces between the sample and the plates is not permitted. The mechanical behavior of the rubber will in fact be governed primarily by its bulk modulus only when the lateral dimensions of the sample are large compared with the sample thickness. In this event the resilience normally associated with the rubber will not be apparent because the bulk modulus will be many times greater than the shear modulus of the material.

DYNAMIC MECHANICAL PROPERTIES OF RUBBERLIKE MATERIALS

When a linear viscoelastic medium is stressed, for example, in shear, the relation existing between small values of stress σ and strain ϵ in the medium may be represented generally by a linear partial differential equation of arbitrary order.

^{*} Reprinted from Noise Control, Vol. 6, pages 18-23, March-April, 1960.

This equation becomes algebraic when stress and strain vary sinusoidally with time, because the *n*th partial derivative with respect to time of stress or strain may be equated to $(j\omega)^n\sigma$ lr $(j\omega)^n\epsilon$, respectively, where $j=(-1)^{\frac{1}{2}}$ and ω is angular frequency, hereafter known simply as frequency. The ratio of stress to strain in the material may therefore be represented by a complex quantity; that is to say the mechanical properties of the material may be represented not by a real, but by a complex shear modulus G^* . The mechanical loss in the material is described by a damping factor, which is defined as the ratio of the imaginary to the real part of the complex elastic modulus.

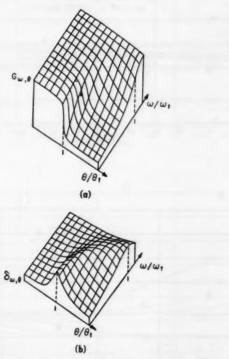


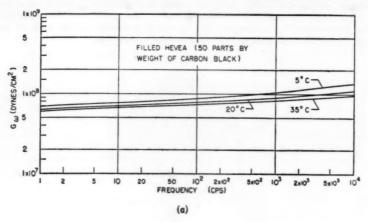
Fig. 2.—The dependence of (a) the dynamic elastic modulus $G_{\omega,\theta}$ and (b) the damping factor $\delta_{\omega,\theta}$ of a rubberlike material upon frequency ω and temperature θ .

The real part of the complex elastic modulus and the damping factor are, in general, functions of frequency and temperature. If these quantities are denoted by $G_{\omega,\theta}$ and $\delta_{\omega,\theta}$, respectively, where θ is temperature, then

$$G^* = G_{\omega,\theta}(1 + j\delta\omega_{,\theta})$$

The real part of the complex elastic modulus of a rubberlike material, hereafter known simply as the dynamic modulus of the material, increases with frequency and when temperature decreases. This may be visualized by reference to Figure 2(a), where the dynamic modulus $G_{\omega,\theta}$ is shown diagrammatically as

a function of ω and θ . The variation of the damping factor $\delta_{\omega,\theta}$ with ω and θ is shown diagrammatically in Figure 2(b). Semiquantitative figures of similar form were first drawn by Nolle¹ for the synthetic rubber Buna N. The quantities ω_t and θ_t are known as the transition frequency and transition temperature, respectively. They refer to the transition of rubberlike materials at sufficiently



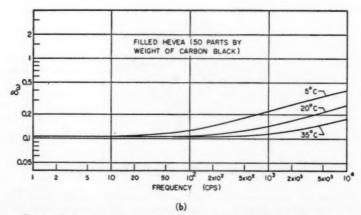


Fig. 3.—The frequency dependence of the dynamic shear modulus and damping factor possessed by natural rubber filled with fifty parts by weight of carbon black.

high frequencies or sufficiently low temperatures to an inextensible and glasslike state. At the so-called rubber-to-glass transition the damping factor of the materials passes through a maximum value, which lies approximately in the frequency or temperature range where the dynamic modulus is increasing too rapidly. The dynamic modulus increases over many decades in frequency at temperatures neighboring room temperature.

The transition frequency of natural and other low damping rubbers occurs at very high frequencies at room temperature so that over the frequency range of interest in vibration isolation, namely, a range of frequencies considerably below ω_i , the damping factor is small, and, in fact, both the dynamic modulus and the damping factor (known simply as G_{ω} and δ_{ω} , respectively, when temper-

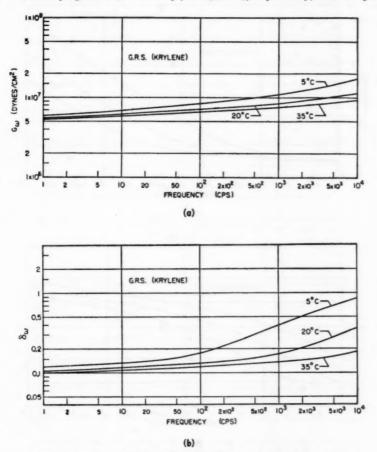


Fig. 4.—The frequency dependence of the dynamic shear modulus and damping factor possessed by a SBR rubber.

ature is constant) may be considered approximately independent of frequency. The frequency dependence of the dynamic shear modulus and damping factor possessed by natural rubber filled with fifty parts by weight of carbon black, and by a synthetic rubber SBR are shown in Figures 3 and 4 at the temperatures 5° C, 20° C, and 35° C. These curves were deduced by the method of reduced variables (see next section) from data published by Fletcher and Gent².

The transition frequency of high damping rubberlike materials is much below that of natural rubber occurring, in general, at frequencies which are normally of interest in vibration isolation at room temperature. The damping factor, therefore, is large in this frequency range, while the dynamic modulus increases rapidly with frequency. The frequency dependence of the dynamic

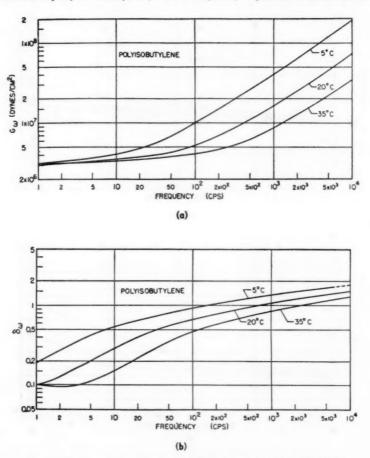


Fig. 5.—The frequency dependence of the dynamic shear modulus and damping factor possessed by polyisobutylene.

shear modulus and damping factor possessed by polyisobutylene—the properties of which should resemble those of unfilled butyl rubber—and plasticized polyvinyl acetate are shown in Figures 5 and 6 at the temperatures 5° C, 20° C, and 35° C. The value of the damping factor in the neighborhood of the transition frequency does not change rapidly with frequency and may sometimes be considered independent of frequency over a limited frequency range. On the

other hand, the dynamic modulus increases rapidly with frequency at a maximum rate proportional to ω^{α} , where α appears to take some value between 0.5 and 1.0 which is characteristic of the material. The values of α for polyiso-

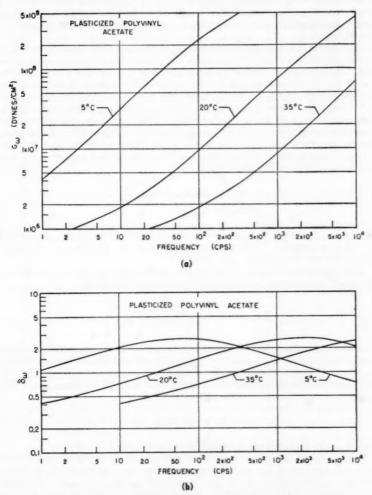


Fig. 6.—The frequency dependence of the dynamic shear modulus and damping factor possessed by plasticized polyvinyl acetate.

butylene and plasticized polyvinyl acetate are approximately 0.68 and 0.93, respectively. Values of G_{ω} and δ_{ω} for these curves were again deduced by the method of reduced variables from data published by Fletcher and Gent², and Williams and Ferry³, respectively.

THE METHOD OF REDUCED VARIABLES

Many attempts have been made to relate the dependence upon frequency and the dependence upon temperature of the dynamic modulus and damping factor possessed by rubberlike materials, and to explain why the variation of the dynamic modulus, $G_{\omega,\theta}$, with frequency is large when $G_{\omega,\theta}$ is strongly temperature-dependent and small when $G_{\omega,\theta}$ varies only slowly with temperature

(see Figures 2-6).

By making the following assumptions, Ferry and coworkers⁴ were able to predict satisfactorily the relation observed between the frequency and temperature dependence of both the dynamic modulus $G_{\omega,\theta}$ and the damping factor $\delta_{\omega,\theta}$. Thus, it was assumed that when a rubberlike material is deformed, the stress in the material is distributed between a variety of molecular mechanisms, each being free to relax exponentially and independently with time. It was assumed also that all the relaxation times exhibit the same dependence upon temperature. If the relaxation times increase by a factor a_{θ} when the temperature changes from some reference temperature θ_{θ} to a temperature θ , then the dynamic shear modulus and the damping factor at the two temperatures were said⁴ to be related in the following manner

$$G_{\omega,\theta} = (\theta \rho / \theta_s \rho_s) \cdot G_{\omega a\theta,\theta s}$$

 $\delta_{\omega,\theta} = \delta_{\omega a\theta,\theta s}$

where ρ and ρ_* are the densities of the material at the absolute temperatures θ and θ_* , respectively. It is generally sufficient² to approximate the ratio $(\theta\rho/\theta_*\rho_*)$ by the temperature ratio (θ/θ_*) .

The dependence of a_{θ} upon θ is found to possess the same general form for a wide range of materials⁵, the approximate relationship being

$$\log_{10}a_{\theta} = -\frac{8.86(\theta - \theta_s)}{\lceil 101.6 + (\theta - \theta_s) \rceil}$$

Consequently, from values of $G_{\omega,\theta}$ and $\delta_{\omega,\theta}$ determined experimentally as functions of frequency and temperature, it is possible to plot master curves referring to a standard temperature θ_s for the so-called reduced shear modulus $[(\theta_s\rho_s/\theta_\rho) \cdot G_{\omega,\theta}]$ and the damping factor $[\delta_{\omega,\theta}]$ in terms of reduced frequency ωa_θ . The temperature θ_s is normally 5 chosen such that

$$\theta_s = \theta_t + (50 \pm 5) \circ K$$

where θ_t is the rubber-to-glass transition temperature of the material.

Once such master curves have been constructed, it is likewise possible to predict that values of $G_{\omega,\theta}$ and $\delta_{\omega,\theta}$ over wide frequency or temperature ranges, although the predictions may become less reliable as the upper and lower limits of the frequencies and temperatures considered become further removed from those at which the measurements were originally made.

In general, it is not possible to determine with a single apparatus the values of $G_{\omega,\theta}$ and $\delta_{\omega,\theta}$ through an extensive range of frequencies. On the other hand, it is generally not difficult to determine these quantities through a relatively wide range of temperatures within which the transition temperature θ_t occurs. The method of reduced variables therefore enables the magnitude of $G_{\omega,\theta}$ or

 $\delta_{\omega,\theta}$ to be predicted through a very broad frequency range if the experiment in which they are determined is conducted at a number of temperatures.

CHOICE OF RESILIENT MATERIALS FOR ANTIVIBRATION MOUNTINGS

It is possible to derive a general equation⁶ from which the transmissibility T of any linear rubberlike material may be obtained once the variation with frequency of the dynamic modulus G_{ω} and the damping factor δ_{ω} of the material

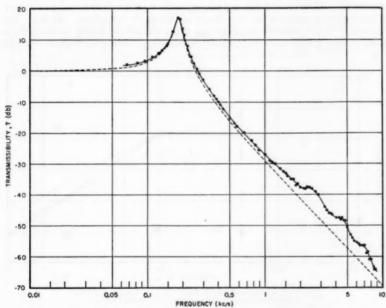


Fig. 7.—The transmissibility of natural rubber containing forty parts by weight of carbon black.

Temperature 19° C. (Reproduced from the British Journal of Applied Physics*.)

are inserted. Thus, if the resonant frequency of the mounting system is ω_0 , and $G_{\omega} = G_0$ at this frequency, then

$$T^2 = \frac{1 + \delta_{\omega}^2}{\left[1 - (\omega/\omega_0)^2 (G_0/G_{\omega})\right]^2 + \delta_{\omega}^2}$$

The frequency ω_0 is normally chosen to fall as far as possible below the frequencies at which the anti-vibration mounting is required to provide isolation-It is desirable also that the transmissibility of the mounting should decrease rapidly as frequency increases above ω_0 . However, the transmissibility of the mounting will be detrimentally increased if G_{ω} or δ_{ω} increase with frequency, because when the frequency ratio ω/ω_0 is large the general transmissibility equation may approximately be written

$$T = (G_{\omega}/G_0)[1 + \delta_{\omega}^2]^{\frac{1}{2}}/(\omega/\omega_0)^2].$$

Only when G_{ω} and δ_{ω} are constant, will T decrease as the square of the exciting frequency, that is, at 12 db per octave. Since the values of the dynamic modulus and damping factor possessed by natural and low damping synthetic rubbers increase slowly with frequency, the isolation afforded by these materials should increase relatively rapidly at high frequencies. The transmissibility of a natural rubber specimen⁶ in compression [Figure 1(b)] is shown in Figure 7. The specimen contains forty parts channel black in one-hundred parts rubber. The broken curve is calculated from the general transmissibility equation assuming that the dynamic modulus and the damping factor of the material are constants. These quantities are chosen such that the theoretical and experimental curves coincide at the observed resonant frequency. At high frequencies "wave effects" are observed when the mount length is equal to or greater than a half-wavelength of the elastic wave passing through the mounting.

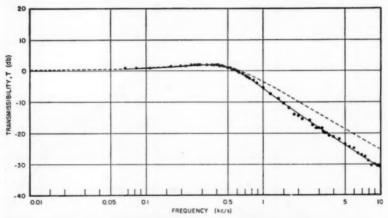


Fig. 8.—The transmissibility of Hycar 1001. Temperature 16.5° C. (Reproduced from the British Journal of Applied Physics.)

The resonant transmissibility of a mounting system may be reduced by employing a high damping mount material. Moreover, if the vibrating item is resiliently mounted upon a nonrigid foundation, a problem not discussed here, a mount of high damping rubber can be valuable in suppressing the natural modes of vibration of the foundation. The damping factors possessed by high damping materials do not, in general, vary rapidly with frequency and therefore do not influence greatly the high-frequency value of transmissibility. However, the dynamic modulus increases very rapidly with frequency and is almost entirely responsible for the poor high-frequency isolation normally associated with these materials. The transmissibility of the copolymer Hycar 1001 measured in compression (Figure 1(b)] is shown in Figure 8. The broken curve is calculated from the general transmissibility equation assuming that the dynamic modulus is directly proportional to frequency ($\alpha = 1$) and that the damping factor is constant. Values of these parameters are again chosen so that the theoretical and experimental curves coincide at the observed resonant frequency.

It may be concluded from this discussion that, ideally, the real part of the complex elastic modulus and the damping factor possessed by an antivibration mount material should vary only slowly with frequency, while at the same time the damping factor of the material should be large.

ACKNOWLEDGMENT

This work was sponsored in part by the Bureau of Ships under a U.S. Navy contract.

REFERENCES

Nolle, A. W., J. Polymer Sci. 5, 1 (1950).
 Fletcher, W. P., and Gent, A. N., Brit. J. Appl. Phys. 8, 194 (1957).
 Williams, M. L., and Ferry, J. D., J. Colloid Sci. 10, 1 (1955).
 Ferry, J. D., Fitzgerald, E. R., Grandine, Jr., L. D., and Williams, M. L., Ind. Eng. Chem. 44, 703 (1952).
 Williams, M. L., Landel, R. F., and Ferry, J. D., J. Am. Chem. Soc. 77, 3701 (1955).
 Snowdon, J. C., Brit. J. Appl. Phys. 9, 461 (1958).
 Harrison, M., Sykes, A. O., and Martin, M., J. Acoust. Soc. Am. 24, 62 (1952).

DETERMINATION OF THE DAMPING CHARACTER-ISTICS OF FABRIC REINFORCED RUBBER STRIPS FOR FLEXURAL WAVES AT AUDIO FREQUENCIES *

FRANCIS M. WIENER AND CREIGHTON M. GOGOS

BOLT, BERANEK, AND NEWMAN, INC., CAMBRIDGE 38, MASSACHUSETTS

INTRODUCTION

Fabric-reinforced rubber is used in such diverse structures as drive belts and automobile tires. Both are statically in tension. Under dynamic excitation bending vibrations occur which give rise, among other things, to the radiation of sound, particularly in the case of tires. The internal damping of the structure can be expected to be one of the important parameters controlling its dynamic behavior. This paper reports the results of a series of experiments to determine the quality factor Q of strips of fabric-reinforced rubber 18 in. in length, 1 in. in width, and of varying thickness and composition. The samples were secured at both ends by clamping the fabric and excited into bending vibrations under static tension. Such a strip approximates a piece of belting or a narrow section through an automobile tire from one bead to the other. For most of the experiments described the types and composition of fabric and rubber were typical of present-day passenger automobile tires. In addition, a few experimental fabrics were also measured. To simplify interpretation of the results the specimens tested did not duplicate the multi-layer configurations common in automobile tires or drive belts, but had simple one-ply or two-ply configurations. Nonetheless, some generalized statements applicable to actual structures can be made based on the results of this study.

EXPERIMENTAL METHOD AND TECHNIQUE

The technique of measuring the quality factor Q and hence the damping by "small-signal" steady-state excitation has many advantages: the results are independent of the level of excitation within wide limits and do not require calibrated transducers or equipment capable of measuring transient decay times. Assuming small damping, i.e. large Q, the overall frequency response characteristic of the system does not influence the results appreciably, since in the vicinity of each resonant mode, the response can be regarded as uniform over the narrow bandwidth under consideration. The test technique used in this study and described below, while related to one of the techniques described by Nolle¹ and to Oberst's method², is especially adapted to the type of specimens tested and, most important, allows the specimen to be subjected to static tension, adjustable at will.

The sample under test was suspended vertically by its reinforcing fabric from a small concrete platform which, in turn, was supported by four braced steel legs as shown in Figure 1. The necessary static tension was supplied by

^{*} Some of the material presented in this paper was the subject matter of a talk entitled "The Damping Characteristics of Fabric-Reinforced Rubber" presented at the 3rd International Congress on Acoustics, September 1959, Stuttgart, Germany.

158

concrete blocks attached to the lower end of the sample. Crossed strings tied to the four corners of the blocks supplied the necessary constraint against pendulum-like oscillations and torsion. Approximately at the center of the sample, a small coil was cemented onto the rubber. The diameter of this coil was small enough so that the drive approximated a point excitation even at the highest frequencies tested. This coil was inserted into the air gap of a magnetized structure and positioned by a cross-slide. Energized from an oscillator, the coil supplied the excitation of the sample into bending vibrations with a minimum of added mass and damping.

The resulting deflections at the driving point were measured by means of a capacitative pickup which measured the change in capacitance between its electrode and a piece of metallic foil cemented onto the sample, as shown in

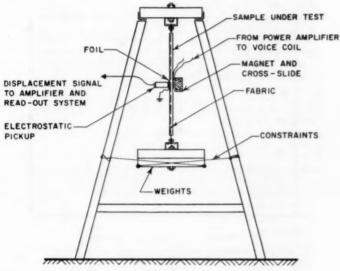


Fig. 1.-Test fixture.

Figure 1. An electronic counter was used to measure the resonant frequency at each mode of vibration and at the corresponding half-power points below and above resonance. In order not to introduce appreciable damping at the end points of the sample, the sample was prepared as follows: The ends of the fabric cords were embedded in a mold filled with a mixture of epoxy resin and fine aluminum particles. After hardening, the resulting flat, rigid plate, which was well separated from the rubber of the specimen, was then used to clamp the specimen into the test fixture.

The bandwidth, and hence the quality factor Q, were measured by observing the displacement near the center of the sample as a function of frequency in the vicinity of the various resonant modes. Following generally accepted usage, Q is defined, for a given mode, as the ratio of the resonant frequency to the bandwidth of the displacement resonant curve at the half-power points, i.e. 3 db "down" from the maximum displacement at resonance. For small damp-

ing, Q so defined is at a given mode inversely related to the damping constant α of the vibrations along the length of the specimen. Moreover, Q is then also directly proportional to the time rate of decay β of the vibrations of the specimen after the excitation at a given mode has been cut off. In fact, the two latter quantities are related by the group velocity \bar{c} of the flexural waves on the speci-

men, evaluated at the mode in question3.

Using the technique described above, the quality factor of a number of fabric-reinforced rubber strips was determined. Samples with various fibers and rubber thicknesses were used covering a range of tensions typical of normal operating conditions in tires. For the thicknesses and tensions used, the frequency of the fundamental mode ranged from about 30 to 70 cps. Measurements at the higher modes could generally be carried out to several hundred cps before adjacent resonance curves began to merge.

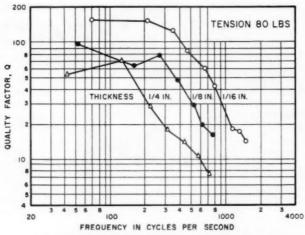


Fig. 2.—Q of fabric-reinforced rubber specimens with two plies of cord as a function of rubber thickness.

RESULTS

Figure 2 shows the results of the measurements of the quality factor Q as a function of frequency made on three different specimens under constant tension. The experimental points obtained show the values of Q for each specimen for the fundamental and higher resonant modes. The reinforcing fabric consisted here of two layers (plies) of parallel cords, fabricated from synthetic fibers. The static Young's modulus of the fibers exceeded that of the rubber by one order of magnitude so that the fabric essentially supported the load. The thickness of the rubber into which the cords were vulcanized varied within the limits of the total thickness indicated.

The results show that the ratios of the frequencies of the first few modes to the frequency of the fundamental follow very nearly the progression of the odd integers. Moreover, they were found to be roughly proportional to the square root of the tension and inversely proportional to the square root of the mass per unit length. This implies that the specimens behave like a string under tensions.

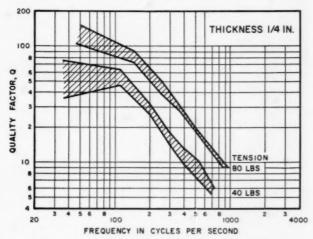


Fig. 3.—Q of fabric-reinforced rubber specimen with one-ply of cord as a function of tension.

sion, excited at the center, with some bending stiffness added by the rubber layer. The graph also indicates that beyond the second resonant mode Q decreases approximately inversely with frequency. This behavior was found to be typical of all specimens tested. It is possible that some of the high values of Q found at the fundamental mode were somewhat in error, because of possible small residual dissipation present at the ends of the sample or elsewhere. This dissipation at the ends becomes even less important as the frequency increases.

Figure 3 shows the results of a series of similar measurements on one speci-

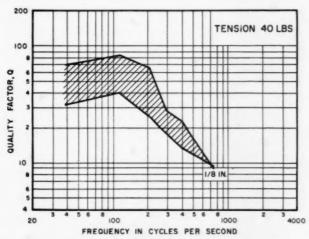


Fig. 4.—Range of values of Q of fabric-reinforced rubber specimens with two plies of cord using different fibers.

men, reinforced by a single-ply fabric, for two different values of the static load. The shading indicates the magnitude of the variability of the data taken under nominally identical conditions. The data show that Q is proportional to the tension within the limits of the experiments. Again, this was found to be

characteristic of all specimens tested.

The influence of the type of fiber used in the reinforcing fabric is illustrated in Figure 4. In that graph results of measurements of Q are shown for several specimens of like construction and a given thickness of rubber, but using different synthetic fibers. Similar data not shown here indicate that the influence of the fiber material decreases as the rubber thickness is increased.

ANALYSIS

A bending wave, traveling in the x-direction along the sample which is "narrow" and "thin" with respect to the wavelength of the flexural waves, can be represented by $y = y_0 \exp{(-i\omega t)} \exp{(ik^*x)}$. The complex propagation constant $k^* \equiv k + \mathrm{i}\alpha$; y is the deflection and $\omega \equiv 2\pi f$ the angular frequency at

the resonant mode in question.

The experimental evidence indicates that all specimens behave very much like a string whose behavior is primarily controlled by tension but with some bending stiffness present. This bending stiffness acts as a perturbation on the simple string behavior and causes the sequence of the measured resonant frequencies at the various modes to be somewhat higher than those calculated for a simple string. The data show that $k \doteq \omega(T/m)^{-1}$ where T is the static tension supported by the fabric and m is the mass of the specimen per unit length. The above expression is the first-order approximation for a string with no losses and with small bending stiffness⁴.

The question arises as to what mechanism is responsible for the damping of the bending waves in the sample. It is well known^{1, 5} that the dynamic Young's modulus of rubber is complex. Hence, the damping could be assigned to the bending waves in the rubber layer of the sample whose bending stiffness

will then be complex2, 6.

On the other hand, one can assume that damping is taking place between the plies of the fabric and in a layer between the fabric and the rubber. This view is all the more plausible because in tires, for example, the cords of the fabric are customarily encased in a thin layer of a soft rubber. The test results on the various specimens for various conditions reported here make it possible

to choose between these two damping mechanisms.

It is convenient and appropriate to express the measured quality factor Q in terms of α , the attenuation constant of the bending waves along the sample. The behavior of the sample at each resonant mode can be shown to be equivalent to that of a simple, damped oscillator. In particular, the damping constant in the time domain β of such an oscillator can be expressed in terms of $Q = \omega/2\pi\Delta f = \omega/2\beta$, assuming small damping (say $Q \ge 5$). The width Δf of the resonance curve between the two "half-power" points is therefore $\Delta f = \beta \pi$. As already mentioned, β and α can be related here via the group velocity $\bar{c} = d\omega/dk$ of the bending waves in the sample, viz. $\beta = \bar{c}\alpha$. Since the samples were found to behave very nearly like a stretched string and not like a bar, there is no appreciable disperson and $\bar{c} = (T/m)^{\frac{1}{\beta}}$. Finally

$$Q = \frac{\omega}{2\alpha} \left(\frac{m}{T}\right)^{\frac{1}{2}} \tag{1}$$

It remains to calculate α for the two cases in question. According to Kerwin⁶, α can be defined as the ratio of the power of the flexural vibrations P_D dissipated per unit length x in the sample to the total power P of the vibrations traveling along the sample, that is, as the fractional decay rate of the power in space.

One has, therefore,

$$2\alpha \equiv -P_D/P \tag{2}$$

Calculating P for the case of a string and P_D for the rubber layer coupled to it, one finds

$$Q \propto T^2/\omega^2 \eta_R B_R \tag{3}$$

where B_R is the bending stiffness and η_R the loss factor of the rubber. In calculating P the power in the rubber bar was neglected. The error incurred is of the order of k^2B_R/T . This result implies that as the tension is varied for a given sample, Q is directly proportional to T^2 for a given frequency. Conversely, for a given tension, Q varies as f^{-2} assuming that $\eta_R B_R$ remains constant. If η_R increases with frequency, as it does for the rubber used here in the frequency range in question, the frequency dependence will be even stronger. These conclusions are contradicted by the experimental evidence and hence this model is not appropriate.

On the other hand, if one assumes that damping is taking place in shear, one finds a different value for P_D . Calculating P_D for this case one obtains

$$Q \propto T/\epsilon_R G_R$$
 (4)

where ϵ_R is the loss factor of G_R , the dynamic shear modulus of the shear layer of rubber.

This expression agrees with experiment, as T is varied. Approximate values of ϵ_R and G_R obtained independently as a function of frequency were inserted in Equation (4) and yielded a frequency dependence of the calculated Q which is similar to the frequency dependence of the measured values of Q for constant tension. It appears therefore reasonable to use this model in accounting for the experimental evidence within the limits of the experiments reported here.

CONCLUSIONS

 The damping of bending waves in fabric-reinforced strips of rubber of the type discussed here appears to be caused primarily by energy loss in shear.

Although care must be taken in extrapolating the results of this study to
practical structures, the above conclusion points up ways for the designer to
control the damping in accordance with the desired dynamic properties of the
finished product.

SUMMARY

The damping characteristics of fabric-reinforced rubber structures for flexural vibrations in the audio frequency range are of interest in studying the dynamic behavior of drive belts and automobile tires. To investigate these characteristics experimentally a strip of the material was secured at both ends by clamping the ends of the fabric and excited electromagnetically near the center into bending vibrations. The resulting displacements were observed by an electrostatic pickup arrangement. The quality factor Q was measured

for the various resonant modes in the frequency range from near 100 cps to near 1000 cps for different specimens as a function of static loading. The results indicate that beyond about 200 cps the observed damping increases with frequency and appears to be primarily due to energy losses in shear. Although the specimens tested did not structurally duplicate tires or drive belts, it is believed that this study points up ways for the designer to control damping in accordance with the desired dynamic behavior of the finished product.

ACKNOWLEDGMENTS

Thanks are due Dr. Jordan J. Baruch for the suggestion of the test technique and the basic design of the test apparatus. The interest and helpful suggestions of Dr. E. M. Kerwin, Jr. and Dr. G. Kurtze are gratefully acknowledged.

REFERENCES

Nolle, A. W., J. Appl. Phys. 19, 753 (1948).
 Oberst, H., Acustica 2, Akus. Beihefte, No. 4, AB181 (1952).
 Slater, J. C., "Microwave Electronics," D. Van Nostrand Co., Inc. New York, 1950.
 Morse, P. M., "Vibrations and Sound," 2nd Ed., McGraw-Hill Book Co., Inc. New York, 1948.
 Nolle, A. W., J. of Polymer Sci. 5, 1 (1949).
 Kerwin, Jr., E. M., J. Acoust. Soc. Am. 31, 952 (1959).

AN ELASTORELAXOMETER FOR LARGE REVERSI-BLE DEFORMATION OF ELASTOMERIC SYSTEMS AND POLYMER SOLUTIONS *

A. A. TRAPEZNIKOV

INSTITUTE FOR PHYSICAL CHEMISTRY, MOSCOW, USSR

INTRODUCTION

There have been numerous investigations of the elastic properties of fluid colloidal systems and polymer solutions. However, elastic deformations were measured only at low shearing stresses and low deformation rates, and the deformations obtained under such conditions could not be truly characteristic of the high elasticity of the system. Most significant in this respect should be the greatest elastic deformations, corresponding to high deformation rates in excess of the maximum relaxation rates of the systems, but these were not known or even suspected to exist in fluid colloidal systems and polymer solutions.

The significance of maximum elastic deformation was first demonstrated in our investigations¹. Oleogels of aluminum soaps and solutions of polyisobutylene rubber in decalin were investigated. Apart from evaluation of limiting (breaking) deformations ϵ_r , corresponding to maximum $P = P_r$ on the stress-deformation $P(\epsilon)$ curves, direct determinations of large elastic (reversible) deformations and their relaxation are of great importance. We used the "silk-thread" method².

Maximum elastic deformations reflect the flexible threadlike structure of the particles, which extend at high deformation rates and are capable of coiling when not under stress. The absolute values of the maximum deformations in many colloidal systems considerably exceed the usual breaking deformations of natural rubber (1000–1200%).

The concept of maximum elastic deformations in fluid systems is also important in connection with the investigations of normal stresses by Weissenberg's method³, which are of considerable current interest. Despite the fact that normal stresses are correlated with elastic shearing deformations, the latter are merely calculated indirectly from normal stresses, or by other methods. Until now reversible shearing deformations at high rates have not been measured directly; no instruments for the purpose have been designed. It should also be noted that in theories of normal stresses arising in fluid systems in steady flow no account at all was taken of the transition beyond the yield value of the structure or beyond the limit of reversible deformations, accompanied by breakdown of the structure before the steady state is established.

It is clear from the foregoing that the development of methods and special instruments for direct measurements of large reversible deformation is a very important task.

APPARATUS

We have developed a new instrument, the elastorelaxometer, based on the coaxial-cylinder principle. The idea of the instrument involves: 1) rotation of

^{*} Reprinted from Colloid Journal, Vol. 21, pages 99-107 (1959); a translation of Kolloidnyš Zhurnal, 21, 108 (1959) by Consultants Bureau, Inc.

the outer cylinder at a constant rate, and the possibility of stopping it automatically at a required angle; 2) measurement of the maximum shearing stress P which develops when the outer cylinder rotates through the required angle; 3) retention of the inner cyclinder in virtually its initial position during rotation of the outer cylinder until its arrest; 4) automatic release of the inner cylinder in a very short time $(0.01-0.05\,\mathrm{second})$ after arrest of the outer cylinder, or after different time intervals; 5) measurement of the angle of rotation of the inner cylinder after arrest of the outer cylinder, determining the elastic recoil of the system under investigation.

To simplify the instrument, the outer cylinder is driven by a gramophone spring mechanism at a rotation rate $\Omega \approx 75$ revolutions/minute. (We have since constructed a new and more powerful model of the instrument, driven by

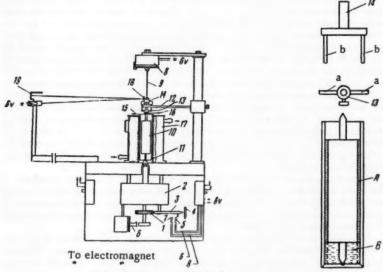


Fig. 1.-Diagram and details of the instrument.

a motor and equipped with gear boxes to give a wider range of Ω . Some of the results for rubber solutions, obtained with the new instrument, have been published.) With an outer cylinder radius $R_2=1.5$ cm (height $L_2=12$ cm) and inner cylinder radii R_1 from 1.3 to 1.45 cm (height $L_1=8.0$ cm) this gives velocity gradients & from 200 to 52.5 sec⁻¹. The instrument is shown schematically in Figure 1. To one of the gear wheels 1 of the drive 2, situated at the lower end of the instrument, there is attached a thrust pointer 3, engaging by its inner end with a cog of the gear wheel 1, and sliding by its outer end along a circular graduated scale 4. This pointer is used to give the desired angle of rotation of the outer cylinder, from 18–20 to 720° (if the pointer is released the cylinder can be rotated continuously at a high rate). On reaching its stop, the pointer closes the contact 5 and, through a relay, switches in the electromagnetic brake 6, which eliminates the slight inertia drag of the outer cylinder. After a short time (0.01–0.05 second) the pointer, moving forward, closes the second contact

7, which switches in the electromagnet 8, situated over the upper end of the

elastic measuring wire 9, through another relay.

The inner cylinder 10 has upper and lower axes with pointed ends. The lower point rests on the bottom of the outer cylinder 11, and the upper point is pressed (not too firmly) against the centering arm 12, which acts as the upper thrust bearing. Instead of the usual permanent linkage between the axis of the inner cylinder and the wire measuring the torque set up by the gel, a removable wire which is easily separated from the cylinder axis is used; it is linked with the inner cylinder by the coupling joint 13 with two projections a, which press against the pegs b of another coupling joint 14, fitted onto the lower end of the wire. The upper end of the wire is inserted into the lid of an electromagnetic clutch which, when the magnet is in circuit, is pulled upward and pulls the

Table I

Angles of Rotation of Inner and Outer Cylinders in Measurement of Elastic Recoil in 2% Aluminum Naphthenate Gel ($\tau_{aging} = 64$ days)

	Rotation angle of outer cylinder	Full rotation angle of inner cylinder	Torsion angle of inner cylinder at start of its free movement φ°		angle of			
				Of outer cylinder relative to the inner $\theta^{\circ} = s - \varphi$	Inner eylinder relative to its initial deviation $\theta^{\circ}_{e} = s_{e} - \varphi$	Rela deform	Shearing	
						Predetermined $\epsilon = \theta/k'$	Elastic recoil ε _θ = θ _θ /k'	$P = C_0 \varphi / 2\pi R_1^3 L \times 10^{-2}$
	39	40	1	38.0	39.0	9.86	10.2	17.3
	59	59	1.33	57.7	57.7	15.1	15.1	23.1
	74	73	1.66	72.3	71.3	18.9	18.7	28.8
	114	113	2.5	111.5	110.5	29.2	28.2	43.3
	141	141	3.17	137.8	137.8	36.1	36.1	54.9
	616	165	4.0	162.0	161.0	42.1	42.1	69.3
	184	193	4.0	180.0	189.0	47.1	49.5	69.3
	213	225	4.0	209.0	221.0	54.8	57.9	69.3
	214	227	4.33	209.7	222.7	54.9	58.9	75.0
	253	239	4.33	248.7	234.7	65.2	61.5	75.0
	269	237	4.33	264.7	232.7	71.9	59.0	78.0
	302	215	4.33	297.7	210.7	77.9	55.1	75.0
	324	213	4.0	320.0	209.0	83.8	54.7	69.3

pegs b from the projections a, so that the inner cylinder is released. The outer and inner cylinders are fitted with pointers 15 and 16 which travel over the graduated upper lid of the thermostat 17, connected with a Hoeppler uitrathermostat.

The torsion angle of the wire measuring the shearing stress is read off from the deflection of the light spot from the mirror 18 on the scale 19. With a rigid wire (in this instance a wire of $C_0 = 99,240$ dynes·cm/radian was generally used) the rotation angle φ of the inner cylinder does not exceed 10–15°, but in most determinations it was less than 5°, so that the deformation of the system $\theta = s - \varphi$ was equal to almost the complete rotation angle s of the outer cylinder, which often exceeded 100°.

If the system under investigation is fully elastic, the inner cylinder should turn through an angle of $\theta_e = s_e - \varphi$ (s_e is the full rotation angle of the inner cylinder), equal to the rotation angle θ of the outer cylinder; if the deformation is partially residual, then $\theta_e < \theta$. In some cases $\theta_e > \theta$, due to inertia overrun of the inner cylinder. If the medium is not elastic, the inner cylinder does not move at all after arrest of the outer cylinder; this was verified with water, mercury, and vaseline oil. The values of θ and θ_e were used to calculate the relative deformations ϵ and ϵ_e (see below). Some data are presented in Table 1.

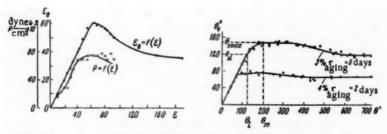


Fig. 2.— $\epsilon_e(\epsilon)$ and $P(\epsilon)$ curves for 2% aluminum naphthenate gel in decalin; $\tau_{\text{aging}} = 64 \text{ days}$. Fig. 3.— $\theta_e(\theta)$ curves for 3 and 4% aluminum naphthenate gels.

EXPERIMENTAL

Elastic recoil and shearing stress.—Figure 2 represents $\epsilon_e(\epsilon)$ and $P(\epsilon)$ curves for 2% gel of aluminum naphthenate in decalin, determined at $R_2=1.50$ cm, $R_1=1.396$ cm. The ratio of the values of P and ϵ_e at the curve maxima shows that the shear modulus $E\approx 130$ dynes/cm²; with the unusually high value of

62 for ε this is a sign of extremely high elasticity of the system.

Figure 3 shows $\theta_e(\theta)$ curves for 3% and 4% gels; it is seen that up to a certain rotation angle $\theta = \theta_t$ of the outer cylinder the values of θ_e are equal to θ , i.e., that the given deformations are fully elastic. Subsequently the $\theta_e(\theta)$ relationship becomes nonlinear; at first θ_e increases a little, passes through a maximum $\theta_{e \max}$ and then gradually diminishes. The lag of θ_e behind θ in the $\theta > \theta_t$ range is the consequence of structural breakdown and relaxation. The fall of θ_e beyond the maximum may also be caused by both these factors, but the first is the chief one. Despite this, the elastic recoil still remains fairly large. The reason is that the disrupted structural elements, undergoing relative displacement in the deformed extended state and giving rise to irreversible deformation, are capable of rapid cohesion at new points, with recoil of their retained elastic deformation. As the deformation increases, the degree of breakdown of the structure grows and elastic recoil diminishes. Moreover, if the deformation time is greater, the relaxation which is mainly associated with contraction of the broken-down structural elements can go further.

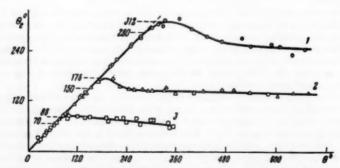


Fig. 4.— $\theta_e(\theta)$ curves for 2% aluminum naphthenate gel ($r_{aging} = 15$ days) with three different inner cylinders of R_1 : 1) 1.300; 2) 1.396; 3) 1.450 cm.

Table 2

Elastic Recoil with Different Gap Widths $R_2=1.50$ cm, $\Omega=6.53$ radians/sec

			Pel	θ_{ex}	ран		te .	ΔR .	Hel.		Hemax.		$\frac{R_{2}^{2}-R_{1}^{2}}{R_{2}^{2}}$
R_1	1/k'	Deg	Rad	Deg	Rad	tel	femax	em	em	tel	cm	6emax	.100%
1,450 1,396 1,300	30,52 15,00 8,04	70 150 280	1,22 2,615 4,88	86 176 311	1,5 3,07 5,45	37,2 39,2 39,2	45,7 46,1 43,8	$0,050 \\ 0,104 \\ 0,200$	1,83 3,92 7,32	36,6 37,7 36,6	2,25 4,60 8,18	45,0 44,2 40,8	6,55 13,3 24,9

Effect of gap width between cylinders on ϵ_e .—Measurements of ϵ_e with different gap widths $\Delta R = R_2 - R_1$ between the cylinders, for three values of $R_1 = 1.30$; 1.396 and 1.45 cm with $R_2 = 1.5$ cm showed that the throw-back angle decreases with decrease of ΔR (Figure 4). The values of $\epsilon = 2\theta R_2^2/(R_2^2 - R_1^2) = \theta/k'$ (Table 2) are similar for all values of ΔR .

Values of $\epsilon_{el} = H_{el}/\Delta R$ and $\epsilon_{e \max} = H_{e \max}/\Delta R$, where $H_{el} = R_2\theta_{el}$ and $H_{e \max} = R_2\theta_{e \max}$, calculated by the simplified formula $\epsilon_e = R_2\theta_e/\Delta R = H/\Delta R$, as the ratio of the linear displacement of the outer cylinder to gap width, coincide (Table 2) with the preceding values for the narrowest gap and are somewhat lower with a wide gap. In general, this proves the reality of enormous elastic deformations and the validity of the formulas used. At the same time, the deformation ϵ_e is in fact the extension deformation of the gel particles.

The use of the first of the two formulas presupposes constancy of the shear modulus E over the entire range of ϵ_e and a distribution of the deformation gradient over the gap characteristic of an ideal elastic Hookian body of constant E at low ϵ_e . In reality E is not constant over the entire range of ϵ_e up to $\epsilon_{e \text{ max}}$, but this lack of constancy is probably of the same type for all gaps and the variations of E are similar at equal values of ϵ_e .

In accordance with our earlier data¹ it may be assumed that variation of the velocity gradient $\dot{\epsilon} = 2\Omega R_2^2/(R_2^2 - R_1^2) = \Omega/k'$, as the result of changes of ΔR , at the fairly large values of $\dot{\epsilon}$ from 52.5 to 200 sec⁻¹ specially used here, has almost no influence on ϵ_e for the given gel.

The agreement between the values of ϵ_e shows that the heterogeneity of the stress field $(R_2^2 - R_1^2)/R_2^2$ (Table 2), which greatly increases with increase of ΔR , has no significant influence on ϵ_{el} and $\epsilon_{e\max}$ for this gel. This is consistent with earlier measurements of E by the method of torsional vibrations for small deformations in 7% gel¹.

Table 3 Elastic Recoil with the Lower Part of the Cylinder Filled with Gel or Mercury; $R_2=1.5$

		Gel aging time, days	Lower part of outer cylinder filled with					
Expt.	Gel composition		Radius of inner cylinder R ₁ , cm	Gel	Radius of inner cylinder, R ₁ , cm	Mercury		
1	2% aluminum naphthenate in decalin	~10	1.4	130-138	1.3	251-260		
2	The same The same, another sample	15 26	1.4	160-164	1.3	336		
3	2% aluminum naphthenate in decalin, with addition of 0.431 g of capryl alcohol The same	2 3	1.4 1.4	191 193	1.4 1.4	21 203		
4	2% aluminum naphthenate in vaseline oil	-	1.4	133-135	1.4	136-137		

In calculation of ϵ_e by means of the above formulas it is assumed that the gel is deformed in the annular gap A (Figure 1). To confirm that the elastic recoil is not due to the column of gel B under the bottom of cylinder R_1 , for which the relative deformation would be calculated from the formula for torsion of a rod as $\epsilon = R_1\theta_e/h$ (where $R_1 = 1.4$ cm, and h is the height of the column B, 2 cm), and which at $\theta_e = 163^\circ$ would be only $\epsilon_e \approx 2.0$ instead of $\epsilon_e = 42.7$, experiments were carried out in which the lower part B between the cylinders was filled with an inelastic liquid-mercury. In this case the gel was poured on top, and was present only in the narrow annular gap A. It was found that when the volume B was filled either with the gel or with mercury the values of θ_e (Table 3) coincided, both for the same cylinder of given R_1 , and for cylinders of different R_1 (with a twofold increase of ΔR , θ_e was also doubled; see Experi-

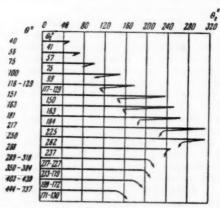


Fig. 5.—Schematic curves representing the character of the motion of the inner cylinder for different predetermined deformations.

ments Nos. 1 and 2, Table 3). This shows that the values of θ_a determined in the instrument are in fact values for the narrow gap A between the cylinders, which justify the above formulas and confirm the existence of enormous relative shearing deformations in high-elastic bodies.

Characters of the motion of the inner cylinder in elastic recoil.—The character of the motion of the inner cylinder after its release differs for different θ , and

depends on transition beyond $\theta_{e \text{ max}}$.

Figure 5 is a schematic representation of the types of motion of the inner cylinder $(M=121.5~{\rm g\cdot cm^2};~R_1=1.396~{\rm cm};~{\rm gel}~{\rm concentration}~2\%;~\tau_{\rm aging}=66~{\rm days})$ for different values of θ and corresponding final angles of rotation of the inner cylinder θ_e . The cylinder displacement θ_e is taken horizontally and the time vertically for each curve. The slope of each line is a measure of the rate of motion. Thus, at $\theta < 116^\circ$ the cylinder first travels rapidly in the forward direction, passes the new equilibrium position $\theta_e = \theta$ by inertia, and returns to it by a reverse movement. At $116^\circ < \theta > 163^\circ$ because of the large inertia over-run in the reverse direction another movement, although slow, appears in the forward direction. In this range of θ the first inertia kicks reach $90-100^\circ$, but in all cases the final position is $\theta_e = \theta$ (within the experimental error limits of $\pm 1-2^\circ$).

At $\theta=181\text{--}268^\circ$ the situation changes. The inertia kicks in the forward and return direction decrease, and the motion in the reverse direction occurs in two stages: most of it is rapid, followed by a virtual halt, and then slow. At $\theta=181\text{--}250^\circ$ the inertia kick in the forward direction decreases, and θ_e is somewhat larger than θ : thus, at $\theta=181^\circ$, $\theta_e=184^\circ$, and at $\theta=217^\circ$, $\theta_e=225^\circ$; i.e., in these cases θ_e is 3-8° higher. At $\theta\geq289^\circ$ the motion of the cylinder changes again; it first moves rapidly in a forward direction through a large angle, then stops, and subsequently moves slowly (through 8-15°) in the same direction. This last fact is very significant. It shows that all the deformation θ_e in this case is truly elastic, as after it has stopped the cylinder can move in the forward direction only under the influence of elastic deformation of the gel. At $\theta=289\text{--}318^\circ$, θ_e is $217\text{--}277^\circ$, and therefore elastic deformations ϵ_e reaching 6000%, found by calculation from θ_e max, can in fact develop the gel. Therefore the somewhat higher values of θ in the range $\theta\geq180^\circ$ are not inconsistent with the possibility of high values of ϵ_e .

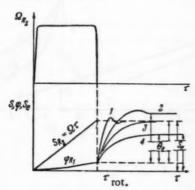


Fig. 6.-Motion of the outer and inner cylinders.

The first rapid jump on the curves for the motion of the inner cylinder might correspond to the "instantaneous" part of the deformation, and the subsequent slow motion to creep (high-elastic part). This subdivision might be useful in a number of cases, but it is very arbitrary, as it depends on the inertia of the cylinder and the time of recording of the deformation.

The types of cylinder motion considered here may be regarded as vibrational and aperiodic damping of a pendulum, where the elastic force is the gel elasticity and the inertia mass is the mass of the cylinder (the gel mass being disregarded). If the cylinder is very light, the gel mass is comparable with the cylinder mass, and must be taken into account. The motion of such a pendulum might conform to the equation

$$M \frac{d^2\theta_s}{d\tau^2} + p \frac{d\theta_s}{d\tau} + \Delta C\theta_s = 0$$
 (1)

under the condition that $p = f(\theta_i\theta)$ and that the gel elasticity in consequence of relaxation is $\Delta C = f(\tau, \theta_\theta)$; for example $\Delta C = \Delta C_0 e^{-\tau/\vartheta}$, when the relaxation time $\vartheta = f(\theta, \theta_\theta)$. A general scheme representing the motion of the outer and inner cylinders is shown in Figure 6. The upper part of the diagram represents

variation of Ω with time, and the lower, the angle of rotation of the outer cylinder $S_{R2} = \Omega \tau_{\rm rot}$ and the angle of rotation of the inner cylinder until the start of its free movement $\varphi(\tau)$, corresponding to change of the shearing stress $P(\tau)$, and also the motion of the inner cylinder after release $s_e(\tau)$. In accordance with the parameters of Equation (1), either oscillation about a new equilibrium position (when $p^2 < 4M\Delta C$) or an aperiodic approach to it (when $p^2 \gg 4M\Delta C$) is possible. The final values of s_e may be either equal to or less than the predetermined s. Therefore, high values of s_e are the consequence of inertia kicks and rapid relaxation ($\Delta C \to 0$). Values of $s_e < s$ are the consequence of structural breakdown and relaxation.

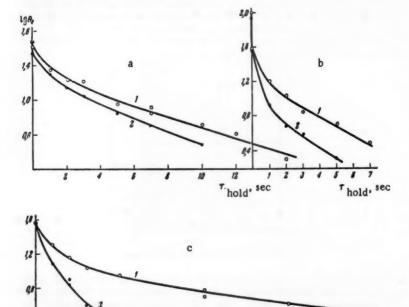


Fig. 7.—θ_r(θ) curves for 2% gel (r_{saing} = 155 days) determined with cylinders of different moments of inertia M: 1) 376.2 g·cm²; 2) 121.5 g·cm²; 3) 26.3 g·cm².

It is evident that the smaller the value of M and, the slower the relaxation, the more exactly the final values of s_e correspond to true s_e . It follows from Figure 5 that with transition through the maximum $\theta_e = \theta_{e \text{ max}}$ the nature of the motion changes from vibrational to aperiodic. This is due to the continuously increasing structural breakdown, accompanied by increase of the damping coefficient p, decrease of ΔC , and increase of the relaxation rate^{1.6}.

The effect of the moment of inertia of the cylinder is confirmed by the curves in Figure 7 for three cylinders of the same $R_1 = 1.40$ cm, and with $M_1 = 376.2$ g · cm² (mass 398 g), $M_2 = 121.5$ g·cm² (mass 81.5 g), solid and hollow stainless-steel cylinders respectively, and $M_2 = 26.3$ g·cm² (mass 23.1 g), a hollow

Duralumin cylinder. The experiments were performed with a low-viscosity gel (1% gel in decalin, $\tau_{\rm aging}=155$ days), in which relaxation is fairly rapid. It follows from Figure 7 that in the $\theta_e < \theta_{e \, \rm max}$ region $\theta_e = \theta$ for the two cylinders of smaller M, but for the heavier cylinder the values are somewhat high at all $\theta < \theta_{e \, \rm max}$. In this range of θ the elastic forces are still large, because structural breakdown is still low. Therefore the system is capable of imparting a fairly high velocity at the initial moment of motion even to the heavy cylinder, and under its influence it passes by inertia through the new equilibrium position. However, the return movement is hindered and the cylinder stops without reaching the new "fixed" equilibrium position $\theta_e = \theta$, and this results in high values of θ_e (Curve 2, Figure 6).

In the range $\theta_e < \theta_{e \text{ max}}$ the values of θ_e for the heaviest cylinder are, on the contrary, least and considerably diminished. This can be attributed to a large decrease of shearing stress beyond $P = P_r$, and to decrease of the relaxation time of the system, leading to a decrease in the velocity of the heavy cylinder

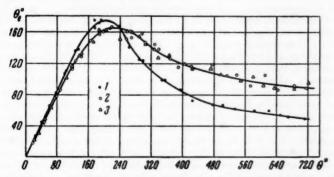


Fig. 8.—Relaxation curves $\log \theta_{\theta} = f(\tau_{hold})$: for 2% aluminum naphthenate gel with addition of 0.215% abryl alcohol, $\tau_{aging} = 76$ days, for $\epsilon = 12$ (a) and $\epsilon_{\epsilon} = 190$ (b); for 1.5% aluminum naphthenate gel, $\tau_{aging} = 80$ days for $\epsilon_{\epsilon} = 12$ (c); i) cylinder of $M_1 = 26.3$ g.-cm²; 2) cylinder of $M_2 = 12.5$ g.-cm².

even in the forward direction (Curve 4, Figure 6). Curve 1, Figure 6 represents vibrational and Curve 3, aperiodic motion when the given value of $\theta_{\epsilon} = \theta$ is exactly reached (cylinders of M_2 and M_3).

The two lighter cylinders, with values of M differing 4.6-fold, give $\theta_e(\theta)$ curves which virtually coincide for all values of θ . This shows that they are suitable for determinations of ϵ_e in this gel, and that $\epsilon_e(\epsilon)$ curves are independent of M. It is obvious that at large values of E and large θ even cylinders of not very low M should give correct values of ϵ_e , but the lightest cylinders should be used in investigations of low-viscosity systems. This is also shown by the curves for relaxation of deformation $\log \epsilon_e = f(\tau_{\text{hold}})$ for 2% and 1.5% aluminate naphthenate gels (Figure 8), the method for determination of which was described earlier. The initial points, corresponding to $\tau_{\text{hold}} = 0$ second and determining the $\epsilon_e(\epsilon)$ curve, coincide for cylinders with $M_2 = 121.5$ g·cm² and $M_3 = 26.3$ g·cm². The curves subsequently diverge, when a part of the elastic deformations and stresses in the system disappear owing to relaxation The small residual stress confers a lower velocity to the heavier cylinder, and the relaxation can proceed even further during this motion. The deviation is more pronounced at lower initial irreversible relaxation times; for example, at lower

gel concentrations (c = 1.5%) or at higher predetermined deformations

 $(c = 2.0\%, \epsilon = 190 > \epsilon_m).$

These results also lead to the conclusion that in investigations of the kinetic elastic properties of colloidal systems the moment of inertia of the cylinder (the acting body) may have an influence, especially with rapidly relaxing systems. In many investigations massive cylinders suspended from thin wires have been used in attempts to increase sensitivity. This can undoubtedly influence the form of the kinetic curves showing development of after-effects. The inertia of the acting body of the instrument should be reduced to a minimum. The type of cylinder motion described above was observed with gels of different compositions, but in some gels of high "dynamic" viscosity (such as aluminum naphthenate in vaseline oil) the motion of the cylinder was in the forward direction only, even at $\theta < \theta_{\theta \max}$.

The effects described have much in common with the types of motion of disks in monomolecular layers on water surfaces, such as highly elastic protein monolayers, in which an increase of the damping decrement was observed with

increase of amplitude and with approach to the yield value.

Some comments on extrusion of the gel from the gap between the cylinders.—It is known that elastic liquids and gels can become twisted on the rod of the inner cylinder and be extruded from the gap. This effect has been studied in detail by Weissenberg³ and by Ward and Lord⁸, and was attributed to normal stresses arising in the system in addition to tangential stresses. The methods used by these workers indicate that the steady-flow stage was investigated, and the initial deformation stage of the system as a "solid" body, with transition beyond the yield value or the maximum elastic deformation not considered at all.

It was noted in this investigation, and also in our earlier studies¹, that up to $\epsilon = \epsilon_{\max}$ or up to $\epsilon = \epsilon_r$, despite the fact that the tangential stress P reaches its maximum value $P = P_r$ at which the normal stress should be greatest, estrusion of the gel does not occur; it begins only after ϵ_e has passed beyond $\epsilon_{e \max}$, on the right-hand descending branch of the $\epsilon_e(\epsilon)$ curve, i.e., in the region of extensive breakdown of the continuous network structure. Consequently, one basic condition for extrusion of the gel and its twisting around the rod is breakdown of the structure, liberation of its individual elements, and further changes of particle configuration in flow.

It should be noted that twisting around the rod occurs only in high-elastic and fluid, i.e., rapidly relaxing, gels. In brittle-elastic gels of the gelatin type when $P = P_r$ and $\epsilon_s = \epsilon_{c \text{ max}}$ is passed the gel merely cracks and is extruded

from the gap in individual pieces, without twisting around the rod.

SUMMARY

 A new instrument, the elastorelaxometer (based on the coaxial-cylinder principle) has been developed, for studies of large high-elastic deformations in

relaxing colloidal gel systems and polymer solutions.

2. The effects of the following were investigated: a) width of the gap between the cylinders; b) moment of inertia of the cylinder (with rapidly relaxing colloidal systems, cylinders of the minimum moment of inertia must be used); c) nature of the liquid in the bottom of the cylinder; d) nature of the motion of the inner cylinder at different ultimate deformations.

3. Values of elastic recoil ϵ_e for different predetermined deformations ϵ have been determined in dilute aluminum naphthenate gels in decalin. It is shown that ϵ_e passes through a maximum, associated with transition beyond the yield

value of the structure, with increase of ϵ . It is shown that ϵ can recah 6000% in 2% gels.

ACKNOWLEDGMENTS

The author thanks technician P. G. Glebov for help in designing and constructing the instrument, and laboratory assistant L. S. Meshcheryakova for carrying out the determinations.

REFERENCES

Trapeznikov, A. A., in the book "New Methods for Physicochemical Investigation of Surface Phenomena" (In Russian) 1, 20; 39 (1950) Proc. Second All-Union Conf. on Colloid Chem. 1950; Prod. Acad Sci. USSR 63, 57 (1948); 74, 525 (1950); Trapeznikov, A. A. and Shlosberg, E. M., Proc. Acad. Sci. USSR 62, 791 (1948); Trapeznikov, A. A., and Fedotova, V. A., Proc. Acad. Sci. USSR, 81, 1101 (1951); ibid. 82, 97 (1952), ibid. 95, 595 (1954); Proc. Third All-Union Conf. on Colloid Chem. Minsk, 1953; Trapeznikova, A. A., and Shalopalkina, T. G., Kolloid, Zhur, 17, 47 (1955).
Trapeznikov, A. A., and Shalopalkina, T. G., Proc. Acad. Sci. USSR 111, 380 (1956).
Weissenberg, K., Proc. First Intern. Congress Rheology, Amsterdam, 1, 29 (1948).
Trapeznikov, A. A., and Assonova, T. V., Kolloid, Zhur, 20, 396 (1958).
Trapeznikov, A. A., and Belugina, G. V., Proc. Acad. Sci. USSR 87, 825 (1952).
Trapeznikov, A. A., Kolloid, Zhur, 20, 476 (1958).
Trapeznikov, A. A., Doctorate Dissertation (Moscow, 1955).
Ward, A. F. H., and Lord, P., Second Intern. Congress Rheology, Oxford, 1953 (London, 1954) p. 214.

DIENE * RUBBER: COMPOUNDING AND TESTING **

WARD A. SMITH AND JAMES M. WILLIS

CHEMICAL AND PHYSICAL RESEARCH LABORATORIES, THE FIRESTONE TIRE & RUBBER Co., AKRON, OHIO

INTRODUCTION

The use of stereospecific catalysts to prepare synthetic polyisoprenes which have the structure (cis-1,4) of natural rubber has been well documented^{1, 2, 3, 4}. It was logical that the catalysts which had been successfully applied to the synthesis of superior polyisoprenes should be tested in the polymerization of butadiene. From this investigation came Diene rubber, a polybutadiene made with an alkyl lithium catalyst.

In the present paper, the development of Diene rubber into superior tire stocks is discussed in detail. The best methods of processing and compounding are described and certain theoretical aspects of the curing reaction with sulfur are brought forth. The results of a large number of tire tests are presented and their relationship to the fundamental laboratory properties of the stocks explained.

BASIC CHARACTERISTICS OF DIENE RUBBER

Comparison to other butadiene polymers.—Diene rubber is distinctly different from usual butadiene polymers-emulsion polybutadiene and butadiene/ styrene copolymers—in several ways. The raw Diene rubber polymer is more waxy in physical appearance and has fewer characteristics of typical elastomers. However, the resilience of Diene rubber is much higher than that of other common polymers. The raw polymer rebound⁷ of Diene rubber at room temperature is exceptionally high compared to natural rubber and synthetic emulsion polymers, and this same increase in resilience is found in cured gum stocks (Table I). The modulus of Diene rubber at rapid deformations (dynamic modulus⁸) is also high, while the modulus at slower deformations (Scott modulus) is no higher, and possibly lower, than that of other polymers at equal states of cure. This high resilience and dynamic modulus found with Diene rubber results in a relative energy absorption (heat build-up) at constant force or constant energy8.9 equal to that of natural rubber and much lower than that found for emulsion polybutadiene or SBR (butadiene/styrene copolymer). Another outstanding property of Diene rubber is its low temperature performance (Table I) which exceeds that of most other polymers.

These same features of Diene rubber carry over into black loaded stocks and more importantly, into stocks based on blends of Diene rubber with natural rubber and SBR. This is illustrated briefly in Figure 1 where the rebound for Diene rubber over a wide temperature range is shown to be considerably higher than that of other polymers in a 50 phr HAF compound.

^{* &}quot;Diene" is a trademark of The Firestone Tire & Rubber Company.

** Reprinted from *Rubber Age 87, 815 (1960). Presented at the 77th Meeting of the Division of Rubber Chemistry, A.C.S., in Buffalo, N. Y., May 4-6, 1960 where it won the Best Paper Award.

Table 1 Comparison of Polymer Properties

	Natural	Direct	CDD	Emulsion polybutadiene		
Steel ball rebound, %	rubber	Diene rubber	SBR 1500	5° C	50° C	
Raw polymer						
@ 73° F, %	73	77	59	59	53	
Cured gumstocks						
@ 73° F	78	84	65	68	67	
@ 212° F	90	84	71	73	76	
Dynamic modulus, psi	57	103	83	73	76	
Internal friction, kps	0.26	0.88	0.9	1.07	0.86	
H_f (rel. energy absorp-						
tion @ constant force)	138	143	225	346	340	
50 phr HAF compounds						
Bell brittle point (° F)	-72	-141	-72	-130	-	

Processing of Diene rubber.—Diene rubber processes very well in blends with other polymers, even if present in rather high percentages. Factory processing operations (mixing, tubing, calendering, tire building, curing, etc.) have been carried out without deviation from normal production practice using stocks containing up to 50% Diene rubber in treads and 40% Diene rubber in bodies. However, Diene rubber used alone has a number of characteristics which make it difficult to handle on rubber processing equipment.

Diene rubber undergoes a marked transition in milling characteristics with a change in temperature. The raw polymer will not process well on a cool mill, being dry and lacking nerve and cohesiveness at temperatures below 110° F. As the temperature is increased, the polymer will gradually smooth out, forming a smooth band at temperatures above 150° F. An increase in Mooney viscosity (ML4 @ 212° F) has an adverse effect on the handling characteristics. Polymers with a Mooney viscosity above 60 will not band smoothly on an openmill even at the higher temperatures.

Butadiene polymers made with a Firestone modified Ziegler catalyst or by the Phillips system^{6, 7}, undergo an opposite change in handling characteristics with temperature. These polymers will form a smooth band on the mill rolls at temperatures below 110° F. Above this temperature, the polymer becomes

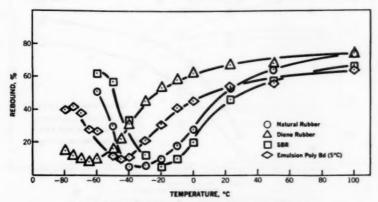


Fig. 1,-Steel ball rebound, %. 50 phr HAF black compounds.

dry, loses cohesiveness and tack, and will not band. As is the case with Diene rubber, the processing becomes worse as the Mooney viscosity of the polymer is increased.

Diene rubber, along with other solution polymerized polybutadienes, is very resistant to breakdown either on the open mill or in a Banbury mixer. Processing aids and chemical peptizers were found to have no effect on the breakdown of Diene rubber.

Black reinforced all-Diene rubber stocks can be mixed satisfactorily in a Banbury mixer but are difficult to mix on a mill, the difficulty increasing with the Mooney of the polymer. The incorporation of carbon black causes the stock to become dry and "loose" on mill rolls and the compounded stock is very difficult to process on warmup mills, tubers and calenders. Processing is improved by the use of high plasticizer levels together with increased black loadings.

BLENDS OF DIENE RUBBER AND NATURAL RUBBER

Processing.—Diene rubber is very advantageously used in blends with natural rubber. Diene rubber/natural rubber blends will process satisfactorily at proper black and oil levels, the maximum ratio of Diene rubber to NR being dependent on the Mooney plasticity of the Diene rubber. Very satisfactory processing is obtained with 50/50 blends of the two polymers if the Mooney plasticity of the Diene rubber is below 90. However, the best overall balance of properties is obtained with polymers having a Mooney plasticity in the range from 20 to 60. For blends containing 75% Diene rubber or higher, best results are obtained with a polymer of 40 Mooney or lower. The processing of Diene rubber/natural rubber blends is further improved by plasticizer levels higher than are normally used in natural rubber compounds. Diene rubber/NR 50/50 stocks designed for use in truck treads should contain at least 10–15 phr of softener. Blending of Diene rubber and natural rubber prior to the incorpora-

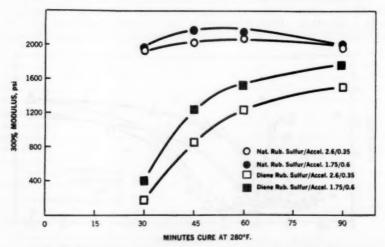


Fig. 2.-Cure curves for natural rubber and Diene rubber (50 phr HAF Black),

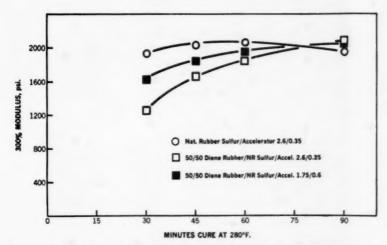


Fig. 3.—Cure curve for natural rubber and 50/50 Diene rubber/natural rubber (50 phr HAF Black).

tion of other compounding pigments is recommended for optimum processing and properties. This is best accomplished by allowing the two polymers to mix briefly in the Banbury mixer before addition of pigments.

Basic reactions with sulfur.—The cure rate of Diene rubber is slower and the induction period longer than that of natural rubber as shown in Figure 2. The cure rate and the level of combined sulfur for a 50/50 Diene rubber/natural

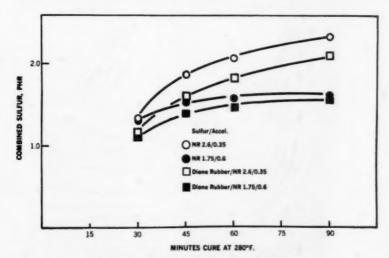


Fig. 4.—Rate of sulfur combination (50 phr HAF Black). (Natural rubber and 50/50 Diene rubber/NR).

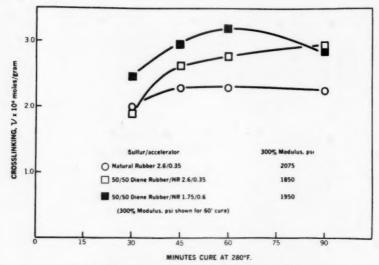


Fig. 5.—Cure rate as measured by crosslinking (50 phr HAF).

rubber blend is more nearly like that of natural rubber when a low sulfur/high accelerator type cure is used (Figures 3 and 4).

Diene rubber and Diene rubber/natural rubber blends require a greater number of crosslinks than are developed with natural rubber compounds.

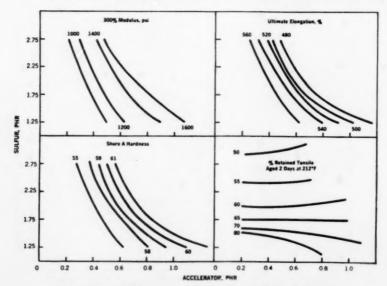


Fig. 6.—Effect of sulfur and accelerator 50/50 Diene rubber/NR, 50 HAF.

This is illustrated in Figure 5, in which it can be seen that the level of crosslinking is higher for the Diene rubber/natural rubber blend even though the modulus is somewhat lower. A higher level of crosslinking and higher modulus is developed with less combined sulfur when the low sulfur/high accelerator level

is used in the blend compound.

Effect of sulfur/accelerator ratio.—The state of cure has a very marked effect on the properties of Diene rubber compounds. The effect of various sulfur/ accelerator ratios on the properties of a 50/50 Diene rubber/natural rubber tread compound is shown in Figures 6 and 7. Satisfactory properties are developed at each of the sulfur levels studied, provided the proper level of accelerator is used. As would be expected, the use of lower sulfur levels results in compounds with improved aging resistance.

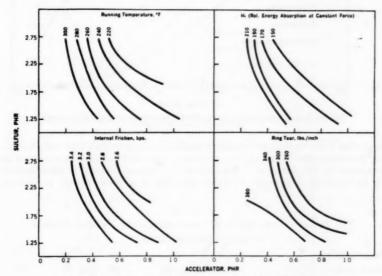


Fig. 7.—Effect of sulfur and accelerator (50/50 Diene rubber/NR, 50 HAF).

Aging characteristics.—In general, Diene rubber/natural rubber blends have better resistance to accelerated oven 10 or bomb 11 aging than does a natural rubber compound. The oxygen absorption rate12 for the Diene rubber blend is very similar to that of natural rubber and higher than that of SBR.

Stress relaxation tests13 were made at 120° C and 50% elongation on natural rubber, Diene rubber, and a 50/50 blend of these polymers. Figure 8 shows the intermittent stress relaxation which is a measure of the combined effect of crosslinking and chain scission. In natural rubber, chain scission is predominant and stress decay occurs. Diene rubber shows a slight increase in stress. Blends of 50/50 Diene rubber/natural rubber resulted in stress behavior such as would be expected from an average of the single polymers.

Ratio of Diene rubber to natural rubber.—The effect on physical properties of various ratios of Diene rubber to natural rubber in a 50 phr HAF black tread stock are shown in Table II. The Diene rubber containing compounds have

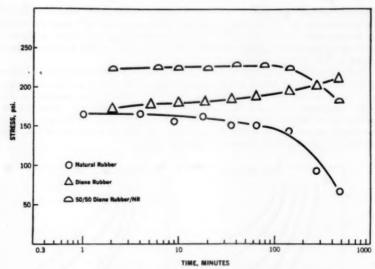


Fig. 8.—Intermittent stress relaxation 120° C 50% extension (50 phr HAF Black).

somewhat lower moduli and tensile strengths, increase in hardness with increasing percentages of Diene rubber, and show a marked increase in resilience as measured by ball rebound. An increase in internal friction is accompanied by an increase in dynamic modulus resulting in a lower energy absorption

TABLE II

THE EFFECT OF THE RATIO OF DIENE RUBBER TO NATURAL RUBBER

(50 HAF—Cured 60' @ 280° F)

(00	mar cure	u 00 @ 200	1		
Natural rubber	100	75	50	25	0
Diene rubber	0	25	50	75	100
Shell SPX 97	3	3	3	3	3
Sulfur	2.6	2.6	2.4	2.4	1.75
Santocure NS	0.35	0.40	0.5	0.6	0.6
Normal stress-strain 300% modulus, psi Tensile strength, psi Ultimate elongation, %	1925 3650 480	2000 3500 440	1725 3175 490	1675 2700 450	1525 2550 440
Shore A hardness	62	63	67	68	65
Forced vibrator @100° C Dynamic modulus, psi Internal friction, kps Rel. energy absorption @ constant force	202 3.0 127	218 3.0 108	277 4.3 97	300 4.6 88	312 4.9 87
Steel ball rebound, % @ 73° F @ 212° F	54 72	58 75	63 74	67 75	69 71

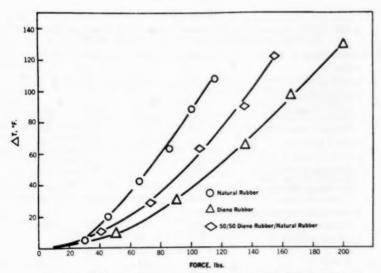


Fig. 9.—Heat build-up at constant force (50 HAF). (Ambient Temp. -100° F.) (Firestone Shear Flexometer).

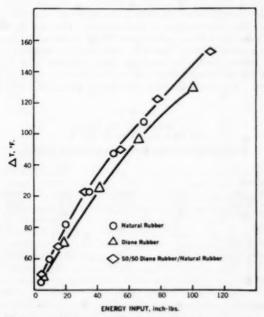


Fig. 10.—Heat build-up at constant energy input. (50 phr HAF. Ambient Temp. -100° F.) (Firestone Shear Flexometer).

TABLE III

THE EFFECT OF AMOUNT OF CARBON BLACK 50/50 BLEND OF DIENE RUBBER AND NATURAL RUBBER. CURED 60' @ 280° F

TOODBIG AND THATCHAD	ACC DESERTE	CORED OO	(a) 200 I	
HAF Black, phr	40	45	50	55
Sulfur	2.4	2.2	2.0	2.0
Santocure NS	0.6	0.5	0.5	0.45
Normal stress-strain 300% modulus, psi Tensile strength, psi	1750 3150	1700 3125	1975 3450	2075 3100
Ultimate elongation, % Shore A hardness	470 65	470 66	480 67	440 68
Forced vibrator @ 100° C				
Dynamic modulus, psi Internal friction, kps Rel. energy absorption @	$\frac{193}{2.3}$	$\frac{237}{3.2}$	289 4.2	324 5.1
constant force	88	98	87	84
Firestone Flexometer—250 lbs, 0	.3 throw (1	4)		
Running temperature, ° F	210	232	248	290
Steel ball rebound, %				
@ 73° F @ 212° F	69 79	$\begin{array}{c} 65 \\ 74 \end{array}$	$\frac{62}{73}$	61 70
Ring tear @ 212° F, lbs/inch	227	316	367	405

(heat build-up) at constant force (H_f) relative to a natural rubber compound. The effect of increased dynamic modulus is also apparent when the heat build-up is measured on the Firestone Shear Flexometer⁹. The heat build-up at constant force is lower for a Diene rubber or a 50/50 Diene rubber/natural rubber blend than for natural rubber (Figure 9). Measured at constant energy input, the all-Diene rubber stock also has lower heat build-up than natural rubber and the 50/50 Diene rubber/natural rubber compound is equal to natural rubber (Figure 10). In view of the fact that tires of Diene rubber/NR blends ran

TABLE IV

A ADDE AV							
THE	EFFECT	OF O	L LEVI	EL			
(50 H.	AF, Cure	ed 60'	@ 280°	F)			

50/50Blend of Diene Rubber and Natural Rubber Shell SPX 97 Oil 0 5 10 15 Normal stress-strain

Normal stress-strain					
300% modulus, psi	2100	1860	1500	1330	1010
Tensile strength, psi	3350	3170	3110	2950	2870
Ultimate elongation %	425	440	500	515	600
Shore A hardness	64	63	60	58	54
Forced vibrator @ 100° C					
Dynamic modulus, psi	237	220	196	170	145
Internal friction, kps	3.8	3.7	3.5	3.2	2.9
Goodrich flexometer					
ΔT , ° F	46.5	43.5	45.5	46.5	44.5
Steel ball rebound, %					
@ 73° F	64	62	59	60	58
@ 212° F	73	72	70	70	68

as cool or cooler than NR controls (Table VII), it appears that the relatively low heat build-up at constant force and constant energy, characteristic of Diene rubber or Diene rubber/NR blends, are more nearly related to heat build-up in service than internal friction, which is relatively high for Diene rubber.

Effect of black and plasticizer level.—The effect of increasing the carbon black loading (HAF) in a 50/50 Diene rubber/natural rubber compound is shown in Table III. As would be expected, an increase in modulus, hardness, and hysteresis loss is noted at the higher black levels. Increasing the plasticizer level at a given black loading will reduce the modulus, hardness, rebound, dynamic modulus and internal friction of the blend compound (Table IV). Very little change is found in the heat build-up as measured on the Goodrich flexometer¹⁵ as the plasticizer is increased up to the 20 phr level.

By the proper choice of black level, plasticizer level and sulfur/accelerator ratio, the compounder should be able to design a Diene rubber/natural rubber stock suitable for his particular requirements.

Table V

Effect of Ratio of Diene Rubber to SBR 1500

(50 HAF, Cured 60' @ 280° F)

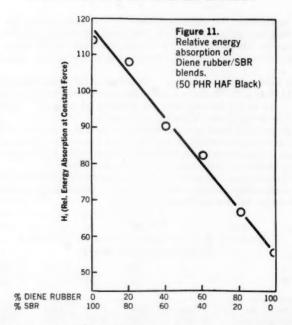
	(00 11/11)	Juica oo	(200 I)			
Diene rubber	100	80	60	40	20	0
SBR-1500	0	20	40	60	80	100
Normal stress-strain						
300% modulus, psi Tensile strength, psi Ult. elongation, %	1800 2700 400	1800 2825 420	$\begin{array}{c} 1625 \\ 3025 \\ 480 \end{array}$	1850 3200 460	2125 3400 440	$2550 \\ 3800 \\ 420$
Shore "A" hardness	70	68	68	67	66	67
Forced vibrator @ 100° C						
Dynamic modulus, psi	394	376	336	324	277	269
H_f (Rel. energy absorption						
@ constant force)	56	67	83	90	108	114
Steel ball rebound, %						
@ 73° F @ 212° F	67 75	63 70	58 68	53 66	50 67	45 65

BLENDS OF DIENE RUBBER WITH SBR

Processing.—Satisfactory processing is obtained when Diene rubber is blended with certain types of SBR. The most satisfactory blends of Diene rubber with SBR polymers result in 20-50 Mooney Diene rubber is used. High levels of plasticizer along with increased loadings of carbon black are a very definite aid to processing of Diene rubber/SBR blends. The use of oilextended SBR polymers is a convenient way to incorporate oil in these blends.

Physical properties.—Diene rubber has unique properties in blends with SBR, exhibiting high rebound and high dynamic moduli, both of these values increasing as the percentage of Diene rubber in the blend is increased (Table V).

This increase in dynamic modulus again results in a marked reduction in energy absorption at constant force as the percentage of Diene rubber is increased (Figure 11). A reduction in tensile strength and an increase in hardness is also noted with increasing Diene rubber content. The same pattern of higher rebound, dynamic modulus, and hardness and lower relative energy



absorption at constant force is found for oil-extended (32 phr oil) blends of Diene rubber and SBR. As mentioned previously, improved processing is obtained with oil extension.

TIRE TESTS

Truck tires.—Polymer usage in large size truck tires is at present restricted mainly to natural rubber due to the necessity of keeping temperature build-up to a minimum in the thick sections involved. The recently developed high cis-1,4 polyisoprenes^{1, 2, 3, 4} duplicate Hevea natural rubber in structure and can be used interchangeably with it in tire stocks. Most other synthetic polymers increase the operating temperature of tire stocks to the detriment of tire performance. Our results show that Diene rubber may be used in blends with Hevea rubber in both the tread and body of truck tires to give lower running temperature and improved tread wear and cracking resistance.

Truck treads based on a 50/50 blend of Diene rubber and natural rubber using HAF black were fleet tested on highways in Texas. A wear improvement of 12% was achieved, over a control stock of natural rubber containing a small amount of SBR, based on an average of 16 tires run a total of 282,200 miles in all positions (Table VI). The wear rating of the Diene rubber tread relative to the control was actually highest in the drive position (tractor rears) which is generally considered to be the most severe test. Cracking was relatively minor with the 50% Diene rubber tread being approximately equal to the control which has excellent cracking resistance. A very limited amount of testing was also carried out on Phillips Cis-4 polybutadiene in the same stock (Table VI).

Tests of 75/25 Diene rubber/natural rubber, HAF black truck tire treads

TABLE VI
TIRE TREAD TESTS OF PBD/NATURAL RUBBER BLENDS
(9.00-20 Truck Tires)

	Wear	Cracking	No.	Total miles
NR plus small amount SBR	100	Very slight	15	336,000
Diene rubber/NR-50/50, HAF	112	Very slight-slight	16	282,000
Phillips' Cis-4 PBD/NR-50/50, HAF	104	Very slight-slight	2	23,000
Diene rubber/NR-75/25, HAF	120	Slight+	5	94,000

in both tractor drive and trailer positions showed wear improvement of 20% over the same control (Table VI), although cracking was slightly worse than

with only 50% Diene rubber present.

Substitution of Diene rubber for natural rubber in truck tire treads resulted in a reduction of the operating temperature of the tire, as predicted by laboratory tests. Tires having Diene rubber/NR treads ran cooler than the controls during both fleet and indoor tests in nearly every case. Typical results (Table VII) indicate a 5–10° F reduction in tire temperature (either shoulder or contained air) when using a 50% Diene rubber tread, with an additional 2–5° lowering obtainable with Diene rubber in the body stocks.

The desirability of the use of Diene rubber in truck tire body stocks is indicated by the indoor test results (Table VII). Particularly noteworthy are the results of the crown break test where 9.00–20 tires with either 25% or 40% Diene rubber in the body and 50% Diene rubber in the tread ran the complete range of the test without failure. Tires built with 25/75-Diene rubber/natural rubber body stocks have run to 60,000 plus miles on a commerical fleet, giving further proof of the durability of such a compound. The 40/60 Diene rubber/natural rubber body stock was evaluated in tires which were run to 30,000 miles without failure.

Laboratory test data on factory mixed truck tire compounds are shown in Table VIII. The low energy absorption at constant force brought about by high dynamic moduli, and also the high rebound of Diene rubber containing stocks, correlate well with the reduced operating temperature in tires. High resistance to crack initiation¹⁶ by Diene rubber containing tread stocks is consistent with reduced cracking in service.

Table VII

Heat Build-up in Diene Rubber Truck Tires
(9.00-20 and 10.00-20)

Fleet test		Shoulder temp.		
Control	7			Par
50/50-Diene rubber/NR Tread	7			4° F Cooler
75/25-Diene rubber/NR Tread	2			7° F Cooler
40/60-Diene rubber/NR in Body Only	2			2° F Cooler
Indoor crown break	Test lim	it	Failure	Contained air temp. at 70 mph, ° F
Control	2 hrs @ 75	mph	Crown break	272
50/50 Diene rubber/NR tread-25/75 Body	4 hrs @ 75		No failure	266
50/50 Diene rubber/NR tread-40/60 Body	4 hrs @ 75		No failure	240
Indoor endurance	Miles run	Failure	Cracking	Shoulder temp.
100% Natural rubber	11,423	None	Severe	199
50/50 Diene rubber/NR tread	10,523	None	Slight	190
25/75 Diene rubber/NR tread and body	9,778	None	Slight	185

TABLE VIII
PHYSICAL PROPERTIES OF TYPICAL DIENE RUBBER/NATURAL
RUBBER TRUCK TIRE STOCKS

	Natural rubber	50% Diene rubber	Natural rubber	25% Diene rubber	40% Diene rubber
Polymer	Tread	stock		Body stocks	
Cure at 280° F, min	60	60	45	45	45
Normal stress-strain					
300% modulus, psi Tensile strength, psi Ultimate elongation, %	1850 3950 520	$1500 \\ 3050 \\ 480$	$\begin{array}{c} 750 \\ 3475 \\ 600 \end{array}$	$\begin{array}{c} 675 \\ 2550 \\ 600 \end{array}$	$\begin{array}{c} 750 \\ 2150 \\ 530 \end{array}$
Stress-strain aged 2 days at 212°	F				
300% modulus, psi Tensile strength, psi Ultimate elongation, %	1475 280	1525 250	$1125 \\ 2800 \\ 490$	825 1425 420	$975 \\ 1275 \\ 330$
Stress-strain at 212° F					
Tensile strength, psi Ultimate elongation, %	$2530 \\ 580$	$\frac{1590}{380}$	$\frac{1310}{560}$	750 38	680 290
Ring tear					
@ 212° F, lbs/in. @ 275° F, lbs/in.	463 360	$\frac{340}{270}$	$\frac{210}{122}$	120 97	110 85
Cure at 280° F, min	60	60	50	50	50
Shore A hardness	59	63	51	52	54
Forced vibrator at 212° F					
Dynamic modulus, psi Internal friction, kps Relative energy absorption at	$\frac{145}{2.3}$	$\frac{193}{3.0}$	$\begin{array}{c} 76 \\ 0.7 \end{array}$	$^{91}_{0.9}$	97 0.8
constant force	189	138	209	190	147
Firestone flexometer					
Running temperature, ° F	237	247	159	168	165
Steel ball rebound					
@ 73° F, % @ 212° F, %	55 73	63 73	71 85	76 84	78 86
Crack initiation at 200° F					
Total number of cracks	88	0			

Passenger tires.—Service tests of 50/50 blends of Diene rubber and oil-extended SBR (41° F, 31 phr oil) in passenger tire treads have shown an average of 12% better wear and less cracking than all SBR treads with the same oil and black contents.

Tread feature	Wear	Cracking	No. tires	Total miles
100% SBR, HAF	100	Slight	8	99,000
50/50 Diene rubber/SBR, HAF 50/50 Firestone modified Ziegler	112	None-V.Sl.	6	75,000
PBD/SBR, HAF	102	None-V.Sl.	4	48,000
75/25 Diene rubber/SBR, HAF	123	Slight	2	24,000

Even better wear performance is obtained if 75% of the polymer blend is Diene rubber. Results of this order have been obtained on both employees' cars (average service) and fleet tests (continuous high speed service).

Other important advantages accrue when Diene rubber is used in passenger tires. The superior low temperature characteristics of Diene rubber give significantly better traction on packed snow when it is blended with SBR in a typical passenger tire tread stock (Table X).

TABLE X

LOW TEMPERATURE CHARACTERISTICS OF TREADS WITH DIENE RUBBER

Polymer	100% Natural rubber	50/50 Diene rubber/NR	100% SBR	50/50 Diene rubber/SBR
Bell brittle point	-72° F	-125° F	-54° F	-103° F
Temp. of 104 Young's modulus	-60° F	−72° F	−36° F	−75° F
Relative lab coefficient of friction on ice (20° F)	100	105	75	101
Traction of tires on snow at 25–30° F	Superior	Excellent	Par	Better

Of equal importance is the contribution of Diene rubber to improved high speed performance and reduced tire operating temperatures through its hysteretic properties (Table XI). As Diene rubber is used in more and more parts of the tire, high speed performance improves and operating temperature drops.

The influence of Diene rubber is also noticed in reduced rolling resistance (horsepower loss) on indoor tests. A 10% reduction in the energy absorbed was achieved with Diene rubber blends in all parts of the tire (Table XI).

TABLE XI
OPERATING CHARACTERISTICS OF 6.00-13 TIRES CONTAINING DIENE RUBBER

		0-4-1-	60	mph	
Feature	High speed failure	Cont. air at 95 mph	HP	Index	
Control	0.1 hr @ 100 mph	200° F	2.14	100	
50/50-Diene rubber/SBR tread on control body	0.4 hr @ 105 mph	197° F	2.00	94	
50/50-Diene rubber/SBR tread, 35% Diene rubber in body	1.9 hr @ 100 mph	192° F	1.94	91	
50/50-Diene rubber/SBR tread, 35% Diene rubber in body and interliner	1.0 hr @ 105 mph	184° F	1.92	90	

This was confirmed by gasoline consumption tests on the highway under carefully controlled conditions. This feature of a tire is becoming more important as the public feels the impact of rising gasoline prices.

CONCLUSIONS

Over 2,000,000 miles of testing on tires containing Diene rubber in blends with natural rubber or SBR show conclusively the advantages of using these

stocks. Important improvements in abrasion and cracking resistance, operating temperature, rolling resistance and gasoline consumption, and traction on snow should be mentioned. At the present time, all of the Diene rubber being manufactured in a pilot plant is being utilized in production of tire stocks. It is certain that this usage will be greatly expanded in the near future when the full scale plant goes on stream.

ACKNOWLEDGMENT

The authors wish to acknowledge the continuing help and guidance of Drs. F. W. Stavely and Glen Alliger throughout this study. Thanks are also due to Sydney Smith for his assistance in obtaining laboratory test data, and to the Firestone Tire and Rubber Co. for permission to publish this paper.

REFERENCES-GENERAL

- F. W. Stavely and others Ind. Eng. Chem. 48, 778 (1956).
 G. Alliger, Willis, J. M., Smith, W. A., and Allen, J. J., Rubber World 134, 549 (1956).
 S. E. Horne, Jr. and others, Ind. Eng. Chem. 48, 784 (1956).
 R. H. Mayor, Saltman, W. M., and Pierson, R. M., Petroleum Ref. 37, 208 (1958).
 Kraus, G., Short, J. U., and Thornton, V., Rubber and Plastica Age 38, 880 (1957).
 H. E. Railsbach, Baird, C. C., and Haws, J. R., Proceedings International Rubber Conference, Washington, D. C., November 1959, p. 502.

REFERENCES—TEST PROCEDURES

- Ball Rebound—Cole, O. D., Trans. Am. Soc. Mech. Engrs. 65, 15 (1943).
 Internal Friction—Dynamic Modulus by Firestone Forced Vibrator—Dillon, J. H., Prettyman, I. B., and Hall, G. L., J. Applied Phys. 15, 309 (1944).
 Firestone Shear Flexometer—Hall, G. L., and Conant, F. S., Firestone Tire and Rubber Co., Report CR-3053 to Federal Facilities Corp., Office of Synthetic Rubber, Research and Development Division, Polymer Science Branch, Washington, D. C., July 15, 1952.
 Oven Aging—ASTM Designation D572-53.
 Oxygen Bomb Aging—ASTM Designation D572-53.
 Oxygen Bomb Aging—ASTM Designation D572-53.
 Oxygen Absorption—Blum, G. W., Shelton, J. R., and Winn, H., Ind. Eng. Chem. 43, 464 (1951).
 Stress Relaxation—J. Applied Phys. 15, 380 (1944).
 Firestone Flexometer—Cooper, L. V., Ind. Eng. Chem. (Anal. Ed.), 5, 350 (1933); Rubber Chem. & Technol. 7, 125 (1934).
 Goodrich Flexometer—ASTM Designation D623-52T.
 Crack Initiation-cut Growth—Prettyman, I. B., Ind. Eng. Chem. 36, 29, (1944).

CIS-1,4-POLYISOPRENE RUBBER BY ALKYL LITHIUM INITIATED POLYMERIZATION *

HUGH E. DIEM, HAROLD TUCKER, AND C. F. GIBBS

INTRODUCTION

The polymerization of isoprene by lithium metal was performed first perhaps as long ago as 1910 by Matthews and Strange¹ in England. However, as late as 1937, Midgley reported that lithium did not polymerize isoprene². At about the same time, Ziegler and his colleagues³ used butyllithium and other organoalkalis to polymerize various dienes, although without identifying cis-1,4-polyisoprene as a product of isoprene polymerization. Many of these products were not rubbers. Recently, Stavely and others¹ reported the polymerization of isoprene by lithium metal to a polymer whose structure consisted of about 94% cis-1,4 units and 6%, 3,4 units. We have found that many alkyl and aryl lithium compounds likewise produce a polyisoprene of 90 to 96% cis-1,4 structure. The July-September issue of Rubber Chemistry and Technology, 1960, pages 595-747, contains a series of articles on rubbers of stereoregular structure and should be consulted for work appearing since the work described here.

EXPERIMENTAL

Polymerizations were carried out in rotating beverage bottles, in laboratory stirred glass reactors under reflux conditions, and in 5-gallon polymerizers. Equipment was cleaned, dried at 140° C, and cooled with argon flushing just prior to charging. Monomer and solvent were charged with an argon pressure siphon, and initiator was added from a hypodermic syringe. Bottle polymerizations were not sampled since rubber gaskets inhibited the polymerization, and aluminum-lined cork gaskets were used. In the bottle polymerizations, reaction temperatures doubtless sometimes rose above the bath temperatures. In the glass reactors, the polymerization temperature, controlled by reflux, increased as monomer was consumed. The contents of the glass reactors could be sampled through a stopcock in the bottom of the flask. In all cases polymer cements were worked up by pouring them into vigorously sitrred methanol containing antioxidant (0.5 part of N, N'-di(2-naphthyl)-p-phenylenediamine and 0.25 part of N, N'-diphenyl-p-phenylenediamine on the rubber). The precipitated rubbers were washed several times in methanol containing antioxidant, and were dried 16 hours at 50° C under vacuum.

Materials.—The success of alkyllithium-initiated polymerization depends upon freedom from impurities. Water, carbon dioxide and oxygen must be rigorously excluded. Such compounds as alcohols, ketones, acids, mercaptans, disulfides, acetylenes, etc. also react with alkyllithiums and must be removed. Ethers should be avoided since they affect the structure of the polymer. As an aid to excluding oxygen and water from polymerization flasks, the expedient

^{*} This paper was presented at the New York meeting, 1957, The Division of Rubber Chemistry, ACS, where it won the Best Paper Award.

of greasing ground joints with a dispersion of lithium in petrolatum was adopted.

Silicone greases are potent inhibitors and must not be used.

Solvents were purified by distillation from sodium dispersion in an argon atmosphere. Commercial isoprene of about 93% concentration was purified similarly. Both solvent and monomer were stored in clean glass bottles under argon. The diffusion of oxygen and/or water vapor through the ground joints of storage bottles was sufficiently rapid that storage of materials for more than a few days resulted in increased catalyst requirements.

Transfers and reactions were continuously blanketed with argon (Air Reduction Sales Company). Lamp-grade nigrogen (General Electric Company)

could be substituted for the argon.

Except for methyllithium, the alkyllithiums were made⁵ by adding an alkylhalide to an excess of lithium at about 35° C under argon. Petroleum ether was the common solvent, although a number of purified hydrocarbons are suitable. Methyllithium was prepared by adding methyl iodide to a solution of n-butyllithium to give a white suspension of methyllithium in petroleum ether. The concentration of each initiator was determined by the double titration method of Gilman6. The titer was redetermined every few days as it continually decreased. Presumably this loss was occasioned by reaction of alkyllithium with oxygen or water vapor diffusing into the storage bottles; alkyllithium solutions (in hydrocarbons) have been stored unchange for months in sealed tubes7. All alkyllithium compounds, except methyllithium, were obtained as clear colorless solutions overlying a blue or purple sediment of lithium halide (byproduct) and unreacted lithium. These solutions were not without some haze when a light beam passed through them. However, neither centrifuging the solutions nor filtering them through a biological filter diminished the haze or the activity of the reagent, and, in any case, the haze was no stronger than that observed with the "pure" solvent from which the solutions were prepared. A haze developed in alkyllithium solutions exposed to the air, and within a few hours a white precipitate formed as the alkyllithium reacted with oxygen and/or moisture. However, no precipitate formed when clear colorless solutions of alkyllithium were added to pure solvent8.

RESULTS AND DISCUSSION

The organolithium compounds which were tested as initiators for the polymerization of isoprene included those in which the organic radical was methyl, ethyl, n-propyl, isopropyl, n-butyl, t-butyl, n-amyl, n-hexyl, n-dedecyl, benzyl and phenyl. All but methyllithium initiated polymerization. In the cases of phenyl- and benzyllithium, reaction was very slow. In every case, the polymer produced was 90 to 96% cis-1,4-polyisoprene. The infrared spectrum of a typical polymer is shown in Figure 1a. Inclusion of sediment from initiator preparation did not appear to affect either the rate of polymerization, or the polymer structure. The sediment alone did not initiate the polymerization. Since the various initiators gave polyisoprenes of similar structure, and it was convenient to prepare n-butyllithium, most of the work was done with that initiator.

The rate of conversion of isoprene to polymer was studied in stirred glass polymerizers in bulk polymerization as well as in solution polymerization. The solvents studied were benzene, heptane and hexane, and they were used in concentrations ranging from 50 to 96 weight per cent. Each of these polymerizations was run at reflux and was sampled periodically until the solution be-

came too viscious to flow from the stopcock. After this, polymerization was allowed to continue until the mass would no longer stir, whereupon methanol was added as a shortstop. Data from three typical runs are recorded in Table I. The initiator levels reported in Table I are expressed as millimoles of n-butyl-lithium per mole of isoprene (mM/M). The "effective initiator" concentration

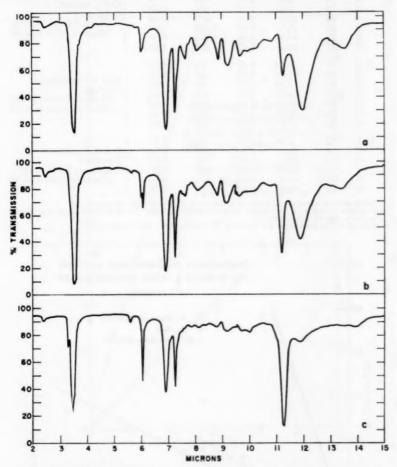


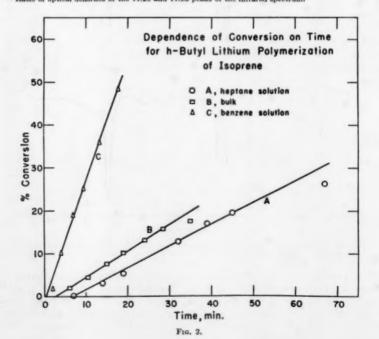
Fig. 1.—Infrared spectra of alkyllithium polyisoprene: a with no added ether; b with 0.01% on the monomer of ethyleneglycol diethylether; c with 0.10% ethyleneglycol diethylether.

will be referred to later. The time-conversion data of Table I are plotted in Figure 2. It is apparent that conversion increased linearly with time, at least to the point where high viscosity prevented further sampling. Probably a decreased rate of diffusion of monomer to the growing chain ends caused the rate of conversion to fall after this point. Induction periods were negligible. The

TABLE I SAMPLED POLYMERIZATIONS OF ISOPRENE WITH N-BUTYL LITHIUM

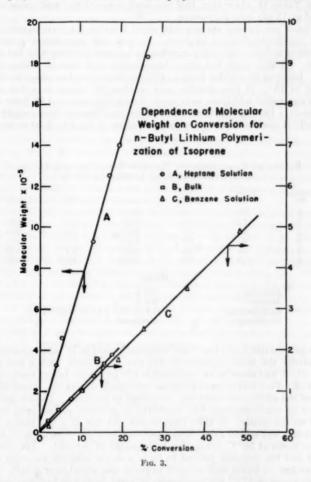
No.	Time, min.	Conv.	DSVa	M. wt. ^b ×10 ⁻³	3, 4-/ 1, 4-°	Remarks
A-1	7	0.30	_		-)
-2	14	3.07	2,40	329	0.49	07 007 1
-3	19	5.33	3.00	460	0.49	85.0% heptane
-4	32	12.8	4.79	920	0.48	Catalyst:
-5	39	16.9	5.80	1,250	0.49	Charged 0.265 mM/M
-6	45	19.5	6.30	1,400	0.50	Effective 0.010 mM/M
-7	67	26.4	7.47	1,830	0.54	J
B-1	6	2.00	0.48	29	0.64)
-2	10.5	4.46	0.73	55	0.65	D 11 D 1
-3	15	7.59	0.94	81	0.63	Bulk Polymerization
-4	19	10.2	1.12	103	0.64	Catalyst:
-5	24	13.1	1.35	137	0.63	Charged 0.146 mM/M
-6	28.5	15.6	1.53	168	0.66	Effective 0.063 mM/M
-7	35	17.5	1.66	189	0.65	}
C-1	2	2.06	0.32	15.6	0.71	1
-2	$\frac{2}{4}$	10.3	1.11	103	0.74	64.5% Benzene
-4	7	19.1	1.58	177	0.74	Cztalyst:
-4	9.5	25.3	2.01	252	0.77	Charged 0.244 mM/
-5	13.5	36.0	2.50	350	0.77	Effective 0.068 mM/M
-6	18	48.8	3.12	489	0.75]

Dilute solution viscosity, 0.1 g/100 ml in toluene at 25° C, Ostwald viscometer.
 Molecular weight from the viscosity-molecular weight curve for Hevea of Carter, Scott and Magat,
 Am. Chem. Soc. 68, 1480 (1940).
 Ratio of optical densities of the 11.26 and 11.95 peaks of the infrared spectrum.



presence of solvent had no effect on the linearity of the time-conversion relation, and it was valid at least to 50 per cent conversion. As a result of high viscosities, samples were not obtained above about 50 per cent conversion.

The relation between molecular weight and conversion was also studied in the polymerizations cited above. The inherent viscosity of each sample and of the final polymer was obtained for each polymerization. Molecular weights



were determined from the measured viscosities and the viscosity-molecular weight equation for Hevea. The data, also recorded in Table I, are plotted in Figure 3. It is evident that the molecular weight is directly proportional to the conversion, even to molecular weights of about 2,000,000. The polymer produced in these polymerizations has a rather narrow molecular weight distribution. In one polymer, separated into fractions by precipitation, the

molecular weights ranged from about 1,080,000 for the lowest four per cent to

1,260,000 for the highest two per cent.

Molecular weight increases with conversion for lithium polymerizations also, but the rate of increase falls continuously as the polymerization progresses. A charge of isoprene polymerized at 50° C with lithium metal was sampled periodically and the molecular weight of the samples was determined. The data, in Table II, show that half the final value of the molecular weight is attained at 12 per cent conversion.

We have run several experiments which bear on the termination of alkyllithium polymerizations of isoprene. In one such experiment isoprene was polymerized to high conversion in refluxing benzene solution with butyllithium catalyst. At this point the vapor temperature was that of boiling benzene, 78° C. Isoprene was added from a syringe, whereupon the vapor temperature dropped to 75°. It rose steadily and reached 78° again in a few minutes. Twenty successive additions were made during the course of an hour with the same result. During this time the solution had become increasingly viscous and finally it could scarcely be stirred. Neither of the two final increments of

Table II Effect of Conversion on Polymer Structure for Isoprene Polymerized with Lithium at 50° C

Sample no.	Time, min.	Conv.	3, 4-/1, 4-	DSV	M. wt×10 ⁻²
1	68	4	0.55		-
2	75	12	0.59	2.7	391
2 3	80	17	0.62	3.0	460
4	85	24	0.67	3.1	481
5	90	35	0.67	3.4	555
6	150	99	0.76	4.5	840
		I	Recipe		
	Isoprene Hexane Li dispersion Shortstop		200 g 800 g 0.8 cc (0.2 g I Methanol	Li/cc disper	rsion)

isoprene polymerized, and the vapor temperature fell to 72° and remained there. Substantially the same experiment was run in a bottle with a polyisoprene cement which had stood in an unopened bottle for a year before more monomer was added. Five additions of isoprene were made during the course of a week and all of the added monomer was converted to polymer. In this case, about ten times as much isoprene was converted to polymer as had been originally charged to the bottle. A third experiment was run in a five gallon reactor. Butyllithium was added to an eleven per cent solution of isoprene in pentane. After two hours at 50° C, conversion had reached 97 per cent. The charge was sampled and the polymer proved to have a dilute solution viscosity of 1.47. After standing 16 hours, half as much isoprene was added as originally charged. After five hours at 5° C, the conversion of total monomer had reached 95 per cent, i.e., 92 per cent of the added monomer had now polymerized. The viscosity of the polymer had increased to 1.94. These experiments support the conclusion that alkyllithium polymerizations are of the type which Prof. M. Swarc had called "living" polymerizations; termination occurs only with impurities or added shortstops. It is interesting in this regard that completely

soluble polymers are always obtained, even with polymers whose molecular

weight must be several millions (viscosities of 9 or 10).

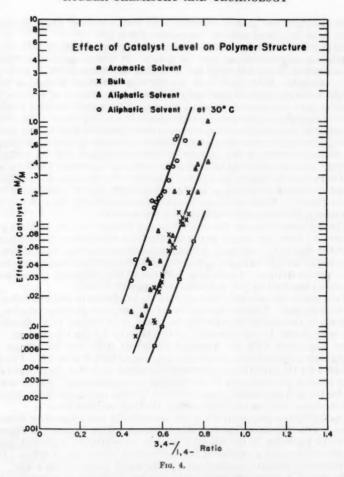
From these data a hypothesis concerning the mechanism of lithium and alkyllithium polymerizations may be drawn. It would appear that lithium polymerization proceeds through the formation of lithium alkyls, or more precisely, alkenyls. With preformed alkyllithium initiators it appears likely that all chains are initiated essentially simultaneously, there is no transfer, and all chains grow continuously at a uniform rate, at least until viscosity increases are great enough to make monomer diffusion a controlling factor. The "effective catalyst" concentration is a concentration calculated from these hypotheses: it is the molar concentration of polymer per mole of monomer charged. The difference between the amount of catalyst charged and the "effective catalyst" concentration (calculated) is attributed to impurities which have reacted with, and destroyed, part of the catalyst. For example, the amount of impurity, calculated as oxygen, would lie between 9 and 21 ppm for the three runs in Table I. While we do not have means of confirming the impurity level analytically, the calculated levels are not unreasonable.

The difference between the mechanisms of lithium and alkyllithium polymerizations, then, lies largely in the fact that new alkyllithium is continuously generated during the course of lithium polymerization; hence new chains are continuously initiated and the actual catalyst level increases during the course of the polymerization. Confirming evidence of this difference in mechanism

is found in the data on polymer structure reported below.

Variation in the polymer structure with the conditions of polymerization has also been studied. Infrared spectra have been obtained on many samples, and the ratio of the optical densities of the peaks at 11.26 and 11.95 claculated. This ratio should be an indication of the ratio of 3,4- to 1,4-polymer. For Hevea it is about 0.25, for Ameripol SN about 0.35, and for lithium and alkyllithium polyisoprenes, ratios have been found from 0.35 to 1.0. The data of Table I for the experiments previously discussed show that the infrared ratio is independent of conversion in alkyllithium polymerizations. This is not the case for the polymerization of isoprene with lithium metal, where the infra-red ratio increases with conversion as seen in the data of Table II.

In alkyllithium polymerizations, the amount of 3,4-structure does, however. decrease with decreasing catalyst concentration. This is shown in Figure 4, where the logarithm of the effective catalyst concentration is plotted against the infrared ratio for a number of polymerizations carried out at reflux. Polymerizations in aromatic solvents give points which fall nicely on a line. The points obtained from bulk polymerizations are scattered more widely about another line. Those obtained from polymerizations in aliphatic solvents are still more widely scattered. In this case, the scatter is largely the effect of polymerization temperature. Bulk polymerizations were, of course, run at 34°, the boiling point of isoprene. The polymerizations in aromatic solvents were all run, coincidentally, at 48° to 52° C. However, polymerization temperatures varied from 45° to 95° for the aliphatic polymerizations. Using the best line (not shown in Figure 4) which may be drawn through the points from polymerizations in aliphatic solvents, it is found that, in general, a point to the right of the line resulted from high polymerization temperature and a point to the left of the line from low temperature. Thus it appears that a reduction in polymerization temperature, as well as a reduction in catalyst, will decrease the amount of 3,4-addition. A number of polymerizations were run in bottles with heptane and butane solvent at 30° C and the effect of temperature was



confirmed. The higher temperature of the polymerizations in benzene may account for the higher infrared ratios found here than in bulk polymerizations run at the same catalyst level. If this difference in infrared ratios is not a specific effect of the solvent, it is nevertheless clear that aliphatic solvents reduce the amount of 3,4-structure in the polymer.

Moreover, it is interesting to note that the order of decreasing 3,4-structure in the polymer resulting from these systems (viz. aromatic solvent, bulk monomer, aliphatic solvent) parallels the order of decreasing dielectric constant. That is, the lowest 3,4 content is obtained from the system in which butyllithium is the least ionized. This is especially significant when compared to the effect of ethers, discussed below.

While higher polymerization temperatures, aromatic solvents, and high catalyst levels all produce small increases in the amount of 3,4-structure, strik-

ing increases are occasioned by the addition of small amounts of ethers to the The effect of aryl ethers is not noticeable much below 1 per cent of the Mixed alkyl aryl ethers show an effect at 0.5 per cent of the Alkyl and cyclic ethers like diethyl ether, dioxane and methylal produce noticeable effects below 0.1 per cent of the monomer. For example, where controls had infrared ratios of 0.65 to 0.70, charges with 0.1 per cent (on monomer) of diethyl ether or dioxane had infra-red ratios well over 1.0. Polyethers such as the diethyl ether of ethylene glycol are the post-potent. At a level of 0.01 per cent on the monomer such ethers give polymers with infra-red ratios well over 1.0 (Figure 1b) and at 0.1 per cent, the polymer produced is mostly of the 3,4-structure (Figure 1c). The minimum amount of these polyethers which will give a discernable increase in 3.4-structure is of the order of one tenth to one quarter of the molar amount of catalyst charged; hence roughly equivalent to the "effective catalyst". The effect of ethers is probably to coordinate with the alkyllithium and increase the extent of ionization.

The 3,4-content of the polymer appears to be controlled by the extent to which the alkyllithium bond is ionized or polarized. Small increases in 3,4content result from the slight increases in the polarization of the carbon-lithium bond brought about by high polymerization temperature, solvents of higher dielectric constant, or larger amounts of initiator. Large increases in 3,4content result from the addition of ethers which coordinate with the lithium ion so that it resembles, in effect, a sodium ion and hence gives polyisoprene typical of sodium polymerization.

CONCLUSION

The mechanism of alkyl lithium polymerization may be pictured as follows, where M refers to monomer:

Initiation: RLi + M
$$\longrightarrow$$
 RMLi
Propagation: RMLi + nM \longrightarrow R(M)_{n+1} Li

In the absence of impurities, there is no termination. The rate of initiation is very fast as compared with the propagation reaction. For lithium polymerization, the initiation step is the generation of lithium alkyls which is slow compared to propagation:

2 Li + M — Li M Li

New catalyst is continuously generated during the polymerization. Hence, the rate of increase in molecular weight drops as the conversion increases. Furthermore, the continuously increasing catalyst level causes an increase in the amount of 3.4-addition as the reaction proceeds.

REFERENCES

Mathews, F. E. and Strange, E. A., Brit. Patent 24,790 (1910).
 Midgley, T., "The Chemistry and Technology of Rubber". Davis and Blake, ed., Reinhold, New York, 1937, pp. 677-704.
 Ziegler, K. and coworkers, Ann. 511, 1-121 (1934); Ann. 542, 90-122 (1939).
 Stavely and coworkers, Ind. Eng. Chem. 48, 778 (1956).
 Gilman et al., J. Am. Chem. Soc. 55, 1252; also Perrine and Rapoport, Anal. Chem. 20, 635
 Gilman and Haubein, J. Am. Chem. Soc. 66, 1515.
 Gilman and Kirby, J. Am. Chem. Soc. 58, 2074 (1937).
 Hsieh and Tobolsky, J. Polymer Sci. 25, 245 ().
 Carter, Scott and Magat, J. Am. Chem. Soc. 68, 1480 (1940).

STUDIES ON THE STRUCTURE OF SKN-26 AND SKN-40 RUBBERS USING OZONOLYSIS METHODS *

A. I. YAKUBCHIK AND A. I. SPASSKOVA

LENINGRAD STATE UNIVERSITY, MOSCOW, USSR

Nitrile butadiene rubbers are produced through copolymerization of 1,3-butadiene and acrylonitrile. Our industry produces three sorts of butadiene rubber: SKN-18, SKN-26, and SKN-40. Vulcanizates produced from these

possess a high stability toward gas and oil.

We have investigated, using ozonolysis, the structure of commercial SKN-26 and SKN-40. The process was carried out in ethyl acetate and the ozonides were degraded using acetyl hydroperoxide. The breakdown products were separated chromatographically giving the following acids: formic, propionic, succinic, butane-1,2,4-tricarboxylic, propane-1,2,3-tricarboxylic, and hexane-1,2,4,6-tetracarboxylic. These acids may be formed, during ozonolysis, as follows: succinic from the -1,4-1,4- links, formic form -1,4-1,2-1,4-, and $-1,4-(1,2)_2-1,4-$, butane-1,2,4- tricarboxylic from -1,4-1,2-1,4- or from a fragment^{1,2} like (1). In ozonolysis studies on rubber, the external double bonds show up in the ozonolysis residues as formic acid and formaldehyde.

$$-CH_{2}-CH=CH-CH_{2}-CH_{2}-CH-CH_{2}-CH=CH-CH_{2}-(I)$$

$$C=N$$

Hexane-1,2,4,6-tetracarboxylic acid may arise from $-1,4-(1.2)_2-1,4$ or from chains (II) or (III):

$$-CH_{\underline{z}}-CH=CH_{\underline{z}}-CH_{\underline{z}}-CH_{\underline{z}}-CH-CH_{\underline{z}}-CH-CH_{\underline{z}}-CH=CH-CH_{\underline{z}}-(II)$$

$$-CH_{\sharp}-CH=CH-CH_{\sharp}-CH=CH-CH_{\sharp}-CH=CH-CH_{\sharp}-(III)$$

$$C=N \qquad CH=CH_{\sharp}$$

Propane-1,2,3-tricarboxylic acid may be formed from -1,4-1,4- branched with an alpha-methyl group, or may arise as an abnormal product³. ⁴ of ozonolysis of -1,4-1,2-1,4-. The presence of propionic acids indicates a profound degradation of the carbon chain of the rubber by the ozonolysis and subsequent oxidation of the ozonides.

The quantities of butane-1,2,4-tricarboxylic and hexane-1,2,4,6-tetracarboxylic acids found among the products, are higher than would be expected to result from -1,4-1,2-1,4- and $-1,4-(1,2)_2-1,4$ chains alone; consequently it is necessary to attribute part of these materials to the structures (I), (II), and (III).

^{*} Translated by J. R. Robinson from Zhurnal Obshchel Khim, 30 (7), 2172-2176 (1960),

Based upon the amounts of acids recovered from the ozonolysis products, we calculated the per cent of the carbon skeleton represented by these; the results are listed in Table I.

The identified acids represent 75.4 and 77.6% of the carbon chain of SKN-26 and SKN-40 respectively, a percentage somewhat higher than expected. Calculation of the carbon from those parts giving origin to the ozonolysis-produced acids is difficult because of the uncertainty of how much, say of butane-1,2,4-tricarboxylic acid, was formed from -1,4-1,2-1,4- chains, and how much came from (I). Thus we cannot account for around 10-15% of the ozonlized rubber. An unknown part is contained in the unidentified acid fractions making up peaks (I) (V) and (X) (Figures 2 and 3, chromatogram 1), and there is certainly some loss during the ozonolysis. It appears from this work that the macromolecules of the rubber are basically formed from parts in which the butadiene molecules are linked -1,4-1,4-,-1,4-1,2-1,4-,

TABLE I

	Wt. of ozonolysis product, g Represents		SKN-40			
				Wt. of ozonolysis products, g		Represents
Acids	Acid	Carbon in the acid	carbon skeleton, % Ac	Aeid	Carbon in acid	carbon skeleton, %
Propionic	0.47	0.23	3.9	0.81	0.39	3.1
Succinic	5.04	2.05	34.5	7.08	2.88	33.3
Butane-1,2,4- tricarboxylic	3.62	1.60	27.0	6.76	2.99	34.5
Propane-1,2,3- tricarboxylic	0.81	0.33	5.6	0.69	0.28	3.3
Hexane-1,2,4,6- tetracarboxylic	0.58	0.26	4.4	0.63	0.29	3.4
Total	10.54	4.47	75.4	15.97	6.83	77.6

 $-1.4-(1.2)_2-1.4-$ and other sections in which one or two residues of acrylonitrile are included among the -1.4- links of the butadiene (I) (II).

EXPERIMENTAL

For the investigation we used samples of commercial nitrile rubber, types SKN-26 and SKN-40. The SKN-26 was leached of antioxidants and low-molecular weight fractions by solution in benzene followed by two precipitations using a 1% benzene solution in alcohol. The SKN-40 samples were purified of antioxidants by extraction with a mixture of toluene and methyl alcohol. The purified rubber was desiccated at 3 m.m. to constant weight, then sealed in ampoules. The clean and dry rubber was handled in a dry atmosphere free of nitrogen oxides.

SKN-26: found, C, 83.37; H, 9.11; N, 7.64% and calculated from this, the acrylonitrile content was 28.8%.

SKN-40: found, C, 81.00; H, 8.70; N, 10.1%. Consequently the acrylonitrile content was 37.9%.

In order to confirm the action of ozone on the nitrile groups in the nitrile rubber, we prepared curves showing the absorption of ozone by the rubber.

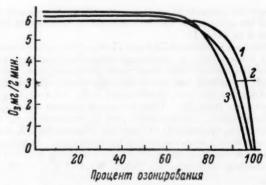


Fig. 1.—Ozone absorption curves. 1—Acrylonitrile, 2—SKN-26, 3—SKN-40. Ord.: O₄, mg/2 minutes; abs.: % ozonization.

The process was performed in chloroform at -20° . The concentration of ozone in the oxygen was 5–6%, and the gas was passed into the rubber solution at a constant velocity of 7 liters per hour. The quantity of ozone taken up was estimated using the absorption curves (Figure 1) which were plotted simultaneously⁵. There was no break in the curves, the absorption of ozone proceeding at a steady rate, corresponding to the theoretical rate based upon the number of double bonds (-C=C-). Ozone was taken up only at the double bonds—the nitrile groups were not affected. In confirmation of this we plotted the ozone uptake by acrylonitrile (b.p. 78–79°). This curve was essentially the same as the ozone-uptake curves for the two types of rubber. From these

TABLE II

			O ₃ absorp-			
		Calcu	lated	Absor	rbed	of that
Material	Batch wt, g.	By double bonds	By nitrile groups	By double bonds	By nitrile groups	for double bonds
SKN-26	0.55	0.355	0.136	0.347		97.8
SKN-40	0.55	0.312	0.162	0.309	-	97.1
Acrylonitrile	0.54	0.490	0.490	0.499	siminar	100.2

curves, and the data of Table II it is evident that the ozone uptake is only at the $-\mathbf{C} = \mathbf{C}$ — positions.

In studying the chemical degradation, the ozonolysis was run in ethylacetate at -20°. The ozone content, in oxygen, was 5-6%; 7.16 g of SKN-26 and 10.7 g of SKN-40 were used. The ozonide products were soluble in the ethylacetate. The solvent was distilled away at 20° (14 mm), the ozonide residue taken up in glacial acetic acid and treated with acetyl hydroperoxide⁴. The acetic acid was then removed from the decomposition products at 20° (5 mm), leaving a mixture of viscous and crystalline substances. The analytical data

Product from	C	Found, %	N
SKN-26	41.00	7.14	4.76, 4.82
SKN-40	42.50, 42.70	6.73, 6.81	3.45, 3.53

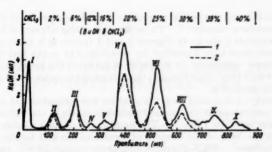


Fig. 2.—Chromatographic separation of the mixture of acid products from the osonolysis of SKN-26 rule (1); a known mixture of acids (2). Peaks: II—propionic, III—acetic, IV—formic, VI—succinic, VIII—butane-1,2,4-fictareboxylic, VIII—propane-1,2,3-fi-ricareboxylic, IX—heart-1,2,4-fi-terracerboxylic acids. The nature of the acids responsible for Peaks f, V and X was not established. Ord.: NaOH (ml.); abs.: Developer (ml.).

The nitrogen analyses are in accordance with the nitrogen content of the ozonized rubber; the SKN-26 sample contains 0.55 g of nitrogen, corresponding to 2.08 g of acrylonitrile, while the ozonolysis product contained 0.51 g of nitrogen, equivalent to 1.93 g of acrylonitrile. The corresponding figures for the SKN-40 were 1.07 g of nitrogen (= 1.93 g of acrylonitrile) in the rubber sample, and 0.95 g of nitrogen (= 1.29 g of acrylonitrile) in the ozonolysis products. This certainly indicates that the —C \equiv N groups are not oxidized either by the ozonolysis process or by the acetylhydroperoxide.

The mixture of acids produced by the ozonolysis and subsequent hydroperoxide treatment was saponified with sodium hydroxide and the acids extracted with ether. 14.73 g of acid was obtained from the SKN-26, 19.85 g from the SKN-40 sample. The acids were separated chromatographically on "MSK" silicagel (a grade having coarse porosity) as described earlier. By gradually introducing solvents of varying polarity for each acid, we developed the solvent system shown (Figures 2 and 3) which adequately separated the acids with satisfactory resolution. In order to help identify the unknown acids, a mixture of known acids was made up and chromatographed under the same conditions. This mixture contained formic, acetic, propionic, succinic, butane-1,2.4-tricarboxylic, and propane-1,2-3-tricarboxylic acids, all of which

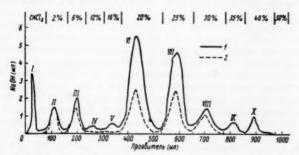


Fig. 3.—Chromatographic separation of the mixture of acid products from the ozonolysis of SKN-40 rubber (1); a known mixture of acids (2). Peaks: II—propionic, III—acetic, IV—formic, VI—succinic, VIII—butane-1,2.4-tricarboxylic, VIII—propane-1,2.3-tricarboxylic iX—hexarboxylic acids. The nature of the acids responsible for Peaks I, V and X was not established. Ord.: NaOH Wml.); abs.: Developer (ml.).

had earlier been found among the ozonolytic degradation products of butadiene and nitrile butadiene rubbers1.2. The separation of this mixutre of known acids into its components is shown in Figures 2 and 3 (curve 2, in each case). The unknown acids were then identified by matching the peaks and the solvent fronts (developer volumes). It is seen that many of the peaks coincide, and the order in which they come through the column is the same in the known and unknown acid mixtures.

The quantity of each acid from the mixture was estimated and expressed in terms of its percentage of the original carbon skeleton of the rubber samples. These data are listed in Table I. The number of terminal double bonds was calculated on the basis of the amount of formaldehyde and formic acid found among the products7. SKN-26 rubber appears to contain 10.8%, and SKN-40, 11.8%, of -1.2 - links.

SUMMARY

It has been established that the macromolecules of SKN-26 and SKN-40 rubbers are constructed from units linked:

REFERENCES

- Yakubchik, A. I., "Academecian S. V. Lebedev," Izd. Akad. Nauk SSSR, 1954.
 Alekseeva, E. N., Zhur. Obahchei Khim. 9, 1426 (1939); 22, 1813 (1952).
 Marvel, C. S. and Schilling. J. Ory. Chem. 16, 838, 854 (1951).
 Yakubchik, A. I., Spasskova, A. I. and Tikhomirov, B. I., Zhur. Obahchei Khim. 28, 918 (1958).
 Yakubchik, A. I. and Kastatkina, N. G., Zhur. Obahchei Khim. 25, 1473 (1955); ibid. 27, 1487 (1957).
 Yakubchik, A. I. and Zykova, S. K., Zhur. Priklad. Khim. 29, 1991 (1956).
 Yakubchik, A. I., Vasil'ev, A. A. and Zhabina, V. M., Zhur. Priklad. Khim. 17, 107 (1944).

OZONATION OF BUTYL RUBBER TO ESTIMATE UNSATURATION *

I. S. UNGAR AND G. A. LUTZ

BATTELLE MEMORIAL INSTITUTE, COLUMBUS, OHIO

INTRODUCTION

In the production of butyl rubber, a rapid reproducible means of measuring the unsaturation in the raw isoprene-isobutylene copolymer, at least on a relative basis, is highly desirable, inasmuch as the curing rate of the polymer and, to some extent, the physical and chemical properties of the finished product are a function of the degree of unsaturation¹⁴.

Many methods have been employed for the determination of unsaturation in isoprene-isobutylene copolymers. These methods include the evaluation of such reagents as nitrosobenzene³, thiocyanogen⁶, iodine monochloride in carbon tetrachloride², iodine monochloride in acetic acid⁴. ⁷⁻⁹, ¹², ¹³, iodine in the presence of mercuric acetate and trichloroacetic acid⁵, and bromine¹¹.

Since ozone has been classified as a "double bond" reagent and recent studies confirm that it reacts rapidly and quantitatively with mono- and polyolefinic unsaturation. It is reagent was investigated for the estimation of the unsaturation in isoprene-isobutylene copolymers, and a method based on its use was developed under standardized conditions.

EQUIPMENT AND MATERIALS

Ozone was produced by passing oxygen or dry air through a Welsbach ozonator. This machine produces a constant concentration of ozone at a given flow rate, pressure, voltage, and cooling-water temperature.

The reactor system consisted of a standard Ace Glass Mini-Lab batch reactor, capacity 100 ml, equipped with a gas inlet through the stirrer, an outlet through a condenser, and a thermometer. Two cold traps were placed between the reactor and the ozone meter.

The ozone concentration was measured by ultraviolet absorption spectrophotometry employing a Welsbach Model C ozone meter. The concentration was read directly on a microammeter in milligrams of ozone per liter of gas. Direct readings were employed in some of the early work. Area measurements (see below) were adopted later as a further refinement of the direct readings.

A recording millivoltmeter was used to record the ozone meter readings. It had a roll speed of 1 inch per minute and a full-scale response of less than 1 second. Area measurement from the chart was measured planimetrically. In this manner, conversion of area to ozone uptake to mole per cent of unsaturation could be readily calculated.

The dry air utilized was obtained from the Matheson Company and had a dew point of less than -80° F. The oxygen (ordinary breathing type) used to obtain a higher output of ozone was obtained from the Linde Company.

^{*} An original conbribution15.

Samples of butyl cements and commercial hexane solvent were furnished by Esso Research and Engineering Company. The commercial hexane solvent had the following composition:

Hydrocarbon component	Per cent by weight
n-Hexane	55
Methylcyclohexane	20
Cyclohexane	3
Methyl pentanes	14
Benzene	8

EXPERIMENTAL

General procedure.—After several preliminary experiments, conditions listed in Table I were chosen as standard for ozonation studies.

Ozonation of solvents.—Carbon tetrachloride and commercial hexane were suitable solvents for the isoprene-isobutylene copolymer. Table II contains

TABLE I EXPERIMENTAL CONDITIONS FOR OZONATION

	Gas employed	
	Dry air	Oxygen
Gas flow.		
cfm	0.04	0.04
1/min	1.13	1.13
Gas pressure, lb/in.2	8	8
Voltagea, volts	105 to 110	90 to 95
Ozone output, mg/l	32	58
Collant temperature, ° C	5 to 10	5 to 10
Reactor temperature, ° C	-3 to -5	-3 to -5
Volume of solution, ml	80	80
Stirring	Vigorous	Vigorous

a As the cooling water temperature changed, the voltage was adjusted to maintain the ozone output constant.

values for the solvent blanks that must be subtracted from copolymer runs if standard conditions (Table I) are used.

Ozonation of octene-1.—Two samples of octene-1 (Phillips, 99 mole per cent) in 80 ml of carbon tetrachloride were ozonated in order to check the accuracy of the method. The results are shown in Table III.

Table II
Ozonation of Solvents Using Dry-Air Feed

Solvent	Area above ozone- output curve, in.2
Carbon tetrachloride	1.05
Commercial hexane	2.74
Refined hexane	0.63

TABLE III
OZONATION OF OCTENE-1 USING DRY-AIR FEED

Sample	Actual ocente-1 present, mg	Octene-1 found by ozonation, mg
1	277	272
2	263	259

TABLE IV

OZONATION OF BUTYL RUBBER SOLUTIONS USING DRY-AIR FEED

Sample	Solvent	Ozone uptake, mg/g of sample	Unsaturation mole per cent
A	Commercial hexane	9.05	1.06
В	Commerical hexane	13.70	1.60
C	Commerical hexane	18.60	2.18
A	Refined hexane	2.95	0.35
В	Refined hexane	5.97	0.70
C	Refined hexane	10.20	1.17
A	Carbon tetrachloride	10.10	1.15
В	Carbon tetrachloride	16.60	1.92
C	Carbon tetrachloride	21.30	2.50

4 Average of 2 runs.

Ozonation of butyl rubber.—Five per cent (by weight) solutions of butyl rubber were prepared in commercial hexane, refined hexane, and carbon tetrachloride. Table IV contains the ozonation results for each sample in the three solvents.

Ozonation of butyl cements.—The cement samples were diluted with the appropriate solvent to 5 per cent (by weight) cement. Ozonation results are shown in Table V.

TABLE V

OZONATION OF BUTYL CEMENTS USING DRY-AIR FEED

Sample	Solvent	Ozone uptake, mg/g of sample	Unsaturation mole per cent
D	Commercial hexane	8.02	0.94
E	Commercial hexane	16.32	1.95
F	Commercial hexane	21.00	2.46
D	Refined hexane	4.68	0.55
E	Refined hexane	9.85	1.15
\mathbf{F}	Refined hexane	14.85	1.75

* Average of 2 runs.

Sample calculation of unsaturation of butyl rubber or cement.—The unsaturation in mole per cent is defined by the following equation:

Unsaturation mole per cent =
$$\frac{(A - B)(C)}{D}$$

where

A = average area above curve for solvent plus rubber or cement, in.2

B =average area for solvent, in.² C =milligrams O_3 per in.² of area

 $D = \text{milligrams } O_3 \text{ required for 1.00 mole per cent unsaturation.}$

(Areas A and B are indicated in Figures 1 and 2.)

Therefore, for 80 g of a 5 per cent solution:

Unsaturation mole per cent =
$$\frac{(2.04 - 0.99)(25.7)}{34.2}$$

= $(0.789 \text{ or } 0.8)$

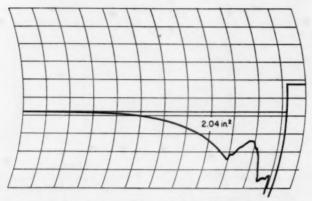


Fig. 1.—Butyl cement diluted with carbon tetrachloride.

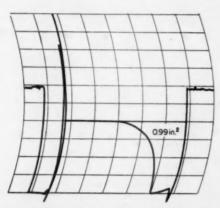


Fig. 2.—Solvent mixture—treated hexane diluted with carbon tetrachloride.

Ozonation time using air and oxygen feeds.—Samples of butyl cements D, E, and F were dissolved in refined hexane and ozonated with an oxygen feed to the ozonator. The voltage was adjusted to maintain the ozone concentration at 58 mg/l. Other conditions were kept constant. Table VI contains comparative data on ozonations employing air under standard conditions and oxygen as described above as feed gases.

 ${\bf TABLE~VI}$ Comparison of Ozonation Time Using Air and Oxygen Feeds

Sample	Area above curve, in.2		Time to reach constant absorption, min	
	Oxygen	Air	Oxygen	Air
D	4.09	3.72	5.75	8.25
E	4.88	4.81	6.75	10.50
F	5.72	5.34	7.50	12.50

TABLE VII
OZONATION OF BUTYL CEMENTS USING OXYGEN FEED

Sample	D	E	F
Solvent mixture	Refined hexane and carbon tetrachloride	Refined hexane and carbon tetrachloride	Refined hexane and carbon tetrachloride
Approximate time, min	5.0-6.0	5.5-6.5	6.0-7.0
Ozone uptake, mg/g of			10.00
sample	6.82	14.77	19.57
Unsaturations, mole per			
cent	0.80	1.73	2,29
Coefficient of variation			
(2 sigma), per cent	6.97	2.58	4.39

[·] Average of 12 determinations.

Ozonation of butyl cements using oxygen feed.—Samples (5 per cent by weight) of butyl cements D, E, and F dissolved in a mixture of refined hexane and carbon tetrachloride were ozonated using oxygen feed. The results are shown in Tables VII and VIII. Twelve determinations were carried out for each sample (Table VIII) in order to obtain a statistical interpretation of the reproducibility of the method.

TABLE VIII

AREA ABOVE CURVE FOR BUTYL CEMENT SAMPLES

		Area above curve, in.2			
Run	D	E	F		
1	2.14	3.32	4.02		
2	2.15	3.36	4.12		
2 3	1.95	3.31	3.97		
4	2.04	3.38	4.07		
5	1.95	3.30	3.97		
6	2.08	3.29	3.90		
7	2.09	3.32	4.11		
8	2.08	3.29	3.92		
8	2.07	3.24	4.16		
10	2.01	3.25	4.08		
11	2.07	3.30	4.12		
12	1.94	3.25	4.15		

DISCUSSION OF RESULTS

Both the commercial and the refined hexane solvents (Table II) contain some ozonizable material. Passing ozonated air through the solvent for as long as 30 minutes under the experimental conditions shown in Table I resulted in no further increase in rate of ozone absorption beyond the initial step. In the case of carbon tetrachloride, which contains little ozonizable material, the rate of ozone uptake rapidly drops to zero. In all cases it is necessary to subtract the solvent blank value from the value of the butyl solutions runs in order to get a reasonable unsaturation value.

The data in Table III show that the ozonation of olefins gives a quantitative measurement of unsaturation under conditions employed in this work. It is believed that the accuracy of the ozonation could have been improved by taking a larger sample of octene-1. Since a low order of unsaturation was being dealt with in the butyl solutions, ozonation of small samples of octene-1 was chosen.

The absolute values of unsaturation of the butyl rubber varied with the

nature of the solvent; the order of apparent unsaturation (Table IV) was refined hexane, commercial hexane, and carbon tetrachloride.

Tables V, VI, and VII show the results of the ozonation of butvl cements dissolved in hexane and mixtures of hexane and carbon tetrachloride. Again, the lowest unsaturation values were obtained using refined hexane. Hexane solutions of cements diluted with carbon tetrachloride (Table VII) gave, as expected, unsaturation values between those obtained using refined hexane and commercial hexane.

Table VI points out that time can be saved by using an oxygen feed instead Under standard conditions, the time required to reach constant absorption with ozonated air (32 mg of ozone per liter) varied from 3 to 13 min-When using ozonated oxygen (58 mg of ozone per liter), the maximum time for reaction decreased to about 7 minutes.

Tables VII and VIII illustrate the precision in unsaturation values that can be achieved by ozonation of butyl cements. Twelve samples each of the butyl cements D. E. and F are diluted with carbon tetrachloride to 5 per cent solutions and treated with ozonated oxygen. The coefficient of variation (2 sigma) varied from 2.58 to 6.98 per cent; that is, the results are reproducible to within 7 per cent. The coefficient of variation (2 sigma) for the results obtained by four laboratories with iodine monochloride varied from 5.65 to 44.1 per cent; with iodine-mercuric acetate it varied from 5.5 to 30.6 per cent. Thus the ozonation method gives a much closer precision of unsaturation values.

CONCLUSIONS

A method has been developed for the estimation of the unsaturation of butyl rubber by ozonation in selected solvents.

Under a given set of conditions the ozonation method is reproducible to within 7 per cent and conceivably could be improved by further refinement.

The unsaturation of a butyl rubber can be estimated in about 10 minutes when using ozonated oxygen and in about 15 minutes when using ozonated air.

ACKNOWLEDGMENT

The authors are indebted to Esso Research and Engineering Company, Linden, New Jersey, who sponsored this work, for permission to publish the results.

REFERENCES

- Badger, G. M., Quart. Revs. (London) 5, 147 (1951).
 Boeseken, J., and Geiber, E. T., Rec. trav. chim. 46, 158 (1927); 48, 377 (1929).
 Bruni, G., and Geiger, E., Atti accad. nas. Lincei (6) 5, 823 (1927); Rubber Chem. Technol. 1, 177 (1928).
 Cheyney, L. E., and Kelley, E. J., Ind. Eng. Chem. 34, 1323 (1942); Rubber Chem. & Technol. 16, 280

- **Stull, S. C. (1928).

 **Cheyney, I. E., and Kelley, E. J., Ind. Eng. Chem. 34, 1323 (1942); Kubber Chem. 40, 1277 (1948).

 **Gallo, S. G., Wiese, H. K., and Nelson, J. F., Ind. Eng. Chem. 40, 1277 (1948).

 **Kaufmann, H. P., and Gaertner, P., Ber. 57, 928 (1924).

 **Kemp, A. R., Ind. Eng. Chem. 19, 531 (1927).

 **Kemp, A. R., and Mueller, G. S., Ind. Eng. Chem. Anal. Ed., 6, 52 (1934).

 **Kemp, A. R., and Peters, H., Ind. Eng. Chem., Anal. Ed., 15, 453 (1943); Rubber Chem. & Technol.

 **Maggiolo, A., Chem. Eng. News 36 (42), 41 (October 20, 1958).

 **Marek, K., Chem. Listy 40 (2), 23-8 (1946).

 **Ogg. R. A., J. Am. Chem. Soc. 57, 2727 (1935).

 **Rehner, J., Ind. Eng. Chem. 36, 118 (1944); Rubber Chem. & Technol. 17, 679 (1944).

 **Rehner, J., Ind. Eng. Chem. 36, 118 (1944); Rubber Chemistry, 110th Meeting, Am. Chem. Soc., Chicago (1946).

 **Presented at Division of Polymer Chemistry, 136th Meeting, ACS, Atlantic City, New Jersey, September, 1959.

STRUCTURE OF THE SPONGY POLYMER OF ISOPRENE*

A. I. SPASSKOVA AND D. I. RABINOVITCH

Isoprene, on storage, is converted to a spongy polymer white in color, lacking in rubber-like properties, insoluble in organic solvents and limited in its swelling properties. S. V. Lebedev has published on the spontaneous polymerization of isoprene. The chemical structure of autopolymerized isoprene has been investigated by Harries. Among the ozonolysis products were levulinic aldehyde and levulinic acid which accounted for 37% of the carbon skeleton of the polymer. In the residue from the distillation of the levulinic compounds Harries proved the presence of peroxide materials whose true chemical nature was not established. The residue was a tarry material.

The purpose of the present work was to establish the chemical structure of the spongy polymer of isoprene produced by polymerization of isoprene in a sealed ampoule under a nitrogen atmosphere at 15-18°. Under such conditions, two high molecular weight polymers are formed of which one is rubberlike and soluble in benzene, chloroform and other organic solvents, while the other one is a crumbly polymer, insoluble in organic solvents, and constituting up to 90-95% of the total mass; the latter is referred to as "spongy" polymer.

The structure of this spongy isoprene polymer has been investigated using the technique of ozonolysis. Degradation of the ozonides was accomplished through catalytic reduction using barium sulfate-palladium in dioxane at atmospheric pressure. Among the products were levulinic aldehyde and levulinic acid, equivalent to 63.7% of the carbon skeleton of the polymer. They are formed from those sections in the macromolecular spongy polymer in which the isoprene molecules are linked -1.4-1.4. However the ozonolysis products include succinic, acetic and formic acids. These latter materials may be formed, during ozonolysis, from sections of the polymer containing -1,2- and -3,4- links. [Catalytic reduction of ozonides is always accompanied by side reactions producing acids. This same process occurs, though slowly, with ozonides on long standing.] The mechanism of the formation of succinate and acetate is unknown; succinic acid may be formed from sections linked -1,4-4,1-, while acetic acid perhaps arises as an abnormal product of ozonolysis. On the other hand, both acids may be formed through secondary reactions from -1,4-1,4-chains. Acetonylacetone has not been found among the reduction products of the ozonides; from this it may be assumed that -4,1-1,4-combinations are completely absent from this macromolecular porous polymer of isoprene. The results of our investigations are shown in Table I.

As pointed out above, 63.7% of the carbon chain of the spongy polymer has been determined as consisting of -1,4-1,4- links; 14.5% shows up as acetic and succinic acids, but to calculate the contribution of the actual parts of the macromolecule from which these acids originate is impossible.

^{*} Translated by J. R. Robinson from Zhur. Obshchel Khim. 30 (7), 2176-2180 (1960).

TABLE I

Ozonolysis product	Wt., g	Polymeric structure from which the product was formed	% of carbon skeleton represented
Levulinic aldehyde	2.97	-1,4-1,4-	40.9
Levulinic acid	1.92	-1,4-1,4-	22.8
Acetic acid	0.96	abnormal product of ozonolysis or a secondary product from a -1,4-1,4- chain.	8.9
Succinic acid	0.60	either from -1,4-4,1 or from -1,4-1,4- as a secondary product	5.5
Formic acid	0.02	-1,2- or -3,4- links	0.1
Residue	1.02		14.0
Total	7.49		92.2

EXPERIMENTAL

Self-initiated isoprene polymerization was carried out, under nitrogen, in sealed ampoules, in the light, at 15–18°. The monomer used had a boiling point of $34.2-34.5^{\circ}$, $n_{\rm p}^{\approx}$ 1.4152. From 38 g of the polymer there was extracted 4.2 g (11%) of a rubberlike material by chloroform. The residual spongy polymer, a crumbly white substance with no elastic properties, was insoluble in organic solvents. Found: C, 87.06, 87.24%; H, 11.77, 11.69%. Calc'd for $(C_5H_8)_x$ C, 88.24; H, 11.76%.

Ozonolysis of this porous polymer was carried out in chloroform at -30° by ozonated oxygen containing 5–6% ozone using an unsealed, constant concentration of ozone⁶. In each run 2 g of polymer was utilized. Ozone was taken up at constant velocity and 1.45 g-mole. was absorbed corresponding to 103% of that calculated for the double bonds present. The quantity of ozone absorbed was allowed for in plotting the absorption curves which were measured during the course of the ozonolysis. Our aim was to produce a transparent, colorless chloroform solution of ozonides. After removal of the solvent, the residue was a colorless, viscous material, which we then subjected to catalytic (Pd/BaSO₄) hydrogenation, under nitrogen, at atmospheric pressure, in dioxane.

Five grams of the spongy polymer of isoprene, produced 8.61 g of ozonide; this was dissolved in dioxane (b.p. 101°; np 1.4215, dp 1.0336, free of peroxides). Catalytic reduction was then accomplished in a Lebedev apparatus, each gram of the ozonized polymer was allowed 1.5 g of the Pd/BaSO₄ catalyst⁸. Fischer has indicated that the reduction of ozonides by this method leads to the formation of carboxylic compounds. At 5° (760 mm) 906 ml of hydrogen [= 889 ml at 0° and 760 mm) was absorbed, which amounts to 54% of the theoretical. This may be due to a significant amount of decomposition of ozonide during the ozonization process itself and during the subsequent distillation to remove the solvent. A solution of the reduced material showed a negative reaction to tests for peroxides and ozonides. The dioxane was distilled away at 25°/10 mm; it had an acid reaction to litmus (and 1 ml of dioxane required 0.8 ml of 0.1 N KOH for neutralization). Separation of the acids in the distilled dioxane was accomplished chromatographically using silicagel type MSK (a fine silicagel of coarse porosity) using techniques reported earlier9. Figure 1 shows the chromatographic separation of these acids which co-distilled with dioxane from the reduced ozonides of the isoprene polymer. For aid in identification, a

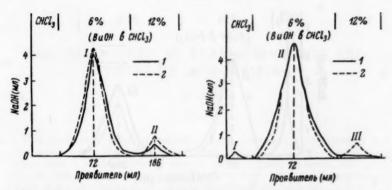


Fig. 1.—Chromatographic separation of the acid mixture which distilled with the dioxane from the products of the catalytic reduction of the osonides of spongy polyisoprene (1); the known mixture of scettic and formic acids (2). I—acetic, III—formic. Ord.: NaOH (ml); abs.: developer (ml).

Fig. 2.—Chromatographic separation of the mixture of acids from the first fraction (1); a mixture of acetic and formic acids (2). II—acetic, III—formic. Ord.: NaOH (ml): abs. developer (ml).

mixture of acetic and formic acids was chromatographed (Figure 1, curve 2). The acids were identified by the position of the peaks¹⁰ (Table II). Through superimposing the chromatograms of the known and unknown acids, it is seen that the peaks coincide, and the order in which they come off the column is retained. Estimating from the chromatograms, the quantities recovered were acetic aicd 0.32 g and formic acid 0.02 g.

The products of the catalytically reduced oxonides from 18 g of polymerized spongy isoprene were also put through the column. The fractions obtained: (1) b.p. 30-35°/10 mm, 11.47 g; (2) b.p. 62-63°/10 mm, 2.97 g.; residue, 3.54 g. The first fraction was acid to litmus and smelled sharply of acetic acid (1 ml required 14.5 ml of 0.1 N KOH for neutralization); there was also present some dioxane. The fraction was chromatographed and Figure 2 shows that the mixture (fraction 1) contained mainly acetic acid, and the quantity was calculated to be about 0.64 g. The second fraction was mainly levulinic aldehyde, b.p. 62-63°/10 mm; np. 5 1.4254. This was characterized through its paranitrophenylhydrazone, m.p. 104-104.5°. (Reported¹¹: b.p. 70°/12 mm; np. 5 1.4256; p-nitrophenylhydrazone, m.p. ~106°.)

Levulinic and succinic acids were found in the residues left after distilling the products of the catalytic reduction of the ozonides of the isoprene polymer. Figure 3 illustrates the chromatographic separation of these acids. The acids were identified by comparison with peaks produced by a known mixture of these acids (Table III), and the quantities were estimated at 1.92 g of levulinic and 0.6 g of succinic.

The levulinic acid was confirmed by chemical analysis on the material from the chromatographic peak. Chloroform and butyl alcohol were recovered from the residues.

TABLE II

	Volume-peaks	
Separated mixture	Acetic	Formie
Acids separated from dioxane	72	186
Known mixture of acids	72	186

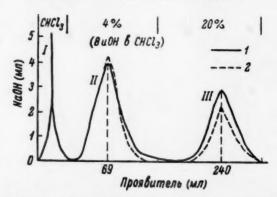


Fig. 3.—Chromatographic separation of the residue left after distilling the products of the catalytic reduction of the osonides from the spongy polymer of isoprene (1); a mixture of levulinic and succinic acids (2). (II)—levulinic, IIII—succinic, Ord.: NaOH (ml); abs.: developer (ml).

Found: Silver, 48.31, 47.98%. Calc'd. $C_5H_7O_3Ag$, Silver = 48.19%. 2,4-dinitrophenylhydrazone of levulinic acid was prepared, m.p. 205-205.5° 12.

The final residue was a tarry substance, wt. 1.02 g (% C, 61.00, 61.30; % H, 8.32, 8.19), representing approximately 14% of the carbon chain of the polymer.

TABLE III

	Volume-peaks	
Separated mixture	Levulinie	Succinic
Acids in the residue	69	240
Known mixture of acids	69	240

On the basis of the quantities of levulinic, succinic, acetic and formic acids and levulinic aldehyde recovered from the products of the catalytic degradation of the ozonides of the isoprene spongy polymer, these comprise about 78.2%of the carbon chain of the polymer (Table I).

SUMMARY

1. The spongy polymer of isoprene was subjected to ozonolysis and 63.7% of the carbon chain was shown to be linked -1,4-1,4-.

2. Acetic and succinic acids were observed as secondary breakdown products of these -1,4-1,4- chains and they amounted to about 14.5% of the carbon skeleton of the spongy polyisoprene.

REFERENCES

- Tilden, Chem. News 5, 265 (1892).
 Mokievakil, V. A., Zhur. Russ. Fiz.-Khim. Obshchestva 30, 895 (1898).
 Lebedev, S. V., ibid. 42, 949 (1910).
 Lebedev, S. V., ibid. 42, 949 (1910).
 Harries, C. D., "Untersuchungen über die natürlichen ünd Künstlichen Kautschukarten", 1919, p. 191.
 Fizcher, G., Düll, H. and Ertel, L., Ber. 65, 1467 (1932).
 Yakubchik, A. I. and Kasatkina, N. G., Zhur. Obshchel Khim. 25, 1473 (1955).
 Lebedev, S. V., Zhim' i Trudy 381 (1938).
 Lebedev, S. V., Zhim' i Trudy 381 (1938).
 Yakubchik, A. I. and Spasskova, A. I., Zhur. Obshchel Khim. 28, 149 (1958).
 Fuchs, I. A. Uspekhi Khim. 17, 45 (1948).
 Harries, C. D., Ber. 31, 43 (1898); 42, 440, 442 (1909).
 Johnson, V. S. et al., "Organic Reactions for Organic Analysis", 1948.

MECHANOCHEMICAL TRANSFORMATION AND SYNTHESIS OF POLYMERS *

A. A. BERLIN

Moscow

The mechanical grinding, milling, mixing, homogenization, freezing and other processes of the physico-mechanical processing of high polymers are widely used in the industries of plastics, rubbers, synthetic fibers, food products, silicates and many other branches of technology. Some of these processes have a great significance in biochemistry, medicine and biology.

An analysis of the available experimental data permits one to reach the conclusion that in the intensive grinding of natural polymers (cellulose1, 2, 3, starch4.5, proteins6 or synthetics (polystyrene7.8, rubber 9-11, polyisobutylene12, etc.) a mechanical scission (cracking) of the macromolecules is observed.

The possibility of macromolecular scission under the grinding of high molecular weight substances is due to the high probability of a localization of mechanical energy at different sections of the polymer chain, which under certain conditions causes internal stresses exceeding the strength of covalent or ionic bonds.

Mechanical breakdown of macromolecules is possible not only with dry or wet grinding, but also by mechanical action on polymer solutions. Thus, for instance, Staudinger has shown that the high speeds and forces of friction developed in forcing a 0.005 molar tetralin solution of polystyrene, average molecular weight = $\bar{M}_{\rm ave}$ = 6.10°, through a platinum capillary bring about a scission of the macromolecules which is revealed13 in a decrease of about 30% in the specific viscosity of the solution.

Forcing a solution of polyisobutylene ($M_{\rm ave} = 3.9 \times 10^4 - 23 \times 10^4$) in dichlorobenzene through a capillary with a diameter of 0.2 mm causes a decrease in the intrinsic viscosity and an increase in the constant of the Huggins equation. An increase in the Mave of the polymer structure formation (crosslinking) and a repeated forcing through is conducive to the mechanical break-

down of the macromolecules14.

It has been established that in mixing together solutions of polymeric substances (starch, gelatine, polyvinyl alcohol, etc.) with high-speed mixers having a rotation speed of over 4000 rpm, a sharp decrease in the intrinsic viscosity [n] is observed, while the degree of scission increases, with an increase in the rotation speed of the mixer, and also with a decrease in the concentration of the solution15. 17

The intensive scission of the macromolecules is brought about by the sound vibration of solutions with ultrasonic vibrations having a frequency of more than 50 kilohertz (kilocycles/sec), with an intensity of 6-10 watts/cm2. cavitation developed by the sound vibration of solutions, the considerable gradients of velocity and the forces of friction reduce the molecular weight of polystyrene, rubber, polyvinyl acetate and nitrocellulose, polymethacrylic acid, proteins and a number of other polymers by a factor of 16-20.

^{*} Translated from Uspekhi Khim, 27, 1, 94-106 (1958).

Nikitin and Klenkova²¹, as well as Berlin and Penskaya^{22, 23}, have shown recently that in freezing and thawing (defrosting) polymers in an aqueous medium, stresses are developed which are due to the mechanical scission of the macromolecules. Thus in the freezing (cryolysis) of high polymers in an aqueous medium, the mobility of the chain links and macromolecules is reduced, the degree of hydration is decreased, and the intermolecular interactions of the polymer chains become intensified. Along with this, the conversion of water into ice involves an increase in the specific volume and a development of mechanical stresses which exceed the strength of the covalent bond.

In the process of thawing (defrosting) of polymers swelled in water, the water penetrates mainly into the places where the polymer chains are more loosely packed, which also creates internal stresses, causing a breakdown of the

high polymer to some degree.

As a result of the freezing of aqueous starch solutions, or of starch swelled in water, at temperatures from -10° to -70° C, a marked increase is noted in the amount of highly soluble fractions, containing low molecular weight sugars and dextrins, together with the formation of fibrous products which are slightly soluble in water, characterized by a high degree of asymmetry and higher copper and iodine number values than those of the original starch^{22, 23}.

These studies have also established that the breakdown of the macromolecules may be brought about by a change in the internal pressure in the freezing

of solutions of polymers in organic solvents15.

The rate and degree of mechanical breakdown depend on the chemical nature and physical state of the polymer, the medium and the conditions of breakdown. An increase in the degree of asymmetry and an increase in the stiffness and the density of packing of the macromolecules facilitate mechanical scission. A rise in temperature and an increase in the flexibility and mobility of the chains makes the breakdown more difficult in the milling and plasticization of polymers¹¹.

The rate of mechanical scission of the macromolecules in a dilute solution

may be determined from the equation:

$$\frac{dx}{dt} = k(P_t - P_m) \tag{1}$$

where x is the number of ruptures of molecule chains; t is the duration of breakdown; k is the rate constant of the reaction; P_m is the final degree of polymerization; and P_t is the degree of polymerization in time t.

In studying the mechanical breakdown of a polymer in concentrated solutions or in the condensed phase, the rate of the process is described by the more

complex equations of the nonintegral series.

Considering the scission-recombination character of the processes occurring in crushed or broken up polymers (see below), it would be correct to determine P_t and P_m for the product subjected to mechanical action in the presence of acceptor radicals. Only in this case can one form a correct conception of the rate and the factors which affect the mechanical scission of the molecule. In this connection, the number of ruptures (in moles) may be found from the equation

$$x = c \left(\frac{1}{P_t} - \frac{1}{P_0} \right) \tag{2}$$

where c is the concentration of the polymer in moles/liter and P_0 is the initial degree of polymerization.

In carrying out the scission in the absence of a solvent, the quantity c may be excluded from Equation (2). In this case x relates to 1 g or base mole.

CHEMICAL TRANSFORMATIONS OF MACROMOLECULES IN THE MECHANICAL BREAKDOWN OF POLYMERS

The energy of mechanical actions on macromolecules of a polymer is expended mainly on the deformation of valence angles and the scission of polymer chains.

These processes reduce the activation energy of the chemical transformations of the polymers broken down, as a result of which the mechanically activated reactions of autoxidation proceed fairly intensively under comparatively mild conditions²⁴, and should be taken into account in the study of mechanochemical transformations of high molecular weight substances. However, in the processes of scission of macromolecular chains which we are considering, mechanically activated reactions have a secondary significance. Actually, the energy necessary for the scission of macromolecules includes the energy consumption in the deformation of valence angles and the breaking of valence bonds, by reason of which the products formed in the mechanical scission of the polymer chains should possess a large chemical potential and enter easily into various chemical conversions.

In view of the fact that under the action of mechanical forces the breaking of macromolecular or three-dimensional structures proceeds not only with covalent bonds but also with ionic ones, we consider that three basic mechanisms of polymer scission are possible: (1) radical, (2) ionic and (3) ionic-radical.

The formation of polymeric radicals (macroradicals) may be expected in the case where the polymer chains contain covalent bonds:

In those cases where less stable ionic bonds enter into the makeup of the polymeric chain or three-dimensional structure, or where the strength of the ionic bonds is reduced by the presence of a medium with a high dielectric constant, a mechanical scission of the macromolecules with the formation of ionic compounds becomes probable:

Finally, cases are possible in principle in which the decomposition of macromolecules proceeds with ionic and covalent bonds, with the formation of radical ions.

The formation of macroradicals in the mechanical breakdown of organic polymers and the possibility of their chemical reactions are noted by Pike and Watson²⁵, Berlin^{26–28}, Kargin and Slonimskii²⁹, Baramboim³⁰ and a number of other research workers.

If one assumes that two radicals are formed by the rupture of each bond, then the total quantity of radicals (in moles/liter) formed by breaking down a polymer solution with a concentration of c moles/liter is determined by the equation

 $[R] = 2x = 2c \left(\frac{1}{P_1} - \frac{1}{P_0}\right)$

where c is the concentration of the polymer in moles/liter; P_1 is the average degree of polymerization after the scission of the polymer with acceptors which inactivate the free radicals; and P_0 is the average degree of polymerization before mechanical breakdown.

The number of radicals contained in c moles per liter of polymer is

$$\left\lceil R'\right\rceil = 2Nx = 2cN\left(\frac{1}{P_1} - \frac{1}{P_0}\right)$$

The polymer radicals formed by a homolytic scission of the macromolecules are capable of further transformations: combinations, disproportionation, reactions with the polymer or the medium. If we consider that, in the mechanical breakdown of a polymer, scissions of the polymer chain may proceed at different points on the macromolecule, then the apparent possibility arises of the formation here not only of monoradicals but also of biradicals. Besides this, a scission of the macromolecules unavoidably leads to the formation of two types of macroradicals, differing in the degree of delocalization of the unpaired electron:

In the polymerization of monomers containing electron acceptor groups on one of the carbon atoms of the double bond, the formation of radicals of type (I) is more economical of energy.

Thus the scission products of polymers contain monoradicals and biradicals of type (I), which are not identical to the macroradicals formed in the poly-

merization of the majority of monomers.

Thanks to the presence in the scission products of at least two different types of radicals, in the mechanical breakdown of polymers different processes of radical inactivation are possible by way of the combinations I-I, I-II and II-II, as well as by disproportionation.

In evaluating the capability of polymer radicals toward one reaction or another, it is necessary to take into account the great influence of spatial or steric difficulties which cause a great flexibility of the chains, the presence of side groups and branchings, as well as the low probability of encounters with the active atoms located at the ends of the macromolecules. Hence when the other conditions are equal an increase in the degree of scission of the macromolecules should lead to the formation of more reactive macroradicals.

The data available^{15, 16, 31, 32} show that in the breakdown of polymers by ultrasonic waves (frequency of 500–1200 kilohertz, intensity up to 8 watts/cm²), just as in the cold mastication on a laboratory masticator of the "worm" type^{34–37}, the quantity of macroradicals formed amounts to about 10⁻⁵–10⁻⁶ moles/liter.

Thus in the systems of interest to us, in addition to the macroradicals, a large quantity of inactivated polymer chains are present, in view of which, besides the combination processes, the acts of chain transfer and the reactions of scission of macromolecules under the action of radicals (initiated scission)

assume a great importance:

(a)
$$\cdots$$
 CH_z — CH_z — \cdots + R · \longrightarrow \cdots — CH_z · + \cdot CH_z — \cdots

(b)
$$\cdots$$
 CH CH_2 \cdots $+$ R : \longrightarrow RH $+$ \cdots C CH_2 \cdots X

where R is a macroradical formed in the mechanical scission of polymer macromolecules.

The initiated scission (a) and chain transfer from the polymer radical to macromolecules (b), the formation of radicals differing in activity, as well as the spatial difficulties in the reaction of the macroradicals, apparently cause a number of specific properties in the products of mechanical scission of macromolecules. Thus in recent time the comparatively low value of the probability of combination W_K of macroradicals formed by the ultrasonic breakdown of polystyrene and polymethyl methacrylate in dilute benzene solutions, in comparison with the quantity W_K in the polymerization of the respective monomers (Table 1), has been shown experimentally^{25, 31}.

TABLE 1

Comparison of the Probability of the Combination of Macroradicals in the Polymerization of Monomers and the Ultrasonic Breakdown of Polymers

	Probability of combination			
Method of forming macroradicals	Polystyrene	Polymethyl methacrylate		
In polymerization	100	40		
In the ultrasonic breakdown of 0.5% polymer solutions	40-53	20		

In relation to what has been said above, the experimentally established fact of the increase in the quantity $\lceil \eta \rceil$ upon storage of products of the cryolytic breakdown of starch^{22, 23}, as well of the change in $\lceil \eta \rceil$ through the prolonged (up to 2 weeks) standing at 20° C of freshly milled polyvinyl chloride³³, should be noted. The process of reducing the plasticity and increasing the $\lceil \eta \rceil$ by the storage of plasticized rubbers, which is known in rubber technology, also indicates the long life duration of the active macromolecules formed by the mechanical breakdown of polymers in the medium of air²⁶.

Considering that the rate of combination (U_K) is proportional to the square of the concentration of free radicals,

$$U_K = k \lceil R \rceil^2$$

while the rate of chain transfer and initiated scission is determined by the equation

$$U_D = k \lceil R \rceil \cdot \lceil P \rceil$$

where [P] is the concentration of macromolecules of the polymer, we reach the conclusion that at low values of [R] and comparatively high concentrations of macromolecules not subjected to scission, $U_D > U_K$, and with high [R] and low [P] values, on the other hand, the rate of combination may exceed the rate of initiated scission.

In the case of forming by the mechanical scission of macromolecules comparatively long-lived macroradicals, a process of initiated breakdown may apparently be observed in the addition of the broken-down polymer to one not broken down, or on storing the polymer substances subjected to intensive mechanical action.

This conclusion is confirmed experimentally. Thus, it is found that the addition of an aqueous solution of starch broken down by freezing to solutions of starch, gelatins and polyvinyl alcohol initiates the breakdown of the polymers mentioned, while an increase in the duration of the experiment beyond a certain limit causes a gradual development of processes leading to an enlargement or coarsening of the polymer chains^{15, 22, 23}.

MECHANOCHEMICAL METHODS OF SYNTHESIS OF POLYMERIC SUBSTANCES

The polymer radicals formed by the mechanical scission of macromolecules may be used for the initiation of reactions of chain polymerization and the synthesis of new block polymers with given physicomechanical and dielectric properties.

The characteristic feature of mechanochemical initiation and block, polymerization is that in this case there is a direct conversion of the mechanical work (A), consumed in breaking up the polymer, into the chemical energy of the activated chains and polymer radicals formed thereby, i.e.,

$$A \ge (\mu_2 - \mu_1)\Delta n$$

where μ_1 and μ_2 are the chemical potentials of the system before and after mechanical breakdown; Δn is the increase in the number of active macromolecules in the mechanical breakdown.

Thus in the processes under consideration, the lowering of the energy barrier of any reaction is basically achieved through mechanical work, and consequently requires almost no additional consumption of heat, light or any other form of energy. Thus, Berlin and Penskaya were the first to achieve a synthesis of a block copolymer of polystyrene (PS) and starch by freezing (from -20° to -70° C) an emulsion of a solution of PS in toluene in 2.5-5% solutions of starch¹⁵.

The product separated after the coagulation of the thawed emulsion gives opalescent solutions in water and toluene, which indicates the formation of a copolymer containing high-polymer blocks of starch and low-polymer blocks of

polystyrene.

After drying, the polymer is only partially soluble in water and toluene, since in this case the intermolecular hydrogen bonds are apparently restored. An analysis showed that the fraction soluble in toluene contains 11-13% of OH groups, while the fraction soluble in boiling water is characterized by a considerably larger hydroxyl content (~18%). The work carried out showed the possibility of block copolymerizations of synthetic and natural materials markedly different in their chemical nature, which opens large scientific and practical vistas for the mechanochemical, and in particular the cryochemical, synthesis of high polymers.

Alexander and Fox have shown the possibility of initiating the polymerization of styrene by vibrating its emulsion in a solution of polymethacrylic acid with sound. This work was the first communication on block copolymeriza-

tion in an ultrasonic field17.

Somewhat later Henglein³¹ established that the addition of polyacrylamide

(up to 0.13 g/liter) to the aqueous solution of acrylonitrile (0.7 g/liter) markedly accelerates its polymerization in a hydrogen medium under ultrasonic sound treatment at a frequency of 500 kilohertz with a sound power of 100 watts and at $18-20^{\circ}$ C.

It has been shown experimentally that in this case the polymerization is initiated by macroradicals formed in the breakdown of polyacrylamide, as well

as by OH radicals.

As the result of the sound treatment of an aqueous solution containing polyacrylamide and acrylonitrile, a polymer is obtained which, in contrast to polyacrylonitrile (PAN), forms in water an opalescent sol which is not coagulated by electrolytes. The high stability of such a system is caused by the biphylic nature of the block copolymer formed by sound treatment, which copolymer

evidently plays the role of a protective colloid.

When benzene solutions of a mixture of polystyrene (PS) and polymethyl methacrylate (PMM)²² are treated with sound in a nitrogen medium, a block-copolymer is formed which, in contrast to polymethyl methacrylate, does not precipitate out on the addition of carbon disulfide. The addition of iodine to such solutions in amounts of 10⁻⁴ mole/liter, or of diphenylpicrylhydrazyl, practically excludes the formation of a copolymer, since in this case the macroradicals formed are inactivated by means of a reaction with the acceptors mentioned.

It is instructive to note that when solutions of PS and PMM are treated with ultrasonic sound in air, the complete inactivation of the macroradicals is not observed; this apparently indicates a capability of peroxide radicals toward combination and chain transfer³².

In 1954 Watson and Wilson³⁴ described the construction and the principle of action of a new apparatus (a masticator) of the "worm" type for the plastici-

zation of rubber and other elastomers.

The polymer, which is loaded between the rotating and immobile disks of the "worm", undergoes the action of very considerable mechanical forces, which cause a scission of the macromolecules and a combination of the ingredients of the compound. The masticator of the worm type was used by Angier and Watson^{35–37} for obtaining various block copolymers of natural as well as synthetic rubbers. Thus when a stock of natural rubber, butadiene-styrene (SKS), butadiene-acrylonitrile (SKN), polychloroprene, polyisoprene, polyurethane ("Vulcallan A") or butyl rubber is processed in a medium of nitrogen in a masticator with the monomers (methylmethacrylate, styrene, acrylonitrile, acrylic and methacrylic acids, acrylates, divinylbenzene, etc.), block copolymers are formed which differ sharply in their properties from the original polymer substances^{36–37}.

In the process of mastication at 18–20° C, a mechanical scission of the polymer chains occurs which gives macroradicals capable of initiating the polymerization of monomers with the formation of block graft copolymers. It has been shown experimentally that the rate of such a mechanochemical block copolymerization is increased with an increase in the amount of polymer (Figure 1). An increase in the processing temperature decreases the rate of copolymerization, since in this case the degree of breakdown of the polymer, and consequently also the concentration of free macroradicals, is decreased. An increase in the speed of rotation of the worms from 76 to 350 rpm causes a heating of the plasticized mass (the temperature is raised accordingly from 32° to 52° C), and consequently a decrease in the rate of macroradical formation and block copolymerization.

The process of mechanochemical block copolymerization is affected by the activity of the polymer radical and monomer formed. Thus, for example, in the mastication of a stock of synthetic rubber and vinyl acetate it was not found possible to obtain a block copolymer. Analogous difficulties are encountered in the processing of polymer-monomer compounds containing butyl rubber, polyisobutylene and polyurethane. The formation of block copolymers by the mastication^{25, 27} of two different polymers in a medium of nitrogen at 30° C has been shown for compounds based on natural and synthetic rubbers.

The products obtained by such processing are distinguished from natural rubber (and the respective elastomers) by their solubility, capability of swelling in polar and nonpolar solvents, and also by the chemical composition of the copolymer, purified by the extraction from it of the ingredients which did not

enter into the reaction.

After a prolonged (up to 8 hours) mastication of a synthetic rubber (SR) and natural rubber, products only partly (30–80%) soluble in organic solvents are formed.

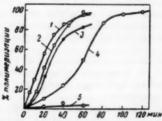


Fig. 1.—Influence of the styrene content of the mixture with rubber and of the mastication temperature on the polymerization rate: I=13.2% styrene, 15° C; 2=33.3% styrene, 15° C; 3=23.3% styrene, 25° C; 4=37.7% styrene, 15° C; 5=37.7% styrene, 25° C. Abecissa: minutes; ordinate: % polymerization.

The chemical and spectroscopic study of the insoluble precipitates and of the fractions going into solution has shown that their composition includes a block copolymer formed in the process of mastication of a compound of natural rubber and synthetic elastomers.

The presence of an insoluble fraction indicates that besides the block copolymers, branched copolymers are also formed. Such products may be formed by the reaction of macroradicals with double bonds or by the chain transfer from the polymer radical to the methylene groups of the natural rubber macro-

molecules.

The preparation of copolymers by low-temperature mastication is not limited only to the case of mixtures of synthetic rubber with natural rubber. In recent times, with this method, block-graft copolymers of styrene-butadiene rubber and polychloroprene³⁷ have been obtained. Kargin, Kovarskaya, Goluben-Kova and Akutin have improved the construction of the masticator and have shown the possibility of a mechanochemical synthesis of copolymers of acrylonitrile rubber with a phenol-formaldehyde resin, epoxy resins and coal-tar pitch³⁸.

The study of the block copolymers obtained has shown that they differ in their thermomechanical properties and solubilities from the initial polymers.

The literature data available thus far does not permit one to form a concept of the physicomechanical and dielectric properties of the block copolymers obtained by freezing, by the action of ultrasonic sound or of the mastication of a mixture of polymers. It has already been noted that in plasticizing elastomers on the roll mill, a mechanical scission of the macromolecules is observed with the formation of polymer radicals, which makes it possible to obtain mechanochemical block copolymers with given physicomechanical and dielectric properties. In relation to this, in order to obtain a material with an increased mechanical strength, we together with I. M. Gilman carried out a plasticization of a block and emulsion polymer in a compound with polyisobutylene, butyl rubber, butvar, polychloroprene, polybutadiene, butadiene-styrene (SKS-30) and butadiene-acrylonitrile (SKN-18, SKN-40) rubbers. This work has shown that at 150-160° C and friction = 1.25, a mechanical breakdown of the polystyrene and the rubbers is observed. The macroradicals formed in the break-

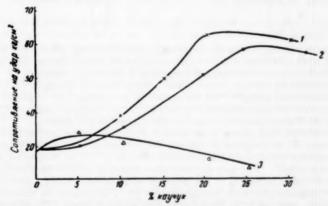


Fig. 2.—Dependence of dynamic flex resistance of polystyrene-rubber block copolymers on the quantity and type of rubber. I—Polystyrene—SKS-30 rubber (SBR); 2—polystyrene—SKN-18 rubber (NBR); 3—polystyrene—SKN-40 rubber (NBR, 40 parts acrylonitrile). Abscissa: % rubber; ordinate: resistance to impact, kg/cm².

down in air at an elevated temperature accept iodine, which indicates the presence of molecules containing unpaired electrons on the carbon atoms. The formation of such radicals in air is possible through a chain transfer:

$$\cdots$$
-CH₂OO, $+\cdots$ -CH₂CH₂- \cdots -CH₂OOH $+\cdots$ -CHCH₂- \cdots

On the basis of the data obtained one may presume that the mechanochemical block copolymerization at elevated temperatures will also take place in a stream of air.

The strongest material is obtained by a joint plasticization of mixtures of polystyrene-SKS-30 and polystyrene-SKN-18. An increase in the quantity of rubber above 20-25% is not expedient, since in this case the major part of the elastomer remains uncombined with the polystyrene, which causes a decrease in the strength characteristics. An increase in the content of polar chain links of acrylonitrile in the rubber prevents the combination with polystyrene and decreases the probability of a combination of differing macroradicals, and consequently lowers the strength of the material (Figure 2).

The fact that under conditions of joint plasticization of polystyrene, with a proper choice of conditions, a reaction of a combination of different macroradicals proceeds with the formation of block copolymers is confirmed by data from the investigation of the thermomechanical properties and on the solubility of the product, which contains combined rubber, in benzene and acetone, as well as by the observed drop in the strength of the material upon the addition of an acceptor radical $[I_2]$ as well as of some dyes (Table 2) on the rubber mill.

Apparently, in view of the fact that some dyes contain mobile atoms of hydrogen or halogens in their molecules, they may play the part of more or less strong macroradical acceptors, thus leading to the scission of the chain and to a decreased probability or complete exclusion of the combination of polymer radicals:

$$-\text{CH}-\text{CH}_2\cdot + \text{AX} \longrightarrow \cdots - \text{CH}-\text{CH}_2\text{X} + \text{A}$$

Thus in coloring polymeric materials by the roll-milling process one should bear in mind that dyes of different classes, even in small addition, may markedly affect the physicomechanical properties of plasticized materials.

In contrast to the dyes, active fillers (carbon black for example) containing active atoms and groups^{39–42} on the surface of the particles, by reason of their reaction with the macroradicals obtained by the mechanical scission of PS and

rubber, form structures which improve the strength of the material.

Considering that phenol formaldehyde resins containing mobile hydrogen atoms may act as acceptors of radicals, the question of the reaction of lacquer resins (phenol aldehyde) with polyvinyl chloride (PVC) in milling on a roll mill was studied³². The data obtained show that as a result of 30-minute processing of such compounds in the presence of plasticizers (20%), part of the phenol formaldehyde resin (approximately 15–17%) cannot be removed by even a very long (up to 24 hours) extraction with methanol. The presence of a stably combined resin in the insoluble residue is also confirmed by the decrease of the Cl content in it (55.6–49%) and the ability to swell in methanol. The addition of a radical acceptor (10⁻² moles of I₂ per base mole) markedly reduces (by a factor of more than 2) the quantity of the product insoluble in alcohol.

A sharp change in the physicomechanical properties of the polymer compound is observed when a stock which consists of teflon, polydimethylsiloxane, benzoyl peroxide and fillers is worked intensively on the rubber mill. In this case a material fairly resistant to benzene is obtained, which possesses a greater tensile strength and especially a greater tear resistance, than an ordinary organosilicon elastomer^{42, 43}. Table 3 gives the properties of such materials.

Table 2

Effect of Some Additives on the Strength of a Polystyrene-Rubber Plasticization Product

	Amount, g	Dynamic flex resistance	Static flex resistance	
Additive	on 100 g resin	kg-em/em²		
No additive	2	53.5	930	
Violet vat dye	0.2	47.6	870	
Pigment "yellow"	0.5	27.5	-	
"Bordeaux" lac dye	0.5	30.9	850	
Crystalline iodine	0.1-0.2	29.9	943	
Channel black	2.0	57.6	835	

Table 3

Composition and Properties of Compounds

	Compound, parts by weight			
	A	В		
Organosilicon elastomer				
("Se-76")	100	100		
Filler	42	42		
Benzoyl peroxide	1.6	1.6		
Teflon TE-3086		10		
Shore A hardness	50	55 (exceeding by 5%)		
Tensile strength, kg/cm ²	52	71.4 (exceeding by 36%)		
Tear resistance, kg/cm	50	190 (excedeing by 280%)		
Elongation at break, %	250	300 (exceeding by $20%$)		

The mechanism by which an organosilicon rubber is strengthened by teflon has not been investigated so far. In this case it is inadmissible that polydimethylsiloxane undergoes scission through mechanical stresses alone, since it follows from experimental data that an organosilicon elastomer in and of itself does not undergo mechanical scission under the conditions of milling. Apparently the process mentioned is related to the scission of polydimethylsiloxane initiated by benzoyl peroxide. The macroradicals formed here may enter into reaction with the radical products of the mechanical scission of polytetrafluoroethylene with the formation of branched and block copolymers.

The mechanochemical methods of synthesis of block copolymers are in the initial stage of development and hence the few papers available thus far do not permit one to form a sufficiently complete conception of the mechanism of the

processes taking place there.

The view developed in a number of papers^{31, 32, 35–37}, that the formation of mechanical block copolymers through acts of combination by polymer radicals, in our opinion, does not explain many of the experimental facts. Actually, it has already been noted above that the concentration of macroradicals formed by ultrasonic seission or by the plasticization of polymers amounts to a quantity of the order of 10⁻⁵ to 10⁻⁶ moles/g^{15, 44}. At the same time, the yields of block copolymers may reach 80–90% of the weight of the polymers subjected to bréakdown. Such a disagreement between the concentrations of active molecules and the yield of block copolymer indicates a chain mechanism of the process of mechanochemical copolymerization and cannot by any means be explained solely by combination or by the possibility of a graft copolymerization through a chain transfer from the polymer radical to the macromolecules.

We consider it more probable that the principal process causing the mechanochemical copolymerization of two polymers is the scission of mechanically activated polymer chains, initiated by macroradicals. For the occurrence of this reaction, very favorable conditions are created by the mechanical scission of polymers. This is indicated by the following: (1) in view of the presence of a comparatively small number of macroradicals and a relatively large quantity of "nonradical" chains, the probability of a reaction between polymer radicals and macromolecules amounts to a considerable quantity; (2) the macromolecules not containing unpaired electrons are activated in the process of mechanical breakdown as a consequence of the deformation of valence angles caused by the intensive mechanical action on the polymer; (3) the rate of the initiated scission should be proportional to the concentration of macroradicals [R] and of "nonradical" macromolecules [P]. In view of this, even with low values of [R] but large [P] values, the initiated scission may proceed fairly intensively.

As a result of the initiated scission, block copolymers are formed and new macroradicals are created which continue this chain process further.

Thus according to the mechanism proposed by us, the process of mechanochemical block copolymerization proceeds in the following manner:

1. Formation of active chains:

$$R \xrightarrow{\downarrow} R + m \xrightarrow{\downarrow} m \xrightarrow{} R^{\cdot} + m^{\cdot}$$

2. Development of chain:

$$R' + m - m \longrightarrow Rm + m'$$
 and so on $m' + R - R \longrightarrow Rm + R'$

- 3. Scission of the chain-
 - (a) As a result of combination:

$$R' + m' \longrightarrow Rm$$

 $m' + m' \longrightarrow m \longrightarrow m$
 $R' + R' \longrightarrow R \longrightarrow R$

(b) As a result of disproportionation:

$$R^{\cdot} + R^{\cdot} \longrightarrow 2R_1; R^{\cdot} + n \longrightarrow R_1 + m_1, etc.$$

(c) As a result of reaction with the medium, the walls of the vessel or with additives:

$$R' + AX \longrightarrow RX + A'; A' + A' \longrightarrow AA$$

In the case of the presence in the macromolecules of bonds capable of reacting with the macroradicals, in addition to the initiated scission, processes of chain transfer may proceed, leading to the formation of branched macromolecules:

The probability of such a process is determined by the activity of the macroradical, the chemical nature of the polymer and the conditions of mechanical breakdown.

The proposed mechanism of mechanochemical block copolymerization clarifies the reason for the seeming contradiction between the concentration of macroradicals and the yield of copolymers; besides this an explanation is found for the known facts indicating that not just any pair of polymeric substances can form block copolymers under the conditions of mechanical breakdown³⁶. From this point of view it is also easy to explain the reason for the inhibiting action of active free radical acceptors, and a number of other experimental facts.

If a polymer is subjected to mechanical breakdown in the presence of a fairly active monomer, the process of block copolymerization also proceeds by a radical chain mechanism. However, in this case the role of initiated scission is reduced to a minimum, since the decisive reaction is the polymerization of a monomer initiated by macroradicals.

The literature considered forms the basis for new principles of the synthesis of polymeric products with given physicochemical and mechanical properties.

The development of mechanochemical methods of synthesis of high polymers is as yet in its initial stage, but nonetheless it is possible to confirm that this method of preparing polymeric substances opens up great possibilities as regards the chemistry and technology of high molecular weight compounds; in particular, this unique method of synthesizing polymeric substances makes it possible to use blocks of both organic and inorganic 46 high molecular wieght substances in preparing polymeric materials.

REFERENCES

- REFERENCES

 1 Staudinger, H. and Dreher, E., Berichte 69, 1093 (1936).
 2 Hess, K., Kiessing, H. and Sunderman, J., Z. phys. Chem. B49, 64 (1941).
 3 Hess, H., Steurer, H. and Fromm, H., Kolloid-Z. 98, 3, 290 (1942).
 4 Lompitt, L. H., Fuller, C. H. F. and Goldenberg, N., J. Soc. Ind. 60, 1 (1941).
 5 Steurer, E. and Hess, H. Z. phys. Chem. VII 193, 3 (4), 248 (1941).
 6 Barambolm, H. K., Nauch. Trudy MTLLP 4, 104 (1954).
 7 Staudinger, H. and Dreher, E., Berichte 69, 1097 (1934).
 8 Staudinger, H. and Dreher, E., Berichte 69, 1097 (1934).
 9 Staudinger, H., Kolloid-Z. 51, 71 (1930).
 9 Zhukov, I. I., Komarov, Ts. A., Gribova, E. I. and Selivanov, I. L., Sint. Kauchuk 5, 4 (1936).
 9 Pike, M. and Watson, W. F., J. Polymer Sci. 9, 229 (1952).
 9 Pike, M. and Watson, W. F., J. Polymer Sci. 9, 229 (1952).
 9 Staudinger, H., Wysokomolekulyarnye organicheskie soodineniya (High Molecular Weight Organic Compounds)", ONTI, 1935, p. 211.
 9 Staudinger, H., "Vysokomolekulyarnye organicheskie soodineniya (High Molecular Weight Organic Compounds)", ONTI, 1935, p. 211.
 9 Morris, W. J. and Schurmann, R., Nature 160, 674 (1947).
 10 Berlin, A. A., "Reports of the 9th Conference on General Questions on the Chemistry and Physics of High Molecular Weight Compounds," I.d. Akad, Nauk SSSR, p. 76, 1956.
 10 Berlin, A. A. and El'tsefon, B. S., Khim. Nauka i Prom. 2, 5, 667 (1957).
 10 Alexander, P. and Fox, M., J. Polymer Sci. 12, 533 (1954).
 11 Graber, P. and Prudhomme, P., J. Chim. Phys. 44, 145 (1948); see also Bull. Soc. Chim. Biol. 29, 122 (1947).
 12 Schmidt, G. and Bautenmüller, E., Z. Electrochem. 49, 325 (1943); 50, 202 (1944).
 13 Kudryavtsev, B. B., "Primenenie ul'traskutsicheskie metody v praktike faishokhimieheskie issledovanie (The Use of Ultrasonic Methods in the practice of Physico-Chemical Investigations)", GTP, 1952; see also Uskekhi Khimii 17, 158 (1948).
 14 Nikitia, N. P. and Klenkova, N. I., "Symposium of Research in the Field of High Molecular Weight Compounds," Izd. Akad. Nauk SSSR, p. 138, 1949.
 15 Wikitia, N. P. and Klenkova,

- Compounds, Iad. Akad. Nauk SSSR, p. 138, 1949.

 "Tesisydokladov Konferentsii MTHMP (Reports of Conference of MTHMP)", 1955, p. 35, Dish-chepromisdat.

 Berlin, A. A. and Penskaya, E. A., Doklady Akad. Nauk SSK 110, 4, 586 (1956).

 Kuzminskii, A. S., Uspekhi Khimii 24, 842 (1955).

 Pike, M. and Watson, W. F., J. Polymer Sci. 9, 229 (1952).

 Berlin, A. A., "Osnovy proisvodatva gasonapolnennykh plastmass i elastomerov (Bases of Production of Gas-Filled Plastics and Elastomers)", Goskhimisdat, 1954, pp. 138, 194.

 "Tesisy dokladov mauchnol konferentsii MTHMP za 1955 g. (Reports of Scientific Conference of MTHMP for 155)", Isd. MTPPT, p. 33.

 Berlin, A. A., Doklady Akad. Nauk SSSR 110, 401 (1956).

 Kargin, V. A. and Slonimskii, G. L., Doklady Akad. Nauk SSSR 105, 751 (1955).

 Barambolm, N. K., "Mekhanicheskaya destruktsiya vysokomolekulyarnykh veshchestv (Mechanical Breakdown of High Molecular Weight Substances)", dissertation, Moscow, 1955.

 Henglein, A., Makromal. Chem. 15, 188 (1955).

 Henglein, A., Makromal. Chem. 15, 188 (1955).

 Berlin, A. A., Petrov, G. S. and Prosvirkina, V. F., Khim. Nauk i Prom. 2, 4 (1957).

 Watson, W. F. and Wilson, D., J. Sci. Instr. 31, 93 (1954).

 Angier, D. J. and Watson, W. F., J. Polymer Sci. 18, 141 (1955).

 Angier, D. J. and Watson, W. F., J. Polymer Sci. 20, 235 (1956).

 Angier, D. J. and Watson, W. F., Trons. Roy. Inst. Rubber Ind. 33, 22 (1957).

 Kargin, V. A., Kovarskaya, B. M., Golubenkova, L. I., Akutin, M. S. and Slonimskii, G. L., Khim. Prom. 12, 13 (1957).

 Kargin, V. A., Kovarskaya, B. M., Golubenkova, L. I., Akutin, M. S. and Slonimskii, G. L., Khim. Prom. 12, 13 (1957).

 Coulson, G. A., J. Chem. Sci. 1953, 1435.

 Coulson, G. A., J. Chem. Sci. 1953, 1435.

 Lavy, M. and Szwarc, M., J. Chem. Phys. 22, 1621 (1954); see also J. Am. Chem. Soc. 77, 1949.(1955); J. Polymer Sci. 10, 106 (1955).

 Rubber World 133, 2 (1955); Materials and Methods 43, 1, 106 (1955).

 Berlin, A. A. and Parin, V. P., Khim. Nauk i Prom. 1, 1, 44 (1956).

COMPOUNDING SBR FOR RADIATION RESISTANCE *

HERBERT R. ANDERSON, JR.

RESEARCH AND DEVELOPMENT DEPARTMENT, PHILLIPS PETROLEUM COMPANY, BARTLESVILLE, OKLAHOMA

I. INTRODUCTION

The need for elastomers which undergo relatively little change in physical properties upon exposure to ionizing radiation has stimulated a great deal of active research in recent years¹⁻¹⁰. Approaches to the problem have included studies of the response of well-known elastomers to radiation, synthesis of new rubbers containing radiation-resistant groups, and the effect of additives. This paper presents results obtained with butadiene-styrene vulcanizates, one of the most resistant to radiation; the results show that by proper compounding techniques resistance to radiation may be increased. Swelling and stress relaxation techniques are applied to determine the effect of styrene content of rubber, oil extension, vulcanization recipe, conditions of cure, additives (antirads), and irradiation atmosphere on radiation damage to polymeric network and the dependent stress-strain properties.

II. EXPERIMENTAL

Vulcanizates were exposed to the gamma-rays from spent fuel elements at the canal facilities of the Materials Testing Reactor at Idaho Falls, Idaho. The cured compounds were separated by sheets of Holland cloth, packed into aluminum cans which were evacuated and purged three times with helium or air, and irradiated under a slight positive pressure. The irradiation was carried out under 16 ft, of water at the ambient canal temperature of ca. 27° C. Comparisons of the radiation resistance of the different vulcanizates without complications introduced by flux variations resulting from decay in activity of the fuel elements can be made by this procedure. All irradiations were performed within three to thirty days after withdrawal of the fuel elements from the reactor. Since much of the lowest energy radiation is absorbed by the intervening water and container walls, the mean energy of the gamma-rays used in this work is estimated at 1.5 m.e.v.; more than 50% of the energy is derived from the barium-lanthanum 140 chain.

The radiation dosages were determined for each experiment by ceric/cerous sulfate dosimetry, and are expressed in roentgens equivalent physical (reps).

Polymers studied were Philprene 1500 (a trademark of Phillips Petroleum Co.), a 50 ML-4 butadiene-styrene copolymer containing 23% bound styrene, and a 47 ML-4 high-styrene analog containing 41% bound styrene. These synthetic rubbers are emulsion copolymers prepared at 5° C. The compounding recipes are shown in Appendix A. A glossary of compounding agents is shown in Appendix B.

^{*} Reprinted from Journal of Applied Polymer Science, Vol. 3, pages 316-330, 1960.

Physical testing of the vulcanizates was carried out by well-known procedures. Degrees of crosslinking were estimated by the equilibrium swelling technique in n-heptane^{11, 12}. Estimates of the amount of scission during irradiation were determined by measurements of stress relaxation^{13–15}. Strips of the vulcanizates were stretched to 100% elongation on an aluminum rack and were allowed to relax 24 hours before measurement of the initial stress. The strips were returned to the rack, placed in an aluminum can, and irradiated in an atmosphere of helium or air; the final tension was determined after removal from the radiation field.

III. GENERAL PRINCIPLES

Irradiation of organic high polymers with ionizing radiation causes both crosslinking and scission. Crosslinking predominates in the butadiene rubbers¹⁶⁻²¹. Estimates of radiation-induced changes in the polymeric network are made by application of the kinetic theory of rubber elasticity.

From statistical theory²²⁻²⁵, the equilibrium stress f in a strip of rubber is

given by

$$f = \nu k T [\alpha - (1/\alpha^2)] \tag{1}$$

where α is the ratio of the extended to the initial length and ν is the number of elastically effective network chains. Equation (1) is useful in a semiquantitative way even when nonequilibrium modulus values are employed, provided the elongation is kept low ($\alpha < 2$). Furthermore, modulus has been found to be related linearly to the number of network chains in carbon black-loaded rubbers for the range of values associated with rubbery vulcanizates¹². One would expect this same linear dependence when a vulcanizate is exposed to radiation. As the change in number of network chains represents the difference of crosslinking and scission, the absolute value of crosslinking and scission is relatively unimportant in determining modulus.

Separate estimates of scission and crosslinking during irradiation are obtained by the measurement of both stress relaxation^{13–15} and equilibrium swelling¹¹. This scheme has been employed by Arnold, Kraus, and Anderson²⁵ to estimate the ratio of crosslinking to scission during gamma-vulcanization. More recently, Kraus²⁷ has shown that deviations of carbon black-loaded vulcanizates from ideal elastic behavior are minimized by measuring the initial (ν_0) and final (ν) number of network chains from equilibrium swelling^{11, 12} and relying on measurements of stress only to determine the stress ratio f/f_0 , where f and f_0 are the final and initial equilibrium stresses in the stress relaxation experiment, respectively. The calculation of the number of scissions s, following the theories of Bueche²⁸ and Berry and Watson²⁹ yields for scission at crosslinks:

$$s = \nu_0 (1 - f/f_0) \tag{2}$$

and for first-order random seission in the main chain:

$$s = \nu_0(f_0/f - 1) \tag{3}$$

The extent of crosslinking r is then

$$r = \nu - \nu_0 + s \tag{4}$$

IV. RESULTS AND DISCUSSION

The results of this work will be divided into two parts. Part I is concerned with the radiation resistance (changes in 100% modulus) of common butadiene-styrene (77/23) rubber tread stocks, which were used to explore the action of vulcanization system, cure temperature, state of cure, irradiation atmosphere, and additives. The useful life of the high-styrene cold-rubber tread stocks which were found to resist radiation in a gamma-ray field was determined by the techniques used in Part I. These results and measurements of swelling and stress relaxation of these vulcanizates to relate network damage to changes in stress-strain properties are presented in Part II.

A complete tabulation of all stress-strain and swelling results of all these vulcanizations are included in Appendix C for possible engineering information.

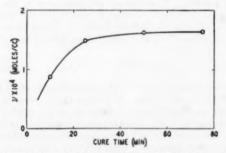


Fig. 1.—Number of network chains vs. cure time at 307° F for a butadiene-styrene (59/41) tread stock (50 phr HAF black) vulcanized with an accelerated sulfur system. For vulcanization recipe see Table I.

PART I. RADIATION RESISTANCE OF BUTADIENE-STYRENE (77/23) TREAD STOCKS

A. Effect of state of cure.—Born and associates1. 2 have emphasized that an evaluation of radiation retarders must be made with vulcanizates at equivalent states of cure, i.e., with optimum physical properties. A similar observation was made independently in our laboratories, where it was found that completeness of cure is, generally, highly desirable for the evaluation of additives. These materials can affect the rate of vulcanization and the yield of crosslinks obtainable from a given recipe. Figure 1 shows a typical change in density of network chains during vulcanization. Once the plateau region of the cure rate curve has been reached there is little change in the 100% modulus [consistent with Equation (1)], tensile strength, and elongation. The amount of curing agent determines the height of the plateau, and, consequently the network chain density with a given compounding recipe. Additives should, preferably, be compared in fully cured stocks, because incomplete vulcanization improves radiation resistance. Born et al.1, 2 explained that this improvement was due to the initial expenditure of radiation to overcome the deficiency in crosslink density. Figure 2 shows the results of a study made with vulcanizates containing two different levels of sulfur to determine if the effect of undercure on radiation resistance is due to the initial crosslink density. These results indicate that curing short of the plateau region (undercuring) produces residual vulcanization intermediates which serve to modify and lessen radiation damage to sulfur-vulcanized rubbers. Such an effect is similar to the results observed

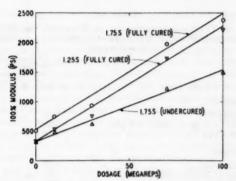


Fig. 2.—Effect of state of cure on the radiation resistance of butadiene-styrene (77/23) tread stocks (50 phr HAF black) in a helium atmosphere. For vulcanization recipe see Appendix A, Table I.

by Kraus²⁷ and Ossefort³⁰ in their studies of the thermal and oxidative degradation of vulcanizates.

B. Effect of sulfur utilization during vulcanization.—Since undercuring of sulfur vulcanizates apparently produces residual intermediates capable of functioning as radiation retarders (antirads), it was of interest to determine the impact of sulfur utilization during vulcanization on radiation resistance. Variations in sulfur utilization were obtained by varying the ratio of sulfur to accelerator at a fixed cure temperature and by curing at different temperatures. The data in Table I reveal that the radiation resistance of a sulfur vulcanizate is greatest when it is undercured at 307° F with a high ratio of accelerator to sulfur, and that it is affected by cure temperature but not by variations in sulfur/accelerator ratios at full cure. Detailed explanation of these results is not possible. The radiation resistance of sulfur vulcanizates appears to be associ-

TABLE I

EFFECT OF SULFUR UTILIZATION DURING VULCANIZATION ON THE RADIATION RESISTANCE OF BUTADIENE-STYRENE (77/23) TREAD STOCKS IN HELIUM ATMOSPHERE

	Santo-	Cure tempera-	Change in 100% modulus, psi, after indicated dosage		
Sulfur, phr	phr	°F	50 Mrep	100 Mrep	
Undercured					
1.25	2.0	307	500	1130	
1.75	1.0	307	670	1300	
2.25	0.7	307	610	1260	
1.75	1.0	280	740	1430	
1.75	1.0	330	830	1680	
Fully cured					
1.25	2.0	307	970	2020	
1.75	1.0	307	1040	2000	
2.25	0.7	307	1030	1950	
1.75	1.0	280	740	1540	
1.75	1.0	330	730	1460	

^e For vulcanization recipe see Appendix A.

TABLE II

EFFECT OF VULCANIZATION SYSTEM ON RADIATION RESISTANCE OF BUTADIENE-STYRENE (77/23) TREAD STOCKS IN A HELIUM ATMOSPHERE⁴

	Change in 100% modulus, psi, after indicated dosage		
Curing agents	50 Mrep	100 Mrep	
Undercured			
Gamma-rays Sulfur (1.75 phr)/Altax (1.8 phr) GMF (5 phr)	970 530 730	1070 1420	
Fully cured			
Gamma-rays Sulfur (1.75 phr)/Altax (1.8 phr) GMF (5 phr)	670 760 770	1470 1460 1500	

^a For vulcanization recipe see Appendix A.

ated intimately with the relative amount and characteristics of crosslinks and with the amount of combined sulfur posutlated to be in the form of five- and six-membered heterocyclic rings³¹.

C. Effect of crosslink type.—Since the mode of preparation of sulfur vulcanizates plays an important role in their radiation resistance, it was of interest to compare the response to radiation of vulcanizates containing carbon-carbon crosslinks with those containing sulfur linkages. The data in Table II show that no significant benefit is obtained by undercuring vulcanizates with carbon-carbon crosslinks, viz., those cured with gamma-rays and p-quinone dioxime. These data are added support for the conclusion that radiation resistance ob-

TABLE III

Effect of Undercuring and Antirads on the Radiation Resistance of Butadiene-Styrene (77/23) Tread Stocks in Various Atmospheres

Change in 100% modulus nei indicated document

	Change	in 100% moduli	s, psi, indicated dosage			
	Hel	ium	Air			
Antirad (5 phr)	50 Mrep	100 Mrep	50 Mrep	100 Mrep		
Undercured						
None	670	1300	600	1340		
Akroflex C	420	870	320	830		
Antiox 4010	580	1040	450	900		
Thio-2-naphthol	470	820	400	790		
2,5-Diphenyloxazole a-Naphthylphenyl-	480	910	290	820		
oxazole	420	920	290	800		
Fully cured						
None	1040	2000	820	2060		
Akroflex C	570	1130	350	840		
Antiox 4010	530	1080	460	1060		
Thio-2-naphthol	490	1010	460	960		
2,5-Diphenyloxazole a-Naphthylphenyl-	570	1140	500	1000		
oxazole	640	1120	450	1010		

· For vulcanisation recipe see Appendix A.

tained by undercuring sulfur vulcanizates is caused by residual sulfur vulcanization intermediates.

D. Combined effect of antirads and undercuring.—Born et al.^{1, 2} and Turner⁶ have discovered a number of compounds which when added to rubber in minor amounts will retard radiation-induced changes in the polymeric network. Some of these compounds and other antirads discovered in this laboratory were incorporated into budadiene-styrene (77/23) tread stocks to determine their effectiveness in the presence and in the absence of undercuring.

Table III and Figure 3 show some of the results of this study. The magnitude of the protection afforded by undercuring is comparable with that obtained with the recommended antirads Akroflex C and Antiox $4010^{1.2}$. These retarders were effective in both fully cured and undercured stocks. Thio-2-naphthol, 2,5-diphenyloxazole, and α -naphthylphenyloxazole, which have not been reported previously as antirads, were equally effective.

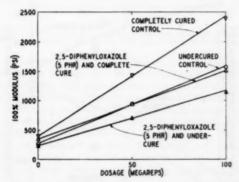


Fig. 3.—Effect of undercuring and antirads on radiation resistance of butadiene-styrene (77/23) tread stocks (50 phr HAF black) in a helium atmosphere. For vulcanization recipe see Appendix A, Table III.

An extensive screening program uncovered additional effective antirads for cold rubber, which with previously reported ones are listed in Appendix D. These additives are arranged according to their ability to resist changes in 100% modulus, which is related to the number of radiation-induced network chains. Akroflex C was used as a reference compound and is arbitrarily given a rating of 1.

Figure 4 shows typical changes in physical properties of these butadienestyrene (77/23) tread stocks by exposure to gamma-rays. The apparent useful lifetime of these vulcanizates in the absence of radiation retarders is approximately 100 Mrep. Corresponding changes in crosslink density and nonequilibrium modulus values demonstrate experimentally the utility of these measurements to provide a fundamental basis for studying network damage to rubber by radiation.

The use of changes in tensile strength values to provide fundamental information about radiation damage to polymers is vitiated by the fact that this property does not depend simply on the number of radiation-induced network chains. Tensile strength also depends on the production of chain ends from scission and the accumulation of short network chains. Figure 4 shows that the over-compensation of radiation-induced scission by crosslinking serves to

minimize changes in tensile strength, which would be drastically decreased in

the absence of compensation.

E. Effect of air.—The radiation resistance of a vulcanizate depends also on the surrounding atmosphere. Previous work has shown that the presence of oxygen during irradiation of polymers tends to stabilize free radicals produced by scission and prevent their recombination³². The data in Table III show that the substitution of air for helium does not necessarily alter the change in 100% modulus, and hence does not affect the balance between crosslinking and scission. The lack of uniform change to the network with this substitution indicates that such changes depend on the interplay of polymer radicals, oxygen, and compounding ingredients during irradiation. Some aspects of this interplay will be discussed in Part II.

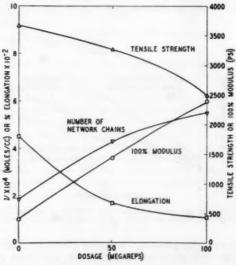


Fig. 4.—Effect of gamma-rays on the physical properties of a completely cured butadiene-styrene (77/23) tread vulcanizate (50 phr HAF black) in a helium atmosphere. For vulcanization recipe see Appendix A, Table III.

PART II. RADIATION RESISTANCE OF HIGH-STYRENE BUTADIENE-STYRENE (59/41) TREAD STOCKS

A. Effect of increased styrene content and oil extension.—Manion and Burton³² show that aromatic groups can exert protective effects by intermolecular energy transfer. Alexander and Charlesby^{34, 35} were able to demonstrate intramolecular energy transfer with a copolymer of isobutylene and styrene. An increase in radiation resistance of butadiene-styrene rubbers would be expected with an increase in styrene content. Extension of the polymeric network with an aromatic oil would be another means of reducing radiation damage by intermolecular energy transfer. Crosslinking would be diminished also by the increase in distance between adjacent polymer chains caused by oil extension. Data in Figure 5 show that the radiation resistance of butadiene-styrene tread stocks increases moderately with styrene content and dramatically with oil extension.

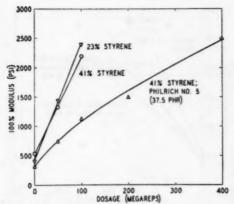


Fig. 5.—Effect of styrene content and oil extension on the radiation resistance of butadiene-styrene tread stocks (50 phr HAF black) in a helium atmosphere. For vulcanization recipe see Appendix A, Table IV.

B. Effect of oil extension, undercure, antirads, and irradiation atmosphere.—The radiation resistances (changes in 100% modulus) of a number of butadiene-styrene tread vulcanizates with high styrene content are shown in Table IV. Typical changes with radiation exposure are shown in Figures 6 and 7. These data show that undercuring and addition of antirads to the vulcanization recipe may be used to advantage to prolong the life of high-styrene cold rubber tread stocks, both in the presence and absence of oil extension. The presence of oil tends to lessen the protection afforded by undercuring and antirads; this result is consistent with the dilution of inhibitor in the rubber matrix. However, the stabilizing effect of oil more than compensates for this disadvantage.

TABLE IV

EFFECT OF OIL EXTENSION, UNDERCURE, ANTIRADS, AND IRRADIATION ATMOSPHERE ON THE RADIATION RESISTANCE OF HIGH-STYRENE BUTADIENE-STYRENE (59/41) TREAD STOCKS ^a

Change in 100% modulus, psi, after the indicated dosage Not oil-extended Oil-extended Helium Air Helium Antirad (5 phr) Mrep Undercure None Akroflex C 710 680 750 740 Antiox 4010 Thio-2-naphthol 2690 2590 490 2,5-Diphenyloxazole g-Naphthylphenyl-oxazole Fully cured 450 450 None Akroflex C 1680 810 730 1750 1110 850 1090 $\frac{1500}{1600}$ Antiox 4010 Thio-2-naphthol 2.5-Diphenyloxasole a-Naphthylphenyl-oxazole

^a For vulcanization recipe see Appendix A, Table IV.

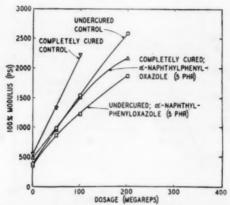


Fig. 6.—Effect of undercure and antirad on the radiation resistance of high-styrene butadiene-styrene (59/41) tread vulcanizates (50 phr HAF black) in a helium atmosphere. For vulcanization recipe see Appendix A, Table IV.

Figures 8 and 9 show typical changes in swelling and stress-strain properties of vulcanizates compounded for radiation resistance. The lack of linearity in the changes in crosslink density and in the dependent modulus values with dosage is indicative of variations in the rate of crosslinking and scission after the vulcanizates have been exposed to a considerable amount of radiation. The apparent decrease in the ratio of crosslinking to scission with dosage serves to prolong the life of a vulcanizate in a radiation field. Comparison of these results with those in Table III and Figure 4 shows that the projected lifetime, i.e., when the elongation reaches 100%, of butadiene-styrene tread stocks has been increased by a factor of 5 to 6 by relatively simple and straightforward compounding techniques.

The data in Table IV show also that substitution of air for helium as an irradiation atmosphere generally causes a slight increase in the lifetime of these

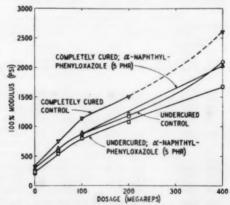


Fig. 7.—Effect of undercure and antirad on the radiation resistance of Philrich-extended (37.5 phr) high-styrene butadiene-styrene (59/41) tread vulcanizates (50 phr HAF black) in a helium atmosphere. For vulcanization recipe see Appendix A, Table IV.

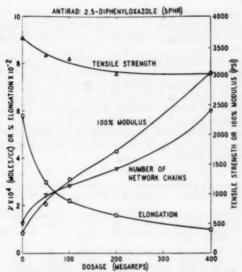


Fig. 8.—Effect of gamma-rays on the physical properties of an undercured butadiene-styrene (59/41) tread vulcanizate (50 phr HAF black) in a helium atmosphere. For vulcanization recipe see Appendix A, Table IV.

vulcanizates in a gamma-ray field; this result is similar to that described in Part I.

C. Network damage during irradiation.—The net effect of radiation on vulcanizates can be surmised from changes in stress-strain properties. Such changes can be explained qualitatively from a knowledge of the effect of cross-linking and scission on these properties. However, to obtain an understanding of radiation damage to vulcanizates, swelling and stress relaxation techniques

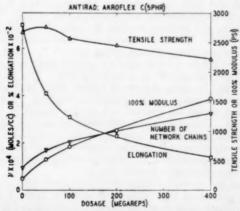


Fig. 9.—Effect of gamma-rays on the physical properties of an undercured Philrich-extended (37.5 phr) butadiene-styrene (59/41) tread vulcanizate (50 phr HAF black) in a helium atmosphere. For vulcanization recipe see Appendix A, Table IV.

must be used to obtain more quantitative estimates of changes in the polymeric network. The relative amounts of the concomitant crosslinking and scission that take place on a microscopic scale have a profound effect on the macro-

scopic properties.

Table V lists the combined results of swelling and stress relaxation results obtained with high-styrene butadiene-styrene tread stocks. Some assumption must be made about the locus of scission to determine the extent of scission. The most consistent results were obtained when calculations were based on the a priori expectation of random scission of main chains [Equation (3)]. A perusal of the data in Table V indicates the following.

(1) Undercuring retards both crosslinking and scission; crosslinking is retarded to a much greater extent, to give a net decrease in the number of radia-

tion-induced network chains.

		Undercured stocks				Fully cured stocks			
Antirad (5 phr)	Dosage, Mrep	v×104, moles/ ee	s×104, moles/ ee	r×104, moles/ cc	7/2	»×104, moles/ ec	a×104, moles/ cc	r×104, moles/ cc	r/a
None	50	1.18	1.09	2.27	2.08	1.66	1.18	2.84	2.40
	100	1.90	1.62	3.53	2.17	2.64	1.67	4.31	2.58
Akroflex C	50	1.18	1.07	2.25	2.10	1.10	1.32	2.42	1.83
	100	1.62	1.61	3.23	2.01	2.00	1.70	3.70	2.18
Antiox 4010	50	1.10	1.03	2.13	2.07	1.22	1.10	2.32	2.11
	100	1.58	1.58	3.16	2.00	1.88	1.61	3.49	2.17
Thio-2-naphthol	50	1.08	0.71	1.79	2.52	1.33	0.78	2.11	2.71
2 mo 2 maphinos	100	1.48	1.16	2.64	2.28	2.32	1.16	3.49	3.01
2.5-Diphenyloxasole	50	1.20	0.96	2.16	2.27	1.12	1.14	2.26	1.98
2,0-Diphenyloxasole	100	1.62	1.40	3.02	2.16	1.86	1.62	3.48	2.15
a-Naphthylphenyl-	50	0.99	1.09	2.08	1.91	1.17	1.06	2.23	2.10
oxazole	100	1.81	1.46	3.27	2.24	1.85	1.60	3.45	2.10

^a For vulcanization recipe see Appendix A, Table IV.

(2) The number of radiation-induced network chains is retarded by the presence of antirads. With the exception of thio-2-naphthol, the antirads protect by retarding crosslinking to a much greater extent than scission in both undercured and fully cured stocks. Thio-2-naphthol is unique in this

group, since it retards crosslinking and scission about equally.

(3) Undercuring and antirads decrease the ratio of crosslinking to scission, r/s, during irradiation. These values are two to three times smaller than those obtained with similar systems without curing agents^{26, 36}. Most of the original network chains are lost by scission after a relatively small dosage compared to the lifetime of these vulcanizates in a radiation field. This indicates a rather dynamic making and breaking of network chains, which gradually accumulate because of the predominance of the crosslinking reaction. The accumulation of network chains causes the gradual and similar change in 100% modulus shown in Figure 8. Retardation of accumulation of network chains by undercuring and antirads increases the longevity of the vulcanizates in a radiation field. The relatively minor changes in tensile strength with dosage indicate that most of the scissions determined by stress relaxation must ultimately lead to crosslinking which compensates for this change.

Table VI lists the network damage results obtained with oil-extended vulcanizates. Comparison of these data with those in Table V show that the presence of an aromatic oil increases the amount of scission and decreases greatly

the amount of crosslinking.

The results are consistent with stabilization of chain ends produced by scission by the aromatic oil and with a decrease in the possibility of crosslinking

of adjacent polymer chains when in the swollen condition.

Undercuring of oil-extended vulcanizates promotes both crosslinking and scission. The residual vulcanization intermediates interact with oil to promote damage to the network. Little change in crosslink density takes place with dosage, because the promotion affects crosslinking and scission almost equally. This explains why undercuring does not provide as much protection in the presence as in the absence of oil.

The action of antirads in oil-extended stocks is different also. All of the antirads, tested with the exception of thio-2-naphthol, retarded both crosslinking and scission to about the same extent; thio-2-naphthol promoted crosslinking and scission to an equal extent. Both types of antirad activity resulted in little net change in crosslink density with increased irradiation to bring little

TABLE VI

RADIATION-INDUCED CROSSLINKING AND SCISSION OF OIL-EXTENDED BUTADIENE-STYRENE [59/41) TREAD STOCKS IN A HELIUM ATMOSPHERE ^a

		Undercured stocks				Fully cured stocks			
Antirad (5 phr)	Dosage, Mrep	ν×10 ⁴ , moles/	s×104, moles/ ee	r×104, moles/ ee	r/s	ν×104, moles/ ee	*×104, moles/ ee	r×104, moles/ ce	7/8
None	10	0.24	0.40	0.64	1.60	0.26	0.43	0.69	1.60
	30	0.62	1.82	2.44	1.34	0.51	1.12	1.63	1.45
Akroflex C	10	0.40	0.34	0.74	2.18	0.30	0.30	0.60	2.00
	30	0.73	0.91	1.64	1.80	0.55	0.97	1.52	1.57
Antiox 4010	10	0.33	0.41	0.74	1.81	0.38	0.27	0.65	2.40
	30	0.56	0.87	1.43	1.64	0.48	0.68	1.16	1.71
Thio-2-naphthol	10	0.27	0.52	0.79	1.52	0.33	0.63	0.96	1.52
	30	0.69	2.38	3.07	1.29	0.76	2.13	2.89	1.36
2,5-Diphenyloxazole	10	0.24	0.41	0.65	1.59	0.21	0.43	0.64	1.49
-,,	30	0.61	1.95	2.56	1.31	0.53	1.30	1.83	1.41
1-Naphthylphenyl-	10	0.25	0.34	0.59	1.73	0.22	0.49	0.71	1.45
oxazole	30	0.58	1.53	2.11	1.38	0.55	1.07	1.62	1.51

⁶ For vulcanization recipe see Appendix A, Table IV.

change in macroscopic properties, e.g., 100% modulus. Apparently, the almost complete compensation of scission by crosslinking during irradiation in this more dynamic network preserves the tensile strength of the oil-extended vulcanizates.

Both undercuring and antirads in general do not greatly affect the ratio r/s of crosslinking to scission, in these oil-extended vulcanizates. Such values are lower in the presence than in the absence of oil. These measurements show that the relatively good radiation resistance of oil-extended stocks is due to a de-

crease in the predominance of crosslinking over scission.

Although quantitative data are not available, the substitution of air for helium as an irradiation atmosphere increased the amount of scission to such an extent that the test samples were completely relaxed after the exposures shown in Tables V and VI. This result is consistent with the findings of others^{37–40}, who propose that the presence of oxygen serves to stabilize free radicals produced as a result of scission. These results combined with changes in 100% modulus shown in Table IV suggest that, even though there are apparent increases in crosslinking and scission, the number of radiation-induced effective network chains is not greatly altered when air is substituted for helium as the irradiation atmosphere.

V. CONCLUSIONS

The radiation resistance of butadiene-styrene cold rubber vulcanizates reinforced with carbon black can be increased materially by increasing the styrene content of the rubber, by extension of rubber with an aromatic oil, by incomplete curing with an accelerated sulfur vulcanization system, and by incorporation of retarders of radiation damage. Incomplete curing produces vulcanization intermediates which are affected by the ratio of sulfur to accelerator and

by cure temperature to retard radiation damage.

Results of swelling and stress relaxation measurements indicate that extension of the polymeric network with an aromatic oil increases the amount of chain scission during irradiation and decreases the amount of crosslinking to produce a correspondingly more radiation-resistant material. These measurements also show that in the absence of oil the decrease in radiation damage obtained by incomplete curing and with antirads is primarily the result of retardation of crosslinking. However, in the presence of oil, incomplete curing promotes and antirads retard radiation-induced crosslinking and scission about equally. Substitution of air for helium as an irradiation atmosphere accentuates the scission reaction to diminish moderately the changes in stress-strain properties.

SYNOPSIS

Compounding techniques to improve the radiation resistance of butadienestyrene tread vulcanizates in a radiation field are described. These include extension of rubber with an aromatic oil, incomplete curing of stocks containing sulfur vulcanization agents, and incorporation of additives. Incomplete curing produces vulcanization intermediates, which are affected by the ratio of sulfur to accelerator and by cure temperature and which are resistant to radiation. A combination of all these factors improved the lifetime of cold-rubber tread vulcanizates by a factor of 5 to 6. Swelling and stress-relaxation techniques are applied to follow quantitatively changes in the polymeric network, which are used to explain changes in stress-strain properties. These techniques indicate that much of the scission that occurs is more than compensated for by crosslinking. Dilution of the polymer network with an aromatic oil decreases the ratio of crosslinking to scission to produce a more radiation-resistant material. In the absence of oil, the decrease in radiation damage obtained by incomplete curing and with antirads is primarily the retardation of the crosslinking reaction. However, in the presence of oil, incomplete curing promotes and antirads retard radiation-induced crosslinking and scission about equally. Substitution of air for helium as an irradiation atmosphere serves to accentuate the scission reaction and to lessen radiation-induced changes in physical properties. A number of previously unreported retarders of radiation damage (antirads) are described.

ACKNOWLEDGMENT

The author would like to thank Dr. G. Kraus for many helpful suggestions and discussions during the course of this work.

APPENDIX A

VULCANIZATION RECIPES FOR RADIATION RESISTANCE STUDIES

Compounding recipes for gamma vulcanizates consisted of rubber, reinforcing filler (50 phr HAF Black), and the antioxidant Flexamine. The com-

pounding recipes used to produce the other chemically vulcanized stocks are given in Appendix Tables I-IV.

APPENDIX TABLE I RECIPE FOR STOCKS OF TABLE I

	Parts
Butadiene-styrene (77/23) ^a	100
Philblack-O (HAF black)	50
Zinc oxide	3
Stearic acid	1
Sulfur	Variable
Santocure	Variable
Flexamine	1

a Philprene 1500.

APPENDIX TABLE II RECIPE FOR STOCKS OF TABLE II

	Parts
Butadiene-styrene (77/23)a	100
Philblack-O (HAF black)	50
Zinc oxide	3
Stearic acid	1
Sulfur	1.75 or 0
Altax	1.8 or 0
G.M.F.	0 or 5
Flexamine	1

⁴ Philprene 1500.

APPENDIX TABLE III

RECIPE FOR STOCKS OF TABLE III AND APPENDIX D

	Parts
Butadiene-styrene (77/23)a	100
Philblack-O (HAF black)	50
Zinc oxide	3
Stearic acid	1
Sulfur	1.75
Santocure	1
Flexamine	1
Antirad (variable)	5

a Philprene 1500.

APPENDIX TABLE IV

RECIPE FOR STOCKS OF TABLES IV, V, AND VI

	Parts
Butadiene-styrene (77/23)°	100 or 0
Butadiene-styrene (59/41)	100 or 0
Philrich No. 5 (highly aromatic)	37.5 or 0
Philblack-O (HAF black)	50
Zinc oxide	3
Stearic acid	1
Sulfur	1.75
Santocure	1
Flexamine	1
Antirad (variable)	5

⁴ Philprene 1500.

APPENDIX B

A GLOSSARY OF COMPOUNDING AGENTS

	CHANGE CONTRACTOR OF THE CONTR	The state of the s	
Altax:	Benzothiazyldisulfide	Flexamine:	Reaction product of a diarylamine ke
Akroflex C:	Phenyl-1-naphthylamine (65%) and N,N' -diphenyl- p -phenylenediamine		tone aldeby de with N, N' -diphenyl-phenylenediamine
	(35%)	GMF:	p-Quinonedioxime
Antiox 4010:	N-Cyclohexyl-N'-phenyl-p-phenylene-	Santocure:	N-Cyclohexyl-2-benzothiazole sulfen-
	diamine		amide

APPENDIX C-1

Physical Properties of Butadiene-Styrene (77/23) Tread Stocks after Various Exposures to Gamma-Rays in Various Atmospheress

				Helium	num			Air		
Antirad (5 phr)	Cure time at 307° F, min	Dosage, Mrep	Mod- ulus,	Tensile strength,	Elon-gation,	noles/	Mod- ulus,	Tensile strength,	Elon- gation,	moles,
None	93	0	970	9740	550	0.03	950	0696	9/	200
	2	20	0+6	2660	061	3 35	850	0000	020	0.00
		100	1570	2890	170	4.80	1590	3270	160	06.4
	45	0	400	3670	450	1.83	420	3780	460	1.75
		20	1440	3270	170	4.31	1240	3330	061	4.00
		100	2400	2490	110	5.50	2480	2750	110	6.10
Akroflex C	13	0	230	2490	099	0.85	240	2600	610	0.91
		20	650	3310	320	2.50	560	3880	420	2.15
		100	1100	2770	200	3.30	1070	3400	240	3.80
	45	0	380	3760	530	1.75	390	4120	520	1.77
		20	950	3310	240	3.80	740	3550	300	2.95
		100	1510	2750	150	4.60	1230	3490	210	4.50
Antiox 4010	18	0	300	3450	570	1.42	290	3210	290	81
		20	088	3220	270	3.40	740	3440	310	2.55
		100	1340	2950	180	4.50	1190	3150	200	3.60
	20	0	370	3780	510	1.70	370	3770	560	1.58
		20	006	3380	250	3.80	830	3590	280	3.05
		100	1450	2890	160	4.70	1430	2720	160	4.15
Thio-2-naphthol	20	0	250	2680	590	1.14	240	2990	089	1.12
		20	720	3500	310	2.95	640	3410	350	2.65
		100	1070	3030	210	4.00	1030	3370	240	3.40
	45	0	270	3200	610	1.36	270	3250	630	1.41
		20	260	3710	300	3.25	730	3970	340	2.95
		100	1280	3290	180	4.40	1230	3490	210	4.50

· For vulcanization recipe see Appendix A, Table III or IV.

APPENDIX C-1—(Continued)

				Helium	un			Air		
Antirad (5 phr)	Cure time at 307° F, min	Dosage, Mrep	Mod- ulus,	Tensile strength,	Elon-gation,	moles/	Mod- ulus,	Tensile strength,	Elon-gation,	"X 104, moles/
,5-Diphenyloxazole	12.5	0	240	2990	650	1.01	230	2460	630	0.72
		20	720	3740	330	2.65	520	3740	440	1.95
		100	1150	3190	210	3.50	1050	3220	220	3.20
	45	0	370	3900	480	1.85	390	3650	460	1.75
		50	940	3440	240	4.05	890	3160	230	3.05
		100	1510	2860	150	4.60	1390	2940	170	4.60
-Naphthylphenyloxazole	13	0	240	2890	630	1.02	220	2330	610	0.80
		20	099	3580	350	2.55	510	3340	380	2.15
		100	1160	2960	200	3.50	1020	3290	230	3.50
	45	0	370	4270	200	1.80	370	3980	510	1.60
		20	1010	3310	230	3.65	820	3400	260	3.05
		100	1490	2630	150	4.50	1380	3200	180	4.50

APPENDIX C-2

PHYSICAL PROPERTIES OF HIGH-STYRENE BUTADIENE-STYRENE (59/41) TREAD SPOCKS AFTER VARIOUS EXPOSURES TO GAMMA-RAYS IN VARIOUS ATMOSPHERES

				Y				1		
Antirad (5 phr)	Cure time at 307° F, min	Dosage, Mrep	Mod- ulus,	Tensile strength, psi	Elon- gation,	noles/	Mod- ulus,	Tensile strength, psi	Elon-gation,	moles,
None	13	0	380	3760	550	1.30	380	3760	550	1.30
		20	940	3920	320	2.16	086	3990	310	2.48
		100	1330	3480	230	2.84	1550	3640	210	3.2
		200	2800	3160	110	4.70	2590	3390	130	3.8
		400	1	3110	75	7.3	1	3120	75	8.0
	45	0	540	4020	440	1.60	540	4020	440	1.6
		20	1220	3880	250	2.88	1330	3530	210	3.2
		100	1810	3410	170	3.48	2220	3030	130	4.2
		200	1	2910	08	6.50	ca. 3380	2690	200	5.6
		400	1	2740	20	12.9	1	2510	40	14.3
Akroflex C	12	0	380	3670	530	1.30	380	3670	530	1.3
		20	750	3610	340	2.32	098	3660	320	2.4
		100	1060	2850	220	2.70	1200	3370	230	2.9
		200	2000	3360	150	3.94	1760	3200	170	3.4
		400	2500	2900	115	5.9	2930	2930	100	6.1
	45	0	200	4290	480	1.60	200	4290	480	9.1
		20	930	3740	290	2.62	1060	3480	250	2.7
		100	1310	3330	220	3.16	1730	3360	170	3.6
		200	2550	3360	130	5.24	2260	3270	135	4.3
		400	1	2650	20	3.5	1	3240	3	8.6
Antiox 4010	12	0	360	3830	580	1.36	360	3830	580	1.3
		20	830	3730	340	2.26	840	3640	330	2.4
		100	1070	3380	270	2.76	1210	3470	240	2.9
		200	1980	3200	160	3.74	1820	3530	180	3.5
		400	2960	3070	105	5.8	3310	3310	100	5.9
	45	0	460	4100	510	1.48	460	4100	510	1.4
		20	950	4030	320	2.60	066	3830	300	2.7
		100	1270	3520	240	3.05	1570	3550	200	3.3
		200	2530	3380	130	4.86	2140	3100	135	4.2
		400	1	2960	00	I I	1	OSSE	20	10

For vulcanization recipe see Appendix A, Table IV.

APPENDIX C-2—(Continued)

Cure at a continued (5 phr) The continue at a continue					Heli	Jelium			Air			
31 0 330 3480 600 1.32 3490 600 50 740 3820 360 2.26 750 3480 600 200 1010 3820 360 2.26 750 3490 230 200 1900 2920 320 110 6.3 3690 240 230 3490 3430 3490 3490 230 3490 3400	Antirad (5 phr)	Cure time at 307° F,	Dosage,	Mod- ulus,	Tensile strength,	Elon- gation,	moles/	Mod-	Tensile strength,	Elon- gation,	10°, moles/	
50 750 740 3420 360 2.25 750 3480 600 100 1010 3590 270 2.25 750 3680 3490 340 200 1900 3800 145 3.56 1150 2470 145 200 1900 2200 1120 380 3180 310 145 100 1120 380 4140 320 2.64 890 3490 140 100 1120 380 4140 320 2.64 890 3490 140 200 1120 3600 240 3.64 380 380 310 140 380 380 380 310 140 380 380 170 140 380 380 170 380 380 170 380 170 380 170 380 170 380 170 180 380 180 180 180 180	Thio-2-nanhthol	23.1	0	086	0016	000	300	and one	rad	0/	99	
75 90 1740 3820 370 2.20 1740 3430 230 200 1900 3010 145 3.56 1140 3430 230 200 1900 3010 145 3.56 1550 2470 140 200 1900 3010 145 3.56 1590 3470 100 100 1120 3800 270 2.24 170 1480 380 3180 <td>Toman June Come</td> <td>10</td> <td>0 0 0 0</td> <td>240</td> <td>00000</td> <td>000</td> <td>1.52</td> <td>330</td> <td>3480</td> <td>909</td> <td>1.32</td> <td></td>	Toman June Come	10	0 0 0 0	240	00000	000	1.52	330	3480	909	1.32	
75 0 390 390 140 350 145 350 1540 240 145 250 145 145 250 145 145 240 145 145 240 145 145 3490 3780 145 145 145 3490 3780 146 1480 380 3780 310 145 470 1480 380 3780 310 145 470 1480 380 170 1480 380 3780 380 170 1480 380 170 1480 380 170 1480 380 170 1480 380 170 170 170 170 170 170 170 170 170 180 380 120 380 120 180 380 180 180 380 180 180 180 180 180 180 180 180 180 180 180 180 180 180 180			89	0101	3500	920	2.20	00/	3660	340	2.40	
75 400 2920 3201 145 355 1550 3470 145 50 390 3780 380 1.35 3920 3780 190 100 1120 380 3780 380 1.35 3920 3780 190 200 1120 360 240 3.06 1480 3490 3780 380 200 1970 3170 145 4.70 1980 3490 170 200 1970 3170 145 4.70 1980 3490 170 200 1970 3170 360 2.22 830 3490 170 100 1050 3470 260 2.80 1250 3280 160 200 1050 3470 260 2.80 1460 3040 170 400 360 380 2.22 83 340 160 400 360 380 2.80 <td></td> <td></td> <td>900</td> <td>00001</td> <td>0000</td> <td>27</td> <td>70.7</td> <td>1140</td> <td>3430</td> <td>230</td> <td>7.80</td> <td></td>			900	00001	0000	27	70.7	1140	3430	230	7.80	
75 400 22920 33200 110 6.3 3920 100 75 400 2390 3780 580 1.35 3920 3920 100 100 1120 3600 240 2.64 890 3450 190 200 1970 3170 145 4.70 1950 3490 370 200 1970 3170 145 4.70 1950 3490 170 200 1970 3170 360 2.22 280 170 400 7.80 3770 360 2.22 830 320 160 400 3020 3240 160 2.80 1250 3280 220 400 3020 3240 160 560 2.84 460 460 160 400 3020 3220 160 2.64 460 3040 170 400 3220 3320 2.64 360 </td <td></td> <td></td> <td>200</td> <td>0061</td> <td>3010</td> <td>145</td> <td>3.56</td> <td>1550</td> <td>2470</td> <td>145</td> <td>3.36</td> <td></td>			200	0061	3010	145	3.56	1550	2470	145	3.36	
15 0 330 3780 580 1.35 336 3780 580 1580 100 1120 360 264 890 3378 580 110 1100 1120 3490 3780 580 110 1100		-	400	2920	3200	110	6.3	30.50	3020	100	00.9	
150 880 1440 320 2.64 890 3450 310 200 1120 3600 240 3.06 1480 3450 190 200 1970 3170 145 4.70 1950 3490 170 200 1970 3170 360 2.22 830 3490 170 100 1050 3770 350 2.22 830 3380 180 200 1050 3270 260 2.22 830 3280 160 40 1050 3270 350 1250 3380 160 40 3020 160 2.80 1710 303 160 40 400 3020 160 5.80 3040 170 50 950 3820 160 1.52 460 401 170 400 1320 3820 220 2.64 950 460 401 170		0/	0	380	3780	580	1.35	390	3780	580	1.35	
12 0.00 11120 3600 240 3.06 1450 3450 190 400 1970 3170 145 4.70 1950 3490 170 400 1970 3170 145 4.70 1950 3490 170 50 780 3770 360 2.22 830 3840 300 100 1050 3470 280 2.22 830 3340 300 400 1050 3470 280 2.22 830 3340 300 400 1056 3470 280 2.22 830 3340 300 400 1056 3470 160 2.80 170 330 160 40 460 4050 100 5.80 3040 170 200 2160 460 460 4010 250 2160 3340 170 200 2160 3340 170 200 2160 33			20	890	4140	320	2.64	890	3930	310	2.68	
12 0 1370 145 4.70 1950 3490 170 400 — 2600 80 7.5 — 2860 170 50 780 3770 280 2.22 830 3840 170 400 1050 3470 280 2.22 830 3340 300 40 1050 3470 280 2.22 830 3340 300 40 1050 3470 280 2.22 830 3340 300 40 1050 340 100 5.80 3040 160 220 220 220 3040 400 160 220 220 2160 3040 170 200 2160 3040 170 200 2160 3040 170 200 2160 320 2160 3040 170 200 2160 320 2160 2160 2160 2160 2160 2160 2160			100	1120	3600	240	3.06	1480	3450	190	3.68	
12 0 330 3630 80 7.5 — 2860 80 12 0 330 3630 580 1.22 330 3630 580 200 1050 3470 260 2.22 830 3340 300 200 1050 3270 360 2.22 830 3380 220 40 1050 3270 160 2.80 1750 3380 160 40 3020 3260 100 5.80 3040 100 160 40 460 4050 460 4050 460 460 460 460 50 950 3820 220 300 2.64 950 460			200	1970	3170	145	4.70	1950	3490	170	4.28	
12 0 330 3630 580 1.22 330 3630 580 100 1050 3470 350 2.22 830 3340 300 200 1950 3270 160 2.80 1750 3380 220 400 3020 3220 160 5.80 3040 3030 160 40 3020 3220 160 5.80 3040 3040 100 100 1320 3020 460 400 3040 100 160 100 1320 3020 264 460 4010 290 100 1320 380 2.64 950 4010 170 200 2530 3040 115 5.00 2160 3910 170 13 0 3580 320 2.18 880 380 290 400 2900 370 270 270 320 220			400	1	2600	08	7.5	1	2860	80	7.7	
45 780 3770 350 2.22 830 3340 300 200 1050 3470 260 2.22 830 3340 300 200 1050 3470 260 2.28 1250 3280 220 200 1050 3470 100 5.80 3040 100 400 3020 3020 460 400 3040 100 100 1320 3920 2.64 950 401 290 100 1320 3890 2.64 950 401 170 200 2530 3040 115 5.00 2160 3910 170 400 2530 3640 115 5.00 2160 3910 170 13 0 3560 3280 2.18 880 3380 160 100 1080 3280 24 27 320 290 400 2900	2,5-Diphenyloxazole	12	0	330	3630	580	1.99	230	0886	200	1 99	
100 1050 3470 250 2.72 250 3240 230			20	700	2770	250	200.0	000	0000	000	1.22	
45 400 3260 3260 1750 3280 220 45 400 3020 3260 160 5.80 1710 3380 220 400 3020 3260 160 5.80 3040 3040 160 50 460 3620 100 1.52 460 401 220 100 1320 3820 2.64 950 401 100 460 401 290 100 1320 3520 2.64 950 4010 290 4010 290 400 2530 3040 115 5.00 2160 3910 170 400 2530 3040 115 5.00 2160 3910 170 10 108 3220 2.18 860 3390 290 40 2090 2770 116 270 320 450 40 400 2900 3150 110			895	000	0770	000	77.77	830	3340	300	2.42	
45 0 460 3240 160 5.80 3040 3030 160 45 0 460 4050 3020 3240 160 160 160 50 950 3920 300 2.64 950 4010 400 405 4010 290 100 <td></td> <td></td> <td>000</td> <td>0001</td> <td>3470</td> <td>260</td> <td>5.80</td> <td>1250</td> <td>3280</td> <td>220</td> <td>2.84</td> <td></td>			000	0001	3470	260	5.80	1250	3280	220	2.84	
45 400 3020 3020 100 5.80 3040 3040 100 50 460 4050 460 1.52 460 4050 460 100 1320 3580 220 2.64 950 4010 290 200 2530 3640 115 5.00 2160 3040 170 200 2530 3640 115 5.00 2160 3040 170 13 0 350 4010 580 7.0 7.0 10 100 1080 3280 2.18 860 3380 290 100 1080 3280 240 2.76 1220 3220 290 450 2900 3150 110 5.7 - 3890 450 45 0 450 3840 280 2.46 960 3410 250 100 1220 3840 280 2.46 <			200	1950	3260	160	3.60	1710	3030	160	3.56	
45 0 460 4050 460 1.52 460 465 460		,	400	3020	3020	100	5.80	3040	3040	100	6.01	
$\begin{array}{cccccccccccccccccccccccccccccccccccc$		45	0	460	4050	460	1.52	460	4050	460	1.52	
100 1320 3580 220 3.00 1490 3040 170 200 2530 3040 115 5.00 2160 3910 170 400 2580 350 4010 580 1.25 350 4010 170 100 1080 3220 2.48 860 3380 290 100 1080 3220 240 2.76 1220 3220 290 400 2900 3150 110 5.7 - 3650 90 45 0 450 3840 280 2.46 960 3410 250 100 1220 3840 280 2.46 960 3410 250 100 1220 3870 2.16 360 360 450 200 250 3840 280 2.46 960 3410 250 200 250 3040 3110 3040 3040			20	950	3920	300	2.64	950	4010	290	2.64	
200 2530 3040 115 5.00 2160 3910 170 400 — 2580 115 5.00 2160 3910 170 13 0 350 4010 580 1.25 350 4010 580 100 1080 3280 240 2.18 860 3380 220 200 2090 2770 126 2.76 1870 3220 220 450 2900 3150 110 5.7 — 3350 160 450 3840 450 110 5.7 — 3350 450 50 950 3840 280 2.46 960 3410 250 100 1220 3870 210 3.04 150 3040 170 200 2590 3640 360 3.04 130 40 3040 130 400 — — 80 3.04 </td <td></td> <td></td> <td>100</td> <td>1320</td> <td>3580</td> <td>220</td> <td>3.00</td> <td>1490</td> <td>3040</td> <td>170</td> <td>33.38</td> <td></td>			100	1320	3580	220	3.00	1490	3040	170	33.38	
13 0 350 4010 580 8.1 — 2820 70 13 0 350 4010 580 1.25 350 4010 580 100 1080 3220 2.18 860 3380 290 200 2090 2770 125 3.76 1220 3220 220 45 0 450 3890 450 1.63 460 3890 450 100 1220 3840 280 2.46 960 3410 250 100 1220 3370 210 3.04 1510 3070 170 200 250 3040 115 5.02 2170 3040 130 400 250 3040 115 5.02 2170 3040 170			500	2530	3040	115	5.00	2160	3910	170	4.56	
$\begin{array}{cccccccccccccccccccccccccccccccccccc$			400	1	2580	80	8.1	1	2820	20	30	
$\begin{array}{cccccccccccccccccccccccccccccccccccc$	a-Naphthyl-	13	0	350	4010	580	1.25	350	4010	580	1 95	
$\begin{array}{cccccccccccccccccccccccccccccccccccc$	phenyloxazole		20	260	3580	320	2.18	098	3380	290	2.94	
$\begin{array}{cccccccccccccccccccccccccccccccccccc$			100	1080	3220	240	2.76	1220	3220	220	3.06	
400 2900 3150 110 5.7 — 3050 90 0 450 3800 450 1.53 480 3890 450 50 950 3840 280 2.46 960 3410 250 100 1220 3370 210 3.04 1510 3070 170 200 2590 3040 115 5.02 2170 3040 130 400 3200 80 6.4 — 2750 70			200	2090	2770	125	3.70	1870	3230	160	000	
$ \begin{array}{cccccccccccccccccccccccccccccccccccc$			400	2900	3150	110	5.2		3050	96	5 80	
950 3840 280 2.46 960 3410 250 1220 3370 210 3.04 1510 3070 170 2500 3040 115 5.02 2170 3040 130 - 3200 80 6.4 - 2750 70		45	0	450	3800	450	1.53	480	3890	450	1.53	
$\begin{array}{cccccccccccccccccccccccccccccccccccc$			20	920	3840	280	2.46	096	3410	250	2.70	
$\begin{array}{cccccccccccccccccccccccccccccccccccc$			100	1220	3370	210	3.04	1510	3070	170	30,00	
3200 80 6,4 - 2750 70			200	2590	3040	115	5.02	2170	3040	130	4.40	
			400	1	3200	98	6.4	1	2750	20	62.5	

For vulcanization recipe see Appendix A, Table IV,

Physical Properties of Oil-Extended; High-Styrene Butadiene-Styrene (59/41) Tread Stocks After Various Exposures to Gamma-Rays in Various Atmospheres. APPENDIX C-3

			-	1				W	J.	
	time at		100% Mod-	Tensile	Flon	×	100%			×
Antirad (5 phr)	307° F.	Dosage,	ulus,	strength,	gation,	moles/	-bod-	Tensile	Elon-	10,
None		days	per	per	%	00	pei	Del	gation,	Moth
one	15	0	210	2700	670	1.04	210	9700	020	0.
		200	550	2700	380	1.56	270	0000	000	5.1
		100	880	2510	260	1.96	750	9730	080	1.0
		200	1170	2310	180	9.50	1930	00000	070	7.7
		400	2100	2100	100	2000	1050	0807	0/1	2.5
	45	0	320	2640	480	0.00	0061	2180	105	3.6
		20	750	0000	200	1.44	320	2640	480	1.4
		100	200	2000	270	2.0.2	720	2720	300	1.0
		000	0411	2030	210	2.65	1040	2400	006	0.4
		200	1510	2410	150	3.10	1790	9910	190	4.0
		400	ca. 2500	2430	95	4.60	2170	2240	105	4.5
Akroflex C	2.5	•	000						000	7.0
	OT	0	200	2680	200	96.0	200	2680	200	00
		25	230	2770	410	1.70	590	9730	310	0.0
		001	740	2580	310	2.04	670	9710	020	0.7
		200	1010	2460	230	9 50	1170	0700	000	7.7
		400	1560	9930	140	0.00	2110	0107	190	7.4
	45	0	330	0000	000	0.50	0/01	0222	130	3.4
		2	000	01.00	020	1.45	330	2940	520	1.4
		35	000	0087	340	1.95	590	2830	360	10
		000	930	2480	230	2.84	780	2680	280	0.4
		200	1210	2430	185	2.95	1470	9300	150	40
		400	2030	2550	120	3.98	1830	2350	130	n co
Antiox 4010	1.4	0	000	0000	000					
		5	077	2830	000	1.10	220	2830	099	11
		397	000	0607	370	1.70	260	2860	410	1 65
		000	200	2400	260	2.25	069	2740	350	50
		200	970	2270	210	2.35	1120	9340	100	0.10
	-	400	1590	2250	140	3.26	1530	0706	140	20.0
	9/	0	290	2810	550	1 30	000	0100	047	3.30
		20	650	2890	350	100	240	0107	000	1.32
		100	068	2480	240	9.44	240	0007	070	20.
		200	1140	9500	010	25.40	050	2410	270	2.38
		400	0000	0000	OTA	6.10	1.580	7380	160	2.99

APPENDIX C-3—(Continued)

Autirad (5 pht) time there are a control of part and part and part and part are a control of part and					Helium				Au		
45 0 180 2350 730 1.23 180 2350 730 2.24 620 2860 420 420 100 670 2860 240 1.80 480 2860 420 420 100 670 2860 240 2.24 620 2860 360 360 200 200 670 2880 140 2.50 1040 2890 360 360 200 2280 140 2.50 1040 2280 120 2280 140 2.50 1040 2280 120 2280 140 2.50 1.92 280 2280 140 360 2.25 280 2280 140 2.60 1.24 220 2280 670 2280 1.92 280 2.00 2.00 2.00 2.00 2.00 2.00 2.00	Antirad (5 phr)	Cure time at 307° F,	Dosage, Mrep	Mod- ulus,	Tensile strength,	Elon-gation,	10*, moles/ cc	Mod- Mus,	Tensile strength, psi	Elon- gation,	moles/
100 100	hio-2-nanhthol	45	0	180	2350	730	1.23	180	2350	730	1.23
100 670 2690 320 2.24 620 2690 360 2200 2280 140 2.56 1040 2330 200 400 1600 2280 140 2.56 1040 2280 120 100 220 2280 670 1.24 220 2280 670 100 740 2800 2.46 670 2280 670 200 970 2800 2.46 670 2280 670 400 1810 2290 120 2.90 1130 2250 180 400 1810 2290 120 2.90 1130 2250 180 50 200 270 2800 120 2.90 1130 2250 180 50 200 280 270 280 270 280 280 50 200 280 270 1.98 620 2220 270 50 630 2490 270 1.98 620 270 280 50 630 2490 270 1.96 280 2470 280 50 630 2490 270 1.96 280 2470 280 50 630 2490 270 1.96 280 2470 280 50 630 2490 290 1.00 2.38 780 290 210 50 600 220 230 1.00 4.02 - 1900 50 600 220 230 1.00 2.02 670 2640 50 600 220 230 1.00 2.02 670 2640 50 640 2260 240 240 240 250 50 640 280 240 240 240 240 50 640 280 240 240 240 50 640 280 240 240 240 50 640 280 240 240 240 50 640 280 240 240 240 50 640 280 240 240 240 50 640 280 240 240 240 50 640 280 240 240 240 50 640 280 240 240 240 50 640 280 240 240 50 640 280 240 240 50 640 280 240 240 50 640 280 240 240 50 640 280 240 240 50 640 280 240 240 50 640 280 240 240 50 640 280 240 50 640 280 240 50 640 280 240 50 640 280 240 50 640 280 240 50 640 280 240 50 640 280 240 50 640 250 50 640 250 50 640 250 50 640 250 50 640 250 50 640 250 50 640 250 50 640 250 50 640 250 50 640 250 50 640 250 50 640 250 50 640 250 50 640 250 50 640 25	The standard of the standard o	2	20	480	2850	440	1.80	480	2860	420	1.80
200 920 2550 240 2.50 1040 2330 200 75 400 1600 2280 670 1.24 220 2280 670 100 740 2280 670 1.24 220 2280 670 200 970 2280 670 1.24 220 2280 670 200 970 280 280 2.46 670 2750 380 400 1810 2290 120 3.94 1730 2170 125 200 970 2250 120 3.94 1730 2170 125 200 980 2720 270 1.98 620 2220 270 100 720 2400 270 1.98 620 2220 270 200 1520 2400 270 1.98 620 2220 270 200 1520 2400 270 1.98 620 2220 270 200 280 2400 270 1.96 520 180 290 200 1800 1900 140 2.78 140 280 280 200 1800 2120 190 2.38 180 280 280 200 1800 2120 2120 1.86 580 2970 130 200 1800 2910 390 1.40 2.78 1470 2170 130 200 1800 2450 210 2.00 670 2550 330 200 2120 2120 2120 1.11 220 2550 330 200 2120 2750 280 1.40 2.00 2800 2800 180 200 2120 2120 2120 2120 2130 1.00 4.02 200 200 2000 2910 390 1.40 2.78 1500 2960 540 200 2000 2800 240 2.00 200 200 190 200 190 200 100 200 2800 2800 240 2.00 200 200 190 200 190 200 100 200 2800 2800 240 2.00 200 200 200 100 200 200 200 200 200 2			100	670	2690	320	2.24	620	2690	360	2.18
75 400 1600 2280 140 3.60 1670 2090 120 75 50 2220 2280 670 1.924 220 2280 670 100 740 2600 280 2.46 670 2280 6670 200 970 2290 120 2.90 1130 2260 260 200 970 2240 270 1.98 620 2230 180 200 720 2240 300 1.58 520 2630 610 75 400 1520 1950 195 2.30 1050 2220 270 75 400 1520 2400 2720 1.86 520 2270 270 100 900 2200 1990 140 2.78 1470 270 125 200 1800 2910 390 1.64 560 2670 390 10			200	920	2520	240	2.50	1040	2330	200	2.85
75 0 220 2280 670 1.24 220 2280 670 1.24 220 2280 670 1.00 200 246 670 2240 2300 2.46 670 2250 280 2750 280 200 200 970 2600 2.46 670 2.46 670 2260 2750 280 200 200 970 2600 2240 2.96 1130 2250 180 200 200 980 2240 200 1.58 520 2620 2750 280 270 200 200 980 2720 1.48 520 2020 2770 125 200 2720 2720 2720 2720 2720 2720 272			400	1600	2280	140	3.60	1670	2090	120	3.78
sole 14 0 2910 390 1.92 500 2750 390 200 740 2600 280 2.46 670 2260 360 200 970 2670 280 2.94 1730 2360 2860 200 970 280 2.90 1.15 200 2580 1.10 1.15 260 2630 2610 1.28 520 2630 360 1.28 1.13 2520 1.29 1.11 2.20 2520 1.20 2630 2610 1.15 200 2630 2740 272 2630 2720 2630 2720 2630 2720 2720 280 2720 280 2720 280 2720 280 2720 280 2720 280 2720 280 2720 280 280 280 280 280 280 280 280 280 280 280 280 280 280 280		25	0	220	2280	670	1.24	220	2280	670	1.24
zole 14 0 2600 280 2.46 670 2260 260 260 260 200 200 200 970 2290 120 2.90 1130 2350 180 180 200 1810 2290 120 2.90 1130 2350 125 180 125 200 260 2240 270 1.58 520 2630 610 220 200 2240 270 1.98 620 2220 270 196 200 2720 270 1.98 620 2220 270 270 196 200 2720 2720 2720 2720 2720 2720 2720			50	570	2910	390	1.92	200	2750	390	1.90
zole 14 0 250 250 120 3.94 1730 2350 180 zole 14 0 200 2530 610 1.15 200 2530 610 100 720 2240 300 1.58 520 2220 270 200 980 2190 195 2.30 1050 2210 120 75 400 1520 120 3.32 1510 1910 125 100 200 250 2720 2770 1.98 620 2270 360 200 1520 1950 1.20 3.32 1510 125 290 170 126 2720 2770 290 2770 290 2770 290 2770 290 2770 290 2770 290 290 290 290 290 290 290 290 290 290 290 290 290 290 290			100	740	2600	280	2.46	670	2260	260	2.42
aole 14 0 2290 120 3.94 1730 2170 125 aole 14 0 200 2530 610 1.15 200 2530 610 100 720 2240 270 1.15 200 2530 610 200 980 2240 270 1.48 620 2220 370 200 980 180 272 120 3.32 1510 130 180 75 400 150 2720 520 1.40 260 2720 520 100 900 270 2790 1.28 580 2470 180 200 1300 1990 140 2.78 1470 2170 130 200 1300 290 120 140 2.78 1470 2170 130 400 2120 250 1.00 4.02 - 1900 96 5			200	970	2670	230	2.90	1130	2350	180	2.98
sole 14 0 200 2530 610 1.15 200 2530 610 100 720 2240 300 1.58 520 2630 360 200 980 2190 272 1.98 620 2220 370 200 980 1520 120 3.32 1510 190 120 75 400 1520 120 3.32 1510 190 120 100 260 2720 27			400	1810	2290	120	3.94	1730	2170	125	4.30
$\begin{array}{cccccccccccccccccccccccccccccccccccc$	5-Diphenvloxazole	14	0	200	2530	610	1.15	200	2530	610	1.15
$\begin{array}{cccccccccccccccccccccccccccccccccccc$			20	540	2240	300	1.58	520	2630	360	1.58
$\begin{array}{cccccccccccccccccccccccccccccccccccc$			100	720	2400	270	1.98	620	2220	270	1.90
$\begin{array}{cccccccccccccccccccccccccccccccccccc$			200	086	2190	195	2.30	1050	2210	180	2.42
$\begin{array}{cccccccccccccccccccccccccccccccccccc$			400	1520	1950	120	3.32	1510	1910	125	3.42
50 630 2490 290 1.86 580 2470 290 200 100 900 2100 190 2.38 780 2080 210 200 1300 1300 140 2.78 1470 2170 130 400 2120 2120 140 2.78 - 1900 95 16 0 220 2570 620 1.11 220 2570 95 200 100 810 2750 290 1.64 560 2570 330 200 1080 2450 210 2.30 1160 2540 200 400 1680 2050 130 3.48 1590 2070 125 40 1680 2050 130 2.30 140 290 2070 125 50 640 2060 130 2.36 870 290 50 100 900 2		75	0	260	2720	520	1.40	260	2720	520	1.40
$\begin{array}{cccccccccccccccccccccccccccccccccccc$			20	630	2490	290	1.86	580	2470	290	1.80
200 1300 1300 140 2.78 1470 2170 130 400 2120 2120 100 4.02 — 1900 95 16 0 220 2570 620 1.11 220 2570 620 100 810 2750 390 1.64 560 2670 380 200 1080 2450 210 2.30 1160 2540 20 45 0 300 2450 230 1160 2540 20 50 600 2860 540 1.40 300 2960 540 100 900 2860 240 1.91 610 2910 360 200 120 260 190 2760 190 2770 216 2710 216 200 123 260 190 276 190 2710 210 2150 2150			100	006	2100	190	2.38	780	2080	210	2.36
400 2120 2120 100 4.02 — 1900 95 16 0 220 2570 620 1.11 220 2570 620 200 810 2750 290 2.02 670 2550 330 200 1080 2450 210 2.30 1160 2540 200 400 1680 2050 130 2.30 1160 2540 200 50 1680 2050 130 3.48 1590 2070 125 400 1680 2050 130 3.48 1590 2070 125 50 640 2750 240 1.40 300 2960 540 100 900 2080 240 2.36 870 2770 270 200 1230 2600 190 2.76 1470 2710 150 200 100 200 190 2.20			200	1300	1990	140	2.78	1470	2170	130	2.98
16 0 220 2570 620 1.11 220 2570 620 100 810 2750 390 1.64 560 2670 380 200 100 810 2750 290 2.02 670 2550 330 200 1080 2450 210 2.30 1160 2540 200 45 0 300 2960 540 1.40 300 2960 540 50 640 2750 240 1.91 610 2910 360 100 900 2080 240 2.36 870 2710 270 200 1230 2600 190 2.76 150 271 150 200 1230 2600 190 2.76 1540 2310 150			400	2120	2120	100	4.02	1	1900	95	3.66
50 600 2910 390 1.64 560 2670 360 200 100 810 2750 290 2.02 670 2550 330 200 1080 2450 210 2.30 1160 2540 2070 125 400 1680 2050 130 3.48 1590 2070 125 50 640 2750 540 1.91 610 2940 540 100 900 2880 240 2.36 870 2770 2770 270 200 1230 2600 190 2.76 1470 2710 150 200 2000 190 2.76 1470 2310 150	-Naphthyl-	16	0	220	2570	620	1.11	220	2570	620	1.11
100 810 2750 230 270 2500 330 200 1080 2450 210 2.30 1160 2540 200 400 1680 2050 130 3.48 1590 2070 125 0 300 2960 540 1.40 300 2960 540 100 900 2760 240 2.36 870 2770 270 100 900 2680 240 2.36 870 2770 270 200 1230 2600 190 2.76 1470 2710 150 200 2600 190 2.76 1470 2310 150	phenyloxazole		020	009	2910	390	1.64	260	2670	360	1.66
400 1680 2480 2480 2480 2480 2480 2560 1700 2570 125 0 300 2960 540 1.40 300 2960 540 100 640 2750 320 1.91 610 2910 360 100 200 2880 240 2.36 870 2770 270 200 1230 2860 190 2.76 1470 2310 150 200 2600 190 2.76 1470 2310 150			38	018	27.30	010	2.02	1160	2550	000	2.02
0 300 2960 540 1.40 300 2960 540 540 1.00 50 2960 540 540 1.00 50 2960 540 540 1.01 610 2910 360 540 50 50 50 50 50 50 50 50 50 50 50 50 50			400	1680	2050	130	3.48	1590	2070	125	3.62
50 640 2750 320 1.91 610 2910 360 100 900 2880 240 2.36 870 2770 270 200 1230 2800 190 2.76 1470 2310 150 200 200 250 150 200 150 150		45	0	300	2960	540	1.40	300	2960	540	1.40
900 2680 240 2.36 870 2770 270 1230 2600 190 2.76 1470 2310 150 000 000 000 000 000 000 000 000 0			20	640	2750	320	1.91	610	2910	360	1.96
230 2600 190 2.76 1470 2310 150			100	006	2680	240	2.36	870	2770	270	2.42
			200	1230	2600	361	2.76	1470	2310	150	2.92

APPENDIX D

RETARDERS OF RADIATION DAMAGE TO BUTADIENE-STYRENE (77/23) TREAD STOCKS IN A HELIUM ATMOSPHERE

Antirad	Ratingb
Azobenzene	1.16
Thio-2-naphthol	1.13
Di-tert-butylhydroquinone	1.10
2,5-Diphenyloxazole	1.06
Azoxybenzene	1.06
trans-Stilbene	1.02
Antiox 4010	1.02
α-Naphthylphenyloxazole	1.02
Akroflex C	1
Hydrazobenzene	1
2,6-Dinitrophenol	0.99
2-Phenylbenzothiazole	0.98
Diphenylacetylene	0.97

 $^{\circ}$ For vulcanization recipe see Appendix A, Table III. $^{\circ}$ Rating = (change in 100% modulus with additive after 100 Mrep)/(change in 100% modulus with Akrofex C after 100 Mrep).

REFERENCES

Born, J. W., WADC Technical Report 55-58, Parts I (1954) and II (1955); Army-Navy-Air Force Conference on Elastomer Research, ACR-Y, Vol. 4, Jan. 11-12, 1956, p. 65.

Born, J. W., Mooney, E. E., and Semegen, S. T., Rubber World 139, 379 (1958).

Bauman, R. G., and Born, J. W., J. Appl. Polymer Sci. 1, 351 (1959).

Harrington, R., Rubber Aps 81, 971 (1957); ibid., 82, 461 (1957); ibid., 82, 1003 (1958); ibid., 83, 472 Bauman, R. G., and Born, J. W., J. Appl. Polymer Sci. 1, 301 (1909).
Harrington, R., and Giberson, R., Modern Plastics 36, No. 3, 199 (1958).
Harrington, R., Rubber Age 81, 971 (1957); ibid., 82, 461 (1957); ibid., 82, 1003 (1958); ibid., 83, 472 (1958).
Turner, D. T., J. Polymer Sci. 27, 503 (1958).
Mullins, L., and Turner, D. T., Nature 183, 1547 (1959).
Morris, R. E., Rubber World 140, 435 (1959).
Meyer, G. E., Rubber World 140, 435 (1959).
Wippler, C., Res., Gen. coautchous 36, 369 (1959).
Flory, P. J., and Rehner, J., J. Chem. Phys. 11, 512 (1943).
Flory, P. J., and Rehner, J., J. Chem. Phys. 11, 512 (1943).
Tobolsky, A. V., D. J. Mets, and Mesrobian, R. B., J. Am. Chem. Soc. 72, 1942 (1950).
Tobolsky, A. V., Prettyman, I. B., and Dillon, J. H., J. Appl. Phys. 15, 380 (1944).
Tobolsky, A. V., and Andrews, R. D., J. Chem. Phys. 13, 3 (1943).
Lawton, E. J., Bueche, A. M., and Balwit, J. S., Nature 172, 76 (1953).
Gehman, S. D., and Hobbs, L. M., Rubber World 130, 643 (1954).
Jackson, W. W., and Hale, D., Rubber Age 77, 865 (1955).
Charlesby, A., and Groves, D., Proc. Third Rubber Technol. Conf., London, 1954, p. 317.
Bopp, D. C., and Sisman, O., ORNL-1373 (1953).
Bopp, D. C., and Sisman, O., Nucleonics 13, 28 (July 1955).
Flory, P. J., Chem. Phys. 18, 108 (1950).
Treloar, L. R. G., Trans. Foraday Soc. 39, 36, 241 (1943).
Flory, P. J., Chem. Phys. 18, 108 (1950).
Arnold, P. M., Kraus, G., and Anderson, H. R., Jr., Kautschuk u. Gummi 12, WT27 (1959); Rubber Plastics Age 40, 836 (1956).
Flory, P. J., Chem. Phys. 18, 108 (1950).
Berry, J. P., and Watson, W. F., J. Polymer Sci. 18, 201 (1955).
Berry, J. P., and Matson, W. F., J. Polymer Sci. 18, 201 (1955).
Berry, J. P., and Groves, C. London A230, 136 (1955).
Alexander, P., and Torns, D., J. Polymer Sci. 22, 343 (1

X-RAY DIFFRACTION COMPARISON OF RADIATION DAMAGE IN RUBBER *

W. E. SHELBERG AND L. H. GEVANTMAN

U. S. NAVAL RADIOLOGICAL DEFENSE LABORATORY, SAN FRANCISCO, CALIF.

This paper describes the use of an x-ray diffraction technique to correlate rubber radiation damage with rubber composition. Correlations between radiation damage and composition are useful as guides for the development of superior radiation resistant elastomers to be used as components of mechanical devices installed in high nuclear radiation fields.

Rubber which is stretched and irradiated in an inert atmosphere is readily damaged by chain cleavage, manifested by loss of crystallinity, possible thinning, decreased x-ray diffraction intensities and eventual rupture (Figure 1)¹. Loss of diffraction spot intensity was used to measure radiation damage in stretched rubber, and was tantamount to loss of crystallinity with little speci-

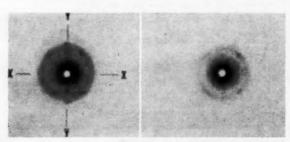


Fig. 1.—Before and after a nearly rupturing dose: x-ray diagrams of a stretched rubber vulcanizate show loss of diffraction intensities upon irradiation. When rubber specimens were positioned on the goniometer of the x-ray diffraction unit with their direction of stretch horizontal, the Geiger counter scanned the amorphous halo along the left hand side of the X axis shown in the pre-irradiation pinhole diagram (left). With the direction of stretch vertical, the counter scanned the upper diffraction spots and the halo between them along the Y axis.

men thinning until just before rupture. Crystalline longevity was determined for an irradiated "standard" rubber under standardized conditions and for other rubbers which were similar to the standard except for an added or substituted ingredient. A greater crystalline longevity connoted a greater radiation resistance, and the standard was used as a basis for comparing radiation resistance and composition.

The experimental work consisted of: firstly, stretching thin strips of rubber specimens 400 per cent and maintaining them immobile, mounted on a special holder; secondly, exposing them in a nitrogen atmosphere to a high irradiance of gamma rays from a kilocurie Cobalt-60 source; and, lastly, periodically as-

^{*} Reprinted from Rubber Age (New York), Vol. 87, pages 263–271, May 1960. This paper was presented before the Division of Polymer Chemistry, ACS, at Atlantic City, N. J., September 17, 1959. The opinions or assertions are the private ones of the authors, and are not to be construed as official or reflecting the views of the Navy Department or the Naval Service at large.

sessing the decrease in diffraction intensities with a Geiger counting x-ray spectrometer.

PREPARATION OF RUBBER SPECIMENS

Table I gives the recipes for the three categories of mill-mixed compounds studied: standard, graphite and additive. The graphite/rubber was similar to the standard except that graphite replaced the carbon black. Seven varieties of additive/rubber were used, and each was made by incorporating 5 parts of a different, potential anti-radiation additive into the standard recipe. Compounds were cured for 20 minutes at 250° F in a tensile mold conforming to ASTM Designation D15-57T, except that the cavity depth was modified to 12 mils by milling the edges.

Hypothetically, a successful anti-radiation additive protects its substrate because the harmful radiation energy absorbed by the substrate is transferred to the additive which dissipates it in a manner harmless to the substrate. The intermolecularly excited additive may dissipate this energy directly as heat or by reradiation, or indirectly through metathetical reactions or decomposition.

TABLE I RUBBER RECIPES

Ingredient	Standard	Graphite, rubber	Additive, rubber**
Deproteinized pale crepe	100.00	100.00	100.00
Sulfur	2.00	2.00	2.00
Zinc oxide (Prontox 166)	3.00	3.00	3.00
Zinc dibutyldithiocarbamate	0.25	0.25	0.25
2-Mercaptobenzothiazole	0.40	0.40	0.40
Graphite*		50.00	
Carbon black (Thermax)	50.00	-	50.00
Potential antiradiation additive**	-		5.00

* The graphite used was Graphite 509 (Asbury Graphite Mills, Asbury, N. J.).

** Seven additives were used: N-cyclohexyl-N'-phenyl-p-phenylenediamine; copper phthalocyanine; phthalocyanine; didodecyl selenide; Carbanthrene Khaki 2G; Indocarbon CLGS CONC CF; Immedial New Blue FBLA Extra CONC CF. The Indocarbon and Immedial New Blue dyes contained sodium chloride whichwas removed by water washing.

Resonant additives or polymer groups seem attractive as anti-radiation protectants. For example, resonant benzene decreases radiation damage of cyclohexane when mixed with it², and the phenyl groups in polystyrene confer excellent radiation stability to the polymer². When some part of the resonant antiradiation additive becomes excited, the excitation energy becomes generally distributed immediately within the molecule. It would seem to be of advantage to have the energy distributed maximally over a large additive molecule, so that its subsequent, generally distributed de-excitation would be less likely to damage some particular bond in the substrate.

The particular additives used were selected on the basis of chemical structures actually or potentially capable of protecting against radiation. N-cyclohexyl-N'-phenyl-p-phenylenediamine was included because Born reported that it substantially improves the retention of tensile strength and ultimate elongation during irradiation of unstretched rubber. Didodecyl selenide was selected since Carroll, Bolt and Calish noted that it retards radiation damage in lubricating oils. Graphite was chosen because of its radiation stability which, it was thought, might be transmitted to the rubber. Copper phthalocyanine and phthalocyanine were picked for their resonance coupled with large molecular size, as well as their chemical, thermal and radiation stabilities which, it

was believed, might confer radiation stability to the rubber. The dye, Carbanthrene Khaki 2G, Form I, was selected because of resonance coupled with large molecular size⁷.

The sulfur dyes, Indocarbon CL and Immedial New Blue, Formulas II and III, respectively, were selected because of their resonance and sulfur side chains^{8, 9}. It was thought that vulcanization might combine these dyes with rubber molecules via sulfur bonds. In this event, successful anti-radiation protection would be hypothesized as due to intramolecular transfer and degradation of absorbed radiation energy.

Formula II

Formula III

APPARATUS AND TEST PROCEDURES

Specifications of test device.—The rubber specimens were stretched on a sample holder which consisted of a base plate, stretching clamps, a top plate and an inert gas well. Front and rear exploded views are shown in Figure 2.

The base plate (A) consisted of a modified stainless steel block, 4.719 in. long, 3.125 in. wide and 0.469 in. thick. A circular well (a) of 1.266 in. diameter and 0.312 in. depth was drilled in the center of one face of the block, and this face became thereby the front face of the sample holder. A second circular well (b) of 0.75 in. diameter and 0.0625 in. depth was drilled in the center of the larger well (a). A 1.15 cm square aperture (c) with sides parallel to those of the block was cut in the center of the small well (b). Other features of the base plate were 0.125 in. tapped holes (d) for attaching the top plate (C) to the rear face; dowel pins (e and f) of 0.125 in, diameter and height for reproducibly attaching the top plate; 0.125 in. tapped holes (g) for securing the inert gas well (D) within the large well (a); holes (h) for attaching the sample holder when completely assembled to the voke-disc of the Geiger counting apparatus, Figure 4; 0.25 in. tapped holes (i) for attaching the stretching clamps; and scribed lines (s) on the rear face for exact centering of the rubber specimen to be stretched, each line parallel to and 0.0875 in, from a long-edge of the base plate.

The stainless steel stretching clamps were made as shown by (B). Each clamp consisted of two side posts (j); binding screws (k); top bar (l); compression screws (m); and press bar (n). The threadless side posts were 0.75 in. long, 0.5 in. O.D. and 0.266 in. I.D. The Allen head, 0.25 in. binding screws (k) penetrated the side posts, matched holes (i) in the base plate, and joined the top bar, side posts and base plate as shown. The top bar was 3 in. long, 0.562 in. high and 0.5 in. wide, and was drilled and tapped for penetration by three 0.156 in. compression screws (m), a median one and one at 0.875 in. on each side. The press bar which moved between the side posts was 2.125 in. long, 0.375 in. high and 0.375 in. wide. The ends of the press bar contoured the side posts, and its bottom side was convex with a 2 in. radius, an important requirement for holding stretched specimens against the base plate without

slippage or cutting.

The stainless steel top plate (C) was 3.688 in. long, 3.125 in. wide and 0.125 in. thick. It was used to compress and immobilize a stretched and clamped specimen against the rear face of the base plate. Compression was effected by screws which penetrated the 0.125 in. holes (d') in the top plate and the tapped holes (d) in the base plate. Holes (h') matched holes (h) in the base plate. The top plate was positioned by holes (e' and f') which matched dowel pins (e and f) in the base plate. Two cavities (o) existed within the top plate, one on each opposite side of the aperture as illustrated. When nitrogen was fed liberally to the cavities via the tubes (p) during x-ray diffraction analysis, the rubber in the aperture was bathed on that side which contacted the top plate.

Nitrogen feed system.—Each cavity was made as follows: A trench—1 cm wide, 1 in. long and 0.062 in. deep—was milled in the top plate starting at the aperture. Next a narrower trench—8 mm wide, 1 in. long and 0.031 in. deep—was milled in the center of the first, which process produced a single trench with shoulders. A steel inlay (q)—1 in. long, 1 cm wide and 0.062 in. thick—having a hole around which the tube (p) had been soldered, was placed on the shoulders and soldered to form the roof of the cavity.

The inert gas well (D) consisted of a brass ring—0.734 in. I.D., 0.531 in. O.D. and 0.312 in. thick—with two 0.062 in. I.D. tubes (r) penetrating a face

at 45 degrees to project 0.008 in. past the well's interior surface, as illustrated in Figure 2. The inert gas well fitted circular well (a) in the base plate and was secured therein by screws through the hole (g') and in the tapped holes (g) in the base plate. The screws could not extend so far into the base plate that they touched the rubber specimen. When nitrogen was applied liberally to the tubes, the rubber in the aperture was bathed on that side which contacted the base plate. The inert gas well was used during x-ray diffraction analysis, but was removed for Cobalt-60 irradiations.

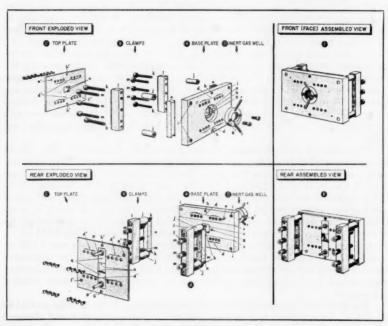


Fig. 2.—Views of sample holder used for rubber specimens, with parts described in the text. Front and rear exploded views are shown on the left, front and rear assembled views of the apparatus on the right.

Procedure for mounting samples—A rubber specimen was mounted on the sample holder by an invariant procedure: The sample holder with its top plate and inert gas well removed was held face down in a vise. A 1.875×0.75 in. piece of latex dental dam about 10 mils thick was placed on the base plate beneath each clamp so that a 1.875 in. side coincided with the edge of the base plate. These rubbers were held tautly with Scotch Brand tape, a short narrow strip of tape over each corner nearest the aperture and a 1.875 in. long, narrow strip along the side at the edge of the base plate. The press bars of the clamps, except their top horizontal surface and upper side surfaces, were also covered with rubber dental dam held tautly by narrow strips of Scotch Brand tape along the sides of the bars.

The rubber specimen for mounting was a long strip of 1.375 in. width, cut with a scalpel and metal template. The strip was extended through both clamps, positioned precisely by the scribed lines on the base plate, Figure 2, and

firmly secured by one clamp. Care was taken not to tighten the screw clamps to the extent of damaging the specimen. A narrow ink dot was placed on the imaginary lengthwise median of the specimen strip near the tightened clamp at a point 0.625 in. from the end edge of the base plate. A second dot was placed on this median toward the aperture and 0.312 in. from the first dot. The ink dots were rewetted and the specimen was stretched through the loose

clamp by winding around a rotating screwdriver.

During this operation the press bar of the loose clamp was held conveniently near its top position by a piece of Scotch Brand tape. The wet dots extended to lines which were kept precisely midway between and parallel to the scribed lines on the base plate as determined with a ruler. This fulfilled the important requirement that the direction of stretch parallel the lengthwise edges of the sample holder, so that orienting the sample holder on the x-ray diffraction unit by means of the edges served to orient the direction of specimen stretch. When stretching approximated a factor of 4, a new ink dot was placed along the midpoint of each extended line, and the exact degree of stretching was measured between the new dots. The clamp was tightened when stretching was exactly a factor of 4. If an extended line and dot became located over the aperture, they were removed carefully with a moist, lintless tissue. The superfluous specimen ends were cut off near the clamps and the top plate attached; the clamps were not touched unnecessarily thereafter. Stretching reduced the thickness of the specimens by approximately one-half of original size.

Irradiating rubber with cobalt source.—The rubber samples were irradiated in a nitrogen atmosphere with a kilocurie Cobalt-60 source. Quadruple samples of each rubber were investigated and irradiated simultaneously. The sample holders were symmetrically positioned about the cylindrical source, and ferrous sulfate dosimetry showed an absorbed dose rate of 1.3 × 10⁵ r/hr at the aperture positions. Irradiations and x-ray diffraction measurement were made at 75°

to 80° F.

A nitrogen atmosphere was provided by sealing the rubber specimens in nitrogen-filled plastic bags. The sample holder was placed on a table so that it was supported by its clamps with its face up. The inert gas well was removed, a dime was set in the circular well [(b) in Figure 2] to protect against possible specimen injury, the tapped holes [(g) in Figure 2] were plugged with short screws, and the dime was removed. The screws could not be long enough to touch the rubber specimen, and were always in place during irradiation.

The sample holder was then placed in a 6 × 11 in., 10 mils thick polyethylene bag. Most of the mouth of the bag was sealed with Scotch Brand tape, the bag was flushed with 15 cu. ft. of nitrogen, and, finally, the mouth was completely sealed with tape. This combination was sealed within a second bag which was filled similarly with nitrogen. All seams on the plastic bags were taped for double sureness against leaks. All corners on the sample holders

were rounded so they would not puncture the bags.

The irradiation schedule consisted of intermittent irradiation, with x-ray diffraction measurement between the increments, continued until the specimen either relaxed and lost its diffraction spots (crystallinity) completely, or ruptured. The specimens were removed from the source only long enough for measurement. The incremental irradiations were of approximately 4 or 8 hours' duration, and quadruple specimen measurement required about 3 hours. Total crystallinity loss was simply revealed when the x-ray spectrometer chart patterns for a horizontally and vertically positioned specimen became identical, as explained subsequently. Total loss of specimen crystallinity usually pre-

ceded rupture by such a short time that it was usually not observed. Partial

loss was always seen.

Occasionally the specimen rendered totally noncrystalline remained intact in the aperture for a while before rupture, but such a specimen was considered a failure from the time its total crystallinity loss was first observed, because of its invariably cracked and damaged appearance. The exact time of specimen rupture or total crystallinity loss within the opaque irradiation chamber could not be determined, but this was of little consequence to the investigation. This time was estimated with sufficient accuracy as the midpoint of the irradiation increment immediately preceding the discovery of these events.

Patterns of diffraction intensity versus angle 2 θ were obtained with the x-ray diffraction units (General Electric Co. XRD-3) modified as shown in Figure 3¹⁰. The following technique was used: Central, maximum intensity

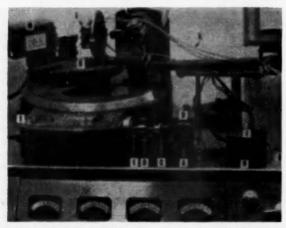


Fig. 3.—Photo of x-ray diffraction unit above the modification for controlling goniometer speed and the sample holder mounted for forward reflection measurement: (A) motor, (B) gear reduction box, (C) flexible coupling, (D) Jacobs Chuck, (E) shaft, (F) remote control, (G) motor switch, (H) x-ray button, (I) usual speed control (not used), (J) horizontally positioned sample holder, (K) sample holder positioner, (L) nitrogen tubes connected to sample holder, (M) Geiger Counter.

x-ray port; nickel-filtered (0.35 mil) copper radiation at 40 kvp and 20 ma (General Electric Co. x-ray tube CA-7); 3-degree beam slit; SPG Soller slit; a 0.05-degree detector slit; a 5-degree target to beam angle; time constant B (6 sec); Speedomax recorder range 1; nitrogen flow past the sample; and a

goniometer speed of 1°/min obtained by modifying the unit.

Modifications for measurement.—The modification is shown in Figure 3 and consists of: a Bodine motor (A) at 10 rpm and 65 in.-oz torque; a 10:1, specially fabricated gear reduction assembly (B); a flexible coupling (C); a 0.25 in., light-duty Jacobs chuck (D); a shaft (E) attached to the vernier of the goniometer driving mechanism and engaging the Jacobs chuck; and remote control (F) for starting-stopping the motor by switch (G) and the X-rays by buttons (H). The motor could only rotate the goniometer to decrease angle 2θ and was fused to stop if the usual speed control (I) was not set in the manual position. The Jacobs chuck was disengaged in order to move the goniometer manually either with our without vernier control.

The rubber specimens were positioned, so that the direction of stretch was horizontal or vertical, by means of a positioner. The sample holder positioner consisted of three main parts as shown in Figure 4: a disc (A); a grooved yoke (B); and a track (C). The stainless steel disc was of 6.25 in. diameter and 0.375 in. thickness. Degree marks were scribed on the edge and numbered from 0 to 360 on one face which thereby became the front of the disc. A rectangular well (a) was milled in the center of the rear face and was 4.734 in. long, 3.141 in. wide and 0.125 in. deep. The 0 and 180 degree scribe marks lay on the disc diameter which was parallel to the long edges of the well. A 4.125 in. by 2.625 in. rectangular hole (b) was centered within the well. The well received the front face of the sample holder (Figure 2), and the sample holder and disc were secured by screws which first penetrated holes (h) in the sample holder, and then the tapped holes (c) in the disc of the positioning attachment.

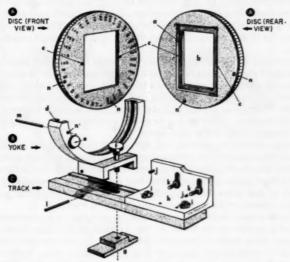


Fig. 4.—Schematic diagram of sample holder positioner illustrates its construction and identifies parts described in the text.

The grooved yoke (B) received the disc and allowed it to rotate with a firm fit. The extent of rotation was given by the degree mark on the disc's edge opposite the knife-edge (d). The screw (e) contacted the front face of the disc and secured it at any position. The yoke was joined to the track (C) by means of screw (f) and bar (g) which had a tapped hole to receive the screw.

The track (C) was 9 in. long. 1.5 in. wide and 0.406 in. thick. The angle bracket (h) was an associated part, permanently joined to the track by dowel pins and Allen head screws (i). The track was attached to the XRD-3 beam slit bracket so that it pointed toward the Geiger counter, and was reproducibly secured by dowel pins (j) and Allen head screws (k). When assembled and attached to the beam slit bracket, the track and bar (g) were suspended 0.187 in. and 0.031 in., respectively, above the rotating support for standard XRD-3 sample holders, as shown previously in the detailed exploded views of Figure 2.

Precise vertical stretching of specimen.—In the assembled apparatus the disc

fit in the yoke with its front face toward the XRD-3 beam slit, which caused the rear (clamp side) of the attached sample holder to face toward the Geiger counter. Figure 3 shows the sample holder positioner, containing the holder in position on the XRD-3 x-ray diffraction unit. The sample holder aperture was positioned precisely over the goniometer pivot point and lined up exactly with the XRD-3 beam and Soller slits. The dowel pin (1) accomplished pivot point positioning conveniently, and the dimensions of the yoke assured aper-

ture-slit alignment.

Furthermore, the dowel pin (m) which matched holes (n) could position the disc in the yoke so that the long edges of the well (a) were either exactly vertical or horizontal. This was tantamount to an exactly vertical or horizontal placement of the attached sample holder and, thus, similar directions of stretch for the rubber specimen. Precisely vertical specimen stretching was important for reproducible, horizontal Geiger scanning through the diffraction spots of measurement interest which always formed on an axis perpendicular to the direction of stretch. The sample holder was always attached to the disc with the same end facing the 0 degree mark on the disc in order to attain constant sample placement.

As illustrated by the x-ray diagram of Figure 1, specimen positioning with the direction of stretch horizontal caused the Geiger counter to scan the rubber amorphous halo and such other concentric diffraction rings which might appear with various vulcanizates. In addition, vertical positioning presented some crystallinity diffraction spots. All specimens were scanned between 2θ angles of 9 and 25 degrees. This region extends just beyond the rubber amorphous

halo and its associated diffraction spots.

Obtaining diffraction patterns.—Â diffraction pattern for the rubber amorphous halo was obtained by subtracting the spectrometer chart pattern for air scatter from the chart pattern for a specimen stretched in the horizontal direction. The chart pattern for air scatter was corrected for a calculated 9 per cent absorption of the x-ray beam by the rubber sample before the subtraction.

Typical spectrometer chart patterns are shown in Figure 5.

A diffraction spot pattern was obtained by subtracting a spectrometer chart pattern for a specimen stretched in the horizontal direction from the corresponding one for a vertical direction of stretch. The subtraction removed the influence of the amorphous halo as well as the influence of air scatter since this was a constant factor. It has been shown previously that the diffraction spot pattern obtained by the subtraction may be considered to be a semi-quantitative diffraction view of the specimen, useful for following and comparing radiation

damage in rubber1.

Counting performance was checked frequently during each series of measurements by scanning a non-stressed, standard rubber sample. The standard sample assembly consisted of a base plate, a piece of rubber and a top plate. The base plate was similar to that of the sample holder, Figure 2, except that holes for attaching stretching clamps were deleted, and that a groove (1 in. wide and 10 mils deep) was milled in the center of the rear face to make it parallel to the short edges of the plate and intersecting the aperture. A 10 mil thick, 1 in. wide strip of the standard rubber was placed in the groove across the aperture and the ends (Scotch Brand) taped to the base plate. The top plate, similar to that for the sample holder except that inert gas cavities were deleted, was then doweled and screwed to the rear face of the base plate. The standard rubber sample assembly was attached to the disc (A) of the sample holder positioner, Figure 4, similarly to the procedure for the sample holder.

Air scatter patterns were determined with a mockup replacing the sample holder in the disc of the sample holder positioner. The mock-up was similar to the aforementioned standard rubber sample assembly, except that the aperture was left vacant.

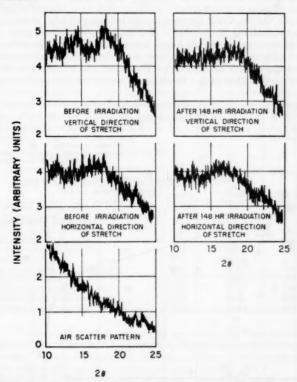


Fig. 5.—Typical x-ray spectrometer chart patterns for N-cyclohexyl-N'-phenyl-p-phenylenediamine/rubber and air scatter are traced in these five charts.

WHAT CAUSES RADIATION DAMAGE

Stretched rubber is extremely sensitive to radiation damage. It is believed that chain seission, manifested by loss of crystallinity and diminution of diffraction spot intensity, dictates the physical-mechanical radiation behavior of stretched rubber. Stress relaxation would make scissions irreversible and their increase would soon weaken the specimen to the point when the chains slip and rupture of the specimen occurs. Crosslinking undoubtedly occurs simultaneously, but at too slow a rate to prevent destruction of the specimen. The extremely low doses which cause rupture in stretched specimens do not produce detectable physical-mechanical changes in unstretched rubber where crosslinking predominates.

Loss of diffraction spot intensity (or crystallinity) due to irradiation is shown in Figure 6 for the standard compound and for rubber containing N-cy-

clohexyl-N'-phenyl-p-phenylenediamine. The curves represent the decrease in peak intensity of that diffraction spot (2 θ , 19°) which lies on the upper Y axis and on the outer shoulder of the amorphous halo in Figure 1. This was the diffraction spot measured for all rubbers. The curves were constructed from numerous diffraction spot patterns corresponding to various irradiation times. For example, the fractional decrease in spot intensity of 0.63, shown in Figure 6 for rubber containing N-cyclohexyl-N'-phenyl-p-phenylenediamine (specimen 3) at an irradiation time of 148 hours, was calculated from the diffraction spot patterns in Figure 7. These, in turn, were derived from x-ray spectrometer chart patterns shown in Figure 5. The other compounds provided similar curves except that they varied in proximity to the standard rubber curve.

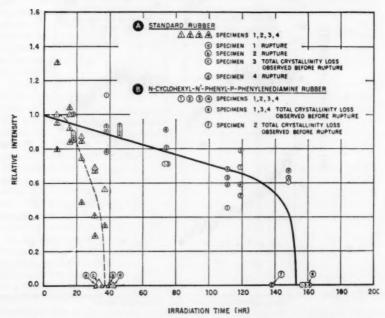


Fig. 6.—Decrease in diffraction spot intensity (peak value at 2 # = 19°) versus irradiation time of rubber containing N-cyclohexyl-N'-phenyl-p-phenylenediamine and standard rubber.

The radiation resistances of the vulcanizates were compared on the basis of their crystalline longevities relative to that of the standard compound. The relative crystalline longevity of a compound was determined from its curve of diffraction spot intensity versus irradiation time, Figure 6. It is defined as the ratio of the area under that curve to the area under the similar curve for the standard compound. A greater longevity connotes a greater resistance. Relative crystalline longevities are given in Table II for all compounds investigated.

The radiation resistance of stretched rubber depends greatly upon composition. Table II shows that the addition of a few per cent of an additive to the standard rubber can markedly increase or decrease relative crystalline longev-

ity. The relative crystalline longevity of the most and least radiation-resistant compound differed by a factor of 9. It has been assumed that the additives used in this study were not destroyed by vulcanization; probable survival was one of the criteria used in their selection.

ADDITIVES ENHANCE RESISTANCE

The stretched N-cyclohexyl-N'-phenyl-p-phenylenediamine/rubber exhibited the best radiation resistance with a relative crystalline longevity of 4. Two studies with unstretched rubber have also shown the usefulness of resonantly stable N-cyclohexyl-N'-phenyl-p-phenylenediamine as an anti-radiation additive for natural rubber. Born has reported that it substantially improves the retention of tensile strength and elongation, and R. E. Morris (Rubber Laboratory, Mare Island Naval Shipyard, Vallejo, Calif.) has found that it decreases compression set significantly. Chain cleavage is believed to pre-

Table II

Relative Crystalline Longevity, Tensile Strength and
Ultimate Elongation for Rubbers

Composition	Relative crystalline longevity	Tensile strength (psi)	Ultimate elongation (%)
N-cyclohexyl-N'-phenyl-p-			
phenylenediamine/rubber	4.00	2900	600
Indocarbon CL/rubber	1.60	2000	500
Carbanthrene Khaki 2G/rubber	1.20	2800	600
Standard rubber	1.00	2100	600
Immedial New Blue/rubber	0.89	2050	550
Graphite/rubber	0.74	1850	500
Phthalocyanine/rubber	0.69	2400	650
Didodecvl selenide/rubber	0.55	2400	650
Copper phthalocyanine/rubber	0.45	2600	600

dominate in irradiated stretched rubber and crosslinking in unstretched. The ability of N-cyclohexyl-N'-phenyl-p-phenylenediamine to protect both stretched and unstretched rubber supports the hypothesis that an additive which can mitigate chain cleavage can also mitigate crosslinking.

The superior radiation resistance of rubber containing N-cyclohexyl-N'-phenyl-p-phenylenediamine was due to the presence of the protective additive rather than to superior initial tensile strength or ultimate elongation. Table II compares relative crystalline longevity, tensile strength and ultimate elongation of all the rubbers, and shows no correlation between these properties. The tensile strengths and elongations are viewed as essentially constant factors for

all compounds tested.

Both oxidative and non-oxidative radiation damage may occur in elastomers, hence the ideal antiradiation additive would protect against both. Oxidative damage arises from radiation-produced ozone. The damage observed in this study was nonoxidative, since the specimens were mill-mixed vulcanizates incorporating essentially no free oxygen, and they were irradiated in an oxygen-free atmosphere. The specimens had no visible air bubbles. It is believed that they contained no free oxygen, only nitrogen, in any possible microbubbles, because the energized molecules and free radicals formed during milling are quite reactive toward oxygen and are expected to remove it, one type of intermediate product being a hydroperoxide at an activated allylic position. The

possibility exists that combined oxygen may rearrange, possibly detrimentally, with mill-mixed rubber on irradiation. The rubber additive, N-cyclohexyl-N'-phenyl-p-phenylenediamine, may be expected to protect against both oxidative and non-oxidative radiation damage, since it is a rubber antioxidant, and it afforded protection against nonoxidative damage, predominantly chain cleavage in this study.

■ Indocarbon CL gave some degree of protection against radiation with a relative crystalline longevity of 1.6, whereas Immedial New Blue did not, with a relative crystalline longevity of 0.89. These sulfur dyes possibly combined

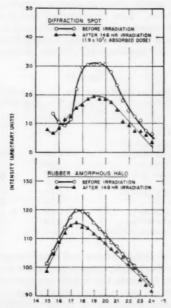


Fig. 7.-Typical x-ray diffraction patterns for Type B rubber of Figure 6.

with the substrate via sulfur bonds, and their sulfur may also have been responsible for a somewhat increased cure. If the Indocarbon CL were chemically combined with the rubber, intramolecular transfer and degradation of absorbed

radiation energy may have been a protective mechanism.

A rubber additive exhibiting resonance and large molecular size does not necessarily afford effective anti-radiation protection. Carbanthrene Khaki 2G, phthalocyanine and copper phthalocyanine illustrate this in that their rubbers gave relative crystalline longevities of only 1.2, 0.69 and 0.45, respectively. Nevertheless it is held that, given the proper chemical structure, a large resonant chemical will protect against radiation by receiving energy intermolecularly from the substrate, distributing it generally over its own large molecular volume, and dissipating it at various sites in amounts insufficient to cause undesirable substrate reactions. Perhaps this hypothetical, large additive should be relatively long, narrow and flat, so that it would not interfere with and

strain the ordered arrangement of stretched chains in the crystalline domain, a phenomenon which would enhance recoil and crystallinity loss after chain scission.

OTHER FACTORS IN MAXIMUM PROTECTION

The presence of a chemically stable and radiation-stable ingredient in a vulcanizate does not necessarily confer protection against radiation. The compounds containing graphite, phthalocyanine and copper phthalocyanine illustrate this by their low relative crystalline longevities of 0.74, 0.69 and 0.45, respectively. Bopp and Sisman's work confirms this observation. They reported^{12, 13} that the physical properties of an irradiated, unstretched elastomer having a radiation stable filler changed at approximately the same rate as the unfilled polymer. Their results with plastics are contradistinctively interesting showing that the addition of radiation resistant fillers (including graphite) to Bakelites improved the retention of tensile strength upon irradiation, while

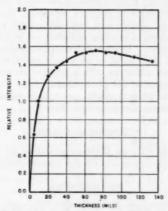


Fig. 8.—Curve for halo diffraction intensity versus rubber specimen thickness demonstrates test technique's sensitivity to halo intensity.

fillers of poor stability had the opposite effect. The poor performance of copper phthalocyanine could not be due to the presence of ionic copper which causes rapid and far-reaching deterioration in rubber. The copper is too tightly bound within this pigment to cause deterioration.

A proficient antiradiation additive for one substrate is not necessarily proficient for another, somewhat similar substrate. Didodecyl selenide, effective with lubricating oils⁵, was tested as an antiradiation additive in rubber on an empirical basis. It produced a compound with a poor relative crystalline

longevity of 0.55.

The decreases in diffraction spot intensity on irradiation, which were observed in this study, have been interpreted as due to a decrease in crystallinity without any appreciable sample thinning, at least until just before rupture. Both crystallinity decreases and sample thinning are capable of lowering spot intensity. As crystallinity is decreased, a shift of x-rays from spot to halo diffraction occurs; but the resulting reinforcement in halo intensity is small, since the spot rays, which are of low intrinsic intensity and low areal distribu-

tion, become integrated uniformly throughout the large areal distribution of the intense halo rays. The x-ray diffraction technique described herein is insensitive to this small reinforcement in halo intensity. However, as shown in Figure 8, it is extremely sensitive to the relatively large changes in halo intensity which are effected by small thickness changes in very thin rubber specimens. Thus, a decrease in halo intensity signifies a decrease in thickness, whether or not there are crystallinity changes.

Figure 7 shows pre-irradiation spot and halo diffraction patterns, as well as patterns taken after a damaging dose—one sufficient to cause a decrease in spot intensity-for the compound containing N-cyclohexyl-N'-phenyl-p-phenylenediamine. These patterns typify over one hundred others which were observed with the various vulcanizates and damaging doses of this study. They show a significant decrease in the diffraction spot peak, but no large decrease in halo intensity.

Bovey has speculated as follows14: "It is conceivable that there may be classes of compounds which absorb ionizing radiation particularly readily and can pass it on to a surrounding polymer structure, thus acting in the same manner as sensitizers for visible and near ultraviolet radiation. Substances which accelerate the action of ionizing radiation on polymers seem to have received little or no attention. It appears that an important field for exploration is open here, one that may be of considerable practical as well as academic interest." Those rubber additives with a relative crystalline longevity of less than unity, which accelerated the predominant chain cleavage reaction in the stretched rubbers of the present study, are hypothesized as belonging to the class of radiation sensitizers mentioned by Boyev.

ACKNOWLEDGMENT

The authors wish to express their appreciation to R. E. Morris for the preparation of rubber specimens and for the measurement of tensile strength.

REFERENCES

- Shelberg, W. E., and Gevantman, L. H., Nature, 183, 456 (1959).
 Harwood, J. J., Hausner, H. H., Morse, J. G., Rauch, W. G., "The Effects of Radiation on Materials",
 Reinhold Publishing Corp., New York, N. Y., p. 252, 1958.
- * Ibid, p. 279.
 * Born, J. W., Diller, D. E., Rowe, E. H., "A Study of the Effects of Nuclear Radiation on Elastomeric Compounds and Compounding Materials", Wright Air Development Center Report 55-58, Part III (June 1957).

- Compounds and Compounding Materials", Wright Air Development Center Report 55-58, Part III (June 1957).

 Carroll, J. G., Bolt, R. O., and Calish, S. R., "Development of Radiation Resistant Oils", California Research-A.E.C. Report No. 11 (June 16, 1958).

 Robinson, M. T., and Klein, G. E., J. Phys. Chem. 61, 1004 (1957).

 Lubs, H. A., "The Chemistry of Synthetic Dyes and Pigments", Reinhold Publishing Corp., New York, N. Y., (1955), p. 467.

 Bidd., p. 320.

 Bidd., p. 324.

 Klug, H. P., and Alexander, L. E., "X-Ray Diffraction Procedures", John Wiley & Sons, Inc., New York, N. Y., (1954), p. 245.

 Fieser, L. F., and Fieser, M. F., "Organic Chemistry" (3rd Ed.), Reinhold Publishing Corp., New York, N. Y., (1956), p. 849.

 Bopp, C. D., and Sisman, O., "Radiation Stability of Plastics and Elastomers", Oak Ridge National Laboratory Report ORNL 1373, Oak Ridge, Tenn. (1953).

 Collins, C. G., and Calkins, V. P., "Radiation Damage to Elastomers, Organic Liquids and Plastics", General Electric Co., Atomic Products Div., Aircraft Propulsion Dept., Engineering Report TID 4500 (11th Ed.), Cincinnati, Ohio, pp. 31, 51 (1956).

 Bovey, F. A., "The Effects of Ionising Radiation on Natural and Syntehtic High Polymers", Interscience Publishers, Inc., New York, N. Y., (1958), p. 60.

VULCANIZATION OF SBR BY GAMMA RADIATION*

P. M. ARNOLD, GERARD KRAUS, AND R. H. ANDERSON, JR.

PHILLIPS PETROLEUM Co., BARTLESVILLE, OKLAHOMA

INTRODUCTION

In spite of recent, active interest in the vulcanization of elastomers by ionizing radiations¹⁻⁷, and the existence of an already considerable literature on radiation effects on high polymers, no systematic investigation of the potentially important gamma ray vulcanization of butadiene/styrene copolymer appears to have been published. The present paper attempts to fill this gap with a detailed study of the physical properties of gamma vulcanizates of this rubber and the dependence of these properties on the characteristics of the network formed during irradiation. In addition, some new results on the promotion of the vulcanization by heavy metal fillers are presented.

EXPERIMENTAL

All radiation vulcanizations were performed by exposing conventionally mixed compounds, containing no chemical curing agents, to gamma radiation from spent reactor fuel elements at the canal facilities of the Materials Testing Reactor at Idaho Falls, Idaho. The uncured compounds were pressed into sheets between Holland cloth or molded into the desired shape in small stainless steel molds. The samples, including the miniature molds, were packed into aluminum cans, evacuated and purged three times with helium, and irradiated under a slight positive pressure of helium. The irradiation was carried out under eighteen feet of water at the ambient canal temperature of ca. 27° C. Figures 1 and 2 illustrate the experimental arrangement.

The distribution of energies from the fission products depends on the age of the fuel element, as the various radioisotopes decay at their characteristic rates. All vulcanization experiments were run with elements three to thirty days after their withdrawal from the reactor. For most of this period the energy spectrum changes relatively little and is roughly as follows:

Energy, Mev	%
>2	5
1.5-2.0	50
0.8-1.5	15
0.6-0.8	15
<08	15

Since much of the lowest energy radiation is absorbed by the intervening water and container walls, the mean energy of the gammas used for vulcanization in the present study is estimated at 1.5 MeV, the bulk (> 50%) of this being derived from the barium-lanthanum 140 chain.

The radiation dosages were determined for each experiment by ceric/cerous

^{*} An English version of the paper which appeared in Kautschuk und Gummi, Vol. 12, pages WT27-32, February 1959.

sulfate dosimetry and are expressed in "roentgens equivalent physical" or reps (93 ergs of energy absorbed per gram). For samples containing only rubber and carbon black this corresponds to the actual dosage received by the sample. Rubber compounds containing heavy metal fillers placed in the same radiation field will, of course, absorb more energy. However, in these cases no attempt was made to calculate the actual dosage. Instead a "nominal dosage" figure was used which is defined as the dosage received by an otherwise identical rubber stock containing no heavy elements placed in the same radiation field for the same length of time. The polymers used in this study were for the most part commercial products, the overwhelming majority of experiments being conducted with Philprene 1500, a 50 ML-4 butadiene/styrene emulsion copolymer prepared at 5° C in the sulfoxylate recipe and containing 23 per cent bound styrene. All other synthetic rubbers were likewise 5° C emulsion polymers. In the following, the abbreviation SBR will be used for all styrene/butadiene copolymers.

Physical testing of vulcanizates was carried out by well known procedures. Degrees of net crosslinking were estimated by the equilibrium swelling method, with n-heptane as the solvent⁸. Stress relaxation during the vulcanization process was measured by stretching gamma-cured rubber strips to 100 per cent elongation on an aluminum rack and allowing these to relax to their equilibrium

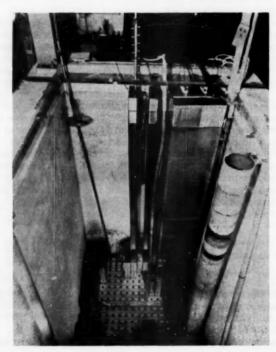


Fig. 1.—Gamma facilities of Phillips-operated materials testing reactor at Idaho Falls. Samples to be the canal constructed in long vertical tubes. Spent fuel elements at the bottom of the canal (in square cans) are grouped around sample tubes to give desired symmetry of radiation field.

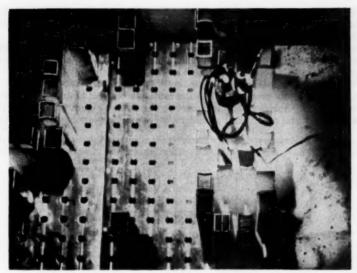


Fig. 2.—Fuel elements at bottom of canal photographed in the light of Čerenkov radiation.

tension in an atmosphere of helium before measuring the initial stress. The strips were returned to the rack, the rack placed into an aluminum can, the assembly irradiated in an atmosphere of helium, and the final tension determined after removal from the radiation field.

Compounding recipes for all gamma vulcanizates consisted merely of rubber, reinforcing filler and, where applicable, promoting filler. The amounts of each are indicated in the Tables. The recipes for the sulfur-vulcanized "control" stocks of Tables III and IV were as follows:

	Table III Controls	SBR control	Hevea control
SBR	100	100	_
Hevea		-	100
HAF black	50	Ministry	-
Silica	MARKET .	60	60
Zinc oxide	3	3	4
Stearic acid	1	2	3
Sulfur	1.25 and 1.75	3	3
N-cyclohexyl-2-benzothiazole sulfenamide	1.1		
Diphenylguanidine		1.5	1.5
Benzothiazyldisulfide	-	0.75	0.75
Triethanolamine	(SMC)	1	1
Antioxidant	1	1	1

GENERAL PRINCIPLES

The general statistical principles involved in radiation crosslinking have been worked out by Charlesby⁵, who tested his theoretical deductions on natural rubber gum irradiated with pile radiation, i.e., both neutrons and gamma rays. These principles apply equally to all chain molecules and are not affected by the type of ionizing radiation used in crosslinking.

To ascertain the effects of radiation crosslinking on the technologically important properties of styrene/butadiene rubber it is necessary to work with filler reinforced vulcanizates, since the utility of gum stocks of these rubbers is extremely limited. The situation is complicated by the introduction of filler effects, but it is felt that this complication must be tolerated if practically significant results are to be obtained.

The net degree of crosslinking produced by gamma radiation is always, at least, approximately proportional to the radiation dosage; however, the crosslinking efficiency varies from one rubber to the next. Figure 3 illustrates the relation for natural rubber and butadiene/styrene copolymer both without and

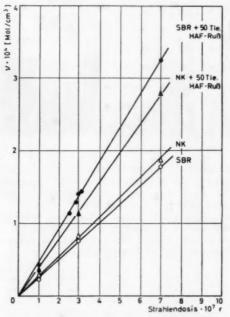


Fig. 3.—Net crosslinking as a function of radiation dosage.

with carbon black. It should be noted that, whereas the carbon black contributes to the apparent crosslinking, this effect in no way obscures the correlation with dosage. The nature of the apparent contribution of fillers to effective crosslinking has been discussed elsewhere. Based on the above and similar data a number of effective crosslinking efficiencies have been calculated for various rubber compounds, Table I. The yields are expressed in G-values which are defined as number of effective network chains formed per 100 electron-volts of energy absorbed. Because of possible scission effects in vulcanization, chain entanglements and filler contributions, these values should not be interpreted as referring to the actual number of chemical crosslinks formed. The yields become smaller when oxygen is not carefully excluded during irradiation. Under exclusion of oxygen, yields are very nearly independent of dose rate. The well known resistance of aromatic compounds to ionizing radiations is

reflected in the low G-values for high styrene rubber and polymer extended with

highly aromatic oil.

Irradiation of organic high polymers with ionizing radiation leads to both crosslinking and scission^{2, 5, 6}. In most hydrocarbon rubbers, butyl rubber excepted, crosslinking predominates. Nevertheless, as long as scission occurs, it will exert an effect on the structure of the network formed. In theory the number of elastically effective network chains, v, is given by the familiar expression:

 $\nu = 2n - 2N$ (1)

where n is the number of crosslinks and N is the number of primary molecules from which the network is formed, with all quantities expressed in moles per unit volume. Scission may occur in the main chain or, less probably, by sever-

TABLE I EFFECTIVE YIELDS OF NETWORK CHAINS FOR VARIOUS GAMMA VULCANIZATES

Rubber	Carbon black	phr	G
SBR ^a	-		2.7
SBR ^a	HAF	50	4.9, 3.80
Hevea			2.9
Hevea	HAF	50	4.2
SBR, oil extended ^b	HAF	50 ^d	2.20
SBR, oil extended	HAF	50d	3.90
SBR, high styrenes	HAF	50	1.50
Bd/MVP/	HAF	50	4.10

Philprene 1500.
Philprene 1712, contains 27.5 parts of highly aromatic extender oil.
Philprene 1708, contains 37.5 parts of naphthenic extender oil.
Based on extended rubber.
Charge ratio 50:50.
Philprene VP-25, a 75:25 copolymer of butadiene and 2-methyl-5-vinylpyridine.
Oxygen not rigidly excluded.

ing a crosslink already formed. Each main chain scission will have the same effect as increasing the number of primary molecules by one while each crosslink broken will cause a corresponding decrease in n. In terms of total scissions of unspecified origin, S, Equation (1) becomes:

$$v = 2n - 2N - 2S \tag{2}$$

By the kinetic theory of rubber elasticity the equilibrium stress in a strip of rubber under tension is proportional to v. If a gamma vulcanizate is irradiated under tension, the stress decays by virtue of scission, but any new crosslinks formed do not contribute to the stress⁹ at the extension prevailing during the The number of scissions will be

$$S = \frac{\nu_1}{2} \left(1 - \frac{f_2}{f_1} \right) \tag{3}$$

where f_1 and f_2 are the initial and final stresses in the relaxation experiment and ν_1 is the initial density of network chains. (Since this paper was first published in its original German version, Scanlan¹⁰ has developed an alternate treatment of network defects which, when applied in the regime of stress relaxation encountered here, yields values for the number of scissions which are approximately twice those given by Equation (3). As pointed out by Scanlan the essential difference between the present (Flory) and Scanlan treatments lies in the status assigned to trifunctional junctions. In the Scanlan theory these are assigned equal effectiveness as constraints on the three elastically active chains as are tetrafunctional junctions; in the Flory theory they are allowed lesser effectiveness. The original Tobolsky⁹ calculation produces values similar to these of the Scanlan theory.) If the final number of network chains, ν_2 , is determined independently, an estimate of the relative magnitudes of crosslinking to scission in the interval between ν_2 and ν_1 may be obtained in the ratio $\Delta n/\Delta S$. Since N is fixed

$$\nu_2 - \nu_1 = \Delta \nu = 2 \, \Delta n - 2 \, \Delta S,$$
 (4)

or

$$\frac{\Delta n}{\Delta S} = 1 + \frac{\Delta \nu}{2 \, \Delta S} \tag{5}$$

Table II illustrates the use of these equations for a typical gamma vulcanization of butadiene/styrene rubber. The ratio $\Delta n/\Delta S$ is approximately 7. This ratio is sensitive to the presence of oxygen, tending to be smaller in experiments carried out under less stringent exclusion of air. Oxygen evidently stabilizes

Table II

Extent of Chain Scission During Vulcanization^o

Dosage interval, Reps×10 ⁻⁷	$_{\nu_1} \times 10^4$ moles/cc	fa/fi	$\Delta S \times 10^4$ moles/cc	Δν×10 ⁴ moles/cc	$\Delta n/\Delta S$
2.5-2.8	1.13	0.982	0.010	0.14	8.0
2.8-3.1	1.27	0.980	0.013	0.15	6.8
3.1 - 3.4	1.42	0.977	0.016	0.18	6.6
2.5 - 5.0	1.13	0.878	0.069	0.80	6.8

a SBR with 50 phr HAF Black.

the radical chain ends, and prevents recombination. Charlesby has estimated the ratio of crosslinking to scission to be in excess of 10:1 for the irradiation of Hevea gum, using the magnitude of the sol fraction as criterion. This method would probably not measure scissions followed by prompt recombination (before the chain ends diffuse apart), whereas the stress relaxation method might count these, depending on how rapidly the severed chain ends pull apart upon removal of the stress. The agreement with Charlesby's estimate must, therefore, be considered as fair. Since our estimate of $\Delta n/\Delta S$ includes both scissions at crosslinks (if such occur at all) and in the main chain, it is apparent that the extent of main chain scission in the absence of oxygen cannot be more than one per seven crosslinks. This would suggest that at comparable degrees of net crosslinking gamma vulcanizates should exhibit similar properties to sulfur cured rubbers except for differences arising from the type of crosslink or from additional filler interaction. This should be particularly true of the dynamic properties of the vulcanizates which are known to be sensitive to both the density of the network chains ν and the free end fraction $2N/(\nu+2N)$. latter quantity increases if N is effectively increased by main chain scission, unless the free chain ends are tied back into the network.

Equations (1) to (5) take no account of physical entanglements of the network chains. Flory¹¹ has suggested an entanglement correction to Equation (1) of the form

$$\nu = g(2n - 2N), \tag{6}$$

TABLE III

PHYSICAL PROPERTIES OF GAMMA CURED SBR TREAD TYPE COMPOUND *

				Original	lan						Oven Age	Oven Aged 24 hrs. at 212° F	at 212° F		
Vulcanization	"X 10°, moles/ ce	300% Mod- ulus, psi	Ten- sile,	Elon- gation,	Shore hard- ness	Resil- ience	Heat buildup	Tear energy, lbs/in.	noles/	300% Mod- ulus, psi	Ten- sile,	Elon- gation,	Shore hard- ness	Resil- ience,	Heat buildup,
						Pr	Properties at	t 25° C							
7, 2.5×107 reps	1.13	1440	2830	540	26	59.5	101.9	120	1.10	1490	2150	390	57	60.2	100.2
7, 2.8 ×107 reps	1.27	1480	2860	530	57	60.5	93.8	96	1.04	1510	3240	530	57	59.6	101.9
7, 3.1 X107 reps	1.42	2010	2850	400	58	64.0	76.0	22	1.35	1940	2860	420	57	61.2	92.4
Sulfur (1.25)b	1.20	1270	2800	510	57	61.4	78.4	245	1.93	2210	3230	400	62	66.2	63.2
Sulfur (1.75)	1.77	2350	3950	460	61	64.2	64.9	140	2.71	3670	4070	330	99	69.4	53.7
						Pro	Properties at	-10° C							
7, 2.5 ×107 reps	1.13	1820	3260	490	1	51.0	1	220	1.10	1940	3080	410	1	48.2	1
7, 2.8 ×107 reps	1.27	1710	3350	540	1	51.5	1	150	1.04	1770	3300	490	-	49.7	1
7, 3.1 X107 reps	1.42	2230	3700	430	-	52.0	1	96	1,35	2030	3120	410	1	51.1	1
Sulfur (1.25)	1.20	1610	3220	490	-	46.5	1	230	1.93	2400	3120	370	ì	46.5	1
Sulfur (1.75)	1.77	3020	4370	410	ļ	45.2	I	140	2.71	3980	4170	310	ı	46.2	
						P	Properties at	J .02 1							
7, 2.5 ×107 reps	1.13	1310	1800	410	1	9.09	1	350	1.10	1200	1530	360	1	61.0	
7, 2.8 ×107 reps	1.27	1380	1810	370	!	64.6	1	235	1.04	1440	1550	320	1	8.09	1
7, 3.1 X107 reps	1.42	1720	1790	310	-	68.6	-	230	1.35	1580	1580	300	1	62.4	1
Sulfur (1.25)*	1.20	1480	2510	450	-	64.6	1	205	1.93	1	2120	270	1	63.8	1
Sulfur (1.75)	1.77	1710	2510	410	1	75.0	-	230	2.71	1	2250	260	1	9.69	1

Philprene 1500 reinforced with 50 phr HAF black (Philblack O).

De Cured 30 minutes at 307° F. For compounding recipes see Appendix.

· Determined at tearing rate of 20 inches/minute by method of Rivlin, Greensmith and Thomas 17-14,

where g is an "entanglement factor". We have chosen to neglect this factor, partly because of the uncertainty of its value, but mainly because entanglements affect both crosslinking and scission in similar manner and we are primarily interested in the ratio of the two events. Entanglements increase the apparent number of crosslinks, but their release on cutting some of the network chains will also lead one to overestimate scission.

The detailed mechanisms of the scission and crosslinking reactions are not completely understood and are beyond the scope of this report. The primary act is undoubtedly the ionization of molecules with ejection of high energy secondary electrons and attenuation of the original gamma photon. This will

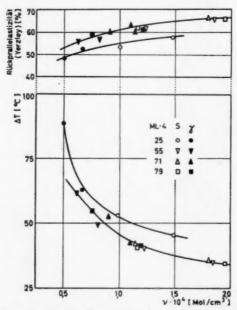


Fig. 4.—Dynamic properties of gamma and sulfur vulcanizates (SBR with 50 phr HAF black).

be discussed further in connection with the promotion of vulcanization by certain fillers. The secondary electrons, by reacting further with the polymer molecules, cause dissociation (scission) and form the free radicals capable of crosslinking.

PHYSICAL PROPERTIES OF GAMMA VULCANIZATES

Table III shows physical properties of typical gamma tread vulcanizates of SBR compared to similar sulfur-cured stocks. It is immediately apparent that the main difference between gamma and sulfur vulcanizates lies in their response to aging. There are, however, other distinctions of interest. The tensile and tear strengths of gamma vulcanizates are noticeably lower than those of sulfur-cured stocks. It has been suggested that this is a consequence of chain scission during vulcanization. This would, indeed, cause a difference

in tensile strength, even at equal densities of network chains (v). However, as pointed out above, such behavior should be accompanied by a degradation in dynamic properties as well. The data of Table III do not show the sulfur vulcanizates to be superior in resilience when compared at equal v. To investigate this question further four experimental copolymers of Mooney viscosity (ML-4) ranging from 25 to 79 were compounded in the recipes of Table III and vulcanized with gamma radiation (dosage 3 and 3.6×10^7 reps) and sulfur (dosage 1.25 and 1.75 phr). The resilience and heat build-up values are shown in Figure 4. The 25 ML-4 polymer yields vulcanizates of poorer dynamic properties at all values of v, reflecting the larger free-end fraction obtained in networks formed from low molecular weight material. Differences between the higher molecular weight polymers appear to be negligible. Significantly, however, the gamma and sulfur vulcanizates fall on the same curves indicating that essentially equivalent networks are obtained at equal values of v. It appears, therefore, that crosslink type rather than network degradation is responsible for the differences in physical properties, a conclusion which is not inconsistent with the relatively low estimate for the extent of scission by the stress-relaxation method.

The data of Table III show that the low temperature resilience of gamma vulcanizates is actually higher than for sulfur stocks. This difference appears to arise out of the fact that viscoelastic effects become more important than network structure at low temperature and is substantiated by the lack of de-

pendence of resilience on the net degree of crosslinking.

The question arises whether the superior retention of stress-strain properties of gamma vulcanizates on aging are entirely due to the absence of a (non-oxidative) post-vulcanization mechanism or whether the vulcanizates are also more resistant to oxidative attack. Stress relaxation and crosslinking measurements after aging in oxygen and nitrogen for 2 hours at 120° C were analyzed along the line developed in the preceding section of this paper for scission during cure and gave the following results for typical gamma and sulfur vulcanizates reinforced with 50 parts of HAF black:

	2 hrs, 1:	20° C, N ₃	2 hrs, 13	20° C, O2	Oxidative, o	omponent
	Sulfur	Gamma	Sulfur	Gamma	Sulfur	Gamma
$\Delta n \times 10^4$, moles/cc.	0.65	0.12	0.61	0.15	(-0.04)	0.03
$\Delta S \times 10^4$, moles/cc	0.36	0.07	0.44	0.18	0.08	0.11

The "oxidative component" of the aging process was obtained by subtracting the appropriate quantity as measured in N_2 from that determined in O_2 . This admittedly somewhat naive calculation assumes that the aging processes are independent and hence additive Whereas this is undoubtedly an oversimplification, the results show quite clearly that in the initial stages of accelerated aging, crosslinking is nonoxidative in both types of vulcanizates and is quite inappreciable in the gamma-cured rubber. The gamma vulcanizate undergoes less total scission on aging but the extent of oxidative scission appears to be about the same as in the sulfur vulcanizate. The comparisons are probably biased slightly in favor of the sulfur-cured rubber as it contained additional antioxidant (1 phr Flexamine) added prior to vulcanization.

On long term aging, scission proceeds to the point where none of the initial chains are left unbroken (total stress-relaxation), but the net effect is strongly in the direction of crosslinking in either type of vulcanizate. This is evident

from measurements on the above vulcanizates taken after 48 hours at 120° C.

		N ₂		O ₂		dative
	Sulfur	Gamma	Sulfur	Gamma	Sulfur	Gamma
$\Delta \nu \times 10^4 = 2(\Delta n - \Delta S) \times 10^4$, moles/ce	3.8	1.2	4.5	1.7	0.7	0.5

Again the main differences appear not to be associated with oxidation. It is concluded that, at least under the conditions investigated here, the superior age resistance of gamma-vulcanized SBR is primarily due to elimination of non-oxidative post-vulcanization effects. Since in sulfur vulcanizates the post-vulcanization over-compensates the scission effect, aging leads to an increase in net crosslinking and hence to improved resilience and heat build-up. The lack of this compensating mechanism in gamma vulcanized rubber aged under relatively mild conditions causes a loss in net crosslinking (aside from possible network degradation due to main chain scission) and with it a loss in the dynamic properties of the vulcanizate. This is shown quite clearly in the resilience and heat build-up data of Table III.

TABLE IV
GAMMA VULCANIZATES REINFORCED WITH SILICA

Rubber	Silica,	Vulcani-	Radia- tion dosage, reps	300% Mod- ulus, psi	Ten- sile, psi	Elon- gation,	Resilience,	ΔT,
SBR ^o Hevea SBR ^o Hevea	60 60 60	Gamma Gamma Sulfur Sulfur	3 ×10 ⁷ 3 ×10 ⁷	1260 1080 850 910	3750 4050 3250 3510	730 810 640 710	50.3 53.2 51.6 66.2	89.8 94.6 73.3 74.3

^a Philprene 1500. ^b Hi-Sil 233.

One of the outstanding features of radiation induced vulcanization is its independence of the retarding mechanism brought into play by so many of the common inorganic fillers in sulfur vulcanization. For example, vulcanizates reinforced with silica or alumina display excellent physical properties. Indeed, it appears that the full reinforcing potential of these fillers may not be realized in sulfur systems because of their inhibitory effect on cure. Gamma vulcanization overcomes this difficulty. Some comparative tests data to support this point are shown in Table IV.

PROMOTION OF VULCANIZATION BY HEAVY METAL FILLERS

As is apparent from the data already presented, the dosage requirement for optimum gamma vulcanization is very large. One method investigated for reducing the dosage requirement involves the use of heavy metal fillers capable of absorbing a greater portion of the incident primary radiation and emitting secondary electrons into the rubber where they cause an increase in the rate of vulcanization. The absorption of gamma rays occurs by three processes—the Compton effect, the photoelectric effect and electron-positron pair production. Absorption by the Compton effect increases linearly with the atomic number of the absorber whereas absorption by the photoelectric effect is insignificant at low atomic numbers but rises very sharply toward the heaviest elements. Pair production is inappreciable for 1.5 Mev gammas. These relations are

[·] Cured 30 min at 307° F.

illustrated in Figure 5. The curves were calculated from data of Davisson and Evans¹⁵ and Heitler¹⁶.

The following simple experiment demonstrates the efficacy of this method for increasing the crosslink, yield in vulcanization. A thin film of gum rubber is irradiated between plates of various metals, adjusted in thickness to transmit equal intensities of gamma radiation. Any differences in crosslinking must then

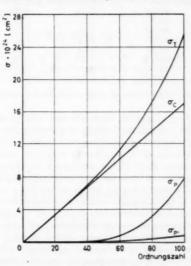


Fig. 5.—Absorption cross sections for 1.5 MEV gamma rays (σ_T total; σ_C Compton; σ_P photoelectric; σ_P ' pair production).

be ascribed to secondary radiations from the metals. Table V shows the result of such an experiment. It is obvious from the data that very substantial increases in crosslink yields can be realized in this manner and that the effect increases with the atomic number of the absorber.

The same principles apply equally to the promotion of vulcanization with fillers, some aspects of which have already been discussed by Gehman and

 $\begin{array}{c} T_{ABLE}\ V\\ G_{AMMA}\ V_{ULCANIZATION}\ of\ G_{UM}\ SBR\ Between\ Metal\ Plates\\ (Nominal\ dosage,\ 3\times 10^7\ reps) \end{array}$

Metal	None	Al	Ni	Mo	Sn	W	Pb
Atomic number	esemen.	13	28	42	50	74	82
$\nu \times 10^4$, moles/cc	0.66	0.72	0.86	0.87	0.89	1.73	1.88

Auerbach⁶ and by Kuzminskii and associates⁷. Table VI illustrates the effect of the atomic number of the promoting filler for a series of metal oxides and for the halides of lead. The results show the expected overall trend with atomic number, but they also indicate that specific effects are not absent (e.g., HgO is more effective than PbO, PbO is more effective than the halides of lead). These might be explained on the basis of dissociation of the filler, giving rise to free radicals capable of adding to the vulcanization effect.

Table VI
Promotion of Gamma Vulcanization with Fillers
(SBR reinforced with 50 phr HAF Black)

Promoter (5.1 mole			$\nu \times 10^4 \text{ (moles/cc)}$	
per cent)	Za	107 reps	3 ×10 ⁷ reps	7×107 repa
None	_	0.27	1.17	2.80
ZrO ₂	40(8)	0.33	1.23	3.25
CdO ₂	48(8)	0.35	1.21	3.37
HgO	80(8)	1.16	2.57	6.50
PbO	82(8)	0.71	2.40	5.80
PbF ₂	82(9)	0.51	1.61	4.50
PbCl ₂	82(17)	0.47	1.73	4.30
PbBr ₂	82(35)	0.51	1.61	4.50
PbI ₂	82(53)	0.59	2.20	6.00

Atomic number of metal; atomic number of oxygen or halogen in parentheses.

Since the absorption of gamma rays per unit volume of rubber compound will vary linearly with the volume loading of the promoter one might expect a similar dependence of induced crosslinking with loading. This is not strictly so (Figure 6), the promotion effect tending to level out somewhat at high PbO loadings, possibly because more of the secondary electrons are reabsorbed by neighboring filler particles as these become crowded together.

The promotion of crosslinking by heavy metal fillers also depends to some extent on their state of subdivision. With particles in the submicron range this effect is not large, but it is nevertheless significant (Table VII). In the example presented the degree of crosslinking increased 18 per cent on reduction of particle size by nearly a factor of two. If the particle size effect is due to self-absorption of the secondary electrons, one would expect it to disappear almost entirely on approaching the state of atomic or molecular dispersion. Experiments with fillers of greatly reduced particle size would be of interest, but have as yet not been performed. The particle size effect might easily account for some of the deviations of the data in Table VII from a simple correlation with atomic number. Comparison of the extent of promotion

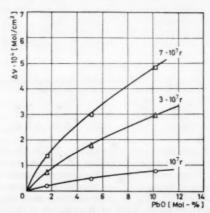


Fig. 6.—Effect of lead oxide loading on production of gamma vulcanization (SBR with 50 phr HAF black).

on initial molecular weight, and to employ Tobolsky's relation, Equation (3), for the interpretation of stress relaxation data in terms of chain scission. Tobolsky's approach should be accurate for small values of χ , but it obviously breaks down when the cuts are sufficiently numerous so that mutual interference occurs. It is extended in this paper so that this limitation is avoided, and it is shown that the discrepancy between Tobolsky's and Flory's results can be readily resolved.

ANALYSIS FOR THE GEL FRACTION

A crosslink will be termed zero-, mono-, bi-, tri-, or tetrafunctional, depending upon whether it joins the ends of none, one, two, three, or four effective network chains. A trifunctional crosslink may thus be either a branch point

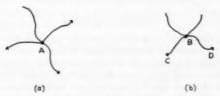


Fig. 1.—Diagrammatic representation of (a) trifunctional crosslink and (b) bifunctional crosslink.

of a polymer or a chemical crosslink at which one of the four chains is ineffective, for example, if it is terminated by a free end (crosslink A in Figure 1 (a)). A bifunctional crosslink is not counted as a physical crosslink because it merely acts as a bridge linking two portions of a chain together. Thus Figure 1b shows only one effective network chain, the crosslink B acting only as a link in the chain CD.

Figure 2 shows tri- and tetrafunctional crosslinks (A and B, respectively). If the chain joining A and B is cut, A becomes bifunctional and ceases to be a crosslink in the sense used here while B becomes trifunctional.



Fig. 2.—Diagrammatic representation of adjacent tetrafunctional and trifunctional crosslinks.

In the determination of the number of effective network chains in the gel in terms of the number of crosslinks and free ends, the final network is considered to arise from the random cutting of chains in a network containing the requisite number of crosslinks, but, initially, with no free chain ends. A necessary restriction is that the cuts are only introduced into effective network chains so that no sol is formed.

If there are N_4 tetrafunctional and N_3 trifunctional crosslinks per unit volume, then the probability of a network chain end being at one of the former is

$$\alpha_4 = 4N_4/(4N_4 + 3N_3)$$

Table VI
PROMOTION OF GAMMA VULCANIZATION WITH FILLERS (SBR reinforced with 50 phr HAF Black)

Promoter (5.1 mole			P×104 (moles/cc)	
per cent)	Z^a	107 reps	3×10 ⁷ reps	7×10 ⁷ repa
None		0.27	1.17	2.80
ZrO ₂	40(8)	0.33	1.23	3.25
CdO ₂	48(8)	0.35	1.21	3.37
HgO	80(8)	1.16	2.57	6.50
PbO	82(8)	0.71	2.40	5.80
PbF ₂	82(9)	0.51	1.61	4.50
PbCl ₂	82(17)	0.47	1.73	4.30
PbBr ₂	82(35)	0.51	1.61	4.50
PbI ₂	82(53)	0.59	2.20	6.00

Atomic number of metal; atomic number of oxygen or halogen in parentheses.

Since the absorption of gamma rays per unit volume of rubber compound will vary linearly with the volume loading of the promoter one might expect a similar dependence of induced crosslinking with loading. This is not strictly so (Figure 6), the promotion effect tending to level out somewhat at high PbO loadings, possibly because more of the secondary electrons are reabsorbed by neighboring filler particles as these become crowded together.

The promotion of crosslinking by heavy metal fillers also depends to some extent on their state of subdivision. With particles in the submicron range this effect is not large, but it is nevertheless significant (Table VII). In the example presented the degree of crosslinking increased 18 per cent on reduction of particle size by nearly a factor of two. If the particle size effect is due to self-absorption of the secondary electrons, one would expect it to disappear almost entirely on approaching the state of atomic or molecular dispersion. Experiments with fillers of greatly reduced particle size would be of interest, but have as yet not been performed. The particle size effect might easily account for some of the deviations of the data in Table VII from a simple correlation with atomic number. Comparison of the extent of promotion

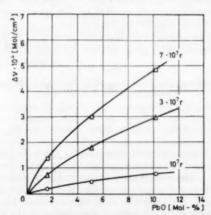


Fig. 6.—Effect of lead oxide loading on production of gamma vulcanization (SBR with 50 phr HAF black).

afforded by either metal plates or fillers with the absorption cross sections of Figure 5 reveals that the crosslink yields do not increase fast enough with the total absorption cross section for the lighter and intermediate elements. This suggests that the absorption through the photoelectric effect contributes more to the promotion of vulcanization than the Compton effect. This may be explained on the basis that in photoelectric absorption the entire energy of the gamma photon is imparted to the secondary electron while the Compton electrons only acquire a portion of the energy of the primary gamma photon.

TABLE VII

EFFECT OF PARTICLE SIZE OF LEAD OXIDE ON CROSSLINKING (SBR reinforced with 50 phr HAF Black)

Lead oxide, mole %	Area average particle diameter, microns	»×104, moles/ee	
5.1	0.52	1.80	
5.1	0.37	1.90	
5.1	0.30	2.12	

The scattered Compton gamma ray stands a much better chance of escaping the sample than the more easily absorbed secondary electrons. In the work of Gehman and Auerbach⁶ barium (atomic number 56) sulfate was the filler of highest atomic number used. The high effectiveness of the photoelectrons was, therefore, not observed.

A large number of fillers have been tried as gamma vulcanization promoters. Of these lead oxide appears to be the most suitable as it does not impair the desirable mechanical properties of the finished vulcanizate. Table VIII shows examples of some typical test data obtained on litharge promoted vulcanizates

Table VIII

Some Properties of Litharge Promoted Gamma Vulcanizates (All vulcanizates reinforced with 50 phr HAF Black)

Rubber	Dosage, reps	PbO,	Mod- ulus, pai	Tensile strength, pai	Ultimate elonga- tion,	Resilience,
SBR	3×10^{7}		1350	2850	580	58.6
	3×10^{7}	2	2460	2890	350	64.4
SBR, oil extended	5×10^{2}	-	700	1560	650	60.8
	3×10^{7}	2	810	1770	610	59.4
Bd/Styrene (50/50)	3×10^7		750	2270	810	53.6
	3×10^{7}	2	1710	2540	460	57.0

^a Philprene 1712, contains 37.5 parts of highly aromatic extender oil.

containing 2 volume parts of promoter per hundred volumes of polymer. In all cases the changes in properties on addition of PbO are in the direction of increased crosslinking, or a lower radiation dosage is required to produce vulcanizates of equivalent properties.

CONCLUSIONS

The vulcanization of butadiene/styrene rubber by gamma radiation is capable of yielding good vulcanizates, differing not too strongly from conventional sulfur vulcanizates in physical properties. The crosslinking reaction

does not appear to be accompanied by an excessive amount of main chain scission. The superior retention of stress-strain properties of gamma vulcanizates during aging appears to be entirely due to the elimination of post-vulcanization effects. The high radiation dosages required for vulcanization may be materially reduced by the use of heavy metal fillers as promoters.

SUMMARY

Experiments on the gamma-radiation vulcanization of butadiene/styrene rubber are described. A systematic investigation of the gamma radiation cure of a tread type compound is presented, which shows the dependence of the physical properties of gamma vulcanizates on the characteristics of the network formed. Swelling and stress relaxation measurements indicate that the crosslinking reaction is not accompanied by an excessive amount of main chain scission. Such measurements show also that the superior retention of stressstrain properties during aging of gamma vulcanizates is due to the elimination of post-vulcanization by chemical curatives. At equivalent crosslinking levels gamma vulcanizates display properties similar to sulfur vulcanizates. Gamma radiation overcomes the inhibition of vulcanization shown by a number of inorganic fillers and appears to enhance their reinforcement potential. ordinarily high radiation dosage requirement for vulcanization may be reduced by incorporating heavy metal fillers into the rubber matrix. Such promotion depends on the atomic number, loading and state of subdivision of the promoting filler.

ACKNOWLEDGMENT

The authors wish to express their appreciation to Dr. C. E. Stoops for many helpful suggestions concerning the irradiation experiments proper.

REFERENCES

- 1 Newton, E. B., U. S. 1,906,402 (1933).
 2 Davidson, W. I., and Geib, I. G., J. Appl. Phys. 19, 427 (1948).
 3 Gehman, S. D., and Hobbs, L. M., Rubber World 130, 643 (1954).
 4 Jackson, W. E., and Hale, D., Rubber Age 77, 865 (1955).
 5 Charlesby, A., Atomice 5, 12 (1954).
 6 Gehman, S. D., and Auerbach, I., Intern. J. Appl. Radiation & Isotopes 1, 102 (1956).
 7 Kuzminskii, A. S., Nikitina, T. S., and Karpov, V. L., J. Nuclear Energy 4, 268 (1957).
 8 Kraus, G., Rubber World 135, 67, 254 (1956).
 9 Tobolsky, A. V., Metz, D. J., and Mesrobian, R. B., J. Am. Chem. Soc. 72, 1942 (1950).
 19 Scanlan, J., J. Polymer Sci. 43, 501 (1960).
 11 Flory, P. J., and Rehner, J., J. Chem. Phys. 11, 512 (1943).
 12 Rivlin, R. S., and Thomas, A. G., J. Polymer Sci. 10, 291 (1953).
 13 Thomas, A. G., J. Polymer Sci. 18, 189 (1955).
 14 Greensmith, H. W., and Thomas, A. G., J. Polymer Sci. 18, 189 (1955).
 15 Davisson, C. M., and Evans, R. D., Res. Modern Phys. 24, 79 (1952).
 15 Heitler, W., "The Quantum Theory of Radiation", Oxford University Press, New York, 1947.

DETERMINATION OF DEGREE OF CROSSLINKING IN NATURAL RUBBER VULCANIZATES. PART III *

L. MULLINS

THE BRITISH RUBBER PRODUCERS' RESEARCH ASSOCIATION, WELWYN GARDEN CITY, HERTS., ENGLAND

INTRODUCTION

The two previous parts of this series^{1, 2} described an attempt to relate the physical properties of natural rubber vulcanizates to their network structure. The first established an empirical relationship between the stress-strain behavior of highly swollen natural rubbers in simple extension, and their equilibrium volume swelling in n-decane. It also examined the effect of changes in initial molecular weight of the unvulcanized masticated rubber on these properties, and an empirical correction making allowance for network flaws due to chainsegments terminated by a crosslink at only one end was obtained. The second part2 gave measurements of the equilibrium volume swelling and the intrinsic viscosity before vulcanization for each of a range of natural rubber vulcanizates which had been prepared by a method which enabled the number of crosslinks to be determined by chemical analysis. These measurements permitted a comparison to be made between (i) the chemical estimate of the actual number of crosslinks introduced and (ii) the number derived from the data on equilibrium volume swelling, by means of the empirical relations derived in Part I. For this purpose, an assumption was made that the stress-strain behavior of highly swollen rubbers was in accord with the predictions of the statistical theory.

Recent studies^{3, 4} of both the stress-strain properties of highly swollen rubbers and the method of determining number-averaged molecular weight from intrinsic viscosity measurements have provided an improved basis for the quantitative determination of the degree of crosslinking from measurements of physical properties. The results described in Parts I and II of this series are reinterpreted here to take account of both of these developments; in addition, the effect of the introduction of a correction for a network defect equivalent to chain entanglements is examined.

MODIFIED BASIS FOR DETERMINATION OF PHYSICAL DEGREE OF CROSSLINKING

STRESS-STRAIN BEHAVIOR OF HIGHLY SWOLLEN RUBBERS

Previous investigations^{1, 5} have shown that the stress-strain behavior of both dry and swollen rubber in simple extension can be described by an expression of the form suggested by Mooney⁶ and Rivlin⁷,

$$f = 2 A_0(\lambda - \lambda^{-2})(C_1 + \lambda^{-1}C_2)$$
 (1)

^{*} Reprinted from Journal of Applied Polymer Science, 2, 1 (1959).

where C_1 and C_2 are parameters characterizing the vulcanizate and the degree of swelling, and f is the force required to extend a sample of rubber of unstrained cross-sectional area A_0 to an extension ratio λ . The value of C_2 was shown to decrease progressively as the degree of swelling was increased until at high degrees of swelling it became exceedingly small and the dependence of force on deformation was then given by

$$f = 2 A_0(\lambda - \lambda^{-2})C_1 \tag{2}$$

and thus followed the predictions of the statistical theory.

Recent studies³ in which stress-strain measurements have been examined up to higher extensions have shown that departures from the simple form of stress-strain curves given by Equations (1) and (2) occur at large extensions. These are due to the finite extensibility of the network chains. With dry rubbers, these departures only became important at large extensions but with highly swollen rubbers, they were present at much lower elongations. Under these conditions they made the determination of accurate values of C_1 extremely

Table I Relationship between C_1 and v_r (Measurements at $25 \pm 0.2\,^{\circ}$ C)

Vul- canizate	$M^{-1} \times 10^{6}$	$\begin{array}{c} C_1,\\ \mathbf{dynes-}\\ \mathbf{cm^{-2}} \times\\ 10^{-4} \end{array}$	$\begin{array}{c} C_{2s} \\ \text{dynes-} \\ \text{em}^{-2} \times \\ 10^{-6} \end{array}$	Dr.
A 1	4.57	1.08	0.70	0.253
2	5.60	1.07	0.75	0.242
3	7.00	0.93	0.63	0.227
4	7.75	0.82	0.54	0.213
5	10.05	0.75	0.47	0.201
B 1	4.60	1.53	0.86	0.285
2	5.70	1.63	0.83	0.292
3	6.40	1.62	0.78	0.292
4	9.20	1.22	0.63	0.259
5	11.20	0.77	0.46	0.213
C 1	6.00	1.10	0.72	0.250
2	7.60	1.02	0.70	0.240
3	9.50	0.85	0.52	0.225
4	11.10	0.72	0.42	0.211
D 1	4.95	1.85	0.87	0.308
2	6.20	1.80	0.80	0.303
3	7.35	1.75	0.78	0.299
4	9.00	1.59	0.72	0.293
5	11.75	1.50	0.65	0.279
E 1	4.80	1.79	0.88	0.304
2	4.80	1.50	0.83	0.283
3	4.80	1.43	0.79	0.277
4	4.80	0.99	0.71	0.238
5	4.80	0.70	0.68	0.204
6	4.80	0.61	0.56	0.192
F i	3.10	1.85	1.01	0.314
2	3.95	1.90	0.94	0.314
- 3	5.12	1.86	0.87	0.314 0.313 0.302
4	7.05	1.67	0.78	0.302
5	9.65	1.57		0.292
H 1	4.20	1.37	0.93	0.271
2	6.00	1.30	0.91	0.273
	6.50	1.22	0.81	0.265
3 4	7.20	1.18	0.80	0.265

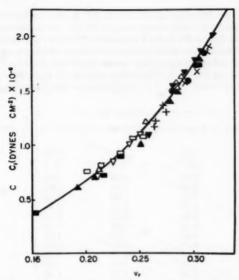


Fig. 1.—Dependence of elastic constant C_1 on the equilibrium volume swelling v_r . (\square) A. (\triangle) B. (∇) C. (\bullet) D. (\blacktriangledown) E. (\times) F. (+) H.

difficult, and resulted in an increase in the apparent value of C_1 and a decrease in the apparent value of C_2 determined by plotting $\frac{1}{2}fA_0^{-1}(\lambda - \lambda^{-2})^{-1}$ against λ^{-1} .

It was shown that values of C_1 varied with swelling in the manner predicted by the statistical theory and that the value of $C_1v_r^{-1}$ remained independent of degree of swelling until, with highly swellen rubbers, these departures due to finite extensibility became significant at low elongations. Thus in this investigation, values of C_1 determined on dry rubbers are used to characterize the network structure. The use of values of C_1 determined on dry rubbers instead of swellen rubbers as previously results in a decrease in the estimated degree of crosslinking by approximately 10%.

DETERMINATION OF INITIAL MOLECULAR WEIGHT

Mullins and Watson³ have recently redetermined the limiting viscosity number-molecular weight relationship for samples of masticated natural rubber and have obtained the following expression

$$[\eta] = 2.29 \times 10^{-7} M^{1.33} \tag{3}$$

which is somewhat different from that previously employed8.

The use of the new relationship for the determination of initial molecular weight makes little difference to the *absolute* value of the empirical correction to be applied for chain ends.

Both of these modifications have been introduced into the previous results. Relationship between C_1 and v_r .—The first step was to provide a new relationship between C_1 and v_r using values of C_1 determined from stress-strain measure-

ments made on dry samples of rubber at 25° C and measurements of their equilibrium volume swelling in n-decane at 25° C. Measurements were made on all the samples examined in Part I following the procedures described there. Compounding details and vulcanization procedures are given in the Appendix. The results obtained on the peroxide vulcanizates are given in Table I and are shown graphically in Figure 1. Here the value of C_1 is plotted as ordinate and the corresponding value of v_r for equilibrium volume swelling is plotted as abscissa.

Vul- canizate	[ŋ], (g/100 ml) ⁻¹	$^{M^{-1} imes}_{10^6} imes$	C_1 , dynes- em ⁻² \times 10^{-6}	C_1 , dynes- em $^{-3} imes 10^{-6}$
A 1	2.82	4.75	1.08	0.70
2	2.30	5.60	1.07	0.75
3	1.71	7.00	0.93	0.63
4	1.48	7.75	0.86	0.54
4 5	1.03	10.05	0.75	0.47
C 1	2.12	6.00	1.10	0.72
2	1.52	7.60	1.02	0.70
3	1.10	9.50	0.85	0.52
4	0.91	11.10	0.72	0.42
D 1	2.70	4.95	1.85	0.87
2	2.05	6.20	1.80	0.80
3	1.60	7.35	1.75	0.78
4	1.19	9.00	1.59	0.72
5	0.86	11.75	1.50	0.65
F 1	4.80	3.10	1.85	1.01
2	3.63	3.95	1.90	0.94
3	2.57	5.12	1.86	0.87
4	1.69	7.05	1.67	0.78
5	1.08	9.70	1.57	
G 1	4.34	3.40	1.31	1.01
2	3.16	4.35	1.30	0.91
- 3	2.38	5.45	1.21	0.90
4	1.22	8.85	1.02	0.78
5	0.80	12.9	0.72	0.57
Hi	3.30	4.20	1.37	0.93
2	2.12	6.00	1.30	0.91
3	1.88	6.50	1.22	0.81
4	1.64	7.20	1.18	0.80

The full line in the figure shows the theoretical relationship derived by Flory-Huggins^{10, 11} to describe the dependence of equilibrium volume swelling on degree of crosslinking. The relation is

$$-\ln (1 - v_r) - v_r - \mu v_r^2 = \rho V_0 M_c^{-1} v_r^4$$
 (4)

Assuming

$$C_1 = \frac{1}{2} \rho R T M_c^{-1} \tag{5}$$

a value⁵ of μ of 0.42 was found to give the best fit to the experimental results. This is to be compared with the value³ of μ of 0.41 determined in Part I.

Dependence of C_1 on initial molecular weight.—The empirical correction for the effect of initial molecular weight was redetermined using values of C_1 obtained on dry vulcanizates and introducing the modified relationship to obtain estimates of the number average molecular weight from intrinsic viscosity data. The six series of rubbers A, C, D, F, H, and G provided vulcanizates which within each series had the same degree of crosslinking but were different in their initial molecular weights. Load-deformation measurements were made at 25° C on dry samples of each of the vulcanizates and from them, values of C_1 and C_2 were determined. The results are given in Table II together with measurements of their intrinsic viscosity prior to vulcanization and estimates of the reciprocal initial molecular weights.

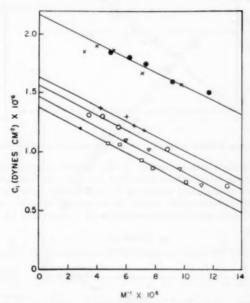


Fig. 2.—Dependence of elastic constant C₁ on the reciprocal initial molecular weight M⁻¹.

The dependence of C_1 on initial molecular weight shown graphically in Figure 2. It will be seen that all of the results can, as previously, be represented satisfactorily by a simple linear dependence of C_1 on M^{-1} , and that the correction for initial molecular weight can now be expressed in the form

$$C_1 = C_1^{\infty} - 6.2 \, M^{-1} \times 10^{10} \, \text{dynes cm}^{-2}$$
 (6)

where C_1^{∞} refers to the extrapolated value for infinite initial molecular weight. Figure 3 gives all of the results plotted to demonstrate this linear relationship between $C_1^{\infty} - C_1$ and M^{-1} .

COMPARISON BETWEEN PHYSICAL AND CHEMICAL DETERMINATIONS OF DEGREE OF CROSSLINKING

Table III gives results on all of Moore and Watson's vulcanizates whose degree of crosslinking fell in the range within which the relationship between equilibrium volume swelling and C_1 had been established. In addition to their

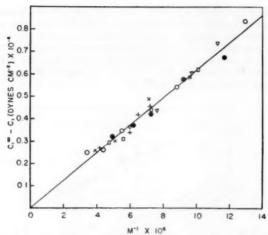


Fig. 3.—Change in elastic constant C_1 with the reciprocal initial molecular weight M^{-1} .

data on the chemical determination of the degree of crosslinking and the equilibrium volume swelling, the table also includes a revised estimate of the initial molecular weight, and values of C_1 determined from the equilibrium volume swelling measurements using the empirical relation established in Figure 1. The table also includes estimates of C_1 corrected for the effect of

Table III
CHEMICAL AND PHYSICAL DETERMINATIONS OF DEGREE OF CROSSLINKING.

Sample (chemical) no $\times 10^{s}$			No correction for entanglements		Correction for entanglements			
	(chemical)	M ⁻¹ ×10⁴ v _r	vr	C_1 , dynes- cm ⁻¹ $\times 10^{-6}$	$C_1^{\circ \circ}$, dynes- cm ⁻¹ $\times 10^{-6}$	M _e -1 (physical) ×10 ^s	C [∞] *, dynes- em ⁻¹ ×10 ⁻⁴	M _e -1* (physical) ×10 ⁵
1 2 3	3.14 3.42 3.44	5.35 5.70 5.70	0.214 0.199 0.144	0.78 0.66 0.62	1.13 1.01 0.97	10.06 8.99 8.63	$0.39 \\ 0.36 \\ 0.33$	3.45 3.20 2.95
5	3.58 3.94	5.35 5.35	$0.219 \\ 0.227$	0.81	1.14	10.15 10.86	0.44	3.90 4.25
6	4.84	5.35	0.240	1.02	1.35	12.02	0.57	5.10
8	4.92 5.74	5.35 5.35	$0.241 \\ 0.252$	1.03	1.36 1.47	12.10 13.08	0.58	5.15 5.85
19	5.76	5.65	0.246	1.08	1.43	12.73	0.63	5.60
10	6.34	5.70 5.70	$0.248 \\ 0.249$	1.10	1.45 1.46	12.91 12.99	0.66	5.85 5.95
12	10.16	5.70	0.293	1.68	2.03	18.07	1.15	10.20
13 14	$10.20 \\ 14.76$	5.70 5.33	0.294 0.333	1.69 2.25	2.04 2.58	18.16 22.96	1.16 1.75	10.30 15.60
21 22	2.20 3.62	5.65 5.35	$0.172 \\ 0.211$	0.47	0.82	7.30	0.28	2.50
23	5.16	5.35	0.211	0.75	1.08 1.31	9.61 11.66	0.40	3.55 4.85
24 25	6.10 6.66	5.33 5.65	$0.261 \\ 0.257$	1.24	1.57 1.57	13.97 13.97	0.60	6.45
26	12.94	5.33	0.326	2.15	2.48	22.07	1.58	14.05
28 29	4.40 5.52	5.35 5.35	$0.232 \\ 0.248$	0.93 1.10	1.26 1.46	11.21 12.99	0.51	4.50 5.65
30	7.52	5.33	0.262	1.25	1.58	14.06	0.76	6.80
31 32	11.98 15.96	5.33 5.33	0.306 0.341	1.83 2.38	2.16 2.71	19.22 24.12	1.27 1.80	11,30 16.00
33	4.02	5.35	0.229	0.91	1.24	11.04	0.49	4.35
34 35	6.66 7.46	5.30 5.33	$0.257 \\ 0.275$	1.19 1.40	1.51 1.73	13,44 15,40	0.70	6.25 7.95
36	11.18	5,33	0.306	1.83	2.16	19.22	1.27	11.30

chain ends using the correction described by Equation (6) together with values of M_e^{-1} (physical) determined using the assumption

$$C_1 = \frac{1}{2} \rho R T M_e^{-1}$$
 (physical)

Values of M_c^{-1} (physical) determined in this way are plotted against the chemical determination of M_c^{-1} in Figure 4. As in Moore and Watson's earlier interpretation of the data, the physical estimate of M_c^{-1} is always greater than the chemical estimate.

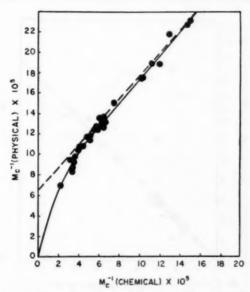


Fig. 4.—Comparison of physical and chemical estimates of the reciprocal chain-segment molecular weight M_e⁻¹.

A possible explanation of the difference between the two estimates, which has previously been discussed by the author² and by Bueche¹², is that the network is subject to restraints other than those resulting from crosslinks. One such form of restraints would result from chain entanglements, which would impose configurational constraints and behave elastically as though they were crosslinks. The consequences of the departures being due to entanglements are now further examined.

CORRECTIONS FOR THE CONTRIBUTION OF CHAIN ENTANGLEMENTS

It is assumed that the measured value of C_1 contains a contribution due to chemical crosslinks and another due to chain entanglements acting as though they were crosslinks. It is further assumed that chain entanglements only contribute to the network if they are in chain-segments bounded by chemical crosslinks at both ends.

The contribution of entanglements to the total number of crosslinks will thus be greater the greater the fraction of rubber linked into the network, and with a highly crosslinked rubber or with rubber of high initial molecular weight, most of the potential entanglements will be effective as crosslinks. Thus in Figure 4, the intercept given by the extrapolation of the linear portion of the plot to zero degree of crosslinking gives an estimate of the maximum contribution of entanglements.

The correction for network flaws due to chain ends should be calculated not on the basis of the apparent number of crosslinks determined from C_1 , which includes both chemical crosslinks and entanglements, but on the basis of the

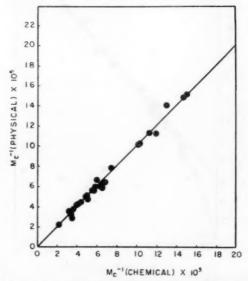


Fig. 5.—Comparison of physical and chemical estimates of the reciprocal chain-segment molecular weight M_c^{-1} after allowance for chain-entanglements.

actual number of chemical crosslinks. If the correction follow the forms shown by theorectical expressions^{13, 14} and is linear with respect to M_cM^{-1} , then the number of effective crosslinks (N_c) will be given by the expression

$$N_e = (N \text{ chemical} \times N \text{ entanglements}) \times (1 - \beta M_c M^{-1})$$
 (7)

where N entanglements is the maximum contribution of entanglements to the number of crosslinks, and M_c is the molecular weight of chain segment between adjacent chemical crosslinks. Or equivalently,

$$C_1 = (C_1^{\infty *} + \alpha)(1 - \beta M_c * M^{-1})$$
 (8)

where α represents the maximum contribution of entanglements to C_1 , and M_c^* is now calculated from the new $C_1^{\infty *}$. Values of α and β were determined to fit the experimental results shown in Figures 2 and 4. The method used in this

determination was one of successive approximations, and it was found that the relation between C_1 and initial molecular weight could be expressed by the relation

$$C_1 = (C_1^{\infty*} + 0.78 \times 10^6)(1 - 2.3 M_c^* M^{-1}) \text{ dynes-cm}^{-2}$$
 (9)

Figure 5 shows the experimental data on the dependence of C_1 on initial molecular weight (previously given in Table II and shown in Figure 2) replotted; but now the full lines in the figure have been drawn using Equation (9). It will be seen that the experimental data can be just as well described by this new relation.

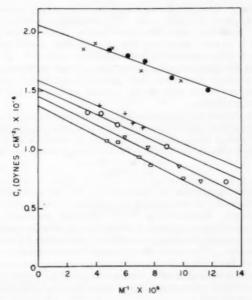


Fig. 6.—Change in elastic constant C_1 with reciprocal initial molecular weight M^{-1} , using Equation (9).

The last two columns of Table III give values of $C_1^{\infty *}$ and M^{-1*} (physical) derived from Moore and Watson's results and using the new empirical Equation (9) and assuming $C_1^{\infty *} = \frac{1}{2} \rho RT M_c^*$, and Figure 5 shows this new physical determination of M_c^{-1*} (physical) plotted against the chemical determination. The line in the figure has a slope of unity and there is now excellent agreement between the new physical estimate and the chemical estimate of M_c^{-1} .

It thus appears that when allowance is made for network flaws due to chain ends and chain entanglements by means of the two empirical corrections determined here, values of C_1 obtained in simple extension on either dry or swollen rubbers can be identified with the value predicted by the statistical theory, namely

$$C_1 = \frac{1}{2}\rho RTM_c^{-1}$$

This remarkable agreement between theory and experiment provides a most satisfactory confirmation of the relationship between the physical properties of

rubber vulcanizates and their chemical structure.

At first sight this complete agreement must be regarded as fortuitous. The simple network model used as a basis for the statistical theory is obviously an oversimplification, but it appears that, in simple extension, deviations from the theory at low and moderate extensions can be completely described by

(i) an extra term in the stored energy function

(ii) a correction for chain ends

(iii) a correction for chain entanglements.

The only one of these three empirical corrections which has any theoretical basis is the correction for chain ends. The empirical correction closely corresponds to the theoretical correction developed by Flory¹² which gives a value of $\beta=2$, but it is now recognized that the network model used in Flory's determination of this correction is not completely realistic¹⁵. It must also be recognized that the three empirical corrections are not independent and that a more refined analysis may alter their relative magnitudes. However, it is considered that the results indicate the general pattern of their contributions to stress-strain properties.

Further theoretical developments may modify the form of the appropriate stored energy function, but it appears unlikely that any simple statistical theory term in a new stored energy function will depart considerably from the value given by the first term in the Mooney-Rivlin form of stored energy function.

SYNOPSIS

Improvement in methods of characterizing the stress-strain properties of vulcanized rubber and of determining its molecular weight prior to vulcanization are described. Experimental results obtained previously by Mullins, Moore, and Watson, in an attempt to relate the physical properties of natural rubber to their network structure, are critically re-examined to take account of these developments. It is shown that if empirical corrections are made for the effect of network flaws due to chain ends and for a second type of network defect equivalent to chain entanglements, then estimates of the degree of crosslinking derived from physical measurements and from chemical determinations are in remarkably close accord.

APPENDIX

The following series of vulcanizates were prepared to give rubbers possessing a wide range of degree of crosslinking and initial molecular weight. In each case (except vulcanizates E1-E6) the compounded stock was divided into a number of equal parts and masticated to give different degrees of breakdown. Compounding ingredients and vulcanization conditions were as follows.

VULCANIZATES A1-A5

Smoked sheet 100, di-tert-butyl peroxide 5 parts by weight. Vulcanization 60 minutes at 140° C.

VULCANIZATES B1-B5

Smoked sheet 100, di-tert-butyl peroxide 7.5 parts by weight. Vulcanization 60 minutes at 140° C.

VULCANIZATES C1-C4

Smoked sheet 100, dicumyl peroxide 2 parts by weight. Vulcanization 90 minutes at 140° C.

VULCANIZATES D1-D5

Smoked sheet 100, dicumyl peroxide 3 parts by weight. Vulcanization 60 minutes at 140° C.

VULCANIZATES E1-E6

The following amounts of di-tert-butyl peroxide were added to 100 parts of masticated smoked sheet. All periods of heating were at 140° C. (1) 2.11 parts (3 hours); (2) 2.02 parts (5 hours); (3) 2.26 parts (14 hours); (4) 2.20 parts (11 hours); (5) 2.18 parts (7 hours); (6) 2.58 parts (7 hours).

VULCANIZATES F1-F5

Smoked sheet 100, dicumyl peroxide 3 parts by weight. Vulcanization 60 minutes at 140° C.

VULCANIZATES G1-G5

Smoked sheet 100, sulfur 3, zinc oxide 5, stearic acid 1, mercaptobenzothiazole 0.5, phenyl-β-naphtylamine 1 parts by weight. Vulcanization 45 minutes at 140° C.

VULCANIZATES H1-H4.

Smoked sheet 100, dicumyl peroxide 3 parts by weight. Vulcanization 60 minutes at 140° C.

ACKNOWLEDGMENT

This work forms part of a program of fundamental research undertaken by the Board of the British Rubber Producers' Research Association.

REFERENCES

- Mullins, L., J. Polymer Sci. 19, 225 (1956).
 Moore, C. G. and Watson, W. F., J. Polymer Sci. 19, 237 (1956).
 Mullins, L., J. Appl. Polymer Sci. in press.
 Mullins, L. and Watson, W. F., J. Appl. Polymer Sci. 1, 245 (1959).
 Gumbrell, S., Mullins, L. and Rivlin, R. S., Trans. Faraday Soc. 49, 1945 (1953).
 Mooney, M., J. Appl. Phys. 11, 582 (1940).
 Rivlin, R. S. and Saunders, D. W., Phil. Trans. Roy. Soc. London, A243, 251 (1951).
 Angier, D. J., Chambers, W. T. and Watson, W. F., J. Polymer Sci. 25, 129 (1957).
 Allen, P. W. and Place, M. A., J. Polymer Sci. 26, 386 (1957).
 Huggins, M. L., J. Am. Chem. Soc. 64, 2716 (1942).
 Flory, P. J., J. Chem. Phys. 18, 108 (1950).
 Bueche, A. M., J. Polymer Sci. 19, 297 (1956).
 Flory, P. J., J. Phys. Chem. 46, 132 (1942).
 Tobolsky, A. V., Prettyman, I. B. and Dillon, J. H., J. Appl. Phys. 15, 380 (1944).

DETERMINATION OF DEGREE OF CROSSLINKING IN NATURAL RUBBER VULCANIZATES. PART IV. STRESS-STRAIN BEHAVIOR AT LARGE EXTENSIONS *

L. MULLINS

BRITISH RUBBER PRODUCERS' RESEARCH ASSOCIATION, WELWYN GARDEN CITY, HERTS., ENGLAND

INTRODUCTION

The statistical theory of rubberlike elasticity predicts that the stress-strain behavior of vulcanized rubber in simple extension is given by

$$f = A_0 \nu k T (\lambda - \lambda^{-2}) \tag{1}$$

where f is the force required to extend a sample of rubber with a density of ν network chains per unit volume to an extension ratio λ , and where k is Boltzmann's constant, T the absolute temperature, and A_0 the unstrained cross-sectional area.

Appreciable deviations from the predictions of the statistical theory occur at low and moderate extensions, and a considerably better description of experimental stress-strain behavior can be obtained by the use of the first approximation of a generalized theory of large elastic deformations developed by Rivlin¹.

For simple extension, this gives

$$f = 2A_0(\lambda - \lambda^{-2})(C_1 + \lambda^{-1}C_2)$$
 (2)

The contribution of the term involving C_1 to the force required to extend rubber has been identified with that predicted by the statistical theory^{2, 3}; thus,

$$C_1 = \frac{1}{2}\nu kT$$

or, alternatively:

$$C_1 = \frac{1}{2} \rho RT M_c^{-1}$$

where ρ is the density of the rubber, M_c the number-average molecular weight of the chain segments of rubber between adjacent crosslinks, and R is the gas constant.

Further deviations from the predictions of Equations (1) and (2) occur at high extensions, and the value of the stress increases much more rapidly than predicted. Flory⁴ and Wood⁵ have associated this rapid upturn of the stress-strain curves with crystallization induced by molecular orientation at high strains. Treloar⁶, Kuhn and his associates^{7, 8}, Isihara, Hashitsume, and Tatibana⁹, and Wang and Guth¹⁰ have shown that deviations of this type result

^{*} Reprinted from J. of Appl. Polymer Sci. 2, 257 (1959).

4.09

naturally from the finite extensibility of network chain segments. At large strains, the use of the Gaussian distribution of chain-segment displacement lengths which was adopted in the derivation of Equation (1) becomes increasingly inadequate and quite unacceptable when the displacement lengths approach the full, extended length of the chain segments. This deficiency of the statistical theory has been dealt with by the introduction of more suitable distributions^{6, 9, 10}.

The quantitative applications of this non-Gaussian statistical theory to stress-strain curves at high extensions has been hampered by inadequacies in methods of determining the network structure. Recent developments in characterization of network structure³ now provide a possibility of quantitatively describing the onset of departures due to finite extensibility; these developments are examined in this paper.

APPLICATION OF NON-GAUSSIAN THEORY TO STRESS-STRAIN BEHAVIOR IN SIMPLE EXTENSION

Treloar⁶ gives a modified stress-strain relationship for simple extension in a series expression the first four terms of which are:

$$f = A_0 \nu k T (\lambda - \lambda^{-2}) \left[1 + \frac{3n^{-1}}{25} (3\lambda^2 + 4\lambda^{-1}) + \frac{297n^{-2}}{6125} (5\lambda^4 + 8\lambda + 8\lambda^{-2}) + \frac{12,312n^{-3}}{2,205,000} (35\lambda^6 + 60\lambda^3 + 72 + 64\lambda^{-3} + \cdots) \right]$$
(3)

The use of Equation (3) to calculate theoretical stress-strain curves is extremely laborious; also, the series cannot be satisfactorily approximated, since it approaches infinity as the chain segments become fully extended. However, its validity in regions where departures due to finite extensibility are small can be readily examined, as in these circumstances the contribution of higher terms in the polynomial becomes vanishingly small.

Departures from the predictions of the simple Gaussian theory, which are given by Equation (1), are described by a function of λ and n; thus, to describe their onset, a relationship between λ^* , the extension at which departures due to finite extensibility give a small but significant correction, and n was derived. An arbitrary value of 2.5 per cent was chosen for the correction, and it was found that for the rubbers used in this investigation it was then sufficient to consider only the first three terms of the polynomial.

Values of the first three terms in the polynomial, viz.,

λ*

$$1 + (3/25)n^{-1}(3\lambda^2 + 4\lambda^{-1}) + (297/6125)n^{-2}(5\lambda^4 + 8\lambda + 8\lambda^{-2})$$

were calculated for values of λ between 1.0 and 4.0 for selected values of n between 50 and 300, with the use of intervals of 0.2 between the values of λ and of

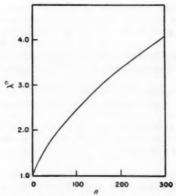


Fig. 1.—Dependence of λ^* on chain segment length π .

50 between the values of n. For each selected value of n, the ratio of the value of the expression to its value at $\lambda = 1$ was determined and conjugate values of λ^* and n, giving a ratio of 1.025 (an increase of $2\frac{1}{2}\%$), were obtained graphically. These are given in Table I, and shown in Figure 1.

STRESS-STRAIN BEHAVIOR AT LARGE EXTENSIONS

EXPERIMENTAL

Measurements were made of the equilibrium stress-strain properties in simple extension at 25° C, according to a procedure described previously^{2, 3}. A range of natural-rubber peroxide vulcanizates chosen to have as wide a range of initial molecular weights (Vulcanizates A-1 to A-5) and degree of crosslinking (Vulcanizates B-1 to B-5 and C-1 to C-5) as conveniently possible were examined. In addition, measurements were made on a range of natural-rubber

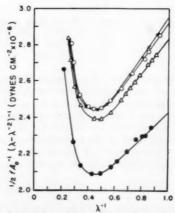


Fig. 2.—Dependence of stress-strain behavior on initial molecular weight: values of $\widehat{M}_{\pi^{-1}} \times 10^{q}$ of (\times) 3.10; (\bigcirc) 3.95; (\triangle) 5.12; (\bigcirc) 7.05.

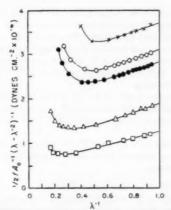


Fig. 3.—Dependence of stress-strain behavior on period of vulcanisation;
(×) 160 min; (△) 80 min; (♠) 60 min; (△) 40 min; (□) 10 min.

accelerated sulfur vulcanizates. Full compounding details and vulcanizing procedures are given in the Appendix.

Values of the number-average initial molecular weight \overline{M}_n , were determined from measurements of the intrinsic viscosity of samples of the compounded stock applied to the limiting viscosity number-molecular weight relationship for masticated natural rubber recently established by Mullins and Watson¹⁵:

$$[\eta] = 2.29 \times 10^{-7} \bar{M}_n^{1.33} \tag{4}$$

STRESS-STRAIN BEHAVIOR OF DRY RUBBERS

Figures 2, 3, and 4 give results obtained on dry samples of peroxide vulcanized rubber. These are plotted as $\frac{1}{2}fA_0^{-1}(\lambda-\lambda^{-2})^{-1}$ against λ^{-1} . The figures

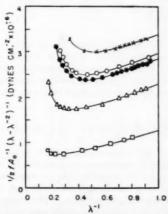


Fig. 4.—Dependence of stress-strain behavior on peroxide concentration: parts of peroxide per 100 parts rubber of (×) 5; (○) 4; (●) 3; (△) 2; (□) 1,

show, respectively, the effect of initial molecular weight, of period of vulcanization, and of concentration of peroxide on the stress-strain behavior. All of the curves show that at low and moderate extensions there is a region where the stress-strain behavior can be described in terms of the two parameters C_1 and C_2 . At higher extensions (smaller λ^{-1}), departures occur, and each curve goes through a minimum, the value of $\frac{1}{2}fA_0^{-1}(\lambda-\lambda^{-2})^{-1}$ thereafter increasing rapidly with further extension.

Figure 2 shows that the value of λ^{-1} at which the minimum occurs is little affected by changes in initial molecular weight. However, Figures 3 and 4 show that the minimum occurs at larger values of λ^{-1} for more highly crosslinked

rubbers.

Table II gives the values of C_1 and λ^* , the extension ratio at which the observed stress-strain curve departs from the linear portion by 2.5 per cent of C_1 , obtained from these curves.

Table II Change in λ^* with Degree of Crosslinking (Peroxide vulcanizates; density = 0.910 g/cm³; measurements at 25 \pm 0.2° C)

Vulcani- zate	$ar{M}_{n^{-1}} imes 10^{6}$	C_{1} , (dynes em ⁻³) $\times 10^{-6}$	λ*	$M_{\mathfrak{o}}$ (physical) $\times 10^{-3}$
A-1	3.10	1.85	2.04	5.72
2	3.95	1.90	2.06	5.51
3	5.12	1.86	2.06	5.49
4	7.05	1.67	2.17	5.73
5	9.65	1.57	2.10	5.71
B-1	5.12	0.56	2.95	10.75
2	5.12	1.27	2.28	7.41
3	5.12	1.86	2.06	5.49
4	5.12	1.93	2.04	5.31
4 5	5.12	2.35	1.82	4.46
C-1	5.12	0.57	3.10	10.76
	5.12	1.04	2.25	8.40
3	5.12	1.86	2.06	5.49
4	5.12	2.06	2.00	5.02
4 5	5.12	2.57	1.82	4.08

In addition, it contains values of the reciprocal of the number-average initial molecular weight \overline{M}_n obtained from intrinsic viscosity data together with estimates of the number-average molecular weight of chain segments between adjacent crosslinks. The values of the latter were obtained by use of an empirical correction for network flaws due to chain ends established previously^{2, 3} and given by the relation

$$C_1 = \frac{1}{2} \rho R T M_c^{-1} \text{ (physical) } [1 - 2.3 M_c \text{ (chemical) } M^{-1}]$$
 (5)

where M_c^{-1} (physical) = M_c^{-1} (chemical) + 0.68 × 10⁻⁴. Here the value of M_c (physical) is the effective number-average molecular weight of the network chain segments and includes the contribution of chemical crosslinks and chain entanglements. It thus describes the effective network which controls the behavior in finite extensibility considerations. The value of M_c (chemical) is the number-average molecular weight of chain segments bounded by chemical crosslinks at both ends.

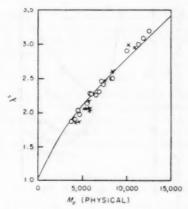


Fig. 5.—Dependence of \(\delta^* \) on chain segment molecular weight of (○) peroxide vulcanizates; (X) sulfur vulcanizates.

Figure 5 shows the values of λ^* plotted against M_c (physical); the full curve in the figure was plotted from the theoretical relation between λ^* and n given in Figure 1 and fitted to the present data by the choice of an appropriate value for the molecular weight of the random link. It was found that a molecular weight of 75 for each link was required to obtain the fit shown in Figure 4 hence

$$M_c = 75n, (6)$$

 $\begin{array}{c} Table\ III \\ Change\ in\ \lambda^*\ with\ Degree\ of\ Crosslinking \\ (Sulfur\ vulcanizates;\ measurements\ at\ 25\ \pm\ 0.2°\ C) \end{array}$

Vulcani-	Density,	$M^{-1} \times 10^{4}$	C_1 , (dynes- em ⁻¹) $\times 10^{-6}$	λ*	(physical) ×10 ⁻³
D-1	0.937	5.15	0.26	3.20	12.46
2		5.15	0.41	3.10	11.87
3		5.15	0.51	3.00	11.36
4		5.15	0.78	2.90	9.99
E-1	0.956	5.00	1.13	2.50	8.39
2		5.00	1.37	2.42	7.30
2 3		5.00	1.37	2.40	7.30
F-1	0.970	6.75	1.05	2.50	8.28
2		6.75	1.35	2.30	7.02
3		6.75	1.69	2.27	6.03
4		6.75	1.49	2.25	6.63
G-1	0.967	7.25	1.74	2.27	5.82
2		7.25	2.32	2.02	4.56
3		7.25	2.35	2.04	4.54
4		7.25	2.37	2.02	4.50
H-1	0.974	5.50	2.68	1.90	4.19
2		5.50	2.98	1.88	3.78
3		5.50	2.43	2.00	4.60

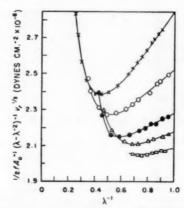


Fig. 6.—Effect of swelling on stress-strain behavior: (\times) $v_r = 1.000$; (\bigcirc) $v_r = 0.753$; (\bigcirc) $v_r = 0.455$; (\bigcirc) $v_r = 0.407$.

Figure 5 also shows values of λ^* and M_c (physical) obtained on a range of sulfur vulcanizates. The results are given in full in Table III.

STRESS-STRAIN BEHAVIOR OF SWOLLEN RUBBERS

In addition, measurements were made on one of the vulcanizates (A-3) at different degrees of swelling. The results are given in Figure 6. These show the expected progressive reduction in the slope of the plot of $\frac{1}{2}fA_0^{-1}(\lambda-\lambda^{-2})^{-1}v^{\frac{1}{2}}$ against λ^{-1} with increase in degree of swelling, but in addition they show that the extension at which the minimum and the following rapid upward sweep of the stress-strain curve occurs is less, the higher the degree of swelling. Table IV gives the values of λ^* obtained from these curves for each degree of swelling.

The theoretical correction for finite extensibility leads to the prediction that the effect of swelling is equivalent to a reduction of the number of links n in the network chain segment to nv_r^{\dagger} , where v_r is the volume fraction of rubber in the swollen vulcanizate. Table IV also includes values of nv_r^{\dagger} , the value of n for this vulcanizate being determined by fitting the value of λ^* obtained on the dry vulcanizate on to the theoretical curve relating λ^* and n given in Figure 1. (For this vulcanizate, it gave a molecular weight of 87 for a random link in the equivalent chain.)

TABLE IV

Change in λ^* with Degree of Swelling (Measurements at $25 \pm 0.2^{\circ}$ C. Vulcanizate A-3, density 0.910 g cm⁻³, M_{\circ} (physical) = 5490. Swelling medium, n-decane)

Volume swelling	λ*	nv, i
1.000	2.06	63
0.855	1.95	55.7
0.753	1.90	51.2
0.585	1.75	43.3
0.455	1.65	36.5
0.375	1.60	34.0

The observed change in λ^{\bullet} with nv_r^{\dagger} is shown in Figure 7. The full line in the figure is once again the theoretical curve given in Figure 1.

The value of n of 63 for M_c (physical) of 5490 corresponds to a molecular

weight of the random link of 87.

DISCUSSION

The results of the dependence of λ^* on the degree of crosslinking which were given in Figure 5 show a most satisfactory agreement between the experimental determinations of the onset of departures which occur at large extensions, and theoretical predictions. They provide confirmation of the validity of the hypothesis that departures at high extensions are due to finite extensibility of the network and not to crystallization.

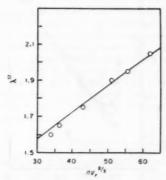


Fig. 7.—Dependence of λ* on degree of swelling.

The results obtained on swollen rubber which were given in Figure 6 provide further confirmation of the general validity of the treatment, and indicate that the effective network structure is the same in both the dry and swollen state.

In addition, the results provide an estimate of the size of the hypothetical random link, which is a basic parameter in the development of the statistical theory. The value of its molecular weight is not precisely determined, but a value of 75 ± 10 includes 90 per cent of the experimental results and is equivalent to 1.1 ± 0.15 isoprene units; this is to be compared with a value of approximately 0.7 isoprene units obtained by Treloar¹¹ from theoretical calculations, approximate values of 1.5 isoprene units obtained by Treloar¹² and 2.2 isoprene units obtained by Saunders¹³ from birefringence studies, and 2.8 isoprene units obtained by W. Kuhn and H. Kuhn¹⁴ from viscosity data and flow birefringence. The most direct determinations are those by Treloar and Saunders and the one described here. Treloar and Saunders both used similar values of the stressoptical coefficient of rubber, and differences in their estimates of the size of a random link are due to differences in their calculated values of the optical anisotropy of a single isoprene unit. A measure of uncertainty of the correct value of this latter quantity still exists. The empirical estimate derived here, from a quite independent method of measurement and analysis, is in sufficiently close accord to justify the belief that the determination is on a sound basis.

The results lead to the two following important practical consequences.

STRESS-STRAIN BEHAVIOR OF HIGHLY SWOLLEN RUBBERS

The curves on the effect of swelling on stress-strain behavior which were given in Figure 6 show that at high degrees of swelling departures due to finite extensibility occur at low elongations. As a result, the linear portions of the stress-strain curves which are used to determine C_1 and C_2 become very limited, and it appears that at very high degrees of swelling departures due to finite extensibility may already be present in swollen but unextended rubbers. This leads to difficulties in determining good estimates of C_1 and C_2 on highly swollen rubbers, and errors due to this cause will result in an increase in the estimated value of C_1 and a decrease in C_2 .

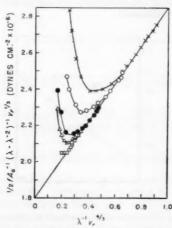


Fig. 8.—Effect of swelling on C_1 and C_2 . (\times) $v_7 = 1.000$; (\bigcirc) $v_7 = 0.753$; (\bullet) $v_7 = 0.585$; (\triangle) $v_7 = 0.455$; (\square) $v_7 = 0.407$.

However, it has been found that the experimental results of the dependence of C_1 and C_2 on degree of swelling can be described by the equation

$$\frac{1}{2}fA_0(\lambda - \lambda^{-2})^{-1}v_r^{\frac{1}{2}} = C_1(\text{dry})v_r^{\frac{1}{2}} + \lambda^{-1}C_2(\text{dry})v_r^{\frac{1}{2}}$$
(7)

and that a plot of $\frac{1}{2}fA_0(\lambda-\lambda^{-2})^{-1}v_r^{\dagger}$ against $\lambda^{-1}v_r^{\dagger}$ gives a single straight line for all experimental data with an intercept on the ordinate of C_1 (dry). The data given in Figure 6 have been replotted in this way in Figure 8 and it will be seen that the two parameters C_1 and C_2 determined on the dry rubber characterize the behavior over the whole range of conditions apart from divergencies which occur at high extensions and high degrees of swelling. The source of both of these divergencies has already been attributed to finite extensibility and it now appears, contrary to previous suggestions², that in the characterization of network structure, values of C_1 obtained on dry vulcanizates are preferred to values obtained on highly swellen vulcanizates.

DETERMINATION OF NETWORK STRUCTURE FROM STRESS-STRAIN MEASUREMENTS

The second practical consequence results from the recognition that the determination of C_1 and λ^* from a single simple extension stress-strain curve

permits the calculation of both the degree of crosslinking and the initial molecular weight of the vulcanizate. The value of λ^* has been shown to reflect the degree of crosslinking and to be independent of initial molecular weight, while the value of C_1 reflects both the degree of crosslinking and network flaws due to chain ends. The determination of these two basic parameters describing network structures was hitherto unattainable from measurements on vulcanized rubbers alone. This development thus provides a new technique which is likely to be of particular value in studies of degradation occurring in vulcanized networks.

SYNOPSIS

Departures from behavior predicted by the statistical theory of rubberlike elasticity, which occur at high extensions, are ascribed to the finite extensibility of network chains. By use of a non-Gaussian statistical theory, a relation is obtained between the extension ratio λ^* , the extension at which departures are small but significant and the degree of crosslinking. Experimental results on the dependence of λ^* on the degree of crosslinking and on the degree of swelling are in good agreement with theoretical predictions. It is shown that the additional determination of λ^* permits the calculation of both the degree of crosslinking and the extent of network flaws due to chain ends, from a single simple extension stress-strain curve. The calculation of these two basic parameters has hitherto been unattainable from measurements on vulcanized rubbers alone. This development provides a new technique of particular value in studies of the degradation of vulcanized networks.

APPENDIX

Compounding details and vulcanization procedures were as follows.

VULCANIZATES A-1-A-5

Smoked sheet 100, dicumyl peroxide 3 parts by weight. The compounded stock was divided into five equal parts which were masticated to give different degrees of breakdown. Vulcanization 60 min at 140° C.

VULCANIZATES B-1-B-5

Smoked sheet 100, dicumyl peroxide 3 parts by weight. Vulcanization 10, 40, 60, 80, and 160 minutes at 140° C, respectively.

VULCANIZATES C-1-C-5

Smoked sheet 100, dicumyl peroxide 1,2,3,4, and 5 parts by weight, respectively. Vulcanization 60 min at 140° C.

VULCANIZATES D-1-D-4

Smoked sheet 100, sulfur 5 parts by weight. Vulcanization 2, 3, 4, and 5 hr at 140° C, respectively.

VULCANIZATES E-1-E-3

Smoked sheet 100, sulfur 4, zinc oxide 5, stearic acid 1 parts by weight. Vulcanization 20, 40, and 60 min at 140° C, respectively.

VULCANIZATES F-1-F-4

Smoked sheet 100, tetramethylthiuram disulfide 6, zinc oxide 5, stearic acid 1 parts by weight. Vulcanization 10, 20, 30, and 40 min at 140° C, respectively.

VULCANIZATES G-1-G-4

Smoked sheet 100, sulfur 4, zinc oxide 5, stearić acid 1, N-cyclohexylbenzthiazylsulfenamide 0.7 parts by weight. Vulcanization 10, 20, 30, and 40 min at 140° C, respectively.

VULCANIZATES H-1-H-3

Smoked sheet 100, sulfur 4, zinc oxide 5, stearic acid 1, mercaptobenzothiazole 0.5, diphenylguanidine 1 parts by weight. Vulcanization 15 and 17 min at 140° C and 4 hr at 100° C, respectively.

ACKNOWLEDGMENT

This work forms part of a program of research undertaken by the Board of the British Rubber Producers' Research Association.

REFERENCES

- Rivlin, R. S., Phil. Trans. Roy. Soc. London, Ser. A, 241, 379 (1948).
 Mullins, L., J. Polymer Sci. 19, 225 (1956).
 Mullins, L., J. Appl. Polymer Sci. 2, 1 (1959).
 Flory, P. J., Ind. Eng. Chem. 38, 417 (1945).
 Wood, L. A., J. Wash. Acad. Sci. 47, 281 (1957).
 Treloar, L. R. G., Trans. Faraday Soc. 50, 881 (1954).
 Kuhn, W. and Kuhn, H., Helv. Chim. Acta 29, 1095 (1946).
 Isihara, A., Hashitsume, N. and Tatibana, M., J. Chem. Phys. 18, 108 (1951).
 Wang, M. C. and Guth, E., J. Chem. Phys. 20, 1144 (1952).
 Treloar, L. R. G., Trans. Faraday Soc. 40, 109 (1944).
 Treloar, L. R. G., Trans. Faraday Soc. 43, 284 (1947).
 Saunders, D. W., Trans. Faraday Soc. 52, 1414 (1956).
 Kuhn, W. and Kuhn, H., Helv. Chim. Acta 26, 434 (1943).
 Mullins, L. and Watson, W. F., J. Appl. Polymer Sci. 1, 245 (1959).

DETERMINATION OF DEGREE OF CROSSLINKING IN NATURAL RUBBER VULCANIZATES. PART V. EFFECT OF NETWORK FLAWS DUE TO FREE CHAIN ENDS *

L. MULLINS AND A. G. THOMAS

BRITISH RUBBER PRODUCERS' RESEARCH ASSOCIATION, WELWYN GARDEN CITY, HERTS., ENGLAND

INTRODUCTION

The statistical theory of rubberlike elasticity predicts that the modulus of a crosslinked polymer network is proportional to the density of chains c^1 , where a chain is the portion of a molecule between successive crosslinks. To a first approximation, the overall length and flexibility of these chains do not affect the modulus, and if there are ν crosslinks per unit volume and four chains terminate at each, then the modulus G is given by

$$G = ckT = 2\nu kT \tag{1}$$

where k is Boltzmann's constant, and T is the absolute temperature.

This relation makes no allowance for the finite length of the molecules before crosslinking, which results in some of the chains being terminated by a crosslink at one end only with the other end free. These terminal chains are elastically ineffective. Flory² has attempted to take account of these network flaws and showed that the number of crosslinks required to link n primary molecules into a single giant molecule was (n-1). Each subsequent crosslink was then assumed to add two chains to the network, and thus the density of chains c was

$$c = 2(\nu - n + 1) \simeq 2(\nu - n)$$
 (2)

Tobolsky³ adopted an alternative approach and considered the introduction of cuts into a network which initially contained no free ends; i.e., n=0. Each cut produced two free chain ends and so was equivalent to increasing the value of n by 1. Thus for linear molecules the introduction of χ cuts resulted in a value of n equal to χ . Tobolsky also assumed that each cut reduced the number of network chains by one and thus

$$c = 2\nu - n \tag{3}$$

The two relations (2) and (3) give a different variation of c with n. Both approaches should be equivalent as it is immaterial whether cuts or crosslinks are introduced first, provided they are put in at random. This has not always been clearly recognized. The usual practice has been to employ Flory's relation, Equation (2), for gel point calculations and for the dependence of modulus

^{*} Reprinted from J. of Polymer Sci. 43, 13-21 (1960).

on initial molecular weight, and to employ Tobolsky's relation, Equation (3), for the interpretation of stress relaxation data in terms of chain scission. Tobolsky's approach should be accurate for small values of χ , but it obviously breaks down when the cuts are sufficiently numerous so that mutual interference occurs. It is extended in this paper so that this limitation is avoided, and it is shown that the discrepancy between Tobolsky's and Flory's results can be readily resolved.

ANALYSIS FOR THE GEL FRACTION

A crosslink will be termed zero-, mono-, bi-, tri-, or tetrafunctional, depending upon whether it joins the ends of none, one, two, three, or four effective network chains. A trifunctional crosslink may thus be either a branch point



Fig. 1.—Diagrammatic representation of (a) trifunctional crosslink and (b) bifunctional crosslink.

of a polymer or a chemical crosslink at which one of the four chains is ineffective, for example, if it is terminated by a free end (crosslink A in Figure 1 (a)). A bifunctional crosslink is not counted as a physical crosslink because it merely acts as a bridge linking two portions of a chain together. Thus Figure 1b shows only one effective network chain, the crosslink B acting only as a link in the chain CD.

Figure 2 shows tri- and tetrafunctional crosslinks (A and B, respectively). If the chain joining A and B is cut, A becomes bifunctional and ceases to be a crosslink in the sense used here while B becomes trifunctional.



Fig. 2.—Diagrammatic representation of adjacent tetrafunctional and trifunctional crosslinks.

In the determination of the number of effective network chains in the gel in terms of the number of crosslinks and free ends, the final network is considered to arise from the random cutting of chains in a network containing the requisite number of crosslinks, but, initially, with no free chain ends. A necessary restriction is that the cuts are only introduced into effective network chains so that no sol is formed.

If there are N_4 tetrafunctional and N_3 trifunctional crosslinks per unit volume, then the probability of a network chain end being at one of the former is

$$\alpha_4 = 4N_4/(4N_4 + 3N_3)$$

and at one of the latter

$$\alpha_3 = 3N_3/(4N_4 + 3N_3) = (1 - \alpha_4)$$

The probability that both ends of a chain segment are at tetrafunctional crosslinks is α_4^2 , that both are at trifunctional crosslinks is α_3^2 , and that one end is of each type is $2\alpha_2\alpha_4$.

If a small number of cuts $\Delta \chi$ is now made in the network, the decrease in N_4 is

$$-\Delta N_4 = 2\alpha_4^2 \Delta \chi + 2\alpha_4 (1 - \alpha_4) \Delta \chi = 2\alpha_4 \Delta \chi$$

and the decrease in the total number of tetra- and trifunctional crosslinks is

$$-\Delta(N_3 + N_4) = 2\alpha_3 \Delta \gamma$$

Thus

$$dN_4/d\chi = -2[4N_4/(4N_4 + 3N_3)] \tag{4}$$

and

If, when $\chi=0$, $N_4=\nu$ (the total number of crosslinks), and $N_2=b$ (the number of branch points) then Equations (4) and (5) give

$$f^{3}/4 = [2 + \gamma + 2f - (2\chi/\nu)]/(4 + \gamma)$$
 (6)

$$t = 2 + \gamma - (2\chi/\nu) - 2f \tag{7}$$

where $f = N_4/\nu$; $t = N_3/\nu$; and $\gamma = b/\nu$. The density of effective network chain segments is given by

$$c = \frac{1}{2}(3t + 4f) \tag{8}$$

Equations (6), (7), and (8) can now be used to determine the related values of c/ν and χ/ν for any given degree of branching b. The procedure is to calculate χ/ν for selected values of f from Equation (6) and then to determine the corresponding values of t from Equation (7) and hence values of c/ν from Equation (8).

Figure 3 shows the derived relation between c/ν and χ/ν for a linear polymer (b=0), together with the relations given by Flory's and Tobolsky's theories [Equations (2) and (3)]. For a linear polymer, $\chi=n$, and the abscissa in Figure 3 is thus equivalent to n/ν . The present theory follows the Tobolsky relation for small values of n/ν , but departs markedly at higher values of n/ν ; eventually the network disintegrates at the same point as predicted by the Flory relation.

With branched polymers, b > 0, but as each molecule contributes more than two free chain ends χ is not equal to n.

In general,

$$\chi/\nu = n/\nu + \gamma/2$$

Thus, for an infinite initial molecular weight

$$\chi/\nu = \gamma/2$$

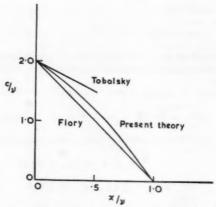


Fig. 3.—Relation between density of network chains per crosslink c/ν and density of cuts per crosslink χ/ν for gel fraction alone.

Figure 4 shows the variation of c/ν with n/ν for $\gamma=1$; this is, when there are equal numbers of crosslinks and branch points. The rate of decrease of c/ν is greater than for a linear polymer and the initial number of network chains greater. The gel point again occurs at $n/\nu=1$.

ANALYSIS FOR THE SOL PLUS GEL FRACTIONS

The results above are expressed in terms of the number of crosslinks and free chain ends in the gel fraction alone. These quantities are not readily measurable and, for experimental comparison, it is more convenient to give them in terms of the total system of sol and gel. To do this it is necessary to know the fraction of the total free ends and crosslinks in the gel. A number of relevant contributions have been made to sol-gel theory⁴⁻⁶, and Charlesby⁷ has given the required relations in a convenient form.

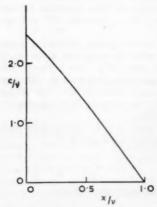


Fig. 4.—Relation between density of network chains and density of cuts for gel fraction of branched polymer $(\gamma = 1)$.

Considering Charlesby's results for a Poisson distribution, which is equivalent to the random cutting assumed in the earlier calculations, in the present notation he gives for linear molecules.

$$n/\nu = 2(1-S)\sqrt{S}/(1-S^2)$$
 (9)

$$n'/\nu' = 2(1-S)\sqrt{S}/(1-\sqrt{S}) \tag{10}$$

and

$$v'/v' = 1 - S^2 \tag{11}$$

where S is the sol fraction and n' and ν' the number of primary molecules and crosslinks in the total system. Equations (9) and (10) permit the calculation

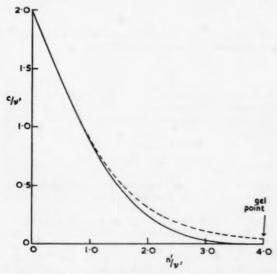


Fig. 5.—Comparison of (—) theoretical relation between c/p' and n'/p' and (—) relation obtained by direct calculation for total system sol plus gel fraction.

of n'/ν' in terms of n/ν , and, as $\chi = n$ for a linear polymer, the relation given in Figure 3 can be used to give the associated values of c/ν ; hence c/ν' can be derived by means of Equation (11).

The full line in Figure 5 shows this relation between c/ν' and n'/ν' and thus describes the efficiency of crosslinks in producing effective network chains as a function of the ratio of the number of primary chains to crosslinks in the total system sol and gel. The gel point now occurs at $n'/\nu' = 4$.

DIRECT CALCULATION OF THE EFFECTIVE NETWORK

The theory above is a development of Tobolsky's approach, and, in view of the discrepancy with Flory's relation, it is of interest to compare its results with those of an alternative method of computing c which has more in common with Flory's treatment.

In this calculation the total system of sol and gel is considered, and c is calculated directly from the number of free chain ends and crosslinks present. A system of successive approximations is used which is accurate when the number of free chain ends is not too great but which breaks down as the gel point is approached. For convenience the calculations will be restricted to a system containing n' linear primary molecules and ν' crosslinks per unit volume. The term "functionality" will now be used in a slightly different sense, a crosslink being termed r-runctional if r of the chains joined there have their other ends at a crosslink, irrespective of whether the chains are elastically effective.

The probability α that the end of a chain is a free end is $2n'/(2n'+4\nu')$, and the probability p(r) that a crosslink should have a functionality r is

$$p(r) = \binom{4}{r} (1 - \alpha)^r \alpha^{4-r} \tag{12}$$

Hence, the number of chains which have one end at an r-functional crosslink and the other terminated by another crosslink is

$$c(r) = r\nu'\binom{4}{r}(1-\alpha)^{r}\alpha^{4-r}$$
 (13)

A first approximation to the effective network structure is given by the determination of the number of chains which have at least one end at a tetra- or trifunctional crosslink and the other end also at a crosslink. This is given by Equation (13) as

$$c = 2\nu'(1 - \alpha)^4 + 6\nu'(1 \times \alpha)^3\alpha$$

$$c/\nu' = 2(1 - \alpha)^3(1 + 2\alpha)$$
(14)

The value of the efficiency of crosslinks given by Equation (14) is an overestimate as it includes a contribution from chains which are terminated by monofunctional crosslinks at the other end. These make no contribution to the network and should be considered as free ends, and thus the functionality of adjacent crosslinks should be reduced accordingly. This leads to the derivation of a second approximation for the effective network structure.

Of the $4\nu'(1-\alpha)$ network chain ends, the probability that one is at a monofunctional crosslink is given by Equation (1) as

$$4\nu'(1-\alpha)\alpha^3/4\nu'(1-\alpha) = \alpha^3 = \beta$$
 (15)

Thus, from Equations (13) and (14) we have for the number of network chains terminating at effective tetra- or trifunctional crosslinks

$$c = 2\nu'(1-\alpha)^4(1-\beta)^4 + \nu'(1-\alpha)^3(1-\beta)^3\alpha + \nu'(1-\alpha)^4(1-\beta)^3\beta$$
 (16)

and

$$c/\nu' = 2(1-\alpha)^3(1-\beta)^3(1+2\alpha+2\beta+2\alpha\beta)$$

respectively.

A further approximation can be derived in a similar fashion by making a correction for network chains which end at a bifunctional crosslink which is then followed by a monofunctional crosslink. These again should be considered as chains terminating in a free end.

It leads to the following expression for the probability that the end of a network chain should be sited at such a link

$$3(1-\alpha)(1-\beta)\alpha^2\beta = \gamma \tag{17}$$

and gives the number of effective chains as

$$c = 2\nu'(1-\alpha)^4(1-\beta)^4(1-\gamma)^4 + 6\nu'(1-\alpha)^3(1-\beta)^3 \times (1-\gamma)^3(\alpha+\beta-\alpha\beta) + 6\nu'(1-\alpha)^4(1-\beta)^4(1-\gamma)^3\gamma$$

and hence

$$c/\nu' = 2(1-\alpha)^{3}(1-\beta)^{3}(1-\gamma)^{3}[1+2(\alpha+\beta+\gamma) - 2(\alpha\beta+\beta\gamma+\gamma\alpha) + 2\alpha\beta\gamma]$$
(18)

Further successive approximations can be derived in a similar way, for example, for tri- and tetrafunctional crosslinks acting effectively as monofunctional crosslinks, which occur when two or three respectively of their chain segments end at monofunctional crosslinks. These corrections become progressively and rapidly smaller and can be neglected in regions sufficiently far from the gel point $(\nu' \gg 4n)$. Then they are only small fractions of 1% of the value given by Equation (18).

These three successive approximations to the value of c/ν' given by Equations (14), (16), and (18) derived by direct calculation are shown by the broken lines in Figure 5.

DISCUSSION

Comparison of the theoretical relation between c/ν' (and n'/ν') with the approximate direct calculation shows a very satisfactory coincidence for the highest degree of approximation used. The curves shown in Figure 5 are almost indistinguishable until n'/ν' is greater than 1.0, but at higher values further approximations are required.

The present approach which makes allowance for the differing functionality of crosslinks resolves the source of the discrepancies between Flory's and Tobolsky's relations [Equations (1) and (2)]. Tobolsky's treatment is correct for a small portion of free chain ends, but due to their mutual interaction, an error is introduced which increases rapidly in magnitude as the proportion of free chain ends increases. Flory's treatment gives the correct gel point, but thereafter his assumption that each further crosslink adds two network chains is unrealistic. This deficiency can be demonstrated by the conversion of two bifunctional crosslinks into trifunctional ones by the introduction of a crosslink between them; in this instance three, not two, effective chains are added to the network.

The present theory can be applied to initially branched polymer molecules. Branching increases the number of effective network chains present for a given number of crosslinks and also results in an increase in the variation of the number of effective network chains with the number of primary polymer molecules.

SYNOPSIS

Previous studies of the effect of flaws due to free chains ends on the elastic behavior of crosslinked polymer networks have considered either (1) the scission of chains in an initially perfect network, or (2) the crosslinking of chains of finite molecular weight. Published relations for the behavior of networks derived in these alternative ways are different. That derived from the first has been preferred for stress relaxation measurements, and that derived from the second for gel point theory. It is shown that the two treatments should be essentially equivalent. Critical consideration of what constitutes an elastically active chain resolves the anomaly of the difference between the two treatments and provides a new relation which should be valid for all ratios of crosslinks to chains ends. The new relation is checked by direct computation of the number of effective chains. This gives satisfactory agreement over the range where approximations, introduced during computation, are small.

ACKNOWLEDGMENT

This work forms part of a program of research undertaken by the Board of the British Rubber Producers' Research Association.

REFERENCES

Treloar, L. R. G., "Physics of Rubber Elasticity", p. 61., Oxford Univ. Press, London, 1949.
 Flory, P. J., Chem. Revs. 35, 51 (1944).
 Tobolsky, A. V., Mets, D. J., and Mesrobian, R. B., J. Am. Chem. Soc. 72, 1942 (1950).
 Flory, P. J., J. Am. Chem. Soc. 63, 125 (1944).
 Stockmayer, W. H., J. Chem. Phys. 12, 125 (1944).
 Flory, P. J., J. Am. Chem. Soc. 69, 30 (1947).
 Charlesby, A., J. Polymer Sci. 11, 513 (1953).

DETERMINATION OF DEGREE OF CROSSLINKING IN NATURAL RUBBER VULCANIZATES. PART VI. EVIDENCE FOR CHAIN SCISSION DURING THE CROSSLINKING OF NATURAL RUBBER WITH ORGANIC PEROXIDES *

C. G. MOORE AND J. SCANLAN

BRITISH RUBBER PRODUCERS' RESEARCH ASSOCIATION, WELWYN GARDEN CITY, HERTS., ENGLAND

INTRODUCTION

In Part II¹ of this series estimates were made of the number of chemical crosslinks introduced into natural rubber during its vulcanization at $110-140^{\circ}$ C with di-tert-butyl peroxide. These estimates were based on the assumption that the sole fate of the polyisoprenyl radicals $(R \cdot)$, derived from reaction of the rubber hydrocarbon (RH) with tert-butoxy or methyl radicals $(R \cdot 2)$, was bimolecular combination to form crosslinks $(R \cdot 3)$, and thus the number of chemically introduced crosslinks was equal to $\frac{1}{2}([t-BuOH] + [MeH])$. Indirect evidence was presented in support of this assumption, based mainly on the reactions of the peroxide with simple olefins^{2,3}. Demonstration of the validity of $(R \cdot 3)$ being the sole stabilization process for polyisoprenyl radicals is important, since is forms the basis for quantitatively relating the "physical"

$$Me_1COOCMe_1 \xrightarrow{\hspace*{1cm}} 2Me_2CO \cdot \xrightarrow{\hspace*{1cm}} 2Me_2C = O + 2 \ Me \cdot \tag{R \cdot 1}$$

$$2R \cdot \longrightarrow R - R$$
 (R·3)

and "chemical" degrees of crosslinking of natural rubber vulcanizates^{1, 4}. Four alternative stabilization reactions of the polyisoprenyl radicals $(R \cdot)$ which warrant consideration, and whose occurrence would necessitate revision of the original calibration^{1, 4}, are: (1) bimolecular disproportionation $(R \cdot 4)$, (2) cyclization to substituted cyclohexenyl or cyclopentenyl radicals and their subsequent disproportionation (see Ref. 1), (3) intramolecular combination of two polyisoprenyl radicals located on the same polyisoprene chain, and (4) unimolecular scission as in $(R \cdot 5a)$ and $(R \cdot 6a)$, followed by stabilization of the new (degraded) polyisoprenyl radical (III $\equiv R' \cdot$) by combination with a like radical $(R \cdot 7)$, or with an original polyisoprenyl radical $(R \cdot)$ to give a trifunctional (branched) crosslink $(R \cdot 8)$:

^{*} Reprinted from J. of Polymer Sci. 43, 23-33 (1960). Present address of Dr. Scanlan is Research Association British Rubber Manufacturers, Shawbury, Shrewsbury, Shropshire, England.

(R·8)

 \rightarrow R' - R

$$R \cdot + R \cdot \longrightarrow RH + R_{-H}$$

(R·4)

$$\begin{array}{c} \left\{ -\mathrm{CH}_{z^{-}}\mathrm{C}(\mathrm{Me}) = \mathrm{CH} - \mathrm{CH}_{z^{-}}\mathrm{CH} - \overset{(a)}{\leftarrow} & -\mathrm{CH}_{z^{-}}\mathrm{C}(\mathrm{Me}) = \mathrm{CH} - \mathrm{CH}_{z^{-}} + \mathrm{CH}_{z^{-}}\mathrm{C}(\mathrm{Me}) - \mathrm{CH} = \mathrm{CH} - & (\mathrm{R} \cdot 5) \\ \mathrm{(II)} & \downarrow & \downarrow \\ \left\{ -\mathrm{CH}_{z^{-}}\mathrm{C}(\mathrm{Me}) = \mathrm{CH} - \mathrm{CH}_{z^{-}}\mathrm{C}(\mathrm{Me}) - \mathrm{CH} = \mathrm{CH} - \overset{(a)}{\leftarrow} & -\mathrm{CH}_{z^{-}}\mathrm{C}(\mathrm{Me}) = \mathrm{CH} - \mathrm{CH}_{z^{-}} + \mathrm{CH}_{z^{-}}\mathrm{C}(\mathrm{Me}) - \mathrm{CH} = \mathrm{CH} - & (\mathrm{R} \cdot 6) \\ \mathrm{(II)} & \mathrm{R} \cdot \cdot + \mathrm{R} \cdot & -\mathrm{CH}_{z^{-}}\mathrm{C}(\mathrm{Me}) - \mathrm{CH}_{z^{-}}\mathrm{C}(\mathrm{R} \cdot 6) - \mathrm{CH}_{z^{-}}\mathrm{C$$

Limited evidence suggesting the negligible intrusion of processes (1) and (2) has been discussed previously¹, although more critical studies are required before acceptance of their nonparticipation. The intramolecular radical combination process (3) will be a very improbable event under the reaction conditions used in Part II¹ and may be neglected. However, the unimolecular scission reactions ($R \cdot 5a$; $R \cdot 6a$), whose possible occurrence has been discussed by Flory⁵ and Craig⁶, will certainly be favored by the weakness of the —CH₂-|-CH₂- bond in (I) and (II), and is anticipated to be a more important competitor for ($R \cdot 3$) in a viscous polymeric system than in a low molecular weight polyisoprene such as 2:6-di-methylocta-2:6-diene or digeranyl (see Ref. 1). Bresler et al.¹ have in fact attributed the polymer degradation they observed when dilute benzene solutions of natural rubber were subjected to attack by free radicals ($R \cdot 5a$; $R \cdot 6a$) or to a radical substitution process as in ($R \cdot 9$); $X \cdot = Me \cdot$ or $Me_2C(CN)$:

$$-CH_{z}-C(Me)=CH-CH_{z}-C(Me$$

In view of the above we now present a re-examination of the data of Part II¹ and report additional data which define more closely the limit to which the crosslinking reaction (R·3) is counteracted by an opposing chain scission reaction. For the latter data use was made of the stress relaxation method for determining the degradation of polymer networks; measurements were made of the fall in tension of a strip of peroxide-vulcanized natural rubber held at constant extended length and subjected to further crosslinking by di-cumyl peroxide at 140° C in an inert atmosphere. To a first approximation, crosslinks introduced into the extended network will not contribute to the tension⁸ and thus any fall in tension will reflect the occurrence of concurrent chain scission.

EXPERIMENTAL METHODS

Preparation of vulcanizates.—Acetone-extracted "highly purified" natural rubber (U. S. Rubber Co.) was vulcanized with 2.0 per cent of pure di-cumyl peroxide at 140° C in a 10×10 cm mold; Sheet A, 0.2 mm thickness, was heated for 20 minutes, and Sheet B, 0.5 mm thickness, for 30 minutes. The vulcanizates were extracted with hot acetone for 24 hours in nitrogen in the dark and then rigorously dried in vacuo. Parts of the sheets were then wrapped in aluminum foil and heated in vacuo (ca. 10^{-5} mm Hg) for 7 days at 140° C; these sheets are designated "preheated" in the following discussion.

Preparation of vulcanizates for further crosslinking under stress.—Di-cumyl peroxide was introduced into strips of the vulcanizates by allowing them to swell overnight in a 5 per cent solution of the peroxide in ethyl acetate, the solvent then being removed in vacuo at room temperature. Samples of vulcanizates used as controls in the stress relaxation experiments were treated similarly to the above in pure ethyl acetate. Oxidation of the vulcanizates during the swelling process was minimized by completely filling the stoppered tubes used with ethyl acetate.

Stress relaxation measurements.—These were carried out at 140° C under a pressure of ca. 650 mm of oxygen-free nitrogen in a stress relaxometer of a type previously described at a measured linear extension of about 100 per cent.

The nitrogen filling was found necessary to prevent volatilization of the peroxide from the strips which was shown to occur rapidly at 140° C in vacuo. Comparison experiments on strips not containing peroxide were made both in vacuo and in nitrogen.

Determination of degree of crosslinking of vulcanizates.—Measurements of the equilibrium volume fraction of rubber in the swollen vulcanizate v_r were made in n-decane at 25° C by the procedure of Moore and Watson¹. Several determinations of v_r were made on the preheated and unpreheated sheets prior

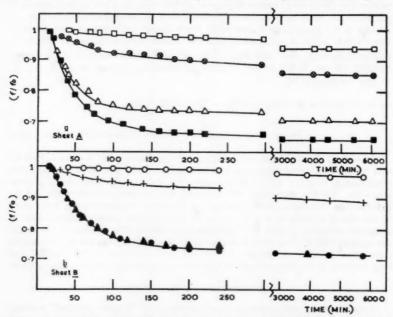


Fig. 1.—Stress relaxation during di-cumyl peroxide crosslinking at 140° C in nitrogen of a stressed peroxide vulcanisate. Relationship of ratio of actual stress: initial stress (f/fs) with time of heating. a. Sheet A. () Preheated control sample—no peroxide present. () Unpreheated control sample—no peroxide present. () Unpreheated sample with peroxide present. b. Sheet B. () Preheated control sample—no peroxide present. () Preheated sample with peroxide present. () Preheated sample with peroxide present. () Unpreheated sample with peroxide present. () Unpreheated sample with peroxide present.

to stress relaxation. The v_r values were converted into values of the elastic constant C_1 of an unswollen vulcanizate by means of the calibration curve of Mullins⁴, the latter being a revised and improved form of that originally published¹⁰.

EXPERIMENTAL RESULTS

Figures 1a and 1b show the stress relaxation (f/f_0) , where f_0 is the initial tension and f the tension at time t) of strips of preheated and unpreheated stressed vulcanizates both in the absence and presence of di-cumyl peroxide under the specified reaction conditions. Identical stress relaxation behavior was observed for samples heated in the absence of peroxide either in nitrogen or in vacuo. Table I details the v_r and C_1 data for the vulcanizates both prior to and following stress relaxation.

DISCUSSION

Kinetic evidence for possible chain scission during peroxide vulcanization of natural rubber.—The occurrence of chain scission of polyisoprenyl radicals according to $(R\cdot 5a)$, $(R\cdot 6a)$, $(R\cdot 7)$, and $(R\cdot 8)$ competitively with their bimolecular combination $(R\cdot 3)$ should in principle be revealed in the overall kinetics of the vulcanization process. This follows from the fact that the rate of chain scission is first order with respect to the concentration of polyiso-

TABLE I

ELASTIC CONSTANTS OF PEROXIDE VULCANIZATES PRIOR TO AND
FOLLOWING STRESS RELAXATION

	FOLLOWING S	TRESS RELA	XATION	
Sheet	Description of vulcanizate	Strip no.	Vr.	C_1 , $\times 10^{-6}$ dynes cm ⁻²
		II	$0.184 \\ 0.166$	0.550 0.440
A	Unpreheated original	III IV V	0.172 0.182	0.480 0.540
		V	0.178	0.515 Mean: 0.505
A	Unpreheated, stress relaxed without peroxide		0.181	0.535
\boldsymbol{A}	Unpreheated, stress relaxed with peroxide		0.267	1.30
A	Preheated		0.169	0.460
A	Preheated, stress relaxed without peroxide		0.180	0.525
A	Preheated, stress relaxed with peroxide		0.315	1.97
В	Unpreheated original	II III IV V VI	0.202 0.206 0.209 0.209 0.205 0.204	0.675 0.700 0.725 0.725 0.700 0.690
\boldsymbol{B}	Unpreheated, stress relaxed without peroxide		0.201	Mean: 0.703 0.670
B	Unpreheated, stress relaxed with peroxide		0.310	1.875
$\frac{B}{B}$	Preheated		0.204	0.690
D	Preheated, stress relaxed without peroxide		0.212	0.750
В	Preheated, stress relaxed with peroxide		0.334	2.325

prenyl radicals, $[R \cdot]$, whereas the rate of crosslinking $(R \cdot 3)$ depends on $[R \cdot]^2$, and so for vulcanization effected by a given initial concentration of peroxide the ratio of chain scission/crosslinking should be lower in the early stages of the reaction than in the later stages when the peroxide concentration is depleted. Figure 2 shows a plot of the elastic constant C_1 versus the yields of tert-butanol plus methane for a series of vulcanizates produced by reaction of natural rubber of essentially constant initial molecular weight and ca. 1.5×10^{-4} mole of ditert-butyl peroxide/g rubber for varying times at 140° C. The data of Figure 2 are those of Moore and Watson', except that the C_1 values are the revised

figures of Mullins⁴. The fact that there is no significant curving of the experimental data in Figure 2 toward the abscissa with increasing extent of reaction suggests that within the sensitivity of the data chain scission is not an important factor.

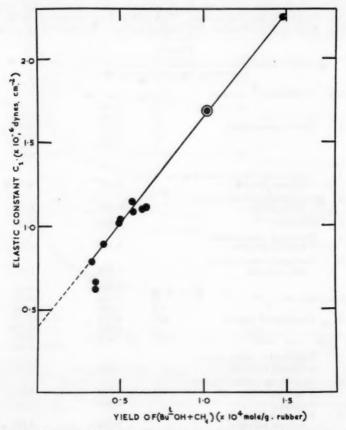


Fig. 2.—Linear relationship of the elastic constant C₁ with the yield of test-butanol plus methane during the vulcanization of natural subber with di-test-butyl peroxide in vacuo at 140° C.

Evidence for chain scission from the stress relaxation experiments.—In contrast to the above conclusions from kinetic data, the stress relaxation experiments, Figures 1a and 1b, which provide a very sensitive measure of network degradation processes, strongly suggest that some chain scission of natural rubber molecules does occur during its vulcanization with di-cumyl peroxide, as was noticed earlier by Berry et al. In the experiments of the above workers and in the present work, considerable stress relaxation was observed in unpreheated extracted peroxide vulcanizates at 140° C in vacuo or in nitrogen in the absence of di-cumyl peroxide, and thus the stress relaxation observed for such

samples in the presence of the peroxide could have been interpreted as being due merely to an acceleration by the peroxide of a network scission process stemming from decomposition of peroxidic groups in the vulcanizate. However, the data now reported (Figures 1a and 1b) on the negligible stress relaxation observed in a preheated peroxide vulcanizate in the absence of peroxide and the marked stress relaxation of such vulcanizates in the presence of peroxide under otherwise identical reaction conditions is strong evidence for chain scission of natural rubber molecules, as envisaged in $(R \cdot 5a)$, $(R \cdot 6a)$, $(R \cdot 7)$, and $(R \cdot 8)$, competing with their crosslinking by the di-cumyl peroxide. Quantitative estimates of the relative amounts of network formation and degradation during peroxide vulcanization can be derived from the present data, although their accuracy is reduced by the rather poor uniformity of vulcanization of the samples used (particularly Sheet A); this feature is difficult to avoid in thin sheets of lightly crosslinked peroxide vulcanizates.

TABLE II

DETERMINATION OF PRIMARY NETWORK DEGRADATION AND SECONDARY NETWORK FORMATION DURING THE CROSSLINKING OF A STRESSED PEROXIDE VULCANIZATE WITH DI-CUMYL PEROXIDE AT 140° C IN NITROGEN

Units for C_1 are (106 dynes cm⁻²); α = extension ratio of stressed samples

		(f//o) final		with and	with and	
Sample	C_1°	without peroxide	with peroxide	with and without peroxide	without peroxide	$-\Delta C_1^{-1}/\Delta C_1^{-1}$
Sheet A						
Unpreheated	0.505	0.85 $(\alpha = 2.01)$	0.70 $(a = 1.96)$	-0.08	0.74	0.11
Preheated	0.460	0.94 $(a = 2.00)$	0.64 $(a = 2.00)$	-0.13	1.45	0.09
Sheet B		,				
Unpreheated	0.703	0.87 $(\alpha = 1.84)$	0.71 $(\alpha = 1.99)$	-0.12	1.16	0.10
Preheated	0.690	0.97 $(\alpha = 1.98)$	0.71 ($\alpha = 1.97$)	-0.18	1.52	0.12

From the initial values of C_1 of the sheets and their final C_1 values after stress relaxation can be calculated the quantity $C_1^{\rm II}$, which provides a measure of the number of elastically effective chains formed during the secondary vulcanization of the extended vulcanizate. According to the "two-network" theory^{8, 11} the final value, $C_1^{\rm III}$, of C_1 for a vulcanizate which has been subjected to both crosslinking and network degradation in an extended state is given by

$$[C_1^{\text{III}}]^3 = [C_1^{\text{I}} + C_1^{\text{II}}/\alpha^2][C_1^{\text{I}} + \alpha C_1^{\text{II}}]^2$$
 (E.1)

where α is the extension ratio, $C_1^{\text{II}} = \frac{1}{2}N_{\text{I}k}T$, $C_1^{\text{II}} = \frac{1}{2}N_{\text{I}k}T$, N_1 and N_{II} being, respectively, the numbers of elastically effective chains per unit volume of the original network remaining after, and of the new network formed by the secondary vulcanization process [see Equation (10) of Ref. 11]. If C_1° is the elastic constant of the original network, then the amount of degradation of this network which occurs during the secondary vulcanization process is given by

$$C_1^{\circ} - C_1^{\mathrm{I}} = C_1^{\circ} (1 - f/f_0)$$
 (E.2)

The results for the two sheets investigated are summarized in Table II. In calculating the amount of primary network degradation which occurs during the secondary vulcanization process, allowance has been made for the network

degradation observed in the absence of peroxide on the assumption that the latter is a concurrent degradation process separate in origin from the peroxide-induced network degradation. The amount of primary network degradation, ΔC_1^{II} , is given by the difference between the values of C_1^{II} in the presence and absence of peroxide, and the amount of secondary network formed, ΔC_1^{II} , is given by the difference in the values of C_1^{II} in the presence and absence of peroxide. The data indicate that during crosslinking by di-cumyl peroxide under the specified reaction conditions degradation of the primary network occurs equivalent to about 10 per cent of the new elastically effective crosslinks formed. If no allowance is made for the network degradation which occurs in the absence of peroxide then the above figure is raised to ca. 15 per cent for the

preheated samples and ca. 20 per cent for the unpreheated samples.

The present results based on the stress relaxation technique are reasonably interpreted in terms of a measure of chain scission of polyisoprenyl radicals according to $(R \cdot 5a)$, $(R \cdot 6a)$, $(R \cdot 7)$, and $(R \cdot 8)$ competing with the crosslinking process (R·3). The alternative scission process [(R·9), where X· is t-BuO· or C6H5C(Me)2O.] proposed by Bresler et al. is believed to be unimportant in the present system since it would require the incorporation of tert-butoxy or cumyloxy groups into the vulcanizate which is contrary to evidence from studies2, 3 on the nature of the crosslinked products obtained from the interaction at 140° C of di-tert-butyl peroxide with mono-olefins (containing R. CH =CH·R' or R·C(Me)=CH·R' groups), diisoprenes, and polyisoprenes including natural rubber. Less critical supporting evidence for this conclusion is the fact that the reacted peroxide in the systems used by Moore and Watson¹ was accounted for close to 100 per cent in terms of tert-butanol, acetone, methane, and ethane. The occurrence of (R.9) where X. is Me2C(CN), as proposed by Bresler et al. 7, is also doubted since recent studies 12 of the reaction of gutta-percha in benzene solution with \(\Gamma^{14}C\)-labeled azoisobutyronitrile at 60° C under rigorous vacuum conditions indicated, contrary to the findings of Bressler et al. on related systems, that there was no degradation (or crosslinking) of the polyisoprene and insignificant incorporation therein of [14C]-Me₂-

C(CN) groups; these results lead one to doubt if the reactions reported by Bresler et al. were conducted under the rigorously anaerobic conditions claimed and suggest that the polymer degradations observed in the presence of Me₂C-(CN) radicals resulted from radical-catalyzed oxidative seission processes.

While the present results are consistent with the scission of some of the polyisoprenyl radicals formed during peroxide vulcanization they do not give any information concerning the ultimate fate of the fragments formed in the scission processes $(R \cdot 5a)$ and $(R \cdot 6a)$; the results are equally consistent with fragments produced in $(R \cdot 5a)$ and $(R \cdot 6a)$ which are located in different parts of the original network undergoing the recombination reactions $(R \cdot 5b)$ and $(R \cdot 6b)$, or with the degraded polyisoprenyl radicals $(R' \cdot)$ being stabilized as in $(R \cdot 7)$ and $(R \cdot 8)$; if the former recombination process occurs, then the amount of network degradation determined above is an overestimate.

The present demonstration of concurrent chain scission and crosslinking during peroxide vulcanization necessitates a revision of the original and modified calibrations relating the physical and chemical degrees of crosslinking of a peroxide vulcanizate; this follows because firstly, the occurrence of chain scission according to $(R \cdot 5a)$, $(R \cdot 6a)$, $(R \cdot 7)$, and $(R \cdot 8)$ means that the original chemical estimate of the degree of crosslinking is too high, and secondly, the original physical estimate of degree of crosslinking for a rubber of "infinite"

initial molecular weight was determined by correcting for the finite initial molecular weight of the rubber prior to crosslinking on the assumption that no scission of the primary rubber molecules occurred during the peroxide vulcanization reaction. Precise correction of the original calibrations cannot be made at this stage because of the quantitative difficulties in interpreting stress relaxation measurements when both crosslinking and chain scission occur simultaneously13 and because of lack of knowledge of the fate of the fragments resulting from the chain scission reactions. Correction of the original calibrations will be further complicated by the fact that if chain scission results from the unimolecular processes $(R \cdot 5a)$ and $(R \cdot 6a)$ then, as discussed above, the relative extents of scission and crosslinking will vary with the concentration of peroxide and thus a variable correction to the original chemical and physical estimates of crosslinking will be required.

SYNOPSIS

The possible scission of natural rubber chains during their crosslinking by

organic peroxides [ROOR; R = t-Bu— or C₆H₅C(Me)₂] at 140° C has been examined: (1) by comparing the kinetics of crosslinking and of peroxide decomposition and (2) by measuring the relaxation in stress of an extended sheet of a peroxide vulcanizate subjected to further crosslinking by di-cumyl peroxide in nitrogen. The former method is too insensitive to establish the occurrence of chain scission, but the latter method indicates that degradation of the primary network occurs during the formation of the secondary network, an effect which is ascribed to the unimolecular scission of polyisoprenyl radicals competing with their bimolecular combination to form crosslinks. Under the reaction conditions prevailing in (2) it is calculated that degradation of the primary network occurs equivalent to about 10 per cent of the new elastically effective crosslinks formed. These findings suggest that minor revision of the existing calibrations1. 4 relating the physical and chemical degrees of crosslinking of a natural rubber vulcanizate is necessary, since the basis of the original chemical estimate was that the sole fate of polyisoprenyl radicals, derived from the reaction of natural rubber with alkyloxy-, aralkyloxy- and methyl radicals, is bimolecular combination. However, the available data, coupled with the present status of stress relaxation theory, are inadequate to permit precise corrections of the existing calibrations to be made at this stage.

ACKNOWLEDGMENTS

We thank Dr. J. Dunn and Dr. L. Mullins for much help during the course of this work which forms a part of the research program of the British Rubber Producers' Research Association.

REFERENCES

- ¹ Moore, C. G., and Watson, W. F., J. Polymer Sci. 19, 237 (1956).

 ² Farmer, E. H., and Moore, C. G., J. Chem. Soc. 1951, 131.

 ³ Farmer, E. H., and Moore, C. G., J. Chem. Soc. 1951, 142.

 ⁴ Mullins, L., J. Appl. Polymer Sci. 2, 1 (1959).

 ⁵ Flory, P. J., "Principles of Polymer Chemistry", p. 456, Cornell Univ. Press, Ithaca, N. Y., 1953.

 ⁶ Craig, D., Rubber Chem. & Technot. 30, 1291 (1957).

 ⁷ Bresler, S. E., Dolgoplosk, B. A., Krol, V. A., and Frenkel, S. Ya., Zhur. Obschei Khim. 26, 2201 (1956);

 Rubber Chem. & Technot. 31, 278 (1958).

 ⁸ Andrews, R. D., Tobolsky, A. V., and Hanson, E. E., J. Appl. Phys. 17, 352 (1946).

 ⁹ Dunn, J. R., Scanlan, J., and Watson, W. F., Trans. Faraday Soc. 54, 730 (1958).

 ¹⁰ Mullins, L., J. Polymer Sci. 19, 225 (1956).

 ¹¹ Berry, J. P., Scanlan, J., and Watson, W. F., Trans. Faraday Soc. 52, 1137 (1956).

 ¹² Allen, P. W., Ayrey, G., and Moore, C. G., J. Polymer Sci. 36, 55 (1959).

 ¹³ Scanlan, J., and Watson, W. F., Trans. Faraday Soc. 54, 740 (1958).

ELECTRON SPIN RESONANCE STUDY OF THE INTER-ACTION OF TETRAMETHYLTHIURAM DISULPHIDE (TMTD) WITH RUBBER AND RELATED COMPOUNDS *

S. E. Bresler, B. A. Dogadkin, E. N. Kazbekov, E. M. Saminskii and V. A. Shershnev

In the article by Dogadkin and Shershnev¹ electron paramagnetic resonance spectra produced in the laboratory of Prof. S. E. Bresler are put forward to confirm the radical mechanism of the interaction of TMTD with raw rubber in the process of vulcanization. After this paper had been printed we learned of the work of B. R. McGarvey² and H. M. McConnel³, in which analogous spectra were observed in solutions containing bivalent copper ions. As a result it is suggested that the electron paramagnetic resonance spectra of stocks of natural rubber with TMTD are affected by admixtures of copper compounds. The amount of copper calculated from the magnitude of the resonance spectrum amounts to 0.1% by weight in relation to the TMTD. The same spectrum is observed on heating a benzene solution of copper acetate and TMTD. Its intensity increases sharply and irreversibly on heating the solution to 100°. corresponding to 10% of the copper contained in the solution.

To clear up the question a spectrum analysis of the specimens which had been investigated was carried out (by Sh. I. Peïzulaev and G. P. Kuznetsova). showing in particular that 10⁻⁵ per cent by weight of copper is contained in the thiuram, while in the rubber polymer the content does not exceed 10⁻⁴ per cent by weight. This content is considerably less than follows from calculation from

the electron paramagnetic resonance spectrum.

The spectrum described is observed on heating a stock of natural rubber with TMTD, but is absent on heating a stock of polyisobutylene with TMTD. although admixtures of copper are contained in the latter as well. If however the stock of polyisobutylene with TMTD also contains geraniol, which may be regarded as a model of the structural units of natural rubber, then we observe the same electron paramagnetic resonance spectrum.

Thus for the electron paramagnetic resonance spectrum described in Ref. 1 to appear, we need the presence of double bonds or labile hydrogen in the vul-

canization system.

The above, it appears to us, shows that a final conclusion as to the nature of the electron paramagnetic resonance spectra observed under the conditions of vulcanization of rubber by TMTD may be reached after a series of supplementary experiments.

REFERENCES

Dogadkin, B. A., and Shershnev, V. A., Vysokomol. Soed. 1, No. 1, 58-67 (1959); RABRM Transl. 738.
 McGarvey, B. R., J. Phys. Chem. 60, 71 (1956).
 McConnel, H. M., J. Chem. Phys. 25, 709 (1956).

^{*} Translated by R. J. Moseley from Vysokomolekularnye Soedineniya, 2, 174 (1960).

SOME ASPECTS OF HIGH TEMPERATURE VULCANIZATION *

G. BIELSTEIN

BRITISH INSULATED CALLENDER'S CABLES LTD., LONDON, ENGLAND

INTRODUCTION

In its simplest form vulcanization can be carried out by conducting the reaction of natural rubber with sulfur at elevated temperatures, and modern practice is in general still based on this procedure. Some 50 years ago, however, it was discovered that the otherwise rather slow curing process could be accelerated by the addition of amines, and a very large number of other vulcanization accelerators has since been introduced. In the course of industrial development the time required for curing rubber was further reduced by raising the temperature of operation. Although temperatures up to 150° C have now become quite usual, some manufacturing techniques are already operated at nearly 200° C and attention has been focused on the study of curing behavior at such a relatively high temperature. A few representative curing systems have therefore been examined and an idealized interpretation of their high temperature behavior is also presented.

At elevated temperature there are two main processes to be considered, namely, vulcanization and reversion. There can be no doubt that vulcanization is the result of chemically crosslinking long-chain rubber molecules. It manifests itself by enhancing the physical properties of the material, such as the modulus and tensile strength, the stability of shape, and the resistance to swelling. Degradation of such molecularly crosslinked rubber networks is called reversion at the curing temperature and aging at service temperatures. A decline in physical properties on continued curing is therefore associated with

reversion.

The quantitative study of high temperature curing is beset by a number of problems. Some of these are a result of a reduction of time scale of the experiments as opposed to those at ordinary curing temperatures. Others arise from the generally increased importance of reversion. It therefore seems desirable firstly to examine the effect of the experimental method on the evaluation and interpretation of the results that have been obtained.

THE INITIAL KINETICS OF CURE 1

In an ideal experiment, each sample of an uncured rubber compound would be uniformly and instantaneously heated to the steady curing temperature; similar cooling would then freeze the state of cure reached after any given time for its subsequent evaluation. Although quenching in cold water will in practice ensure a sufficiently abrupt termination of cure, the beginning is less certain, as there will always be a gradual, asymptotic approach to the final curing temperature.

^{*} Reprinted from Transactions of the Institution of the Rubber Industry, Vol. 36, pages 29-44 (1960).

For conventional rubber compounds the heat of vulcanization is known to be far too small to cause any significant change in temperature. Let it therefore be assumed that the temperature T at a point in the rubber sample will change from an initial value T_a , usually the room temperature, to the steady curing temperature T_b according to Newton's rule:

$$\frac{dT}{dt} = \beta(T_b - T) \tag{1}$$

where t is the time of cure and β is a constant. As $T = T_a$ when t = 0, this integrates to

$$-\log_{\epsilon} \frac{T_b - T}{T_b - T_c} = \beta t \qquad (2)$$

Plotting $\log_{10} (T_b - T)$ against t should thus produce a straight line of slope β and this was confirmed by the following simple experiment (Figure 1).

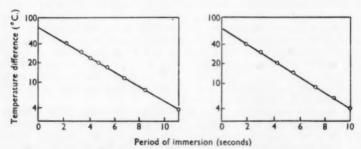


Fig. 1.—Temperature difference between inner and outer surface of rubber tubing plotted logarithmically against period of immersion at 100° C.

The cold junction of a thin wire thermocouple was threaded into a loop of very small rubber tubing and immersed in water at room temperature. The hot junction was placed directly into a beaker of boiling water. When the rubber tubing containing the cold junction was transferred to the boiling water, the temperature difference between the two thermocouples decreased and readings of this were obtained with a previously calibrated galvanometer.

Using the Arrhenius equation it can be shown that in a system undergoing a temperature change from T_a to T_b according to Newton's rule the instantane-

ous rate constant k for a chemical reaction is given by

$$k = e^Q \cdot k_b \tag{3}$$

and

$$Q = \frac{1 - \frac{\log_{e} A_{b}}{\log_{e} k_{b}} \cdot \frac{T_{b} - T_{a}}{T_{b}} \cdot e^{-\beta t}}{1 - \frac{T_{b} - T_{a}}{T_{b}} \cdot e^{-\beta t}}$$
(4)

where k_b is the rate constant at the final temperature T_b and A is the frequency factor of the reaction.

A correspondingly modified rate equation for crosslinking can in fact be integrated in terms of a numerically tabulated function. Instead of showing a very gradual change, such a calculation has revelaed that the extent of reaction remains negligible during an apparently well-defined heating-up period and then proceeds as if the steady curing temperature had been reached instantaneously. The heating-up period may therefore be discounted from the overall curing time with virtually no effect on the subsequent kinetics of cure.

In practice, however, the temperature of a rubber sample will not always be uniform and the concept of an apparent heating-up period followed by a sudden onset of curing must become an approximation. The experimental technique was therefore arranged so as to reduce all these end effects as far as possible.

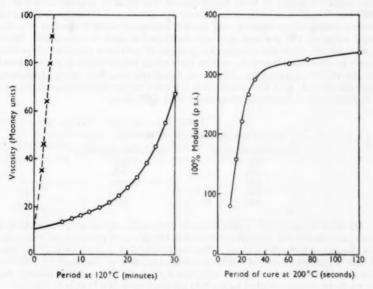


Fig. 2.—Polychloroprene compound.

EXPERIMENTAL

Thin round filaments were extruded from the rubber compound and cured by exposure to saturated steam. The condensation of steam thus ensured efficient and direct heating of the rubber. On completion of cure each filament was automatically quenched in cold water. The apparatus was developed from that previously described by Mason², and consisted essentially of a short iron pipe with suitable inlet and outlet valves. It is worth noting that the pressure of saturated steam at 200° C already amounts to about 15 atmospheres and would have to be almost trebled to reach 250° C.

The cured rubber filaments were cut into known lengths, and the average cross-sectional area of each length determined by weighing. The stress-strain properties were then assessed by measurement of the retractive force one minute after extension by 100 per cent³.

VULCANIZATION OF A POLYCHLOROPRENE COMPOUND

A relatively simple curing behavior was shown by a technical polychloroprene compound. As a vulcanizing system this compound contained zinc and magnesium oxides in the usual proportions of 5 phr and 4 phr respectively, together with 2 phr of a condensed aldehyde-amine accelerator. A Mooney scorch test at 120° C produced quite typical results, and the compound cured well at 200° C (Figure 2). However, the outstanding feature was that no reversion occurred on continued curing (the broken scorch curve was obtained

using 6 phr of accelerator).

Further series of vulcanizates were prepared at 185° C, 170° C, 155° C and 140° C. A qualitative examination of the data revealed that the gradation of cure obtained at any of these temperatures was broadly analogous to that at 200° C. The results entirely confirmed the absence of reversion over the extensive curing range studied, and allowed estimates to be formed of the ultimate values of 100 per cent modulus developed at each temperature. These figures do not show the systematic decrease of optimum physical properties, which is sometimes found on raising the curing temperature of conventional, natural rubber compounds. Moreover, the nearly constant values of ultimate modulus indicate that the crosslinking efficiency of the vulcanizing agents used is independent of temperature up to at least 200° C.

TABLE I
POLYCHLOROPRENE COMPOUND

Ultimate 100% modulus, psi		
355		
375		
360		
375		
350		

In order to carry out a quantitative evaluation of the modulus data it is useful to consider the relation between the 100 per cent modulus and the cross-link density of the vulcanizates. The use of modulus as a measure of the state of cure in pure gum natural rubber vulcanizates has been discussed by Fletcher, Gee and Morrell⁴. At constant compound viscosity the crosslink density was shown to be linearly related to the 100 per cent modulus, that is to say,

$$1/M_c = a \cdot F + b \tag{5}$$

where M_c is the molecular weight of rubber between crosslinks, F is the 100 per cent modulus, and a and b are constants. The same general relationship may also be expected to apply to other rubber vulcanizates with a degree of approximation characterized by their hysteresis. In consequence it should be possible to examine the chemical processes which occur during vulcanization and result in the introduction of crosslinks.

A number of investigators have found the overall chemical processes to be kinetically of the first order, and for a nonreverting pure gum natural rubber compound Gee and Morrell demonstrated first order kinetics directly in terms of the measured 100 per cent modulus⁵. It is a feature of kinetic analysis that any linearly related parameter of a first order chemical reaction will exhibit a first order time dependence with the identical specific rate constant (Figure 3). If therefore the modulus after curing time t is expressed as a percentage P of

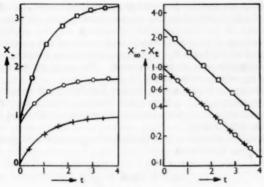


Fig. 3.-First order kinetics.

the ultimate value, i.e., as the reduced modulus, we should have

$$\log_{\epsilon} (100 - P) = \text{constant} - k t \tag{6}$$

where k is the specific rate constant.

The applicability of this equation to the modulus results obtained with the polychloroprene compound was tested by plotting the difference of the reduced modulus values from 100 per cent logarithmically against the time of cure.

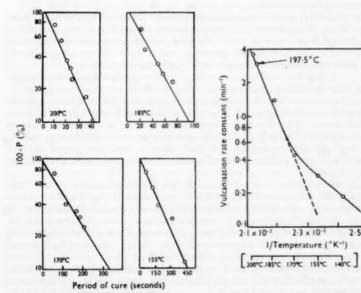


Fig. 4.—Rate of vulcanization of polychloroprene compound.

Fig. 5.—Temperature dependence of vulcanization of polychloroprene compound.

This was carried out for the five curing temperatures used, and straight lines could satisfactorily be fitted to the experimental points (Figure 4). As the reduced modulus of the unvulcanized compound may be neglected and the scorch curve indicated no definite delay in the onset of vulcanization, it was to be expected that at the lower curing temperatures these fitted lines should also intercept the ordinate axis at 100 per cent. The small lateral shift observed at 200° C has already been explained.

It therefore seems reasonable to believe that chemical crosslinking can in this case be represented by a first order process. Using Equation (6), the specific rate constant at each temperature can thus be determined directly from

the slope of the fitted lines.

The temperature dependence of the rate of chemical reactions was given by Arrhenius and may be written

$$\log_e k = \log_e A - \frac{E}{R \cdot T} \tag{7}$$

where k is the rate constant at absolute temperature T, E the energy of activation, R the gas constant and A the frequency factor. The five rate constants which had been obtained were therefore plotted logarithmically against the reciprocal absolute temperature of vulcanization (Figure 5). Whereas it was verified by inspection that the deviation of the points from any single straight line was much larger than the experimental variation indicated by the preceding evaluation, the data can be well fitted by two intersecting straight lines. The energy of activation is calculable by reference to the Arrhenius equation and was almost exactly 10 kcal/mole for the lower and 30 kcal/mole for the higher curing temperatures.

The unusual type of temperature dependence found in this case has been interpreted by Hinshelwood as the consequence of two alternative, simultaneous reactions⁶. In a system of the chemical and physicochemical complexity such as that of this polychloroprene compound it is, of course, not possible to

assign these two activation energies to a simple pair of reactions.

However, it is known that substances which accelerate vulcanization can act by lowering the energy of activation, and also that the rate of an apparently first order vulcanization determining process may vary with the stoichiometrical excess of accelerator present. In view of the considerable effect which accelerator concentration had in fact been found to have on the scorch behavior of the compound (Figure 2), it could be inferred that the aldehyde-amine accelerator used actually participated in that reaction, which exhibited the low activation energy of 10 kcal/mole and determined the overall rate of vulcanization at the lower curing temperatures.

From this important basic supposition follows an immediate consequence concerning the other alternative reaction, which showed an activation energy of 30 kcal/mole. By virtue of being an alternative process to the above, it must also be independent of any reactants peculiar to the other process. In other words, the speed of that vulcanization process, which at the higher curing temperatures is faster and therefore rate determining, may thus be expected

not to vary with the concentration of accelerator used.

In the limiting case it should then be possible to omit the accelerator altogether without affecting the rate of vulcanization at the higher temperatures. This simple test was carried out at a curing temperature of 197.5° C and the first order rate constant determined in the smae manner as before. From Fig-

ure 5 it can be seen that the value at 197.5° C is in complete agreement with those previously obtained for compound containing the aldehyde-amine accelerator.

It is, of course, conceivable that other vulcanization accelerators, which operate satisfactorily at conventional temperatures, may also become ineffective at high curing temperatures. Provided that the crosslinking efficiency of the curing system is not greatly changed, this could depend on the frequency factor as well as on the activation energy of the rate determining step in the accelerated vulcanization process. Although the finding predicted in this investigation supported the rather tentative explanation that was offered, the latter must be treated with some reserve, particularly as regards any generalization. Nevertheless, this example demonstrates very clearly that the curing behavior of a rubber compound actually observed at high temperatures may significantly differ from that suggested by any studies which are limited to normal curing temperatures, e.g. less than 150° C.

CURING BEHAVIOR OF A SULFUR-BASED COMPOUND

Had the polychloroprene compound shown any definite degree of reversion, it would undoubtedly have been much more difficult to evaluate its vulcanization behavior. Reversion does in fact generally occur in the case of all those rubber compounds in which elemental sulfur is the crosslinking agent. A natural rubber compound that is typical of this class has been formulated by the American Chemical Society; per 100 parts of rubber this ACS1 compound contains 6 parts of zinc oxide, $3\frac{1}{2}$ parts of sulfur, and $\frac{1}{2}$ part each of stearic acid and mercantobenzthiazole.

Pure gum natural rubber compounds do not extrude well, and in order to obtain satisfactory filaments for high temperature curing, all such natural rubber compounds were prepared from superior processing pale crepe, which had been exhaustively extracted with acetone. It was considered that the very small amount of bound sulfur remaining after extraction (found 0.05 per cent) would be of no consequence compared with the extent of sulfur crosslink-

ing during vulcanization.

Some consideration must firstly be given to the curing behavior at temperatures below 150° C. Although rubber compounds of this type already show a certain measure of reversion, its effect during the main part of the vulcanization process is then still relatively small. From data published by Lorenz⁷ it was possible to calculate the apparent crosslink density of a range of vulcanizates. In view of the linear relationship between the apparent and the chemical crosslink density, which is implicit in the results of the calibration experiments by Mullins, Moore and Watson³, these values could be treated in the represented as a first order process. An interesting feature is the marked increase of both the rate and the efficiency of crosslinking in the presence of zinc stearate.

In terms of 100 per cent modulus, Gee and Morrell have also reported first order vulcanization, and their results already indicated that continued curing produced only partial reversion. More recently Ellis and Welding drew particular attention to the limiting value reached, and subject to this they took reversion as well as vulcanization to be first order processes. These were important observations, and the question arose of whether they would also

apply to high temperature curing.

Experiments were therefore carried out at 197.5° C. On inspection the

modulus results indicated that reversion had not become excessive but allowed useful measurements after very long periods of cure (Figure 7). There could be no doubt that a definite and substantial lower limiting value was being approached; this was easily obtained by extrapolation. Vulcanization of the ACS1 compound also appeared still to be a much faster process than reversion.

For a simple graphical evaluation of the data it was in fact necessary that vulcanization should practically have ceased during at least a reasonable part of that period over which reversion was still operative. When the difference between the observed modulus and the estimated lower limiting value was plotted logarithmically against the time of cure, a straight line was obtained (Figure 8). This indicated that the original requirement had been met, and the rate constant for reversion was thus given by the slope of the fitted line.

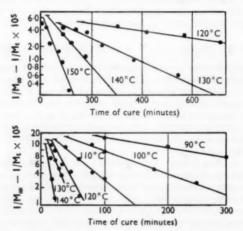


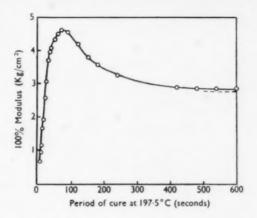
Fig. 6.—Kinetics of crosslinking. Upper plot is for the recipe: rubber 100, zinc oxide 4.5, sulfur 3.5, MBT 2.3. Lower plot is for the recipe: rubber 100, ZnO 4.5, sulfur 3.5, zinc stearate 3.3 and MBT 2.3.

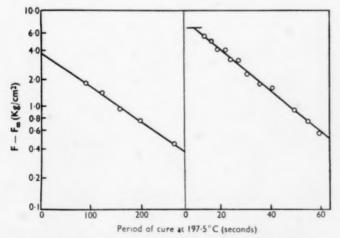
Vulcanization was then evaluated in a similar manner, except that the limiting value appropriate to each time of cure was taken from the extrapolated portion of the reversion line. A straight line could again be fitted to the points (Figure 8), and its slope gave the rate constant for vulcanization. At conventional curing temperatures where both the extent and the relative rate of reversion are small, an approximate correction is to use the intercept of the reversion line as a constant limiting value for vulcanization.

In an ideal experiment the vulcanization and reversion lines would intersect at the ordinate axis, whereas in practice they were found to reach the same value at a small positive time of cure. This upper limiting value is obviously equivalent to zero modulus, but the corresponding time of cure does not necessarily denote the onset of vulcanization. Theoretical values of 100 per cent modulus for uncured, pure gum natural rubber compounds have been calculated by Gee and Morrell¹¹, and taking this into consideration the apparent heating-up periods of the rubber samples were estimated to have been less than 2 seconds.

Before entering into any further aspects of interpretation it will be useful to examine the results given by a so-called sulfur-free compound containing TETD

(tetraethylthiuram disulfide) and zinc oxide. Although such compounds are noted for the absence of reversion at conventional temperatures, it was plainly exhibited by the curing behavior at 197.5° C (Figure 9). A substantial lower limiting value was again indicated, and its value estimated as before by extra-

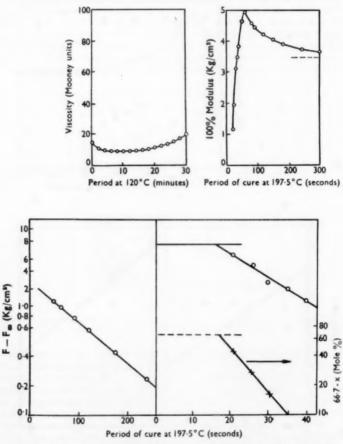




Figs. 7. and 8.—ACS1. compound for the recipe: S.P. pale crepe 100, ZnO 6, sulfur 3.5, stearic acid 0.5, and MBT 0.5.

polation. In addition to the modulus data, the zinc diethyldithiocarbamate formed during vulcanization was determined by conductometric titration of acetone extracts with hydrochloric acid. A Mooney scorch test was also carried out and showed a relatively gradual increase of the compound viscosity at 120° C.

The modulus results were evaluated graphically according to the same procedure as that employed for the ACS1 compound. Both reversion and vulcanization could again be characterized by straight lines giving the respective rate constant. However, the evaluation drew attention to an important difference (Figure 10). The time of cure corresponding to zero modulus had changed



Figs. 9 and 10.—TETD vulcanization for the recipe: pale crepe 92, ZnO 5, and TETD 3.

from approximately 4 seconds to about 16 seconds, and neither the apparent heating-up time nor the negative modulus value calculated for the uncured rubber compound could account for more than a small part of this period. Taking the formation of the dithiocarbamate as a first order process with an established limit of 66.7 mole per cent, a similar delay in the appearance of dithiocarbamate was also found. This delay period is another phenomenon of this curing system which had not been observed for conventional temperatures. It suggests that

crosslink formation is preceded by a process of lower activation energy, which may in some way be associated with the believed localization of reaction at the zinc oxide-rubber interface¹².

INTERPRETATION OF VULCANIZATION AND REVERSION

Any evaluation of such data as those which have been presented poses the question of their interpretation in terms of the fundamental processes, which together constitute the overall curing behavior. Each of these processes may in turn comprise a number of individual chemical steps, one of which will, of course, be rate determining. However, a first order process does not necessarily imply a unimolecular reaction, but probably contains some bimolecular rate determining step with an invarient concentration of one reactant, as for instance the rubber hydrocarbon.

The salient features which have emerged are that the state of crosslinking can be represented to increase exponentially during vulcanization while decreasing exponentially due to reversion towards a substantial limiting value. A formal equation relating the crosslink density to the time of cure will therefore consist of one exponential term for vulcanization, another exponential term for reversion, and a constant term for the ultimate limiting value. Equations of this type have been derived by making a simple assumption to explain the existence of a finite limit.

Firstly it was assumed that an equilibrium is set up between the rupture of crosslinks X and their formation from the degradation product B by first order processes with rate constants of k_2 and k_3 respectively. Vulcanization was also taken to be a first order process with rate constant k_1 , and the potential crosslinks A are in fact related to the quantity of unreacted curing agent. Initially there are only the potential crosslinks A_0 ; ultimately these decrease to zero and the observed crosslinks reach their limiting value $X \infty$. Using these conditions an equation of the requisite form is obtained. Thus if

$$A \xrightarrow{k_1} X \xrightarrow{k_2} B$$

where X = observed crosslinks, A = potential crosslinks, B = ruptured crosslinks, and t = time of cure, it can be shown that

$$X = \frac{k_3}{k_2 + k_3} \cdot A_0 - \frac{k_1 - k_3}{k_1 - k_2 - k_3} A_0 e^{-k_1 t} + \left(\frac{k_1 - k_3}{k_1 - k_2 - k_3} - \frac{k_3}{k_2 + k_3} \right) \cdot A_0 e^{-(k_2 + k_3)t}$$
(8)

In the second scheme it was assumed that both stable crosslinks X' as well as unstable crosslinks X'' are formed during vulcanization and that degradation of the latter then takes place; their sum equals the observed crosslinks X. Taking first order processes for every case and introducing A_0 and X^{∞} , another equation of the same general form was derived. Again if

$$X' \xleftarrow{k_4} A \xrightarrow{k_5} X'' \xrightarrow{k_6} B$$

where X' = stable crosslinks, X'' = unstable crosslinks, X = X' + X'' = observed crosslinks, A = potential crosslinks, B = ruptured crosslinks and t = time of cure, it can be shown that

$$X = \frac{k_4}{k_4 + k_5} A_0 - \left(\frac{k_4}{k_4 + k_5} + \frac{k_5}{k_4 + k_5 - k_6} \right) A_0 e^{-(k_4 + k_5 t)} + \frac{k_5}{k_4 + k_5 - k_6} A_0 e^{-k_6 t}$$
(9)

Although there are basic differences between the concepts underlying these two simple reaction schemes, the final Equations (8) and (9) are mathematically equivalent. No explicit allowance has been made for degradation by chain scission, which is, however, implied in as far as it is crosslink activated.

TABLE 2
FIRST ORDER RATE CONSTANT

Description of rate constant		ASC1 compound	TETD compound	
Graphical evaluation	Vulcanization	2.6 min-1	3.8 min ⁻¹	
	reversion	0.55 min^{-1}	0.54 min ⁻¹	
1 Reaction scheme	k_1	2.6 min^{-1}	3.8 min ⁻¹	
	k_2	0.28 min^{-1}	0.15 min^{-1}	
	k_1	0.27 min ⁻¹	0.38 min ⁻¹	
2 Reaction scheme	k_4	1.3 min ⁻¹	2.7 min ⁻¹	
	k_b	1.3 min ⁻¹	1.1 min ⁻¹	
	ke	0.55 min ⁻¹	0.54 min ⁻¹	

The procedure employed for evaluating the modulus data can now be examined by reference to Equations (8) and (9). The lower limiting value is seen to correspond to the first term. By neglecting the second term, which is associated with vulcanization, reversion could be treated as a first order process. In view of the linear relationship between 100 per cent modulus and crosslink density, the rate constant given by the reversion line may thus be identified with the exponent of the third term. Vulcanization was then evaluated by means of the difference between the second and the other two terms of each equation, so that the rate constant for vulcanization may be identified with the exponent of the second term.

The determination can only be completed by applying an additive correction for the 100 per cent modulus of the uncured rubber compound to both the lower and upper limiting values. This gives the ratio $X \propto /A_0$, which equals that of k_3 to $(k_2 + k_3)$ or k_4 to $(k_4 + k_5)$ respectively (Table 2).

The two reaction schemes may of course be combined by considering with the previous notation

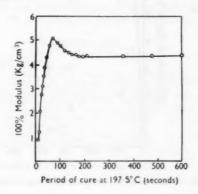
$$X' \xleftarrow{k_4} A \xrightarrow{k_5} X'' \xrightarrow{k_2} B$$

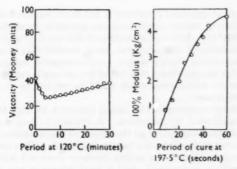
and in this case an equation of the requisite form is again obtained. The rate constant for vulcanization is then given by $(k_4 + k_5)$ and that for reversion by $(k_2 + k_3)$, but additional information would be required to evaluate the four individual rate constants.

OTHER CURING SYSTEMS

The wider scope of high temperature curing will be illustrated by only a brief reference to two other curing systems. They were both examined in pure gum compounds prepared from superior processing crepe, and curing was carried out at 197.5° C.

In one case a typical quinoid system was used, and this consisted of approximately equimolecular quantities of dibenzoyl-p-quinonedioxime and red lead. The modulus data (Figure 11) at once showed the existence of a substantial





Figs. 11 and 12.—Quinoid vulcanization for the recipe: S.P. pale crepe 92, red lead 5.25, dibenzoyl-p-quinonedioxime 2.75.

and well-defined limiting value, but further inspection already indicated that the graphical method of evaluation must fail because of the similar rate of vulcanization and reversion. Although the oxidizing action of red lead is necessary for crosslinking to occur, neither the scorch measurements at 120° C nor the initial gradation of the modulus curve for 197.5° C suggested any major delay in the onset of cure such as that which had been observed for high temperature TETD vulcanization (Figure 12).

The curing system chosen for the second sample contained dicumyl peroxide and hydrated lime. Owing to the sulfur crosslinks originally built into superior processing crepe, some reversion had been anticipated (Figure 13). However, on comparing the decrease of modulus on continued curing with the behavior shown by the previous compound, it seemed likely that the observed reversion was largely associated with the curing system.

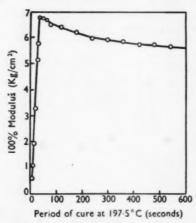


Fig. 13.—Peroxide vulcanisation for the recipe; S.P. pale crepe 95, lime 3.7, dicumyl peroxide 1.35.

CONCLUSION

From the various examples presented it will have become evident that very rapid vulcanization of rubber compounds can generally be carried out at temperatures near 200° C. Although estimates of this are frequently based on the behavior at conventional temperatures, their unreliability was well demonstrated by vulcanization studies with a polychloroprene compound. In this case curing at high temperatures was found to produce a fundamental change in the vulcanization mechanism which could be related to the action of the vulcanization accelerator.

For most rubber compounds the curing behavior at high temperatures is considerably complicated by reversion. A relatively simple graphical procedure usually allows a separation of the effects of vulcanization and reversion by which the overall curing behavior can be evaluated. Two reaction schemes have been devised to explain the salient features observed with sulfur cross-linked natural rubber compounds, and a breif reference was made to other curing systems.

SUMMARY

When a thin rubber sample is heated to a high curing temperature, the initial kinetics of cure as derived from Newton's rule can be represented by a well-defined time delay at the final curing temperature. This facilitates quantitative studies for which it is also shown that first order changes in crosslink density can be assessed by modulus measurements.

The vulcanization rate constants thus determined in the case of a polychloroprene compound indicate the apparently different action of the vulcanization accelerator at conventional and at high temperatures, which allows a fundamental interpretation to be advanced. Partial reversion at high temperature is shown for both the ACS1 and a thiuram-cured natural rubber compound, and using an appropriate graphical method, vulcanization and reversion can be evaluated as first order processes. Two simple overall reaction schemes are developed to fit the experimental data with only three calculated rate constants. Quinoid and peroxide curing systems are also examined.

ACKNOWLEDGMENT

Acknowledgments are due to the Director of Research of British Insulated Callender's Cables Ltd., for permission to publish the results of this work.

REFERENCES

- 1 A detailed account is to be published later.
 2 Mason, J., Trans. Inst. Rubber Ind., 29, 148 (1953).
 3 Flory, P. J., Rabjohn, M., and Schaffer, M. C., J. Polymer Sci. 4, 225 (1940).
 4 Fletcher, W. P., Gee, G., and Morrell, S. H., Trans. Inst. Rubber Ind. 28, 89 (1952).
 5 Gee, G., and Morrell, S. H., Trans. Inst. Rubber Ind. 28, 111 (1952).
 6 Gee, G., and Morrell, S. H., Trans. Inst. Rubber Ind. 28, 111 (1952).
 7 Lorens, O., and Echte, E., Kautschuk und Gummi 10, WT24, WT82 (1957).
 8 Mullins, L., Moore, C. G., and Watson, W. F., J. Polymer Sci. 19, 225-254 (1956).
 9 Gee, G., and Morrell, S. H., Trans. Inst. Rubber Ind. 28, 109 (1952).
 10 Gee, G., and Morrell, S. H., Trans. Inst. Rubber Ind. 28, 109 (1952).
 11 Gee, G., and Morrell, S. H., Trans. Inst. Rubber Ind., 28, 114 (1952).
 12 Scheele, W., and Stange, P., Kautschuk und Gummi, 9, WT110 (1956).

THE MECHANISM OF DISULFIDE DECOMPOSITION UNDER VULCANIZATION CONDITIONS *

I. A. Tutorskii, L. B. Ginsburg, B. A. Dogadkin

THE M. V. LOMONOSOV INSTITUTE OF FINE CHEMICAL TECHNOLOGY, MOSCOW, USSR

A homologous decomposition of several organic disulfides that are used as vulcanization accelerators^{1, 2, 3} for rubber, such as MBTS (2,2'-dibenzothiazolyldisulfide) or TMTD (tetramethylthiuram disulfide) is observed at the temperatures encountered during vulcanization. The mechanism of decomposition has been examined insufficiently. The majority of studies assumed that only the less stable S-S bonds are split while the C-S bonds are not involved. However, lately there have been indications that cleavage of the C-S bonds may be possible. Thus, in the exchange of the sulfur of the sulfide bonds of MBTS and the corresponding monosulfide with elemental sulfur, the values of the activation energy for the exchange reaction of the di- and monosulfides are close to each other (23-24 kcal/mole)4. Besides this, at 130° an exchange5 between elemental sulfur and the sulfurless vulcanizate obtained with MBTS

In the following work the mechanism of the decomposition of MBTS was studied with S35 under the conditions of vulcanization.

EXPERIMENTAL

Vulcanization with MBTS.—The vulcanizing action of MBTS in the absence of sulfur was first mentioned in papers from our laboratory and has been examined in detail by us2. In the present work vulcanizates of mixes of sodium butadiene rubber containing 1 and 2 parts per hundred parts rubber by weight (phr) were used.

The technical rubber SKB-30 S was purified from alkali and other low molecular weight impurities by the following method. First, the following mix was prepared on the micromill: Rubber 100; stearic acid 5 phr, PBNA 1 phr. The mix was heated for 3 hours at 70° in an air thermostat and then extracted with a binary mixture of ethanol-toluene azeotrope in a cold extraction apparatus for 5 hours under a stream of pure nitrogen. Purification of the heated mix in this manner lowers the alkali content of the rubber below the point where it will influence the kinetics of vulcanization.

Sulfurless vulcanization was accomplished through the use of MBTS labeled with S35 in the disulfide bridge. The MBTS was obtained by oxidizing MBT (2-mercaptobenzothiazole), labeled in the sulfhydryl group, with gaseous chlorine⁶. The specific activity of the sulfur used to synthesize the MBT was 0.4 millicuries per gram. The resulting MBTS possessed a specific activity

of 5100 impulses/minute/mg.

The compound was prepared on a micromill enclosed in a hermetically sealed cabinet filled with argon (the oxygen content of the argon was 0.1%).

^{*} Translated for Rubber Chemistry & Technology from Zhurnal Fizicheskol Khimil 33, 1401 (1959) by Robert L. Dunning.

The compounds were wrapped in cellophane packets and vulcanized in an electrically heated press at $143^{\circ} \pm 2^{\circ}$. The amount of MBTS bound to the rubber was determined radiometrically³. The activity of the specimens of the vulcanizate at various cure times was 513–1450 impulses/minute as compared to a background of 33–40 impulses/minute. The total amount of sulfur of the MBTS bound to the rubber was determined by oxidizing the vulcanizate with a mixture of HNO₂ and Br₂ in the presence of MgO followed by a determination of the SO₄⁻ ion as barium sulfate⁹.

In Figure 1 is presented the kinetics of the combining of MBTS during the vulcanization of a compound consisting of 100 phr rubber and 2 phr DBTDS at 143°. Curve 1 corresponds to the amount of bound MBTS determined radiometrically while curve 3 corresponds to the amount determined chemically. The radiometric method gives the quantity of sulfur of the disulfide

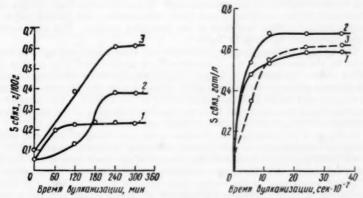


Fig. 1.—The kinetics of combination of sulfur during sulfurless vulcanization with MTBS at 143°:

1—disulfide; 2—thiazole; 3—total sulfur.

Fig. 2.—The kinetics of combination of elemental sulfur during vulcanization in the presence of MBTS at 143°: 1—0.5% MBTS; 2—1.5% MBTS; 3—1.5% MBTS and 5.0% ZnO.

bridges bound to the rubber while the chemical method gives the total amount of bound sulfur. By subtracting from the value of the total sulfur the corresponding value of the disulfide bridge, the amount of sulfur as thiazole rings bound to the rubber is determined (Curve 2 in Figure 1). As may be seen from these data, the total amount of bound sulfur is more than double the amount of disulfide bridge sulfur. There is also observed a period of low activity in the

reaction bonding the thiazole sulfur to the rubber.

Sulfur vulcanization in the presence of MBTS.—In order to examine the mechanism of the decomposition of MBTS during sulfur vulcanization a mix was prepared from MBTS which was labeled in the thiazole ring with S²⁵. This compound¹⁰ was prepared by oxidizing MBT containing the labeled S in the thiazole ring with gaseous chlorine. The specific activity of the sulfur used in the synthesis was 0.8 millicuries/g. The specific activity of the MBTS labeled with S³⁵ only in the thiazole ring was 6300 impulses/minute/mg. The activity of the specimens of vulcanizate registering on the counter varied from 400 to 2300 impulses/minute depending on the amount of MBTS introduced. By marking the MBTS molecule in the thiazole ring the possibility of an ex-

Table 1
Composition of the Compounds of Purified Rubber

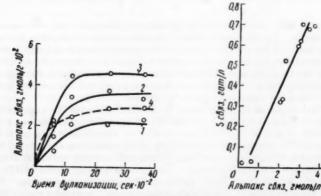
		Comp	pound	
Ingredient	1	2	3	4
Rubber	100	100	100	100
MBTS*	0.5	1.5	2.0	1.5
Sulfur	2.0	2.0	2.0	2.0
Zinc oxide		-	execute	5.0

* Having labeled sulfur in the thiazole ring.

change between the S²⁵ atoms of the accelerator and elemental sulfur is excluded thus allowing one to simultaneously follow the kinetics of the addition of sulfur and accelerator to the rubber. Ordinary nonactive sulfur recrystallized from benzene was used in the vulcanizates. The purification of the rubber, the preparation of the compounds and their vulcanization was carried out in a manner similar to that described in the preceding section. The composition of the compounds is shown in Table 1.

The amount of bound sulfur (elemental and that introduced into the compound by the accelerator) was determined by a method analogous to that described above; the amount of bound MBTS was determined radiometrically. The amount of bound elemental sulfur corresponds to the difference between the total bound sulfur and the bound sulfur of the MBTS. The number of crosslink chains was calculated from the maximum swelling of the vulcanizates in xylene according to the equation of Flory and Rehner¹².

In Figure 2 are presented the kinetics of the combining of elemental sulfur during the vulcanization of compounds containing various amounts of MBTS at 143°; in Figure 3 are presented the kinetics of the combining of the MBTS during vulcanization of the same compound. As may be seen, the addition of sulfur and accelerator to the rubber takes place in a like manner. A linear relationship is found between the amount of bound sulfur and the bound MBTS (Figure 4). The rate constant for the addition of MBTS calculated from



Fro. 3.—The kinetics of combination of MBTS during vulcanization at 143°: 1—0.5% MBTS 2—1.5% MBTS; 3—2.0% MBTS; 4—1.5% MBTS and 5.0% ZnO.
Fro. 4.—The dependence of bound sulfur on the combined MBTS.

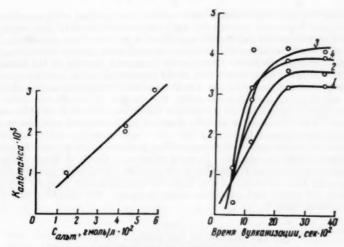


Fig. 5.—The dependence of the rate constant for the combination of MBTS on the initial concentration.

Fig. 6.—The kinetics of the formation of crosslinks during vulcanisation in the presence of MBTS (the numbers on the curves correspond to the compound numbers in Table 1).

the straight portion of the kinetic curve is a linear function of the concentration of MBTS (Figure 5).

In Figure 6 are shown the kinetics of crosslink formation during vulcaniza-The number of sulfur atoms and molecules of MBTS occurring per crosslink remains approximately constant in the main period of vulcanization

In order to obtain direct experimental data showing the manner in which the bond in the MBTS molecule ruptures, the distribution of activity between the vulcanizate and its acetone extract was studied. The extracted vulcani-

TABLE 2 SULFUR VULCANIZATION IN THE PRESENCE OF MBTS LABELED WITH S⁸⁵ IN THE THIAZOLE RING

Compound*	Cure time, min	Bound elemental sulfur, g-atoms/g ×10 ⁹	Bound MBTS g-mol/ g×10 ³	Number of cross- links, v/2 g-mol/ g×10s	No. of S atoms per erosslink	No. of MBTS molecules per cross- link	Bound 8 Bound MBTS
1	0	0.0231	0.280	-	-	_	8.25
	10	0.496	0.749	**	-	-	66.4
	20	0.555	1.044	1.820	30.5	0.575	53.1
	40	0.614	1.118	3.259	18.8	0.343	54.9
	60	0.612	1.508	3.280	19.2	0.459	40.06
2	0	0.0253	0.335	1000	-	_	7.55
	10	0.552	1.36	0.37	66.9	2.72	40.60
	20	0.691	3.43	4.18	16.5	0.822	20.20
	40	0.711	3.70	3.45	20.6	1.072	19.20
	60	0.721	3.23	3.48	20.6	0.930	22.30
3	0	0.033	0.771		-	-	4.28
	10	0.341	2.07	1.186	28.8	1.74	16.48
	20	0.536	2.40	3.169	16.9	0.75	22.35
	40	0.610	2.960	3.640	16.7	0.81	21.0
	60	0.625	3.01	3.978	15.7	0.75	20.70

^{*} The composition of the compounds is shown in Table 1. ** The vulcanizate dissolved in xylene.

zate and the material in the acetone extract was oxidized with a mixture of HNO3 and Br2 in the presence of MgO, after which the SO4 ions were precipitated as benzidine sulfate, the activity of which was then measured. thickness of the benzidine sulfate layer was in all cases greater than 20 mg/cm² i.e. greater than the limit. Because the measured activity of the benzidine sulfate was lower than that which would correspond to the activity specified by the presence of the active sulfur in the accelerator molecule as a result of the presence of nonactive elemental sulfur, the quantity of nonreactive sulfur occurring in the vulcanizate or extract was taken into account in all of the calculations. The values of the activity obtained in this manner were determined only by the relationship between the active and nonactive sulfur in the accelerator molecules and their decomposition products which go into the extract or remain in the vulcanizate. In cases where only the S-S bonds splits, the activity must be equally distributed between the vulcanizate and the extract because in the formation of the identical benzothiazolyl radicals the ratio between the active and nonactive sulfur is equal. The results obtained are presented in Table 3.

Table 3

The Distribution of the Activity Between the Vulcanizate and the Extract

	Compo	und 1*	Compound 4*			
Time of vulcanisa- tion, min	Activity of vulcanizate, imp./min	Activity of extract, imp./min	Activity of vulcanizate, imp./min	Activity of extract, imp./min		
10	10520	19380	1350	2010		
20	6370	21850	2050	6030		
40	**		2400	327		
60	**	-	*****			

^{*}The composition of the compound is shown in Table 1.

**The precipitation of benzidine sulfate was not successful because only a small amount of sulfur went into the extract.

As may be seen, in the first stages of vulcanization the activity of the extract significantly exceeds the activity of the vulcanizate. After 20 minutes the reverse is true: the activity of the extract becomes less than that of the vulcanizate.

DISCUSSION OF THE RESULTS

In investigations of the mechanism of vulcanization one encounters great difficulties because it is impossible to isolate and identify the reaction products in such insoluble high molecular weight systems. Besides this, the usual methods of analysis do not distinguish between the bound elemental sulfur and the bound sulfur of the accelerator because these methods are based upon a simple chemical decomposition of the vulcanizate. The present work a radiometric method is used which opens up the new possibility of studying the mechanisms of these complicated reactions.

As is seen in Figures 2 and 3, the combining of the sulfur and accelerator with the rubber occurs in a parallel manner. A similar case¹⁰ was mentioned by us in vulcanization in the presence of MBT. After all of the sulfur was added, a sharp reduction in the addition of MBTS to the rubber is observed in spite of the fact that there is a significant amount of free accelerator remaining in the compound. The limit to the amount of bound MBTS is near 75% of

that introduced and does not depend on the concentration of the accelerator in

the compound.

During the main period of vulcanization there is on the average 2-3 molecules of bound MBTS (Table 2) for every crosslink. These results may be explained by taking into account the nonproductive decomposition of the accelerator in the scission reaction in which the bezothiazolyl radicals combine with the polymer radicals:

Besides this, there is the possibility of an exchange reaction between the MBTS and di- or polysulfide bonds of the vulcanizate acting to reverse the vulcanization process:

$$R-S-SR'+Ar-S-S-Ar-\longrightarrow R-S-S-Ar+R'-S-S-Ar$$

Thus, during vulcanization synthesis and scission occur at the same time whereupon the relationship between the rates of these processes determines the effectiveness of vulcanization, a fact that has been shown repeatedly by us¹³.

There is great interest in the question of where the MBTS molecule cleaves: there the split occurs symmetrically at the S—S bond or unsymmetrically at the C—S bond with the formation of two nonidentical radicals. As has already been shown above, the latter possibility has been born out by the fact, revealed by E. N. Gurianova⁴, that the activation energy for the exchange reaction between elemental sulfur and MBTS and di-benzothiazolylmonosulfide are equal. Besides this, the exchange of the MBTS vulcanizates with elemental sulfur, occurring at elevated temperatures⁵, already makes the assump-

tion that a split in the C-S bond is possible.

From Figure 1 it is evident that the amount of bound sulfur determined by the chemical method (total bound sulfur) is more than double that determined by the radiometric method (sulfur in the disulfide bridges). The obtained results suggest that there is an unsymmetrical seission of the MBTS since in the other case the total amount of bound sulfur would be exactly twice that of the bound disulfide sulfur. Besides this, the S-shaped character of the curve of the bound thiazole sulfur may serve as an indication of the accumulation in the extract of a product rich in disulfide sulfur in comparison to the original MBTS. Such a product might be 2-benzothiazolylhydrodisulfide, the existence of which has been established by us earlier¹⁴. Thus, during sulfurless vulcanization, along with the split in the disulfide bond the MBTS also, apparently, experiences an unsymmetrical scission with a split of the C—S bond:

The benzothiazolyldisulfide radical (II) accepts a hydrogen from an α -methylene group of the rubber molecule and is converted to benzothiazolyl-

hydrodisulfide. The concentration of the latter in the compound gradually increases whereupon this compound goes into the extract causing the S-shaped

curve for the bound thiazole sulfur.

Data on the distribution of the activity of the sulfur of the accelerator between the extract and the vulcanizate, obtained during the study of sulfur vulcanization, also bears witness to the fact that an unsymmetrical split in the MBTS occurs. During this, the activity of the extract significantly exceeds that of the vulcanizate in the main period of vulcanization (to 20 minutes) (Table 3). After all of the sulfur has combined, the reversed is observed: the activity in the vulcanizate exceeds that of the extract. Evidently the distribution of the thiazole and disulfide sulfur between the extract and the vulcanizate essentially depends on the concentration of the free sulfur in the compound. As is well known, sulfur is an excellent acceptor for free radicals. The radicals that are formed during the cleavage of the MBTS react with the sulfur with the formation of benzothiazolylpolysulfide radicals:

$$C_0H_4$$
 S
 $C \cdot + S_0 \rightarrow C_0H_4$
 S
 S
 S
 S_0
 S
 S_0

The polysulfide radical reacts with the rubber which in turn splits off a sulfur atom from the polysulfide chain since the latter S—S bond is the weaker:

$$C_0H_4$$
 S
 $C - S_0 + Ka \rightarrow C_0H_0$
 S
 $C - S_7 + KaS$.

The bonding of the benzothiazolyl radicals to the rubber is possible only under conditions of complete depolymerization of the polysulfide chains, i.e, when all of the free sulfur in the compound has been used up. Then the bonding of the benzothiazolyl radicals to the rubber starts and, consequently, the part of the thiazole sulfur in the vulcanizate that determines the activity significantly increases:

C₆H₄

$$\begin{array}{c}
N \\
C \cdot + \sim CH_2 - CH = CH - CH_2 \sim \rightarrow \sim CH_2 - CH - \dot{C}H - CH_2 \sim \\
C \\
N \\
C_6H_4$$

Besides this, during vulcanization of the compound it is possible to accumulate 2-benzothiazolylhydrodisulfide to some extent due to the extraction of a hydrogen atom from the α -methylene group of the rubber by the benzothiazolyldisulfide radicals. The transference of the latter compound to the extract makes sure that the larger portion of the disulfide sulfur will be in the extract, i.e., to cause a decrease in sulfur activity.

Thus the experimental data conclusively show that together with the

cleavage of the disulfide bond of MBTS, there is also possible a nonsymmetrical split of the C-S bond. The thus formed nonequivalent radicals enter into competition with the sulfur or rubber during which the relative extent of this or that reaction depends on the concentration of the free sulfur and thus changes in various phases of vulcanization.

The distribution of the activity of the sulfur between the extract and the vulcanizate is determined by the relative extents of each reaction in the complicated step by step elementary reactions that lead to the effect of vulcaniza-

tion.

CONCLUSIONS

1. 2,2'-dibenzothiazolyl disulfide (MBTS) labeled in the thiazole ring with

the S35 isotope was synthesized.

2. During vulcanization of purified sodium butadiene rubber with MBTS the accelerator is observed to combine with the rubber simultaneously with the sulfur reaction. When all of the sulfur is combined the bonding of the accelerator is sharply retarded in spite of the fact that there is a significant amount of free MBTS left in the reacting mixture.

3. There is a linear relationship between the bound sulfur and the combined

accelerator.

4. The rate constant for the combining of MBTS with the rubber increases linearly with the concentration of the accelerator. The limiting quantity of combined MBTS is about 75% of that introduced and does not depend on the concentration of the accelerator.

5. During sulfurless vulcanization with MBTS labeled with S35 in the disulfide bridge the quantity of combined accelerator determined chemically exceeds that determined radiometrically by more than two times which indicates

that there is an unsymmetrical seission of the MBTS.

6. During vulcanization with sulfur in the presence of MBTS labeled in the thiazole ring the ratio between the activity of the extract and the vulcanizate is significantly greater than unity. After all of the sulfur is combined this ratio becomes less than unity. An explanation of this phenomenon is reported.

BIBLIOGRAPHY

- Guthford, H. G. and Selwood, P. W., J. Am. Chem. Soc. 70, 278 (1948).
 Dogadkin, B. A. and others. Doklady Akad. Nauk SSSR 92, 61 (1953). Rubber Chem. & Technol. 27, 920 (1953); Kolloid. Zhur. 17, 215 (1955); Rubber Chem. & Technol. 29, 917 (1956).
 Bresler, S. E., Prisdilova, V. I. and Khainman, V. Ya., Zhur. Techh. Fiz. 24, 577 (1954); Rubber Chem. & Technol. 29, 946 (1956); Scheele, W., Kolloid.-Z. 146, 14 (1956); Bielstein, G., Scheele, W., Kolloid.-Z. 147, 152 (1956).
 Gurianova, E. N., Dissertation in Physical Chemistry at the L. Ya. Karpova. Institute, Moscow, 1956.
 Dogadkin, B. A. and Feldshtein, M. S., "Materialy Konferentsii po Vulkanizatsii" (Material Conference on Vulcanization) Yaroelval, 1956.
 Guryanova, E. N. and Kaplunov, M. Ya., Doklady Akad. Nauk SSSR 94, 53 (1954).
 Dogadkin, B. A. and others. Kolloid. Zhur. 19, 421 (1957).
 Dogadkin, B. A., Tarasova, Z. N. and Kaplunov, M. Ya., Zavodskaya Lab. No. 4, 296 (1955).
 Franta, J., "Gumarenska technologia", Praha, 1953.
 Dogadkin, B. A., Tutorskii, I. A. and Pevzner, D. M., Doklady Akad. Nauk SSSR 112, 449 (1957); Rubber Chem. & Technol. 31, 751 (1968).
 Gurianova, E. N., Sb "Vulkanizateiya Resim" (Vulcanization of Rubber), p. 109, Goskhimizdat, Moscow, 1954.
 Flory, P. and Rehner, J., J. Chem. Phys. 11, 512 (1953).

Flory, P. and Rehner, J., J. Chem. Phys. 11, 512 (1953).
 Dogadkin, B. A., "Ychenie o Kauchuke" (Study of Rubber) p. 294, Mashizdat, Moscow, 1938; "Khimiya i Fizika Kauchuka", p. 298, Gosakhimizdat, Moscow, 1947; Dogadkin, B. A. and Tarasova, Z. N., Doklady Akad. Nauk SSSR, 85, 1069 (1952).
 Dogadkin, B. A. and Tutorskii, I. A., Doklady Akad. Nauk SSSR 108, 259 (1956).

THE SHAPE OF SPECIMEN AND THE MEASUREMENT OF PERMANENT SET *

SHIRO YABUTA

MUTSUBISHI RUBBER COMPANY, LTD., NAGATA, KOBE, JAPAN

From a rheological point of view, there are doubts with regard to the effects of shape of the specimen, the testing temperature, and the time scale on the determination of permanent set according to JIS K6301¹ or ASTM D412-51T². Especially, whether a specimen in tension is subjected to stress uniformly or not is most important in the determination of set. Distributions of stresses in two different types of specimens have now been studied both mechanically and photoelastically. The results are reported here.

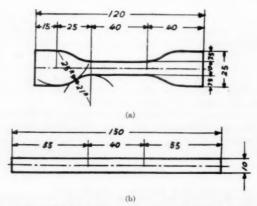


Fig. 1.—Specimens for the measurement. (Figures in mm.) (a) JIS #1 dumbbell-shaped specimen. (b) Rectangular strip specimen.

Experimental and results.—Dimensions of two types of specimens, one having a dumbbell shape (JIS #1) and the other those of a simple rectangular strip, are shown in Figure 1. Both types were cut from a vulcanized rubber sheet of about 2 mm. thickness. The JIS-type specimens were cut by the JIS die, which had the same dimensional tolerance as in ASTM D412-51T. For the mechanical measurement a soft NR vulcanizate (compound A) having 45 degrees JIS-Hardness and low modulus was used in order to get a better idea of the deformed dimensions of the specimen. For the photoelastic determination a transparent NR vulcanizate (compound B) which also has low modulus was used. Table I gives the formulas of the two compounds.

^{*} Translated by J. Tsurugi from J. Soc. Rubber Ind., Japan, 33, 173 (1960). The present address of the above is Japan Synthetic Rubber Co., Kansai Processing Research Institute, Kamitezaki, Suma, Kobe, Japan.

TABLE I COMPOUNDS TESTED

	A	В
Smoked sheets #1	100.0	-
Pale crepe	_	100.0
Zinc oxide	5.0	-
Transparent zinc carbonate		1.5
Stearic acid	1.0	1.0
Sulfur	3.0	1.0
Morpholine disulfide		1.0
Dibenzothiazolyl disulfide	1.2	0.5
Hexamethylenetetramine	-	0.3
Tetramethylthiuram monosulfide	40000	0.05
Titanium dioxide	20.0	-
Light calcium carbonate	40.0	-
Total parts	170.2	105.35
Press cure, 10 mins. at 60 psi.		

Mechanical measurements.—For both a JIS specimen and a rectangular one the length between specimen bench marks (40 mm) was divided into eight parts of equal length and each part was numbered in order as indicated in Table II. When each specimen was stretched to 300%-elongation, the length of each deformed part was measured and compared with the original one. Deformation ratio I in these tables represents A_0/A , where A_0 is the original

Table II
Measurements of Deformation of JIS #1-Specimen

No. of divided parts	1	2	3	4	5	6	7	8
Original thickness, mm	1.89	1.92	1.96	1.98	2.00	2.02	2.04	2.05
Deformed length of each part, mm	19.2	20.8	20.7	20.4	20.5	20.5	19.5	19.5
Deformed width of each part, mm	5.31	5.18	5.13	5.13	5.13	5.13	5.13	5.16
Deformed thickness of each part, mm	1.03	1.00	1.02	1.03	1.04	1.06	1.07	1.07
Original sectional area. (A ₀), mm ²	18.9	19.2	19.6	19.8	20.0	20.2	20.4	20.5
Deformed sectional area, (A) , mm ²	5.47	5.18	5.24	5.28	5.33	5.43	5.49	5.52
Deformation ratio-I. (A_0/A)	3.46	3.70	3.74	3.75	3.75	3.72	3.73	3.72
Deformation factor, f	0.96	0.98	1.00	1.00	1.02	1.04	1.04	1.04
Deformation ratio-II. $\lceil (A_0/A) \cdot \rceil$	3.32	3.61	3.74	3.76	3.81	3.82	3.86	3.83

cross sectional area in mm², and A the area after deformation. However, since the value of A_0/A is considered to be affected by the thickness of the specimen, it is necessary to minimize this effect by using a correction factor f, i.e., the ratio of average thickness throughout the specimen to the thickness of each part. The former can be calculated by using the average thickness of each part listed in Table II and III. Deformation ratio II $[(A_0/A) \cdot f]$ is considered to represent the corrected stress concentration on the deformed specimen.

Table III
Measurements of Deformation of Rectangular Strip Specimen

No. of divided parts	1	2	3	4	5	6	7	8
Original thickness, mm Deformed length of each part, mm Deformed width of each part, mm Deformed thickness of each part, mm Original sectional area, (As), mm ² Deformed sectional area, (As), mm ³ Deformation ratio-1, (As/A) Deformation factor, Deformation ratio-11, [(As/A)·f]	1.60	1.62	1.65	1.67	1.67	1.66	1.66	1.66
	21.0	20.0	20.0	19.9	19.8	20.0	20.0	20.0
	5.8	5.8	5.8	5.8	5.8	5.8	5.8	5.8
	0.80	0.83	0.85	0.85	0.85	0.84	0.85	0.85
	16.0	16.2	16.7	16.7	16.7	16.7	16.6	16.6
	4.64	4.81	4.93	4.93	4.93	4.87	4.93	4.93
	3.45	3.37	3.35	3.39	3.39	3.41	3.39	3.39
	0.93	0.99	1.01	1.02	1.02	1.01	1.01	1.01
	3.37	3.33	3.37	3.45	3.45	3.45	3.43	3.43

Photoelastic measurements.—Because the above mechanical method is not very accurate, it may not lead to precise results. The transparent NR vulcanizate was used to determine photoelastically the variations of stress and strain distribution. Isochromatic patterns of two types of specimens at 100%-elongation were photographed, and are indicated in Figures 2 and 3. The thicknesses of the two specimens were in the range of 1.50 to 1.55 mm. The black points on the specimens shown in Figures 2 and 3 were bench marks.



Fig. 2.—Isochromatic pattern of JIS #1-specimen at 100%-elongation.

Discussion.—It is very interesting to note how the deformation of each part varies, especially to note how the curved parts of the JIS type specimen affect the deformation of parts located near the center of the specimen. The deformation ratio-II of each part was plotted in Figure 4 against the successive

number of each part.

It is concluded that the JIS-specimen deforms less uniformly than the rectangular specimen. The deformation of each part of the latter varies in narrow range as compared with that of the former as shown in Figure 4. The determination of the thickness of the deformed specimen was carried out with a dial gauge at several points on each part and the mean value was taken as an average of the thickness. This may lead to not so accurate results. Nevertheless, such a simple method reveals the influence of specimen shape on deformation. Rectangular specimen is considered preferable to a dumbbell one.



Fig. 3.—Isochromatic pattern of rectangular strip specimen at 100%-elongation.

According to the theory of photoelasticity³⁻⁶, when polarized light falls vertically on the surface of a rubber sheet subjected to biaxial plane stresses, the following relation holds

$$n_1 - n_2 = \frac{2\pi}{45 kT} \frac{(n_0^2 + 2)^2}{n_0} (\alpha_1 - \alpha_2) (\sigma_1 - \sigma_2) = C(\sigma_1 - \sigma_2)$$
 (1)

Hence,

$$C = \frac{2\pi}{45 kT} \frac{(n_0^2 + 2)^2}{n_0} (\alpha_1 - \alpha_2)$$
 (2)

where the terms used have the following meanings: $n_1 - n_2$ difference between principal refractive indexes, n_0 average refractive index in the absence of stress,

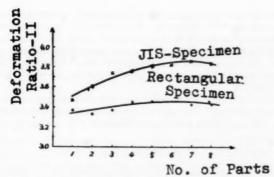


Fig. 4.—Deformation ratio-II vs. number of divided parts.

 $\alpha_1 - \alpha_2$ difference between principal polarizabilities of molecular elements, $\sigma_1 - \sigma_2$ difference between principal plane stresses, C stress-optical coefficient, k Boltzmann constant, T absolute temperature.

Therefore, the difference between principal plane stresses can be obtained by the determination of either the difference between principal refractive indexes $(\Delta n = n_1 - n_2)$ or the retardation δ .

$$\delta = \frac{2\pi}{\lambda} (n_1 - n_2)t \tag{3}$$

where λ is wave length of light and t is the optical path difference.

Above all, the monochromatic fringe method is suitable for the determination of δ by using the standardized optical system having two polarizers and two quarter wave plates. In this case, the δ value can be obtained by the measured fringe order N.

At the photoelastic analysis, the relation between N and $(\sigma_1 - \sigma_2)$ is

$$N = \alpha(\sigma_1 - \sigma_2)t \tag{4}$$

where α is the photoelastic sensivity. Therefore, the $(\sigma_1 - \sigma_2)$ distribution of each part can be obtained by the measurement of fringe order N.

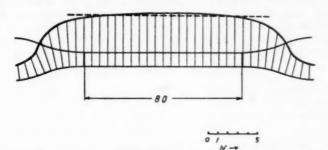


Fig. 5.—Distributions of principal stresses on the free boundaries of JIS-specimen.

The distributions of principal stresses on the free boundaries of the specimen are obtained and shown in Figure 5. The broken line in Figure 5 denotes the average stress between bench marks. It is seen from the figure that stresses in the central part of the JIS-specimen are larger than those in the curved parts, that is, the former part is subjected to more stress than curved part. The same observation was obtained also by the simple mechanical method mentioned above.

On the other hand, the rectangular specimen, having approximately 10 mm width, deforms uniformly. Variations of stress concentrations are not observed in this case, although slight changes are considered to exist owing to heterogenity of the stock.

CONCLUSIONS

Stress distributions in an ASTM or JSI-specimen and a rectangular strip specimen were investigated. It is concluded that the dumbbell type specimen is not suitable for the determination of permanent set, because of the considerable variations of stress concentration due to the influence of the curved parts on the parallel part. The strip specimen, deforming uniformly, is preferable to the dumbbell specimen.

ACKNOWLEDGMENT

The author wishes to express his hearty thanks to Dr. Kawata of Aeronautic Research Institute, Tokyo University for instruction and to Dr. Kase for kind discussion and encouragement.

REFERENCES

JIS K6301-1958. Japanese Industrial Standard, "Physical Testing Method for Vulcanized Rubber".
 ASTM D412-517, "Tentative Method of Test for Tension Testing of Vulcanized Rubber".
 Kuhn and Grün, Kolloid-Z. 101, 248 (1942).
 Treloar, Trans. Faraday Soc. 42, 273 (1956).
 Kubo, J. Phys. Soc. Japan 2, 84 (1947).
 Kawata, J. Sci. Res. Inst. 35, 5 (1959).

A NEW INDENTOR HYSTERESIMETER *

G. TANGORRA

PIRELLI RUBBER LABORATORIES, MILAN, ITALY

INTRODUCTION

The ever increasing importance of dynamic properties in the application of high polymers and vulcanized elastomers in particular, justifies the vast amount of special equipment which has been developed for their measurement¹. Just to mention a few examples, there have been the two methods put forward by Oberto and Palandri², the research work done by Cooper⁵ and by Marvin³, as well as the complete survey of the theory and suggested methods by Gehman⁴.

The technologist is often more concerned with rating vulcanized materials by the simplest, quickest and most reproducible method, rather than with the absolute values of dynamic parameters. Perhaps this accounts for the success of the hardness and rebound tests, both performed on the surface of the test piece with suitable indentors. The data obtained from tests of this kind are more or less closely correlated with the results of more complex tests and with

the specific parameters of the material.

The purpose of this paper is to describe a device for the dynamic testing of elastomers, the principle of which has not been found in the literature already examined. It can be included in the above class of instruments, combining as it does, speed and efficiency in operation with an adaptability to a wide range of materials. This device permits the determination of the equivalent stiffness and damping of the material simultaneously from the same test piece. It has the remarkable advantage of allowing dynamic tests to be carried out merely by being placed on the flat surface of a test piece, with the same ease as carrying out a hardness test and could therefore be adapted for almost general use. It might also be said that this instrument bears the same relation to more complex dynamic tests as a hardness test to a static shear modulus determination, and so in a certain sense represents an improvement over the rebound test.

As will be seen later, the apparatus should, if suitably constructed, have a remarkable range of linearity and operate with a slight preloading of the indentor. As the energy involved is negligible, practically no thermal effect is present; therefore the response is almost invariant with the time. Furthermore the resonance frequency and consequently the measured stiffness are independent of the hysteresis of the material under examination because a velocity measurement is used instead of the usual measurement of amplitude.

THEORY OF THE APPARATUS

A mechanical model having a single degree of freedom is considered, which consists of a mass m and a spring of stiffness k in parallel with a damper which has a damping constant c. When a sinusoidal force of root mean square value F and angular frequency ω is applied to the mass

Force =
$$\sqrt{2} F \sin \omega t$$
 (1)

^{*} An original contribution.

the motion is defined by the familiar differential equation

$$m\frac{d^2x}{dt^2} + c\frac{dx}{dt} + kx = \sqrt{2} F \sin \omega t \qquad (2)$$

The steady state instantaneous displacement x is obtained from the following expression

$$x(t) = \frac{\sqrt{2} F \sin (\omega t - \theta)}{\sqrt{c^2 \omega^2 + (k - m \omega^2)^2}}$$
(3)

with

$$\theta = \tan^{-1} \frac{c\omega}{k - m\omega^2} \tag{4}$$

The amplitude of x has a resonance peak at angular frequency ω_{RX} :

$$\omega_{RX} = \sqrt{\frac{k}{m} - \frac{c^2}{2m^2}}$$
 (5)

with the r.m.s. value:

$$X = \frac{F}{c\sqrt{\frac{k}{m} - \frac{c^2}{2m^2}}}$$
 (6)

Now if the velocity \dot{x} of the mass is obtained from Equation (3) by taking the derivative with respect to time, the following result is obtained:

$$\dot{x}(t) = \sqrt{\frac{\sqrt{2} F \cos (\omega t - \theta)}{c^2 + \left(\frac{k}{\omega} - m\omega\right)^2}}$$
 (7)

which at resonance, obviously different from Equations (5) and (6), gives the angular frequency ω_B :

$$\omega_R = \sqrt{\frac{k}{m}}$$
(8)

and the r.m.s. velocity:

$$\dot{X}_{R} = \frac{F}{c}$$
(9)

These expressions are simpler than those referring to displacement x, the first being independent of the damping and the second of the stiffness. It may be shown furthermore, that the resonance curve plotted with logarithmic abscissas is symmetrical with respect to ω_R .

By applying a velocity transducer to the mass of the mechanical model an ideal condition is achieved for recording under resonance conditions the unknown values of stiffness k and damping c, when the mass m is known.

In fact, introducing frequency $f = \omega/2\pi$, into Equation (8) the stiffness is found to be

$$k = 4\pi^2 m f_R \tag{10}$$

and the damping from Equation (9):

$$c = F/\dot{X}_R \tag{11}$$

The most direct way of applying the preceding considerations to a mechanical model of known mass, the stiffness and damping of which are unknown, is perhaps to electromagnetically impose a sinusoidal force with adjustable frequency, and observe the electromotive force induced in an electromagnetic transducer by the vibration of the mass itself.

The preceding theoretical discussion can be usefully extended, by introducing, instead of the parameters k and c, the real, K', and the imaginary, K'', components of the complex stiffness. As is well known, for a parallel or Kelvin element the following relations are valid:

$$K' = k \quad K'' = \omega c$$

In general, since the mechanical behavior of a vulcanizate may be more complex than that of a single Kelvin element, it is observed experimentally that the above parameters are functions not only of course of the temperature, but also of the frequency and amplitude of oscillation. For small strains and a limited frequency range several authors^{1,5,2} agree in stating that the components of complex stiffness are nearly constant. This means that the stiffness is constant and that damping is inversely proportional to frequency.

Knowledge of both dynamic parameters k and c, even if limited only to the resonance frequency, permits the total dynamic behavior of the material under examination to be determined. No specific parameter has yet been introduced; it may be thought that relations of the type

$$c = \eta \lambda \quad k = G \lambda \quad (K' + jK'') = (G' + jG'') \lambda \tag{12}$$

where η viscosity of material, G shear elastic modulus, G'+jG'' complex elastic modulus and λ has the dimensions of a length, must hold for the specific magnitudes related to a material. The parameter λ should, for conditions of perfect linearity, be a constant dependent only on the shape and dimensions of the indentor. As this must be verified through comparisons with results on samples subjected to a homogeneous strain, and as the initial conditions include constant force and not constant deformation, the experience so far acquired does not admit a general conclusion on this point.

PRINCIPLE AND CALIBRATION OF THE APPARATUS

The apparatus (Figure 1) consists essentially of a rod of nonmagnetic, nonconductive material containing two cylindrical permanent magnets near its ends. The rod is held at the top by a centering spring of practically negligible vertical stiffness, while it rests, at the bottom, on the testpiece or article's surface by means of a suitable indentor. Two coils are held by a support around the two magnets. The bottom coil is connected with an electronic oscillator which can supply it with a sinusoidal current of variable amplitude and frequency; the top coil is connected with a high impedance AC voltmeter measuring the induced voltage. The instantaneous force acting axially on the rod is:

$$F\sin\omega t = AI\sin\omega t \tag{13}$$

where I is the r.m.s. value of the current and A is a constant related to motor magnet and coil characteristics. The r.m.s. voltage V read on the voltmeter is proportional to the r.m.s. value of the axial velocity of the rod through another

constant of proportionality B related to detector coil and magnet characteristics:

$$\dot{X} = BV \tag{14}$$

When velocity resonance conditions are reached, its frequency introduced in Equation (10) gives the unknown stiffness; while from Equations (11), (13), and (14) one has:

$$c = \frac{A}{B} \frac{I}{V} = C \frac{I}{V} \tag{15}$$

If the apparatus constant C = A/B is known, it is possible to calculate the unknown damping c, as the r.m.s. value I of the current may be measured by switching the voltmeter so as to measure the voltage drop across the known

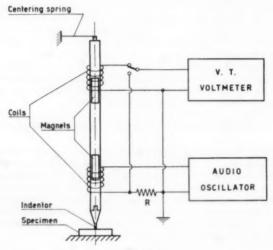


Fig. 1.-Principle of apparatus.

resistance R. As far as the calibration is concerned, the following considerations aim at putting the operator in a position to assess the equivalent stiffness and viscosity factors, namely the parameters relative to the testpiece under the particular stress conditions, considered as a pure Kelvin's model having lumped constants. For this purpose any form of the indentor could be used, but among the various types tested, the flat tip Shore A type was chosen because it showed a good linear behavior even for noticeable strains, and also because it is easily available, being already standardized for hardness measurements.

As may be seen from Equation (10) above, the knowledge of mass m of the vibrating rod is sufficient to compute the stiffness factor with no other calibration. The determination of constant C is less obvious, and can be performed either by computing A and B separately, or by a second method leading to the knowledge of C directly.

Determination of constants A and B.—With the aid of a precision balance and a d.c. ammeter, the axial force F due to a known direct current I in the

excitation coil is measured. The ratio F/I, as may be seen from Equation [13] is the constant A, which can be expressed for instance, in MKS units, in

newtons per ampere.

In order to obtain constant B, the rod is vibrated preferably on a soft material at a known angular frequency ω_c and, with the aid of a microscope equipped with an ocular micrometer, the complete amplitude $2\sqrt{2} X_c$ of the oscillation is measured, while the r.m.s. voltage V_c is read on the voltmeter.

The r.m.s. velocity being $\omega_c X_c$ it follows that

$$B = \frac{\omega_c \cdot X_c}{V_c}$$

which can be expressed, for instance, in meters per weber.

Direct determination of constant c.—Equation (7) may be more suitably put in the form:

$$\dot{x}(t) = \frac{\sqrt{2} F \cos(\omega t - \theta)}{c \sqrt{1 + \left(\frac{\omega_{R/\omega} - \omega/\omega_R}{2\beta}\right)^2}}$$
(16)

where the damping factor is:

$$\beta = c/2\sqrt{km} \tag{17}$$

For those angular frequencies ω_{D1} and ω_{D2} for which

$$\omega_R/\omega_D - \omega_D/\omega_R = f_R/f_D - f_D/f_R = 2\theta \tag{18}$$

Equation (16) becomes

$$\dot{x}(t) = \frac{F}{c} \cos \left(\omega_D^t - \theta\right)$$

It is sufficient, therefore to perform the determination on any viscoelastic testpiece (together with the resonance voltage V, current I and frequency f_R) of the two frequencies f_{D1} and f_{D2} (Figure 6) at which the output voltage is about 0.707 of the resonance voltage. From Equation (18) the damping factor β of the system is obtained, and from Equations (8) and (17) one has

$$c = 2m\omega_R\beta$$

which compared with Equation (15) gives:

$$C = 2m\omega_R \beta \frac{V}{I}$$

all the terms of which are known.

In order to prevent any mistake originating from variations of the damping as a function of frequency, an average value could be given to β computed from ratios $\omega_R/\omega_{D1} - \omega_{D1}/\omega_R$ and $\omega_R/\omega_{D2} - \omega_{D2}/\omega_R$. If the determination is performed repeatedly on various testpieces, the C factor may be obtained with adequate accuracy.

For greater accuracy both calibration systems can be used. In this way under other similar conditions (shape and size of the indentor, material and thickness of testpiece, temperature, etc.) two instruments of equal mass, which can differ because of the output and measuring system, lead to the same stiffness and damping values.

DESCRIPTION OF THE INSTRUMENT AND TESTING METHOD

Column A (Figure 2) solidly connected with platform B is held vertical by means of two levelling screws and a spherical level. With lever C, the operator can raise or lower D in which the body E of the instrument slides with low friction, being always guided in a vertical position. Under working conditions body E of the instrument containing the two exciter and detector coils, presses with all its weight (about 0.7 kg) on the testpiece under examination through a

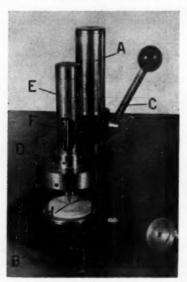


Fig. 2.—Electromechanical vibrator of hysteresimeter (presser ring G removed to show indentor H).

metal presser ring G (O.D. 25 mm, I.D. 8 mm). Rod F, with the two permanent magnets near the coils, rests its weight (about 0.054 kg) on the testpiece through the hole drilled in the center of metal ring G. When the instrument comes to rest, rod F is raised by a centering conical seat located near its lower end; under working conditions, when body E is lowered, rod F is released and rests on the testpiece by means of indentor H. Centering is ensured by an extremely thin sheet steel top spring, which introduces a negligible vertical stiffness. As the apparatus described here is the first prototype, it is still open to improvements which will be added as they suggest themselves.

The apparatus is necessarily completed (Figure 3) by a low frequency oscillator and a high impedance voltmeter which may be chosen from among many models available on the market; at this stage it may be pointed out that the electrical system is largely responsible for the accuracy and constancy of the apparatus, as the mechanical part may be built very economically with a



Fig. 3.—Complete indentor hysteresimeter.

high standard of precision. The electronic oscillator used had an output of about 0.1 W and a range of frequencies from 20 to 20,000 c/s, of which only the range 20–500 c/s was used, with regulated constant amplitude; an electronic voltmeter with several ranges the lowest of which was 1 mV was used. A unit containing only the useful ranges of the oscillator and voltmeter and a single power supply could of course be constructed.

The measurement is made by changing the oscillator frequency, having set a constant input current, until the voltmeter reading reaches its maximum value; this value together with that of frequency and input current is noted and through Equations (10) and (15) the equivalent stiffness and damping are calculated.

The test is fast and simple enough to allow a skilled operator to make several determinations per minute. This constant force procedure can be replaced by a constant velocity procedure. Under resonance conditions, in fact, the output voltage can be brought always to the same value by varying the input current. In this instance, as shown by Equation (15), the equivalent damping is proportional to the r.m.s. exciting current.

Similarly, by means of a more complex system, it is possible to render the rod vibration amplitudes constant, by setting output voltages proportional to frequencies.

The differences among the results obtained from the three above mentioned methods will, of course, be more or less noticeable according to the degree of linearity of the testpiece-indentor system and are an indication of the linearity itself.

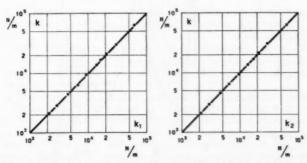


Fig. 4.—Stiffness determined with constant force (k) versus stiffness determined with constant velocity (k_1) and constant displacement (k_2) .

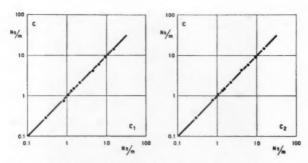


Fig. 5.—Damping determined with constant force (c) versus damping determined with constant velocity (c₁) and constant displacement (c₂).

On the basis of the above said criteria the indentor tip of the Shore A type (flat circle 0.8 mm diameter) was selected. With this indentor differences obtained with different methods both for stiffness (Figure 4) and for damping (Figure 5) proved to be negligible. Excellent linearity was obtained with the majority of elastomers on which measurements were made up to an exciting current of 5mA, corresponding to a force of about 10 mN, and a vibration amplitude, according to materials tested, from 0.1 to 0.001 mm. Consequently in subsequent testing the constant force system was used, as it is faster and simpler.

The length λ introduced previously in Equation (12) is, for the Shore A indentor, of the order of magnitude of 10 mm; further tests are being made in order to better define its values.

As an example two full resonance curves plotted under conditions of equal \dot{X}_R on two widely different elastomers are shown (Figure 6); solid points correspond to angular frequencies ω_{D1} and ω_{D2} . The instrument constants were respectively: A = 1.1 N/A; B = 0.32 m/Wb; $C = 3.45 \text{ N/A} \cdot \text{Wb/m}$.

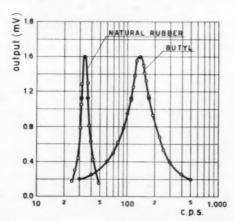


Fig. 6.—Resonance curves for two rubber vulcanized compounds at equal velocity.

FIRST EXPERIMENTAL RESULTS

Mention is briefly made here of some results obtained with the first prototype of the apparatus. Far from considering the initial survey as complete a few results are merely mentioned as examples of the way in which the instrument can be adapted for research or testing work.

Effect of the test piece thickness.—Tests on different compounds show no effect of testpiece thickness above 8 mm and a slight effect, only for softer materials, between 8 and 4 mm; further reduction in thickness gives an increase in both stiffness and damping. Although it is possible to use reduced thickness by reducing the indentor dimensions and the mass of the vibrating rod, the dimensions chosen seem to be convenient for the majority of practical applications.

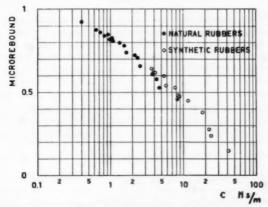


Fig. 7.—Experimental correlation between dynamic damping and microrebound for many rubber vulcanized compounds.

Effect of the surface conditions of the testpiece.—Tests carried out on molded, ground, talc-dusted, wet, soaped, and oiled testpieces did not yield noticeable discrepancies. On the other hand considerable variations in parameters were observed for small swelling with solvents or because of an irregular surface level.

Mechanical history of the testpiece.—Carbon black loaded testpieces previously stressed, showed a considerable reduction in both parameters.

Nonlinearity.—Beyond the linearity range used in experimentation, a reduction in stiffness is noted as well as an increase in viscosity, shown differently by the various elastometers. It is hardly necessary to point out that at a given time the impressed acceleration can exceed the acceleration due to gravity and the reading loses its meaning.

Effect of frequency.—For the same compound, the parameters obtained at different frequencies with heavier or lighter vibrating rods have shown in a small range (50–120 c/s) a constant stiffness and an almost inversely proportional reduction in damping with increasing frequencies. In order to disengage the static load on the testpiece from the mass of the vibrating rod, and to extend, in consequence, the frequency interval, a similar apparatus is being constructed which can assume different tilts from the vertical.

Correlation with Oberto's microrebound6 .- A large group of elastomers (Figure 7) shows sufficiently close correlation between rebound and the logarithm of their damping. It does not seem opportune to discuss the significance of this alignment at length here; but while further research work is being carried out it seems interesting to stress experimental comparison between two such widely different types of test.

Effect of temperature on the instrument.—Owing to its simple construction and remotely controlled input and output, the instrument can be easily placed in a thermostat in order to study the effect of the temperature on a testpiece.

The instrument has been used in the range 20 to 110° C without any appreciable change of its constants.

CONCLUSIONS

Although the apparatus described here is not without limitations, it has some obvious advantages over the previously described dynamic tests.

Owing to the simplicity and rapidity of the test as well as to its apparent standardization possibilities, it seems probable that it could prove of practical use in technological and industrial fields.

ACKNOWLEDGMENT

The author thanks Dr. S. Eccher and Dr. V. Zerbini for their valuable suggestions and encouragement during the development of this work, Mr. G. Della Vedova for his cooperation and Pirelli S.p.A. for sponsoring this publication.

REFERENCES

- Dillon, J. H., and Gehman, S. D., India Rubber World 115, 61, 217 (1946).
 Oberto, S., and Palandri, G., Rubber Age 63, 725 (1948).
 Marvin, R. S., Ind. Eng. Chem. 44, 696 (1952).
 Gehman, S. D., Ruber Chem. & Technol.. 30, 1202 (1957).
 Cooper, D. H., "Method of Applying the Results of Dynamic Testing to Rubber Antivibration Systems", W. Heffer & Sons, Cambridge, 1959.
 Oberto, S., Proc. Intern. Rubber Conf. Washington, 1959, p. 162.

APPARATUS STUDY OF PORE FORMATION KINETICS IN VULCANIZATION *

M. A. ALBAM AND A. P. PISARENKO

The investigation of the processes of formation of microporous vulcanizates is a complex matter, since pore formation depends upon a whole ensemble of simultaneous chemical and physical processes some of which are: the decomposition of the blowing agent with the formation of gaseous products; the solution of these gases in the rubber hydrocarbon; the formation of an independent gaseous phase inside the compounded rubber stock and the foaming of the vulcanizate, which changes its elastic and plastic properties in the course of vulcanization; the escape of the gas.

The biggest difficulty is the lack of a satisfactory procedure for investigation. Many specialists have investigated the kinetics of various pure blowing agents, but this differs from the kinetics of the decomposition of a blowing agent in various media, including a compounded rubber stock^{1, 2, 3, 5, 6, 7, 8}. In other investigations⁴ the force of the blowing action has been assessed from the size of the pressure exerted from the direction of the compounded stock upon a steel diaphragm. Nevertheless this method does not enable us to investigate the kinetics of the process or the influence of external pressure acting upon the compounded stock.

All the methods proposed hitherto for investigation of the decomposition of blowing agents enable us merely to judge the relative amount of gas liberated by the various blowing agents, or else the action of whatever blowing agent in the "foaming" of the compounded stock. But with these methods it is impossible to determine the actual amount of gas formed in the compounded stock in

the vulcanization period.

The investigation of the escape of gas from the stock in the process of vulcanization is very important for the investigation of the kinetics of pore formation. We can determine the actual internal pressure of the gas in the cells of the stock if we simultaneously consider the amount of gas which has escaped from the compounded stock. An attempt to determine indirectly the gas which had escaped, from the loss of weight of the specimens, has been made by Hofmann and Mehring¹ but their method does not enable us to establish at what point of the vulcanization process the gas escapes. The specimen of vulcanized rubber loses in addition to the gas a considerable amount of certain volatile substances and, in particular, water, which were contained in the compounded stock in the form of the hygroscopic moisture attached to the ingredients and in addition formed as a result of chemical interactions between the components of the compounded stock. The method is therefore nonapplicable.

The staff of the All-Union Artificial Leather Research Institute (Vsesoyuzn. Nauchno-Issled. Inst. Iskusstv. Kozhi) were given the assignment of developing a method of investigation which would make it possible to study the kinetics of the processes governing pore formation, under the industrial conditions for

^{*} Translated by R. J. Moseley from Legkaya Prom., 18, No. 2, 30-2 (1958); RABRM translation 811.

vulcanization of microporous rubbers. For this we designed in collaboration with Matveev a special mold consisting of a steel cylinder into which there fits a pressure-tight ram. The upper part of the cylinder is recessed to take a flanged sleeve which with the cylinder wall forms a socket into which there is fitted a vulcanized rubber ring of circular cross-section. The ring is compressed from above by the sleeve, the sleeve being adjusted by means of stud bolts through the ram.

Under the action of the sleeve the rubber ring is compressed against the lower and outer walls of the socket and against the side surface of the ram. In the middle portion of the cylinder below the rubber ring and above the lower end of the ram there is made an annular recess communicating with a gas vent. The lower part of the cylinder consists of a flat cavity in which there is placed the specimen of compounded rubber stock containing the blowing agent.

To measure the temperature of the compounded stock inside the specimen,

a needle thermocouple is inserted through the wall of the cylinder.

When the mold is placed between the heated platens of a press decomposition of the blowing agent and "foaming" of the compounded stock take place. The increase in the height of the specimen may be recorded by means of an indicator measuring the extent of the movement apart of the platens of the press.

On escaping from the rubber specimen the gas passes around the ram and into the annular recess and thence by way of the gas vent to a measuring cylinder. The rubber ring does not allow gas to escape. Because the annular recess is connected with a space which is under atmospheric pressure, a slight turn of the stud bolts by hand is sufficient to give the necessary tightness. In this case the force of friction of the ram on the rubber ring is insignificant even in com-

parison with slight pressure of the press.

By means of the apparatus described it is possible to determine the amount of gas which is formed in the decomposition the blowing agent contained in the compounded stock. For this purpose a specimen of stock containing blowing agent but no vulcanizing agent is heated in the mold at a given platen temperature and external pressure for a given time. Then the external pressure and the amount of gas which has escaped is measured in the measuring cylinder, and also according to the reading of the platen indicator we determine the amount of gas remaining within the mold, including that within the compounded stock. Here it is necessary also to take into account that a portion of the gas remains

in the compounded stock in a dissolved and sorbed state.

The term dissolved is not altogether correct for compounded rubber stocks. Melikhova⁹, while investigating the sorption of gas in filled vulcanizates of synthetic rubber, found that the amount of absorbed gas in them considerably exceeds the amount of gas which dissolves in an unfilled vulcanizate containing the same amount of rubber hydrocarbon. She explains this by the idea that the excess gas sorbed by the filled vulcanizate over and above that normally dissolved in the rubber phase comprises gas occluded by particles of filler and contacting in the form of microbubbles those parts of the particles of filler which are not wetted by the rubber phase. We have adopted Melikhova's term sorption instead solution implying by sorbed gas the weight of gas which is within the compounded stock and that outside which does not show itself as an independent gaseous phase having its own volume.

We may also employ the apparatus under discussion with some accuracy for the determination of the coefficient of sorption of the compounded stock at the temperature of vulcanization. The gas which forms in the compounded stock is partly in the form of an independent gaseous phase, and partly in a sorbed state; the sorption of the gas as we understand it obeys the Henry Law like solubility⁸. At the beginning of gas formation the whole of the gas will be sorbed by the compounded stock, while the volume of this stock does not increase.

The foaming of the stock begins only when the stock is fully saturated with the gas sorbed in it. The higher the exernal pressure upon the stock, the greater the amount of sorbed gas and the lower the amount taking part in pore formation. At a certain sufficiently high external pressure all the gas which has been formed will be in the sorbed state, and there will be no foaming at all. This fact may be made use of for an approximate determination of the coefficient of sorption of a compounded rubber stock at the temperature of vulcanization.

Having determined by raising the external pressure at what level there is a complete absence of increase in the volume of the stock (determined on the platen indicator) and having measured after releasing the pressure the amount of gas liberated from the stock, we can calculate the coefficient of sorption. For greater accuracy this determination is carried out simultaneously for compounded stocks of one type with different amounts of blowing agent, for which the saturation state sets in at different external pressures.

Knowing the coefficient of sorption, we determine and take into account the amount of gas which results from the decomposition of the blowing agent and which remains in the sorbed state in the stock after the pressure is released.

To determine the composition of the gas the apparatus is connected to a gas analyzer or samples of gas are taken in gas pipettes for subsequent analysis.

With the apparatus described it is possible to study the kinetics of the process of decomposition of a blowing agent in a compounded rubber stock, as a function of the temperature of vulcanization, the external pressure acting on the rubber, and other factors. For this we must carry out for all the given conditions a series of tests of different duration, and plot a kinetic curve on the basis of the results.

We found that the time for gas to escape from a compounded rubber stock not containing a vulcanizing agent can be measured in seconds. Since for accurate results it is necessary for the escape of gas after release of the external pressure to take place very rapidly, it is desirable to study the kinetics of decomposition of a blowing agent with a stock not containing sulfur or accelerators.

By using this apparatus, it is possible to study the course of alteration of the volume of a microporous stock during vulcanization and simultaneously follow the process of escape of gas from the rubber, and also to investigate the process of escape of gas on releasing the pressure, i.e., at the instant of discharging the specimen from the mold. By making use of the data on the kinetics of decomposition of a blowing agent in a stock, on the alteration in volume of the stock and the escape of gas in the process of vulcanization, and knowing the coefficient of sorption of the compounded stock, it is possible to calculate the alteration in the internal pressure in the process of vulcanization of microporous rubber.

The study of all these questions is highly important for the development of a theoretical basis for the production of molded microporous parts which do not change in size on discharging from the mold or shrink in the course of time.

The practical significance of this method is that the investigation of the process of pore formation is carried out under conditions corresponding fully to the actual manufacturing conditions of press curing. Thus the results of the investigations may be used directly to achieve the production of light micro-

porous rubbers, and in particular in developing a rational method of producing such rubber in the form of molded shoe sole parts.

REFERENCES

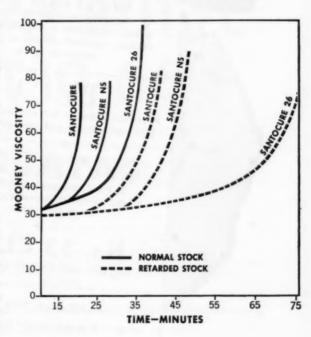
- Hofmann, G. and Mehring, R., Plaste u. Kautschuk, 3, No. 3, 58-60 (1957).
 Safrai, B. A. and Chelusheva, K. P., Nauchno-Issled. Trudy TsNIKZ, 1954, Sb. 6, p. 3-15 (Research Transactions of the Central Leather Substitute Research Inst.)
 Safrai, B. A., Solomatin, A. V., Clazkov, I. I. and Shalaeva, I. A., Nauchno-Issled. Trudy TsNIKZ, 1955, Sb. 7, p. 3-15.
 Cooper, A., Trans. Inst. Rubber Ind. 18, No. 2 (1942).
 Pryer, W. R., Rev. gén. caout., 27, 721-24 (1950).
 Lober, F., Angev. Chem. 34, No. 3, 65-76 (1952).
 Safran, G., Plaste u. Kautschuk 4, No. 3, 102-6 (1957).
 Seltlinger, S. A., Uspekhi Khin, 20, No. 2, 2(13-20 (1951).
 Melikhova, N. A., Summary of a thesis, Moscow Lomonosov Institute of Light Chemical Technology.

3 SANTOCURE® sulfenamide accelerators answer your need for compounding "flexibility"--- can give you

THE ONE DELAYED-ACTION CURE FOR BEST SPEED... SAFETY... ECONOMY

Three Monsanto sulfenamide accelerators offer you wide, dependable margins of processing safety. Within this range of delayed-action vulcanization which they provide, one of them is virtually certain to give you the most efficient and economical production you can achieve—without sacrificing processing speed or affecting your cure cycle at normal temperatures.

To fit your exact needs, let Monsanto help you compound the one delayed-action curing system for best speed, safety and economy. Chances are, Monsanto can cut your losses from premature curing of stock due to high temperature in prolonged mixing or processing operations. To see for yourself, just write or phone:



See how Santocure, Santocure NS, and Santocure 26 compare in this Mooney viscosity test... give long delayed action for greatest safety from scorch in a fast-curing natural rubber stock. Tread stock formulations and test data furnished on request.

Monsanto Chemical Company Rubber Chemicals Department Akron 11, Ohlo

Phone: HEmlock 4-1921



OUTSTANDING PRODUCTS

WHITETEX

A new white and bright pigment for rubber, synthetic rubber or plastics, especially vinyls.

BUCA

A proved pigment for compounding ALL types of natural and synthetic rubber.

CATALPO

A tried and proved product for compounding rubber and synthetic rubber.

No. 33 CLAY

For wire and vinyl compounding

For full details, write our Technical Service Dept.

Southern Clays, Inc.

33 RECTOR STREET,

NEW YORK 6, N. Y.

WHAT'S NEWS IN RUBBER

NOW IN COMMERCIAL PRODUCTION AN IMPORTANT NEW POLYMER ENJAY BUTYL HT 10-66

New Enjay Butyl HT 10-66 (formerly MD-551) is an elastomeric isobutyleneisoprene copolymer containing reactive chlorine. New HT 10-66 can be cross-linked by a variety of conventional and novel vulcanizing techniques, using either the carbon-to-carbon double bonds or the reactive chlorine, or both. Vulcanization of HT 10-66 is usually more rapid than unhalogenated Butyl polymers. Vulcanizates show the same inertness to environmental attack characteristic of Enjay Butyl rubber. Stable cures make HT 10-66 especially suitable for service at high temperatures.

NEW ENJAY BUTYL

- · Covulcanization with other elastomera
- · Fast cure rate
- Sensitivity to a wide variety of cure systems
- · Non-toxic cure systems
- Excellent low compression set character
- · Exceptional heat aging properties

. . . PLUS THESE WELL-KNOWN PROPERTIES OF BUTYL:

- · Good flex and abrasion resistance
- · High tear strength
- · Resistance to chemicals
- Low permeability Resistance to aging, ozone and oxidation

For more information, write Room 1222, Enjay Chemical Company, 15 West 51st Street, New York 19, New York

EXCITING NEW PRODUCTS THROUGH PETRO-CHEMISTRY

ENJAY CHEMICAL COMPANY

A DIVISION OF HUMBLE OIL & REFINING COMPANY



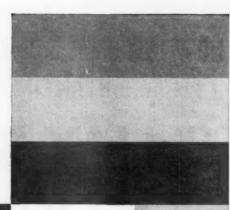
CARBON BLACKS

Wyex EPC
Easy Processing Channel Black
Arrow MPC
Medium Processing Channel Black
Essex SRF
Semi-Reinforcing Furnace Black

Semi-Reinforcing Furnace Black Modulex HMF High Modulus Furnace Black Aromex CF Conductive Furnace Black

Aromex HAF
High Abrasion Furnace Black
Aromex ISAF
Intermediate Super Abrasion Furnace Black

Arovel FEF
Fast Extruding Furnace Black
Arogen GPF
General Purpose Furnace Black



CLAYS

Suprex Clay
High Reinforcement
Paragon Clay
Easy Processing
Hi-White R
White Color
LGB
Very low grit, high reinforcement
LGP
Very low grit, easy processing
Polyfil C, X* and F*
Fine particle, light color,
water fractionated
'este overlieble in spery-dried form



RUBBER CHEMICALS

Turgum S, Turgum S8
Natuc
Buttac
Resin-Acid Softeners
Aktone
Accelerator Activator
Zeelex 23*
White Reinforcing Figment
Sylp syniloble in spray-dried form





J. M. HUBER CORPORATION 630 Third Avenue, New York 17, N. Y. Now You Can Greatly Increase Warehouse Space at No Increase in Cost With ... AZODOX... High Apparent Density Zinc Oxides



- Easier to Handle
- · Stacks Higher, Safely
- Less Bag Breakage
- · Close-Packed. **Unitized Shipments**

AZODOX stores in much less space than other zinc oxides. That's because you get many more pounds of AZODOX per cubic foot of pigmentup to 62 lbs. per cubic foot! Save valuable space for other purposes with every ton of AZODOX you buy.

In the manufacture of AZODOX, an exclusive process removes excess, space-wasting air from between individual particles of zinc oxide. Actual pigment density and every other desirable property remain unchanged. High apparent density AZODOX flows freely yet dusts less, incorporates fast and disperses thoroughly.

AZODOX is available in the following grades at no additional cost over conventional zinc oxides:

	Bulk Density ibs./cu. ft.	Rate of Activation	Reinferce- ment Properties
AZODOX-44 (Conventional)	60	Medium	High
AZODOX-55 (Conventional)	60	Fast	High
AZODOX-55-TT (Surface Treated)	62	Fast	High
AZODOX-550 (Conventional)	58	Medium	High

For technical data, fill in and mail this coupon.

American Zinc Sales Company 1515 Paul Brown Bldg. St. Louis 1, Mo.

Please send me technical information about

- ☐ AZODOX-44 ☐ AZODOX-55-TT
 - ☐ AZODOX-550
- ☐ AZODOX-55 ☐ 15 types of AZO brand zinc oxides

Company.....

Address.....

City.....Zone....State.....



Distributors for AMERICAN ZINC. LEAD AND SMELTING CO. Columbus, Ohio . Chicago . St. Louis . New York Call

for

Laboratory Reagents

Fast Service . . Glassware, Thermometers, Hydrometers and Microscopes.

JE 5-5175

for

Laboratory Design Service

Complete Laboratory Design Service . . . Fume Hoods, Lab Tables, Microscope Tables, etc.

JE 5-5175

AKRON CHICAGO MEMPHIS
LOS ANGELES NEWARK

411



The C.P. Hall Co. CHEMICAL MANUFACTURERS



NATURAL CRUDE RUBBER IN LIQUID FORM — 100% SOLIDS

Available in HIGH and LOW VISCOSITIES



INCORPORATED

A SUBSIDIARY OF H. V. HARDMAN CO., INC.

595 CORTLANDT STREET
BELLEVILLE 9, N. J.

ST. JOE

"Controlled-Analysis"

ZINC OXIDES For The RUBBER INDUSTRY



Direct Reporting On Baird-Atomic Spectrometer

RUBBER GRADE - FAST CURING TYPES

BLACK LABEL No. 20

Very fine particle size, giving maximum reinforcement and activation in rubber. For highest quality rubber goods.

RED LABEL No. 30

Excellent reinforcing and activating properties in rubber. Having fewer extremely fine particles, it is easier to incorporate than Black Label No. 20.

RUBBER GRADE - SLOW CURING TYPES

RED LABEL No. 31

Slow curing type for long flat cures and excellent scorch resistance. Good activating and reinfarcing

GREEN LABEL No. 42

General purpose type. Excellent activating and moderate reinforcing properties. Faster rate of incorporation into rubber than Black Label No. 20 or Red Label No. 30.

GREEN LABEL No. 43

Large particle size type for easy incorporation.
Good activating and reinforcing properties.

GREEN LABEL No. 42A-3

Somewhat larger in particle size than Red Label No. 31 for easier incorporation; otherwise, similar in general characteristics.

RUBBER GRADE - SURFACE TREATED TYPES

BLACK LABEL No. 20-21

GREEN LABEL No. 42-21

These grades are made from Black Label No. 20 and Green Label No. 42, respectively, by surface treating with a nontaxic hydrophobic high molecular weight

organic material. They disperse in a rubber mix rapidly and thoroughly, developing physical properties, in vulcanized rubber comparable to standard Black Label No. 20 and Green Label No. 42.

GREEN LABEL No. 46

ATEX GRADE

BLACK LABEL No. 20

Very fine particle size, giving minimum settling out in water dispersions and maximum activation in Latex Compounds.

GREEN LABEL No. 12

Heavily-calcined Black Label No. 20 type, containing few extremely fine particles. Less reactive than Black Label No. 20 and produces low viscosity water dispersions which do not readily thicken.

Low pH type used in foam latex where zinc axide is used for both activation and as a supplementary gelling agent. RED LABEL No. 30

0 type, con-

Intermediate particle size, having fewer extremely fine particles than Black Label No. 20. Less reactive than Black Label No. 20, producing lower viscosity water dispersions which do not readily thicken.

GREEN LABEL No. 43

Medium particle size for easy wetting. In pellet form this grade is particularly advantageous in preparing pourable 70% zinc axide water dispersions.



St. Joe's Distributor Network Puts St. Joe ZnO On Your Decretes

AKRON, O.
ALBERTVILLE, ALA
BALTIMORE, MED
BOSTON, MASS.
BUFFALO, N. Y.
CNICAGO, ILLINOIS
CINCAGO, ILLINOIS

DENVER COLD DETMOIT, MICH. GREENVILLE S. C. MOASTON, TES. HUNTINGTON, W VA. MACKSONVILLE, FLA. KAMEAS CITY, MO. LITTLE ROCK, ARK. LONG ISLAND CITY, N. Y.
LUS ANGELES, CAL.
MEMPHYS, TEAM,
OKLAHOMA CITY, OKLA.
OMAMA, NES.
PHILADELPHIA AREA, PA.
PICTIERUMON AREA, FA.
PICTIERUMON AREA, FA.
PICTIERUMON AREA, FA.

ET LOUIS, MO 17. PAUL MINN. BAN ANTONIO, TEX. SAN FRANCISCO: CAL BERTILE, WASH. FRENTON, N. J. FULSA, OKLA.

Write for the same of the St. Ine distributor secret you

ST. JOSEPH LEAD CO.

250 Park Avenue * New York 17, N. Y. Plant & Laboratory: Josephtewn (Monaco) Po

SNO-198 A

VULCANIZED VEGETABLE OILS RUBBER SUBSTITUTES



REPRESENTED BY

HARWICK STANDARD CHEMICAL CO.

Akron — Boston — Trenton — Chicago — Denver — Pico Rivera (Cal.) —
Albertville (Ala.) — Greenville (S. C.)

ADVERTISE in

RUBBER CHEMISTRY AND TECHNOLOGY

KEEP YOUR NAME AND YOUR PRODUCTS CONSTANTLY BEFORE THE RUBBER TECHNOLOGIST

Advertising rates and information about available locations may be obtained from George Hackim, Advertising Manager, c/o R C & T, General Tire & Rubber Company, Chemical Division, Akron 9, Ohio

RUBBER CHEMISTRY AND TECHNOLOGY IS SUPPORTED BY ADVERTISING FROM THESE LEADING SUPPLIERS

INDEX TO ADVERTISERS	PAGE
American Zinc Sales Company	23
Cabot Corporation (Opposite Inside Front Cover)	1
Carter Bell Mfg. Company, The	26
Columbia Southern Chemical Company	18
Columbian Carbon Company (Opposite Title Page)	16
DPR, Incorporated	24
DuPont, E. I., Elastomer Chemicals Department (Chemicals)	14
Eastman Chemical Products, Inc	6
Enjay Chemical Company	21
General Tire & Rubber Company, Chemical Division	10
Goodrich, B. F., Chemical Company	7
Goodrich-Gulf Chemicals & Company	
(Opposite Inside Back Cover)	28
Goodyear Tire & Rubber Company, Chemical Division	5
Hall, C. P., Company, The	24
Harwick Standard Chemical Company (Inside Back Co	ver)
Huber, J. M., Company	22
Monsanto Chemical Company	19
Naugatuck Chemical Division (U. S. Rubber Company)	
Chemicals	9
New Jersey Zinc Company, The (Outside Back Co	ver)
Pacific Smelting Company	8
Phillips Chemical Company (Philblack)	4
Phillips Chemical Company (Philprene)	11
St. Joseph Lead Company	25
Scott Testers, Inc.	15
Southern Clays	20
United Carbon Company(Inside Front Co	ver)
Witco Chemical Company	2-13

You get preferred service from Goodrich-Gulf

Fast—Warehouses in Chicago, Akron, Newark, and Neosho, Missouri, backed by giant plants in Institute, West Virginia, and Port Neches, Texas, are geared to give you quick service. Most rubber product manufacturers are within a 24-hour delivery range of Ameripol stocks.

Complete—You have the most complete selection of polymers available: non-pigmented hot, cold, and oil-extended types; micro-black masterbatch cold, and oil-extended types. Packaged in bales to suit your requirements; selected polymers available in crumb form.

Progressive—Extra values with Ameripol include technical assistance, packaging improvements to cut your handling costs, dependable quality to simplify your processing. And Goodrich-Gulf's polymer development program helps you gain a competitive edge.



For this preferred service call . . .



Goodrich-Gulf Chemicals, Inc.

Cleveland: 1717 East Ninth Street • Phone: TOwer 1-3500 New York: 200 East 42nd Street • Phone: Murray Hill 7-4255 Chicago: 6272 West North Avenue • Phone: NAtional 2-3722

RUBBER and PLASTICS COMPOUNDING

COLORS:

- STAN-TONE PE
 POLYETHYLENE
 (Less than 50%
 Pigment Concentration)
- STAN-TONE MB5
 (Rubber Masterbatch)
- STAN-TONE PEC (Polyester Paste)
- STAN-TONE PC PASTE (Pigment in Plasticizer)
- . STAN-TONE DRY COLORS
- STAN-TONE GPE
 POLYETHYLENE
 (50% Pigment Concentrate)

FILLERS

Dependable uniformity in compounding material means certainty in

product development and production runs. You can rely on consistent quality with Harwick Standard ma-

2000000000000

compounding problems,

For technical as-

terials.

SOFTENERS

EXTENDERS

PLASTICIZERS

RESINS:

- . TERPENES
- . COUMARONE INDENES
- . MODIFIED STYRENES
- . AROMATIC HYDRO-CARBONS

HARWICK STANDARD CHEMICAL CO.

60 SOUTH SEIBERLING STREET AKRON S OHIO

ALBESTYRILE MAY. 461 BOYLSTON IS, MAIS. CHICAGO 25, ILLINOIS GREENFILLE, S.C. PICO RIVERA, CALIF. TEENTON 9, MA OLD GUNTERSWELLE MAY. 461 BOYLSTON ST. 2731 W. LAWEENCE AVE. 1 MOTTINGBIASH 88. 2225 FARALHOUNT GLVD. 2395 E. STATE ST.

HORSE HEAD

HORSE HEAD AMERICAN PROCESS
ZINC OXIDES — Derived from Zinc Ore

the MOST COMPLETE

Special-3	For better color and brightness in white and linted rubber goods and pressure-sensitive adhesives.
XX-4	Tires, tubes, mechanicals, footwear; highest thermal conductivity.
XX-178	Washed, Cure rate approaches that of XX-78. Used in low moisture-absorbing stocks.
XX-203	White rubber compounds, especially white sidewalls.
PROTOX-166	Faster mixing, better dispersion than XX-4. Uses: tires, tubes, mechanicals, footwear, later, insulated wire, etc.
PROTOX-167	Faster mixing, better dispersion than XX-4. Uses: tires, tubes, mechanicals, footwear, insulated wire, etc.
PROTOX-267	Free-flowing, non-dusting, low bulk for easy handling. Uses: same as PROTOX-167.

MORSE HEAD FRENCH PROCESS ZINC OXIDES — Derived from Zinc Metal

Line of White Pigments

XX-78	Relatively coarse particle size, easy mixing. Uses: white and linted rubber goods, insulated wire, packings, latex.
KADOX-15	High surface area provides optimum activation. Latex, mechanicals insulated wire, transparent rubber, cut thread.
KADOX-25	Highest purity. For can-sealing compounds and lacquers used in food industries.
KADOX-72	Lower surface area, easier mixing, but less active than KADOX-15. Latex, mechanicals, insulated wire, footwear, tires.
KADOX-215 (pelleted)	Developed specifically for aqueous dispersions for the latex industry
PROTOX-168	Fixter mixing, better dispersion than KADOX-72. Uses: same as KADOX-72.
PROTOX-169	Faster mixing, better dispersion than KAOOX-15. Uses: same as KADOX-15.
PROTOX-268	Free-flowing, non-desting, few bulk for easy handling. Uses: tires, tubes, mechanicals, footweer, insulated wire, etc.

HORSE HEAD TITANIUM DIOXIDES



A-410(Anatase)	Water-dispersible type. For general use in islest and dry rubber compounds.
A-420 (")	Preferred HORSE NEAD anatase grade for whitewells of lires, for latex, and for compounds designed for low water absorption.
A-430 (")	For general use in dry rubber compounds and latex. Preferred NORSE HEAD anatase grade for plastics.
R-710 (Rutile)	Water-dispersible type. For general use in nea-lire compounds and in latex.
R-730 (")	For non-tire compounds designed for low water absorption. Preferred HORSE HEAD grade for superior aging properties in plantics.
R-750 (")	Uses in rubber are similar to these of R-730. In plactics, it furnishes outstanding dispersion and high resistance to aging.

THE NEW JERSEY ZINC COMPANY
160 Front Street • New York 38, N.Y.

